PB86-167186

Symposium on the Transfer and Utilization of Particulate Control Technology (5th). Volume 4

Research Triangle Inst.
Research Triangle Park, NC

Prepared for

Environmental Protection Agency
Research Triangle Park, NC

Feb 86

U.S. Department of Commerce
National Technical Information Service
NTIS

PB86-167186

EPA/600/9-86/008d
February 1986

Proceedings: Fifth Symposium on the Transfer and Utilization of Particulate Control Technology

Volume 4

Franklin A. Ayer, Compiler

Research Triangle Institute
P.O. Box 12194
Research Triangle Park, North Carolina 27709

EPA Cooperative Agreement CR810152

EPA Project Officer:
Dale L. Harmon
Air and Energy Engineering Research Laboratory
Research Triangle Park, NC 27711

EPRI Project Manager:
R.F. Altman
Air Quality Control Program
Coal Combustion Systems Division
Palo Alto, California 94304

Prepared for:

U.S. Environmental Protection Agency
Office of Research and Development
Washington, DC 20460

Electric Power Research Institute
3412 Hillview Avenue
Palo Alto, California 94304

REPRODUCED BY
NATIONAL TECHNICAL
INFORMATION SERVICE
U.S. DEPARTMENT OF COMMERCE
SPRINGFIELD, VA. 22161

AIR AND ENERGY ENGINEERING RESEARCH LABORATORY
OFFICE OF RESEARCH AND DEVELOPMENT
U.S. ENVIRONMENTAL PROTECTION AGENCY
RESEARCH TRIANGLE PARK, NC 27711

TECHNICAL REPORT DATA

(Please read Instructions on the reverse before completing)

1. REPORT NO. EPA/600/9-86/008d	2.	3. RECIPIENT'S ACCESSION NO. PB86 167186/AS

4. TITLE AND SUBTITLE Proceedings: Fifth Symposium on the Transfer and Utilization of Particulate Control Technology; Volume 4	5. REPORT DATE February 1986
	6. PERFORMING ORGANIZATION CODE
7. AUTHOR(S) Franklin A. Ayer, Compiler	8. PERFORMING ORGANIZATION REPORT NO. EPRI CS-4404, V1-4
9. PERFORMING ORGANIZATION NAME AND ADDRESS Research Triangle Institute P.O. Box 12194 Research Triangle Park, North Carolina 27709	10. PROGRAM ELEMENT NO.
	11. CONTRACT/GRANT NO. CR810152
12. SPONSORING AGENCY NAME AND ADDRESS EPA, Office of Research and Development* Air and Energy Engineering Research Laboratory Research Triangle Park, NC 27711	13. TYPE OF REPORT AND PERIOD COVERED Proceedings; August 1984
	14. SPONSORING AGENCY CODE EPA/600/13

15. SUPPLEMENTARY NOTES AEERL project officer is Dale L. Harmon, Mail Drop 61, 919/541-2429. EPA-600/9-84-025a, b, and c were proceedings for the fourth symposium. (*) Cosponsored by EPRI.

16. ABSTRACT The proceedings document the Fifth Symposium on the Transfer and Utilization of Particulate Control Technology, held August 27-30, 1984, in Kansas City, MO. The symposium was sponsored by EPA's Air and Energy Engineering Research Laboratory (formerly the Industrial and Environmental Research Laboratory), located in Research Triangle Park, NC, and EPRI's Coal Combustion Systems Division, in Palo Alto, CA. The symposium provided for the exchange of knowledge and to stimulate new ideas for particulate control with the goal of extending the technology and aiding its diffusion among designers, users, and educators. Fabric filters and ESPs received the major attention, but novel concepts and advanced technologies were also explored. Volume 1 covered the plenary session, advanced energy applications, economics, and novel concepts. Volume 2 was devoted to electrostatic precipitators. Volume 3 dealt with fabric filters. Volume 4 described fugitive emissions, dry SO2, and operation and maintenance.

17. KEY WORDS AND DOCUMENT ANALYSIS

a. DESCRIPTORS		b. IDENTIFIERS/OPEN ENDED TERMS	c. COSATI Field/Group	
Pollution	Economics	Pollution Control	13B	05C
Particles	Processing	Stationary Sources	14G	13H
Aerosols	Leakage	Particulate	07D	
Electrostatic Precipitators		Fabric Filters	13I	
Filtration		Fugitive Emissions		
Fabrics			11E	

18. DISTRIBUTION STATEMENT Release to Public	19. SECURITY CLASS *(This Report)* Unclassified	21. NO. OF PAGES 506
	20. SECURITY CLASS *(This page)* Unclassified	22. PRICE

EPA Form 2220-1 (9-73)

NOTICE

This document has been reviewed in accordance with U.S. Environmental Protection Agency policy and approved for publication. Mention of trade names or commercial products does not constitute endorsement or recommendation for use.

ORDERING INFORMATION

Requests for copies of this report should be directed to Research Reports Center (RRC), Box 50490, Palo Alto, CA 94303, (415) 965-4081. There is no charge for reports requested by EPRI member utilities and affiliates, U.S. utility associations, U.S. government agencies (federal, state, and local), media, and foreign organizations with which EPRI has an information exchange agreement.*

(*) Copies of this report are available to the public through the National Technical Information Service, Springfield, Virginia 22161.

Copyright © 1986, EPRI CS-4404, V1-4, "Proceedings: Fifth Symposium on the Transfer and Utilization of Particulate Control Technology, Volumes 1-4." Since this work was, in part, funded by the U.S. Government, the Government is vested with a royalty-free, non-exclusive, and irrevocable license to publish, translate, reproduce, and deliver that information and to authorize others to do so.

NOTICE

This report was prepared by the Electric Power Research Institute, Inc. (EPRI). Neither EPRI, members of EPRI, nor any person acting on their behalf: (a) makes any warranty, express or implied, with respect to the use of any information, apparatus, method, or process disclosed in this report or that such use may not infringe privately owned rights; or (b) assumes any liabilities with respect to the use of, or for damages resulting from the use of, any information, apparatus, method, or process disclosed in this report; or (c) is responsible for statements made or opinions expressed by individual authors.

ABSTRACT

These proceedings are of the Fifth Symposium on the Transfer and Utilization of Particulate Control Technology, held August 27 to 30, 1984, in Kansas City, Missouri. The symposium was sponsored by EPA's Air and Energy Engineering Research Laboratory (formerly Industrial Environmental Research Laboratory), located in Research Triangle Park, North Carolina, and the EPRI Coal Combustion Systems Division, located in Palo Alto, California.

The objective of the symposium was to provide for the exchange of knowledge and to stimulate new ideas for particulate control with the goal of extending the technology and aiding its diffusion among designers, users, and educators. Fabric filters and electrostatic precipitators were the major topics, but novel concepts and advanced technologies were also explored. The organization of sessions was as follows:

- Day 1
  - --Plenary session
  - --ESP: Performance Estimating (Modeling)
  - --FF: Practical Considerations
  - --Economics
  - --Novel Concepts
- Day 2
  - --ESP: Performance Enhancement I
  - --FF: Full-Scale Studies I (Coal-Fired Boilers)
  - --Fugitive Emissions I
  - --ESP: Performance Enhancement II
  - --FF: Full-Scale Studies II (Coal-Fired Boilers)
  - --Fugitive Emissions II
- Day 3
  - --ESP: Advanced Technology I
  - --FF: Fundamentals/Measurement Techniques

--Dry SO_2 Removal I

--ESP: Advanced Technology II

--FF: Advanced Concepts

--Dry SO_2 Removal II

- Day 4

--ESP: Fundamentals I

--FF: Pilot-Scale Studies (Coal-Fired Boilers)

--Operation and Maintenance I

--ESP: Fundamentals II

--Advanced Energy Applications

--Operations and Maintenance II

Volume 1 contains 19 papers presented at the Plenary, Advanced Energy Applications, Economics and Novel Concepts Sessions.

Volume 2 contains 33 papers presented at the ESP: Performance Estimating (Modeling), ESP: Performance Enhancement I and II, ESP: Advanced Technology I and II, and ESP: Fundamentals I and II Sessions, plus one unpresented paper.

Volume 3 contains 24 papers presented at the FF: Practical Considerations, FF: Full-Scale Studies I and II (Coal-Fired Boilers), FF: Fundamentals/Measuring Techniques, FF: Advanced Concepts, and FF: Pilot-Scale Studies (Coal-Fired Boilers) Sessions.

Volume 4 contains 29 papers presented at the Fugitive Emissions I and II, Dry SO_2 Removal I and II, and Operations Maintenance I and II.

PREFACE

These proceedings for the Fifth Symposium on the Transfer and Utilization of Particulate Control Technology constitute the final report submitted to EPA's Air and Energy Engineering Research Laboratory (AEERL), Research Triangle Park, North Carolina, and to the Coal Combustion Systems Division, EPRI, Palo Alto, California. The symposium was conducted at the Hyatt Regency Hotel at the Crown Center in Kansas City, Missouri, August 27-30, 1984.

This symposium (the first jointly sponsored by EPA and EPRI) was designed to provide a forum for the exchange of knowledge and to stimulate new ideas for particulate control with the goal of extending technology and aiding its diffusion among designers, users, educators, and researchers. In the opening session, an address was given on the regulatory framework for future particulate technology needs followed by a series of addresses on the impact of coming particulate requirements on the utility industry and the iron and steel industry as well as the viewpoint of large and small manufacturers. There were subsequent technical sessions on electrostatic precipitator performance estimating (modeling), ESP performance enhancement, ESP advanced technology, ESP fundamentals, practical considerations for fabric filters, fabric filter full-scale studies (coal-fired boilers), fabric filter fundamentals/measurement techniques, fabric filter pilot-scale studies (coal-fired boilers), fugitive emissions, dry SO_2 removal, operation and maintenance, and advanced energy applications. Participants represented electric utilities, equipment and process suppliers, state environmental agencies, coal and petroleum suppliers, EPA and other Federal agencies, educational institutions, and research organizations.

The following persons contributed their efforts to this symposium:

- Dale L. Harmon, Chemical Engineer, Particulate Technology Branch, Utilities and Industrial Power Division, U.S. EPA, AEERL, Research Triangle Park, North Carolina, was a symposium co-general chairman and EPA project officer.

- Ralph F. Altman, Ph.D., Project Manager, Coal Combustion Systems Division, EPRI, Chattanooga, Tennessee, was a co-general chairman and EPRI project manager.

- Franklin A. Ayer, Consultant, Research Triangle Institute, Research Triangle Park, North Carolina, was the overall symposium coordinator and compiler of the proceedings.

TABLE OF CONTENTS

VOLUME 1, PLENARY, ADVANCED ENERGY APPLICATIONS, ECONOMICS, AND NOVEL CONCEPTS

VOLUME 2, ELECTROSTATIC PRECIPITATION

VOLUME 3, FABRIC FILTRATION

VOLUME 4, FUGITIVE EMISSIONS, DRY SO_2, AND OPERATION AND MAINTENANCE

VOLUME 1
PLENARY, ADVANCED ENERGY APPLICATIONS, ECONOMICS, AND NOVEL CONCEPTS

Page

Session 1: PLENARY SESSION 1
Everett L. Plyler, Chairman

The Regulatory Framework for Future Particulate Technology Needs 2
Sheldon Meyers

The Impact of Coming Particulate Control Requirements on the Utility Industry 9
George T. Preston

The Impact of Coming Particulate Control Requirements on the Iron and Steel Industry. 16
Earle F. Young, Jr.

The Impact of Particulate Control Requirements: Large Manufacturer's Viewpoint 22
Herbert H. Braden
Paper presented by Gary R. Gawreluk

Future Particulate Regulations: The View of the Small Manufacturer 33
Sidney R. Orem

Session 2: ADVANCED ENERGY APPLICATIONS. 36
George A. Rinard, Chairman

Page

High-Temperature, High-Pressure Electrostatic Precipitation, Current Status. 37
P. L. Feldman* and K. S. Kumar

Test Results of a Precipitator Operating at High-Temperature and High-Pressure Conditions 50
Donald E. Rugg*, George Rinard, Michael Durham, and James Armstrong

Evaluation and Development of Candidate High Temperature Filter Devices for Pressurized Fluidized Bed Combustion. . . . 64
T. E. Lippert*, D. F. Ciliberti, S. G. Drenker, and O. J. Tassicker

High Temperature Gas Filtration with Ceramic Filter Media: Problems and Solutions 79
Ramsay Chang

The Development and High Temperature Application of a Novel Method for Measuring Ash Deposits and Cake Removal on Filter Bags. 92
David F. Ciliberti*, Thomas E. Lippert, Owen J. Tassicker, and Steven Drenker

Session 3: ECONOMICS 107
John S. Lagarias, Chairman

Economics of Electrostatic Precipitators and Fabric Filters 108
Victor H. Belba*, Fay A. Horney, Robert C. Carr, and Walter Piulle

Estimating the Benefits of SO_3 Gas Conditioning on the Performance of Utility Precipitators When Burning U.S. Coals 126
Peter Gelfand

Microcomputer Models for Particulate Control 135
A. S. Viner*, D. S. Ensor, and L. E. Sparks

The Impact of Proposed Acid Rain Legislation on Power Plant Particulate Control Equipment. 142
William H. Cole

Session 4: NOVEL CONCEPTS. 158
Dale L. Harmon, Chairman

*Denotes speaker

Page

Particle Charging with an Electron Beam Precharger 159
J. S. Clements*, A. Mizuno, and R. H. Davis

Charging of Particulates by Evaporating Charged Water Droplets 175
G. S. P. Castle*, I. I. Inculet, and R. Littlewood

Role of Electrostatic Forces in High Velocity Particle Collection Devices 187
H. C. Wang, J. J. Stukel*, K. H. Leong, and P. K. Hopke

Hot-Gas Fabric Filtration 500° F - 1500° F, No Utopia but Reality. 201
Lutz Bergmann

The Prediction of Plume Opacity from Stationary Sources. . . . 211
David S. Ensor*, Ashok S. Damle, Philip A. Lawless, and Leslie E. Sparks

APPENDIX: Attendees 234

VOLUME 2
ELECTROSTATIC PRECIPITATION

Session 5: ESP: PERFORMANCE ESTIMATING (MODELING) 267
Leslie E. Sparks, Chairman

Microcomputer Programs for Precipitator Performance Estimates. 268
M. G. Faulkner*, J. L. DuBard, R. S. Dahlin, and Leslie E. Sparks

Analysis of Error in Precipitator Performance Estimates. . . . 283
J. L. DuBard* and R. F. Altman

Use of a Mobile Electrostatic Precipitator for Pilot Studies. 299
Robert R. Crynack* and John D. Sherow

Prediction of Voltage-Current Curves for Novel Electrodes--Arbitrary Wire Electrodes on Axis. 314
Phil A. Lawless* and L. E. Sparks

Numerical Computation of the Electrical Conditions in a Wire-Plate Electrostatic Precipitator Using the Finite Element Technique. 328
Gregory A. Kallio* and David E. Stock

*Denotes speaker

Page

Session 6: ESP: PERFORMANCE ENHANCEMENT I 345
Ralph F. Altman, Chairman

A Field Study of a Combined NH_3-SO_3 Conditioning System on a Cold-Side Fly Ash Precipitator at a Coal-Fired Power Plant. 346
Robert S. Dahlin*, John P. Gooch, Guillaume H. Marchant, Jr., Roy E. Bickelhaupt, D. Richard Sears, and Ralph F. Altman

Conditioning of Power Station Flue Gases to Improve Electrostatic Precipitator Efficiency. 362
Gernot Mayer-Schwinning* and J. D. Riley

Pilot-Scale Study of a New Method of Flue-Gas Conditioning with Ammonium Sulfate. 375
Edward B. Dismukes*, E. C. Landham, Jr., John P. Gooch, and Ralph F. Altman

Power Plant Plume Opacity Control. 390
J. Martin Hughes* and Kai-Tien Lee

Pulse Energization System of Electrostatic Precipitator for Retrofitting Application 404
Senichi Masuda* and Shunsuke Hosokawa

Session 7: ESP: PERFORMANCE ENHANCEMENT II. 419
B. G. McKinney, Chairman

Practical Implications of Pulse Energization of Electrostatic Precipitators. 420
H. Milde*, J. Ottesen, and C. Salisbury

Laboratory and Full-Scale Characteristics of Electrostatic Precipitators with Rigid Mast Electrodes 437
H. Krigmont*, R. Allan, R. Triscori, and H. W. Spencer, III

Full Scale Experience with Pulsed Energization of Electrostatic Precipitators. 458
K. Porle* and K. Bradburn

New Life for Old Weighted Wire Precipitators: Rebuilding with Rigid Electrodes. 479
Peter J. Aa* and Gary R. Gawreluk*

*Denotes speaker

Page

Pulsing on a Cold-Side Precipitator, Florida Power Corporation, Crystal River, Unit 1 495
Joseph W. Niemeyer*, Robert A. Wright, and Wayne Love

Session 8: ESP: ADVANCED TECHNOLOGY I 499
Norman Plaks, Chairman

Field Study of Multi-Stage Electrostatic Precipitators 500
Michael Durham, George Rinard, Donald Rugg, Theodore Carney, James Armstrong*, and Leslie E. Sparks

Optimizing the Collector Sections of Multi-Stage Electrostatic Precipitators. 513
George Rinard*, Michael Durham, Donald Rugg, and Leslie Sparks

Ceramic-Made Boxer-Charger for Precharging Applications. . . . 525
Senichi Masuda*, Shunsuke Hosokawa, and Shuzo Kaneko

Precipitator Performance Enhancement with Pulsed Energization 539
E. C. Landham, Jr.*, James L. DuBard, Walter R. Piulle, and Leslie Sparks

Aerosol Particle Charging in a Pulsed Corona Discharge 554
James L. DuBard* and Walter R. Piulle

Session 9: ESP: ADVANCED TECHNOLOGY II. 569
Walter R. Piulle, Chairman

Performance of Large-Diameter Wires as Discharge Electrodes in Electrostatic Precipitators. 570
P. Vann Bush*, Duane H. Pontius, and Leslie E. Sparks

Technical Evaluation of Plate Spacing Effects on Fly Ash Collection in Precipitators. 586
Ralph F. Altman*, Gerald W. Driggers, Ronald W. Gray, and James L. DuBard, and E. C. Landham, Jr.

Electrical Characteristics of Large-Diameter Discharge Electrodes in Electrostatic Precipitators. 599
Kenneth J. McLean* and Leslie E. Sparks

Laboratory Analysis of Corona Discharge Electrodes and Back Corona Phenomena. 610
P. Vann Bush* and Todd R. Snyder

*Denotes speaker

Page

Session 10: ESP: FUNDAMENTALS I 627
Grady B. Nichols, Chairman

The Onset of Electrical Breakdown in Dust Layers 628
Ronald P. Young*, James L. DuBard, and Leslie E. Sparks

Bipolar Current Probe for Diagnosing Full-Scale Precipitators. 643
Senichi Masuda*, Toshifumi Itagaki, Shigeyuki Nohso, Osamu Tanaka, Katsuji Hironaga, and Nobuhiko Fukushima

A Method for Predicting the Effective Volume Resistivity of a Sodium Depleted Fly Ash Layer 658
Roy E. Bickelhaupt* and Ralph F. Altman

Analysis of Air Heater-Fly Ash-Sulfuric Acid Vapor Interactions 676
Norman W. Frisch

Session 11: ESP: FUNDAMENTALS II. 698
Philip A. Lawless, Chairman

Experimental Studies of Space Charge Effects in an ESP 699
D. H. Pontius* and P. V. Bush

An Electrostatic Precipitator Facility for Turbulence Research 714
J. H. Davidson* and E. J. Shaughnessy

On the Static Field Strength in Wire-Plate Electrostatic Precipitators with Profiled Collecting Electrodes by an Experimental Method. 730
C. E. Akerlund

The Fluid Dynamics of Electrostatic Precipitators: Effects of Electrode Geometry. 741
E. J. Shaughnessy*, J. H. Davidson, and J. C. Hay

VOLUME 3
FABRIC FILTRATION

Session 12: FF: PRACTICAL CONSIDERATIONS. 751
Wallace B. Smith, Chairman

Fabric Screening Studies for Utility Baghouse Applications . . 752
Larry G. Felix* and Randy L. Merritt

*Denotes speaker

Page

Tensioning of Filter Bags in Reverse Air Fabric Filters. . . . 769
Robert W. Tisone* and Gregory L. Lear

Sound of Energy Savings. 784
N. D. Phillips* and J. A. Barabas

Solving the Pressure Drop Problem in Fabric Filter Bag Houses 797
Carl V. Leunig

Session 13: FF: FULL-SCALE STUDIES (COAL-FIRED BOILERS) 807
Robert P. Donovan, Chairman

Emission Reduction Performance and Operating Characteristics of a Baghouse Installed on a Coal-Fired Power Plant 808
David S. Beachler*, John W. Richardson, John D. McKenna, John C. Mycock, and Dale Harmon

Evaluation of Sonic-Assisted, Reverse-Gas Cleaning at Utility Baghouses 823
Kenneth M. Cushing*, Larry G. Felix, Anthony M. LaChance, and Stephen J. Christian

Sonic Horn Application in a Dry FGD System Baghouse. 839
Yang-Jen Chen*, Minh T. Quach, and H. W. Spencer III

Full Scale Operation and Performance of Two New Baghouse Installations 853
C. B. Barranger

Session 14: FF: FULL-SCALE STUDIES II (COAL-FIRED BOILERS). . . 867
Robert C. Carr, Chairman

Performance of Baghouses in the Electric Generating Industry 868
Wallace B. Smith* and Robert C. Carr

Flue Gas Filtration: Southwestern Public Service Company's Experience in Design, Construction, and Operation. 893
John Perry

Start-Up and Operation of a Reverse-Air Fabric Filter on a 550 MW Boiler 902
R. A. Winch and L. J. Pflug, Jr.*

*Denotes speaker

Page

Update on Australian Experience with Fabric Filters on Power Boilers 920
F. H. Walker

Session 15: FF: FUNDAMENTALS/MEASUREMENT TECHNIQUES 937
David S. Ensor, Chairman

Modeling Baghouse Performance. 938
David S. Ensor*, Douglas W. VanOsdell, Andrew S. Viner, Robert P. Donovan, and Louis S. Hovis

Measurement of the Spatial Distribution of Mass on a Filter 952
Andrew S. Viner*, R. P. Gardner, and L. S. Hovis

Laboratory Studies of the Effects of Sonic Energy on Removal of a Dust Cake from Fabrics. 964
B. E. Pyle*, S. Berg, and D. H. Pontius

Cleaning Fabric Filters. 981
G. E. R. Lamb

Session 16: FF: ADVANCED CONCEPTS 994
John K. McKenna, Chairman

Modeling Studies of Pressure Drop Reduction in Electrically Stimulated Fabric Filtration 995
Barry A. Morris*, George E. R. Lamb, and Dudley A. Saville

Flow Resistance Reduction Mechanisms for Electrostatically Augmented Filtration 1007
D. W. VanOsdell*, R. P. Donovan, and Louis S. Hovis

Laboratory Studies of Electrically Enhanced Fabric Filtration 1020
Louis S. Hovis*, Bobby E. Daniel, Yang-Jen Chen, and and R. P. Donovan

Pressure Drop for a Filter Bag Operating with a Lightning-Rod Precharger 1034
George E. R. Lamb* and Richard I. Jones

New High Performance Fabric for Hot Gas Filtration 1048
J. N. Shah
Paper presented by Peter E. Frankenburg

*Denotes speaker

Page

Session 17: FF: PILOT-SCALE STUDIES (COAL-FIRED BOILERS). . . . 1059
Louis S. Hovis, Chairman

The Influence of Coal-Specific Fly Ash Properties Upon Baghouse Performance: A Comparison of Two Extreme Examples 1060
Stanley J. Miller* and D. Richard Sears

Top Inlet Baghouse Evaluation at Pilot Scale 1081
Gary P. Greiner* and Dale A. Furlong

Development of Woven Electrode Fabric and Preliminary Economics for Full-Scale Operation of Electrostatic Fabric Filtration. 1082
James J. Spivey*, Richard L. Chambers, and Dale L. Harmon

ESFF Pilot Plant Operation at Harrington Station 1101
Richard L. Chambers*, James J. Spivey, and Dale L. Harmon

VOLUME 4
FUGITIVE EMISSIONS, DRY SO_2, AND
OPERATION AND MAINTENANCE

Session 18: FUGITIVE EMISSIONS I 1119
Chatten Cowherd, Jr., Chairman

Technical Manual on Hood Capture Systems to Control Process Fugitive Particulate Emissions 1120
E. R. Kashdan*, J. J. Spivey, D. W. Coy,
H. Goodfellow, T. Cesta, and D. L. Harmon

Pilot Demonstration of Air Curtain Control of Buoyant Fugitive Emissions 1132
Michael W. Duncan*, Shui-Chow Yung, Ronald G. Patterson,
William B. Kuykendal, and Dale L. Harmon

Characterization of Fugitive Particulate Emissions from Industrial Sites 1147
K. S. Basden

Evaluation of an Air Curtain Secondary Hooding System. 1161
John O. Burckle
Paper presented by William F. Kemner

*Denotes speaker

Page

Session 19: FUGITIVE EMISSIONS II. 1172
Michael J. Miller, Chairman

Technical Manual on the Identification, Assessment, and Control of Fugitive Emissions. 1173
Chatten Cowherd, Jr.*, John S. Kinsey, and William B. Kuykendal

Quantification of Roadway Fugitive Dust at a Large Midwestern Steel Mill. 1188
Keith D. Rosbury and William Kemner*

Evaluation of Street Sweeping as a Means of Controlling Urban Particulate. 1200
T. R. Hewitt

Windbreak Effectiveness for the Control of Fugitive-Dust Emissions from Storage Piles--A Wind Tunnel Study. 1210
Barbara J. Billman

Evaluation of Chemical Stabilizers and Windscreens for Wind Erosion Control of Uranium Mill Tailings. 1227
Monte R. Elmore* and James N. Hartley

Session 20: DRY SO_2 REMOVAL I. 1245
Richard G. Rhudy, Chairman

Modeling of SO_2 Removal in Spray-Dryer Flue Gas Desulfurization System 1246
Ashok S. Damle* and Leslie E. Sparks

Fabric Filter Operation Downstream of a Spray Dryer: Pilot and Full-Scale Results 1275
Richard G. Rhudy and Gary M. Blythe*

Novel Design Concepts for an 860 MW Fabric Filter Used with a Dry Flue Gas Desulfurization System. 1303
Michael F. Skinner, Steven H. Wolf, John M. Gustke*, and Donald O. Swenson

Start-Up and Operating Experience with a Reverse Air Fabric Filter as Part of the University of Minnesota Dry FGD System 1315
J. C. Buschmann*, J. Mills, and W. Soderberg

*Denotes speaker

Page

Spray Dryer/Baghouse Experiences on a 1000 ACFM Pilot Plant. 1325
Wayne T. Davis*, Gregory D. Reed, and Tom Lillestolen

Session 21: DRY SO_2 REMOVAL II 1337
Theodore G. Brna, Chairman

Design and Operation of the Baghouse at Holcomb Station, Unit No. 1. 1338
B. R. McLaughlin* and R. D. Emerson

An Update of Dry-Sodium Injection in Fabric Filters. 1357
Richard G. Hooper*, Robert C. Carr, G. P. Green, V. Bland, L. J. Muzio, and R. Keeth

Removal of Sulfur Dioxide and Particulate Using E-SOX. 1366
Leslie E. Sparks*, Geddes H. Ramsey, Richard E. Valentine, and Cynthia Bullock

Comparison of Dry Injection Systems at Normal and High Flue Gas Temperatures 1382
Robert M. Jensen*, William Dunlop, George C. Y. Lee, and Duane Folz

Acid Rain Control Options - Impact on Precipitator Performance. 1397
Victor H. Belba*, Fay A. Horney, and Donald M. Shattuck

Session 22: OPERATIONS AND MAINTENANCE I 1412
Richard D. McRanie, Chairman

Comparison of U.S. and Japanese Practices in the Specification and Operation and Maintenance of Electrostatic Precipitators. 1413
Michael F. Szabo*, Charles A. Altin, and William B. Kuykendal

Operation and Maintenance Manuals for Electrostatic Precipitators and Fabric Filters 1427
Michael F. Szabo*, Ronald D. Hawks, Fred D. Hall, and Gary L. Saunders

An Update of the Performance of the Cromby Station Fabric Filter. 1448
M. Gervasi*, J. R. Darrow, and J. E. Manogue

*Denotes speaker

Page

Critical Electrostatic Precipitator Purchasing Concepts. . . . 1463
Charles A. Altin* and Ralph F. Altman

Reducing Electrostatic Precipitator Power Consumption. 1481
Joseph P. Landwehr* and George Burnett

Session 23: OPERATIONS AND MAINTENANCE II. 1494
Peter R. Goldbrunner, Chairman

Design Considerations to Avoid Common Fly Ash Conveying Problems 1495
Gus Monahu* and Walter Piulle

Feasibility of Using Parameter Monitoring as an Aid in Determining Continuing Compliance of Particulate Control Devices. 1510
Joseph Carvitti*, Michael F. Szabo, and William Kemner

Air Pollution Control: Maintenance Cost Savings from the Washing, Patching and Reuse of Bags Used in Fabric Filters. 1530
Frank L. Cross, Jr.
Paper presented by Lutz Bergmann

Optimizing the Performance of a Modern Electrostatic Precipitator by Design Refinements 1537
Donald H. Rullman* and Franz Neulinger

Weighted Discharge Electrodes - A Solution to Mechanical Fatigue Problems. 1567
John A. Knapik

PAPER PRESENTED AT THE FOURTH SYMPOSIUM ON THE TRANSFER AND UTILIZATION OF PARTICULATE CONTROL TECHNOLOGY BUT NOT PUBLISHED IN PROCEEDINGS

Measurement of the Electrokinetic Transport Properties of Particles in an Electrostatic Precipitator. 1584
Wallace T. Clark III*, Robert L. Bond, and Malay K. Mazumder

UNPRESENTED PAPER

Electrostatic Precipitator Bus Section Failure: Operation and Maintenance. 1596
Louis Theodore, Joseph Reynolds, Francis Taylor, Alan Filippi, and Steve Errico

*Denotes speaker

Session 18: FUGITIVE EMISSIONS I

Chatten Cowherd, Jr., Chairman
Midwest Research Institute
Kansas City, MO

TECHNICAL MANUAL ON HOOD CAPTURE SYSTEMS TO CONTROL PROCESS FUGITIVE PARTICULATE EMISSIONS

by: E.R. Kashdan, J.J. Spivey, and D.W. Coy
Research Triangle Institute
Post Office Box 12194
Research Triangle Park, N.C. 27709

H. Goodfellow and T. Cesta
Hatch Associates, Ltd.
21 St. Clair Avenue East
Toronto, Canada M4T1L9

D. L. Harmon
Industrial Environmental Research Laboratory
U. S. Environmental Protection Agency
Research Triangle Park, N.C. 27711

ABSTRACT

This paper describes highlights from an ongoing effort to prepare a technical manual for hood systems to control process fugitive particulate emissions. General design considerations are presented as well as specific considerations for buoyant plumes. Two hood systems used for control of emissions from electric arc furnaces illustrate design methods and provide case studies.

This paper has been reviewed in accordance with the U.S. Environmental Protection Agency's peer and administrative review policies and approved for presentation and publication.

INTRODUCTION

The objective of this program is to develop a technical manual for hooding systems used to control process fugitive particulate emissions. This paper presents highlights of the technical manual effort.

Process fugitive particulate emissions are defined as "particulate matter which escapes from a defined process flow stream due to leakage, materials charging/handling, inadequate operational control, lack of reasonably available control technology, transfer or storage"(1). Control of process fugitives may be attempted by using hooding systems that are supplemental to primary control or using the primary hood system itself. In either case, the hood plays a vital role. The particulate control device is usually a high efficiency device capable of collecting most of the process fugitive particulate matter that is captured. Therefore, overall control is limited by the capture efficiency of the hood system.

The following paper reviews general design considerations for process fugitive hood systems, as well as design methods (both generally and specifically for buoyant plumes) and provides two brief case studies of hood systems employed for electric arc furnaces. The technical manual will include four or five detailed case studies.

DESIGNING HOOD SYSTEMS

CLASSIFICATION OF HOODS

Hoods are classified in several ways such as by function, by geometry, or by supposed (actual) method of operation. Terms such as "receiving hood," "exterior hood," "freely suspended hood," "canopy hood," and "push-pull hood" illustrate the naming of hoods, but the terms are often used very loosely. For purposes of the technical manual and also for designing hoods, it is more important to consider the source/hood interaction than to develop a detailed system of nomenclature for all possible hoods.

For the technical manual, the elementary distinction is made between local and remote hoods. Remote hoods (often termed "canopy hoods") are located at large distances from the source and are used on hot sources. The nature of the hot source determines the design considerations as discussed below. Local hoods are placed near the source. The design of these local hoods will depend again on the type of source to be controlled, although distinctions are often made on the basis of location of the exhaust, for example, "side-draft" or "downdraft." Local hoods often employ sides to enclose the source. In effect, a totally sided hood is an "enclosure."

CLASSIFICATION OF SOURCES

For purposes of designing a hood system for control of process fugitive particulate emissions, sources of particulate emissions may be classified as processes giving rise to buoyant plumes, nonbuoyant plumes, or plumes having significant particle inertia. The distinction among these categories should not be made rigid. Sources giving rise to buoyant plumes will generally be hot (on the order of 500 °F or greater[1]), and the initial plume rise may reach a velocity on the order of 500 ft/min. Nonbuoyant sources are generally cold processes, or at least not very hot. For the nonbuoyant source, the plume will not exhibit strong plume rise and is likely to be deflected easily by cross-drafts, even when it is close to the source. Plumes with significant particle inertia are generally nonbuoyant, but the motion of the particulate matter itself entrains additional air. Examples clarify these definitions. Charging and tapping operations from large electric arc furnaces produce typical buoyant plumes of process fugitive emissions. Cold scarfing or rolling mills are examples of sources producing nonbuoyant plumes. Materials handling operations, such as dumping or conveying, create process fugitive emissions having significant particle inertia. Design of hoods (usually enclosures) for these sources requires that due allowance be made for the entrained air which results from the momentum of the materials.

EVALUATION OF EXISTING HOODING SYSTEMS

For purposes of the technical manual, it is necessary to distinguish good and bad hood designs from good and bad system performance. A good hood design is not simply one that performs well. A good hood design is one that is based on a set of principles or rules which may therefore be repeated on hood systems for other sources. In other words, a well-designed hood is based on a model which provides a conceptual framework of the way the hood works or will work when installed. A bad design is one which was not based on any principles and is therefore generally not repeatable for different sources. This important distinction between design and performance is summarized in Table 1. From Table 1, it can be seen that good hood designs may be designed on the basis of a correct model, a limited model, or an incorrect model. The correct model is perfect in the sense that, as shown in Table 1, it always produces a hood system which performs acceptably. In actual practice, the correct model does not exist and probably never will exist because of the complex behavior of particulate plumes. However, the correct model category represents a goal towards which the second category of "limited models" may strive. A limited model basis of design does provide a conceptual framework of the performance of hood systems, but because of complexities in actual installations, the limited model may or may not produce a hood system with acceptable performance. The third category under good designs in Table 1 represents systems based on an incorrect model. Here, a conceptual framework is provided, but because the model does not correctly represent plume/system behavior, hood systems based on an incorrect model will not perform acceptably. Note that using these definitions, good designs may or may not produce acceptably working hood systems.

---

[1] Readers more familiar with the metric system may use the metric conversion table at the end of this paper.

TABLE 1. EVALUATION OF HOOD SYSTEMS WITH REGARD TO DESIGN AND PERFORMANCE

	Performance	
	Acceptable	Unacceptable
Good design		
Correct model	X	
Limited model	X	X
Incorrect model		X
Bad design		
Overdesign	X	
No model		X

Bad designs, as shown in Table 1, may be of two types. A hood, after all, is not a sophisticated device, and frequently a particular hood system was installed by simply fitting some structure into available space and exhausting it. These "designs" are bad designs because no model is provided, and the design is, therefore, not repeatable for different sources. Generally, designs not based on a model will not perform satisfactorily unless they are of the other type of bad design, that is, those based on overdesign. For this type of design, if an excessive exhaust rate is used on most hood systems, even without a design basis, acceptable performance will result. However, hoods that are overdesigned waste both energy and control device capacity. It is apparent in Table 1 that merely examining the performance of various hood systems implies nothing about the adequacy of the design. The significance of Table 1 will become apparent in the following section in which design methods are discussed.

DESIGN METHODS FOR HOOD SYSTEMS

Hood systems for process fugitive particulate emissions may be designed by any one or a combination of five different methods. In increasing order of sophistication, these methods are: design by precedent, design by rule-of-thumb, design by mathematical model, design by diagnosis of an existing system, and design by physical scale models. In design by precedent, a particular hood system installation that performs satisfactorily is copied. Design by precedent will generally result in an acceptably working system, but (see Table 1) the copied system will be either a good design based on a limited model or an overdesigned system. Failures in performance using this method will be because the limited model does not apply to the case at hand. In design by rule-of-thumb, many working systems are surveyed and the elements common to most of them are put together to form a working design rule(s). In this method, both limited model designs and overdesigns will be examined. It is likely that overdesigned systems will become more apparent and are less apt to be copied. However, if the working rule provides an incorrect model, the resulting hood system will not perform satisfactorily. Design by mathematical model will always be a good design because the basis of the design can be examined. Performance, however, is not guaranteed because the model may be limited or incorrect. Examination of hood systems is not necessarily part of this method, in contrast to other methods. Design by diagnosis of an existing site is more specialized than the other methods discussed. Measurements and observations of the hood installation are made, usually because the system is not performing well. This method actually represents an attempt to classify the hood system within the context of Table 1. Depending on the results, certain remedies may be applied to the hood system, or an entirely new design may be necessary, in which case, another design method will be invoked. Lastly, design by physical scale model may be considered a more sophisticated analysis and may be applied to existing or planned sites. The hood design will be scaled hydrodynamically as a physical model in a water tank or wind tunnel, or perhaps as a full-scale mock-up of a hood system.

In a subsequent section, two case histories provide examples of the application of some of these design methods.

DESIGNING REMOTE HOODS FOR BUOYANT PLUMES

The remainder of this paper is devoted to considerations in the design of remote hoods for buoyant plumes. Design considerations have been discussed by Bender (2), Goodfellow and Bender (3), and Hemeon (4) and are reviewed below.

Process fugitive particulate emissions from intermittent processes, such as charging of furnaces, are huge surges of plume lasting only a short duration. During charging, the plume flow rate is much greater than the hood suction rate so that fume simply spills out of the hood (4). Increasing the hood suction rate to accommodate the peak surges represents a wasteful overdesign. An alternative discussed by Bender (2) is to construct a deep hood to temporarily store the fume during the peak periods. Once the charging operation has been completed, the hood will slowly evacuate the stored plume.

Remote hoods fail in other ways besides spillage. As the plume rises, dilution with clean air (entrainment) reduces the plume velocity thereby making the plume susceptible to building cross-drafts. These drafts may cause the plume to be partly or totally deflected away from the hood. This failure in performance was mentioned by Hemeon (4) and considered quantitatively by Bender (2). Because cross-drafts depend on prevailing wind direction, building orientation, concurrent processes in the building, and other factors, no simple mathematical model will predict their behavior. Another common cause of failure in remote canopy hoods arises because the path between the furnace and hood is obstructed by cranes, walkways, etc. The rising plume diverges around these obstacles causing additional plume spreading. The result may be that the hood face area is not sufficient to accommodate the width of the plume. Again, simple mathematical models cannot account for plume spread. Ignoring the effect can result in poor performance. This consideration is illustrated in one of the following examples.

CASE HISTORIES

ELECTRIC ARC FURNACE CONTROL SYSTEM DESIGNED BY DIAGNOSIS AND MATHEMATICAL MODEL

A canopy hood system was designed for an 80-ton electric arc furnace in a steel plant as shown in Figure 1. The installed system was diagnosed by Hatch Associates in an effort to improve system performance and meet proposed opacity regulations. The basis of the original design was a mathematical model which provided estimates of the required exhaust rate and plume width based on input parameters of furnace heat release and source-hood geometry.

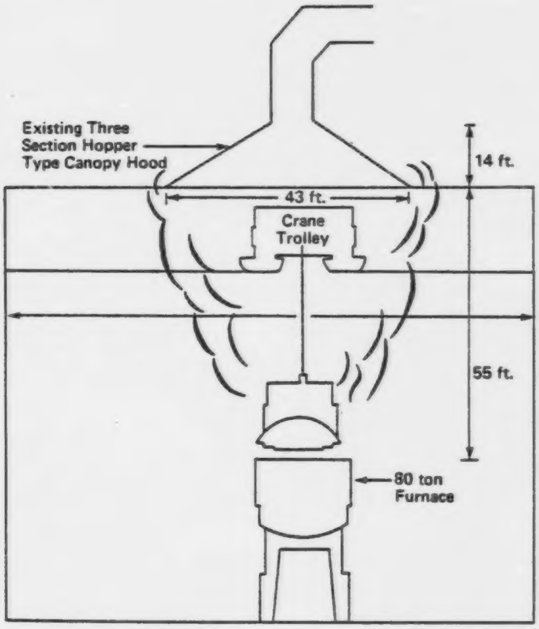

Figure 1. Canopy hood system for fugitive emission control on 80-ton electric arc furnace (Case 1).

The rate of heat release (q) is calculated from a rate of temperature drop for ladle and furnace of 10° F/min:

$$q = 75 \text{ tons} \times 2000 \frac{\text{lb}}{\text{ton}} \times \frac{0.12 \text{ Btu}}{\text{lb - °F}} \times \frac{10° \text{ F}}{\text{min}} \qquad (1)$$

$$q = 180{,}000 \text{ Btu/min.}$$

It is assumed that this heat release is equal to the rate of convectional heating of the rising plume--then the plume flow rate is calculated from the following equation (which actually applies to continuous rather than intermittent processes (4)):

$$Q = 7.4 Z^{1.5} q^{1/3}, \qquad (2)$$

where

Q = plume volume at hood face (acfm)

Z = height (ft) of hood above virtual plume source.

This latter quantity is taken as

$$Z = Y + 2B \qquad (3)$$

where

Y = source to hood face distance (ft)

B = source diameter (ft).

For furnace charging for this source, $Z = 91$ ft, hence, $Q = 360{,}000$ acfm. For ladle tapping, $Z = 96$ ft, hence, $Q = 384{,}000$ acfm. The diameter (D) of the plume at the hood face was estimated from Hemeon (4) by means of the following correlation equation:

$$D = Z^{0.88}/2 \qquad (4)$$

which for this case is $D = 27$ ft (charging). The diameter of the installed hood system was chosen as 43 ft. The system operated at a suction rate of 212,000 acfm (subsequently measured); this rate was well below the calculated required exhaust rate of about 400,000 acfm.

The first step in diagnosis of the system was detailed observations of plume behavior during charging and tapping. These observations revealed that during charging, the plume was severely deflected by the crane trolley. Charging the furnace when it was hot, especially with combustible scrap, produced a spectacular plume that spilled from the hood. Conversely, charging a relatively cold furnace produced a slowly rising plume that was easily deflected by cross-drafts. During tapping, the same problems of cross-drafts and deflection around the crane trolley caused the plume to miss the hood. These observations are illustrated in Figure 2 which shows the approximate boundaries of the charging and tapping plumes relative to the location of the existing hood. From Figure 2, the plume cross-sectional area at the canopy hood face is estimated to be 1740 ft^2. Plume photography was used to quantitatively estimate the velocity of the plume, yielding a value of 530 ft/min measured at the hood face. Evidently, the peak plume flow rate is estimated as 1740 × 530 = 922,000 acfm.

As indicated previously, it would be wasteful to match the hood suction rate to the peak plume flow rate. Instead, a working minimum hood face velocity of 300 ft/min is selected, indicating a required suction rate of 520,000 acfm (1740 ft^2 × 300 ft/min). To accommodate the plume surges during charging, a pool-type hood addition shown in Figure 3 is recommended

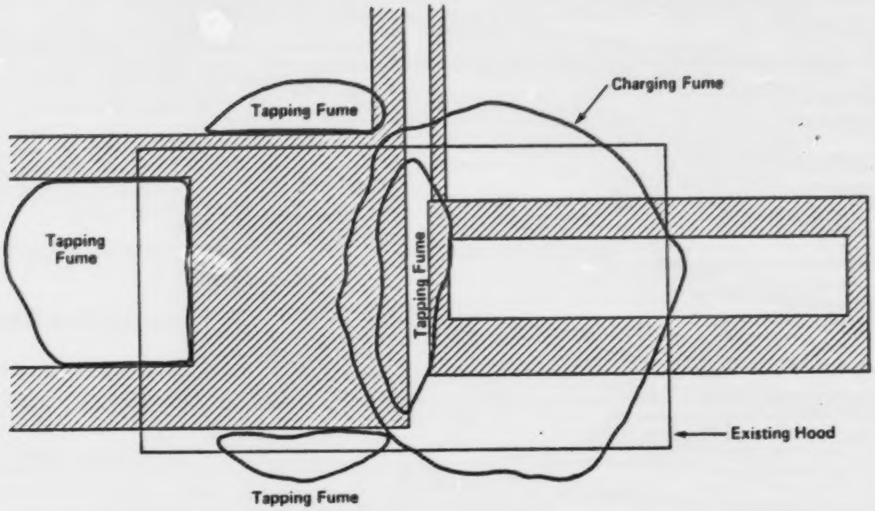
Tapping Fume
Charging Fume
Tapping Fume
Tapping Fume
Existing Hood
Tapping Fume

Figure 2. Fume interference diagram showing plume boundaries relative to original hood (Case 1).

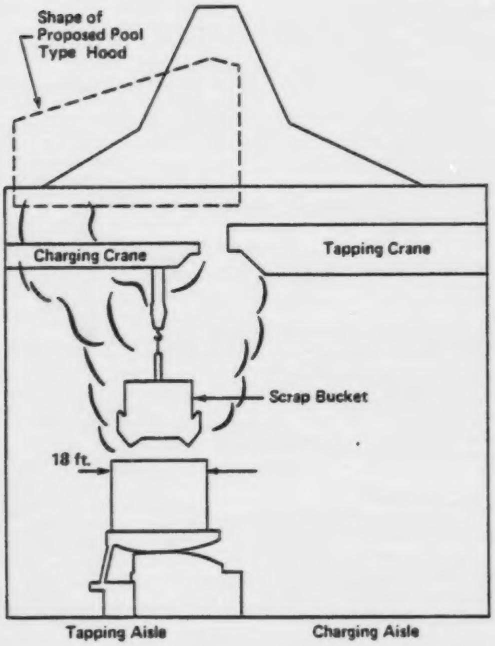
Shape of Proposed Pool Type Hood
Charging Crane
Tapping Crane
Scrap Bucket
18 ft.
Tapping Aisle
Charging Aisle

Figure 3. Proposed pool-type hood addition to accommodate plume surges (Case 1).

so as to provide additional storage capacity. The required storage capacity is calculated from the plot of charging plume flow rate shown in Figure 4. The shaded area under the curve is measured as 30,000 ft^3, which is taken as the required storage capacity.

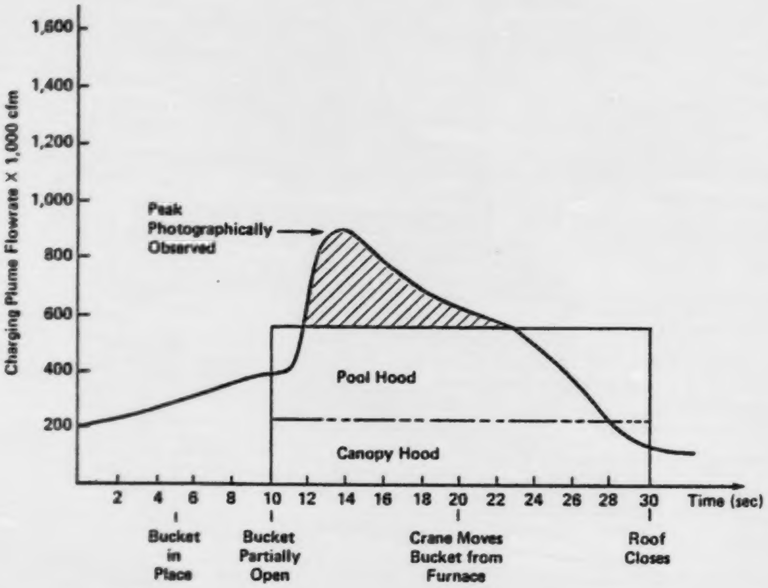

Figure 4. Plot of charging plume flow rate with time (Case 1).

For better capture of tapping plumes, Figure 5 shows a proposed curtain system extending 16 ft from the tapping crane. This modification would be expected to reduce cross-draft deflection and improve capture because the distance between the ladle and hood effectively is decreased. A more detailed analysis of this modification is provided in the technical manual.

Based on calculations too lengthy to be recounted here, final recommended exhaust rates were 695,000 acfm for the modified system (pool hood), and 491,000 acfm for the hood system as originally installed.

ELECTRIC ARC FURNACE CONTROL SYSTEM DESIGNED BY PRECEDENT

Figure 6 shows a different canopy hood system above a 150-ton electric arc furnace. The hood geometry was based on the designer's observations of one working system (5). In this case, a new furnace was added to an existing plant. The working hood system was deep with 60° sides. This feature was incorporated in the present system as shown in Figure 6. The effect of the 60° sides produced a hood with greater storage capacity, thereby reducing plume spillage. The width of the hood was determined by projecting a line, 15° from the vertical, from the furnace roof ring and ladle lip to the desired height of the canopy hood (5). Selected hood face dimensions were

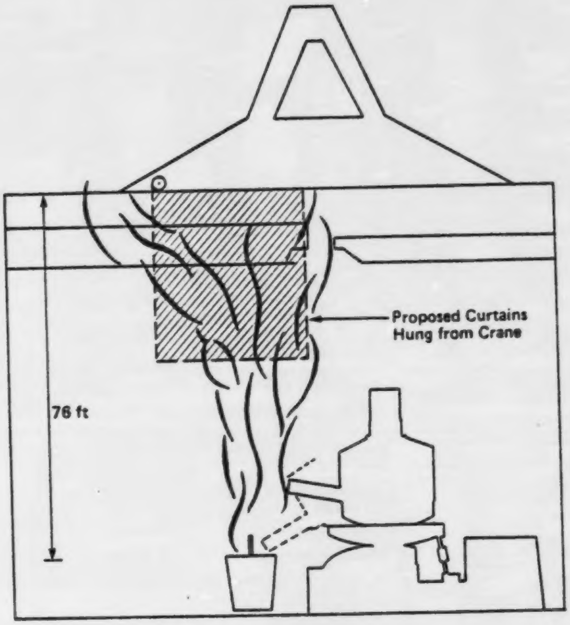
Proposed Curtains
Hung from Crane
76 ft

Figure 5. Proposed curtain system to improve tapping fume capture (Case 1).

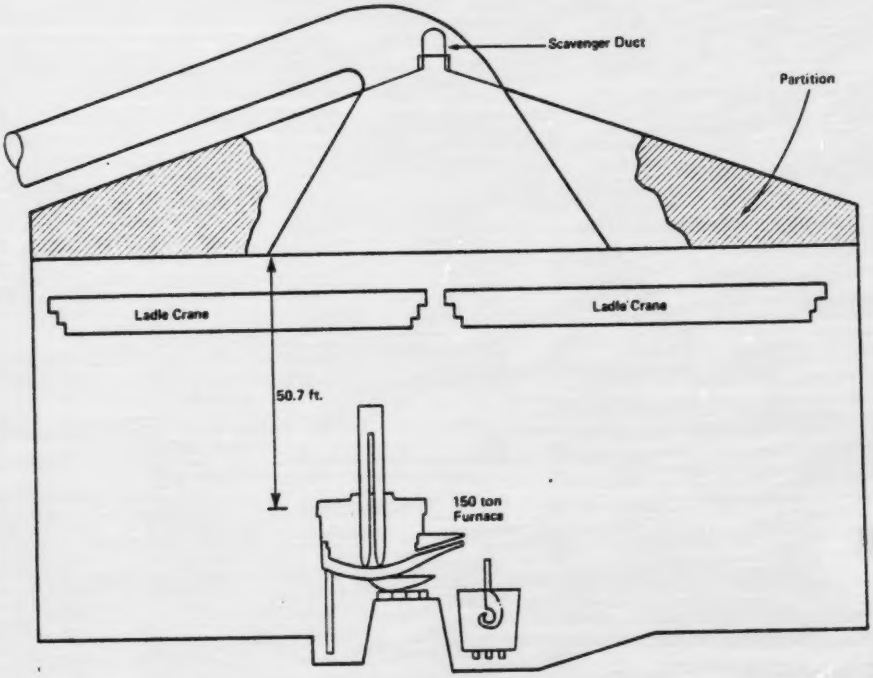
Scavenger Duct
Partition
Ladle Crane
Ladle Crane
50.7 ft.
150 ton
Furnace

Figure 6. Canopy hood system used for fugitive emission control on 150-ton electric furnace (Case 2).

72 ft × 60 ft. Design exhaust rate was determined from a nominal face velocity of 150 ft/min multiplied by the hood face area resulting in a value of 650,000 acfm (150 × 72 × 60).

Other features of this installation are solid baffles and a scavenger duct system. The scavenger duct system was installed at the request of the State regulatory agency who reviewed the design. The solid baffles, which tend to reduce the effects of cross-drafts, are sheet metal partitions suspended on purlins from the melt shop roof to the level of the crane. Two scavenger ducts on either side of the canopy hood collect emissions that are deflected beyond the hood sides; these ducts are shown in Figure 6.

Simple calculations may be performed for this canopy system, as with the previous example. From Equations (1) and (2), assuming again 10° F/min and $Z = 99$ ft, an estimated plume flow rate of $Q = 520,000$ acfm results. Relative to this calculated value, the design exhaust rate does not appear excessive.

Recent tests of this canopy hood system indicated the design performed quite well: over the 2 days of testing, the highest 15-second interval opacity observed at the roof monovent was 15 percent and the highest 6-minute average was 3.5 percent (6). Operating exhaust rates were 550,000 acfm through the canopy and 50,000 acfm through the scavenger ducts. The excellent performance of this system is likely because the system provides storage capacity for plume surges and minimizes cross-drafts. Suggested modifications in the previous example appear to be realized in the design of this system.

FUTURE WORK

In addition to the cases considered in this paper, the technical manual will provide case studies of control of hot processes by local hoods and control of a nonbuoyant source with significant particle inertia. It is anticipated that the design methodology and case studies in the manual will greatly aid regulatory officials in their review of both existing and new sites. Industry personnel may also become more aware of the difficulties in designing hood systems.

METRIC EQUIVALENTS

Nonmetric	Times	Yields metric
°F	5/9 (°F-32)	°C
°F/min	0.556	°C/min
ton	907	kg
lb	0.454	kg
Btu/lb-°F	4186	J/kg-K
Btu/min	1055	J/min
cfm	1.7	m^3/hr
ft	0.30	m
ft^2	0.093	m^2
ft^3	28.32	L
ft/min	0.00508	m/s
in.	2.54	cm

REFERENCES

1. Jutze, G.A., Zoller, J.M., Janszen, T.A., Amick, R.S., Zimmer, C.E., and Gerstle, R.W. Technical Guidance for Control of Industrial Process Fugitive Particulate Emissions. EPA-450/3-77-010 (NTIS PB272288), U.S. Environmental Protection Agency, Research Triangle Park, North Carolina, 1977, pp. 1-3.

2. Bender, M. Fumehoods, open canopy type -- their ability to capture pollutants in various environments. Am. Ind. Hyg. Assoc. J. 40: 118, 1979.

3. Goodfellow, H.D., and Bender, M. Design considerations for fume hoods for process plants. Am. Ind. Hyg. Assoc. J. 41: 473, 1980.

4. Hemeon, W.C.L. Plant and Process Ventilation. Industrial Press, Inc., New York (1963).

5. Walli, R.A., Rostik, L.F., and Lincoln, R.E. A market mill approach to environmental control -- Chaparral's experience. Paper presented at 1983 Spring Conference, Association of Iron and Steel Engineers, Dallas, Texas. April 11-13, 1983.

6. Terry, W.V. Site Visit -- Chaparral Steel Corporation, Midlothian, Texas. (MRI Project 4663-L). Letter to: Dale A. Pahl, U.S. EPA, Research Triangle Park, North Carolina, August 31, 1982.

PILOT DEMONSTRATION OF AIR CURTAIN CONTROL OF BUOYANT FUGITIVE EMISSIONS

Michael W. Duncan, Shui-Chow Yung, Ronald G. Patterson
Air Pollution Technology, Inc., San Diego, CA
and
William B. Kuykendal, Dale L. Harmon
U.S. EPA
Industrial Environmental Research Laboratory
Research Triangle Park, NC

ABSTRACT

Typical systems for controlling buoyant fugitive emissions involve hooding at the source, or total building enclosure and evacuation. A simpler and cheaper method is to divert the emissions with an air curtain (and fans for some cases) into a control device located near the source. Under sponsorship of the U.S. EPA, Air Pollution Technology, Inc. is demonstrating the technical and economic feasibility of using an air curtain transport system for controlling particle emissions from mold pouring operations at a Naval foundry in San Diego, California.

The system uses an air curtain to capture and convey the buoyant fugitive emissions to a filter unit. High Efficiency Particulate Air (HEPA) filters in the filter unit collect the particles. The system is currently being tested, and early results indicate that the air curtain capture efficiency is 91 to 100%.

INTRODUCTION

Fugitive emissions are air pollution emissions which have not passed through a stack or duct. They are diffuse and typically come from many small sources rather than a single large source. One method for controlling buoyant fugitive emissions is to gather and convey them to conventional air pollution control devices. Typical systems of this type involve hooding at the local source of emissions, or total building enclosure and evacuation. These systems usually require high capital and energy costs, especially when there are many small, diffuse sources.

A simpler and cheaper method is to divert the emissions with air curtains (and fans for some cases) into a control device located near the source. An air curtain is a wedge-shaped flow field of air that is formed by blowing air through a slot. A major advantage of air curtains over hoods is that, for a given volumetric flow rate, an air curtain can cause air movement at a much greater distance than hoods (about 30 times greater). Another advantage is that air curtains allow free movement of equipment and personnel.

Air Pollution Technology, Inc. has developed a system for controlling buoyant, fugitive particle emissions. This system uses air curtains to capture and convey the emissions to a device that collects the particles. System testing is now underway at an industrial site.

DEMONSTRATION SITE

SITE SELECTION CRITERIA

The criteria considered in the selection of the demonstration site were:

1. The fugitive particle source requires free access around it, thus making fixed hooding impractical.
2. The emission should occur commonly and constitute a significant source of pollution.
3. The site has enough space to facilitate the installation of the pilot plant system.
4. The site should be near San Diego, California (to minimize travel costs).

SITE SEARCH

To find potential demonstration sites, these agencies were contacted: San Diego County Air Pollution Control District, California Air Resources Board, and the Southern California Chapter of the American Foundrymen's Society. Several foundries in San Diego, Orange, and Los Angeles Counties were considered and visited.

SELECTED SITE

Site Operation and Layout

The selected site is a Naval maintenance foundry in San Diego. This foundry pours steel, stainless steel, cast iron, aluminum, bronze, brass, and other metals. The production rate of the foundry is approximately 45 to 450 kg/day (100 to 1,000 lb/day), with an average of about one pour per day.

The layout of the selected foundry is shown in Figure 1. It has separate areas for mold preparation, mold shakeout, metal melting, and mold pouring. Metal melting is carried out in six induction furnaces, with capacities ranging from 82 to 295 kg (180 to 650 lb) per melt.

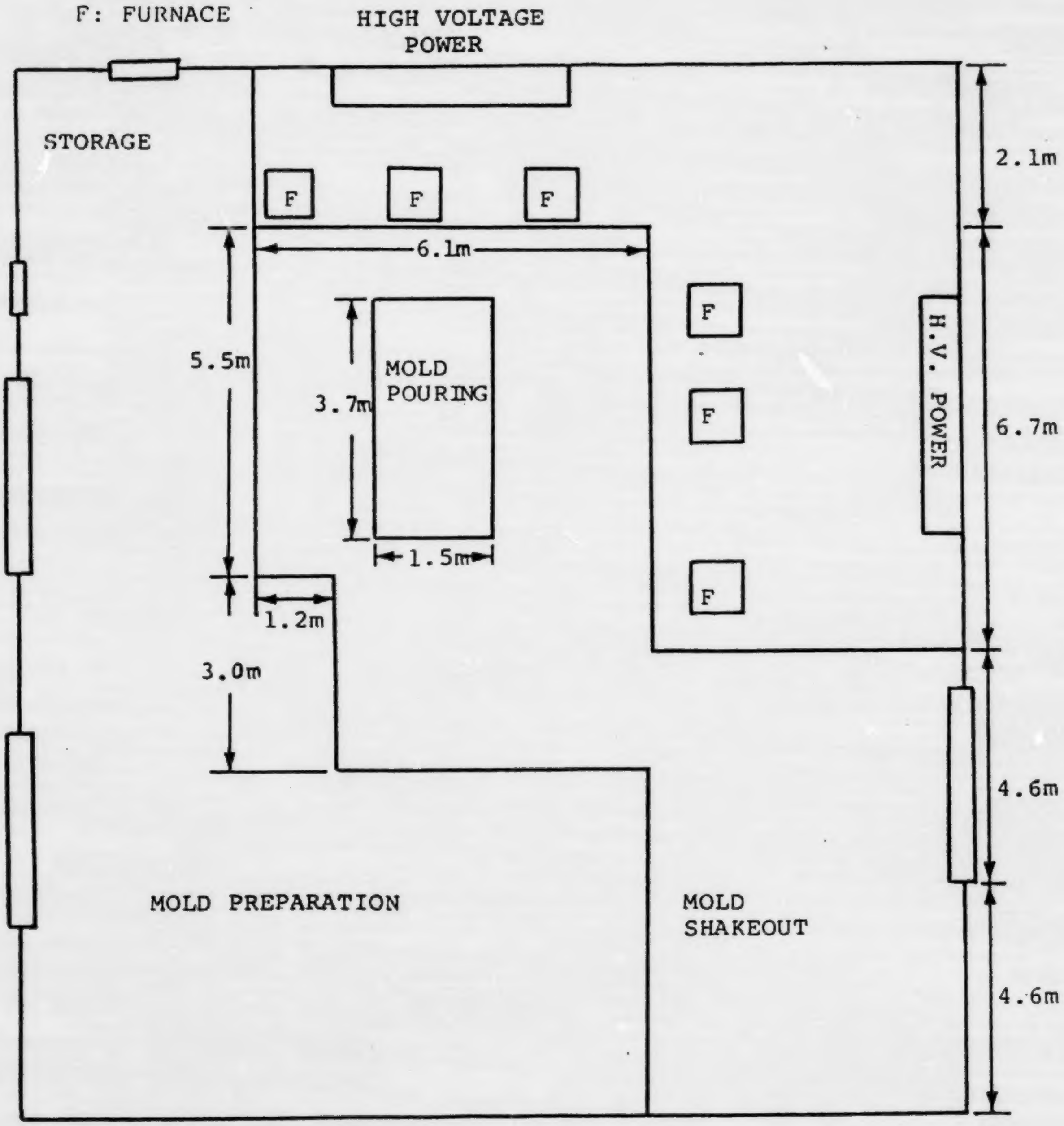
F: FURNACE
HIGH VOLTAGE POWER
STORAGE
F
F
F
6.1m
5.5m
3.7m
MOLD POURING
1.5m
1.2m
3.0m
F
F
F
H.V. POWER
2.1m
6.7m
4.6m
4.6m
MOLD PREPARATION
MOLD SHAKEOUT

Figure 1. Foundry layout.

After melting, the metal is poured into "air-set" sand molds which are usually arranged in a row. Typical lengths, widths, and heights of the molds range from 0.5 to 1.2 m (1.5 to 4 ft). Pouring operations last about 1 to 2 minutes.

After pouring, the metal cools in the mold for about 24 hours. After cooling, the molds are transferred to the shakeout area, where the cast parts are removed from the molds.

Emission Characteristics

The major emissions are the metal fumes from the crucible during the pouring and smoke from combustion of the mold binder. Sampling of the mold emissions indicated that a typical mold emits 7 to 10 g/hr (0.015 to 0.022 lb/hr) of particles with a mass median diameter of 0.2 to 0.4 µm aerodynamic.

The temperatures and velocities of some mold plumes were measured at 15 to 112 cm (6 to 44 in.) above the molds. At 30 cm (12 in.) above the molds, the plume rise-velocities were 3 to 56 cm/s (5 to 110 ft/min), and the temperatures were 25 to 32°C (77 to 90°F).

PILOT PLANT DESCRIPTION

The air curtain control system uses air curtains to deflect crosswinds, to contain buoyant plumes, and to convey emissions. A generalized arrangement for the air curtain control system is shown in Figure 2. The horizontally oriented air curtain unit contains the buoyant plume. The two vertical air curtains deflect crosswinds. The fan moves the emissions to the particle collection device.

Since the location of the demonstration pilot plant is indoors, vertical air curtains are not required. Also, since the volume of the plume is relatively small, a fan is not required. The pilot plant arrangement is shown in Figure 3. A single, horizontally oriented air curtain is used to capture and convey the mold plume. Both the air curtain unit and the filter unit are portable and have adjustable-height legs.

AIR CURTAIN UNIT

The design of the air curtain was based on the following equations (1).

Air Curtain Flow Field Equations

The equations for the air curtain flow field are:

$$u_c = 2.45\ u_s\ (w/x)^{1/2} \qquad (1)$$

$$u_a = u_c\ /\ 1.86 \qquad (2)$$

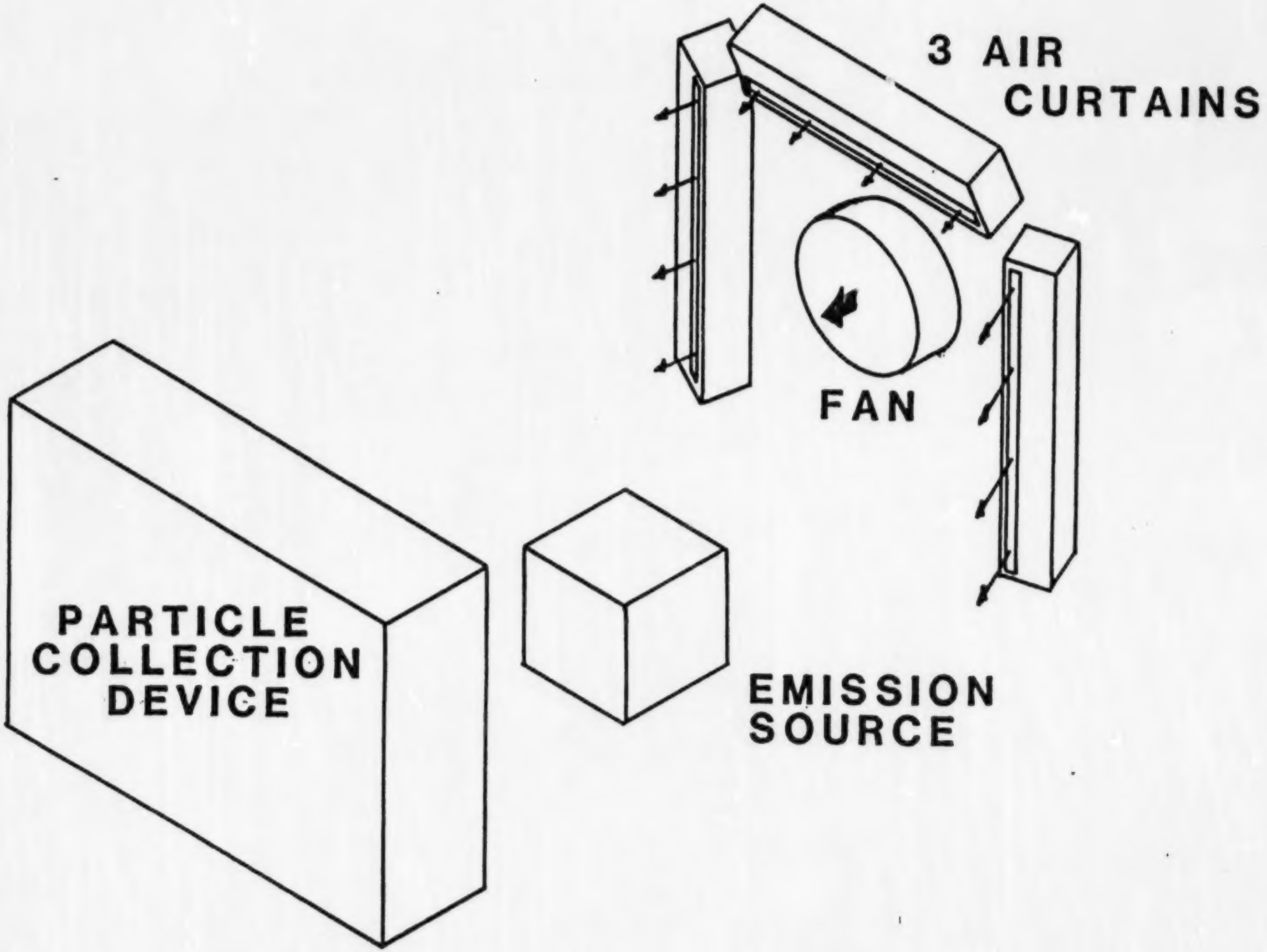
3 AIR
CURTAINS
FAN
PARTICLE
COLLECTION
DEVICE
EMISSION
SOURCE

Figure 2. Generalized air curtain control system.

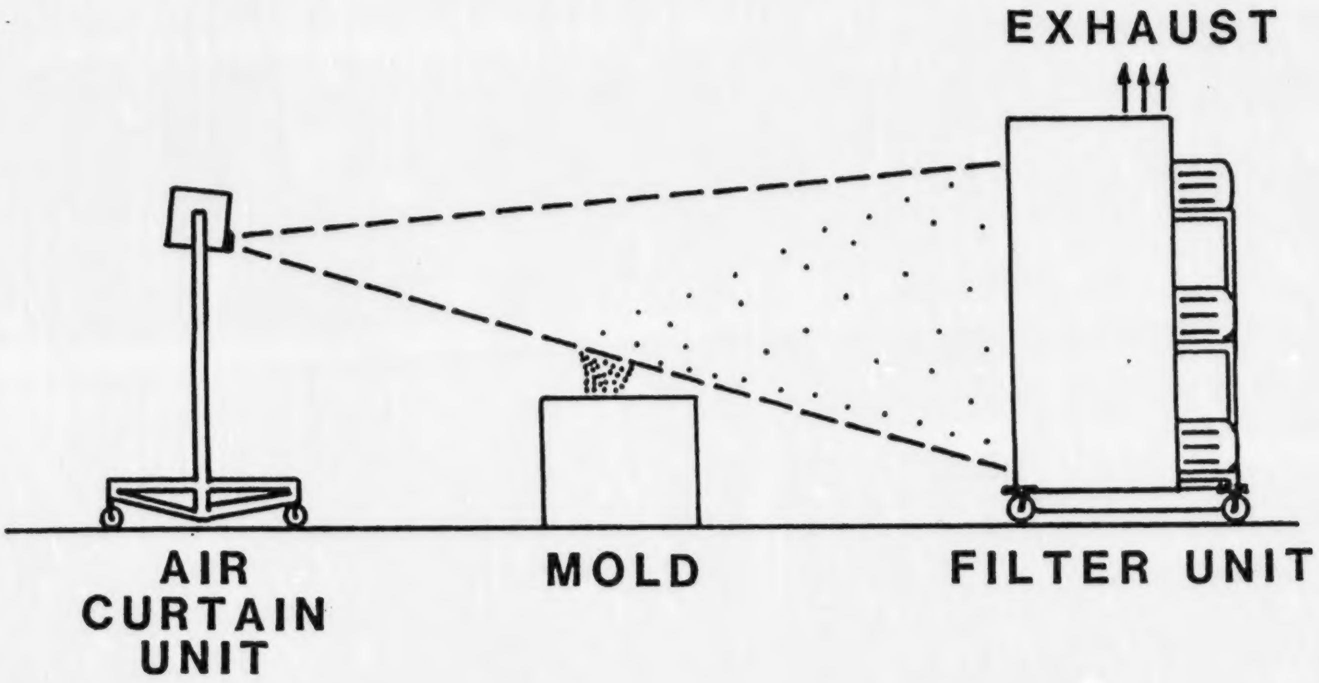
EXHAUST
AIR CURTAIN UNIT
MOLD
FILTER UNIT

Figure 3. Pilot plant arrangement.

$$b = 0.22\ x \qquad (3)$$

$$Q_s = u_s\ A_s \qquad (4)$$

$$Q_x = 0.66\ Q_s\ (x/w)^{1/2} \qquad (5)$$

where: u_c = centerline velocity of air curtain at distance x from slot, cm/s

u_s = slot exit velocity, cm/s

w = slot width, cm

x = distance from slot, cm

u_a = average velocity of air curtain at distance x from slot, cm/s

b = half-width of air curtain at distance x from slot, cm

Q_s = slot volumetric flow rate, cm^3/s

A_s = cross-sectional area of slot, cm^2

Q_x = volumetric flow rate of air curtain at distance x from slot, cm^3/s.

Equation (2) indicates that the cross-sectional velocity distribution of an air curtain is independent of slot width and slot exit velocity. Also, equation (3) shows that the expansion angle of an air curtain is independent of the slot width and slot exit velocities. Thus, from equation (1), it can be concluded that:

$$\text{Air Curtain Strength} \propto \text{Air Curtain Velocities} \propto u_s\ w^{1/2} = S \qquad (6)$$

where: S = a relative indicator of air curtain strength.

Plume Trajectory Equations

The following equations for a buoyant plume with negligible exit momentum flux were used to determine the plume elevation within the air curtain.

$$z = \frac{1.6\ F^{1/3}\ x_s^{2/3}}{u_w} \qquad (7)$$

and $$F = \frac{g\ A\ u_g\ (d_a - d_g)}{d_a} \qquad (8)$$

where:

z = vertical rise of plume, cm

x_s = horizontal distance downstream of source, cm

u_w = crosswind velocity, cm/s

g = acceleration of gravity = 981 cm/s²

A = cross-sectional area of the plume, cm²

u_g = plume rising velocity, cm/s

d_a = air curtain density, g/cm³

d_g = plume air density, g/cm³

Air Curtain Trajectory Equation

The equation for the air curtain centerline elevation is:

$$\frac{z}{b_o} = \frac{0.1\ g\ b_o\ (T_g - T_a)}{u_o^2\ T_a} (x_c\ /\ b_o)^{2.5} \qquad (9)$$

where:

z = vertical coordinate, cm

g = acceleration of gravity = 981 cm/s²

b_o = air curtain half-thickness, cm

T_g = air curtain gas temperature, K

T_a = ambient air temperature, K

u_o = average air curtain velocity where the hot plume and jet stream meet, cm/s

x_c = horizontal coordinate, cm.

Air Curtain Power Requirements

To investigate the power requirements of an air curtain, the energy equations for air curtain manifolds of Yung et al. (1) were used. Assuming that the gas velocities within the manifold are negligible in comparison to the slot exit velocities, it can be concluded that:

$$\text{Manifold Static Pressure} = p_m \propto u_s^2 \qquad (10)$$

and

$$\text{Air Curtain Blower Power Requirement} \propto Q_s \, p_m$$

$$\propto (u_s \, w) \, (u_s^2)$$

$$\propto w \, u_s^3 = P \qquad (11)$$

where: u_s = slot exit velocity, cm/s

Q_s = slot volumetric flow rate, cm^3/s

P = a relative indicator of air curtain power requirement.

The relationship between "Air Curtain Strength" and "Air Curtain Power Requirement" is illustrated in Figure 4, where S and P are plotted as functions of slot width and slot exit velocity. Figure 4 shows that for any given level of air curtain strength, the power requirement decreases as the slot width increases.

Air Curtain Design

The air curtain design is based on the emission source parameters of Table 1. The design values for the first four parameters are larger than the measured values to include extra capacity in the design.

The first step of the air curtain design was to compute plume and air curtain trajectories for various combinations of air curtain slot widths and slot velocities. Then for the combinations that yielded trajectories which met the maximum height requirement of the particle control device, their S values (from equation 6) were computed. These values indicated that the order of magnitude of S required for the pilot plant's air curtain was 2,000 $cm^{1.5}/s$.

A commercial air curtain unit that exceeded this S value was selected. Only one size of slot width was available for the desired S range, so the power requirement guideline of a wider slot for lower power was not important. The selected air curtain unit has an adjustable slot velocity, and has S values from 1,835 to 3,670 $cm^{1.5}/s$. Based on the design mold size of 107 cm (42 in.), a 152 cm (60 in.) air curtain slot length was selected, allowing 23 cm (9 in.) of plume drift on each side of the mold.

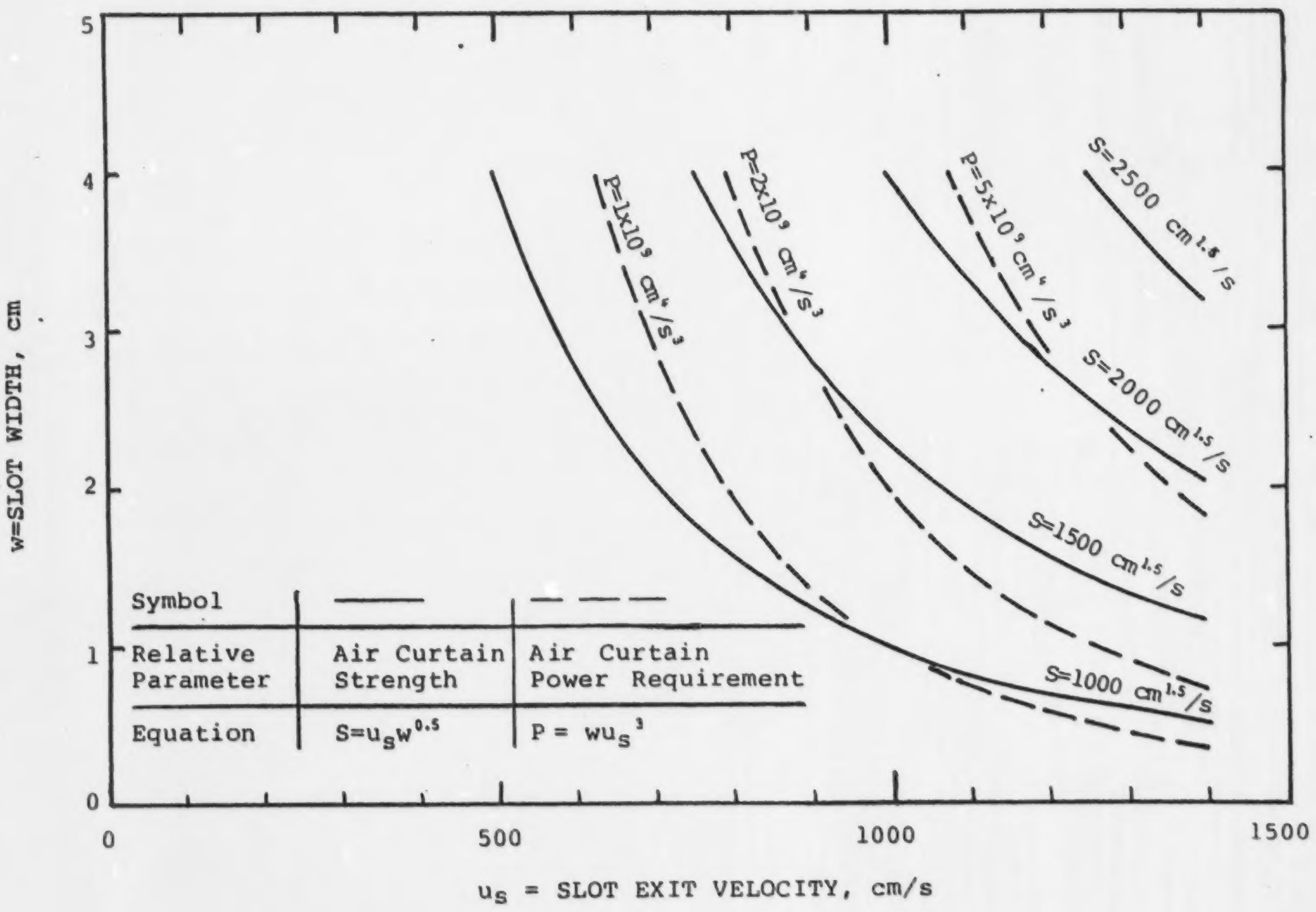

Figure 4. Air curtain power requirement and strength as functions of slot width and slot exit velocity.

TABLE 1. AIR CURTAIN DESIGN PARAMETERS

PARAMETER	MEASURED VALUE	DESIGN VALUE
Temperature at 30 cm (12 in.) above mold	32°C (90°F)	93°C (200°F)
Plume rise velocity at 30 cm above mold	3 to 56 cm/s (5 to 110 ft/min)	84 cm/s (165 ft/min)
Cross-sectional area of plume	undefined	2800 cm^2 (3 ft^2)
Largest mold size	76cm X 76cm X 81cm high (30" X 30" X 32" high)	107cm each side (42" each side)
Distance from air curtain slot to particle collection device	305 to 396 cm (10 to 13 ft)	305 to 396 cm (10 to 13 ft)
Distance from air curtain slot to mold plume centerline	61 to 335 cm (2 to 11 ft)	61 to 335 cm (2 to 11 ft)
Maximum height of particle collection device	270 cm	270 cm

To verify the adequacy of the air curtain design and to determine the required size for the inlet of the particle collection device, an air curtain duct from previous work was modified and tested with a smoke generator. Visual observation indicated that the air curtain adequately captured the smoke. At 396 cm (13 ft) from the air curtain slot, the velocity distribution of the air curtain and the horizontal and vertical expansion of the smoke were measured. At 396 cm (13 ft) from the slot, the height of the air curtain was 180 cm (6 ft), and its width was 180 cm (6 ft). The portion of the air curtain that contained smoke had a height of 180 cm (6 ft) and a width of 120 cm (4 ft).

FILTER UNIT

A previous, developmental version of the air curtain emission control system used charged spray scrubber for the particle collection device. However, the mass median diameter of the foundry mold emissions (0.2 to 0.4 µm aerodynamic) is too small for charged spray scrubbing to be effective.

In selecting the particle collection device, two types were considered: HEPA (High Efficiency Particulate Air) filters, and fabric bags. The HEPA filters were selected because they require less space than fabric bags. The HEPA filters use glass microfiber paper that is pleated.

Series 95 HEPA filters were selected. They have a collection efficiency of 95% when tested with 0.3 µm, thermally generated, dioctylphthalate smoke, in accordance with Federal Standard 209B.

The filter unit of the pilot plant is illustrated in Figure 5. To form a 183 cm by 183 cm (6 ft by 6 ft) filter panel, nine filter modules, each 61 cm by 61 cm (2 ft by 2 ft), were used. The depth of the modules is 29.2 cm (11.5 in.). A prefilter, of the pleated paper type and 5 cm (2 in.) deep, is used upstream of each HEPA filter. Nine centrifugal fans with dampers are used to pull the air through the filters.

PILOT PLANT TESTS

The overall performance of the pilot plant depends on both the ability of the air curtain to capture the particles and the ability of the filter unit to collect the particles. Consequently, two types of tests are used to evaluate the pilot plant: air curtain capture efficiency tests, and filter collection efficiency tests.

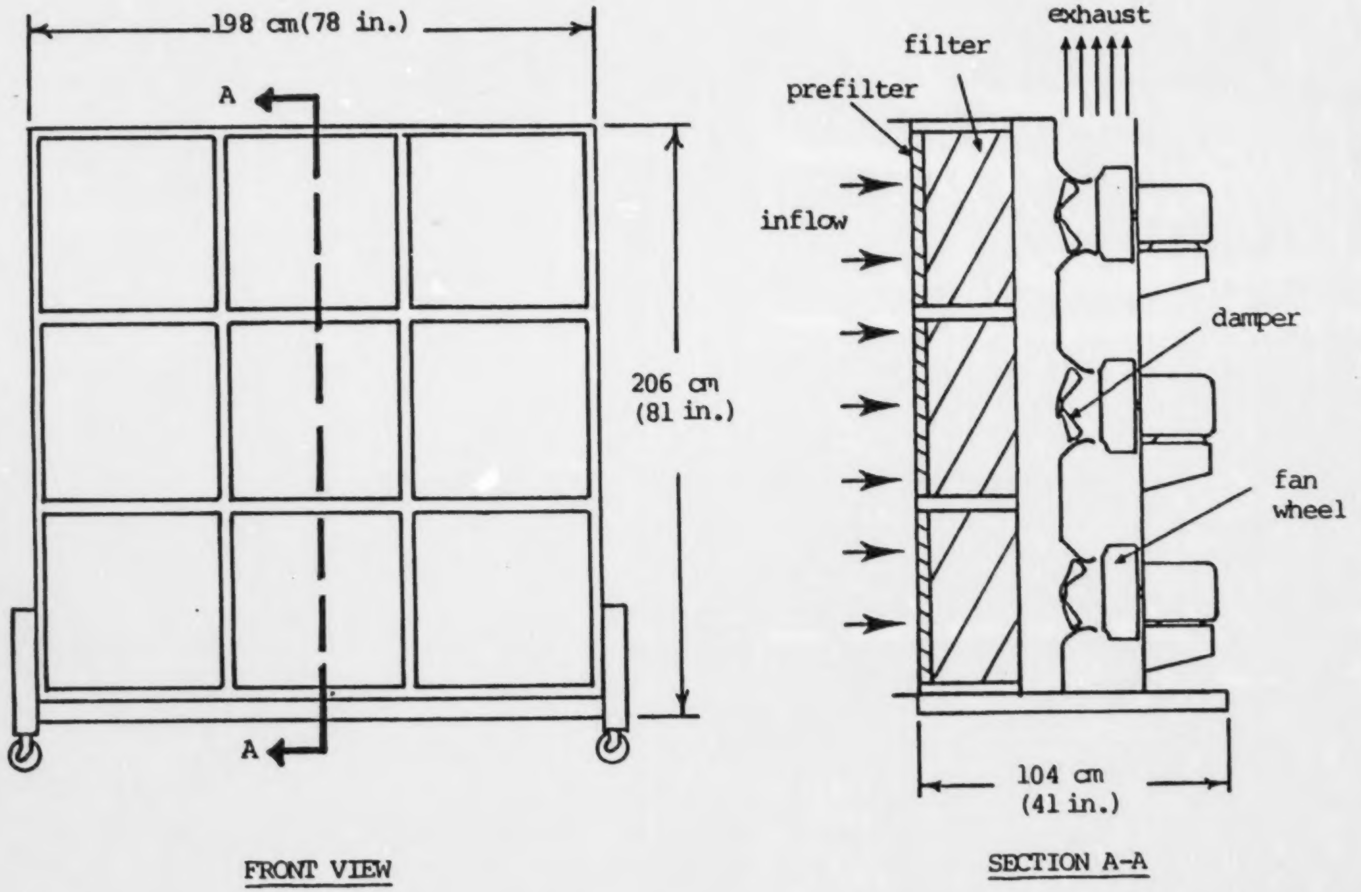
198 cm(78 in.)
A
A
206 cm
(81 in.)
exhaust
filter
prefilter
inflow
damper
fan
wheel
104 cm
(41 in.)

FRONT VIEW

SECTION A-A

Figure 5. Filter unit of pilot plant.

AIR CURTAIN CAPTURE EFFICIENCY TESTS

Method

To determine air curtain capture efficiency, the mold emission rate and the portion of this captured by the air curtain need to be known. The mold emission rate varies widely from mold to mold, and cannot be measured while the pilot plant is operating; so measuring the particles to determine the capture efficiency is not feasible.

Because the particles from the molds are very small, they behave like a gas. Therefore, the capture efficiency is determined using sulfur hexafluoride (SF_6) as a tracer gas. A temporary duct of rectangular cross section was added at the filter unit outlet for sampling and velocity measurement. The duct exhausts into existing hooding that carries the exhaust to an outdoor location where the SF_6 cannot return to the air curtain area. For each test, a mixture of SF_6-in-air (of a certified concentration) is injected into the mold plume at a controlled and measured rate. At the temporary duct, velocities are measured, and syringe samples of gas are taken, using a 4 by 5 array of 20 duct traverse points. The SF_6 concentrations of the samples are measured with an electron capture gas chromatograph.

For all of the capture efficiency tests, the air curtain unit is set at 370 cm (12 ft) from the filter unit. The volumetric flow rate of the filter unit is set at about 115% of that of the air curtain flow field at the filter unit inlet.

The air curtain capture efficiency is calculated according to this definition:

$$\text{Air Curtain Capture Efficiency} = \frac{\text{Total volumetric flow of } SF_6 \text{ measured at filter unit outlet, at standard temperature and pressure}}{\text{Volumetric flow of } SF_6 \text{ injected above mold, at standard temperature and pressure}}$$

Accuracy

To determine the accuracy of the capture efficiency test method, tests were performed in which the SF_6-in-air mixture was injected into the filter unit at three points between the bottom row of filters and the bottom row of dampers. Six of these tests were performed. Three of the tests had problems with tracer gas recirculation or velocity meter breakdown. For the three good tests, the measured amounts at the outlet were 94.0%, 93.5%, and 106.4% of the injected amounts. This indicates that the accuracy of the air curtain capture efficiency test method is no better than + or - 6%.

Results

This testing is currently underway, and seven tests have been made, with five of the tests having problems with high SF_6 concentrations in the background samples taken before and after each test. The capture efficiencies of the two good tests are 105.0% and 91.0%. Capture efficiencies greater than 100% are impossible, so the 105.0% value has at least 5% error.

FILTER COLLECTION EFFICIENCY TESTS

Particle concentrations at the inlet and outlet of the filter unit are too low to allow direct measurement of the particle collection efficiency. Consequently, a small, series 95 HEPA filter, 30 cm by 30 cm by 29 cm deep (12 in. by 12 in. by 11.5 in. deep), will be tested in ductwork that will capture the mold emissions with a hood. The particles will be measured with both cascade impactors and an electrical aerosol size analyzer. The electrical aerosol size analyzer is based on the "diffusion charging-mobility analysis" principle. It measures the number of particles larger than 7 particle diameters, ranging from 0.01 to 0.32 µm. The filter collection efficiency tests have not started yet.

CONCLUSIONS

The air curtain transport system provides an effective method for controlling the buoyant emissions of foundry molds. Early test results of the demonstration pilot plant indicate that the air curtain capture efficiency is 91 to 100%.

REFERENCES

1. Yung, S., J. Curran, and S. Calvert. Spray Charging and Trapping Scrubber for Fugitive Particle Emission Control. EPA-600/7-81-125, (NTIS PB82-115304), U.S. Environmental Protection Agency, Research Triangle Park, North Carolina, 1981.

CHARACTERIZATION OF FUGITIVE PARTICULATE EMISSIONS
FROM INDUSTRIAL SITES

by: K. S. Basden
School of Chemical Engineering & Industrial Chemistry;
University of New South Wales
Kensington, N.S.W. 2033
Australia.

ABSTRACT

One of the problems of modeling fugitive particulate matter emissions from various industrial sites, such as quarries or open cut coal mines, coal loaders, ore transport lines or stockpiles, etc., is to obtain reliable source emission data. If such data are available there are numerous dispersion equations, or models and programmes based thereon, which may be used to predict airborne concentrations or ground deposition rates around the sites as functions of appropriate meteorological parameters. This paper reviews briefly some recently completed work on this subject in which "conventional" instruments such as hi-vol samplers and deposition gauges have been used. However the principal objective is to describe current work involving a small portable cascade impactor and related portable manually-operated instruments to determine the nature and emission rates from component sections of the sites, as opposed to the overall average values obtained with long sampling period instruments.

INTRODUCTION

Much work has been done during the past 20 years in developing quite reliable dispersion equations by means of which pollutant concentrations at receptor sites may be computed. (1)(2)(3)(4) The input parameters, in addition to various meteorological factors, include a source emission term. This term may vary in its dimensions or units depending upon the type of model to which it applies: for example it may be mass only (e.g. kg) for an instantaneous point source, or mass per unit length per unit time (e.g. kg/(m)(s)) for a continuous line source, and so on. Other units for source emission terms depend upon the dimensional requirements of the equation which defines the appropriate model.

For many dispersion problems the source emission rate is obtained easily. For example, in a combustion situation where the effluent leaves a stack as an elevated continuous point source, the pollutant evolution rate is calculated readily from the known fuel composition and rate of burning. Similar considerations apply for other models involving continuous or instantaneous point, line or area sources. However, with fugitive dusts, in general, the production rate cannot be measured or calculated directly, and hence must be inferred by making downwind concentration measurements and "back calculating" in order to arrive at a source factor. Stated in another way, it is not possible to weigh a section of roadway, for example, before and after a truck has passed over it, in order to determine directly the loss in weight which could be attributed to fugitive dust entrainment and dispersal. However, in some instances involving wind entrainment of material from the surface layers of static features, such as stockpiles or roadways, etc., threshold velocities and emission factors have been obtained by isokinetic sampling from a portable open-bottom wind tunnel which has been placed directly onto the surface concerned (5)(6)(7). Although such a method could be classified as indirect, it nevertheless should yield reliable and reproducible data. Unfortunately a similar technique cannot be used for surfaces involved in draglining or shotfiring, etc., therefore rollback methods from downwind receptor airborne concentrations have been utilised to achieve a source emission factor. Accordingly, numerous papers have appeared over recent years on this subject, and all of these, of which the present writer is aware, have utilized hi-vol samplers either with or without associated deposit gauges (dustfall jars) in a variety of receptor configurations in order to establish numerical values for emission data.

THE CURRENT STATUS OF WORK IN NEW SOUTH WALES

In recent years the N.S.W. State Pollution Control Commission (SPCC), inter alia, has expressed concern about the fugitive emissions from various open-cut coal mines and related developments principally in the Hunter Valley and to a lesser extent in the Western District coalfields.(8) In view of the projected increase in production associated with the opening of new sites, largely to supply a growing export market for metallurgical and steaming coal, the SPCC has conducted a substantial monitoring campaign to establish present and future pollution levels. The latter, which consist of isopleths of both airborne concentration ($\mu g/m^3$) and fallout rate [g/(m²)(month)] have been obtained principally with the USEPA Climatological Dispersion Model (CDM) - a part of the UNAMAP package - using modified input parameters.

The input factors, which have been considered to be representative of emission rates from the Hunter Valley area without the imposition of dust control procedures, are stated (8)(9) to be based upon a frequently-quoted USEPA publication (10) after modification to correlate with the results of monitoring around a particular Hunter Valley mine site. The factors and a qualifying statement are reproduced from references (8) and (9) in Table 1.

TABLE 1. EMISSION FACTORS FOR UNCONTROLLED OPERATIONS (8)(9)

Operation	Emission Factor
Haul Trucks	4.0 kg per vehicle kilometre travelled
Blasting of Overburden and Coal	Blast (Kg/blast) $= \frac{758\ A^{0.8}}{M^{1.9} D^{1.8}}$ where A is area to be blasted m² D is the depth of blast, m M is moisture content, %
Loading by Truck and Shovel:	
Overburden	0.01 kg per tonne of Overburden
Coal	0.02 kg per tonne of Coal
Drilling	0.6 kg per hole
Truck Dumping:	
Overburden	0.02 kg per tonne of material
Coal	0.06 kg per tonne of material
Exposed Areas	0.4 kg per hour per hectare
Top-soil Removal	14 kg per scraper hour
Dragline	0.02 kg per m³ of material

"These are preliminary figures only, and more work is required to gain complete confidence in emission factors for conditions in NSW coalfields. In particular, the figure for dragline operations has not been verified at this stage, so additional caution is required in the use of this factor."

At the recently-held Eighth International Clean Air Conference in Melbourne, Victoria, May 6 - 11 (1984), four papers on fugitive dust in the Hunter Valley were presented (9)(11)(12)(13), two by consultants and two by officers of the SPCC, which indicates the growing level of concern of this subject.

In addition to this work, an independent study into dust emission from open-cut collieries recently was undertaken over a two year period by technical staff of the School of Chemical Engineering and Industrial Chemistry, University of New South Wales, with partial support from the Electricity Commission of New South Wales. Emission factors have been obtained for a number of operations such as dragline removal of overburden, blasting, transport on unpaved and unwatered non-haulage roads, truck and shovel overburden loading and coal loading, and overburden drilling prior to blasting. The units reported are in g/s or g/(s)(m) as the case may be for various short and long term time-averaging periods, and where appropriate they also are given for differing Pasquill-Gifford stability categories. At the time of writing these data have not been cleared for publication and hence are not reproduced in this Paper. However, it can be mentioned that the figures were obtained in the usual way by rollback calculation from results of hi-vol samplers (some fitted with 5- and 6-stage parallel slot cascade impactor heads) stationed at appropriate downwind receptor sites.

DEVELOPMENT OF INSTRUMENTS FOR ACQUISITION OF SHORT-TIME SPECIFIC EMISSIONS

In the work referred to in the previous Section, considerable difficulty has been experienced in transporting, setting up and servicing the hi-vol samplers and associated motor-generator sets (M-G sets which provided operating power) at sites for which access is difficult. In addition, such instruments normally have to run for several hours at least (more if cascade impactor heads are installed) in order to obtain a "weighable" sample. It has been found that this leads to difficulties in characterizing the plume from a unique source, as during the "exposure time" dusts from other operations or from general "background" continues to arrive at the receptor site. The latter, i.e. "background", could have a disproportionate influence if the source under investigation temporarily were to lapse or to fluctuate in output over the sampling period.

Accordingly, the feasibility of two other "simple" and readily-portable instruments which would sample a much smaller volume of air over a shorter time period, and which would involve a particle number "count" rather than a particle "weight", has been investigated. With the well-known mathematical relationships which exist to convert from number to mass distributions and vice versa, a mass basis distribution would be obtainable readily from the number distribution. A further advantage of the procedure would be the immediate availability of a particle size distribution, not only by number but also by mass which is a required parameter for "tilting plume" dispersion models.

To demonstrate the theoretical feasibility and the mathematical operations associated with the proposal, a hypothetical example may be taken. Assume a particulate plume to be log-normally distributed with a mass geometric mean particle diameter (D_{pgm}) of 10 μm and a geometric standard deviation (σg) of 2.0 - a highly likely and realistic assumption. Also assume that the atmospheric concentration of the particulate cloud (X) is $100 \mu g/m^3$. (A real plume would be substantially attenuated to yield such a low value). What would be the total number of particles and the size distribution by number, of this particulate population, in 1.0 liter of atmosphere? (Note that a hi-vol sampler would have to pass $1000\ m^3$ of atmosphere to collect 100 mg or 0.1 g on its 200 x 250 mm (8 x 10 inch) filter which itself would weigh over 3 grams. This would take 12 to 15 hours.)

The solution is as follows. Firstly the initial distribution is plotted on a log probability graph, and this immediately yields the cumulative percent undersize as a function of particle diameter. To obtain the related number distribution, the number geometric mean diameter is obtained from the well known relationship:

$$\ln D_{pgm}(N) = \ln D_{pgm}(V) - 3\ln^2\sigma_g \qquad (1)$$

which yields the result that $D_{pgm}(N) = 2.36\ \mu m$. (At this stage $D_{pgm}(V)$ is synonymous with $D_{pgm}(M)$ [V≡volume; M≡mass]. If the sizing is by aerodynamic diameter this situation remains; if not a density (ρ) correction is made later as shown in equations (2) and (3).) A line is drawn through the 2.36 µm intersection with the 50% locus on the probability scale, parallel to the original mass distribution (as σ_g is the same) and this yields the number distribution for later reference.

The relationship between total particle mass (M_p) and the log-normal number distribution is as follows.

$$M_p = \frac{\pi\ \rho\ N}{6\sqrt{2\pi}\ \sigma_u}\int_{-\infty}^{\infty} \exp(3u)\ \exp\left[\frac{-(u-\bar{u})^2}{2\ \sigma_u^2}\right] du \qquad (2)$$

for which the solution is:

$$M_p = \frac{\pi}{6}\rho N\ \exp(3\bar{u})\ \exp\left[\frac{9}{2}\sigma_u^2\right] \qquad (3)$$

where N = particle number; $u = \ln D_p$; $\bar{u} = \ln D_{pgm}(N)$; $\sigma_u = \ln \sigma_g$. Substituting -12.9568 for $\bar{u}$; 0.69315 for σ_u; 1.0×10^{-10}kg for M_p (i.e. 100 ng which will be in 1.0 L) and $1000\ kg.m^{-3}$ for ρ it is found that N = 1670 particles with a size distribution as given on the log probability plot: i.e.

4% or 67 particles ≥ 8 µm
6% or 100 " = - 8 + 6 µm
10% or 167 " = - 6 + 4 µm

20% or 335 particles = - 4 + 2.8 µm
20% or 335 " = - 2.8 + 2.0 µm
28% or 468 " = - 2.0 + 1.0 µm

and the remaining 12% are ≤1.0 um. The plot also indicates that this 12% of the number which is ≤1.0 µm in diameter constitutes only 0.05% of the mass.

Therefore, if a sample of about a liter or two in volume is drawn through a cascade impactor or a filter, and the particle numbers, as a percentage of the whole in appropriate size ranges are determined, both the mass distribution and the total concentration in $\mu g/m^3$ are rapidly and easily obtained by the reversal of the abovementioned procedure. Accordingly equations (1) (2) and (3) are the key to the whole procedure. Equation (1) is well known, but equations (2) and (3) are more obscure. Because of this it was planned originally to provide the formulation of (2) and its solution to yield (3) in an Appendix to this paper, but this could not be done because of space limitations. The subject is to be covered in the oral presentation.

DESCRIPTION OF INSTRUMENTS AND METHOD OF USE.

The simplest piece of equipment which could be devised to achieve the abovementioned objective consists of a membrane filter in a suitable holder connected to a hand-operated pump of known capacity, as illustrated in Figure 1. The swept volume of the pump is adjustable and for this work is set at 333.3 mL or one third of a liter. In the field new membrane filters are placed directly into the holder from the original package, by means of membrane filter forceps. Exposed filters are placed singly in suitable sealed cartridges or containers for transport back to the laboratory. Each filter is exposed by drawing through it an appropriate volume of the cloud of particulate matter, the volume varying according to circumstances. Typically from 1 to 5 liters (i.e. 3 to 15 strokes of the pump) are utilised, taking about 5 to 8 seconds to withdraw the handle for one stroke. This gives a face velocity of between approximately 20 and 13 cm/s respectively, so if facing into any type of a breeze isokinetic conditions would not prevail. However, it is considered that departure from isokinetic conditions should have negligible effect on the collection of particles of the size range of interest, although care in sampling in high wind conditions should be exercised.

In the laboratory the filters are rendered transparent by exposure to glyceryl triacetate or acetone, etc., according to various techniques long established but principally used in the determination of airborne asbestos fibers. The procedure used by the writer is outlined briefly in the Appendix. After covering in a suitable manner with a cover slip, the now transparent filter is examined by a microscope fitted with a calibrated eyepiece graticule, of which several designs are available. A stage micromoter is used for calibrating the graticule. The numbers of particles in various size ranges, in a statistically significant number of randomly - or rule - selected fields of view of known area, are recorded; and when

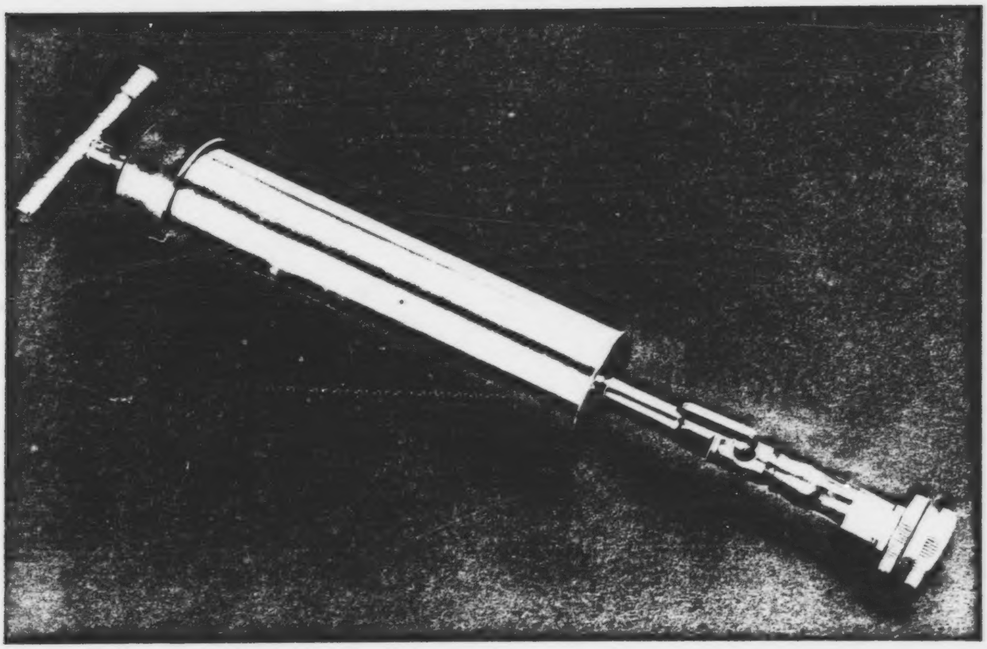

Figure 1. Hand pump with membrane filter holder.

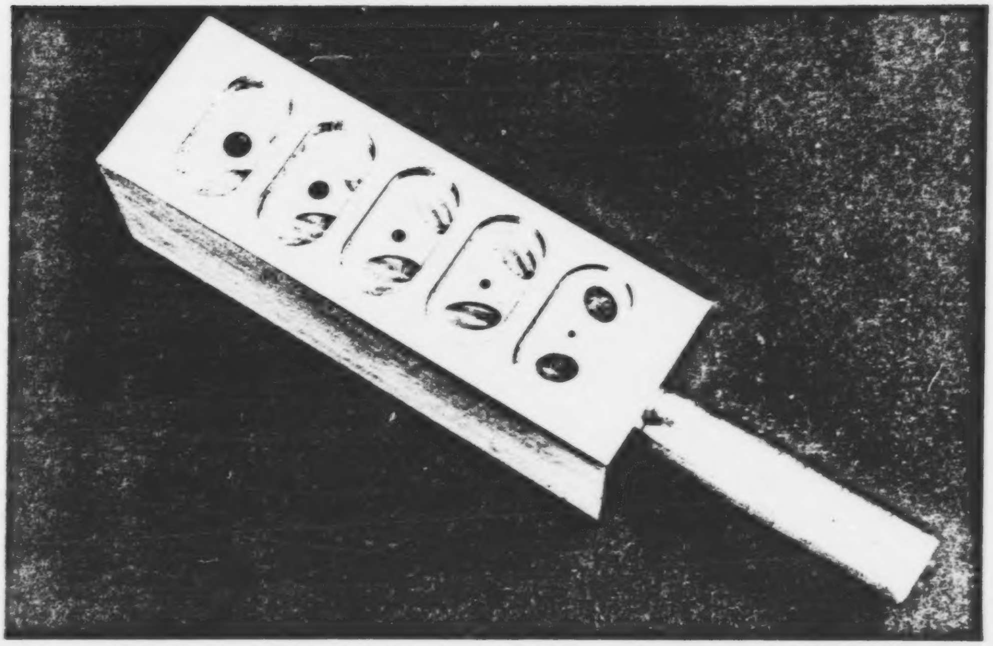

Figure 2. Cascade impactor - front view.

these are related to the total exposed area of the filter, the number distribution for the sampled volume of air is established. The techniques of counting the numbers of particles in various size ranges, from a heterogeneous mixture in the field of view of the microscope, have been well established for more than half a century. (14)(15) However, the writer feels that this now may be a "dying art", as various industrial hygiene workplace atmosphere dust regulations are being converted from a number to a mass concentration basis, with a concominant change from microscopes to micro-balances in many laboratories.

The cascade impactor (Figure 2) was developed in an endeavour to facilitate further the assessment of a heterogeneous mixture of unsegregated particle sizes. The only novel or unusual design feature associated with this impactor compared with the multitude which have been in existence since the 1940's, is that all 5 of the stages impact onto the one 75 x 25 mm (3 inch x 1 inch) microscope slide. The slide covers the front face shown in Figure 2; it is held in place by a cover and a clamp. The smooth, lightly greased surface of the slide makes such a close contact with the smooth flat upper surface of the impactor that a leak-proof seal is provided. On applying suction, the air enters the enlarged orifice on the back (Figure 3) and passes through the block via a converging conduit and impacts on the slide in the first oval-shaped depression. The air then passes up the two sloping holes which meet above the second orifice, through which it passes to impact against the slide in the second oval depression. This is repeated for all 5 stages with the orifice diameters and the separation distance decreasing at each stage. An in-line membrane filter holder with filter may be attached at the outlet not only to capture the sub-micrometer material leaving stage 5 (a proper assessment would require electron microscopy), but also to check on larger particle carry-through, etc. The 50% cut-sizes (i.e. D_{p50}) vary with air flow rate according to well known design principles (16), but with the 1.33 liters/minute which has been decided upon arbitrarily for this instrument, the 50% cut-sizes are as shown in Table 2. In each stage the orifice-to-slide separation distance is equal to the orifice diameter (except in stage 1 where it is about 10 per cent less).

TABLE 2. DATA FOR CASCADE IMPACTOR AT A FLOW RATE OF 1.33 LITERS/MIN.

Stage	Orifice diameter mm	D_{p50} μm Aerodynamic diameter
1	3.556	7.5
2	2.540	4.5
3	1.575	2.2
4	1.321	1.6
5	0.813	0.8

The air may be drawn through the impactor head by a number of devices, provided that the flow is steady and uniform at the calibration value. An

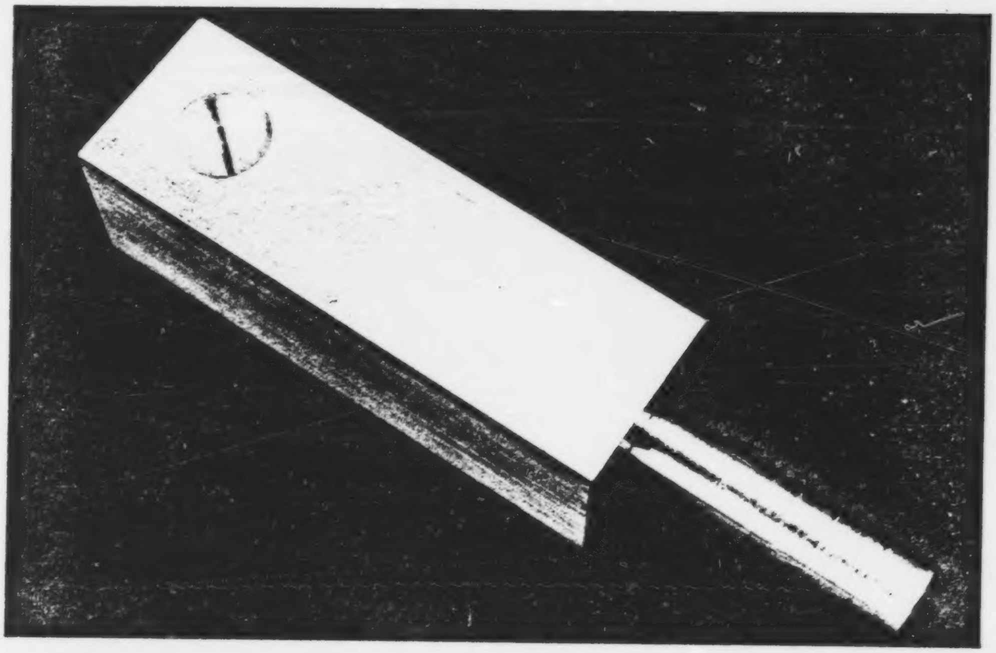

Figure 3. Cascade impactor - rear view.

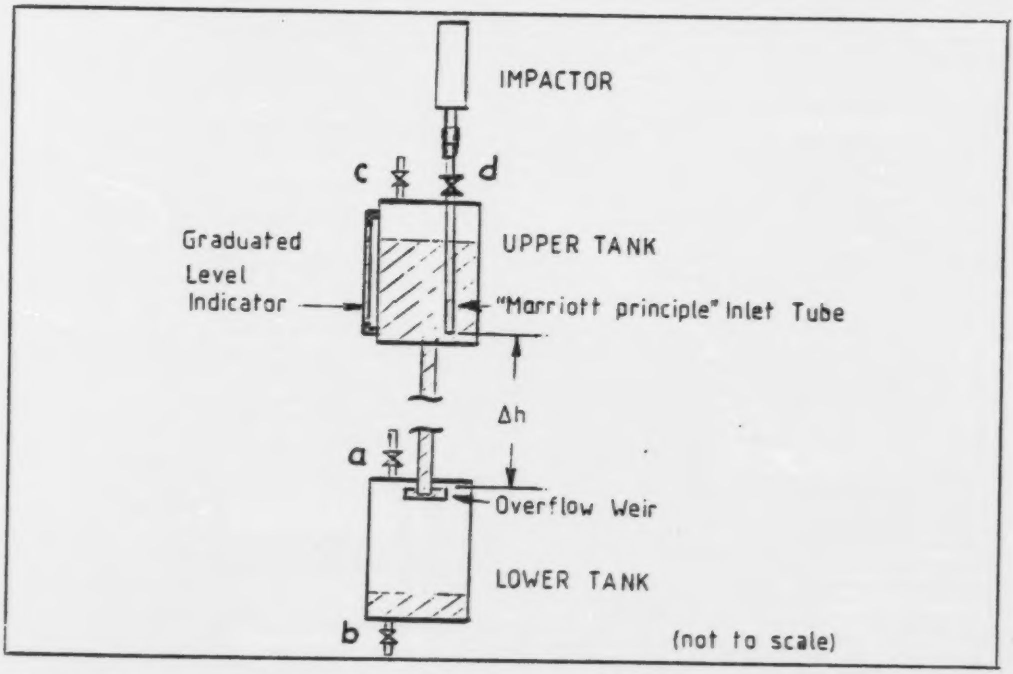
IMPACTOR
c
d
Graduated
Level
Indicator
UPPER TANK
"Marriott principle" Inlet Tube
Δh
a
Overflow Weir
LOWER TANK
b
(not to scale)

Figure 4. Diagram of dual tank aspiration system.

appropriately-adjusted battery operated pump for a "personal sampler" would be satisfactory. However the initial work with this instrument utilised water aspiration. The system is shown diagrammatically in Figure 4. Because of the "Marriott principle" of the air inlet to the top tank continuing via a tube to an outlet near the bottom of the top tank, and the water on entering the lower tank overflowing a constant-level weir near that tank's inlet, the suction head is always constant irrespective of the actual water levels in the tanks, and is equal to the vertical separation between the base of the air inlet tube in the top tank and the overflow weir in the lower tank. With this cascade impactor, the resistance to flow is such that a vertical separation of 52 cm. is required to produce the flow of 1.33 L/min.

When the upper tank needs to be refilled, the air-escape (a) in Figure 4 is closed, the lower tank is inverted above the upper one on a stand provided for that purpose, valves (b) and (c) are opened and the water flows back. On closing valves (b) and (c), restoring the tank to its lower position, and opening (a), the system is ready to function again as and when the main flow-valve (d), which is connected to the impactor, is turned on. The system may be left in the state of readiness with (d) closed almost indefinitely.

This system functions very successfully, and in the field is reasonably portable. However, subsequently it has been found that the hand pump of Figure 1 can be relied upon to draw air uniformly and very successfully through the impactor at the required flow rate, so plans to build another more easily transportable and reversible water aspirator system have been abandoned. In using the hand pump, the piston must be withdrawn uniformly in 15 seconds in order to provide a flow rate of 1.33 L/min. Accordingly, the piston stem has been engraved with 15 equally-spaced marks (which are about 12 mm or ½-inch apart); therefore, if the stem is withdrawn so that the marks appear at 1 second intervals - as timed by a watch or a pocket metronome - the required flow rate is achieved. It is found that the friction provided by the tightly-fitting piston together with the additional resistance caused by the suction head contributes to a uniformity and smoothness of movement which facilitates this operation.

As mentioned above the slides are very lightly greased to reduce particle bounce on impact. The amount of bounce that has been detected even with perfectly clean slides is almost negligible, but with the light grease coating it is less. A minute amount of vaseline - less volume than the head of a pin, or a barely-visible streak 1 or 2 mm long put on with the point of the pin, - is all that is required. With a scrubbed finger tip which has been rinsed in distilled water and dried by being dabbed on a clean membrane filter, this minute amount of vaseline is spread over the entire 3 x 1 inch slide, which then is placed with others similarly prepared in a dust-free microscope slide box to await exposure at the investigation site.

The spots of dust particles when viewed under the microscope show a gratifying uniformity of size, but unless the numbers are comparatively few they may be difficult to count because the particles are concentrated non-uniformly over a small area of the slide. For comparative or for semi quantitative purposes, the superficial number density of particles may be approximated within acceptably close limits by comparison with a series of previously-prepared (or manually drawn) standards. However a laboratory procedure which has been found to be useful not only to facilitate the counting of the particles but also to increase the counting accuracy is as follows. It consists of causing the particles to re-deposit uniformly over a known area of the slide, which means that the number of particles in a known fraction of the area (as delineated by a calibrated eyepiece graticule), averaged from a small but statistically significant number of observations, is all that is required. The re-deposition is obtained by surrounding each spot with a "wall" of about 7 or 8 mm internal diameter made from PVC laboratory tubing; adding about 0.05 to 0.1 mL of an appropriate liquid and subjecting the resulting system to ultrasonic vebrations for about 5 minutes in order to detach the particles from the surface and cause them to become suspended in the liquid. After evaporation of the liquid a uniform distribution of particles over the known area is obtained. The "liquid" found to be most effective, after trials involving several organic liquids, is doubly-filtered distilled water with a small concentration (of the order of units of mg/L) of soap (sodium stearate), with the water in the ultrasonic bath heated to about 70 - 80°C. The practical aspects of performing this operation are to be illustrated during the oral presentation of this paper. However in passing it is of interest to note that the lengthy exposure to the ultrasonic bath is required to dislodge the particles from the slide surface, as even on a perfectly clean ungreased slide they adhere so tenaciously that strong jets of organic liquids and boiling detergent-containing water are capable of removing only a small fraction of the finer sized deposits.

CONCLUSIONS

A method has been described which permits primary airborne particulate matter concentrations to be determined over a wide range of values. The field operations are simple and utilise readily portable manually operated equipment. The hand pump, with cascade impactor head and membrane filter holder, together with holders for many filters and prepared microscope slides, fit in a carrying case less than half the size of a small attache case. Sampled air volumes may range from less than 1 liter to probably a maximum of 10 or more liters, requiring times from several seconds to about 15 or 20 minutes per determination, depending on whether filter or impactor are used. This is short enough to be able to characterize the fugitive emissions from a single source or operation, but probably not long enough to give a time-averaged airborne concentration at a considerable downwind distance because of the effect of turbulent eddies, etc. Accordingly, for the latter purpose several determinations should be made at appropriate time intervals, and the results averaged.

A disadvantage of the method is the slightly more complex laboratory procedure which is involved, but this may be offset by a more-or-less permanent record which remains. The cover-slip covered membrane filters, appropriately labeled, may be retained ad infinitum and the assessments checked by others. The cascade impactor slides also may be kept for a considerable time, but so far no technique has been devised for applying a cover-slip over the spots in such a manner as to ensure that the particles therein are not disturbed.

Finally, a comment should be made about the application of this technique to the determination of source emission factors, which is the subject of the early part of this paper.

Firstly, in our work we have been inclined to doubt the reliability of using rollback calculations from receptor concentrations to source emission, because of the input of subjective judgment in allocating appropriate horizontal and vertical dispersion parameters. From the result so obtained other receptor concentrations are predicted by an appropriate model again using subjectively-allocated dispersion parameters, thereby doubling the unreliability factor - whatever that may be.

Secondly, although we are not aware of any work to support or deny this view, we believe that a fugitive dispersion episode may be divided into three parts, as follows. (i) The initial mechanical raising of the dust into the atmosphere by the moving vehicle, dragline, explosive blast, etc. Some of this material immediately will fall back to ground, but the remainder remains suspended. (ii) For a short, but probably variable finite time, this suspended material uniformly fills a hypothetical "box" the dimensions of which perhaps could be determined by aerodynamic theory, wind tunnel tests or more simply by photography of the actual operation. (iii) At the conclusion of this short finite time, the action of the wind and its eddies produces the traditional Gaussian model of a spreading plume by horizontal and vertical turbulent diffusion, giving downwind time averaged concentrations predictable with varying degrees of reliability by the existing multitude of equations.

Thirdly, we believe that with the short-time sampling capability of the instruments described, attention could be given, possibly for the first time, to part (ii) of the paragraph above; namely if an observer could get sufficiently close to a dust-producing operation to measure the initial uniform concentration in the "box" before Gaussian turbulence mechanisms attenuated the concentration, and the "box" dimensions could be established (e.g. by slow-speed cinematography, say 1 frame/s) then a source emission factor readily could be determined. For example, a truck moving along a haulage road would constitute an "instantaneous line source", and the units of the emission term of the appropriate equation would be g/m or similar. Suppose the sampling method described herein gives a result of 8 mg/m^3 when the initial "box" is shown to be a cylinder of effective cross sectional area $4m^2$. Accordingly an emission factor of 2 mg/m could be allocated to that type of truck moving at the same speed on the same type of road.

It is not the purpose of this paper to follow this subject any further as a new study programme in this field is required.

The work described in this paper was not funded by the U.S. Environmental Protection Agency and therefore the contents do not necessarily reflect the views of the Agency and no official endorsement should be inferred.

APPENDIX

A note on the method of preparation of membrane filters for microscopy as developed and utilised by the present writer.

The filter is placed on a clean microscope slide, and on it is placed a smooth-edged stainless steel ring of the same diameter and about 3 or 4 mm high. (These rings are prepared by cutting 3 or 4 mm slices off a commercial 25 mm dia (1 inch) stainless steel tube.) The ring very effectively prevents any distortion in the shape of the filter during the subsequent process.

The slide with the filter and ring then are placed on a stand 8 or 10 mm high in a glass Petri dish in which the base has been covered with acetone. The lid is placed on the Petri dish and it is allowed to stand for about 15 - 20 minutes or until the filter becomes quite transparent. At the end of this time the slide is removed and the ring - which now has adhered to the transparent filter - is gently removed by inserting a knife or spatula blade under one edge and twisting so as to raise the ring directly from the surface.

A cover slip, with the surface wetted with acetone, is placed carefully on the filter so as to exclude air bubbles and is gently pressed down. This results in a quite transparent filter with the particles all in situ in their original locations and in the focal plane of the objective lens of the microscope. The slide so produced may be handled, observed and stored probably indefinitely. When the slides are no longer required they may be stood in a beaker of water for about 20 - 30 minutes after which the cover slip may be moved gently sideways whereupon it frees itself from the transparent filter. The latter then peels off the slide like a piece of clear plastic so both the slide and cover slip are returned to use.

REFERENCES

1. Slade, D.H. (Ed.) Meteorology and Atomic Energy 1968. U.S. Atomic Energy Commission Office of Information Services, 1968. 439 pp.

2. Turner, D.B. Workbook of Atmospheric Dispersion Estimates PB-191482 U.S. Dept. of Commerce National Technical Information Service, 1970. 83 pp.

3. Air Pollution Control Association, Proceedings Speciality Conference. Dispersion Modeling from Complex Sources, Greater St. Louis Section, April, 1981. 334 pp.

4. Benaire, M.M. Urban Air Pollution Modelling. Macmillan Press, U.K., 1980. 405 pp.

5. Gillette, D.A. Tests with a portable wind tunnel for determining wind erosion threshold velocities. Atmos Environment 12: 2309, 1978.

6. Cowherd, C.Jr. Emission factors for wind erosion of exposed aggregates at surface coal mines. Paper 82 - 15.5 presented at 75th Annual Meeting of the Air Pollution Control Association, New Orleans, Louisiana, June 20 - 25, 1982.

7. Cowherd, C.Jr. A new approach to estimating wind-generated emissions from coal storage piles. In: Proceedings: Fugitive Dust Issues in the Coal Use Cycle - Speciality Conference, Western Pennsylvania Section, Air Pollution Control Association, April, 1983. p. 4 - 16.

8. State Pollution Control Commission. Air pollution from coal mining and related developments. ISBN 0 7240 5936 9. December, 1983. 27 pp.

9. Nguyen, H., Ross, I.B., and Dean, M. Problems encountered in developing a model to predict dust emission levels around open cut coal mines in the Hunter Valley of New South Wales. In: Eighth International Clean Air Conference, Clean Air Society of Australia & New Zealand, Melbourne, Vic. 1984. p.251 - 69.

10. Axetell, K.Jr. and Cowherd, C.Jr. Improved emission factors for fugitive dust from Western Surface Coal Mining sources, Vols. 1 and 2. E.P.A. Contract No. 68-03-2924. U.S. Environmental Protection Agency, Cincinnati, Ohio, July 1981.

11. Zib, P. Modelling air quality for fugitive dust from open sources in Australia. In: Eighth International Clean Air Conference, Clean Air Society of Australia & New Zealand, Melbourne, Vic. 1984. p.217-224.

12. Beer, T. Modelling dust from open-pit coal mining. Ibid, p.225-238.

13. Dean, M. and Train, W.J. Recent studies on the modelling, appraisal and control of dust from open cut coal mines in New South Wales. Ibid, p.239 - 250.

14. Davies, C.N. Dust is Dangerous. Faber & Faber, London, 1st Ed., 1954, 116 pp.; p.29 - 42.

15. Jacobs, M.B. The Analytical Toxicology of Industrial Inorganic Poisons. Wiley Interscience, New York, 1967. 943 pp.; p.228 - 56.

16. Fuchs, N.A. Aerosol Impactors (A Review) In: Shaw, D.T. (Ed.) Fundamentals of Aerosol Science, Wiley Interscience, New York, 1978. 372 pp.; p.1 - 83.

EVALUATION OF AN AIR CURTAIN SECONDARY HOODING SYSTEM

by: John O. Burckle
U. S. Environmental Protection Agency
Office of Research and Development
Industrial Environmental Research Laboratory
Cincinnati, Ohio 45268

ABSTRACT

A prototype secondary hooding system, based upon air curtain technology, has been installed in a domestic primary copper smelter to capture fugitive emissions from the converter. Tests have been conducted by the USEPA to evaluate its effectiveness for capture of low-level fugitive particulate, including trace metals, and sulfur dioxide. These tests demonstrated that this system was capable of providing effective control of emissions during most of the converter cycle, achieving an overall capture effectiveness of 94%. The Office of Air Quality Planning and Standards has proposed the air curtain secondary hooding system as Best Available Control Technology for converter fugitive emissions. This paper is based upon the work reported in EPA-600/2-84-042a,b (NTIS order number PB-84-160514 for Volume I and PB-84-160522 for the Appendices).

This paper has been reviewed in accordance with the U.S. Environmental Protection Agency's peer and administrative review policies and approved for presentation and publication.

INTRODUCTION

Copper converting is a batch operation conducted in two stages to convert copper matte produced in a smelting furnace into blister copper. The Pierce-Smith converter, used in all but one U.S. smelter, is acknowledged to be the major source of fugitive emission in the smelter. These fugitive emissions first enter the workplace and, because they are present in relatively high concentrations, are considered hazardous to worker health. They are emitted from the smelter at relatively low levels through roof monitors and other openings in the building. These low level emissions cause deterioration of the air quality and are believed to cause adverse health impacts on the general population suffering prolonged exposure. While some dispersion and dilution of the fugitives occur upon leaving the smelter workplace, the ambient exposure concentrations are high relative to a well dispersed emission from a tall stack.

A number of approaches to the control of these emissions have been attempted by industry with unsatisfactory results. The major barrier to the development of an acceptable secondary hood has been the inability to design a system capable of permitting crane and ladle access while simultaneouly providing for reasonably effective capture of fugitive emissions.

The air curtain (Figure 1) is formed by blowing air from a supply plenum or a row of nozzles which is especially designed to form an air sheet, or curtain, with as little turbulence as possible. This curtain is directed over the open space, well above the converter, which permits crane access. On the opposite side of the space, the curtain and entrained air are captured by an exhaust system. Fumes which rise from the source are directed into the suction plenum by the curtain. Air is also pulled into the curtain from both above and below. Since all air flow is inward, into the curtain, a high capture efficiency is achievable with a properly designed and operated curtain.

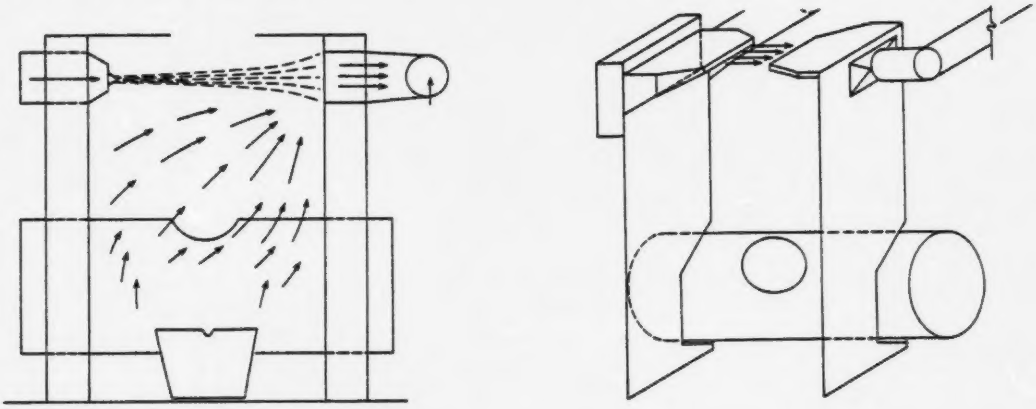

Front View

Perspective View

Figure 1. Air Curtain Operating Concept

TEST PROGRAM

The test program was designed to estimate the effectiveness of capture of the converter fugitives not controlled by the primary hood. The effectiveness of capture was evaluated using three techniques.

- mass balance using sulfur hexafluoride as a tracer
- opacity of emissions escaping through the slot
- observation of visible emissions

The testing was complicated by the fact that the smelter is operated on a Supplementary Control System (SCS) basis. This means that production is curtailed to maintain sulfur dioxide ambient concentrations below that required by local regulations. When production is curtailed, the normal converter operation is discontinued and the hot metal is held without processing to minimize the generation of sulfur dioxide emissions to the atmosphere. Because of curtailment, it was not possible to plan to sample through a complete converter cycle, as it may have been interrupted and put on "hold" at any time. Therefore, the tests were designed to synthesize a converter cycle by appropriately taking composite samples to represent a total cycle. Based on this approach, the test sample may be composed of "pieces" of more than one actual cycle. The test sequence employed is shown in Figure 2. Three complete "composite" cycles had been planned, but because of extensive curtailments, only two were completed.

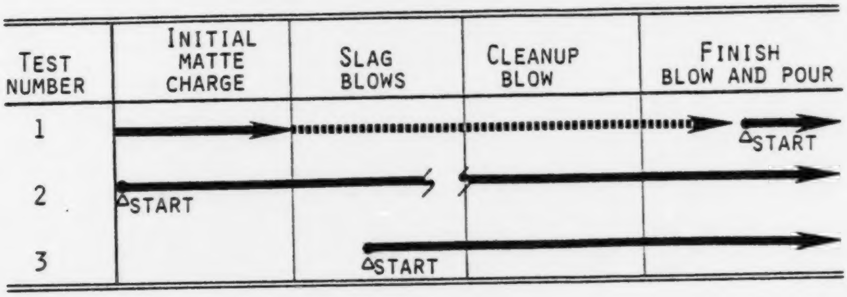
TEST NUMBER
INITIAL MATTE CHARGE
SLAG BLOWS
CLEANUP BLOW
FINISH BLOW AND POUR
1
2
3
START
START
START

Figure 2. Test Sequence

TRACER EXPERIMENTS

Sulfur hexafluoride was injected into various points within the air curtain control volume, defined by the top, sides, and front of the air curtain structure and the converter and primary hood which formed the back of the structure (Figure 3). The tracer experiments were of two types, those in which the tracer was injected into the air curtain volume above the converter (the upper portion of the air curtain control volume and those in which the tracer was injected below the plane of top of the converter and near the front of the air curtain side walls (the lower portion of the air curtain control volume).

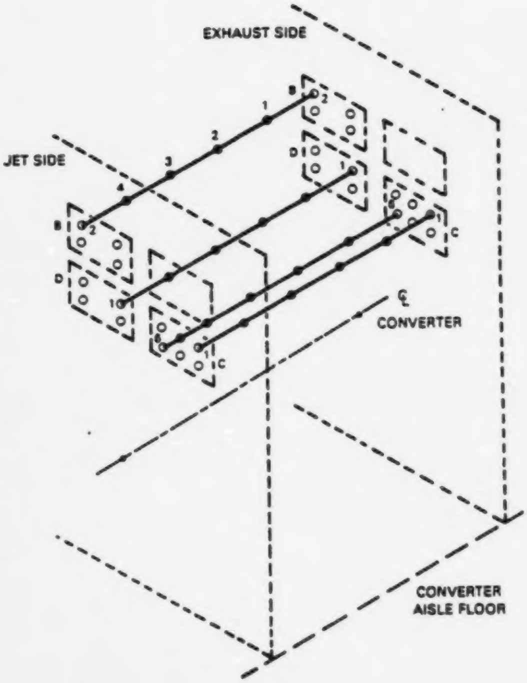
EXHAUST SIDE
JET SIDE
1
2
3
4
B
D
C
℄ CONVERTER
CONVERTER AISLE FLOOR

Figure 3. Tracer Injection Matrix.

The recovery efficiencies measured in the first test (Table 1) for individual tracer releases above the converter varied from 69 to 119 percent, and the overall average efficiency for the 45 tests was 94 percent. The port through which the releases of the tracer were made did not have any effect on the average collection efficiency. The average collection efficiency of all releases made through a given port ranged from 93.0 percent for Port C-6 to 95.4 percent for Port C-1. This difference was not statistically significant. The variability between the average collection efficiency of the replicates made at a given position (between the jet side and the exhaust side) was statistically significant. The greatest difference occurred at Port D-1, where the average collection efficiency ranged from 83.3 to 105.7 percent. The collection efficiencies for Positions 1 and 2 (near the exhaust side) were approximately 96.6 percent and were generally higher than those for Positions 3 and 4 (near the jet side) which were approximately 91.6 percent.

TABLE 1. TRACER COLLECTION EFFICIENCY WITHIN THE AIR CURTAIN CONTROL AREA

	Position				
	Exhaust		Jet		
PORT	1	2	3	4	Average
B-2	97	102	94	97	97.5
B-2	89	95	89	96	92.2
B-2	94	97	79	94	91.0
AVERAGE	93.3	98.0	87.3	85.7	93.6
D-1	91	105	98	91	96.2
D-1	89	119	-	90	99.3
D-1	93	93	98	69	88.2
AVERAGE	91.0	105.7	98.0	83.3	94.2
C-6	95	94	-	93	94.0
C-6	101	93	96	81	92.8
C-6	94	97	89	90	92.5
AVERAGE	96.7	94.7	92.5	88.0	93.0
C-1	97	93	-	94	94.7
C-1	95	105	95	91	96.5
C-1	97	95	97	90	94.8
AVERAGE	96.3	97.7	96.0	91.7	95.4
OVERALL AVERAGE					94.0

For the second test (Table 2), a replicate of the first, the overall average tracer recovery efficiency was 96.0 percent. Again, the port through which the tracer releases were made had no effect on the average tracer recovery efficiency of the air curtain hood. The average efficiency varied from 94.5 percent at Port C-6 to 98.0 percent at Port B-2 (Figure 4). For positions within the matrix, the average collection efficiency varied from 80.7 percent at Position 4, Port D-1, to 106 percent at Position 2, Port D-1. As in the first test series, the recovery efficiencies were consistently higher for positions near the exhaust side than for positions near the jet side (Figure 5).

TABLE 2. TRACER COLLECTION EFFICIENCY WITHIN THE CONTROL AREA

PORT	POSITION				AVERAGE
	Exhaust		Jet		
	1	2	3	4	
B-2	103	99	95	93	97.5
B-2	95	107.5	81	87	92.6
B-2	101	103	119	92	103.8
AVERAGE	99.7	103.2	98.3	90.7	98.0
D-1	106	106	96	65	93.2
D-1	101	111	92	88	98.0
D-1	106	97	89	89	98.2
AVERAGE	104.3	106.0	95.0	80.7	96.5
C-6	104	102	101	81	97.0
C-6	93	106.5	95	79	93.4
C-6	96	99	93	95	93.2
AVERAGE	97.7	102.5	96.3	81.7	94.5
C-1	105	103	99	93	100.0
C-1	95	96	84	91	91.5
C-1	99	103	104	69	93.8
AVERAGE	99.7	100.7	95.7	84.3	95.1
OVERALL AVERAGE					96.0

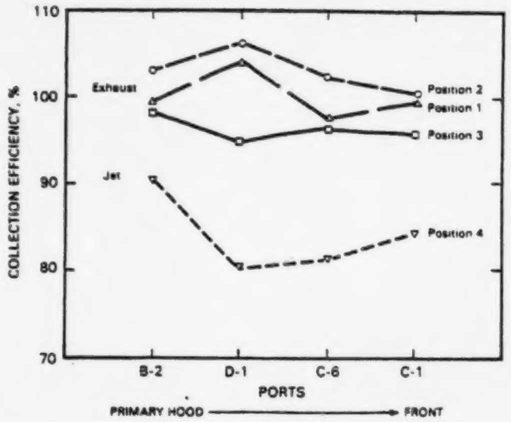

Figure 4. Comparison of Collection Efficiency and Matrix Point Injection.

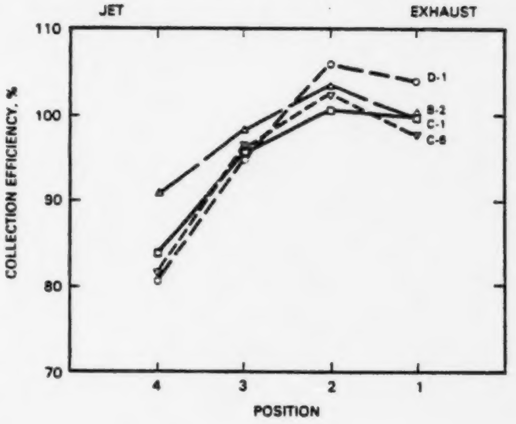

Figure 5. Comparison of Collection Efficiency and Matrix Injection Point.

The tracer recovery efficiencies for the various converter operating modes were also measured. The results are presented in Table 3, with the data for Test 1 given in the first line for each entry and those for test 2 in the second. With the exception of cold additions, the average recovery efficiencies were not affected by the operating mode of the converter; averages varied from 92.8 during blowing to 95.0 during slag skimming. Two special tests were conducted during slag skimming where the tracer was injected just above the top of the converter at the front of the jet side baffle wall. The average collection efficiency measured was 94.5 percent, which is comparable to that reported for the releases on the three-dimensional matrix in the space above the converter.

TABLE 3. SUMMARY OF TRACER CAPTURE EFFICIENCY WITHIN AIR CURTAIN CONTROL AREA

CONVERTER CYCLE	BLOW	SLAG SKIM	MATTE CHARGE	COLD ADD	IDLE	COPPER POUR
Number of Injections	19 27	9 7	7 6	3 3	7 4	- 4
Mean, %	92.8 96.7	95.0 94.3	93.1 94.2	102.0 96.7	93.4 100.0	- 88.5
Standard Deviation, %	8.47 10.06	4.87 8.08	3.13 9.54	14.7 20.4	3.6 11.4	- 9.6

For the third experiment, several series of tests involving the release of tracer into the lower portion of the air curtain control volume near the front of the air curtain side walls were conducted (Table 4). The first series (three tests) involved the release of the tracer material at a location slightly above the ladle near the jet side of the hood. The average recovery efficiency was 64.3 percent.

For the second series (6 tests), the tracer was released at a location slightly above the ladle and very close to the wall on the exhaust side. During slag skimming the recovery efficiency measured (four tests) ranged from 52 to 79 percent for an average of 63.5 percent. During matte charging the average recovery was 68.5 percent.

In the third series, the tracer material was also released at a location slightly above the ladle, but farther from the wall on the exhaust side. The collection efficiency measured for the seven tests ranged from 30 to 89 percent, with an overall average of 58.7 percent. It should be noted that the samples for tests conducted during operation in the blowing mode yielded the lowest recovery efficiencies, i.e.; 32, 33, and 33 percent. These values would be expected because the hooding system was in the low flow mode and there was no thermal lift to enhance the collection efficiency.

In the final series of tests, the tracer was released very near the ladle on the exhaust side of the hooding system. Recovery efficiencies were determined for 53 releases of the tracer material and ranged from 27 to 128 percent, with an overall average of 70 percent. Recovery varied from 38 percent for the 6 tests performed during blowing to 84 percent for the 28 tests performed during slag skimming. The difference between average collection efficiencies for the several operating modes is statistically significant.

TABLE 4. SUMMARY OF TRACER CAPTURE EFFICIENCIES SPECIAL TESTS

TEST	NUMBER OF RELEASES	COLLECTION EFFICIENCY, % MEAN	STANDARD DEVIATION	RANGE
Converter Mode				
Blowing	6	33.0	5.0	27-42
Matte Charge	17	61.8	27.6	35-91
Slag Skimming	28	84.0	18.4	52-128
Cold Addition	6	61.5	18.3	49-76
Idle	8	53.8	22.7	30-95
Copper Pour	4	80.8	16.9	61-98

OPACITY MEASUREMENTS

An opacity monitor was mounted on the top of the air curtain below the crane rail in order to obtain information on emissions escaping capture by the air curtain and passing through the slot. A total of 86 discrete observations were made with results ranging from a low of 2% to a high of 54% opacity for the major converter operations (Table 5). During slag and finish blowing, no attenuation of the the monitor's light beam was observed resulting in zero percent opacity. The instrument output range was 0 to 20 milliamps which corresponds to 0 to 98.4% opacity. The relationship of the instrument output to opacity was exponential, with 6 milliamps corresponding to 50% opacity. Therefore emissions during the test program were in the lower end of instrument response. No correlation between opacity and capture effectiveness could be made because of emissions from the front of the air curtain system.

TABLE 5. SUMMARY OF OPACITY OF EMISSIONS ESCAPING AIR CURTAIN

CONVERTER OPERATION	NUMBER OF OPERATIONS OBSERVED	OPACITY, %		
		AVERAGE	LOW	HIGH
COLD ADDITION CHARGE (Reverts and Cold Dope)	14	21	5	54
MATTE CHARGE	25	14	5	34
SCRAP COPPER CHARGE	5	18	9	28
BLISTER COPPER CHARGE (Imperfect Anodes)	4	9	9	9
SLAG SKIMMING	31	18	2	50
BLISTER COPPER POUR	9	9	5	17
TOTAL	86			

VISUAL EMISSIONS

Two observers visually monitored the air curtain capture effectiveness by noting the location, approximate opacity, duration, and significance of visible emissions. Their estimates of capture efficiency were within 5 to 10% with only a few exceptions. Most variability in the estimates occurred for those operations involving rapid evolution of emissions over a short period, such as roll-in, roll-out and pouring. A summary of the average of the observations for the various conventer operating conditions (Table 6) displays these same trends indicated by the tracer experiments and indicates a reasonably effective capture of fugitives.

TABLE 6. SUMMARY OF VISUAL OBSERVATIONS OF CAPTURE EFFICIENCIES

CONVERTER EVENT	Observer No. 1 No. of Events Observed	Observer No. 1 Estimated Hood Capture Efficiency, %	Observer No. 2 No. of Events Observed	Observer No. 2 Estimated Hood Capture Efficiency, %
Roll-In Roll-Out	21	77	20	76
Blow-Hold	14	96	5	90
Matte-Charge	42	94	33	91
Slag Skim	34	78	30	82
Copper Pour	12	92	12	85
Other Additions	42	95	26	85

DISCUSSION OF RESULTS

Visual observation and tracer injection results reveal the importance of the thermal lift phenomenon. It is obvious that only those fumes which are carried upwards and into the path of the air curtain will be captured an carried out through the exhaust duct. The fumes are carried upward by the air flow created by the air curtain and by thermal lift.

Visual observations of hood capture efficiency were made by assessing the overall capture effectiveness while tracer recovery tests only provide information regarding the portion of the control volume into which the tracer is injected. This situation pertains for the following reasons. Because of the narrow converter aisle, the air curtain side walls were not extended sufficiently into the aisle area to completely enclose the ladle within the air curtain control volume during the skimming and pouring operations (Figure 6). When rapid fume evolution occurred,a considerable portion of the fume could escape capture by the air curtain system. Such fume appeared to be escaping from that portion of the ladle which was outside of the air curtain control volume. Tracer recovery tests performed in the upper control area during such an event would not account for this "spillage" and would

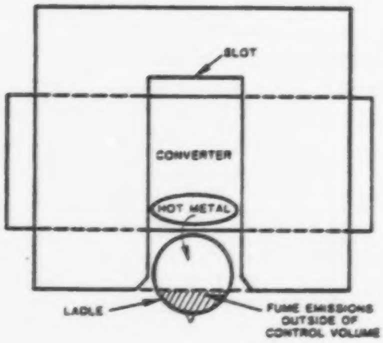

Figure 6. Top View of Air Curtain Hooding System (Primary Hood Omitted)

probably show a greater recovery efficiency than an overall visual assessment. For this reason, it is necessary to use both observation of visible emissions in conjunction with the tracer to quantify capture effectiveness. Visible emissions observation revealed that converter and crane operations introduce significant variablity in estimating overall hood capture efficiency particularly for skimming operations. For example, as visually determined, hood capture effectiveness increased considerably (greater than 90 percent) during skimming operations when the overhead crane operator held the receiving ladle next to the converter while the converter was slowly rotated to the discharge position. In contrast, when the receiving ladle was placed on the ground during skimming operations and the slag discharge rate was rapid, considerable fume spilled into the converter aisle. Converter and overhead crane operating techniques were inconsistent throughout the entire test program.

The third tracer experiment was conducted to characterize hood capture effectiveness in the lower portion of the air curtain control volume. The data clearly show the effects of increased exhaust side air volume and thermal lift from hot gases during converter roll-out modes. Also, the data indicate that determination of tracer recovery from the lower portion of the control volume is heavily dependent upon the relation between injection location and converter operation. Tests performed during the blowing operation, which is conducted with the primary hood closed and little heat escape, ranged from 27 to 42 percent. During charging, the primary hood is raised and a ladle of hot matte or cold scrap is raised above the converter and positioned over the mouth partially blocking it (i.e. as a cork is placed into a bottle). In this operation, the tracer injection probe was below the ladle and near the side of the air curtain enclosure. The tracer recovery measured was 61.8% for charging of matte and 61.5% for cold additions. During slag skimming and copper pouring, it was usual practice to set the ladle on the floor in front of the converter and pour at any convenient rate. Here, the tracer was injected above and to the left of the ladle. Tracer recovery efficiencies of 84 and 81 percent respectively, were measured for converter discharge operations.

CONCLUSIONS

In summary, the visual observation and tracer recovery data indicated that the fugitive emission capture effectiveness of the secondary hood is greater than 90 percent, averaging about 94% overall. The capture effectiveness during converter roll-in and roll-out and slag skimming operations is more variable than other converter modes since fugitive emissions generated during these events are more dependent upon converter and crane operations. It is also evident that capture efficiencies of 90 percent or better are achievable for these events under the proper crane and converter operating conditions to minimize fume "spillage" into the converter aisle.

Thermal lift plays a significant role in increased collection efficiencies for fume generated in the lower portion of the control area. Also, the lower tracer recovery efficiencies for the various converter roll-out modes are indicative of fume "spillage" outside of the control area.

It is believed that no practical correlation can be made between opacities recorded by the observers and the transmissometer. The transmissometer was mounted perpendicular to the longitudinal axis of the slot, whereas the position of the visual observers was such that their view was parallel to the longitudinal axis of ths slot, which resulted in a considerably longer path length through the escaping emission. The apparent opacity increases as the path length through the emissions increases. Also, when positioned in front of the converter, the overhead crane interfered with visual observations above the slot area.

Session 19: FUGITIVE EMISSIONS II

Michael J. Miller, Chairman
Electric Power Research Institute
Palo Alto, CA

TECHNICAL MANUAL ON THE IDENTIFICATION, ASSESSMENT, AND CONTROL OF FUGITIVE EMISSIONS

by: Chatten Cowherd, Jr.
John S. Kinsey
Midwest Research Institute
Kansas City, Missouri 64110

William B. Kuykendal
U.S. Environmental Protection Agency
Research Triangle Park,
North Carolina 27711

ABSTRACT

To assist control agency personnel and industry personnel in evaluating fugitive emission control plans and in developing cost-effective control strategies, the U.S. Environmental Protection Agency is funding the preparation of a technical manual on the identification, assessment, and control of fugitive particulate emissions. This paper summarizes the organizational structure and content of the technical manual. The organizational structure follows the steps to be undertaken in developing a cost-effective control strategy for fugitive particulate emissions. The procedural steps are the same whether the sources of interest are contained within a specific industrial facility or distributed over an air quality control jurisdiction. In line with the results of a survey of 84 potential industrial and regulatory users, the manual will emphasize open dust sources (rather than process sources) and preventive control systems (rather than emission capture/removal systems). This paper also summarizes the quality and extent of published performance data for control systems applicable to open dust sources and process sources. The scheme developed to rate performance data reflects the extent to which a control efficiency value is based on mass emission measurement and reported in enough detail for adequate validation.

This paper has been reviewed in accordance with the U.S. Environmental Protection Agency's peer and administrative review policies and approved for presentation and publication.

INTRODUCTION

Because early control strategies based primarily on the reduction of stack emissions have not achieved desired improvements in particulate air quality, the need to base control strategies in part on the reduction of fugitive emissions has become apparent. Fugitive emissions refer to those air pollutants that enter the atmosphere without first passing through a stack or duct designed to direct or control their flow.

Fugitive particulate emission sources may be separated into two broad categories: process sources and open dust sources. Process sources are those associated with industrial process operations that alter the chemical or physical characteristics of feed materials. Examples would be charging and tapping emissions from metallurgical furnaces and emissions from crushing of mineral aggregate. Such emissions normally occur within buildings and, unless captured, are discharged to the atmosphere through forced or natural draft ventilation systems. However, a process source of fugitive emissions can occur in the open atmosphere (e.g., scrap cutting). Open dust sources are those that entail generation of fugitive emissions of solid particles by the forces of wind or machinery acting on exposed materials. Open dust sources include industrial sources of particulate emissions associated with the open transport, storage, and transfer of raw, intermediate, and waste materials, and nonindustrial sources such as agricultural tilling, unpaved roads and parking lots, and paved streets and highways.

To assist control agency personnel in evaluating fugitive emissions control plans and to assist industry personnel in the development of cost-effective control strategies, the U.S. Environmental Protection Agency is funding the preparation of a technical guidance document on the identification, assessment, and control of fugitive particulate emissions. The document will describe the procedures for developing a cost-effective strategy for control of fugitive particulate emissions within any specific setting. Also, it will provide sources of data or in some cases actual data needed to implement the procedures.

Cost-effectiveness is defined as the annualized cost of control divided by the reduction in total annual particulate emissions, as a result of the fugitive emissions control system being employed. Control costs include the capital, operating, and maintenance costs associated with the control system over its useful life. Alternatively, cost-effectiveness might be expressed as the annualized cost of control divided by improvement in air quality (annual or 24-hr worst case) at a reference receptor point.

USER SURVEY

In November of 1983, an 11-question survey form was distributed to potential industrial and regulatory users for the purpose of identifying user needs and preferences relative to the content and format of the technical guidance document. Survey forms were provided to each member of the program advisory panel, who distributed them to representative users within the respective industry or regulatory agency of that panel member.

Eighty-four responses to the survey were received, consisting of 32 survey forms completed by regulatory personnel and 52 forms completed by industrial users. Those responding to the survey represented a broad cross-section of government and industry users.

With regard to the function(s) which the document should serve, the majority of the users thought that it mainly should be used as a source of data on control techniques, efficiencies, costs, etc. The document should also be a basic reference for developing fugitive emission control strategies.

The users rated the presentation of information on control options and control efficiencies as being most important with cost data also being of considerable interest. The need for data on operation and maintenance costs of fugitive emission control systems was viewed as greater than the need for data on capital equipment costs.

User opinion indicated that the document should include "how to" sections on the selection of control alternatives, estimation of control system performance, and the determination of allowable control trade-offs, with the calculation of control costs and cost-effectiveness also being of interest. Most users responding to the survey thought that any trained technical person should be capable of utilizing the document. Also, there was a clear preference for data to be presented in the form of equations rather than nomographs or tables.

The preponderance of the users indicated that the text of the guidance document should emphasize open dust sources and preventive control systems of demonstrated effectiveness. Users indicated that open dust sources had the largest influence on air quality either at the property line (industrial users) or on an overall basis within their area of jurisdiction (regulatory users).

In summary, open dust sources were viewed by the majority of users, whether industrial or regulatory, as deserving of the greatest emphasis in the proposed technical manual. The most pressing data needs to be addressed by the document appear to focus on the control performance (efficiency) achievable with available control technology.

LITERATURE REVIEW

A literature review was conducted to define the quality and extent of performance data for fugitive particulate emission control systems. For industrial emission sources, the review focused on surface mining and those processing industries that are generally recognized as accounting for the most significant sources of fugitive particulate emissions, as listed below:

Iron and steel plants
Lime manufacturing
Coal-fired power plants
Ferrous foundries
Primary aluminum production
Primary copper smelters
Primary lead smelters
Primary zinc production
Secondary aluminum smelters
Secondary lead smelters
Secondary zinc production
Secondary copper, brass/bronze production
Cement manufacturing
Ferroalloy production
Rock products
Asphalt concrete plants
Grain storage and processing

For nonindustrial sources, the review focused on unpaved roads, paved roads, and construction operations. Agricultural operations were excluded from the review.

The literature review was begun by a survey of technical documents relating to fugitive particulate emissions and controls. These documents included: final reports on original research investigations of fugitive emission controls; proceedings of air pollution technical conferences; and compendia of performance and cost data on fugitive particulate emission controls. Many of these documents were published either by the U.S. Environmental Protection Agency or U.S. Bureau of Mines. References 1-3 are examples of compendia documents surveyed.

The following sections summarize the quality and extent of performance data for fugitive particulate emission controls, as determined from the literature review. This discussion is broken down by the type of control (preventive measures, capture/removal methods) as defined in each subsection. A summary of published control performance data, delineated by test method, is presented in Table 1. Factors considered in evaluating the quality of performance data are described later in this paper.

TABLE 1. SUMMARY OF AVAILABLE TEST DATA FOR FUGITIVE PARTICULATE EMISSION CONTROL[a]

Type of fugitive emission control technique	Type of fugitive emission source	No. of Valid Tests Reported by Measurement Method						No. of test reports[d]
		Exposure profiling	Upwind/ downwind	Wind tunnel	Tracer method[b]	Per- sonnel sampling	Vicinity sampling[c]	
Preventive measures:								
Wet suppression (water)	Materials transfer					31		3
	Aggregate crushing				37			2
	Unpaved roads	14						2
Wet suppression (surfactant or foam)	Materials transfer					57		2
	Aggregate crushing					1		1
Surface stabilization (chemical)	Unpaved roads	141	68					7
	Storage piles			22				2
Surface cleaning	Paved roads	10						1
Wind screens	Erodible surfaces		12					2
Capture/removal methods:								
Capture/collection systems	Metallurgical processes				6			1
	Banbury mixer				3			1
Plume aftertreatment (charged fog)	Materials transfer		6			32	310	4
	Cotton gin/press						22	1
	Coke screen						52	1
	Torch - cutting						132	1

---

[a] Based on literature search conducted during the study.
[b] Control efficiency determined through the use of a tracer.
[c] Samples collected near or immediately downwind of source with no ambient background determined.
[d] Number of original test reports containing control efficiency data.

PREVENTIVE MEASURES

Preventive measures for the control of fugitive particulate emissions include those measures which eliminate or substantially reduce the injection of particles into the surrounding environment. Preventive measures are independent of whether the particulate is emitted directly into the ambient air (as is the case with open dust sources) or into the interior of a building, eventually reaching the atmosphere through various openings in the structure (e.g., roof monitors). The main types of preventive measures include: enclosure of process equipment/material flows but without evacuation; application of dust suppressants to materials prior to or during handling; stabilization of exposed materials (e.g., storage piles, unpaved roads); cleaning of paved roads; and wind screens.

The two methods for preventing emissions from process sources are passive enclosures (i.e., enclosures without ventilation) and wet suppression. Wet suppression encompasses the use of both water sprays and foams. It was found in the literature review that only a few of the published values of control efficiency for either preventive method are based on mass emissions data. In several tests of wet suppression systems, the basis for the control efficiency value was the reduction of respirable dust in the vicinity of the operation. Estimated control efficiency values have been developed from visible emissions (VE) data and engineering judgement.

Besides passive enclosures, the major preventive control methods for open sources include wet suppression, surface stabilization (chemical or physical) of unpaved roads and storage piles, and cleaning of paved roads. It is important to note that the latter two methods entail periodic rather than continuous control application.

The control of dust emissions from unpaved roads has received the widest attention in the literature. Exposure profiling and upwind/downwind sampling have been used to measure control efficiencies for watering and for a range of chemicals which bind the surface material or increase its capacity for moisture retention. Most of these studies have been performed on roads in iron and steel plants or surface coal mines. Because of differences in the dust suppressants, application parameters, and traffic conditions from one study site to another, the composite set of published control efficiency values for unpaved roads should be applicable to a wide range of source and control conditions.

In contrast to controls for unpaved roads, there are very few published values for control measures applicable to paved roads. A limited number of exposure profiling tests have been performed to determine the control efficiency achieved by vacuum sweeping, water flushing, and water flushing followed by broom sweeping of steel plant paved roads. The efficiency of an improved vacuum sweeper has been measured indirectly by quantifying the reduction in surface loading on two city streets.

To test the effectiveness of controls for wind erosion of storage piles and tailings piles, wind tunnel measurements have been performed. Although most of this work has been carried out in laboratory wind tunnels, portable wind tunnels have been used in the field on storage piles and tailings piles. A limited amount of upwind/downwind testing has also been performed to measure the effectiveness of wind screens.

CAPTURE/REMOVAL METHODS

Capture/removal methods for the control of fugitive particulate emissions include those methods which capture and remove the particles after they have become airborne. Again, this classification is irrespective of whether such emissions are generated inside or outside of a building. The major types of capture/removal processes include capture and collection systems and plume aftertreatment.

Capture and collection systems have three primary components: (a) a hood or enclosure to capture emissions that escape from the process; (b) a dust collector that separates entrained particulate from the captured gas stream; and (c) a ducting or ventilation system to transport the gas stream from the hood or enclosure to the air pollution control device.

For several industrial categories, information is available on the application of canopy hood/enclosure capture systems to control fugitive emissions. However, minimal quantitative data (based on mass flow measurements) are available on capture system efficiency, which is critical to the determination of overall control efficiency, as illustrated in Figure 1.

Typically, available mass data are limited to captured emissions (measured at the collector inlet) and collector outlet emissions. These mass emissions data provide information sufficient to evaluate collection device efficiency and to permit comparison of different types of collectors. However, these data do not provide adequate information for evaluating overall control efficiency.

Because capture efficiency is the most critical factor in the control of process fugitive emissions by capture/collection systems, this lack of data poses a significant problem. With the data presently available, it is necessary to rely on one of two methods to evaluate capture efficiency: (a) observation of visible emissions; or (b) calculation of mass emissions reduction from an estimate of the uncontrolled emission rate (i.e., emission factor) and the measurement of captured emissions. The evaluation of visible emissions escaping capture often has been used to estimate control system capture efficiency in conjunction with EPA studies in support of New Source Performance Standards.

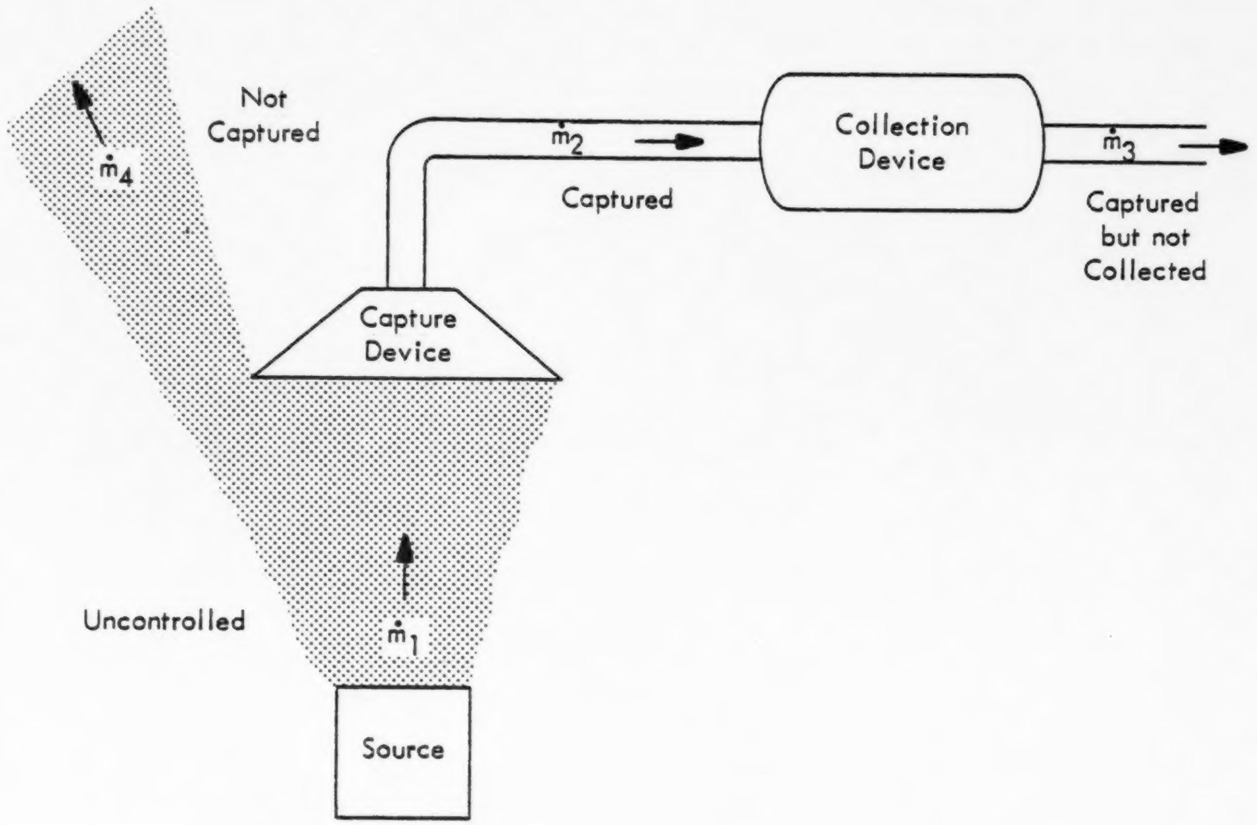
Not Captured
$\dot{m}_4$
$\dot{m}_2$
Captured
Collection Device
$\dot{m}_3$
Captured but not Collected
Capture Device
Uncontrolled
$\dot{m}_1$
Source

$$\text{Control Efficiency (\%)} = \frac{\dot{m}_1 - (\dot{m}_3 + \dot{m}_4)}{\dot{m}_1} \times 100$$

$$\text{where} \quad \dot{m}_1 = \dot{m}_2 + \dot{m}_4$$

Figure 1 - Emissions quantification requirements for performance evaluation of capture/collection system.

Plume aftertreatment refers to the injection of fine water droplets into a dust plume to capture and agglomerate the suspended particles by impaction and/or electrostatic attraction such that gravitational settling can occur. Plume aftertreatment systems can use water sprays with or without the addition of a surfactant as well as with or without the application of an electrostatic charge (charged fog).

A significant amount of research has been conducted by the U.S. Bureau of Mines (BuM) on plume aftertreatment systems used to control respirable dust (particles < 10 μm) in underground mining. A number of studies have also been conducted under the sponsorship of the EPA relative to the use of charged fog for the control of fugitive dust emissions.

QUALITY RATING SCHEME FOR CONTROL EFFICIENCY VALUES

The proposed quality rating scheme for control efficiency values is similar to the A through E rating model developed by EPA for AP-42 emission factors.[4] The scheme entails the rating of test data quality followed by the rating of the adequacy of the data relative to the characterization of uncontrolled and controlled emissions.

To be assigned an A quality rating, a control efficiency value must be based on mass emission tests performed by a sound methodology and reported in enough detail for adequate validation. In addition, enough tests must be performed at appropriate sampling points to quantify the average uncontrolled and controlled mass emission rates for the specific source/control combination in question. Finally, values for the parameters needed to characterize the source operation and the control system must be reported. At the other extreme, a control efficiency value based only on estimation is assigned an E rating.

After the test data supporting emission rate values are evaluated, the adequacy of the testing strategy in support of control efficiency determination must be assessed. If the test data quantifying uncontrolled and controlled emission rates are rated equally, then the resulting control efficiency value is rated the same as the test data. Otherwise, the control efficiency value is rated equal to the less reliable of the controlled and the uncontrolled emission test data.

In the case of a capture/collection system applied to a process source of fugitive emissions, the controlled emissions are made of: (a) that portion of the uncontrolled emissions which are not captured, plus (b) that portion of the uncontrolled emissions which are captured but not collected. This was illustrated in Figure 1 for a canopy hood. Frequently testing is performed at the inlet and outlet of the collection device, but there is insufficient information to determine the overall control efficiency.

For preventive control measures and plume aftertreatment, either of two study designs may be used to determine the control efficiency. A

Type 1 design entails the measurement of source emissions with and without the application of control. In a Type 2 design, emissions from identical sources are measured, one with control and the other without control. It must be shown that the two sources are identical in terms of their uncontrolled emissions.

The question of the representativeness of the source operation and control system being tested is germane only if a widely applicable control efficiency value is being sought. In such a case, the value should be based on tests of several source/control facilities of the same type which typify a particular industry. However, unless the variability of the determined control efficiency values from one facility to another is small, it is preferable to list each value separately with the corresponding source/control parameters. This opens the possibility of developing a statistical performance model which mathematically relates the observed variance in control efficiency to the variances in the source/control parameters.

CONTROL COST-EFFECTIVENESS ANALYSES

When evaluating a particular control strategy for fugitive particulate emissions, analysis of the costs over the useful life of the mechanical equipment is important. The most informative method for comparing cost data is on a cost-effectiveness basis. Cost-effectiveness in air pollution control is defined as dollars expended per mass of emissions reduced or:

$$CE = \frac{D}{ER}$$

where: CE = cost-effectiveness (\$/mass of emissions reduced)

D = control technique cost (\$/year)

ER = emissions reduction (mass of emissions reduced/year)

The cost of implementing a particular control technique includes several components shown graphically in Figure 2. Purchase and installation costs must include freight, tax, and borrowed money. The operation and maintenance costs should reflect increasing frequency of repair as the equipment ages along with increased costs due to inflation for parts, energy, and labor. Costs recovered from tax credits should also be considered as income.

The slopes of the lines in Figure 2 have little significance except to show an increasing or decreasing cost trend over time. The slope of the tax deduction for loan interest assumes the equipment was funded by a loan to be repaid on an installment basis beginning at the time the equipment was purchased. The equipment could have been funded by a bond program with

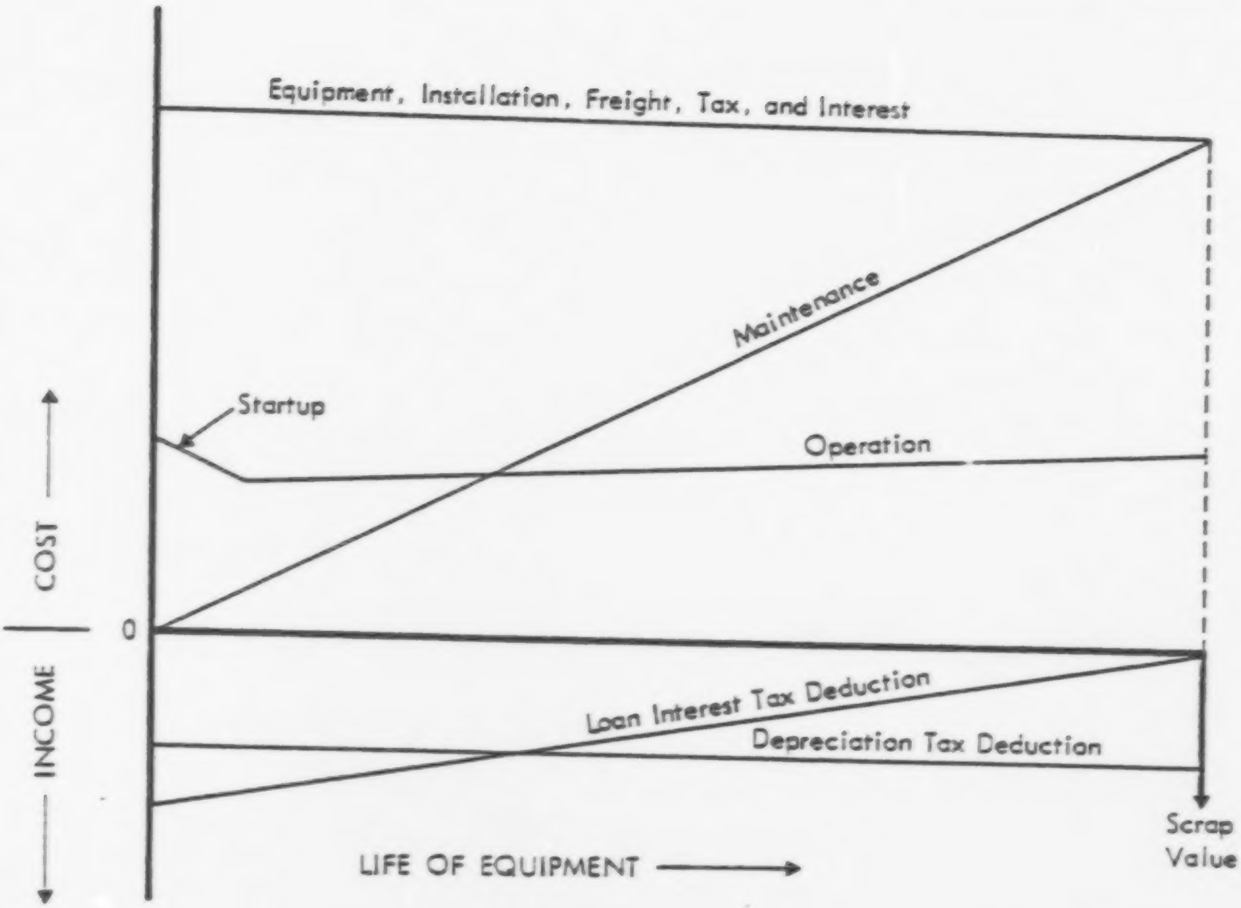

Figure 2 - Graphical presentation of fugitive emission control costs[5].

bonds maturing at different times causing the interest paid to increase, remain constant, or decrease with time in a continuous or step fashion.

Cost-effectiveness also includes the emissions reduction achieved by the control method selected. This is assumed to be constant except in the case of various types of control measures for open dust sources which require repeated application. In this instance, the emissions reduction of a specific control technique decays with time until the technique finally yields no reduction over the uncontrolled state. This can be defined as the life of the control technique, which should not be confused with the lifetime of the control equipment.

For example, the determination of optimum use of vacuuming of a particular paved road might include the following rationale. The efficiency of vacuuming decays from the initial value immediately after cleaning to zero as the surface dust loading builds up to its uncontrolled (equilibrium) value. Although the highest control efficiency would be achieved by continuous use of the available vacuum trucks, operating costs would be at a maximum. If the decay of control efficiency to zero took 3 days, a single vacuuming of the road each day would produce about two-thirds of the maximum emission reduction at a fraction of the cost.

In the overall selection process, each candidate control measure should be analyzed to determine those operating parameters which correspond to its optimum cost-effectiveness for the particular source being considered. Finally, the control measure selected for implementation should be the one with the most favorable optimized cost-effectiveness.

ORGANIZATION OF TECHNICAL DOCUMENT

The proposed organization of the technical document follows the steps to be undertaken in developing a cost-effective control strategy for fugitive particulate emissions. Whether the sources of interest are contained within a specific industrial facility or distributed over an air quality control jurisdiction, the procedure is the same.

In line with the results of the user survey, the organization of the technical document (i.e., chapter designations) reflects an emphasis on applicable control technology and control system performance. Also greater emphasis in terms of chapter length will be placed on controls for open dust sources rather than process sources. This will, in fact, be consistent with the larger body of available data on the performance of open dust source controls (focusing on controls applicable to unpaved roads).

The chapter content of the technical document is summarized as follows:

- Chapter 1 (Introduction) will present background information underlying the need for the document, followed by statements of the purpose and scope of the document.

- Chapter 2 (Source Classification and Identification) will define terms used to identify sources of fugitive particulate emissions, followed by descriptions of generic source categories, and finally a matrix classifying specific sources by generic category within each major industry.

- Chapter 3 (Preparation of an Emissions Inventory) will present a review of the standard procedures used to develop an emissions inventory, except that the discussion on evaluation of control performance will contain a new, more definitive quality rating scheme to be applied in Chapters 5 and 6.

- Chapter 4 (Identification of Control Alternatives) will identify control alternatives by generic category, ending with a matrix of feasible alternatives for specific sources within each major industry.

- Chapter 5 (Estimation of Control System Performance--Open Sources) will document and rate published performance data on open source controls, identifying the parameters which affect control performance. This will be followed by a compilation of performance data for control alternatives applicable to each generic source category.

- Chapter 6 (Estimation of Control System Performance--Process Sources) will document and rate published performance data on process source controls, identifying the parameters which affect control performance. This will be followed by a compilation of performance data for control alternatives applicable to each generic source category.

- Chapter 7 (Estimation of Control Costs and Determination of Control Cost-Effectiveness) will describe procedures for estimation of capital, operating, and maintenance costs and the methodology for calculating cost-effectiveness. This will be followed by examples for representative controls of open dust sources and process sources.

- Chapter 8 (Estimation of Air Quality Impact/Improvement) will describe the standard procedures for predicting the improvement in air quality resulting from the implementation of specific controls.

- Chapter 9 (Review of Overall Methodology and Procedures) will review the procedures described in Chapters 2 through 8.

Although the presentation of control system performance and cost data in equation form was a clear user preference, this will be possible only to the extent that reliable performance and cost models have been developed. Such is more likely to be the case for cost estimation as opposed to performance estimation. While emission factor models (i.e., predictive equations) have been developed for uncontrolled open dust sources, the approach of defining empirical relationships between control efficiency and source/control system parameters has not been widely pursued because of inadequacies in the available data.

In Chapters 5 and 6, the following protocol will be used for presenting published control efficiency values (in tabular form):

1. For a given combination of emission source and control system, each control efficiency value will be presented with a reliability rating (A through E) based on the degree to which the value was determined from a sound, adequately documented testing program.

2. To properly define the representativeness (applicability) of a control efficiency value, the distinguishing source emission and control system parameters will be specified with the efficiency value. The reader will be cautioned that the reliability rating must be reduced if the control efficiency value is applied to a source/control combination in the same category but with one or more parameters which differ significantly from those specified. It is possible that more than one control efficiency value may be presented for the same generic source/control combination if the specified source/control parameters are not equivalent for the available efficiency values.

3. Each control efficiency value will be referenced to the original source of the information, whether test data or rationale for an estimate. This will eliminate the confusion which has resulted from the referencing of more recent documents which may (or may not) reference the original source of the control efficiency value. As a general rule, no value will be listed which cannot be traced to an original reference document which is accessible to the public.

Statements similar to the above apply to the presentation of control system cost data. However, as stated earlier, it is much more likely that cost estimating techniques can be modeled; i.e., expressed in the form of mathematical equations. In fact, it is anticipated that some of these relationships may be broadly applicable within a generic source/control combination. Nevertheless, such relationships will always call for geographic-specific rates; e.g., the cost of labor and energy.

ACKNOWLEDGEMENT

The work upon which this paper is based was performed pursuant to EPA Contract No. 68-02-3922. William B. Kuykendal and Dale L. Harmon have served as EPA project officers for this study.

REFERENCES

1. PEDCo Environmental. Technical guidance for control of industrial process fugitive particulate emissions. EPA-450/3-77-010 (NTIS PB272288). U.S. EPA, Research Triangle Park, NC, March 1977.

2. Reasonably available control measures for fugitive dust sources. Ohio EPA, Columbus, OH, September 1980.

3. Currier, E. L. and Neal, B. D. Fugitive emissions from coal-fired power plants. CS-3455, Project 1402-19. Electric Power Research Institute, Palo Alto, CA, June 1984.

4. Technical procedures for developing AP-42 emission factors and preparing AP-42 sections. U.S. EPA, OAQPS/Air Management Technology Branch, Research Triangle Park, NC, April 1980.

5. Cuscino, T., Jr., Muleski, G. E., and Cowherd, C., Jr. Iron and steel plant open source fugitive emission evaluation. EPA-600/2-83-110 (NTIS PB84-110568). U.S. EPA, Research Triangle Park, NC, October 1983.

QUANTIFICATION OF ROADWAY FUGITIVE DUST AT A LARGE MIDWESTERN STEEL MILL

by: Keith D. Rosbury
William Kemner
PEDCo Environmental, Inc.
14062 Denver West Parkway
Golden, CO 80401

ABSTRACT

The purpose of this research was to quantify roadway emissions in a major Midwestern steel mill that has over 80 miles of roads within its boundaries. The research took place in two phases. First, a field survey consisting of 515 vehicle counts and 165 roadway silt/surface loading samples was completed. Also, all regular vehicle movements (e.g., transport of tar from the coke plant to the blast furnace, hot roll shipments) were identified by origin, destination, trip path, and vehicle type. These 200 movements were each quantifiably related to a scaling parameter of plant production (e.g., coke production, sinter production) reported in the plant's Daily Report of Operation. The second phase consisted of the design and application of a computer program that assigned the 200 regular vehicle movements for the plant road system. The computer-assigned vehicle trips were calibrated against the 515 vehicle counts taken during the field survey. After calibration, the computer output for each roadway section (approximately 300) listed plant area, road classification, measured silt and surface loading, length, calculated vehicle miles traveled/shift by vehicle type, calculated average emission rate, and calculated emissions/shift. When plant operations change, as reflected in the Daily Report of Operations, all vehicle miles traveled and emission data can be adjusted accordingly.

INTRODUCTION

The quantification of roadway fugitive particulate emissions from industrial plants requires the input of various parameters, one of which is traffic volumes for each street segment. These data are difficult to obtain. For example, a particular Midwestern steel mill contains approximately 80 miles of road in a complicated street network with over 200 intersections, nine gates, and 11 external parking lots. Counting each street segment by vehicle type, weekday, Saturday, Sunday, and three shifts is, for all practical purposes, impossible. A method was needed that would allow the extrapolation of a subset of counts to all roadway segments.

In addition, the steel industry in general is rapidly changing; efforts are constantly being made to optimize production and employment. The Midwestern mill under study is no exception. Several operations have been eliminated or reduced in scope, and corresponding reductions in employment and vehicular traffic have resulted. Because further production changes will occur, the method for quantifying traffic should also permit adjusting traffic levels to changing levels and methods of production.

The method developed to meet these requirements was a computerized program that related all vehicle movements to plant operations reported in the mill's Daily Report of Operations (DRO). This program required the identification of approximately 200 regular truck movements, called vectors (e.g., transporting tar from the coke plant to the blast furnace, moving coal from shaker to storage, hot roll shipments). The vectors were tied to scaling parameters of plant production reported in the DRO, such as coke production, sinter production, ingot production, etc. Each vector was quantifiably related to a scaling parameter by use of a scaling factor. For example, for the vector describing Hot Strip Mill Scale to Blending Area, it was determined that 0.0005 trip/ton of hot strip mill production were made by a rear-dump truck with a 25-ton capacity on weekday second shift.

The computer predicted truck trips by shift and day of the week on each road segment or link by use of the vectors, scaling parameters, and scaling units. These predicted values were compared with 515 actual vehicle counts made during the field survey. The vector analysis was then calibrated to the vehicle counts on a vehicle-specific, link-specific basis.

DATA COLLECTION

PRESURVEY

The presurvey involved gathering information on or for the following subjects.

Vector/Scaling Parameter Analysis

Implementation of the vector/scaling parameter analysis required a detailed knowledge of all plant functions, including their locations and inter-relationships. Extensive interviews were conducted with plant personnel and plant contractors. For many operations, material flow diagrams were developed that identified material movement locations, quantities, truck sizes, and number of trips. Material balances were prepared to verify the reasonableness of certain vector densities or to calculate densities where no data were available. For example, pellet fines from the screening operation were calculated to determine the number of trips for hauling fines to the sinter plant. Many of the haul routes were verified by traffic counts made during the presurvey.

Road Classification

Almost all paved roads in the plant have unpaved shoulders. Surface loading and silt, however, vary widely throughout the plant depending on spillage, type of material being hauled over the road, particle fallout from the air, and wind erosion from adjacent areas. Because their large numbers prevented sampling every individual road link in the plant, a decision was made to classify all roads by type according to paved/unpaved, type of material hauled over the road, adjacent wind erosion, and the amount of surface loading as determined by visual examination (medium, heavy, very heavy). Based on these criteria, 17 paved road and 16 unpaved road types were delineated. All roads in the plant were assigned to one of the 33 categories. Two to 15 road samples were taken at random locations along a portion of the roads in each category, and these measurements were then applied to all roads in that category.

Count Locations

Count locations were determined after driving the plant roads several times, consulting with plant personnel, and examining a map of the plant showing all roads and all building locations by name. Approximately 50 intersections, 6 external gates, and 11 external parking lots were identified as count locations after a review of the locations with the plant personnel.

Vehicle Types

A plant inventory identifying all plant vehicles by type and weight was obtained from plant personnel. These data were supplemented by observations of nonplant vehicles (product haulers, vendors, contractors) traveling within the plant. A preliminary vehicle type list was compiled and reviewed with plant personnel for accuracy.

Miscellaneous Data

A number of additional miscellaneous data items were also collected. These included:

(1) Gate passes showing the origin and destination of vehicles coming into the plant.
(2) Employee travel/month from expense reports.
(3) Vendor passes.

(4) Aerial photographs and numerous maps.
(5) Copies of DRO's.
(6) Employment records.

FIELD SURVEY

Vehicle Counts

The result of the vehicle portion of the presurvey was a facility map marked with coded count locations and a daily schedule of required counts to be taken. Vehicle counts were taken at each coded intersection according to the daily schedule. Counts were also taken during off-shift periods and on weekends. For a given intersection, each road link was numbered from 1 to 6, depending on the number of links. For each counting period at an intersection, a safe location that permitted a good view of each link was selected. From this location, each vehicle crossing the intersection was counted and classified by type and by the origin and destination links used. Twenty different vehicle classifications were used during the counts. Each counting period lasted 30 minutes to 4 hours.

Counts were also taken at six external plant gates and at hourly employee external parking lots. At the external gates, counts were 3 to 4 hours in duration over a shift change. A total of 11 parking lots were counted several times to determine the number of cars actually parking in each lot.

Road Surface Samples

The predictive emission factor equations require data on the dust-emitting aggregate materials being disturbed by the action of wind or machinery. For unpaved roads, the silt content is required. For paved roads, silt content and surface loading data are required. The sampling and analysis procedures used to acquire these data were structured identically as laid out in American Society for Testing and Materials (ASTM) Standards when practicable. When this was not possible, an attempt was made to develop the procedure in a manner consistent with the intent of the majority of pertinent ASTM Standards.

ANALYSIS PROCEDURES

VEHICLES

Extrapolation of Short-Term Counts

When the data from all of the counts had been compiled, the next step was to convert the short-term counts to equivalent counts by shift. Some of the vehicle classifications in the preliminary vehicle list were combined to form 12 new categories, which represent the final vehicle classifications for the remaining analyses. These final classifications are shown in Table 1.

The next step was to compile all of the counts from the field data forms into the new categories by road link. During this process, the individual

TABLE 1. FINAL VEHICLE CLASSIFICATIONS

Vehicle Category	Work Schedule, min/shift 1	2	3	Weight, tons*	Wheels
1. Flatbed-over the road	0	450	120	24.5	18
2. Flatbed-lowboy, coil	400	400	400	57.0	20
3. Scow	400	400	400	25.6	6
4. Trailer-dump	400	400	400	22.5	20
5. Straddle carrier	400	400	400	12.5	4
6. Tanker	0	450	120	25.8	18
7. Service vehicle, 10 to 15 tons	400	400	400	14.3	10
8. Utility	400	400	400	7.6	6
9. Passenger/pickup	420	420	420	2.9	4
10. Bus	180	180	180	8.8	6
11. Miscellaneous (< 5 tons)	400	400	400	2.0	4
12. Miscellaneous (> 5 tons)	400	400	400	15.0	9

*Represents 50/50 percent split of loaded and unloaded vehicles. Vehicle weight data obtained from plant vehicle inventory.

counts for each intersection were further subdivided into weekday, Saturday, and Sunday counts.

The following general equation was used to convert a single short-term count into an equivalent shift count:

$$\begin{array}{c}\text{Equivalent}\\ \text{Shift count}\end{array} = \frac{\text{Short-term count}}{\text{Time of count}} \times \begin{array}{c}\text{Shift work}\\ \text{schedule}\end{array} \qquad \text{(Eq. 1)}$$

For each type of vehicle, a work schedule was defined for each shift, as shown in Table 1. The work schedules had to be assumed for most of the vehicle types; actual schedules were available only in the case of two specific bus routes.

Finally, based on the values in Table 1, the actual vehicle counts, and the time of each count, Equation 1 was applied to the field data for each vehicle category to obtain the equivalent shift count by shift and weekday, Saturday, or Sunday. In general, Equation 1 was applied directly to the short-term counts by vehicle category. When more than one count was taken for a specific shift and day of the week, however, the total vehicle count and total counting time from the multiple counts were calculated for each vehicle category before Equation 1 was applied.

When all the calculations were completed, the counts for each vehicle type were plotted by road link on a separate map. This resulted in 12 separate maps of the facility, one for each vehicle category.

Calibration of Vector/Scaling Parameter Analysis to Vehicle Counts

Truck Traffic--

As mentioned previously, the truck traffic was predicted by a vector/scaling parameter procedure. The scaling parameters used are shown in Table 2. The model-predicted truck traffic from the vector/scaling parameter analysis required calibration to match the ground counts. Discrepancies between the model-predicted values and the counts can be attributed to one or more of the following factors:

(1) Inaccurate scaling factor.
(2) Wrong trip path from origin to destination.
(3) Improper vehicle type in vector.
(4) Errors in vehicle count, consisting of improper extrapolation of ground counts, counts taken when a particular activity was not being performed, and counts taken during atypical operational patterns.

The model-predicted values by vehicle type and shift were plotted on a map along with corresponding expanded ground counts, and the values were compared. When differences were found, the four sources of possible error were examined. This consisted of recontacting various plant personnel to verify scaling factors, trip paths, vehicle operations, and plant operations during the survey period. The calibration was performed iteratively, and a total of three model runs were required to obtain acceptable calibration results.

TABLE 2. SCALING PARAMETER VALUES USED IN ANALYSIS

Production	Scaling parameter value (21 Shifts)
Coke	42,423
Blast furnace 13	55,646
Total raw steel	100,800
Blast furnaces 4 and 6	34,423
Galvanizing lines	4,075
Ingot production	61,050
BOP ingots, cast slabs	41,854
Sintering	44,027
Plate mill	4,715
Bar and structural	2,033
Primary mills	51,365
Hot strip mill	62,685
Hot metal	90,069
Tin cold reduction	7,584
Electro-galvanizing	8,964
Picklers	52,472

Autos, Light-Duty Trucks, and Utility Vehicles--

A significant amount of traffic in the plant throughout the day consists of automobiles and light-duty trucks. This traffic includes supervisory personnel traveling from place to place, maintenance vehicles, construction personnel, nonroutine deliveries, etc. A portion of it involves plant personnel using private automobiles. On almost all individual road links, automobiles and light-duty trucks account for over one-half of the vehicle count. Because the majority of these trips are nonroutine and do not follow regular patterns, a vector/scaling parameter approach was not feasible; the auto, light-duty truck, and utility vehicle traffic was therefore input directly.

Adequate counts were available to assign weekday second-shift values to each link. Although counts were not available for many links on off-shifts, 266 counts were taken during the eight off-shift periods. To calculate auto and light-duty truck traffic for off-shift periods for each of eight areas in the plant (the same areas used for exposed-area sampling), ratios of weekday second-shift traffic to each of the other eight shift periods were calculated. This resulted in eight sets of eight distribution factors to assign auto and light-duty truck traffic.

The same procedure was used to develop an additional eight sets of eight distribution factors for utility vehicles. This was necessary because the counts indicated that the shift distributions of the two vehicle categories were significantly different.

VECTOR/SCALING PARAMETER MODEL DESCRIPTION

As mentioned in the Introduction, the Vector/Scaling Parameter Model was developed for this specific application. The program contains two basic data files, a link data file, and a vector file, which are summarized in Table 3.

TABLE 3. MODEL DATA FILE INDEX

Link data file	Vector data file
Link identifier	Vector number
Area	Description
Category	Origin and destination centroid
Silt, percent	Vehicle type
Surface loading, lb/mile	Scaling parameter and value
Average speed, mph	Scaling factor
I-Factor	Shift allocation factor
Number of lanes	Links used by vector
Link length, miles	
Auto and utility vehicle shift allocation factors	

The conceptual procedure for the model is as follows:

(1) Read link data file.
(2) Print link description.
(3) For link 000/000, identify all vectors using link.
(4) Obtain trips/shift by vehicle type from each vector.
(5) Combine trips from all vectors and print number of vehicles by shift. Sum columns for vehicles/shift.
(6) Multiply number of trips/shift by link length to obtain vehicle miles traveled (VMT)/shift. Print. Multiply weekday values by 250 (10 holidays assumed), and Saturday and Sunday values by 52 to obtain VMT/year. Print.
(7) Calculate emission rate for each vehicle type using vehicle characteristics and unique link characteristics (silt, surface loading, speed, I-Factor). EPA emission factors are used. Print.
(8) Calculate weighted average emission rate. Print.
(9) Multiply average emission rate by VMT/shift to obtain TSP, tons/shift. Print.
(10) Multiply values to obtain total suspended particulates (TSP) in tons/year. Print.

A link summary printout is shown in Figure 1.

CALCULATION OF EMISSIONS

Emissions for vehicular traffic were calculated by using EPA Emission Factors (1). For unpaved roads, the equation used was:

$$E = k(5.9) \quad \frac{s}{12} \quad \frac{S}{30} \left(\frac{W}{3}\right)^{0.7} \left(\frac{w}{4}\right)^{0.5} \frac{d}{365} \qquad \text{(Eq. 2)}$$

where
E = Emissions, lb of $\leq$ 30-micrometer particulate
k = particle size multiplier (dimensionless) = 0.80
s = silt content of road surface material, %
S = mean vehicle speed, mph
W = mean vehicle weight, tons
w = mean number of wheels
d = number of days with less than 0.254 mm (0.01 in.) of rainfall per year = 222

For paved roads the following equation was used:

$$E = k(0.090)\ I \quad \frac{4}{n} \quad \frac{s}{10} \quad \frac{L}{1,000} \left(\frac{W}{3}\right)^{0.7} \qquad \text{(Eq. 3)}$$

where
E = Emissions, lb of $\leq$ 30 micrometer particulate
I = industrial augmentation factor (dimensionless)
n = number of traffic lanes
s = surface material silt content, %
L = surface dust loading, lb/mile
W = average vehicle weight, tons

```
                              *L I N K  S U M M A R Y*

              Node A/Node B : 225/230                          Average speed, mph : 20
              Area : 5                                         I factor : 3.5
              Category : 40                                    Number of lanes : 2
              Silt, % : 7.9                                    Link length, miles : 0.11
              Surface loading, lbs/mile : 2464


                                                        NUMBER OF TRIPS
                              ================================================================================
                                            WEEKDAY                  SATURDAY                  SUNDAY
                              Shift->    1        2        3        1        2        3        1        2        3
                              --------------------------------------------------------------------------------
F.B. OTR                                 0        0        0        0        0        0        0        0        0
F.B.- LB, coil                           0        0        0        0        0        0        0        0        0
Scow                                     4       33        4        4        4        4        4        4        4
Trailer - dump                          15       67       15       15       15       15       15       15       15
Straddle                                 0        0        0        0        0        0        0        0        0
Tanker                                   9        9        9        9        9        9        9        9        9
Service veh., 10-15t                     0        4        0        0        0        0        0        0        0
Utility                                  8      136       57        0       42        0        0        7        7
Passenger / P.U.                        30      412      119       50      202       59       41       32       44
Bus                                     20       20       20        0        0        0        0        0        0
Misc., <5t                               0        0        0        0        0        0        0        0        0
Misc., >5t                               0       15        0        0        0        0        0        0        0

Vehicles / shift                        86      696      224       78      272       87       71       67       79
Vehicles / year                      21500   174000    56000     4056    14144     4524     3692     3484     4108

VMT / shift                           9.46    76.56    24.64     8.58    29.92     9.57     7.81     7.37     8.69
VMT / year                         2365.00 19140.00  6160.00   446.16  1555.84   497.64   406.12   383.24   451.08

Avg. vehicle weight, tons            11.58     7.57     7.26    10.48     5.80     9.69    11.02    12.21    10.80
Avg. vehicle wheels                   9.00     6.41     6.36     8.79     5.68     8.30     9.27     9.79     8.91

Avg. emission rate, lb/vmt            2.54     1.86     1.83     2.20     1.54     2.15     2.41     2.59     2.35
TSP, tons/shift                       0.01     0.07     0.02     0.01     0.02     0.01     0.01     0.01     0.01
TSP, tons/year                        3.00    17.79     5.63     0.51     1.20     0.54     0.49     0.50     0.53
                              ================================================================================
```

Figure 1. Link summary printout.

It should be noted that the paved road emission factor contains no term for dry days (d) as the unpaved road emission factor does. This is arguable. The EPA suggests dry days not be used with paved roads because rainfall increases track-on from shoulders and unpaved roads and thus increases emissions. Conversely, the I-Factor of 1.0 for roads with curbs versus 3.5 for roads with unpaved shoulders already increases emissions by a multiplier of 3.5 times. No field testing has been done to validate or invalidate the use of the dry days term with paved roads.

RESULTS

Paved road emissions for the entire plant for a single weekday, Saturday, and Sunday were calculated to be 50.8, 16.9, and 12.0 tons/day, respectively. Corresponding values for unpaved roads are 8.0, 4.9, and 3.8 tons/day, respectively. Weekday second shift accounted for 68 percent of weekly emissions. The average emission rates for paved and unpaved roads were calculated to be 2.1 and 6.9 lb/VMT. A dust control program incorporating paved road sweeping/flushing, and unpaved road dust suppressants was in place at the plant during the time of the survey.

Comparative EPA-sponsored field testing is limited. In two tests at a steel plant on a paved road without curbs, the average emission rate was 2.1 lb/VMT (2). Uncontrolled emissions from unpaved (crushed-slag) roads were measured in nine tests at an average of 6.8 lb/VMT (3). These values are remarkably close to the values calculated as a result of this study.

Beyond the use of the data for an emissions inventory, the calibrated Vector/Scaling Parameter Model has other potential uses as a planning and estimating tool. First, as production levels change in the plant over time, the DRO values can be input to the model to predict new roadway emission levels for a revised emission inventory. Secondly, the model could be very useful at optimizing emission control expenditures. The emissions by link data very clearly show the major roadway emission locations throughout the plant. Conversely, these data also indicate where control dollars are being spent on roadways with little traffic. By varying control expenditures on specific road segments, the model can predict changing emission levels. Because the data also show emission levels by the vehicle type that may be associated with a specific activity, causes for high surface loadings can sometimes be identified or routes certain vehicle types take can be changed to cleaner roads to reduce emissions. Thus, the calibrated Vector/Scaling Parameter Model is not only useful for producing an initial emission inventory, it can also be used to revise emission inventories in future years and to optimize roadway dust-control expenditures.

Because the work described in this paper was not funded by the U.S. Environmental Protection Agency, the contents do not necessarily reflect the views of the Agency and no official endorsement should be inferred.

REFERENCES

1. U.S. Environmental Protection Agency. Fugitive Dust Emission for AP-42. Prepared for Industrial Environmental Research Laboratory, Research Triangle Park, N.C. 27711. 1982.

2. Energy Impact Associates. A Study of Controlling Fugitive Dust Emissions from Non-Traditional Sources at the United States Steel Corporation Facilities in Allegany County, Pennsylvania. Prepared for U.S. Steel Corporation. 1981.

3. U.S. Environmental Protection Agency. Iron and Steel Plant Open Source Fugitive Dust Evaluation. EPA-600/2-79-103. Prepared by Midwest Research, Kansas City, Missouri. 1979.

EVALUATION OF STREET SWEEPING AS A MEANS OF CONTROLLING URBAN PARTICULATE

by: T. R. Hewitt, P.E.
CRS Sirrine, Inc.
Research Triangle Park, North Carolina

ABSTRACT

Street sweeping using a vacuum street sweeper was found to be a highly effective method of reducing particulate concentrations in two northern U.S. urban locations. The effectiveness of street sweeping was measured by determining the percentage reductions in monitored TSP concentrations. Reductions measured at one location were used to predict reductions at a second location where sweeping was being considered. Monitoring results during the first year of sweeping at the second location showed that sweeping achieved greater reductions than predicted. Average annual TSP concentrations were reduced 15-38% at the two locations.

OVERVIEW

Street sweeping can be an effective method for reducing total suspended particulate (TSP) concentrations in urban areas. How effective sweeping can be is not well documented because little experience and data are available. CRS Sirrine, Inc. conducted an analysis to predict the effectiveness of street sweeping as a means to reduce TSP background levels at a northern U.S. project site where sweeping was being considered. Historical monitoring data from another northern location where sweeping had been instituted were gathered and analyzed. The historical data were used to predict the reductions in TSP background that could be achieved by a street sweeping program at the project site.

A sweeping program was ultimately instituted at the project site based on the predictions made. Monitoring data from the first year of sweeping shows that significant TSP reductions were achieved and that sweeping was at least as effective as predicted.

This paper describes the analytical procedure used to measure and predict the effectiveness of street sweeping, presents the predicted reductions at the project site, and presents the actual results from the first year of the newly instituted sweeping program. This paper demonstrates the effectiveness of street sweeping at two discrete locations where TSP monitoring data is available for periods before and after sweeping was instituted.

BACKGROUND

Many areas with TSP standard attainment problems are urban areas with industrial sources of particulate matter. In developing plans to assure air quality standards are met, we sometimes find that TSP background levels are relatively high and that background consumes 50-75% of the 24-hour air quality standard of 150 μ/m^3. Without some method of reducing the background, the cost for industrial particulate matter sources to meet standards can be astronomical.

CRS Sirrine faced the problem of high background in a populated area where a single existing industrial source was required to demonstrate and assure attainment of air quality standards. High-volume TSP sampler filter pads showed that many of the high readings were caused by mineral particulates suspected to be generated from street traffic. Since the town surrounding the source had no street sweeping program and since the paved streets were often observed to be dusty, a street sweeping program was identified as a potential method of reducing background TSP levels.

Street sweeping is an effective strategy for reducing fugitive dust levels in areas with paved streets. The two most common methods of street sweeping are vacuum sweeping and mechanical sweeping. Vacuum sweepers are clearly superior because a high volume of air flow through the apparatus assures that the dust entrained in the sweeping process is collected. Conversely, mechanical sweepers stir up dust during operation and collect only a portion of the deposited material. Mechanical sweeping sometimes causes increased TSP concentrations during sweeping operations because some deposited particles are entrained by the wind and not collected. Vacuum sweeping was judged to be a a reliable method of removing deposited particulate matter otherwise subject to re-entrainment by wind and traffic action and is the method upon which this analysis is based.

SUMMARY

A statistical analysis of TSP monitoring data in an urban area in the northern U.S. showed that a sweeping program markedly reduced TSP background levels. The annual (geometric) average TSP level was reduced by 15% and the statistically calculated maximum 24-hour average TSP level was reduced by 35%.

Similar reduction percentages were predicted at the project site, also a northern location with high background levels. TSP monitoring results after the first year show annual and 24-hour values were reduced 37% and 53%, respectively. The first year data suggest sweeping at the project site may be even more effective than originally predicted using off-site data.

MEASURING STREET SWEEPING EFFECTIVENESS

Street sweeping effectiveness was measured by determining the percent reduction in TSP background levels achieved by the sweeping program. Reductions in the geometric average of TSP readings were used to measure the annual average TSP background reductions. Reductions in the statistically determined "maximum" TSP values, described below, were used to measure the 24-hour average TSP background reduction. Data were compiled from two samplers located in the business district. Data from March through October for the two years before (1978-1979) and after (1980-1981) the sweeping program began were also subjected to statistical analysis. March through October is the street sweeping season in the northern climate and is also the season when the highest TSP background concentrations are recorded. TSP reductions achieved during the sweeping season are another measure of sweeping effectiveness.

A statistical method of measuring TSP reductions was necessary because each grouping of data sets contained different numbers of values. The following analytical procedures were used to measure effectiveness.

Then, the reduction percentages achieved at the off-site location were simply applied to existing measured background levels at the project site to predict future background levels at the site after instituting a sweeping program.

ANNUAL AVERAGE

FIGURE 1 shows the annual geometric average of all 24-hour TSP readings taken at the two off-site monitors for two years before and two years after sweeping was instituted. The sweeping programs reduced the annual average TSP by 15%. The annual average measurement procedure, using all TSP readings, gives a diluted representation of sweeping effectiveness since sweeping occurred during only seven months of each year. Isolating the sweeping season data gives a better representation of the average reduction.

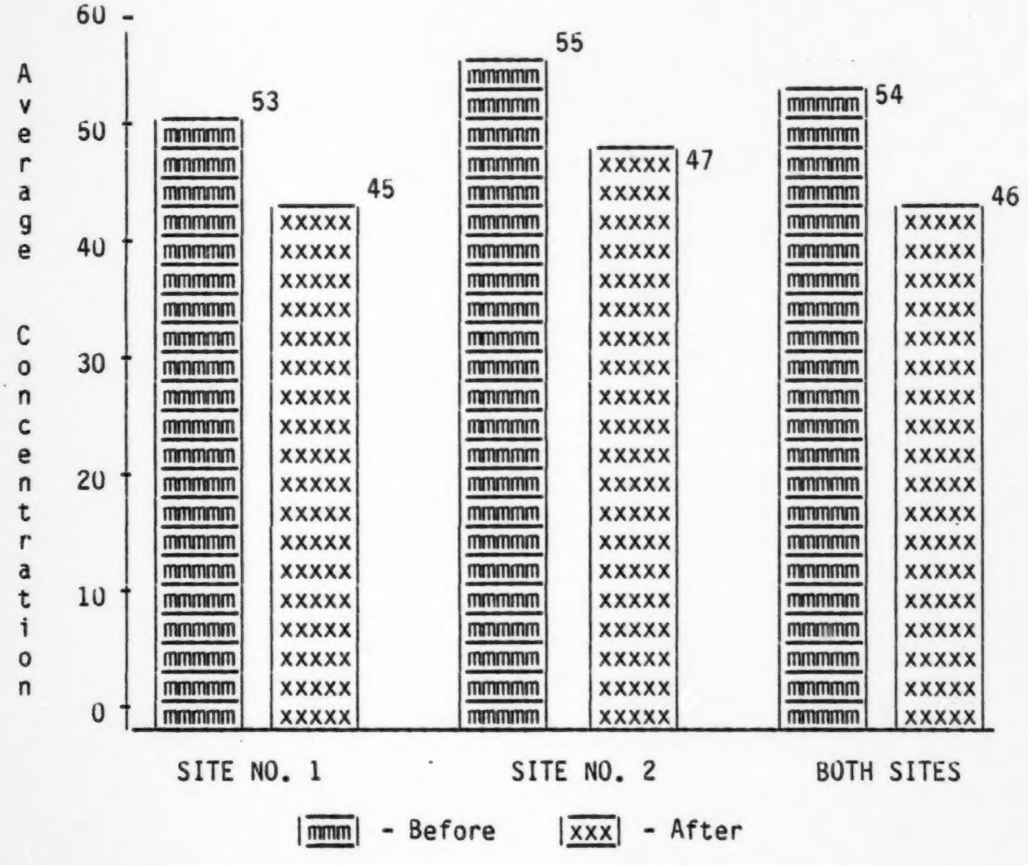

Figure 1. Reduction in Annual Average TSP Readings Before and After Street Sweeping Program Institution

SWEEPING SEASON AVERAGE

The street sweeping season (March-October) average more directly shows how sweeping can reduce the average TSP concentrations. FIGURE 2 shows sweeping season geometric average of TSP readings before and after sweeping was instituted. The average reduction during the sweeping season was 20%.

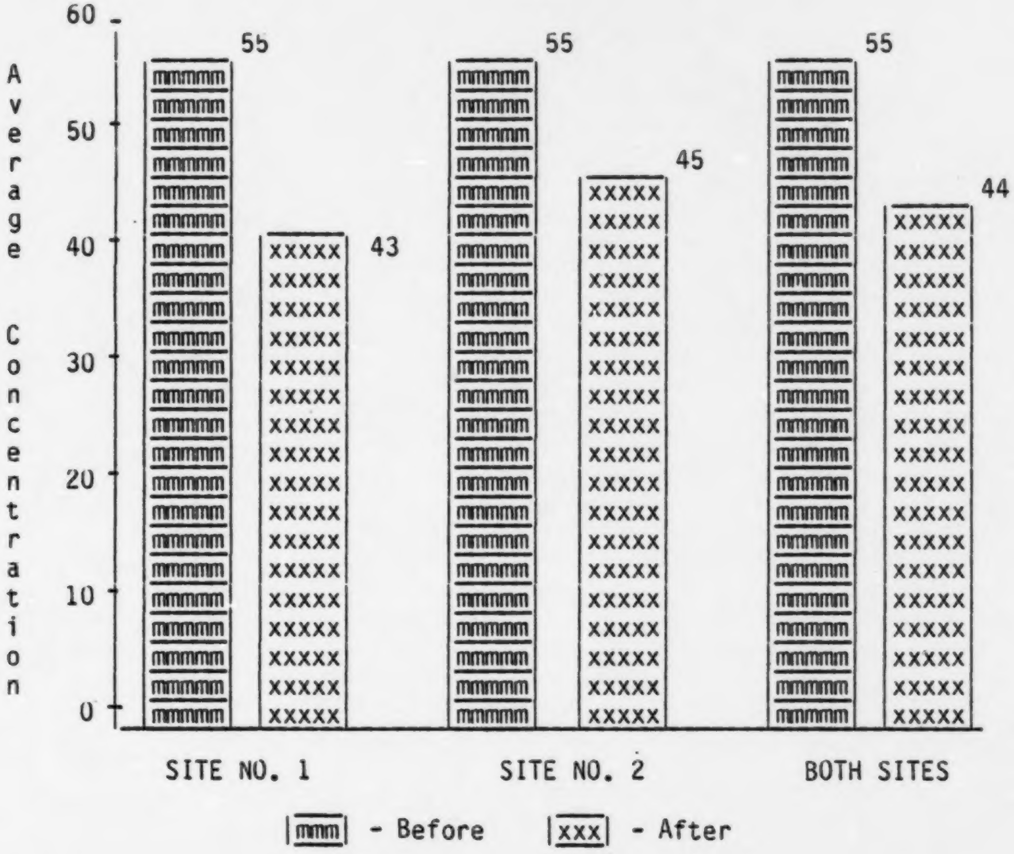

Figure 2. Reduction in Average* TSP Values Before and After Street Sweeping Program Institution Sweeping Season Only

* Geometric Mean

For comparison, FIGURE 3 shows the geometric average of TSP readings for the nonsweeping months at each monitor. Average values were essentially the same at each location before and after sweeping, showing that the year-to-year differential in overall TSP readings is probably not a factor in the analysis.

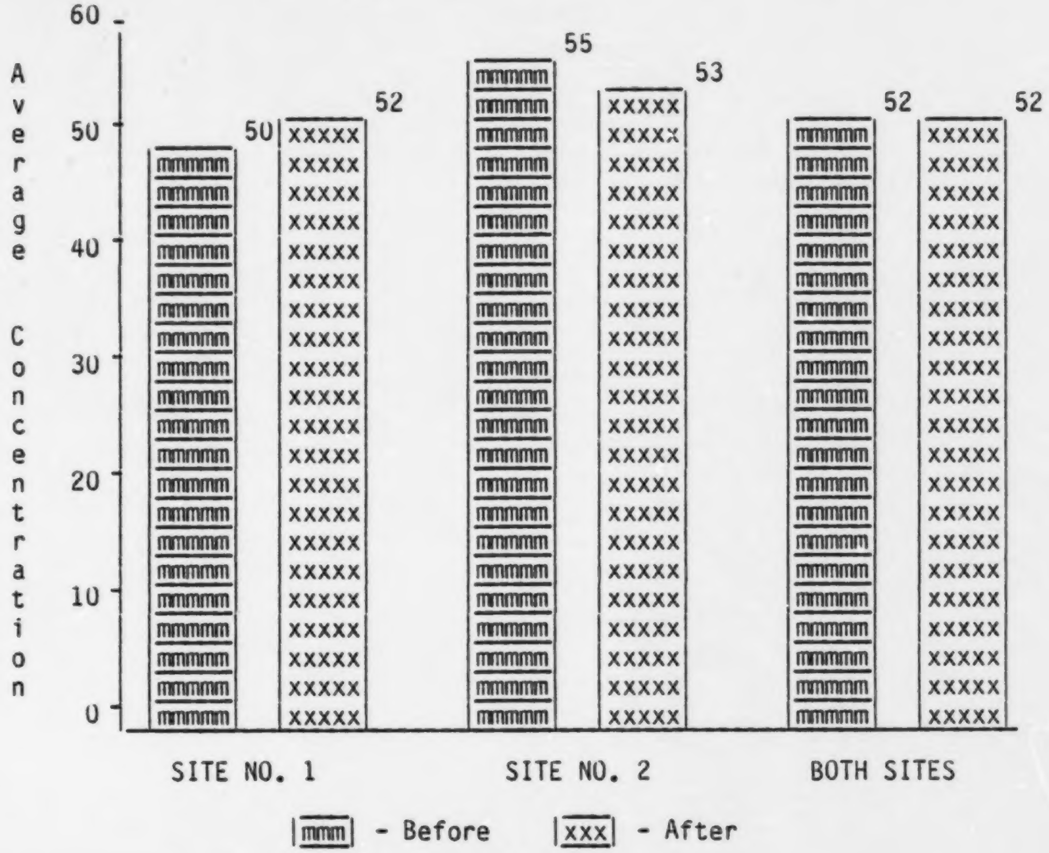

Figure 3. Non-Sweeping Season Average TSP Values

24-HOUR MAXIMUM

While the seasonal and annual average calculations generally show how sweeping can reduce the TSP levels, the most meaningful reduction from a regulatory viewpoint is the reduction in the highest 24-hour background concentrations. Twenty-four-hour background is often defined as the highest or second highest value in the data set. Since background values are determined subjectively on a case-by-case basis, a standard statistical method is used to show that the 35% reduction was achieved in the highest 24-hour values. The statistical analysis used to determine the extent by which 24-hour levels were reduced by sweeping is described below.

The data sets before and after sweeping was instituted each contained readings from two consecutive sweeping seasons. The two data sets are different in size:

Before: 223 values
After: 569 values

Meaningful comparison of the two data sets of different size and different sampling frequency required use of a statistical frequency distribution method.

The goal of the analysis was to determine the reduction in the maximum 24-hour TSP concentration. Since the data are a random sampling of naturally occurring conditions, direct comparison of the maximum recorded values was not meaningful. Therefore, the Log-Pearson III method was used to statistically determine the 99% confidence limit (the TSP concentration that will be be exceeded 99% of the time) for the two sets. The reduction in the 99% limit concentrations between the "after" and "before" periods is a statistical representation of the reduction in the maximum TSP concentration achieved by street sweeping.

The Log-Pearson III method is a gamma transformation of data that produces a probability distribution. The Log-Pearson III method was selected because the natural skewness of a data set is accounted for in the gamma transformation, whereas in a lognormal transformation, skewness is removed. Since this analysis compares two different data sets (the "before" and "after" TSP readings), it was desirable to allow the natural skewness of each data set to remain a factor in the analysis. Sweeping may affect the skewness of monitor data, and skewness could be accounted for in determining the extent of reduction in the maximum value accomplished by sweeping.

The 99% confidence level 24-hour TSP concentration before sweeping was 175 $\mu g/m^3$. After sweeping was instituted, the 99% confidence level value fell to 113 $\mu g/m^3$, a reduction of about 35%. FIGURE 4 shows a graphic distribution of the data for the two periods.

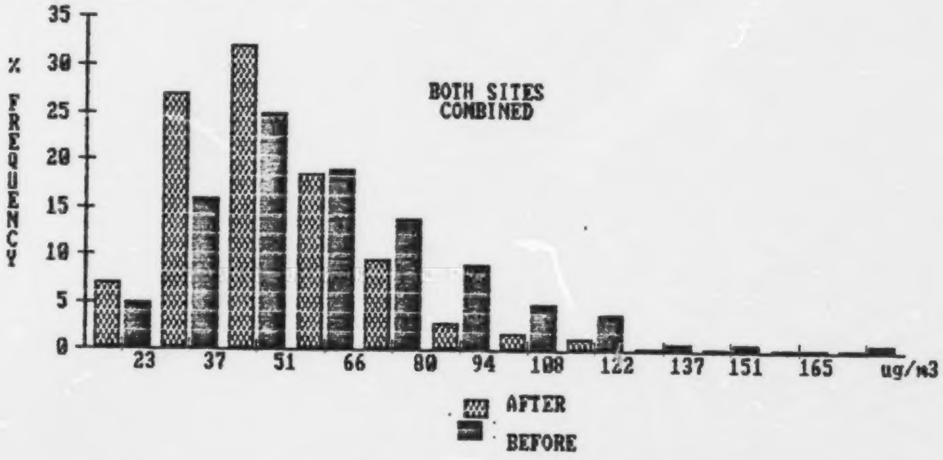

Figure 4. TSP Value Histogram Before & After Sweeping Program Institution

FIGURE 5 shows the relative reductions in maximum values at each location.

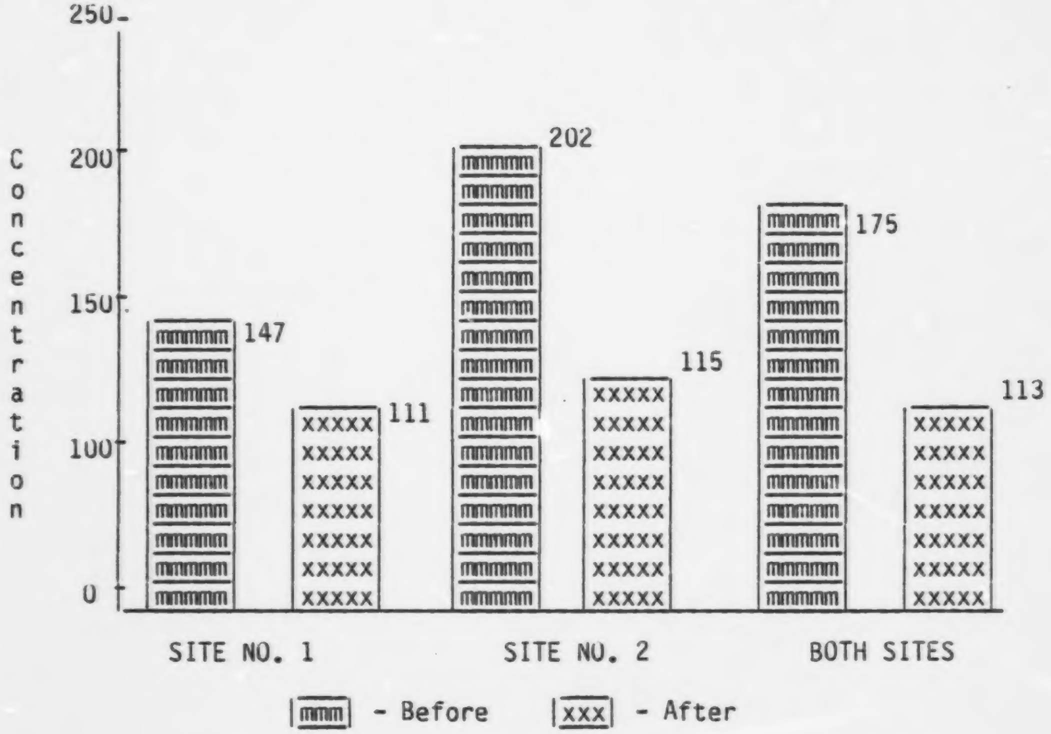

Figure 5. Reduction in Maximum* TSP Values Before and After Street Sweeping Program Institution

* Maximum TSP values are represented by the 99% confidence limit value in the data set.

PREDICTING SWEEPING EFFECTIVENESS

Two years of monitoring data at the project site provided the following measures of TSP background prior to the sweeping program:

24-Hour Average: 106 $\mu g/m^3$

Annual Average: 41 $\mu g/m^3$

The background data had been analyzed to assure that no local point source had contributed to the readings. Petrographic analyses of qualified background hi-vol filter pads showed mineral contributions as high as 85%, strongly suggesting that sweeping would be effective.

The project site location was a small-town business district with conditions similar to those of a sample off-site location where sweeping effectiveness was measured. Since the highest background values were reduced 35% in the sample data, a similar reduction was predicted at the project site.

The predicted 24-hour TSP background after sweeping program institution was calculated to be 69 $\mu g/m^3$, a reduction of 38 $\mu g/m^3$. Annual background was predicted to be reduced 15% to 35 $\mu g/m^3$.

SWEEPING PROGRAM RESULTS

A street sweeping program was instituted at the project site in April 1983. The first year of sweeping is complete and the TSP monitoring data confirms the predictions made in the analysis. The results are shown in Table 1.

TABLE 1. TSP Concentrations At The Project Site

	YEAR BEFORE SWEEPING	YEAR AFTER SWEEPING	REDUCTION
99% Confidence Limit	190	89	53%
Geometric Average	42	26	38%

A full sweeping season has not occurred since implementation; therefore, sweeping season averages for comparison are not available.

The initial results show that actual TSP reductions at the project site exceeded those predicted based on data from the other location. This is not surprising given the large mineral contribution found on the TSP filter pads at the project site. Note, however, that this analysis is for only one year of data before and one year after sweeping, and involved 52 and 38 background data points, respectively. Nonetheless, the effectiveness of vacuum street sweeping is clearly confirmed by the first year results.

CONCLUSIONS

Vacuum street sweeping is an effective, relatively inexpensive method of reducing TSP background levels in areas with paved streets and moderate or heavy traffic. This analysis is an attempt to use after-the-fact data in technology assessment. Therefore, the many variables that could affect the results were not controlled. Applying these results to locations with markedly different characteristics may yield different results. However, given the state-of-the art predictive methods used in estimating fugitive emissions and modeling air quality impacts of fugitive dust sources, the results of this analysis are suitable for use in air quality permitting analyses. Furthermore, a more purely scientific measurement of sweeping effectiveness may not be possible because of the climatic and physical variables that would be encountered from year to year and site to site.

Street sweeping is also an economical method of air quality improvement. With a capital cost of less than $100,000, a sweeper can reduce maximum 24-hour background concentrations substantially, as demonstrated at the two locations analyzed here.

The work described in this paper was not funded by the U.S. Environmental Protection Agency and therefore, the contents do not necessarily reflect the views of the Agency and no official endorsement should be inferred.

WINDBREAK EFFECTIVENESS FOR THE CONTROL OF FUGITIVE-DUST EMISSIONS FROM STORAGE PILES -- A WIND TUNNEL STUDY

by: Barbara J. Billman
Department of Marine, Earth, and Atmospheric Sciences
North Carolina State University
Raleigh, NC 27695-8208

ABSTRACT

Results of wind-tunnel experiments to determine the optimal windbreak porosity, size, and location for storage-pile fugitive-dust emission control are presented. A neutrally stratified, rural atmospheric boundary layer was simulated in the wind tunnel. A cone made of non-erodible material was used to represent an idealized storage pile shape. Straight sections of windbreak material of various combinations of porosity, height, length, and location were placed upwind of the pile. Wind speeds near the pile surface at various locations were measured with thermistors. Wind speed was isolated here as the primary factor affecting particle uptake. The surface averaged wind speed reduction and a windbreak effectiveness factor based on the relationship between the cube of the wind speed and particle uptake are given for each windbreak. All windbreaks used caused wind speed reductions. The largest and most solid windbreak caused the greatest reduction, but similar wind speed reductions were given by several smaller windbreaks. A 50% porous windbreak of height equal to the pile height and length equal to the pile diameter at the base, located one pile height from the base was found to be quite effective in reducing wind speeds over the entire pile surface. Windbreak effectiveness decreased as the angle between the windbreak and the wind direction decreased.

This paper has been reviewed in accordance with the U.S. Environmental Protection Agency's peer and administrative review policies and approved for presentation and publication.

INTRODUCTION

Total suspended particulate (TSP) levels in many regions of the country do not meet the National Ambient Air Quality Standard; fugitive dust from sources such as storage piles, materials transfer points, unpaved roads, and agricultural tilling contribute significantly to TSP levels in some regions.

Many states regulate fugitive dust emissions by forbidding visible fugitive dust beyond the property line surrounding the source; some states have more strict regulations (e.g. 1, 2). Although limiting emissions from a fugitive dust source may not be required, a given industrial facility may use the Environmental Protection Agency (EPA) "bubble" policy to their benefit by controlling fugitive dust rather than the more costly process of upgrading the particulate controls on their stacks to make them more efficient.

Early air pollution control efforts emphasized controlling emissions from stacks rather than fugitive emission sources because the greater bulk of pollutants came from stacks. Now that efficient control methods for particulate matter from stacks are available, control methods for fugitive dust sources are being tested. The EPA Industrial Environmental Research Laboratory (IERL), Particulate Technology Branch, has requested that the EPA Environmental Sciences Research Laboratory (ESRL), Fluid Modeling Section, conduct a wind tunnel study to assess windbreak effectiveness for the control of fugitive dust from storage piles. No effort was made here to simulate fugitive dust emissions. Effects of windbreak porosity, height, length, and location on wind speed at a conical storage pile surface have been determined. The wind speed patterns were analyzed to determine the optimal windbreak parameters and to develop windbreak design guidelines.

BACKGROUND

FUGITIVE DUST EMISSIONS

Mechanical forces by such implements as bulldozers acting on the pile surface and by falling material impacting the surface, freezing and thawing, etc. create particles that may become airborne. Storage-pile fugitive-dust emission rate depends upon the stored material's bulk density, moisture content and particle size distribution, storage pile geometry, wind velocity near the pile surface and other parameters. However, particle uptake does not occur unless the wind speed is greater than a given value, the threshold velocity, which is dependent upon the type of stored material, its moisture content and particle size distribution.

Bagnold (3) suggested that the particle uptake rate is proportional to the cube of the wind speed. Gillette (4), in a wind tunnel test of the effects of sandblasting, wind speed, soil crusting, and soil surface texture on wind erosion, showed that the soil particle flux is proportional to the cube of the friction velocity (u_*), where u_* is determined from the mean velocity profile over a horizontal surface,*

$$u = \frac{u_*}{k} \ln \frac{z}{z_o} , \qquad (1)$$

where u is wind speed at height z, z_o is the surface roughness, and k is von Karman's constant (~0.4).

Blackwood and Wachter (5) suggested that storage pile emission rate, Q (mg/s), may be expressed as

$$Q = (cu^3 \rho_b{}^2 s^{0.345})/(PE)^2, \qquad (2)$$

where u is wind speed (m/s), ρ_b is bulk density (g/cm^3), s is pile surface area (cm^2), PE = Thorntwaite's precipitation-evaporation index (6), and c is a constant.

Wind erosion emissions from active storage piles may also be estimated from the EPA emission factor (7)

$$EF = 1.9 \left(\frac{S}{1.5}\right)\left(\frac{365-p}{235}\right)\left(\frac{f}{15}\right) , \qquad (3)$$

where EF is the TSP emission factor (kg/day/hectare), S is silt content (% of particles < 75 μm in diameter), p is number of days with > 0.25 mm precipitation per year, and f is the percentage of time that the unobstructed wind speed exceeds 5.4 m/s at the mean pile height. This equation is based on sampling emissions from sand and gravel storage piles and hence gives less accurate estimates when applied to other stored materials such as coal, coke, or limestone.

To summarize, particle uptake, hence storage pile emission rate, clearly depends upon the ambient wind speed. Previous studies indicate that uptake is highly sensitive to wind speed, being related to the cube of the speed and the threshold velocity. If the wind speed over a given area of a storage pile is reduced, then fugitive dust emissions from that area will also be reduced. The current study isolates the single variable, wind speed, as the primary factor affecting emission rates and attempts to evaluate the effectiveness of windbreaks in reducing particle uptake. A complete assessment, of course, would require an analysis of all factors, including material type, particle size distribution, moisture content, etc.

FLOW ABOUT WINDBREAKS

Rows of trees or hedges have been used to protect homes and agricultural fields from high winds for many years (e.g. 8). Wind tunnel and field experiments have shown that windbreaks produce large areas of reduced wind speed in their lee.

Figure 1 shows typical streamlines for flow about solid and porous windbreaks. Recirculation regions are evident both upwind and downwind of the solid windbreak; they are regions of low velocity and high turbulence intensity (Figure 1(a)). As porosity (ratio of open to total cross-sectional area) increases, the downwind recirculation region becomes smaller and moves

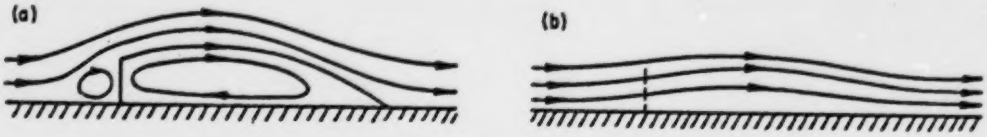

Figure 1. Sketches of streamlines about windbreaks: (a) solid, (b) porous.

downstream (9); the upwind recirculation region is eliminated. Air incident on the porous windbreak flows over and through the windbreak. A region of reduced wind speed is evident in Figure 1(b). Speeds near the surface are typically reduced to half the upstream value for a distance of 10 to 12 windbreak heights downstream of a porous windbreak (10, 11). Greater magnitudes and larger areas of wind speed reduction occur with smoother upstream terrain and lower turbulence in the approach flow (10).

OPTIMAL WINDBREAK SIZE AND POROSITY

Very little information on the use of windbreaks as a storage-pile fugitive-dust control method is contained in the literature. Results of a water flume test indicated that the windbreak height should be at least 1.4H, where H is the pile height (12). However, the author did not state whether more than one windbreak height was used. Details of windbreak length with respect to the pile length and/or width and windbreak position were not given, nor was the atmospheric boundary layer simulated. Cai et al. (13) conducted a wind tunnel study using a two-dimensional windbreak and pile. Combinations of two windbreak heights, two porosities, and two positions were tested. The wind tunnel speed and model pile size were chosen to match the full-scale Reynolds number, one of the wind-tunnel-modeling similarity criteria. The optimal windbreak was shown to be 33% porous, of height 0.5H, placed 3H from the pile base. In this study the atmospheric boundary layer was not simulated, although the flow was turbulent.

TYPICAL STORAGE PILE SHAPES

No two storage piles have the same shape and size, and active piles have constantly changing dimensions. For purposes of the present study, windbreak effects on two typical, but idealized, pile geometries are studied, with the results being generally applicable to many full-scale piles. Results of modeling a conical pile of height 11 m, base diameter 29.2 m, and slope 37° are reported here. Experiments modeling an oval, flat-topped pile of height 11 m, base dimensions 63 m x 78 m, having 37° slopes are in progress and their results will be reported in the future.

WIND TUNNEL MODELING

Simulating the lower part of the atmospheric boundary layer (ABL) under strong winds and determining model size and free-stream wind speed are necessary to assure that wind tunnel results will be valid for the full-scale case under investigation. Simulated atmospheric boundary layers are typically created in wind tunnels through the use of vortex generators (14) or a trip fence and surface roughness elements (e.g. 15).

Model shape must be geometrically similar to that of the prototype. Model size and free-stream wind speed should be determined from matching the model and full-scale Reynolds numbers ($Re=U_0L/\nu$, where U_0 is free-stream speed, L is a characteristic length, and ν is kinematic viscosity). However, with typical scale reductions, the model Re is typically 3 to 4 orders of magnitude less than the full-scale Re. Very high wind speeds in the tunnel are generally required to match full-scale Re, but are often impractical. Fortunately for wind tunnel modeling, "geometrically similar flows are similar at all sufficiently high Reynolds numbers" (16). That is, for Re greater than some minimum value, the turbulent flow structure described in terms of characteristic length and velocity scales is independent of Re. Since atmospheric flows are almost always aerodynamically rough, they are also Re-independent. Model surfaces are generally roughened to make them aerodynamically rough with roughness elements of size greater than approximately $400\nu/U_0$, (17). In practice, a given series of velocity measurements are made for various free-stream speeds. If the data scaled by the free-stream speed from all the data sets coincide, the lowest free-stream wind speed may be used.

The model length scale is in many cases determined by matching the length scale to boundary layer depth (δ) ratio, L/δ, of the model and prototype. If the model height is much less than the boundary layer depth, then the boundary layer depth in the wind tunnel per se is not important. Jensen (18) finds matching the ratio of model height to surface roughness length (z_0) is more important.

Further details on similarity criteria and guidelines on modeling may be found in Snyder's (17) discussion of fluid modeling.

METHODOLOGY

WIND TUNNEL BOUNDARY LAYER GENERATION AND MODEL SIZE

The experiment was conducted in the EPA Meteorological Wind Tunnel, a low-speed, open-return tunnel having a test section 2.1 m high x 3.7 m wide x 18.3 m long. A neutrally stratified simulated ABL was generated by a 15.3 cm high trip fence placed 22.3 cm from the test section entrance. Gravel roughness composed of pebbles having typical diameters of 1 cm covered the tunnel floor downstream of the fence. The boundary layer is characterized by a depth of approximately 1 m, a roughness length (z_0) of 0.1 mm, and a friction velocity (u_*) of $0.048U_0$. The velocity profile in the surface layer is described by Equation 1.

A full-scale neutrally stratified ABL is typically 600 m high and has a surface layer depth of 100 m (19). Since the typical pile height (11 m) is well within the surface layer, matching L/δ is not important. Jensen's criterion gives the relevant model length scale. The model pile had to be small enough to be within the surface layer but large enough to construct windbreaks of height the same order as the pile height and to facilitate measurements. The result was a model pile 11 cm high (37° slope and base diameter of 29.2 cm). The pile could not be roughened with the same gravel as that covering the floor of the tunnel because the 1 cm gravel was too large with respect to the pile size. Gravel having diameter less than 4 mm was used instead. With a free-stream speed of 4 m/s, the roughness Reynolds number criterion discussed earlier was met with the 4 mm gravel. The terrain surrounding actual piles is also usually rougher than the pile surface.

Vertical velocity profiles obtained with a hot-wire anemometer upstream of the model pile and at the crest of the pile (at several ambient wind speeds) indicated that the flow was Re-independent at a free-stream wind speed of 4 m/s.

PILE-SURFACE WIND-SPEED MEASUREMENT SYSTEM

Wind speeds near the pile surface at various locations were desired since wind speed at the surface affects particle uptake and varies from location-to-location. Unfortunately, it is difficult to measure the wind speed near a roughened, sloping surface, particularly when the wind direction at the measurement point is unknown and difficult to determine. Pitot-static tubes and hot-wire anemometers require certain orientation with respect to the wind for accurate results. Heated thermistor beads were used here for several reasons. First, several thermistors could be mounted on the pile, eliminating the tedious task of moving a hot-wire from location to location, orienting it properly and placing it the same distance from the surface for each sample. Once the thermistor was fixed at the pile surface, errors resulting from differences of thermistor orientation and height, and effects of local roughness elements were minimized by comparing wind speed reduction at a specific point on the pile. Since the thermistor bead is an ellipsoid, its output is independent of wind direction as long as the flow is normal to the thermistor axis.

The resistance-temperature relationship for thermistors is expressed as

$$R = R_o \exp[\beta(T^{-1} - T_o^{-1})], \qquad (4)$$

where R and R_o are the resistances at temperature T and T_o, respectively, and β is a constant dependent on the thermistor material. Each thermistor was calibrated in a hot oil bath.

The electric circuit consisted of a constant power supply of voltage E and thermistor-resistor pairs in parallel with the power supply (Figure 2). The voltage across each series resistor is the output voltage (V_i). Voltages V_i and E were digitized and processed on a PDP 11/40 minicomputer.

Thermistor anemometers operate under the same basic principle as do hot-wire anemometers, that is, the heat loss from the sensor is a function of wind speed. Rasmussen (20) has shown that

$$i^2 R = K(T_T - T_a), \qquad (5)$$

where i is current through the thermistor, R is thermistor resistance, T_T and T_a are thermistor and ambient temperature, respectively, and K is the dissipation factor. K is a function of the wind speed and the properties of

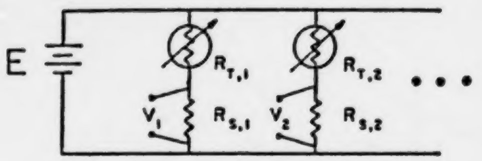

Figure 2. Thermistor circuit.

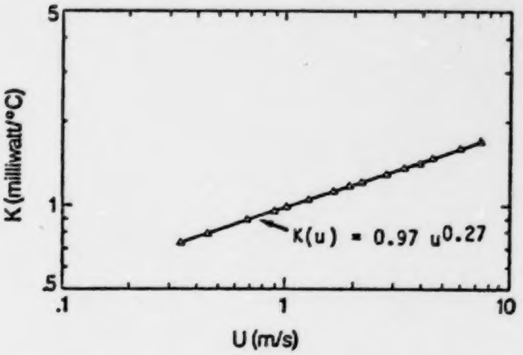

Figure 3. Dissipation factor vs. wind speed for a Fenwal GB31J1 thermistor.

the fluid surrounding the thermistor, and was determined experimentally as follows. A Fenwal GB31J1 thermistor was placed in the center of a smaller wind tunnel (1 m x 1 m x 4 m). At each wind speed, E and V_i were measured. From those, i, R and T_T were calculated. T_a was measured with a YSI model 4320 temperature sensor. Hence, K at each wind speed was calculated. By varying the wind speed from 0.3 m/s to 8 m/s, the functional relationship of K (mW/°C) to u (m/s) was found to be (Figure 3)

$$K = 0.97u^{0.27}. \qquad (6)$$

Hence, thermistor output is related to wind speed. It was assumed that this relationship was valid for all the thermistors used in this project.

Nine thermistors (Fenwal GB31J1) were mounted at different elevations on the pile normal to and about 2 to 3 mm above the surface in the arrangement shown in Figure 4. The thermistor diameters were about 1 mm and their lengths were about 1.5 mm. Each run consisted of measuring the wind speed with the nine thermistors, rotating the pile 30°, measuring the wind speed at these nine positions, etc., through 360°, resulting in 108 data points per run.

WINDBREAK SPECIFICATIONS

50%, 60%, and 70% porous synthetic material is commercially available for use in windbreaks. Tests with these three porous materials were desired for the present study but the open areas of the 60% and 70% porous material were too large (25 mm x 12 mm, 25 mm x 25 mm) with respect to the overall windbreak size for direct use in the wind tunnel. Hence other windbreak material having the same aerodynamic drag or pressure drop coefficient as the more porous commercial material was desired. Caput el al. (21) have used the pressure drop coefficient c_p to account for the porosity and size and shape of the windbreak openings. The pressure drop coefficient is defined as

$$c_p = \Delta p/(0.5\rho u^2) \qquad (7)$$

where Δp is static pressure drop across the material, ρ is air density, and u is reference wind speed, here, that upstream of the material.

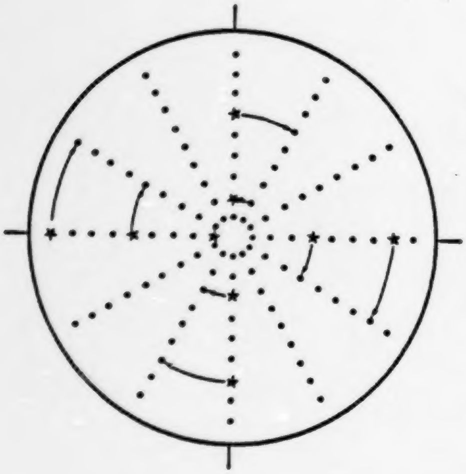

Figure 4. Top view of conical pile. Stars: Thermistor positions on pile. Dots: Effective thermistor positions due to pile rotation.

The pressure drop coefficient of the three windbreak materials and a 16 x 18 mesh nylon screen (65% porous) were determined through tests in the smaller wind tunnel. The material was placed 1 m from the entrance to the test section and fully covered the cross section. The pressure drop was measured with pitot-static tubes placed upstream and downstream of the material. The pressure drop coefficient, independent of wind speed for speeds greater than 2 m/s, of the 50%, 60%, and 70% porous materials and the mesh screen are 5.5, 2.2, 1.4, and 1.8, respectively. The mesh screen was used as a high porosity screen, as its c_p was midway between that of the 60% and 70% screens. Note that c_p of the 50% porous windbreak material is much higher than that of the others.

The windbreaks and pile used are shown in Figure 5. Note that the windbreak height and length are given in terms of the pile height and base diameter, respectively, and that the position is the distance between the windbreak and the upstream pile base, given in terms of pile heights. All combinations of the parameters result in six windbreaks of each porosity placed at two different distances from the pile, i.e. a total of 24 cases. For these cases, the windbreak was placed normal to the air flow and the tunnel floor. Upon completion of the 24 tests, one windbreak was placed at angles of 20° and 40° to the air flow.

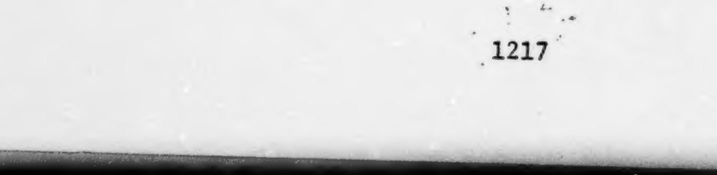

Windbreak Specifications	
Porosity	50%, 65%
h	0.5H, 1.0H, 1.5H
L	1.0D, 1.5D
P	1H, 3H

Figure 5. Geometry of pile and windbreaks.

RESULTS

Discussion of the results is divided into three sections: the wind speed distribution for the unprotected (no windbreak) case, for cases with the air flow in the direction of the windbreak normal, and at an angle to the normal. Relative windbreak effectiveness may be assessed by several methods. The location of regions of greatest wind speed reduction, the magnitudes of the reductions, and an area-averaged reduction may be determined. The maximum wind speed and a factor based on the relationship between the cube of the speed and particle uptake may also be used. Finally, depending on the threshold speed, emissions may not occur over a fraction of the pile surface. The results will be discussed in terms of these methods.

WIND SPEED DISTRIBUTION: NO WINDBREAK

Figure 6 shows the top view of the pile with contours of normalized wind speed, u/u_r, where u is the wind speed at the pile surface measured with the thermistor and u_r is the wind speed at the equivalent full-scale height of 10 m in the absence of the pile. 10 m was chosen as the reference height rather than 11 m, the pile height, because 10 m is the standard height to which "surface" wind speed measurments are usually referenced. Note that the air flow in the figure is from the left. The areas of maximum wind speed are near the top of the upwind face but toward the sides of the pile. A high speed region ($u/u_r > 0.75$) is on the upstream face, extending from near the crest down both sides. The area of minimum wind speed is in the lee near the top of the pile with regions of low wind speed extending down the pile on both sides of the centerline. High speeds along the pile sides are expected because the flow is accelerating round the pile. The flow separates on the lee side, resulting in a region of low-speed recirculating flow.

INCIDENT WIND NORMAL TO THE WINDBREAK

Wind Speed Reduction

Figures showing normalized wind speed for all the windbreak cases are not included here because the change in wind speed due to a windbreak is of more interest. The wind speed at a given location on the pile surface for a case with the windbreak is some fraction of that in the unprotected case. The amount by which the wind speed is reduced is called the wind speed reduction factor R_i and, in percent, is defined as

$$R_i = \frac{u_i(\text{no windbreak}) - u_i(\text{windbreak})}{u_i(\text{no windbreak})} \times 100, \qquad (8)$$

where u_i is the wind speed at the i-th location on the pile. R_i is zero when the windbreak causes no change in the wind speed, and 100% when the wind speed is zero due to the windbreak. R_i of 25% means that the wind speed resulting from the windbreak's presence is 25% less than the wind speed in the unprotected case. It is important to remember that the combined effects

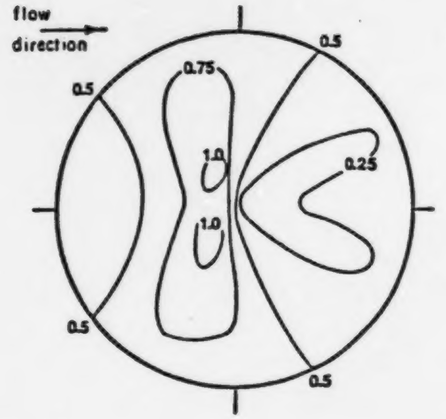

Figure 6. u/u_r for no windbreak case.

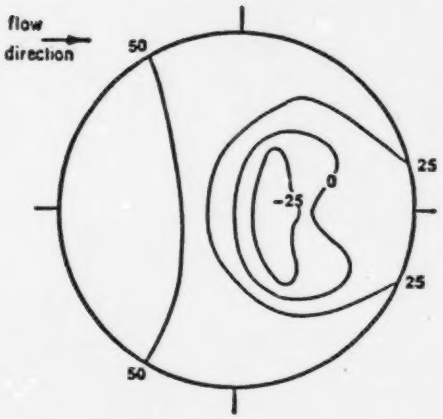

Figure 7. Wind speed reduction factor for the 65% porous windbreak of height 0.5H and length 1.0D placed 1H from the pile base.

of windbreak height, length, porosity, and position, as well as turbulence in the approach flow, and pile shape and surface roughness determine the wind speed distribution over the pile surface. Some of these factors will be considered here.

Effect of Height--

Figure 7 shows contours of wind speed reduction factor R_i resulting from the 65% porous screen of height 0.5H, length 1.0D, located 1H from the pile base. Referring also to Figure 6, it is seen that in the areas of maximum wind speed of the no windbreak case, this windbreak reduced the wind speed by 25%, but that in the area of minimum wind speed without the windbreak, the windbreak increased the speed by approximately 25% (negative reduction factor). In terms of fugitive dust control, the increase is probably not significant because the wind speed would be low in this region unless the reference speed (u_r) were very high. Wind speed was reduced by at least 50% on most of the upstream face. This general pattern of high wind speed reduction in the lower portion of the upstream face and increase in the upper lee region was typical of all the windbreaks of height 0.5H, but not of the higher windbreaks.

For higher windbreaks, the area of greatest wind speed reduction was the upper part of the windward side, with typical reductions of at least 50%. In general, reductions in the lee were at least 25%. The reduction pattern for windbreaks of the same porosity, length, and position did not differ significantly when the windbreak height was increased from 1.0H to 1.5H, except for the least porous windbreak located farther from the pile. In that case, the highest windbreak caused the greatest reductions over much of the pile.

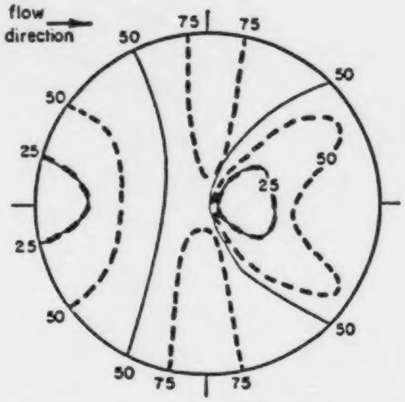

Figure 8. Wind speed reduction factor for the windbreak of height 1.0H and length 1.0D placed 1H from the pile base with porosity 65% (solid line) and 50% (dashed line).

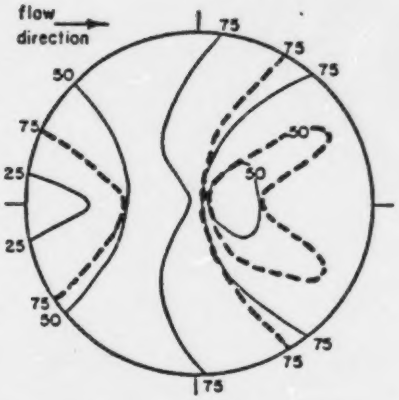

Figure 9. Wind speed reduction factor for the 50% porous windbreak of height 1.5H and length 1.5D placed 1H (solid line) and 3H (dashed line) from the pile base.

Effect of Length--

Increasing length is expected to effect greater reductions at the pile sides. This was observed with the 50% porous windbreaks, although the difference was slight as the length was increased from 1.0D to 1.5D. Length is important if the incident wind is not normal to the windbreak (see later discussion).

Effect of Porosity--

For a given windbreak height, length, and position, greater wind speed reductions occured for the less porous (50%) windbreak, particularly on the windward face of the pile. The reduction factors for the two windbreaks of height 1.0H and length 1.0D located at the 1H position are shown in Figure 8. The distributions are quite similar in shape, with larger reductions in the 50% porous case.

Effect of Position--

The effect of windbreak position appears to be related to windbreak height. Windbreaks of height 0.5H caused greater wind speed reduction in the lower part of the windward face and sides when placed 1H, rather than 3H, from the pile base. Windbreaks of height 1.0H placed 3H from the pile caused greater wind speed reduction on the windward face but less reduction in the lee. Windbreaks of height 1.5H placed 3H from the pile caused even greater wind speed reductions on the windward face. This may be due to the observation that the sheltered area downwind of a windbreak increases in size and the area of minimum wind speed moves downwind as the windbreak height increases. Unfortunately, no velocity measurements were made here in the absence of the pile downstream of any of the windbreaks. Figure 9 shows the wind speed reduction distribution for the 50% porous windbreak of height 1.5H and length 1.5D at the two positions. Clearly, larger areas of high reduction occurred for the 3H case.

Averaged Wind Speed Reduction Factor

An area-averaged wind speed reduction factor $\overline{R}$ may be calculated from the individual R_i's for a given windbreak case:

$$\overline{R} = \sum_i (R_i A_i) / \sum_i A_i, \qquad (9)$$

where A_i is the surface area surrounding the i-th thermistor location. If the fugitive dust emission rate is proportional to the wind speed, then the averaged reduction factor is a measure of the reduction in emissions from those in the unprotected case.

The averaged reduction factors are given in Table 1. $\overline{R}$ is better than 20% in all cases, with averaged reductions of 21-36% for the windbreaks of height 0.5H, and for heights greater than 0.5H, 42-51% and 57-70% for 65% and 50% porous windbreaks, respectively. Differences between the heights 1.0H and 1.5H and the two lengths were within the experimental scatter except for higher, less porous windbreaks placed farther from the pile. As expected, in those cases, the larger windbreak was better. The windbreak locations closer to, and farther from, the pile were better for the windbreaks of height 0.5H and 1.5H, respectively.

TABLE 1. AREA-AVERAGED WIND SPEED REDUCTION FACTOR ($\overline{R}$) FOR THE VARIOUS WINDBREAK CASES

	65% porous windbreak				50% porous windbreak			
position:	1H		3H		1H		3H	
length:	1.0D	1.5D	1.0D	1.5D	1.0D	1.5D	1.0D	1.5D
height								
0.5H	26	25	21	22	36	36	27	26
1.0H	45	42	48	47	60	60	57	62
1.5H	45	43	51	51	60	58	62	70

Maximum Wind Speed

Since the maximum wind speed, independent of position, is related to the maximum particle emission rate (neglecting other factors which affect emissions), it may be used to assess the relative effectiveness of the various windbreaks. The values of maximum wind speed normalized by the wind speed at the equivalent full-scale height of 10 m in the absence of the pile for the 24 cases are given in Table 2. Note that this ratio, u_{max}/u_r, is 1.16 for the unprotected (no windbreak) case.

All the windbreaks gave a lower u_{max}/u_r, which is desired for fugitive dust control. Windbreaks of height 0.5H caused much higher u_{max}/u_r than did the higher windbreaks. Differences in u_{max}/u_r between windbreaks of height

1.0H and 1.5H, for the same porosity, length, and position, were not nearly as great as for those between 0.5H and 1.0H. Comparing u_{max}/u_r for the three heights, given the other parameters, at the 1H position, this value is a minimum for the 1.0H height, but at the 3H position, it is a minimum for the 1.5H height. The minima indicate that for these cases, the pile was located near the area of minimum wind speed for that particular windbreak height. In general, for a given windbreak height, length, and position, the 50% porous windbreak caused lower u_{max}/u_r than did the 65% porous windbreak. Placing a given windbreak a distance 3H from the pile base was more effective than placing it 1H from the pile for nearly all the cases tested here. The longer windbreak is more effective for the higher, less porous windbreaks placed farther from the pile.

TABLE 2. u_{max}/u_r FOR THE VARIOUS WINDBREAK CASES

	65% porous windbreak				50% porous windbreak			
position:	1H		3H		1H		3H	
length:	1.0D	1.5D	1.0D	1.5D	1.0D	1.5D	1.0D	1.5D
height								
0.5H	0.91	0.93	0.91	0.94	0.90	0.93	0.82	0.86
1.0H	0.55	0.59	0.54	0.56	0.31	0.34	0.37	0.27
1.5H	0.56	0.60	0.50	0.52	0.39	0.42	0.25	0.17

Windbreak Effectiveness Factor

A windbreak effectiveness factor E may be defined by analogy to the averaged wind speed reduction factor

$$E = \sum_i \left[\frac{u_i(\text{no windbreak})^3 - u_i(\text{windbreak})^3}{u_i(\text{no windbreak})^3} \right] A_i \times \frac{100}{\sum_i A_i} . \qquad (10)$$

The windbreak effectiveness factor is the percent by which the emission rate is reduced due to a given windbreak, assuming that the emission rate is proportional to the cube of the wind speed, other factors being equal. Referring to Table 3, many of the same qualitative results as with the averaged wind speed reduction factor are apparent. The windbreaks of the lowest height would be least effective, the increase in windbreak length beyond 1.0D is not important, and the optimum position is related to the windbreak height.

Although the highest effectiveness factor of 95% corresponds to the 50% porous material of height 1.5H, length 1.5D, located 3H from the base of the pile; the effectiveness of the more economical windbreak of the same porosity, height 1.0H and length 1.0D is only slightly lower. Clearly, the latter would be preferable on the basis of cost effectiveness. Any location between 1H and 2H from the base of the pile could be chosen depending on the convenience.

TABLE 3. WINDBREAK EFFECTIVENESS FACTOR FOR THE VARIOUS WINDBREAK CASES

	65% porous windbreak				50% porous windbreak			
position:	1H		3H		1H		3H	
length:	1.0D	1.5D	1.0D	1.5D	1.0D	1.5D	1.0D	1.5D
height								
0.5H	44	44	34	36	50	46	39	34
1.0H	81	78	80	80	90	87	84	86
1.5H	81	78	87	86	88	89	89	95

An Example with a Threshold Velocity

Drawbacks to the averaged wind speed reduction factor and windbreak effectiveness factor as defined here are that through averaging over the entire pile surface, effects in the region of high wind speeds (high dust emission rate) without a windbreak are no more important than effects in other regions; and that the lower the wind speed, the better. But if the wind speed is lower than the threshold value for fugitive dust uptake, it does not matter how much lower the wind speed is.

An example calculation was made using the u/u_r wind tunnel data assuming a reference wind speed (u_r) of 10 m/s and a threshold velocity of 2.8 m/s. With no windbreak, 22% of the pile surface area had wind speeds less than the threshold. With all the 65% porous windbreaks and the 0.5H high 50% porous windbreaks, 40-65% of the pile surface area would have no dust emissions. The area increased to 77-100% for the other 50% porous windbreaks. Again, length made no significant difference. Note that the percentage surface areas calculated here would increase with a lower reference speed and/or a higher threshold velocity.

INCIDENT WIND AT AN ANGLE TO THE WINDBREAK

Since the wind direction is constant in a wind tunnel, a windbreak oriented at an angle to the tunnel centerline simulates a full-scale case of a fixed windbreak with the air flow at an angle to the windbreak different from normal. Figure 10 shows u/u_r contours for the 50% porous windbreak of height 1.0H, length 1.0D, placed 1H from the pile base for wind directions normal to the windbreak, and at 20°, and 40° to the normal. The windbreak positions are also shown in the figures. The maximum u/u_r was 0.31, 0.69, and 1.12 for the 0°, 20°, and 40° cases, respectively. For the 20° case, a region of high wind speed (u/u_r greater than 0.5) was observed on the side of the pile opposite the windbreak, indicating that the windbreak length and position are important. For the 40° case, the region of u/u_r greater than 0.5 was much larger than that for the 20° case; indeed the wind speed pattern is approaching that of the unprotected case (Figure 6). Clearly, windbreak effectiveness decreases with increasing angle of flow from the normal.

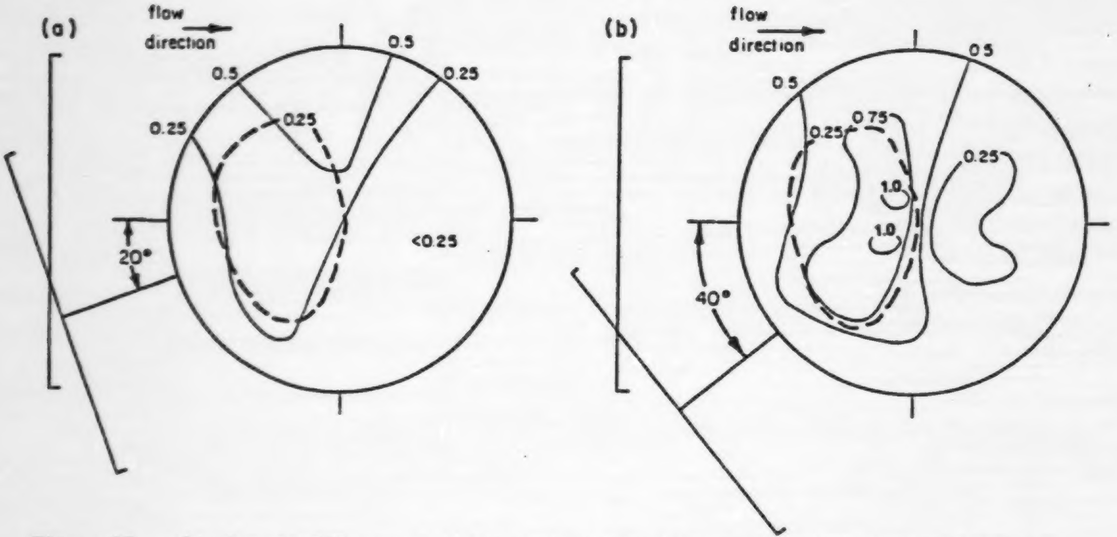

Figure 10. u/u_r for the 50% porous windbreak of height 1.0H and length 1.0D placed 1H from the pile base oriented normal (dashed lines), and at (a) 20° (solid line) and (b) 40° (solid line) to the flow direction.

CONCLUSIONS

This wind tunnel study has shown that windbreaks normal to the wind direction placed upwind of a conical storage pile reduce wind speeds near the surface of the pile and hence should reduce fugitive dust emissions. Large wind speed reductions occurred with the less porous windbreak material, windbreaks at least as high as the pile and as long as the pile base diameter. Optimal windbreak location appears to be related to windbreak height; low windbreaks located close to the pile and higher windbreaks located farther from the pile effected greater reductions than when placed at other positions. Of the windbreaks tested, the largest 50% porous windbreak placed farther from the pile appears to be best in terms of greatest wind speed reduction. However, all the 50% porous windbreaks at least as high as the pile had similar overall effects. Windbreaks of height 0.5 times the pile height reduced the wind speed over the entire upstream face of the pile, but not as much on the upper half as did the higher windbreaks. Windbreak length and position are more important in determining effectiveness when the air flow is not normal to the windbreak. With the particular windbreak used here, fairly high wind speed reductions resulted when the windbreak was placed at an angle of 20° to the air flow, but at 40°, little reduction occured.

ACKNOWLEDGEMENTS

This work was conducted under a cooperative agreement, CR-807854, between the North Carolina State University and the U.S. Environmental Protection Agency, Dr. S.P.S. Arya, principal investigator, and Dr. W.H. Snyder, project officer.

REFERENCES

1. The Bureau of National Affairs, Inc., Environment Reporter. 336:0553-0554, Rule 302(f), 1983.

2. The Bureau of National Affairs, Inc., Environment Reporter. 411:0516-0517, R336.1371, R336.1372, 1982.

3. Bagnold, R.A. The Physics of Blown Sand and Desert Dunes. Methuen, London, 1941, 265 pp.

4. Gillette, D. A wind tunnel simulation of the erosion of soil: Effect of soil texture, sandblasting, wind speed, and soil consolidation on dust production. Atmos. Environ. 12: 1735, 1978.

5. Blackwood, T.R. and Wachter, R.A. Source assessment: Coal storage piles. EPA-600/2-78-004k, U.S. Environmental Protection Agency, Cincinnati, Ohio, 1978. 83 pp.

6. Thornthwaite, C.W. The climates of North America according to a new classification. The Geographical Review. 21: 633, 1931.

7. U.S. Environmental Protection Agency. Supplement No. 14 for Compilation of Air Pollutant Emission Factors, 3rd ed., AP-42, Research Triangle Park, North Carolina, 1983.

8. Van Eimern, J., Karschon, R., Razumova, L.A., and Robertson, G.W. Windbreaks and shelterbelts. WMO Technical Note No. 59, 1964. 188 pp.

9. Perera, M.D.A.E.S. Shelter behind two-dimensional solid and porous fences. J. Indus. Aerodyn. 8: 93, 1981.

10. Raine, J.K. and Stevenson, D.C. Wind protection by model fences in a simulated atmospheric boundary layer. J. Indus. Aerodyn. 2: 159, 1977.

11. Carnes, D. and Drehmel, D.C. The control of fugitive emissions using windscreens. In: Proceedings of the Third Symposium on the Transfer and Utilization of Particulate Control Technology. Vol. IV. Atypical Applications. EPA-600/9-82-005d, U.S. Environmental Protection Agency, Research Triangle Park, North Carolina, 1982. p. 135.

12. Davies, A.E. A physical modelling approach to the solution of fugitive emission problems. In: Proceedings of the 73rd APCA Annual Meeting. Montreal, 1980. Paper 80-68.11.

13. Cai, S., Chen, F.F., and Soo, S.L. Wind penetration into a porous storage pile and use of barriers. Environ. Sci. Technol. 17: 298, 1983.

14. Counihan, J. An improved method of simulating an atmospheric boundary layer in a wind tunnel. Atmos. Environ. 3: 197, 1969.

15. Arya, S.P.S. and Shipman, M.S. An experimental investigation of flow and diffusion in the disturbed boundary layer over a ridge; Part I: Mean flow and turbulence structure. Atmos. Environ. 15: 1173, 1981.

16. Townsend, A.A. The Structure of Turbulent Shear Flow. Cambridge Univ. Press, Cambridge, England, 1956, 315 pp.

17. Snyder, W.H. Guideline for fluid modeling of atmospheric diffusion. EPA-600/8-81-009, U.S. Environmental Protection Agency, Research Triangle Park, North Carolina, 1981. 185 pp.

18. Jensen, M. The model-law for phenomena in a natural wind. Ingenioren, Int. Ed. Vol. 2, No. 4, 1958.

19. Counihan, J. Adiabatic atmospheric boundary layers: A review and analysis of data from the period 1880-1972. Atmos. Environ. 9: 871, 1975.

20. Rasmussen, R.A. Application of thermistors to measurements in moving fluids. Rev. Sci. Instrum. 33: 38, 1962.

21. Caput, C., Belot, Y., Guyot, G., Samie, C., and Seguin, B. Transport of a diffusing material over a thin wind-break. Atmos. Environ. 7: 75, 1973.

EVALUATION OF CHEMICAL STABILIZERS AND WINDSCREENS FOR WIND EROSION CONTROL OF URANIUM MILL TAILINGS

by: Monte R. Elmore and James N. Hartley
Pacific Northwest Laboratory
Richland, WA 99352

ABSTRACT

Potential wind erosion of uranium mill tailings is a concern for the surface disposal of tailings at uranium mills. Wind-blown tailings may subsequently be redeposited on areas outside the impoundment. Pacific Northwest Laboratory (PNL), under contract to the U.S. Nuclear Regulatory Commission, is investigating techniques for fugitive dust control at uranium mill tailings piles.

Laboratory tests, including wind tunnel studies, were conducted to evaluate the relative effectiveness of 43 chemical stabilizers. Seventeen of the more promising stabilizers were applied to test plots on a uranium tailings pile at the American Nuclear Corporation-Gas Hills Project mill site in central Wyoming. The durabilities of these materials under actual site conditions were evaluated over time. In addition, field testing of commercially available windscreens was conducted. Test panels were constructed of eight different materials at the Wyoming test site to compare their durability. A second test site was established near PNL to evaluate the effectiveness of windscreens at reducing wind velocity, and thereby reduce the potential for wind erosion of mill tailings. Results of the laboratory and field tests of the chemical stabilizers and windscreens are presented, along with costs versus effectiveness of these techniques for control of wind erosion at mill tailings piles.

The work described in this paper was not funded by the U.S. Environmental Protection Agency and therefore the contents do not necessarily reflect the views of the Agency and no official endorsement should be inferred.

INTRODUCTION

The uranium milling process generates large quantities of solid wastes, or tailings, that contain radionuclides, toxic elements found in the original ore, and residual chemicals used in the milling process (1). The most common method of tailings disposal is to deposit the waste material from a slurry into open ponds. In most cases, a raised pile is formed over time by the repeated deposition of spigotted tailings.

Many active and inactive uranium mill tailings piles are subject to potentially severe wind erosion if the surface of the tailings pile is not properly stabilized. Windblown tailings have been found at distances up to several kilometers from impoundment sites. Excluding radon, these fugitive dust emissions are the largest potential source of offsite radiation exposure and the proper selection of control techniques is necessary to reduce such emissions to "as low as reasonably achievable" (ALARA) levels.

Pacific Northwest Laboratory (PNL)[1] is therefore investigating the effectiveness, durability, and practicability of methods to minimize the wind erosion of exposed tailings surfaces. Results of this study, which is sponsored by the Office of Nuclear Regulatory Research of the U.S. Nuclear Regulatory Commission (NRC), will provide technical information needed in formulating plans for the short-term stabilization of uranium mill tailings over a wide range of site and environmental conditions.

WIND EROSION CONTROL BY SURFACE STABILIZATION

A number of techniques have been tried for controlling wind erosion of tailings. The simplest concept for surface stabilization is water sprinkling. Some mill operators use irrigation-type sprinkler systems distributed across the tailings surface. The binding action from the increased surface tension of the wetted particles, however, is often not sufficient to prevent wind erosion entirely. The wetting and drying from cyclic sprinkling also tends to make the surface more fragile, actually increasing the wind erosion potential. In addition, maintenance and operation of sprinklers can be expensive, and the arid climate at most uranium mill sites often limits the availability of water.

Another stabilization method is to cover the tailings with a layer of straw, bark, soil, or rocks to protect the fine tailings from direct exposure to the wind. This method may be suitable for an inactive tailings pile, but is not considered cost effective for the short-term stabilization requirements at an active uranium mill. Man-made materials such as plastic films and woven fabrics, or geotextiles, have been developed for the same purpose, but have not been demonstrated to be practical.

---

[1] Operated for the U.S. Department of Energy by Battelle Memorial Institute under Contract DE-AC06-76RLO 1830.

Vegetation has often been used to stabilize wind-blown soils, and a significant research effort has focused on developing methods to revegetate mine spoils and tailings piles (2-4). However, vegetative covers are generally more useful for longer-term stabilization of inactive areas because of the time, effort, and soil conditions required to establish plant cover.

Perhaps the most widely used control method is to treat the surface with some form of erosion-resistant binder. Chemical stabilizers are generally available and have been employed at many mill sites. These stabilizers bind the surface particles either by forming protective continuous films over the surface or by reacting with the particles to form a crust or large agglomerates of particles that resist blowing. Chemical stabilizers include surfactants (wetting agents that merely increase the effectiveness of water sprinkling), hygroscopic salt solutions, petroleum resin emulsions, asphalt products, wood pulp by-products, and synthetic resin emulsions (5).

The typical method of applying chemical stabilizers is to dilute the concentrates with water and spray the solution onto the surface. The dilution factors and rates of application depend on the requirements of the job and the characteristics of the blowing material. Although the chemicals are often expensive, the advantage of spraying is its simple application method, which involves common spray equipment. Major disadvantages of surface stabilization in general are that the stabilizers must be applied to the entire surface area and often must be frequently renewed.

LABORATORY TESTING

The objective of the laboratory evaluation was to determine the effectiveness and durability of commercially available stabilizers, and to select the more effective ones for field testing at a uranium mill tailings pile. Most of the laboratory studies were conducted using a wind tunnel to compare the relative resistance of stabilized simulated tailings (sand) samples to wind erosion. Various stabilizer dilution and application rates were tested. The effects of temperature (freeze/thaw) cycling and wet/dry cycling were evaluated, as well as the stabilizers' resistance to water erosion and ultraviolet (UV) degradation. Table 1 summarizes the wind tunnel studies from which stabilizers were selected for field testing (6). The stabilizers selected for the field test were those with positive cumulative scores from the laboratory tests (with exceptions as noted in Table 1) and are listed in Table 2.

FIELD TESTING

The durability of the selected chemical stabilizers was field tested at the Federal American Partners (FAP) uranium mill in central Wyoming, now known as American Nuclear Corporation-Gas Hills Project. Fifteen stabilizers selected from the laboratory tests were initially applied to test plots in August 1982. In September 1983, two other recently identified materials were also applied to similar test plots (along with one of the previous year's stabilizers, providing a means of comparing both years). The test plots were then periodically monitored for about one year.

TABLE 1. SUMMARY RATINGS OF LABORATORY WIND TUNNEL TEST RESULTS*

Product	Test A	Test B	Test C	Test D	Test E	Test F	Cumulative Rating
8803	0	-3	0		0	-1	-4
8820	0	-3	0		-1	-1	-5
Aerospray-70	0	0	0	0		+1	+1
AMS-2200	0	0	0	-3	0	0	-3
Coherex	0	+1	0	+1	0	+1	+3
CPB-12	+1	+1	0	0	0	0	+2
Dust Binder C-266	+1	0	+1	+1	0	0	+3
Dust Gard	+1	+1	0	+1	0	0	+3
Dust Loc VMX-50	0	0	+1	+1	0	+1	+3
ESI-BOND	0	0	+1	-1	+1	+1	(+2)
Gantrez AN-119	0	0	0	0	0	0	0
Gantrez ANM-139	+1	0	0	0	0	-2	-1
Gantrez AN-169	+1	0	+1	0	0	-3	-1
Hercobind DS-3	+1	+1	0	+1	0	-3	0
Hydrodyne C	-3			-3			-6
IDA-656	0	0	0	-1	0	0	-1
Liquid Dust Layer	+1	-1	-1	-1	0	0	-2
M-166	-1	+1	0	0	0	0	0
M-167	0	0	+1	+1	0	+1	+3
Marloc	+1	0	+1	0	0	0	+2
Orzan A	+1	0	0	0	0	0	+1
Orzan S	0	0	0	0	0	-1	-1
Pentron DC-5	+1	0	+1	-1	0	0	(+1)
Polyco 2151	0	+1	+1	+1	0	0	+3
Rezasol 5411-B	+1	0	0	0	0	-1	0
Sandstill	0	0	0	0	0	-1	-1
Sandstill I	0	+1	0	0	0	0	+1
Soil Gard	0	0	0	0	0	+1	+1
SP-301	0	+1	0	-2	+1	+1	(+1)
SP-400	0	+1	+1	+1	0	0	+3
Suferm	0	+1	-3	0	0		-2
TPC 2245	0	0	-1	0	-3	0	-4
V-4100 Binder	0	0	0	0	0	0	0
Wallpol 40-133	+1	+1	+1	0	0	+1	+4

* Tests are identified as follows:

A - normal application rate tests
B - one-half normal application rate tests
C - temperature cycling tests
D - $750/ha rate tests
E - inclined sample tests
F - wet/dry cycling tests.

Materials selected for field testing were those with positive cumulative ratings. Numbers in parentheses indicate that the material had a negative score in one or more tests. Even though the cumulative rating was positive, the stabilizer was therefore rejected from the field testing. Source: Ref.(6).

TABLE 2. CHEMICAL STABILIZERS SELECTED FOR FIELD TEST

Stabilizer	Manufacturer	Composition*
Aerospray 70	American Cynamid	Polyvinyl acetate emulsion
CPE-12	Wen Don Corporation	Acrylic polymer emulsion
Coherex	Witco Chemical Co.	Petroleum resin emulsion
Dust Binder C-266	Union Carbide Corp.	Synthetic polymer emulsion
Dust Gard	Great Salt Lake Minerals	Hygroscopic chloride brine
Dust Lok VMX-50	American Energy	Polyvinyl acetate emulsion
Hydromulch	Conwed Corporation	Wood fiber mulch
M-167	Dowell/Dow Chemicals	Latex polymer emulsion
Marloc	Reclamare Co.	Polyvinyl acetate emulsion
Orzan A	Crown Zellerbach	Ammonium lignin sulfonate
Polyco 2151	Borden Chemicals	Vinyl acetate/acrylic emulsion
Retain†	Dubois Chemicals	Asphalt emulsion
SP-400	Johnson and March Corp.	Latex polymer emulsion
Sandstill II	Energy Systems	Petroleum resin emulsion
Soil Gard	Walsh Chemicals	Styrene butadiene emulsion
Soil Sement†	Midwest Industrial Supply	Synthetic polymer emulsion
Wallpol 40-133	Reichold Chemicals	Vinyl acetate/acrylic emulsion

* The actual chemical compositions of most of the products is proprietary information.

† Applied at the Wyoming field test site in September 1983.

Three synthetic polymer emulsions were found to be the most effective at the Wyoming test site: Wallpol 40-133 (Reichold Chemicals), SP-400 (Johnson and March Corp.), and CPB-12 (Wen Don Corp.) (7). The field-tested stabilizers are ranked in order of observed durability in Table 3.

The durability rating is based on the observed amount of stabilized surface remaining on each test plot after one year of exposure to climatic conditions at the Wyoming test site. An expected effective service life for each stabilizer was then assumed to be equivalent to the durability rating. In other words, a rating of 10 represents an expected lifetime of one full year, and a rating of 4 represents an expected lifetime of 4/10 of a year. The expected effective lifetime is only an approximation, since insufficient data were available on the condition of the stabilizers at certain times of the year. For example, during the winter months the stabilizer test plots were often covered with snow for long periods, and frequent monitoring trips to the test site were not possible.

COSTS OF LARGE-SCALE CHEMICAL STABILIZATION

The costs to chemically stabilize a tailings pile will vary greatly depending on the site location, size and condition of the tailings pile, and

TABLE 3. CHEMICAL STABILIZERS GROUPED BY RELATIVE EFFECTIVENESS AFTER EXTENDED WEATHERING*

Group	Stabilizer	Composition	Relative Durability
I	Wallpol 40-133	Vinyl acetate/acrylic	7-10 (good)
	SP-400	Latex emulsion	
	CPB-12	Acrylic emulsion with conditioners	
II	Sandstill II	Petroleum resins/surfactant	4-6 (fair)
	Soil Gard	Styrene butadiene	
	Dust Loc VMX-50	Acrylic latex	
	Dust Gard	$MgCl_2$ brine	
	Aerospray-70	Polyvinyl acetate	
	Orzan A	Ammonium lignin sulfonate	
	Coherex	Petroleum oils and resins/ surfactant	
	Marloc	Polyvinyl acetate	
	Soil Sement	Latex emulsion	
III	Hydro Mulch	Wood fiber mulch	0-3 (poor)
	Retain	Asphalt emulsion	
	Dust Binder C-266	Synthetic polymer emulsion	
	Polyco 2151	Vinyl acetate/acrylic	
	M-167	Latex, sufactant, propylene glycol	

* From Ref. (7).

type of stabilizer selected. Table 4 shows the range of material costs for the field tested stabilizers. These costs are based on 1984 estimated prices of the materials delivered to the Wyoming test site in quantities sufficient to treat a 40-ha (100-acre) tailings pile.

Large-scale stabilization costs, also shown in Table 4, are based on costs estimated by FAP for a similar stabilization project in July 1982, which was performed with a two-man crew and a tank truck fitted with a pump and hose for spraying. The crew was able to apply 1 to 2 tank loads during an 8-hour shift. The expected coverage for one tank-load of the stabilizer, applied according to the manufacturer's directions, was approximately 1.67 ha (4.13 acres). The estimated costs for truck and crew was $66/hr, or a labor and equipment charge of $160 to $320/ha. The time and effort required to treat a given area would not vary significantly for any of the stabilizers, so a conservative estimate of $320/ha is used for all materials. Applications costs are a significant portion of the total for only the least expensive materials.

TABLE 4. ESTIMATED APPLICATION COSTS OF CHEMICAL STABILIZERS FOR A LARGE-SCALE STABILIZATION PROJECT

Chemical Stabilizer		Material Costs, $/ha*	Large-Scale Stabilization Costs	
			$/ha†	$/ha/yr‡
1	Aerospray 70	3280	3600	7200
2	SP-400	3170	3490	4360
3	Dust Lok VMX-50	2790	3110	6220
4	Wallpol 40-133	2690	3010	3762
5	Dust Gard	2260	2580	5160
6	CPB-12	1980	2300	3290
7	Marloc	1910	2230	5580
8	Dust Binder C-266	1880	2200	7330
9	Soil Sement	1730	2050	5130
10	Sandstill II	1630	1950	3250
11	M-167	1580	1900	19,000
12	Soil Gard	1350	1670	2780
13	Coherex	1250	1570	3930
14	Hydro Mulch	810	1130	3770
15	Retain	670	990	4950
16	Polyco 2151	480	800	2670
17	Orzan A	360	680	1700

* Stabilizer costs are based on delivered price to the field test location in central Wyoming, and on amount required to stabilize a 40-ha site. Delivered costs will vary with location.

† Includes expected labor and equipment charges of $320/ha based on FAP estimate for a similar large-scale project at FAP mill in 1982 using two operators and a 10,000-gal spray truck (7).

‡ Cost per hectare per year is based on relative durability of the stabilizers as observed from the Wyoming field test, shown in Figure 1. The value of relative durability is taken here as a fraction of the test year that each stabilizer remained effective, so a stabilizer with a rating of 5 out of 10 would need to be applied twice a year.

When the relative observed durabilities of the materials are plotted against the estimated large-scale application costs, as in Figure 1, it can be seen that the longer-lasting stabilizers tend to be the more expensive ones, with some exceptions. However, any stabilizers falling on a diagonal line drawn through the origin are considered to be equally cost effective. That is, a less expensive stabilizer can be applied more often to produce a chosen level of erosion control (compared to a more expensive one on the same line) at an overall equivalent cost. For example, stabilizer 4 was given a durability rating of 8. Its applied cost is $3010/ha to apply and lasts for 8/10 of a year. Stabilizer 13 was given a rating of 4 with an applied cost of $1570/ha, and so could be applied twice as often for approximately the same cost and degree of erosion protection. Those chemicals below the diagonal

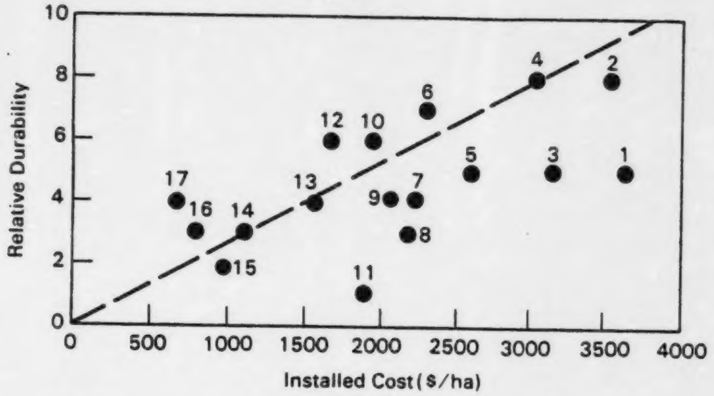

Figure 1. Cost versus relative durability of field-tested chemical stabilizers. Numbers correspond to numbered stabilizers listed in Table 4.

line would then be less cost effective in this case, and those lying above the diagonal would likely be more cost effective. However, the final selection of a particular chemical stabilizer will depend on site-specific requirements for the mill (i.e., frequency at which previously stabilized tailings are covered by new slurry) in addition to weather, mill location, price and availability of stabilizers, and other such factors.

WIND EROSION CONTROL BY WIND VELOCITY REDUCTION

In early experiments, Bagnold (8) observed that about 75% of the total movement of blowing sands occurred through saltation, the forward bounding movement of wind-blown particles too large to remain suspended in the air (100 to 500 μm). Size distribution analysis of tailings, particularly the more erodible beach sands, predicts that the primary mechanism for tailings erosion will also be saltation. Bagnold (8), Belly (9), and Gillette (10) have shown the horizontal flux of particles from various soil types to be proportional to the cube of the wind velocity. Therefore, cutting the wind speed in half should reduce sand erosion to one-eighth the original amount. (This is true if, by reducing the horizontal wind speed, the surface shear force is similarly reduced). Wind speed reduction on large open areas can be accomplished using windscreens.

Windscreens can be constructed to protect a tailings pile from erosion by lowering the wind velocities to the leeward of the screen below the threshold velocity of the surface particles. The design and siting of a windscreen, however, is critical for proper performance, and should consist of the optimal combination of several factors, including:

* windscreen height and length
* windscreen permeability
* size and shape of openings in the screen
* location of the screen on the tailings pile.

In general, the area behind some windscreens where the wind velocity is reduced to one-half the incident wind extends 10 to 20 times the windscreen height downwind. Thereafter, the velocity gradually increases until it again reaches the full upwind velocity.

A solid wall would result in a small sheltered area behind the barrier, due to the increased turbulence caused by diverting the entire flow of air over the barrier. A porous barrier, on the other hand, absorbs some of the momentum of the wind and allows some of the flow to pass through at a lower velocity. This "bleed flow" smooths the wind flow across the sheltered area, decreasing the shear acting on the tailings surface. Turbulence in the wind flow can also be created by surrounding terrain features and obstacles, and should be taken into account for proper siting of a windscreen.

Virtually all research indicates that an aerodynamic porosity of 50% is close to the optimal value to produce the largest sheltered area. Most commercially available windscreens attempt to reflect this finding; however, the actual measurement of porosity may vary with the manufacturers. (Optical porosity, which is often how porosity is measured, may vary considerably from true aerodynamic porosity).

To date there has been relatively little reported experience with windscreens to reduce wind erosion of storage or tailings piles. However, the use of windscreens to protect highways from blowing and drifting snow is an effective established practice, and many of the principles that govern the use of snow fences should also apply to the use of windscreens on tailings piles (11, 12).

In addition to wind velocity reduction, another potentially important use of windscreens is the recapture of wind-blown tailings on the downwind perimeter of the tailings pile. This system might serve as an effective backup for chemical stabilizers or windscreens, or when other measures are not practical. A downwind screen should not have to be very tall, since most of the eroded tailings would be particles in saltation and would be within 1 to 2 meters of the surface.

WINDSCREEN FIELD TESTING

Due to the size of the materials, laboratory wind tunnel studies of available windscreens were not feasible; therefore, windscreen evaluations were conducted entirely at field test sites. One test was established at the Wyoming test site to evaluate the durability of the windscreens under actual conditions. Test panels of eight commercially available windscreens (Table 5) were erected so as to be exposed to strong prevailing southwest winds. Another field test was established near PNL to study the relative effectiveness of three screen types: 1) vertical wood-slat (Canadian-style) snow fence, 2) woven polyester cloth, 50% porosity - small openings (Julius Koch Dusttamer), and 3) rigid extruded plastic mesh screen, 50% porosity - large openings (DuPont Canada L-300).

TABLE 5. WINDSCREENS EVALUATED AT WYOMING TEST SITE

Windscreen	Distributor	Description	Cost, $/m*
Agrinet wind/ shade screen	Hydrolic Enterprises Casper, WY	Woven polyester	4.40
Athalon snow control fence	Athalon Products Denver, CO	PVC-coated stainless steel wire and fiberglass	11.50
DuPont Canada	Flasher Handling Corp. Buffalo, NY	High-density polyethylene	
L-300 fence		2-in. mesh	4.35
L-36		1/8-in. mesh	5.05
CE-121		3/8-in. mesh	8.25
L-38		3/4-in. mesh	6.20
Julius Koch Dusttamer	KPN International Newton, CT	Woven polyester	13.00
"Canadian" wood-slat snow fence	(generally locally available)	Vertical wood slats and wire	2.60

* Cost per linear meter of a 1.22-m (4-ft) high fence.

Durability Tests

The results of the windscreen durability test conducted at the Wyoming site indicate that there is considerable variation in durability of the tested materials (Table 6). These observations were made after exposure of the screens to nine months (September 1983 to June 1984) of severe weather conditions. The materials were ranked according to their observed relative durability. The most durable materials appeared to be the DuPont Canada materials; in particular the L-300. The least durable were the Julius Koch Dusttamer and the wood-slat snow fence. The poor performance of the Dusttamer, however, was not consistent with the results of other tests of this material. Poor durability was not the result of the material itself but rather of the special slide-lock mounting posts supplied for the material. When sharp edges cut the material soon after the fence was constructed, the damaged section was replaced. Then, during high spring winds, the aluminum posts fatigued from the wind loading and broke off at ground level. No other signs of degradation were evident. The vendor has since been testing other types of mounting posts to eliminate this problem.

TABLE 6. RESULTS OF WINDSCREEN DURABILITY TEST*

Windscreen	Observations†	Ranking‡
Agrinet	Stretched considerably after installation, but no deterioration	5
Athalon	Broken wires and torn cloth from constant winds	6
DuPont Canada		
L-300	Some breaks where stapled to wooden posts, otherwise good shape	1
L-36	Stretched but no degradation	2
CE-121	Stretched like L-36 but otherwise in good condition	3
L-38	Less stretch than L-38 and CE-121; no visible deterioration	4
Dusttamer	Aluminum mounting posts fatigued and broke, causing rips in cloth	8
Wood slat	Wires and slats broken in several places	7

* Installed 9-1-83.

† Observations made during 6-1-84 site visit (9 months exposure to relatively constant winds 10 to 20 m/s).

‡ Ranking based only on durability (1 highest, 8 lowest). Cost, ease of installation, and other factors were not considered.

The deteriorated condition of the wood-slat fence, on the other hand, was less surprising. The wires and wood slats were broken in several places. The other materials showed varying amounts of stretching and some breaking due to the high winds; none showed obvious signs of deterioration from UV exposure, freezing, or other factors.

Performance Tests

The field test at PNL was initiated in November 1983 to evaluate the relative effectiveness/performance of some of the windscreens, and was monitored through July 1984. Wind velocity reductions over a sandy surface were measured behind each of the three screens, and the extent of the leeward zone of reduced velocity was determined (Figure 2). Velocity reduction measurements were normalized with simultaneous measurements taken at the same heights on an identical upwind tower (Figure 3.) The relative size of the zone of reduced wind velocity was considered a measure of their effectiveness at

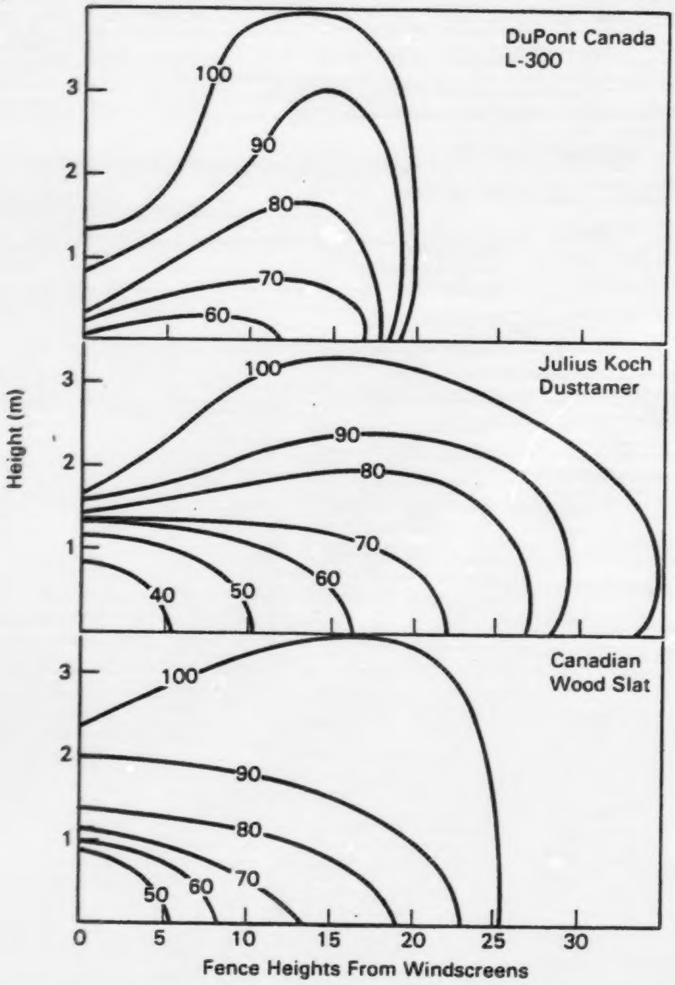

Figure 2. Windscreen velocity reductions above a smooth sand surface at the PNL field test site downwind of three types of windscreens. Curves are labeled as percentages of upwind velocity.

reducing wind erosion. The one with the largest protected zone (i.e., the most effective) was the Julius Koch Dusttamer, which continued to be at least somewhat effective at distances up to 35 times the height of the screen (35 screen heights) measured downwind of the screen. Following were the wood-slat snow fence and the DuPont Canada material in that order. These two had a protected zone of approximately 25 screen heights. This result was not unexpected, since these materials are designed more for capture of suspended particulates than for wind reduction. In this application the DuPont Canada L-300 might perform better than the wood-slat fence, since the height of its protected zone is greater.

To construct a system of windscreens that will effectively protect an area from most potential wind erosion events, the maximum expected velocities

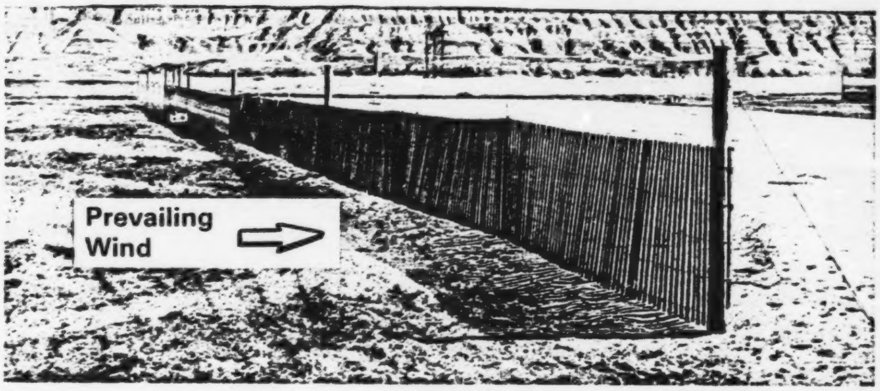

Figure 3. Windscreen field test at PNL evaluating wind reduction performance of 3 windscreens: wood slat (foreground), Dusttamer, and DuPont Canada L-300.

and directions of possible winds must be known. These can be estimated from past weather data for the site. (See the "Case Studies" in the following section.) Given that a 50% reduction would protect an area from all expected erosion-causing events, a series of parallel screens, separated by the distance shown by intersection of the 50% isotach and the surface, would be erected. In addition, however, the design must account for any increased turbulence created by local terrain, which can decrease the efficiency of a screen.

WINDSCREEN CONSTRUCTION COSTS

The costs to construct windscreens for wind erosion protection are complicated by the probability of weather events and the effects of local terrain features on turbulence in windflow patterns. However, some analyses can be made from the results of the field tests. The material costs for the eight tested windscreens ranged from \$2.60 to \$13.00 per linear meter for a 1.2-m-high screen, as shown in Table 5. Based on the field test experience and data from one of the suppliers, a two-man crew and equipment should be able to install about 60 to 75 meters of screen per hour. Using the \$60/hr estimate for manpower and equipment calculated for chemical stabilization, the installation costs are estimated to be \$0.80 to \$1.00/m.

From the results of the performance tests, the cost to protect an area with a single prevailing wind direction (a common occurrence at many mill sites) would range from \$1500 to \$6000/ha (\$600 to \$2400/acre). Highly variable winds would require more extensive windscreen installations, which would substantially increase the costs. The design of a windscreen system is quite flexible; it can range from low free-standing fences to portable modules to massive permanent installations, whichever is most suitable for a particular application. This flexibility offers the mill environmental engineers and operations personnel a wide range of control options.

In general, a windscreen system is expected to cost more, initially, than some chemical stabilizers. Windscreens have the advantage, however, of being essentially passive. They do not need to be powered or renewed, and they do not contain chemicals that may adversely affect the mill process or environment. They should last considerably longer than chemicals (perhaps three to five years or longer if properly maintained). If so, windscreens may be more cost effective than chemical stabilizers, again depending on site-specific factors.

HYPOTHETICAL CASE STUDIES

PURPOSE

This section provides examples to compare the use of chemical stabilizers and windscreens on a hypothetical uranium mill tailings pile that incorporates features common to the majority of existing tailings piles. However, it must be understood that specific conditions at actual sites will vary from this model, and would necessitate the development of site-specific erosion control plans.

ASSUMPTIONS

For the hypothetical tailings pile in this evaluation, the following parameters were assumed:

* size - 40.5 ha (100 acres)

* shape - square, 636 x 636 m

* height - 20 m above surrounding level terrain

* status - currently inactive, no ponded water, tailings sufficiently consolidated to support stabilization equipment

* location - similar to Wyoming field-test site since information is available on delivered prices of materials and environmental conditions

* climate - semiarid, seasonal
  - annual rainfall 25 to 40 cm
  - summer high temperatures ~35 to 40°C
  - winter low temperatures ~-30°C
  - peak winds 22 m/s from one prevailing direction (west)
  - light variable winds do not cause erosion of tailings

- material availability - chemical stabilizers and windscreens tested at Wyoming test site available at same prices; equipment necessary to apply chemical stabilizers and to construct windscreens already available.

CASE 1: CHEMICAL STABILIZATION

The cost to initially stabilize a tailings pile, presented in Table 4, ranges from $680 to $3600/ha for the field-tested stabilizers. The annual cost to apply chemical stabilizers, based on their expected effective lifetimes, ranges from $1700/ha/yr to $19,000/ha/yr, as previously shown in Table 4. Therefore, the annual costs to stabilize a 40-ha tailings pile under the same conditions as the field test could range from a low of $68,000/year to a high of $760,000/year. Areas of high wind shear, such as at the crest of dikes, would require heavier or more frequent applications, and would increase the overall costs.

CASE 2: WINDSCREENS

The proper use of windscreens for effective wind erosion control, as previously discussed, requires more detailed information on wind, site topography, and windscreen performance than for chemical stabilization. However, some of the assumptions made about the hypothetical site will simplify the model for the purpose of this illustration.

The Julius Koch Dusttamer windscreen was selected for this analysis. Previous studies, including the PNL field test, show this type of screen to have one of the largest sheltered zones behind the windscreen (Figure 2). Additionally, a screen such as one of the DuPont Canada materials could be used on the downwind perimeter of the pile to recapture blowing particles if necessary.

In general, the threshold velocity for this type of particulate tailings material, as measured 3 m or higher above the ground, would be about 11 m/s (25 mph). Recorded peak wind speeds are assumed to be 22 m/s (50 mph) from the west. Therefore, to prevent blowing tailings the minimum design for a windscreen system would be to place parallel screens across the pile at separations which provide 50% velocity reduction on the surface.

As seen in Figure 2, for the Dusttamer windscreen the 50% isotach (where the resultant wind velocity is reduced to 50% of the incoming wind velocity) extends laterally to about 10 times the fence height (10H). Assume that the raised tailings pile would not increase the turbulence in the wind flow. (In reality the elevated tailings pile would probably result in accelerated wind flow and increased turbulence along the crest of the upwind dike.) For proper windscreen installation, then, the first row would be placed along the crest of the upwind dike. The next parallel row would be constructed at a distance of about 10H from the first screen. Succeeding screens would only have to be placed at intervals of approximately 35H, or at the 100% isotach; since at that point the incoming wind to each succeeding screen is only 50% of the original upwind velocity. This spacing of parallel windscreens is illustrated in Figure 4.

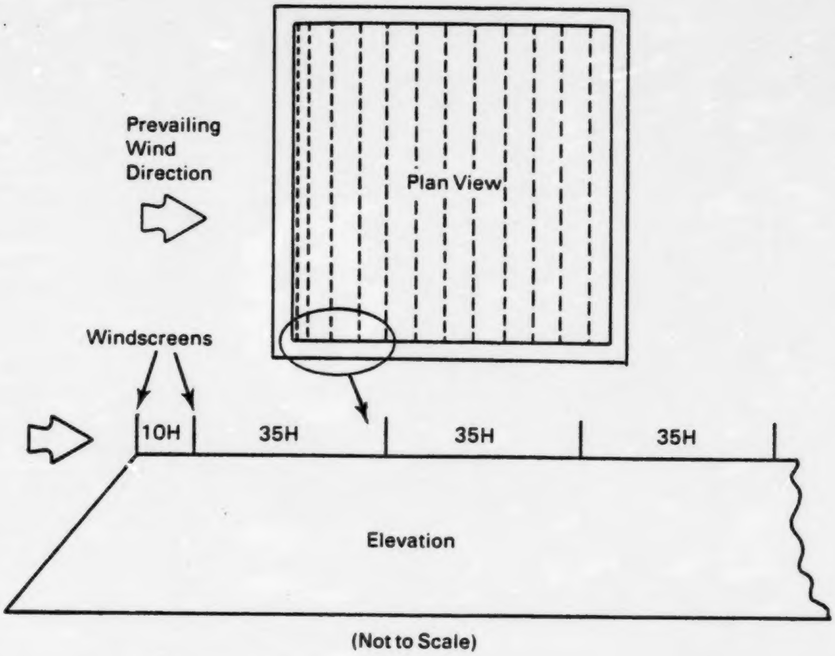

Figure 4. Illustration of hypothetical tailings pile showing parallel rows of windscreens constructed perpendicular to prevailing wind direction.

For a 1.2-m windscreen this system would require 15 rows of windscreens across the tailings pile for total protection from the expected winds, or a total of 9540 m of screen. At $13.00/m (Table 5) the total installed cost for the 40-ha site would be $124,000, or $3000/ha. The costs for a somewhat taller windscreen, 1.8 m (6 ft), may be less, since fewer rows would be required and the installation time might therefore be shorter. (A 1.8-m screen is assumed to require about the same time and effort to install as a 1.2-m screen.) However, screens much taller than 1.8 m increase the installation costs to the point of impracticality unless there were other justifications, such as accessibility of the tailings after erection of the screens.

DISCUSSION

Although the initial cost of a windscreen system may be more than for some chemical stabilizers, the long-term (3- to 5-year) cost should be less, even including maintenance costs. With proper maintenance most windscreen systems should last a minimum of 3 to 5 years, giving an annual cost of $27,000 to $45,000/yr for the site, including some estimate for maintenance. These estimated costs are substantially less than the expected annual cost to chemically stabilize the 40-ha site, even using the most cost effective (as tested) stabilizer. In addition, some windscreen systems may qualify as capital investments for most companies, which then may qualify for investment tax credits. Also, new tax laws may allow depreciation of the system costs over a period of a few years. These factors help to further reduce the actual cost of a windscreen system. Chemical dust suppressants are not subject to the same tax incentives.

These comparisons of chemical stabilizers and windscreens for wind erosion control of tailings piles are highly simplified. The assumptions made for these examples are reasonable, but certainly much more information would have to be considered to make a proper selection of a wind erosion control system for a specific site. However, this analysis does illustrate that the use of a series of parallel windscreens (a relatively new technology for erosion control) across an erodible surface may be more cost effective than the more conventional method of chemical stabilization. Under certain circumstances, careful analysis may show that a combination of both chemicals and windscreens may provide the optimal method of control.

REFERENCES

1. Schwendiman, L.C., Sehmel, G.A., Horst, T.W., Thomas, C.W., and Perkins, R.W. A field and modeling study of wind-blown particles from a uranium mill tailings pile. NUREG/CR-1407, PNL-3345, Pacific Northwest Laboratory, Richland, Washington, 1980.

2. Leroy, J.C. How to establish and maintain growth of tailings in Canada — cold winters and short growing seasons. In: Tailings Disposal Today, Proceedings of the International Tailings Symposium. Miller Freeman Publications, San Francisco, California, 1973.

3. Dean, K.C. and Havens, R. Comparative costs and methods for stabilization of tailings. In: Tailings Disposal Today, Proceedings of the International Tailings Symposium. Miller Freeman Publications, San Francisco, California, 1973.

4. Johnson, M.S. and Bradshaw, A.D. Prevention of heavy metal pollution from mine wastes by vegetative stabilization. The Institution of Mining and Metallurgy Transactions, London, England, April 1977.

5. Li, C.T., Elmore, M.R., and Hartley, J.N. A review of fugitive dust control for uranium mill tailings. NUREG/CR-2856, PNL-4360, Pacific Northwest Laboratory, Richland, Washington, 1983.

6. Elmore, M.R. and Hartley, J.N. Laboratory testing of chemical stabilizers for control of fugitive dust emissions from uranium mill tailings piles. NUREG/CR-3697, PNL-5025, Pacific Northwest Laboratory, Richland, Washington, 1984.

7. Elmore, M.R. and Hartley, J.N. Field testing of fugitive dust control techniques at a uranium mill tailings pile - 1982 field test, Gas Hills, Wyoming. NUREG/CR-3510, PNL-4798, Pacific Northwest Laboratory, Richland, Washington, 1983.

8. Bagnold, R.A. The physics of blown sand and desert dunes. Methuen and Co., Ltd., London, England, 1954.

9. Belly, P. Sand movement by wind. Defense Documentation Center for Scientific and Technical Information, 1964.

10. Gillette, D.A. On the production of soil wind erosion aerosols having the potential for long-range transport. Special Issue of Journal de Researches Atmospheriques, the Nice Symposium of the Chemistry of Sea-Air Particulate Exchange Processes, Nice, France, 1973.

11. Tabler, R.D. Predicing profiles of snowdrifts in topographic catchments. In: Proceedings of the Western Conference, 43:87-97, April 1975.

12. Tabler, R.D. Self-similarity of wind profiles in blowing snow allows outdoor modeling. Journal of Glaciology 26:94, 1980.

Session 20: DRY SO_2 REMOVAL I

Richard G. Rhudy, Chairman
Electric Power Research Institute
Palo Alto, CA

MODELING OF SO_2 REMOVAL IN SPRAY-DRYER FLUE-GAS DESULFURIZATION SYSTEM

by: Ashok S. Damle and Leslie E. Sparks*
Research Triangle Institute
Research Triangle Park, NC 27709

*U.S. Environmental Protection Agency
Industrial Environmental Research Laboratory
Research Triangle Park, NC 27711

ABSTRACT

This paper presents a mathematical model of the SO_2 removal process in a spray-dryer flue-gas desulfurization system. Simultaneous evaporation of a slurry droplet and absorption/reaction of SO_2 in the droplet are described by the corresponding heat- and mass-transfer rate relations. Dissolution kinetics of lime particles within a slurry droplet is included in determining the overall SO_2 removal rate. The model identifies several parameters which need to be estimated or determined from experimental data. The model predictions of the effects of major parameters, such as approach to saturation and stoichiometric ratio on the SO_2 removal efficiency, follow observed trends. Comparison of the model predictions with one set of pilot-plant data shows very good agreement.

This paper has been reviewed in accordance with the U.S. Environmental Protection Agency's peer and administrative review policies and approved for presentation and publication.

INTRODUCTION

Spray drying technology for SO_2 absorption/removal from flue gases has been advanced for the past few years. In spite of a large amount of pilot-plant testing and a few full-scale commercial applications, however, there is still a lack of comprehensive predictive modeling of this process. A review of qualitative mechanisms so far proposed was published recently (1, 2). Semi-empirical relationships have been developed to relate SO_2 removal efficiency of the spray dryer system with stoichiometric ratio and approach to saturation (3, 4). Such relationships, due to the empirical parameters, tend to be specific for the spray dryer system used to obtain them.

This paper presents a simple mathematical model describing various processes occurring in a spray-dryer flue-gas desulfurization (FGD) system. The overall process is subdivided into subprocesses contributing to SO_2 removal. Various parameters required for such a model are identified. An overall qualitative picture is described first in this paper, followed by modeling of the different subprocesses.

OVERALL PROCESS

In a spray-dryer SO_2 removal system, a conventional spray dryer is typically used to contact SO_2-laden flue gas with spray droplets of a slurry or a solution of a suitable sorbent. A typical schematic of a spray dryer system is shown in Figure 1. Rotary or pneumatic atomizers are used to inject the sorbent slurry/solution. Amount of sorbent added depends upon stoichiometric ratio to be used and the inlet flue gas SO_2 concentration. Amount of water added into the system is controlled by inlet flue gas temperature and humidity, and the desired approach to saturation at the spray dryer outlet. Lime slurry is typically prepared in a slaker to obtain a slurry of fine-grained lime particles. Although lime is predominantly used as a sorbent, some studies have also been conducted with sodium carbonate and bicarbonate which are highly soluble and are therefore injected in a solution form. Flue gas is usually introduced at the top of spray dryer cocurrently with the sorbent, but other configurations are also possible. The flue-gas residence time is typically about 10 seconds. After the spray dryer, the flue gases, along with flyash and dried sorbent/product particles, pass through particulate control equipment, such as a baghouse or an electrostatic precipitator. Some particulate collection may also occur in the spray dryer itself.

In the spray chamber, two processes occur simultaneously: water evaporates from the droplet; and SO_2 is absorbed in, and reacts with, the alkaline sorbent. The flue gas is typically humidified adiabatically to within 20° to 60°F* of its saturation temperature. The sorbent in the spray droplets, along with the reaction products, is evaporated to apparent dryness up to a certain equilibrium moisture content and entrained in the flue gas. The

---

*Use the equation °C = 5/9 (°F-32) to convert to the equivalent metric unit.

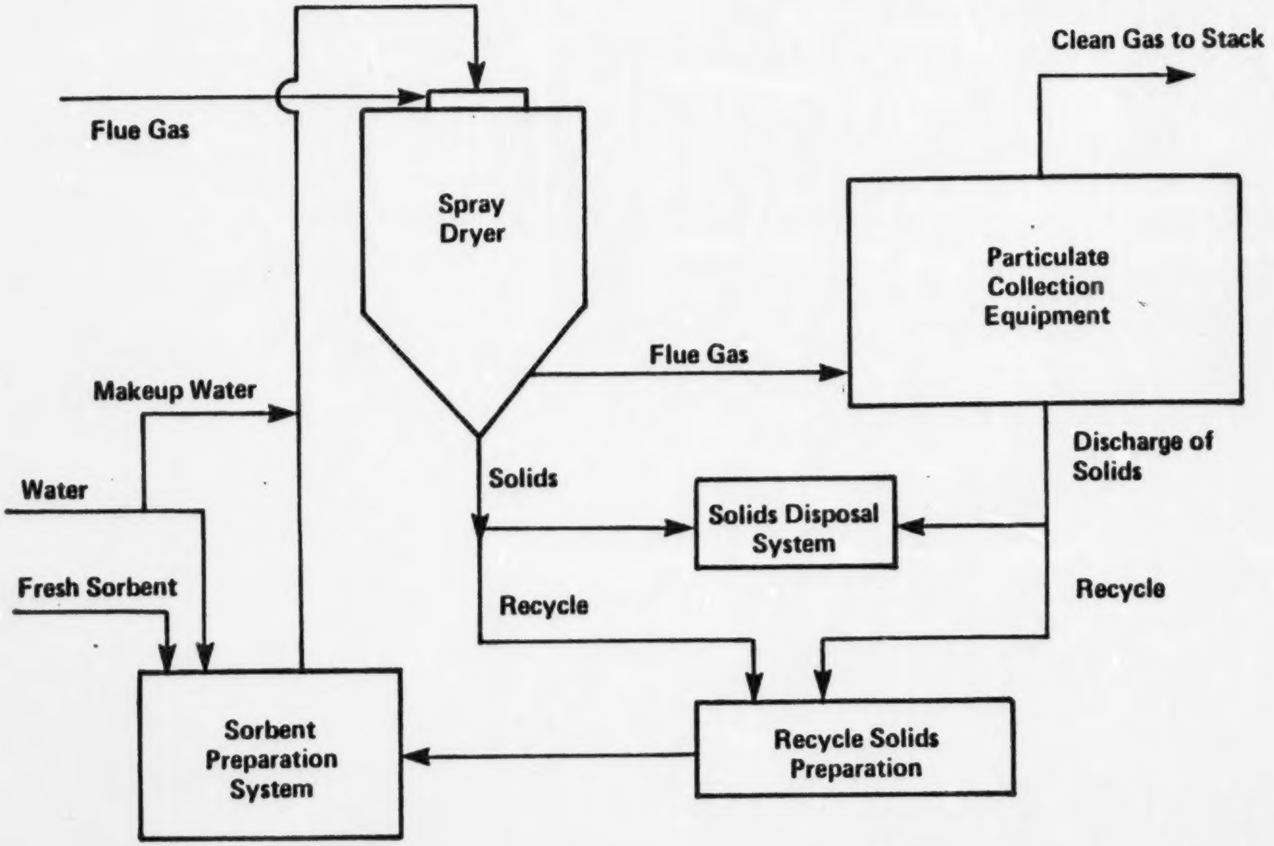
Flue Gas
Spray Dryer
Clean Gas to Stack
Particulate Collection Equipment
Flue Gas
Makeup Water
Water
Fresh Sorbent
Solids
Solids Disposal System
Discharge of Solids
Recycle
Recycle
Sorbent Preparation System
Recycle Solids Preparation

Figure 1. Simplified flow diagram of a spray-dryer FGD system.

resulting solid particles are removed in a particulate collection device. The amount of water evaporated from a droplet is determined by the operating conditions of the dryer-inlet gas temperature, inlet gas relative humidity, approach to saturation temperature, and corresponding equilibrium moisture content of the solid. SO_2 may be removed by the sorbent both during and after drying of droplets. It is commonly believed that most of the SO_2 is removed before the slurry droplets are dried. Spray dryer operation nearer to flue-gas saturation condition and higher stoichiometric ratios improve SO_2 removal efficiencies. SO_2 removal may continue through the particulate collection equipment as gas passes through filter cake in the baghouse or over the deposits on the collection plates in case of an electrostatic precipitator. A portion of the waste particulate discharge from the spray dryer and the particulate collection device may be recycled into the spray dryer's feed slurry to increase the sorbent utilization.

Although droplet evaporation and SO_2 absorption occur simultaneously, the droplet drying process is more or less independent of the SO_2 absorption process. On the other hand, the SO_2 absorption/reaction process has been observed to be strongly related to the drying process and droplet moisture content. Thus, the drying process may be considered first to estimate the drying time of a droplet, rate of drying, and the droplet moisture content with time. The SO_2 absorption is then considered to determine the rate of absorption/reaction and the SO_2 removal during the droplet drying process. SO_2 absorption/reaction occurs both before and after drying of the droplets in the spray chamber and continues through the particulate collection device until the dried droplet is deposited.

DRYING OF DROPLETS

When sorbent is introduced in the slurry form, the slurry feed to the spray absorber is usually 60-95 percent moisture and contains finely divided, solid, sorbent particles suspended in liquid medium. The drying behavior of a slurry droplet with freely moving sorbent particles is similar to that of a solution droplet. In line with conventional drying theory (5), the evaporation from a slurry/solution droplet may be expected to proceed in two stages. In the first stage, the solid's concentration does not affect evaporation rate, and this stage continues until the moisture level falls below a critical moisture content. During this stage, similar to the conventional constant drying-rate stage, the rate of evaporation is solely determined by the resistance of the gas film surrounding the droplet to the transfer of water vapor. In case of a solution droplet, the solid phase appears during this stage as the amount of water remaining in the droplet is reduced. In the second stage, the solid's concentration reduces the rate of drying, since the moisture must diffuse through the solid matrix. During this stage, there is a change from water as a continuous phase, initially in the droplet, to the solid matrix as a continuous phase; the solid individual particles touch each other and are no longer mobile in the droplet. The drying continues until the droplet moisture content reaches an equilibrium with the surrounding gas atmosphere. The drying behavior of droplets in a spray chamber has been studied extensively, at least for the first stage (6, 7, 8, 9, 10). The drying processes in the two stages are considered in the following section.

CONSTANT RATE OF DRYING PERIOD

The rate of droplet drying in this period is determined by the simultaneous heat transfer from gas phase to the droplet, and mass transfer from the droplet to the gas phase. The heat and mass transfer processes between a droplet and surrounding gas phase have been studied extensively (11, 12). The respective transfer coefficients may be determined by the widely used empirical correlations by Ranz and Marshall (12):

$$Sh = 2 + \alpha\, Re^{\beta} Sc^{\gamma} ,$$

$$Nu = 2 + \alpha\, Re^{\beta} Pr^{\gamma} , \qquad (1)$$

where Sh = Sherwood Number for mass transfer ($k_d d_d/D$); Nu = Nusselt Number for heat transfer (hd_d/k); Re = Reynolds Number based on droplet diameter and relative velocity between droplet and air ($d_d v\rho/\mu$); Sc = Schmidt Number ($\mu/\rho D$); Pr = Prandtl Number ($C_p \mu/k$); k_d = gas-phase mass-transfer coefficient; d_d = droplet diameter; D = gas-phase diffusivity; h = convective heat-transfer coefficient; k = gas-phase thermal conductivity; v = relative velocity between droplet and gas phase; ρ = gas-phase density; μ = gas-phase viscosity; and C_p = gas-phase specific heat. The best fit values for constants α, β, and γ, as given by Ranz and Marshall (12), are 0.6, 0.5, and 0.33, respectively.

To use the above correlations, the relative velocity between air and a droplet, v, is required. The movement of droplets in a spray chamber is highly complicated, but may be broken down into two stages: 1) deceleration, and 2) free fall, with respect to air. Droplets often have very high initial velocity leaving the atomizer and are first decelerated due to the resistance of the surrounding air to a steady-state free-fall velocity. In the second stage the droplet may be considered to move at the free-fall velocity. The deceleration time depends upon the droplet diameter and is usually very short. For example, a 100-μm droplet may be decelerated from 67 m/sec to 5 m/sec within 0.0185 second (6), and for smaller droplets less time would be required. Since this period is usually of short duration (less than 0.1 second), its contribution to drying of the droplet and SO_2 removal may be ignored. The free-fall velocity of the droplets in the air may be approximately determined by Stokes' Law as:

$$v = \frac{(\rho_1 - \rho)\, g\, d_d^2}{18\, \mu} , \qquad (2)$$

where, ρ_1 = density of droplet and g = acceleration due to gravity. Ideally, a three-dimensional momentum balance equation should be considered for the droplet and gas phase to determine droplet trajectories and relative velocities in the spray chamber. However, only one-dimensional gas phase and droplet flow is considered here for model simplicity.

If the effect of relative velocity is ignored ($v = 0$), Equation (1) simplifies to:

$$Sh, Nu \approx 2 . \quad (3)$$

For droplet temperature T_d, bulk gas temperature T_g, bulk water vapor mole fraction $x_{g,w}$, and equilibrium vapor-mole fraction at droplet surface $x_{d,w}$ (see Figure 2a), the respective rates of mass (N_w) and heat transfer (Q) are given by:

$$N_w = k_d \, \pi d_d^2 \, c(x_{d,w} - x_{g,w}) , \quad (4)$$

and

$$Q = h \, \pi d_d^2 \, (T_g - T_d) , \quad (5)$$

where c = mean molar density of the gas phase, N_w = the molar rate of mass transfer (evaporation of water), Q = rate of heat transfer, and h = heat transfer coefficient.

The above equations, however, do not take into account the effect of water evaporation on the heat and mass transfer rates. For a quiescent droplet-gas system ($v = 0$) (Figure 2b), a rigorous analysis, taking into account the above effects, leads to the following expressions:

$$N_w = 2\pi \, D_{water\text{-}air} \, c \, d_d \, \ln\left[\frac{1 - x_{g,w}}{1 - x_{d,w}}\right], \quad (6)$$

and

$$Q = 2\pi \, k \, d_d \, (T_g - T_d) \left(\frac{\varepsilon}{e^{\varepsilon} - 1}\right) , \quad (7)$$

where e = base for natural logarithm, and ε = dimensionless heat-transfer rate factor and, for water, is given by:

$$\varepsilon = \frac{9}{\pi} \frac{N_w C_p}{k \, d_d} , \quad (8)$$

where C_p = specific heat of water vapor.

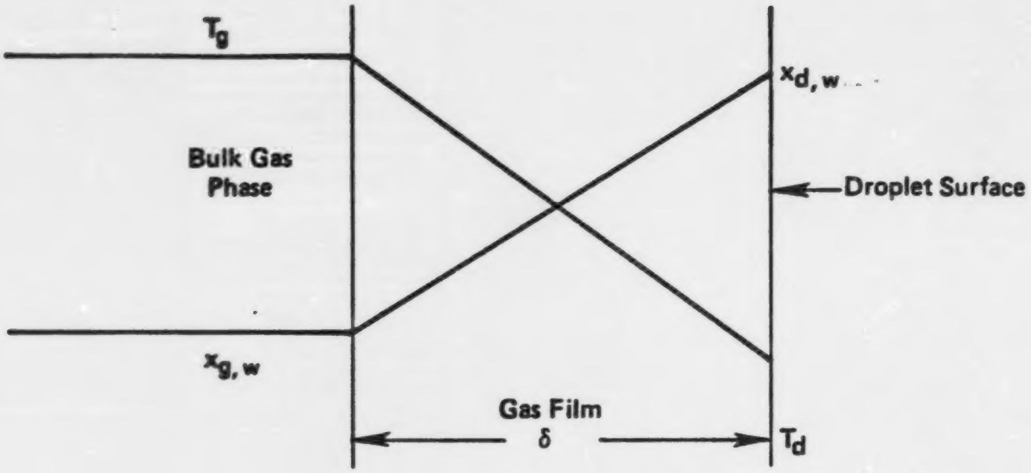
T_g
$x_{d,w}$
Bulk Gas Phase
Droplet Surface
$x_{g,w}$
Gas Film
δ
T_d

Figure 2a. Gas-phase concentration and temperature gradients near a moving droplet.

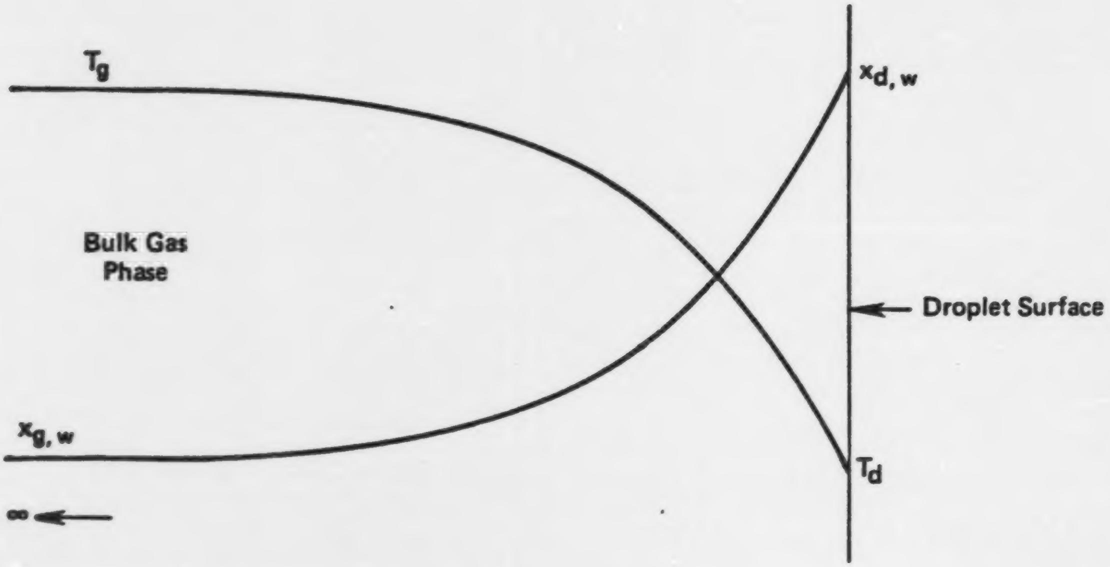
T_g
$x_{d,w}$
Bulk Gas Phase
Droplet Surface
$x_{g,w}$
T_d
∞

Figure 2b. Schematic of quiescent droplet-gas system.

Equations (6) and (7) take into account the effect of evaporation of water on the rates of heat and mass transfer, and they approach Equations (4) and (5) for low droplet Reynolds Number when Sh, Nu ≈ 2, and for low rates of water evaporation.

FALLING RATE OF DRYING PERIOD

The constant rate-drying process continues until the moisture content of the droplet falls below a critical moisture content at which the solid's concentration begins to influence the drying rate. Critical moisture content of the droplet is also a property peculiar to its solids properties such as hygroscopicity (13). The critical moisture content may be considered as the one at which the solid particles begin to touch each other and form a continuous phase. The drop diameter then does not change during further drying (14). This period continues until the moisture content reaches an equilibrium value.

In this period, drying is controlled by diffusion of moisture through the solid matrix. The drying rate may be assumed to fall linearly between the critical-moisture content and equilibrium-moisture content, and may be expressed by:

$$\text{Rate of Drying} = \left(\begin{array}{c}\text{Rate of drying based on}\\ \text{gas-phase resistance alone}\end{array}\right)\left(\frac{X - X_e}{X_c - X_e}\right) , \qquad (9)$$

where X = droplet moisture content at time t, wt. % dry basis; X_e = equilibrium-moisture content, wt. % dry basis; and X_c = critical-moisture content, wt. % dry basis. The rate of drying, based on gas-phase resistance alone, is determined using equations developed earlier in this paper. The parameters, critical-moisture content and equilibrium-moisture content, depend upon the solid's content and their properties and must be determined experimentally. The critical-moisture content for lime, clay, etc., is typically in the range of 25-60 percent moisture. Solid's properties, such as hygroscopicity and deliquescent nature, and the relative humidity of surrounding gas determine the equilibrium-moisture content. For given solids, equilibrium-moisture content varies linearly with respect to relative humidity of the surrounding gas phase.

In a given spray-dryer system, the final moisture content at the spray-dryer exit may be expected to be close to the equilibrium-moisture content. The final moisture contents in droplets at the spray-dryer exit were reported by Felsvang (15) from a pilot-plant study and were found to depend upon the approach to saturation temperature and the droplet size. The fact that moisture content depends on droplet size indicates that the larger droplets did not reach an equilibrium state by the end of spray drying in this particular study. The measured moisture contents in this study ranged from 0.5 to 1.5 percent for "very fine" droplets and 0.5 to 3.0 percent for "fine" droplets. There seem to be a lot of variations in measured values of solid's moisture content at the spray-dryer outlet as reported in the literature.

For example, Stevens et al. (16) reported measured values of moisture content which ranged from 5 to 20 percent, which is almost an order of magnitude higher than those in Felsvang's (15) work. Stevens et al. (16) also reported variations in moisture content with residence time and atomizer speed for the same approach to saturation, indicating that the droplets had not reached an equilibrium-moisture level.

Determination of equilibrium-moisture content is very important to estimate the drying time of the droplet in this second period. This is also critical for prediction of SO_2 removal, as the aqueous reactions may be assumed to continue until the droplet reaches low enough moisture content. High equilibrium-moisture content may enhance continued SO_2 removal after the droplet is "dried" to its equilibrium moisture value.

The critical-moisture content divides the total drying time in the above-mentioned two stages and is thus important as different drying-rate relations apply in each stage. The drying time required for each stage may be determined using the appropriate drying-rate expression and the parameters, critical- and equilibrium-moisture content of solids.

SO_2 ABSORPTION/REACTION IN SPRAY DRYER

Absorption and reaction of SO_2 in a sorbent droplet occurs both before and after drying of the droplet up to an equilibrium-moisture content. Presence of moisture during wet-droplet stage plays an important role as it provides an aqueous medium for absorption and fast ionic reaction of SO_2. The lack of moisture in dry-particle stage considerably reduces the rate of SO_2 removal as absorption and reaction in solid phase is likely to be slower. This is especially true for the lime sorbent which has a low reactivity in solid phase. The mechanisms of SO_2 removal in the two stages are distinctly different and, therefore, will be considered separately.

WET-PARTICLE STAGE

During the wet stage, moisture in the droplet participates actively in the overall SO_2 removal process. SO_2 is transported from the bulk-gas phase to the droplet surface by gas-phase diffusion process. The dissolved SO_2 migrates from the interface to the interior of the droplet by liquid-phase diffusion and reacts with the dissolved sorbent. If a sparingly soluble sorbent, such as lime, is used, dissolution of sorbent also becomes important. If the ionic reaction between sorbent and SO_2 is considered as very fast, both species may migrate to a reaction plane or zone in the bulk liquid as shown in Figure 3. The dissolution process will not be present in case of a highly soluble sorbent, but the overall process may still be represented by Figure 3 by replacing the equilibrium-solubility sorbent concentration by the bulk liquid-phase sorbent concentration.

The above picture is easier to visualize for a wet droplet with a moisture content greater than the critical moisture content when the sorbent particles are freely moving. The above processes become less obvious during further drying as the water phase becomes discontinuous. Nevertheless, for

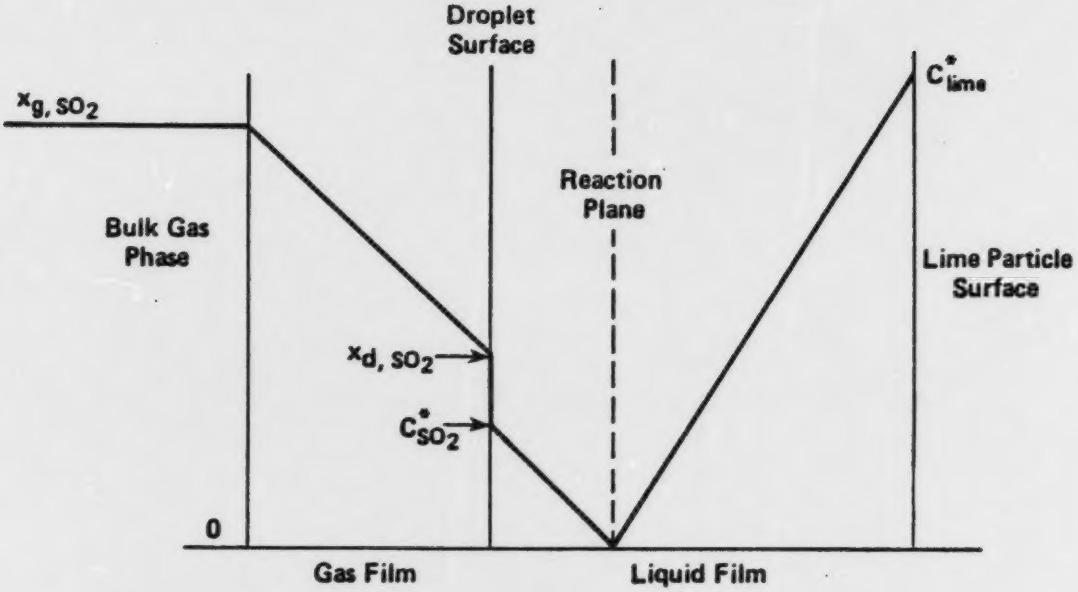
Droplet Surface
x_{g, SO_2}
C^*_{lime}
Reaction Plane
Bulk Gas Phase
Lime Particle Surface
x_{d, SO_2}
$C^*_{SO_2}$
0
Gas Film
Liquid Film

Figure 3. Schematic of SO_2 absorption/reaction in a wet droplet.

model simplicity, the moisture held within particle interstices may still be assumed to provide enough aqueous medium for the SO_2 absorption process. SO_2 removal during the wet stage by the above mechanism may be assumed to continue till the moisture content in the droplet falls to a certain low level, the lower limit being the equilibrium moisture content. After that, the droplet may be considered as a dry-porous solid to determine further SO_2 removal. Specific steps that are involved in the removal of SO_2 during a wet-droplet stage may be described as follows:

1. Transfer of SO_2 from bulk-gas phase to droplet/particle surface. The rate of transfer in this step is controlled by the resistance of a gas film around the droplet.

2. Dissolution of SO_2 into the liquid phase in the droplet, and transfer of dissolved SO_2 from the droplet surface to interior liquid. The transfer rate is controlled by the liquid-film resistance in this step.

3. Dissolution of lime into the liquid phase.

4. Ionic reaction between dissolved SO_2 and dissolved lime in liquid phase.

Gas-Film Resistance

Diffusion of SO_2 from the bulk-gas phase to the droplet surface is similar to water evaporation from the droplet surface, and similar correlations apply.

The Sherwood Number for mass transfer is given by:

$$Sh = 2 + 0.6\ Re^{0.5}\ Sc^{0.33}\ , \qquad (1')$$

and in a limiting case for small droplets and low Reynolds Number (as discussed earlier in this paper), $Sh \approx 2$. The rate of SO_2 transfer, N_s, from gas phase to droplet surface would then be given by:

$$N_s = k_d(\pi d_d^2)\ c\ (x_{g,s} - x_{d,s})\ , \qquad (10)$$

where $x_{g,s}$ and $x_{d,s}$ are mole fractions of SO_2 in gas phase at the bulk gas and at the droplet surface, respectively [see also Equation (4)].

The above formulation does not, however, take into account the effect of water evaporation on SO_2 diffusion. This may be done in a rigorous analysis for a quiescent droplet-air system which gives the rate of SO_2 mass transfer under condition, $N_w >> N_s$, as:

$$N_s = \frac{x_{g,s} N_w}{F - 1} - \frac{N_w x_{d,s} F}{F - 1} , \qquad (11)$$

where $F = \exp (N_w / 2\pi \, D_{SO_2\text{-air}} \, c \, d_d)$.

The rate of SO_2 transfer from gas phase to droplet surface, as given by Equations (10) and (11), is strongly dependent on SO_2 concentration in the bulk-gas phase.

Liquid-Film Resistance

No good correlations are available to estimate the liquid-phase resistance in the droplet to the mass transfer. An order of magnitude estimate may be obtained. For a droplet diameter of 25-50 μm containing primary lime particles of the order of 1-5 μm, the liquid-film thickness, δ, at the surface contributing this resistance may be considered to be of the order of 1 μm. The liquid-phase mass transfer coefficient may then simply be obtained as the ratio of diffusivity of SO_2 in liquid and δ:

$$k_1 = \frac{D_{SO_2\text{-water}}}{\delta} \approx 0.17 \text{ cm/sec} , \qquad (12)$$

Important consideration should be given to the enhancement of this liquid film mass-transfer coefficient due to the very fast reaction of dissolved SO_2 with dissolved lime in the bulk liquid. From the theory of mass transfer with chemical reaction in liquid phase (17), this enhancement may be expected to be on the order of ϕ:

$$\phi = 1 + \frac{D_{\text{lime-water}} \, C^*_{\text{lime}}}{D_{SO_2\text{-water}} \, C^*_{SO_2}} , \qquad (13)$$

where D = diffusivity, and C^* = equilibrium solubility concentration.

Calculations using typical diffusivity and solubility values indicate that, due to this enhancement factor, ϕ, the liquid-phase resistance to SO_2 mass transfer is two orders of magnitude smaller compared to gas-phase resistance (18). Therefore, the liquid-phase resistance may be ignored in model simulations without significant error.

Dissolution of Lime

This step is obviously required only for sorbents such as lime which are sparingly soluble in water. Rate of dissolution of lime may be approximately estimated using the diffusivity of lime in water, its solubility, and the average distance between lime particles in the droplet. Based on a simple film model (Figure 3), the rate of lime dissolution from a single lime particle, R_p, suspended in a lime slurry droplet is given by:

$$R_p = D_{\text{lime-water}} \# d_p^2 \left(\frac{C_1^* - C_1}{\delta}\right) , \tag{14}$$

where d_p = average primary lime particle diameter; C_1^* = equilibrium solubility concentration of lime in water; C_1 = concentration of lime in bulk solution; and δ = liquid film thickness responsible for lime dissolution and may be approximated to half of the interparticle distance between lime particles suspended in a droplet.

For particle diameter, d_p, and moisture-volume fraction, w, the film thickness, δ, based on interparticle distance, may be given for a cubical particle arrangement as:

$$\delta = d_p\left(\frac{0.973}{(1-w)^{1/3}} - 1.0\right). \tag{15}$$

For fast reaction between dissolved SO_2 and lime, both the species diffuse to a reaction front where $C_1 \approx 0$. The rate of lime dissolution from all lime particles in a droplet, R_d, assuming a discrete primary lime particle-size distribution with I size channels, is given by:

$$R_d = \sum_{i=1}^{I} R_{p,i} \, n_i , \tag{16}$$

where $R_{p,i}$ = rate of lime dissolution from a single lime particle of size $d_{p,i}$, and n_i = number of lime particles of size $d_{p,i}$ in a droplet. The above equations are of course approximate, and better correlation should be developed by carrying out lime-dissolution experiments.

Liquid-Phase Reaction Rate

For a finite liquid-phase reaction rate for the reaction between dissolved SO_2 and sorbent, it may be necessary to consider its effect on overall removal of SO_2. Since the concentration of dissolved sorbent (e.g., lime) is usually in large excess to dissolved SO_2 concentration, the reaction rate may be expected to depend predominantly on liquid-phase SO_2 concentration. The rate of reation in such a case may be expressed by:

$$N_s = k_r \frac{\pi d_d^3}{6} w\, C_{SO_2,l}$$

$$= k_r \frac{\pi d_d^3}{6} w \frac{c\, x_{d,s}}{H} , \tag{17}$$

where k_r = volumetric reaction rate coefficient; w = volume fraction of liquid in droplet; $C_{SO_2,l}$ = liquid-phase SO_2 concentration; c = molar density of gas phase; $x_{d,s}$ = mole fraction of SO_2 in the gas phase at the droplet surface; and H = Henry's Law constant.

Equation (17) may be combined with Equation (10) to obtain a reduction factor, ψ, for the gas-phase mass transfer:

$$\psi = \frac{1}{1 + \frac{6H\, k_d}{d_d w\, k_r}} = \frac{\text{rate of mass transfer with finite liquid-phase reaction rate}}{\text{rate of mass transfer with gas-phase resistance alone}} . \tag{18}$$

For infinite liquid-phase reaction rate ($k_r \longrightarrow \infty$), of course $\psi = 1$.

In case of infinite liquid-phase reaction rate, the controlling mechanisms of SO_2 removal will be determined by relative values of N_s and R_d as given by Equations (11) and (16) for SO_2 gas-phase mass transfer and lime dissolution rate, respectively. If $N_s \geq R_d$, the overall SO_2 removal rate will be controlled by lime dissolution rate and given by R_d. On the other hand if $N_s < R_d$, the gas-phase mass-transfer resistance to SO_2 transfer will control its removal rate.

Effect of Product Precipitation

In developing above relations, the effect of product formation is ignored. The reaction products of lime (e.g., $CaSO_3$ and $CaSO_4$) have low solubility and would therefore precipitate within the droplet. As this precipitation may take place on existing lime particles, it may affect the lime dissolution rate. In deriving relationships for the rate of lime dissolution, it was assumed that all the particle surface area is available for dissolution. The reduction in lime dissolution rate would be directly proportional to surface area of a lime particle obstructed by product precipitation. In the early stages of drying, this effect would tend to be minimal because of the mobility of lime particles within a droplet and also due to the low level of product formation. This effect would increase significantly as the solid phase becomes the continuous phase, since the immobility would allow the precipitated product layer to build up on the lime particle surface. A simpler way to account for this effect in the model is to ignore it in the early stages until moisture content falls to the critical moisture content, and in later stages consider the dissolution rate to be proportional to the lime fraction remaining in the solid phase.

DRY-PARTICLE STAGE

As the droplet dries and moisture content approaches the equilibrium moisture level, diffusion of SO_2 into the solid matrix becomes important. Primary sorbent particles form a continuous solid-phase matrix and become immobile, and the SO_2 removal process thus becomes that of SO_2 diffusion through solid matrix with chemical reaction. Analysis of SO_2 absorption during this dry-particle stage may be carried out in a rigorous approach of diffusion of SO_2 into a spherical solid matrix with chemical reaction. For this approach, both the diffusivity of SO_2 in the solid matrix and the reaction coefficient are needed. The local reaction rate depends upon the local SO_2 concentration, reaction-rate coefficient, and local mass fraction of lime in the solid. Such rigorous analysis may be simplified for cases in which either the diffusion process in the solid matrix or the chemical reaction in the solid matrix is dominant over the other. For a fine porous sorbent particle, the diffusion process may be considered to be much faster compared to the reaction rate, in which case the SO_2 concentration throughout the particle will be uniform and equal to the gas-phase concentration. The reaction will then proceed throughout the volume of the particle, and may be expressed by a bulk-volume reactivity (K_r) for the entire dried particle. This reaction coefficient would depend upon the moisture content in the particle, primary lime particle size or available surface area, and the diffusivity of SO_2 in the solid material. In a specific dry-scrubbing application, the solid reagent, its source, and preparation method are set, and this leaves only the moisture content of the particle as a variable process parameter.

The rate of SO_2 removal by a single particle with this approach is given by:

$$N_s = K_r \left(\frac{\pi d_d^3}{6}\right) C_{SO_2,g} \, C_{\text{remaining lime}} , \qquad (19)$$

where K_r = f (moisture content). Such a correlation between K_r and moisture content should be obtained by well-designed experiments. This approach is simple and may also prove practical to use. The gas-phase SO_2 concentration, $C_{SO_2,g}$, depends upon the rate of SO_2 removal by the dried particles and is determined by overall gas-phase mass balance. The concentration of remaining lime with time is determined by the above rate relation and mass balance over the particle.

SPRAY-DRYER INLET AND OPERATING PARAMETERS

The rate relations developed earlier in this paper describe the mass- and heat-transfer interactions between a single droplet/particle and the surrounding gas phase. The rate of drying and SO_2 removal are interrelated to bulk-gas and droplet properties. In addition, the bulk-gas properties also depend upon gas-inlet conditions, prescribed operating conditions, and gas flow and mixing within a spray chamber.

INLET-GAS SPECIFICATIONS

The primary inlet flue-gas specifications required are: 1) volumetric gas-flow rate; 2) inlet flue-gas temperature; 3) flue-gas composition and its molecular weight; 4) amount of water vapor present or the absolute humidity of the flue gas, or the adiabatic saturation temperature; and 5) SO_2 concentration.

Also important is the particulate-phase concentration/size distribution in the inlet flue gas and its available alkalinity. However, the dry-particulate phase with its alkaline content, entering the spray chamber along with the flue gas, is not considered to be effective in SO_2 removal in the spray chamber. Its contribution primarily comes when recycled in the slurry along with fresh lime sorbent or other reagent.

OPERATING PARAMETERS

There are basically five primary operating parameters which influence the bulk-gas properties at the spray-dryer outlet and SO_2 removal in the spray chamber:

1. Approach to saturation temperature at the spray-dryer outlet.

2. Stoichiometric ratio of fresh lime (sorbent) added in the atomized slurry to the amount of SO_2 in the inlet flue gas.

3. Recycle ratio of solids collected in spray dryer and particulate collection equipment in the spray-dryer feed slurry.

4. Droplet size distribution in sorbent feed slurry/solution.

5. Method of slurry preparation (slaking)--primary lime particle size distribution.

In the spray chamber, the gas is cooled and humidified (almost) adiabatically by evaporation of the water from the droplets. The temperature and absolute humidity of the gas phase at the spray-dryer outlet is then given by following the adiabatic saturation line on the air-water psychrometric chart, from the flue-gas inlet conditions (ignoring any heat losses). Thus, prescribing the approach to saturation temperature at the spray-dryer outlet determines the temperature and absolute humidity of the flue gas at the spray-dryer outlet.

The amount of moisture retained by the solids at the spray-dryer outlet is negligible compared to the amount of water evaporated. Thus, the amount of water added in the slurry per unit amount of inlet flue gas is simply obtained from the gas-phase humidities at the spray-dryer inlet and outlet.

The stoichiometric ratio in spray-dryer FGD operations is usually defined as moles of fresh lime or sorbent added in the slurry per mole of SO_2 in the inlet flue gas. Thus, setting the stoichiometric ratio determines the amount of fresh lime/sorbent used per unit amount of inlet flue gas. The recycle ratio further determines the amount of recycled solids (from particulate collection/spray dryer) accompanying the fresh lime in the slurry. These three parameters fix the amount of total solids and water added in the slurry per unit amount of inlet flue gas, thus setting the solids concentration in the slurry.

The methods used for lime slaking, slurrying of recycled solids, and slurry preparation determine the average primary particle size in the slurry. The recycle ratio and the amount of active reagent in the waste solids influence the active available alkaline content in the primary lime particles in the slurry. This in turn determines the equilibrium concentration of lime in the solution. The method of atomization, slurry concentration, and slurry feed rate determine the size distribution and average size of the atomized droplets as well as total number of droplets generated per unit amount of flue gas.

The amount of SO_2 in the flue gas at spray-dryer outlet is the result of the operating parameters. It is a design parameter, and the purpose of this modeling and experimental pilot-plant study is to predict it as a function of various operating variables.

GAS-FLOW PATTERN AND MIXING IN SPRAY DRYER

The inlet and operating conditions specify the bulk-gas properties at the inlet and outlet. However, the rates of heat and mass transfer depend upon the local properties of the bulk gas in contact with the spray droplet. The local bulk-gas properties (temperature and SO_2 and water-vapor concentrations) are determined by the gas-flow pattern and mixing within the spray chamber. With the completely backmixed gas-flow pattern, the bulk-gas properties throughout the spray chamber are uniform and same as at the spray-dryer outlet. At the other extreme, when the spray dryer is operated as an ideal plug-flow system, the bulk-gas properties change gradually with the local rate of change of a property depending upon the local rate of transfer.

Plug-flow systems generally give greater transfer rates compared to backmixed systems. In a spray-dryer application, this means that the droplets will dry faster in a plug-flow system as opposed to a backmixed system. This indicates a shorter time span for wet-droplet stage in plug-flow spray-dryer application. The initial rate of SO_2 removal in wet-droplet stage in a plug-flow system would be higher than that in a backmixed system but will be operative for a shorter time period. Thus for SO_2 removal, plug-flow systems offer higher initial SO_2 removal rates, whereas backmixed systems offer longer drying times.

The actual gas-flow pattern and mixing would be intermediate of the above two extremes. Usually a deliberate attempt is made for efficient gas mixing in a spray dryer by employing efficient gas-distribution systems, such as a dual gas-dispersion system. In such situations, the gas mixing is more closely approximated by the well backmixed case, with uniform gas-phase temperatures and compositions in the spray chamber.

MASS AND ENERGY BALANCES

Evaporation of water from droplets, and absorption and reaction of SO_2 in droplets, change the bulk properties and composition of both the gas phase and droplets. The rate relations developed earlier in this paper must be coupled with material and energy balances for both the gas phase and droplets to develop differential equations to describe the rate of change in the bulk properties (composition, mass, temperature, droplet diameter, etc.). These differential equations then must be integrated over the spray-dryer residence times of gas phase and droplets to obtain the overall removal of SO_2 in the spray chamber.

All the initial parameters/properties of the droplet and gas phase are established by the gas-phase inlet conditions and spray-dryer operating parameters just discussed in this paper. After establishing the initial conditions, the gas phase and the droplets are "followed" from the spray-dryer inlet to outlet to determine total change in both.

Since the rigorous two-dimensional momentum balance equation is not considered in the present model, it is enough to consider one-dimensional flow of droplets from top to bottom of spray dryer. The droplets may be assumed to be uniformly distributed across the spray chamber cross section. The spray droplets may also be assumed to have the same residence time and mean velocity as that given by the gas-phase volumetric flow rate and mean velocity. In case of plug-flow type gas-flow pattern, the gas phase is also assumed to travel cocurrently with the droplets from the top to bottom of the spray dryer. In case of backmixed-flow type gas-flow pattern, the gas phase is assumed to be uniformly mixed throughout the spray chamber and its properties are assumed to be those at the outlet. The spray droplets in this situation are exposed to constant gas atmosphere throughout the residence time.

The differential equations describing the rate of change in droplet properties, with respect to residence time or distance travelled in the spray dryer, can easily be derived using the rate relations developed before. For a broad droplet-size distribution, the size distribution may be divided into discrete size channels with a certain mean droplet size for each channel. Since the rate of transfer processes depend upon the droplet size, the differential equations for droplets need to be written for each size channel in the distribution.

Similar differential equations describing the rate of change in gas-phase properties, with respect to residence time or distance travelled in the spray dryer, can also be easily derived for a plug-flow type gas-flow pattern. In the derivation of these equations, effect of entire droplet-size distribution on the gas phase needs to be considered. No such gas-phase balance equations are required for a completely backmixed gas-flow pattern since all the gas-phase properties are assumed to be uniform and the same as those at the spray-dryer outlet. The gas-phase temperature and humidity at the spray-dryer outlet are determined by operating conditions; however, the outlet SO_2 concentration is not known a priori. Therefore, a trial-and-error procedure is required to determine the efficiency of SO_2 removal and outlet SO_2 concentration in case of a backmixed type gas-flow pattern.

COMPUTER PROGRAM

To solve the material and energy balance equations just described in this paper, using the rate relations developed earlier in this paper, a computer program, "SPRAYMOD," was written in Basic language. The computer program was developed on a desk-top microcomputer.

The program basically has three sections. In the first section, a menu input format is used to enter all the input data regarding specifications and operating variables. After input, the data is printed out for verification. In the second section, gas-phase overall material and energy balances are carried out to establish all the initial conditions for both the droplet and the gas phase. All the dependent variables are then initialized.

In the third section, the differential equations for the droplets and for the gas phase (plug-flow option) are solved by a simple, explicit, finite-forward-difference scheme. The time step is controlled so that a maximum change during a time step in the droplet temperature or the droplet weight is less than 1% of the function value. This criterion ensures accurate solution in spite of the simple numerical scheme used for the solution. The program has two options regarding the gas-flow pattern: 1) backmixed flow and 2) plug flow. The backmixed-flow case requires a trial-and-error procedure to determine SO_2 removal efficiency. The backmixed flow assumption is often close to the real situation.

The program essentially follows a single spray droplet suspended in the bulk-gas phase with time. The changes in droplet and bulk-gas properties (e.g., droplet diameter) are related to rates of mass and heat transfer. The bulk-gas physical properties required in various rate relations are evaluated at the mean temperature of the gas film surrounding the droplet. The properties of the liquid phase, such as vapor pressure, are evaluated at the droplet temperature, which is assumed to be uniform throughout the droplet.

At initial time, T = 0, all the bulk gas and droplet properties are initialized. If the backmixed flow option is used, first trial value of SO_2 removal efficiency needs to be specified. At each time increment, the derivative functions are determined and the time step, DT, is established.

The amount of water evaporated and SO_2 absorbed in time DT are then evaluated. Corresponding changes in all gas-phase and droplet variables during time step DT are determined. The calculations continue until no more SO_2 is removed by droplets or till the time reaches the residence time value.

PHYSICAL PARAMETERS NEEDED FOR THE MODEL

To determine the rate of drying of droplets, it is necessary to know the drying characteristics of the solids involved, i.e., the critical-moisture content and equilibrium-moisture content at 100% relative gas-phase humidity. Other important parameters needed are the reaction-rate coefficients for both solid-phase and liquid-phase reactions between SO_2 and sorbent, which should be determined from well designed experimental studies. The droplet-size distribution strongly affects the gas-phase transfer coefficient and the drying times. The sorbent-dissolution rate, in case of a sparingly soluble sorbent such as lime, depends strongly upon the sorbent particle-size distribution in the slurry, which in turn depends upon the lime-slaking and slurry-preparation system. The gas-phase inlet conditions and spray-dryer operating parameters needed for model simulations were discussed earlier in this paper.

COMPARISON OF MODEL PREDICTIONS WITH PILOT-PLANT DATA

The predictions of SO_2 removal efficiency of a spray-dryer system by the model presented in this paper were compared with a set of pilot-plant data under various operating conditions. The pilot-plant data set used for comparison here was collected by Cottrell Environmental Sciences, Inc., at the Comanche Station of Public Service Company of Colorado (16). One of the difficulties in obtaining a suitable data set for comparison was lack of complete information in various reported pilot-plant and full-scale studies. This particular data set was chosen because of its availability and extent of information; these pilot-plant studies were recently published by Stevens et al. (16).

In addition to various operating parameters, some physical parameters need to be specified in model simulations. The drying characteristics of solids used were: critical-moisture content of 30% by mass and an equilibrium-moisture content of 15% by mass at 100% relative gas-phase humidity. The critical-moisture content value was considered to be at which the solid spheres start touching each other in the droplet, whereas the equilibrium-moisture content value was approximately determined from the measured moisture contents of spray-dryer solids in this pilot-plant study (16). The information regarding reaction coefficients was not available in this report. For model simulations, the solid-phase reactivity was considered to be zero and that of liquid-phase reaction taken to be infinite. No measured atomized droplet-size distribution was available in this study, and the mean-droplet size inferred from the measured spray-dryer outlet solid-size distribution was taken as 50 μm (monodispersed). The lime particle-size distribution in slurry was available and was approximately monodispersed with a mean size of 4 μm. The gas-flow pattern in model simulations was assumed to be completely backmixed.

The model comparison with the data is shown in Table 1 and Figure 4. The agreement was very good, with most of the model prediction being within ±10% of data values. With closer approach to saturation, however, there was an underprediction of SO_2 removal efficiency. This is believed to be due to neglecting the solid-phase reactivity, which is expected to be significant at closer approach to saturation, due to increased amount of equilibrium moisture in solids.

Case Studies

Additional model simulations were carried out to study the effect of stoichiometric ratio, approach to saturation, and inlet gas-phase temperature on SO_2 removal efficiency under otherwise similar operating conditions. All the physical parameters used were the same as just described.

Figure 5 shows the effect of stoichiometric ratio on SO_2 removal efficiency as predicted by the model. As expected, the efficiency increases with increasing stoichiometric ratio, with a leveling off at higher ratios. The leveling off occurs due to reduced moisture content at higher stoichiometric ratios, which reduces the drying time and thus offsets the availability of greater amount of sorbent.

Closer approach to saturation at the spray-dryer outlet leads to improved performance of the spray dryer as seen in Figure 6. This is primarily due to increased amount of water in feed slurry, which increases the drying time of droplets.

Although marginal, the gas-inlet temperatures have an influence on SO_2 removal efficiency. Figure 7 indicates that higher inlet temperature increases removal efficiency. This is due to higher water requirements to cool and humidify the gas. This increases the moisture content in feed slurry and hence the drying time.

Numerous reported observations in the literature (4, 16) follow similar trends as shown in these simulations.

Figure 8 shows a typical time history of a spray droplet in the spray dryer under the following operating conditions:

- Inlet gas temperature ≈ 160°C
- Amount of water at inlet ≈ 6.4% by volume
- SO_2 concentration at inlet ≈ 800 ppm
- Approach to saturation temperature ≈ 15°C
- Average droplet diameter ≈ 50 μm
- Primary lime particle size ≈ 4 μm
- Stoichiometric ratio ≈ 1.0
- No recycle

TABLE 1. COMPARISON OF SO_2 REMOVAL EFFICIENCIES PREDICTED BY MODEL TO THOSE OBSERVED IN RESEARCH COTTRELL PILOT-PLANT DATA (16)

Run Number	Inlet Gas Temperature (°F)*	Adiabatic Saturation Temperature (°F)*	Approach to Saturation (°F)*	Stoichiometric Ratio	Inlet SO_2 Concentration (ppm)	Observed SO_2 Removal Efficiency (%)	SO_2 Removal Efficiency Predicted by Model (%)
101	334	125	69	3.26	780	57.7	58.6
104	340	125	33	1.69	710	76.8	70.4
105	301	126	74	2.36	780	44.9	46.4
107	300	126	52	2.70	730	56.2	61.4
109	307	126	62	1.28	800	45.0	36.3
111	301	126	34	1.62	780	65.4	65.4
112	307	126	22	1.55	750	81.3	79.8
115	256	126	31	1.56	770	61.0	64.0
116	261	127	15	1.30	800	71.2	77.5
118	340	125	15	1.31	810	82.7	86.4
120	341	124	61	1.35	790	49.4	39.2
125	262	126	18	0.71	800	65.0	50.0
126	264	126	18	0.99	800	67.5	62.6
130	340	125	20	1.17	800	73.8	68.8
131	342	123	22	0.72	800	55.0	42.0

Note: Recycle ratio = 0.

*Use the equation °C = 5/9(°F - 32) to convert to the equivalent metric unit.

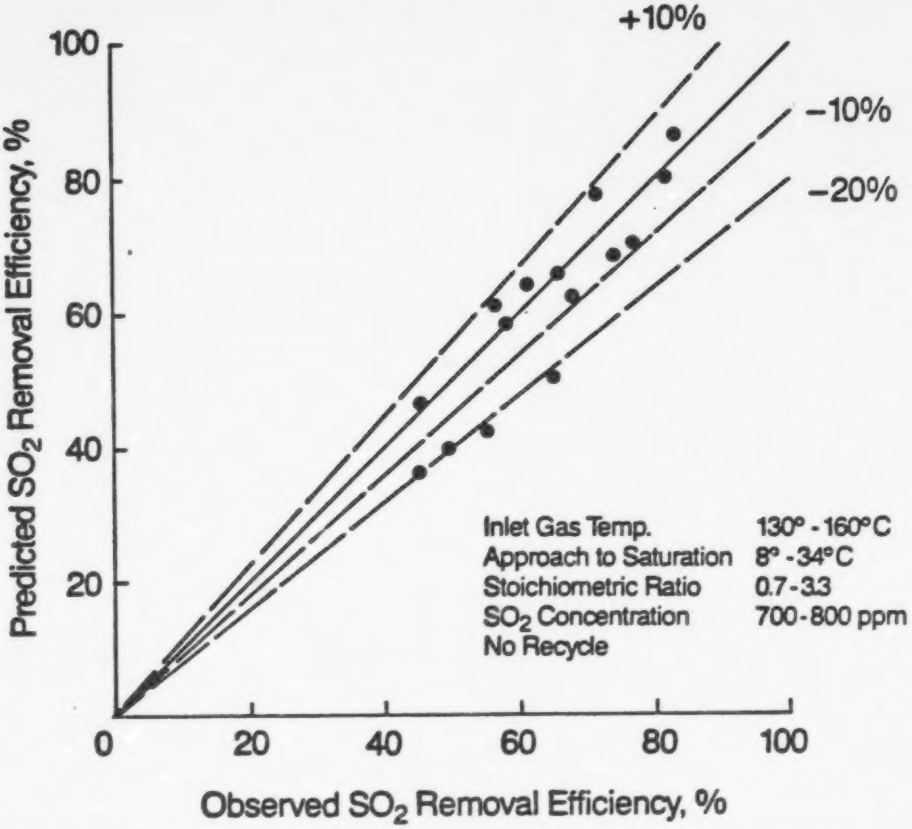

Figure 4. Comparison between predicted and observed SO_2 removal efficiencies under various operating conditions. Source of data points: Stevens et al. (16).

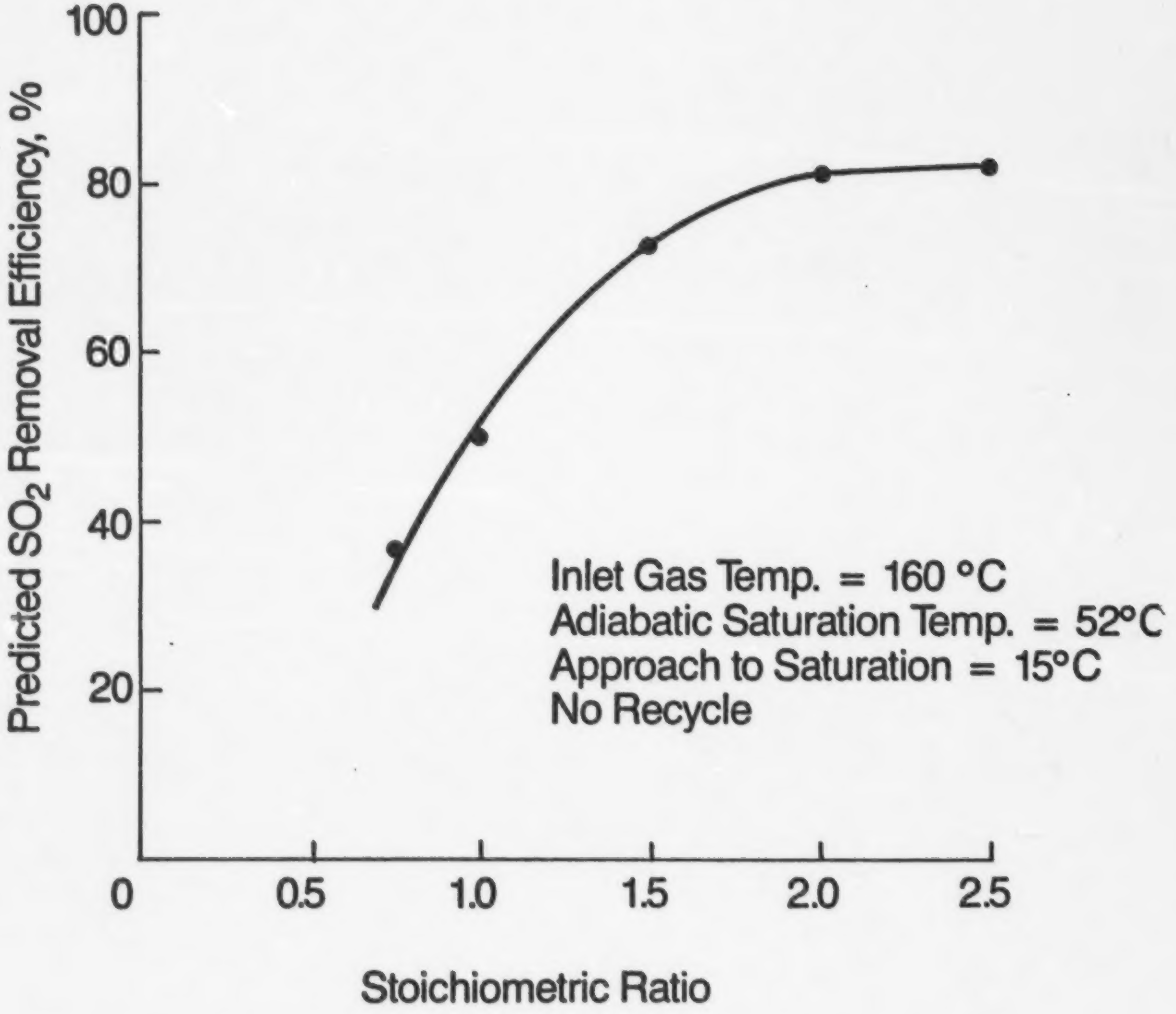

Figure 5. Effect of stoichiometric ratio on SO_2 removal efficiency (points represent cases simulated by the model).

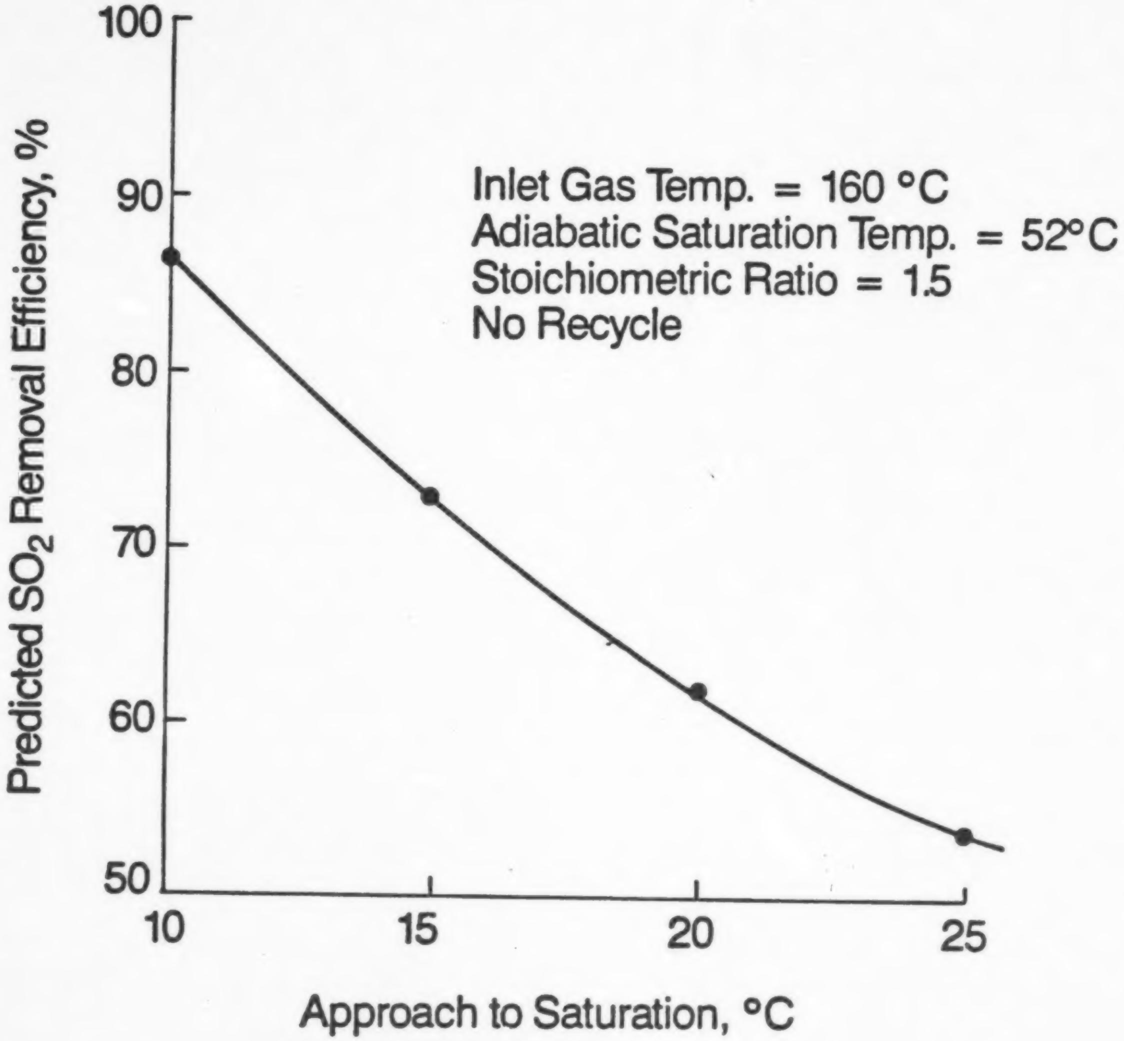

Figure 6. Effect of approach to saturation on SO_2 removal efficiency (points represent cases simulated by the model).

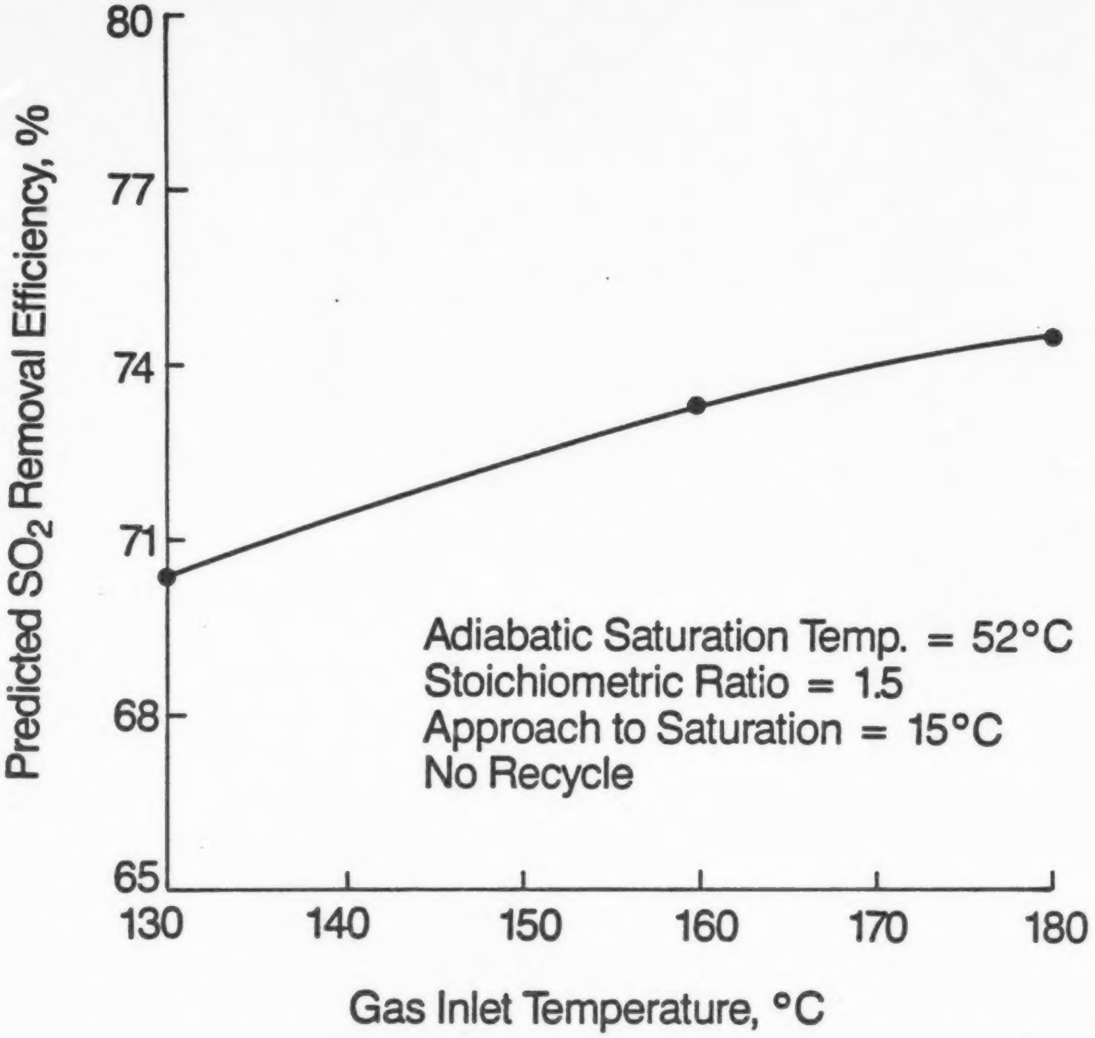

Figure 7. Effect of gas-inlet temperature on SO_2 removal efficiency (points represent cases simulated by the model).

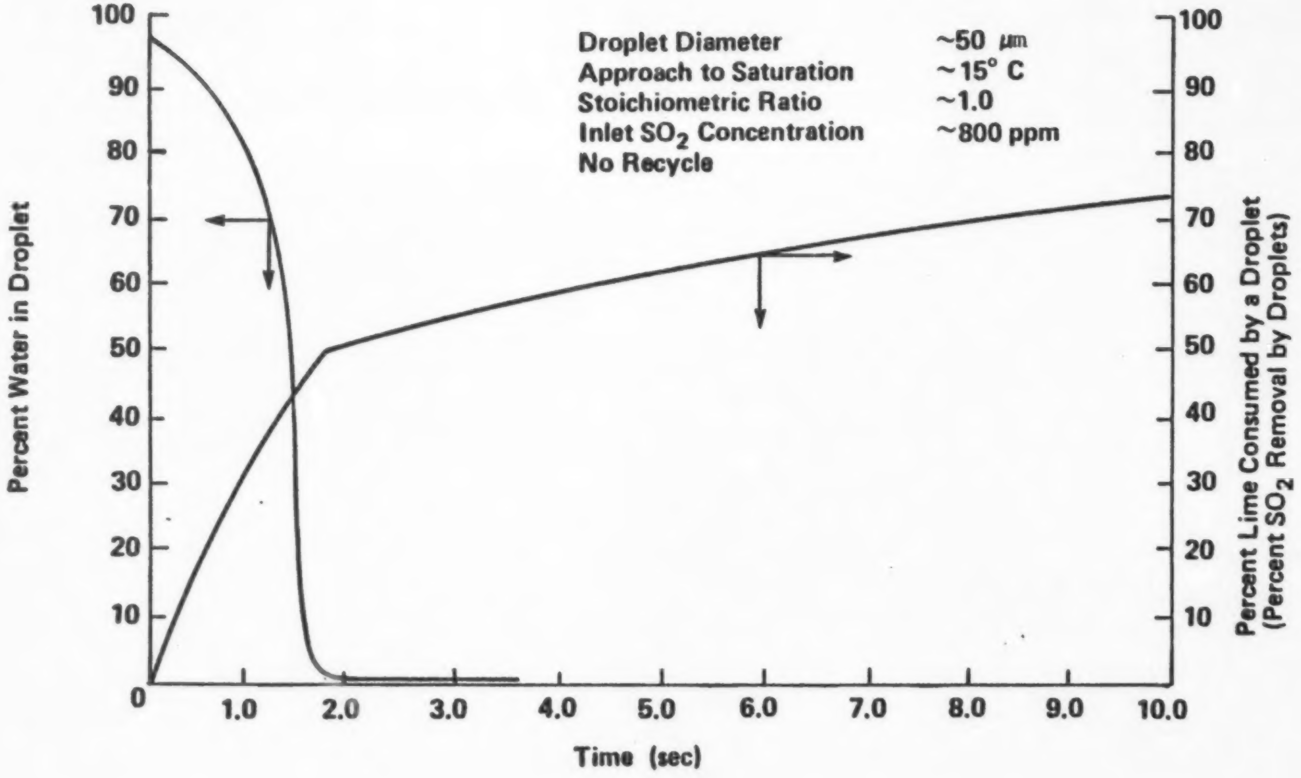

Figure 8. Evaporation of water and SO_2 absorption by a droplet in a spray dryer.

- Mass fraction of active sorbent in feed	≈ 1.0
- Critical moisture content	$\approx 50\%$
- Equilibrium moisture content at 100% relative humidity	$\approx 3\%$
- Completely backmixed flow system in spray chamber	
- Volumetric reaction coefficient at 2% residual moisture in solids	$\approx 1\times10^7$ cm^3/gmole-sec

The simulation shows that, in this particular case, the slurry droplet loses most of its moisture in the first couple of seconds, with the moisture content eventually approaching its equilibrium level. Most of the SO_2 is absorbed in the first stage of drying with SO_2 removal continuing at a slower rate in the dry stage.

SUMMARY AND CONCLUSIONS

1. A quantitative model is developed for various processes influencing SO_2 removal in a spray-dryer system.
2. A computer program, "SPRAYMOD," is written to solve resulting equations and to predict SO_2 removal efficiency of a spray-drying system.
3. Simulation case studies show expected trend of SO_2 removal efficiencies with various operating parameters, such as stoichiometric ratio and approach to saturation.
4. Comparison with one set of pilot-plant data shows good agreement between model predicted and observed SO_2 removal efficiencies.
5. Several key parameters influencing the process have been identified. Parameters, such as reaction-rate coefficients and critical- and equilibrium-moisture contents, need to be determined experimentally.

REFERENCES

1. Apple C., and Kelly, M.E. Mechanisms of dry SO_2 control processes. EPA-600/7-82-026 (NTIS PB82-196924), April 1982.
2. Getler, J.L., Shelton, H.L., and Furlong, D.A. Modeling the spray absorption process for SO_2 removal. Journal of the Air Pollution Control Association, 29(12), p.1270, December 1979.
3. Downs, W., Sanders, W.J., and Miller, C.E. Control of SO_2 emissions by dry scrubbing. Presented at the American Power Conference, Chicago, IL, April 21-23, 1980.

4. Samuel, E.A., Lugar, T.W., Lapp, D.E., Murphy, K.R., Brna, T.G., and Ostop, R.L. Process characterization of SO_2 removal in spray absorber/baghouse systems. *In*: Proceedings: Eighth Symposium on Flue Gas Desulfurization, New Orleans, LA, November 1983, Volume 2, EPA-600/9-84-017b (NTIS PB84-223049), July 1984.

5. Perry, R.H., and Chilton, C.H. (editors). Chemical engineers handbook. *In*: 5th Edition, Chapter 20. McGraw-Hill, New York, 1973.

6. Sjenitzer, F. Spray drying. *Chem. Eng. Sci.*, Vol. 1, No. 3, pp.101-117, 1952.

7. Kerkhof, P.J.A.M., and Schoeber, W.J.A.H. Theoretical modeling of the drying behavior of droplets in spray dryers. *In*: A. Spicer (ed.), Advances in Preconcentration and Dehydration of Foods. Wiley, New York, 1974.

8. Marshall, W.R., Jr. Heat and mass transfer in spray drying. *Trans. ASME*, Vol. 77, pp.1377-1385, 1955.

9. Gauvin, W.H., and Katta, S. Basic concepts of spray dryer design. *AIChE J.*, Vol. 22, No. 4, pp.713-724, 1976.

10. Crowe, G.T. Modeling spray-air contact in spray-drying systems. *In*: A.S. Mujumdar (ed.), Advances in Drying, Vol. 1. Hemisphere Publishing Corp., Washington, 1980.

11. Froessling, N. *Gerlands Beitr. Geophys.*, 52, 170, 1938.

12. Ranz, W.E., and Marshall, W.R., Jr. Evaporation from drops. *Chem. Eng. Prog.*, Vol. 48, pp.141-46, 173-80, 1952.

13. van Brakel, J. Mass transfer in convective drying. *In*: A.S. Mujumdar (ed.), Advances in Drying, Vol. 1. Hemisphere Publishing Corp., Washington, 1980.

14. Parti, M., and Palancz, B. Mathematical model for spray drying. *Chem. Eng. Sci.*, Vol. 29, pp.355-362, 1974.

15. Felsvang, K. Results of high sulfur dry-FGD operation. Presented at the Joy/Niro Seminar, Minneapolis, June 1982.

16. Stevens, N.J., Manavizadeh, G.B., Taylor, G.W., and Widico, M.J. Pilot-scale parametric testing of spray dryer SO_2 scrubber for low-to-moderate sulfur coal utility applications, EPA-600/7-84-045 (NTIS PB84-175959), March 1984.

17. Danckwerts, P.V. Gas liquid reactions. McGraw-Hill, New York, 1970.

18. Damle, A.S. Modeling of SO_2 removal in spray dryer flue-gas desulfurization system. Draft report, submitted to U.S. Environmental Protection Agency under Cooperative Agreement No. CR-808936-02-0, July 1984.

FABRIC FILTER OPERATION DOWNSTREAM OF A SPRAY DRYER: PILOT AND FULL-SCALE RESULTS

Richard G. Rhudy
Electric Power Research Institute
Palo Alto, California 94303

Gary M. Blythe
Radian Corporation
Austin, Texas 78766

ABSTRACT

The Electric Power Research Institute (EPRI) is conducting an independent evaluation of spray drying FGD technology to confirm the process capabilities and to provide the electric utility industry with reliable design and operating information for spray dryer systems. This paper summarizes the results to date for the operation of a fabric filter downstream of the spray dryer.

Few bag related problems have been experienced and the pressure drops have been lower than expected. Some corrosion on the fabric filter walls has occurred. SO_2 removal across the fabric filter is strongly influenced by recycle. Cooling tower blowdown water can be a positive, negative, or neutral influence depending on its compositon and whether it is used for slaking or dilution. The addition of $CaCl_2$ to the atomizer feed slurry can improve fabric filter SO_2 removal.

INTRODUCTION

Of the 19 utility-scale spray drying systems that have been awarded, 14 will use a fabric filter for particulate collection downstream of the spray dryer. While fabric filters have become an accepted particulate control technology for use in the utility industry, the effects of operating a spray dryer upstream on fabric filter operation and maintenance are not well documented.

Spray dryer operation causes several changes in the fabric filter inlet gas. These include reduced flue gas temperature, increased particulate loading, higher flue gas moisture content, and a potentially altered particulate size distribution. Many questions arise concerning the effects of these changes on the fabric filter. For example, how are fabric filter pressure drop, particulate removal, and bag life characteristics changed? Is there an increased potential for corrosion? Most of the spray drying systems will employ recycle, where material collected in the spray dryer and/or fabric filter is mixed with lime fed to the spray dryer. How does recycle affect fabric filter operation?

In addition to potential spray dryer effects on fabric filter operation and maintenance, the impact of the fabric filter on SO_2 removal needs to be determined. If all of the alkali fed to the spray dryer is not utilized there, how much additional reaction occurs within the fabric filter? How does the air-to-cloth ratio or compartment cleaning cycle affect the SO_2 removal in the fabric filter? Furthermore, can SO_2 removal considerations affect the choice of optimum values for air-to-cloth ratio or cleaning cycle? Will the use of cooling tower blowdown (CTB) water or chemical additives in the spray dryer affect either the SO_2 removal or the operation of the fabric filter?

The Electric Power Research Institute (EPRI) is conducting a program to evaluate the use of spray drying technology in flue gas desulfurization systems for the utility industry. The program includes both pilot- and full-scale studies of the technology. One of the most important objectives of this work is to resolve questions about the interaction between the spray dryer and the fabric filter. Results from this program have been presented previously (References 1, 2, 3, 4). This paper will highlight the fabric filter related results from over 2 years of pilot-scale testing, a full-scale field test, and from the reported experience on several operating full-scale systems.

PROCESS DESCRIPTION

In typical FGD applications of spray dryers, a slurry of water and lime is sprayed through an atomizing device, usually a rotary atomizer, into a drying vessel. Flue gas enters the vessel cocurrently with the atomized slurry, and SO_2 is absorbed as the slurry droplets dry. Some of the dried material falls out at the bottom of the spray dryer, but most leaves the drying vessel with the flue gas and enters a particulate collection device, usually a fabric filter. In most systems, some of this product is reslurried and recycled to the spray dryer to increase SO_2 removal, improve droplet drying characteristics, and minimize the lime requirements. A flow diagram for a typical spray drying system is shown in Figure 1. A summary of the design and operating characteristics of the fabric filters currently operating downstream of spray dryers in utility FGD systems is presented in Table 1. Reference will be made to this table throughout the paper.

At the Arapahoe Test Facility, EPRI has a 2 1/2 MW spray dryer/fabric filter pilot plant which uses one compartment of a 10 MW pilot-scale fabric filter for particulate collection. Details of the pilot spray dryer and fabric filter are presented in Reference 3. The use of a single compartment rather than a multi-compartment unit has facilitated a better understanding of how the fabric filter operates during each filtering and cleaning cycle. In addition to the pilot-scale study, field testing has been performed at the full-scale 100 MW spray dryer/fabric filter demonstration system at the Northern States Power Riverside Station. Details of that system are presented in Reference 4.

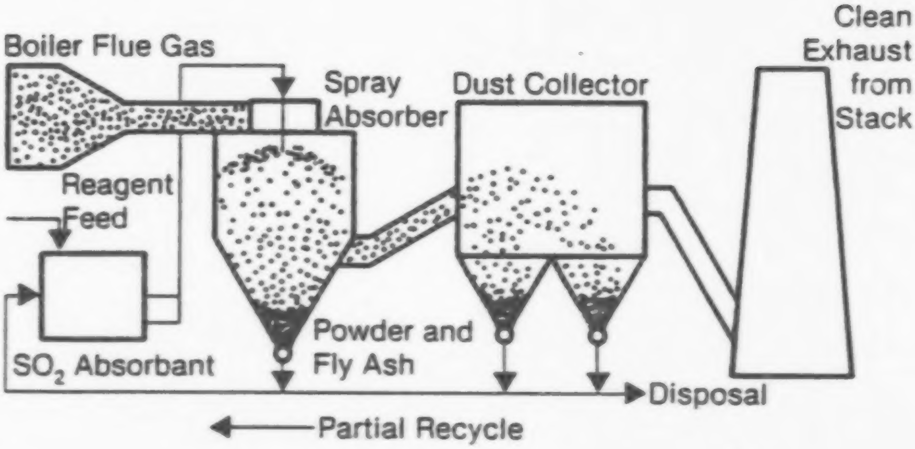
Boiler Flue Gas
Spray Absorber
Dust Collector
Clean Exhaust from Stack
Reagent Feed
SO_2 Absorbant
Powder and Fly Ash
Disposal
Partial Recycle

Figure 1. Process Flow Diagram for a Spray Dryer/Baghouse FGD System.

TABLE 1. OPERATIONAL FABRIC FILTERS DOWNSTREAM OF SPRAY DRYERS

Unit/Utility	Start Date	System Supplier	Gross[2] Air-to-Cloth Ratio ACFM/FT² Design	Gross[2] Air-to-Cloth Ratio ACFM/FT² Current	Cleaning Cycle	Cloth Material (WT, OZ/YD)	% of Gas Bypassed Around Spray Dryer Design	% of Gas Bypassed Around Spray Dryer Current	Fabric Filter ΔP,[4] in. H2O Design	Fabric Filter ΔP,[4] in. H2O Current	Fabric Filter Solids Recycled Design	Fabric Filter Solids Recycled Current	Approach to Saturation °F Design	Approach to Saturation °F Current	Spray Dryer Outlet Temperature °F Design	Spray Dryer Outlet Temperature °F Current	Baghouse Inlet Temperature °F Design	Baghouse Inlet Temperature °F Current	Type of Baghouse Cleaning
Antelope Valley 1 Basin Electric Power	5/27/83 6/8/83	Joy/Niro	2.3	2.2	1/2 hr.	Fiberglass with teflon coat (10)	3.2 Before APH[3]	0	4	5.5	Yes	Yes	33	33	185	167	185	167	Reverse Gas
Coyote 1 Montana-Dakota Utilities	3/81 4/81	Rockwell/ Wheelabrator	2.5	2.6	1/30 min.	Acrylic (6 and 10)	0	0	3	4-5	No	No	50	90-120	180	220	180	220	Shaker
Holcomb 1 Sunflower Cooperative	6/16/83 8/19/83	Joy/Niro	1.6	1.6	1/3 hr. or Δp=6"	Fiberglass with teflon coat (10)	0	0	3.5	4	Yes	Yes	30	50	160	175-180	180	175-180	Reverse Gas
Rawhide 1 Platte River Power	1/13/84 3/1/84	Joy/Niro	1.8	1.8	1/hr. or Δp=6"	Fiberglass with teflon coat (10)	10 After APH	0	4.8	<4	Yes	Yes	35	50-60	165-170	180-200	165-170	180-200	Reverse Gas
Riverside 6,7 Northern States Power	2/81 3/1/84	Joy/Niro	1.8	1.3	1/hr.	Fiberglass with teflon coat (10)	0	0	6	1.5-2	Yes	Yes	Var	25	143-153	150-160	143-153	150-160	Reverse Gas
Shiras 3 City of Marquette	4/14/83 5/12/83	General Electric	1.5	1.6	1/8 hr. or Δp=5"	Fiberglass with acid resist coat	3 Before APH	3 Before APH	6.0	5-6	Yes	No	25	33-40	153	165-170	155	200	Reverse Gas
Stanton 10 United Power	7/22/82 8/28/82	Research/ Cottrell	1.6	1.7	1/hr.	Fiberglass with silicone-graphite-teflon finish (16)	0	0	6	4.6 with 2 hours/ compt.	No	No	30	40	170	173	170	175	Reverse Gas

FOOTNOTES

1. 1st date is flue gas only, 2nd date is start of spray drying
2. All compartments in operation
3. APH = air preheater
4. Flange to flange at full or normal load

RESULTS

PRESSURE DROP

An initial concern about operating a fabric filter downstream of a spray dryer was that during upsets in operation, water would be carried out of the dryer vessel and enter the fabric filter. This water would then wet the material on the bags, causing chemical reactions that would blind the bags. It was thought that once wetted, the bags would have to be replaced. To date, though, bag failure due to the effects of water carryover has not been a problem.

For example, upset operation at the EPRI pilot plant resulting in water running out of the bottom of the spray dryer vessel, i.e., saturated gas reaching the fabric filter, has not resulted in bag problems. One moisture problem did occur during a system shutdown at the Antelope Valley 1 Station. In this case moisture in ambient air was allowed to enter the fabric filter. Under these conditions, the moisture had a chance to react with the material on the bags. However, hand cleaning the bags restored the normal pressure drop characteristics and no bags had to be replaced.

One question posed earlier in this paper was: what impact will the spray dryer upstream have on the pressure drop performance of a fabric filter? Plotted in Figure 2 are the average tube sheet pressure drop versus air-to-cloth ratio for a number of full-scale fabric filter systems. Data from systems with and without spray dryers upstream are presented. Note that pressure drops are lower for the fabric filters with spray dryers upstream. It should be noted that the pressure drop versus air-to-cloth data for the spray drying systems are based on flange-to-flange measurements by the utilities involved. The data for the systems without spray dryers, all from Reference 5, just include tubesheet pressure drop values. In order to make the data from all sources comparable, 1/2 to 1 inch of water was subtracted from the flange-to-flange pressure drop measurements, with the highest pressure drops receiving the largest correction. This correction

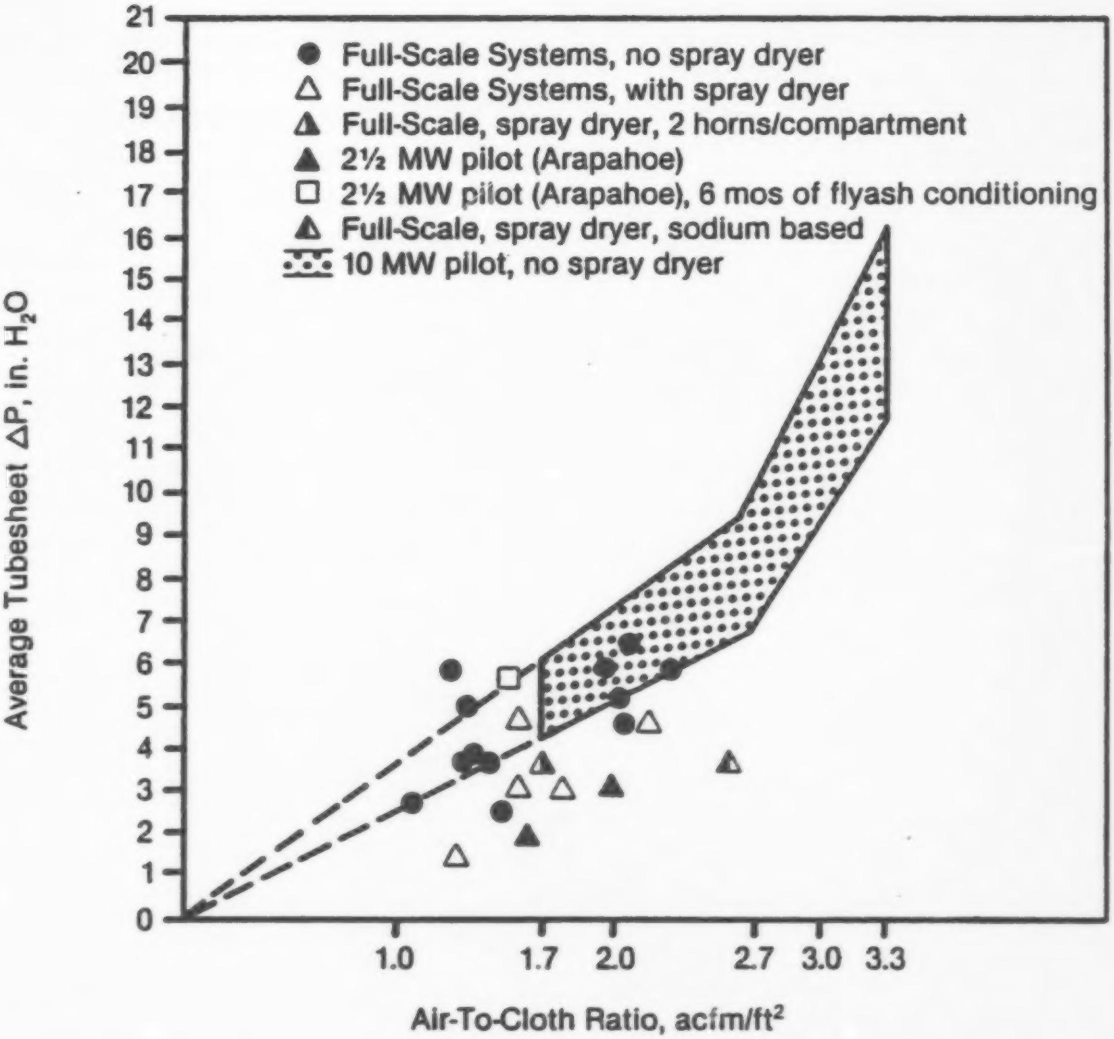

Figure 2. Pressure Drop Data for Pilot- and Full-Scale Fabric Filters.

was an estimate of the magnitude of compartment entrance and exit losses, etc. Even without this correction, the spray drying system flange-to-flange pressure drops are lower than tubesheet pressure drops for the systems without spray dryers.

Data from the 2 1/2 MW pilot plant are also represented in Figure 2. The shaded area represents data from compartments without the spray dryer upstream. Data from the compartment with the spray dryer upstream are plotted as individual points. Data are presented for both the original bags in this compartment, which were conditioned with operation on fly ash only for approximately 6 months before the spray dryer pilot plant was started up, and for a new set of bags that were immediately placed into service downstream of the spray dryer. Note that for the bags started up with the spray dryer in operation, the pressure drop compares well with the full-scale spray dryer system data, while the bags conditioned for 6 months with fly ash only compare more closely with the pilot- and full-scale data for systems without spray dryers. The majority of the full-scale systems start up the spray dryer within 1 1/2 months of first sending untreated flue gas to the fabric filter (see Table 1).

These data appear to indicate that the permanent cake initially formed on the bags may dominate the long term pressure drop characteristics. If so, in order to maintain minimum pressure drop values, utilities and vendors may want to start up the spray dryer as soon as possible after the fabric filter is operational.

It should be noted that the pressure drops are similar or lower for the fabric filters downstream of a spray dryer, even though the particulate loadings are much higher for these systems. The operation of the spray dryer, in either once-through or recycle operation, significantly increases the particulate loading at the fabric filter inlet. This increase in loading is shown clearly in Table 2, for both pilot plant and full-scale data. Particulate loadings at the inlet to the fabric filter are 1.5 to 5.5 times higher than the fabric filter would otherwise see. The spray dryer inlet

TABLE 2. MASS LOADING TEST RESULTS

Location	Run No.	Nominal Spray Dryer Inlet SO_2 Level, PPM	Recycle[1] Ratio lb/lb $Ca(OH)_2$	Reagent[2] Ratio, Mole Ca/mole S In	Approach Temp, °F	Average Mass Loading, gr/DSCF Spray Dryer Inlet	Average Mass Loading, gr/DSCF Spray Dryer Outlet	Ratio of Outlet/Inlet Mass Loading	Comments
Arapahoe	1	1000	2.8	0.91	20	2.75	9.29	3.4	
Arapahoe	2	400	12.3	0.90	20	3.83	9.65	2.5	
Arapahoe	3	400	2.5	1.07	21	3.04	4.53	1.5	
Arapahoe	4	1000	0	1.17	19	3.87	6.44	1.7	
Arapahoe	5	1000	2.5	0.92	20	2.69	8.65	3.2	High inlet gas flow
Arapahoe	6	1000	2.0	1.03	30	2.06	6.10	3.0	
Riverside	7	800	12.5	0.71	18	3.5	17.9	5.1	75% SO_2 removal
Riverside	8	800	10.7	0.82	18	3.9	11.4	2.9	90% SO_2 removal
Riverside	9	2000	2.0	1.33	18	3.1	15.6	5.0	
Riverside	10	2000	3.2	0.98	18	2.9	15.9	5.5	Chloride addition

[1] Recycle Ratio = $\frac{\text{lb recycle material}}{\text{lb of } Ca(OH)_2 \text{ solids in fresh lime feed}}$

[2] Reagent Ratio = $\frac{\text{lb-Mole } Ca(OH)_2 \text{ in fresh lime feed}}{\text{lb-mole } SO_2 \text{ in spray dryer inlet gas}}$

values in Table 2 represent typical fabric filter loadings without spray dryer operation.

The similar or even reduced pressure drop may result from the difference in particulate size distribution when the fabric filter is operating downstream of the spray dryer. Particulate size distribution data collected at the Arapahoe pilot plant indicate that much of the increase in mass loading across the spray dryer is in the larger particle sizes and therefore would be expected to have a minimal impact on the fabric filter pressure drop. Several measurements using both impactors and series cyclones, performed at the inlet and outlet of the spray dryer, indicate that there is little difference in the the spray dryer inlet and outlet mass loading below about 1 μm particle diameter. The concentration is increased above 1 μm particle diameter, and for particles with diameters above 10 to 20 μm, the increase in loading can be as great as an order of magnitude.

Using impactor and series cyclone data, increases in mass loading across the spray dryer by size fraction were calculated, and are presented in Table 3. These results summarize the change in mass loading across the spray dryer for particles less than and greater than 10 micron aerodynamic diameter using the impactor data and for particles less than and greater than 7 micron aerodynamic diameter using the series cyclone data. Also, the overall increase in mass loading is presented for each case.

For all four tests, the mass loadings for the smaller (less than 7 or 10 μm) particles only moderately increases, or slightly decrease, while in most cases the mass loadings for the larger particles increase by a substantial margin. The decreases in the mass loadings of the smaller particles may reflect process variations from measurement to measurement or minor inaccuracies in the measurement methods, rather than indicating a true decrease in the number of these particles across the spray dryer. The data clearly show, however, that the mass loadings of the larger particles are substantially increased across the spray dryer, with the loadings increased by a factor of two to seven in the impactor data, and by 20 to 160 percent in the

TABLE 3. CHANGE IN MASS LOADING ACROSS DRYER BY SIZE FRACTION USING BRINKS IMPACTOR AND SERIES CYCLONE SIZE DISTRIBUTION DATA

Test	Particle Size		Mass Loading, gr/DSCF				Change Across Spray Dryer	
			Spray Dryer Inlet		Spray Dryer Outlet			
No.	Impactor	Cyclone	Impactor[1]	Cyclone	Impactor	Cyclone	Impactor	Cyclone
1	<10μ	<7μ	1.2	0.7	1.6	0.7	+ 33%	0
	>10μ	>7μ	1.5	3.0	7.7	7.9	+410%	+160%
	Overall	Overall	2.7	3.7	9.3	8.7	+240%	+140%
2	<10μ	<8μ	1.7	0.9	1.4	1.2	− 18%	+ 30%
	>10μ	>8μ	1.2	3.5	8.3	7.4	+590%	+110%
	Overall	Overall	2.9	4.4	9.7	8.6	+230%	+ 90%
3	<10μ	<6μ	1.4	0.4	0.9	0.4	− 36%	0
	>10μ	>6μ	1.6	2.4	3.6	3.3	+125%	±40%
	Overall	Overall	3.0	2.8	4.5	3.7	+ 50%	+ 30%
4	<10μ	<6μ	1.8	0.4	2.2	0.5	+ 22%	+ 20%
	>10μ	>6μ	2.1	3.4	4.2	4.0	+100%	+ 20%
	Overall	Overall	3.9	3.8	6.4	4.5	+ 64%	+ 20%

[1] Uses impactor distribution data and Method 17 mass loading data

series cyclone data. These calculations further verify that the spray dryer has little impact on the mass loading of smaller particles, but can greatly increase the mass loading of larger size fractions.

FABRIC FILTER CORROSION

When utilities were first considering spray dryer-based dry FGD technology, many feared that fabric filter corrosion might occur by either of two mechanisms. The first mechanism would involve sulfuric acid present in the flue gas condensing in the spray dryer and corroding downstream equipment. The second mechanism would involve moisture carried over from the spray dryer during upset conditions. It was feared that this moisture would collect on downstream surfaces, absorb flue gas SO_2, and ultimately form corrosive sulfuric acid. However, neither of these mechanisms appear to directly contribute to fabric filter corrosion, as each would be expected to result in corrosion upstream of the fabric filter bags, or on the "dirty" side of the compartment. Instead, corrosion has been noted on compartment walls on the downstream or clean side of the bags. This corrosion is apparently the result of condensation of flue gas moisture on cold spots at the outlet side of the fabric filter. As mentioned above, moisture condensed will absorb flue gas SO_2 forming sulfuric acid.

Corrosion on the outlet side of the bags has been especially noted at the EPRI pilot plant. Corrosion was first noted on all of the internal walls of the clean side of the fabric filter compartment after 8 months of spray dryer pilot plant operation. After 13 months, three bags had fallen to the floor of the fabric filter due to corrosion and failure of the bag caps. All three fallen bags were located adjacent to the walls. Examination of the remaining bags indicated that several other caps on bags near the walls were severely corroded. Corrosion was particularly noted on the door to the compartment, where air inleakage promotes cold spots. Sonic measurements indicated that the compartment walls have lost less than 10 percent of their original thickness in spite of the apparent severity of the corrosion at some spots.

Thermocouples installed throughout the compartment confirmed that during cold weather, the temperature of the compartment walls can fall below the water dew point of the flue gas. Data for selected thermocouples are shown in Table 4 for a range of ambient temperatures.

While the corrosion experienced on the EPRI pilot unit at Arapahoe has been significant, there are several conditions at Arapahoe that would probably not be experienced on a full-scale fabric filter. First, the pilot-scale fabric filter compartment has a high surface area to volume ratio and therefore a higher flue gas temperature drop than would be experienced in a full-scale installation. Second, because the compartment is part of a pilot unit, it goes through numerous start-ups and shutdowns, passing through the water dew point of the flue gas each time. In addition, since the compartment shares no common walls with other compartments, all four walls of the compartment are exposed to ambient temperatures. Finally, the four compartment fabric filter was originally designed to clean hot gas (250°F to 300°F) rather than gas which is close to saturation. Consequently, the compartment walls are insulated with only a 2-inch thickness of fiberglass batts.

The design of the reverse gas system for the pilot fabric filter compartment may also contribute to the corrosion problem. The compartment is cleaned once every three hours using clean gas from the other three compartments which are treating hot, fly ash-laden gas. Between cleanings, there is no reverse gas flow in the run of ductwork between the compartment and the reverse gas recirculation header. The gas temperature in this ductwork has been measured as low as 100°F just prior to cleaning. Since this is below the flue gas dew point, it is suspected that water condensation may be occurring. When the reverse gas flow through this short run of ductwork begins as cleaning is initiated, this moisture may be carried into the compartment. This moisture may further aggravate corrosion within the compartment. Traces of water flow on the compartment wall below the reverse gas duct inlet, and evidence of impaction of droplets on the tops of bag caps have been observed. In order to protect the walls of the fabric filter

TABLE 4. AMBIENT TEMPERATURE EFFECTS ON FABRIC FILTER TEMPERATURES

	Temperature (°F)		
	Case 1	Case 2	Case 3
Ambient	82	36	9
S.D. Outlet	138	135	137
Fabric Filter Outlet	132	124	125
Approximate Dewpoint (F.F. Outlet)	108	104	104
T_1 (Top Interior Wall)	117	107	-
T_5 (Bottom Interior Wall)	125	113	96
T_8 (Bottom Exterior Wall)	125	117	109
T_9 (Bag 16-Cap)	136	130	-
T_{10} (Bag 36-Cap)	133	124	-

compartment at Arapahoe from further corrosion damage, the walls were sandblasted and covered with a relatively inexpensive vinyl ester coating. (Cook 931-B-301). In addition, test patches were covered with two more expensive epoxy coatings (ConChem-Fibercrete AR and Martek-Duromar HPL3100). These patches are located on the compartment door - the most extreme service condition. After 7 months the vinyl ester coating has shown some deterioration at the tubesheet, in some of the compartment corners, and on the compartment door. Both epoxies are holding up well.

Some corrosion has also been noted on the fabric filters at the full-scale Riverside and Stanton systems. Improvement of the insulation has corrected most the problems on these systems. Several coatings have also been applied on compartment doors at Riverside. The best experience at Riverside has been with an epoxy (Glidden self priming mastic 5256/5257). This coating has performed well after 10 months of service.

While it would appear that corrosion of compartment walls and doors and bag caps may be a significant problem on the clean side of fabric filters operated downstream of spray dryers, there are several methods available for reducing the severity of the problem. Installation of adequate insulation - especially around doors, structural members and possibly between compartments - has proven effective in several instances. Techniques to increase the fabric filter inlet flue gas temperature such as flue gas bypass around the spray dryer, other forms of reheat, or operation of the spray dryer at higher exit temperatures may also be quite effective. The latter technique may result in a reduced SO_2 removal, both in the spray dryer and in the fabric filter. Minimizing stagnant runs of reverse gas duct-work between cleaning cycles may also reduce the potential for corrosion. If none of these techniques are completely effective, coatings - at least in areas of severe service conditions - may provide protection from further corrosion damage.

SOLIDS TRANSPORT

One area that has received little attention, but deserves highlighting, is the fabric filter solids transport system. As indicated by the mass loading values in Table 2, the fabric filter downstream of a spray dryer will handle much higher particulate mass loadings which will result in corresponding higher waste solids transport rates. Proper design of this system will be critical. Its malfunction can, aside from causing fabric filter operating problems, limit system SO_2 removal because of the loss of recycle. The EPRI pilot fabric filter solids transport system is a pressurized pneumatic system and no problems have been experienced. However, the systems starting up use various transport methods - mechanical, and pressure and vacuum pneumatic systems. It will be important to determine the best method for solids transport to assure reliable operation of these systems.

SO_2 REMOVAL

The importance of SO_2 removal in the fabric filter has been established in EPRI pilot- and full-scale data presented in previous papers (References 2, 3, and 4). At removal levels above 80%, the baghouse contributes significantly to the overall system removal (see Figure 3a). This contribution appears to be predominantly a function of reagent ratio when operating at a 20°F approach--i.e., the same curve applies regardless of varying between once through and recycle (Figure 3b) and increasing inlet SO_2 concentration (Figure 3c). Because these SO_2 removal data are calculated based on the percentage of the inlet SO_2 concentration to the spray dryer that is removed, they do not reflect the effects of the changing inlet SO_2 concentration at the fabric filter inlet. A better understanding of what affects fabric filter SO_2 removal can be achieved by comparing SO_2 removal across the fabric filter as a percentage of the actual fabric filter inlet SO_2 concentration.

Calculating the percent SO_2 removal based on the SO_2 concentration at the inlet to the fabric filter is straightforward, as the fabric filter

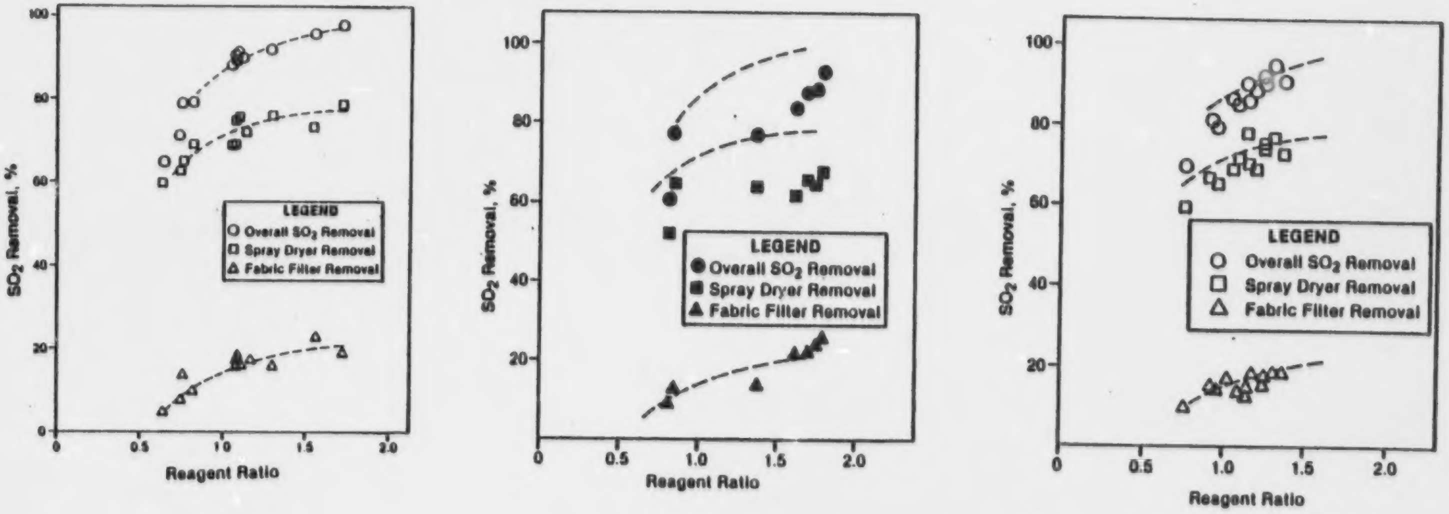

3 (a)

3 (b)

3 (c)

Figure 3. SO_2 Removal vs. Reagent Ratio for Various Test Conditions: (a) 350 ppm inlet SO_2, 2:1 Recycle Ratio, (b) 350 ppm, Once-Through Operation, and (c) 1000 ppm Inlet SO_2, 2:1 Recycle Ratio

Notes: (1) SO_2 removal across fabric filter is calculated as a percentage of the spray dryer inlet SO_2.
(2) Dashed lines in figures represent best fit of 350 ppm, 2:1 recycle data (i.e., Figure 3a data).

inlet and outlet SO_2 levels can be directly measured. However, reagent ratio values based on fabric filter inlet conditions can only be estimated.

The assumption made for calculating fabric filter reagent ratio values in this paper is that the reagent available in the fabric filter is the fresh reagent added in the spray dryer less the amount reacted with the SO_2 removed in the spray dryer. This available reagent is a maximum estimate since certain factors are not considered. First, the calculation assumes that no lime drops out at the spray dryer bottom or in the fabric filter hopper. However, some lime drops out at both locations. The amount will depend on the flue gas rate, approach to saturation, recycle rate, etc. In particular, once-through operation appears to lead to increased drop out in the dryer. Second, the calculation assumes that all unreacted lime is available for reaction with flue gas SO_2. However, some lime may be totally encapsulated with calcium sulfite and gypsum salts, so that it is not readily available for reaction. Also, some of the lime will have reacted with flue gas CO_2 to form $CaCO_3$. The availability of this $CaCO_3$ for subsequent reaction with flue gas SO_2 is not clear.

In spite of these obvious shortcomings, the available reagent calculated appears to be a good indicator of the relative amount of alkali that is available for reaction in the fabric filter.

Under the assumptions just outlined, trends in fabric filter SO_2 removal at different operating conditions become more apparent. Several of the more important variables - inlet SO_2, inlet gas temperature, recycle ratio, make-up water quality, and additives - will be discussed. Also, the apparent effects of the choice of fabric filter cleaning cycle duration will be discussed. In the case of inlet SO_2 level, it should be kept in mind that when 350 ppm, 1000 ppm, and 2000 ppm tests are discussed, these are concentrations at the inlet to the spray dryer. Actual values at the inlet to the fabric filter ranged from 70 to 180 ppm for the 350 ppm tests, 240 to 510 ppm for the 1000 ppm tests, and 560 to 800 ppm for the 2000 ppm tests, with the lower values generally occurring at the highest reagent ratios.

INLET SO_2 AND SPRAY DRYER INLET TEMPERATURE

Plotted in Figure 4 are the SO_2 removal across the fabric filter vs. the estimated maximum fabric filter reagent ratio for the 350 ppm, 1000 ppm and 2000 ppm inlet SO_2 tests on the 2 1/2 MW pilot plant. The 350 ppm data are shown for three levels of recycle ratio - 0 (once-through), 2:1 and 9:1 to 12:1, while for the 2000 ppm tests, data at 275° and 325°F spray dryer inlet temperature are plotted.

Fabric filter SO_2 removal can be compared as a function of inlet SO_2 for tests with a recycle level of 1:1 to 2:1; a 20°F approach and a spray dryer inlet temperature of 275°F. The removals drop as the inlet SO_2 increases. The drop is about 4 to 8 percentage points between 350 and 1000 ppm, and between 1000 and 2000 ppm. Interestingly, when the spray dryer inlet temperature is increased to 325°F for the 2000 ppm tests - more typical for high sulfur operation - the fabric filter SO_2 removal increased about 20 percentage points. The cause for this increase is unknown, although the recycle ratio increase from 1:1 to 2:1 and may be a major factor in the improvement. Also, the spray down across the spray dryer is increased by nearly 50°F. This leads to a higher relative humidity at the fabric filter inlet, which has been reported to remove SO_2 removal across a fabric filter (Reference 6).

Recycle has a dramatic impact on fabric filter SO_2 removal, as shown in Figure 4. For the 350 ppm tests, increasing the recycle ratio from 0 (once-through) up to 9:1 to 12:1 resulted in an SO_2 removal improvement of up to 54 percentage points at a fabric filter reagent ratio of 1.0. As shown in the plot, at high reagent ratios the improvement is reduced.

The 2:1 recycle tests showed removal improved by 29 percentage points relative to once-through operation at a fresh reagent ratio of 1.0. At this recycle ratio, the measured potential alkali associated with the recycled material would make the effective reagent ratio about 1.4. Increasing from 1 to 1.4 on the once-through curve would only result in 6 percentage points

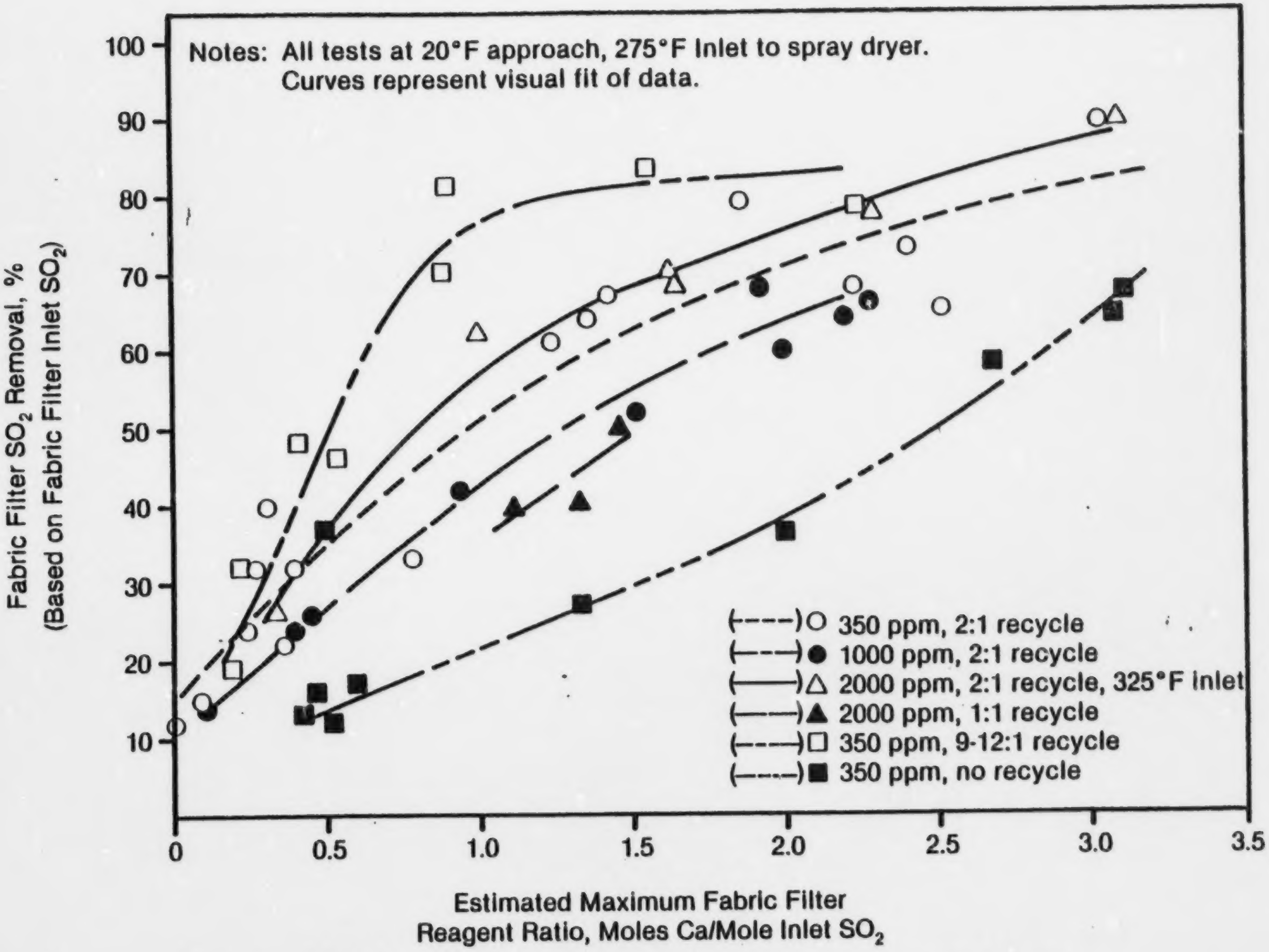

Figure 4. Fabric Filter SO_2 Removal Data From the Arapahoe Pilot-Scale System, Showing the Effects of Inlet SO_2 Level, Recycle Ratio, and Inlet Temperature.

of SO_2 removal increase, so recycle apparently has additional positive effects on SO_2 removal beside strictly increasing the amount of alkalinity available. At high recycle ratios a significant amount of potential reagent material is contained in the material recycled. This results in raising the estimated maximum fabric filter reagent ratio by a factor of 3 to 5. This amount of alkali corresponds well to the improvement in SO_2 removal resulting when increasing the recycle ratio from 2:1.

WATER QUALITY

Shown in Figure 5 are the fabric filter SO_2 removal versus estimated reagent ratio for a series of tests using both simulated and real cooling tower blowdown (CTB) waters for makeup to the system. The compositions of the CTB's used are shown in Table 5. Results varied significantly depending on the CTB composition and on whether the water was used only for dilution of the atomizer feed slurry or for both dilution and slaking fresh lime. CTB1 always showed improved SO_2 removal. It is believed that the high chloride content of this CTB was the main reason for the improvement, since the 1000 ppm sulfate present was expected to degrade performance when used for slaking. The reason for this belief will be explained in the section on additives. CTB2, representing a sidestream softened water, gave the same or improved performance relative to service water when used for dilution. The four tests plotted had different scale inhibitors added to the water, but it is not known if their presence resulted in the large amount of scatter between the four points. Future tests are planned to further investigate the effect of scale inhibitors. The third water, CTB3, has a high sulfate concentration - 2400 ppm. As expected, the results show no effect on SO_2 removal when this water is used for dilution, but significantly reduced SO_2 removal when used for slaking. This water was intended to simulate the actual CTB at a full-scale unit, so a comparison could be made between actual and simulated CTB. The results were somewhat surprising. The actual CTB performed better when used for dilution and worse when used for slaking and dilution. The reason for this is not known; however, the scale inhibitor used at the full-scale unit was added to the simulated CTB, but the

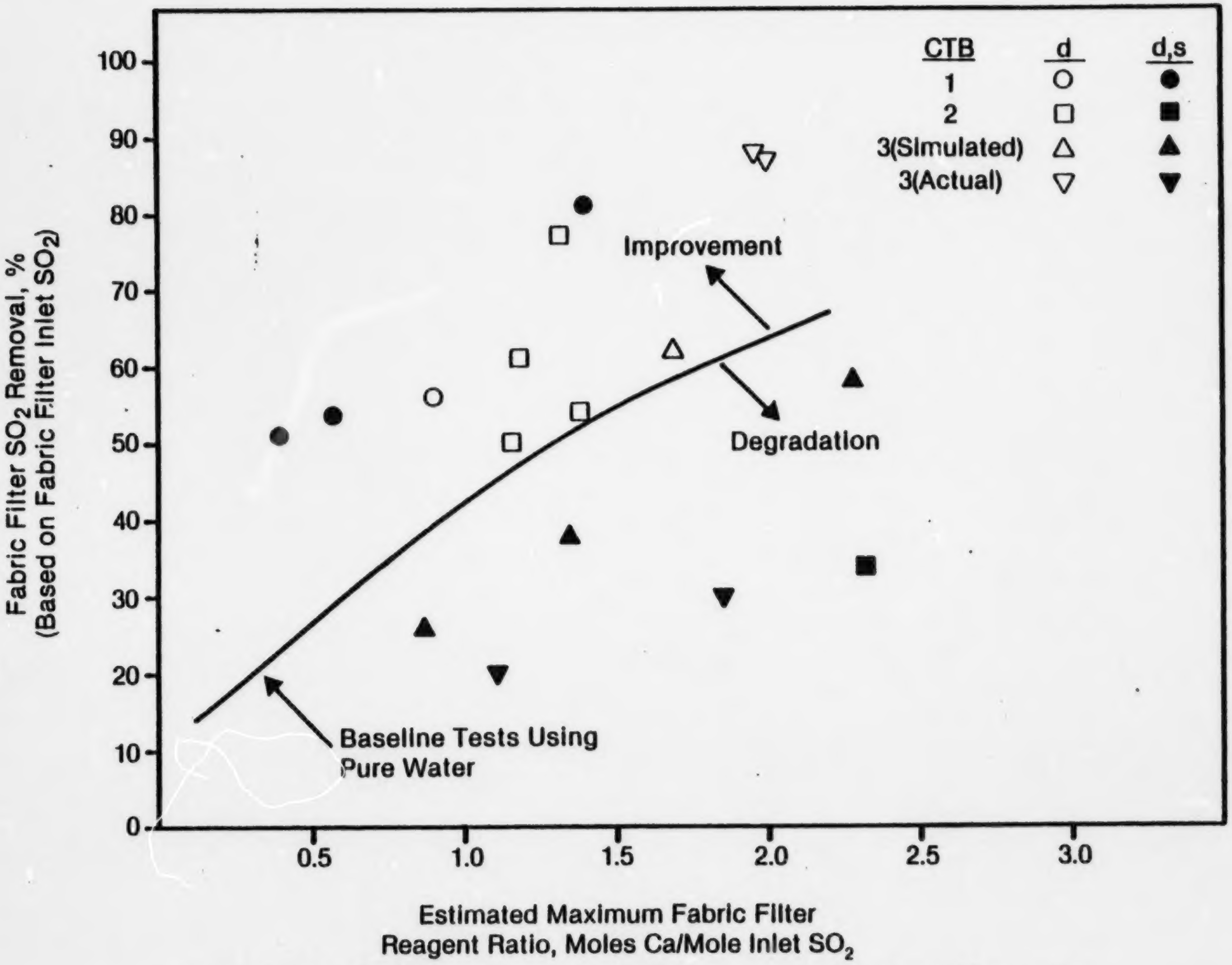

Figure 5. Fabric Filter SO_2 Removal Data From the Arapahoe Pilot-Scale System, Showing the Effects of System Make-up Water Quality.

TABLE 5. COOLING TOWER BLOWDOWN COMPOSTIONS

	Simulated			Actual
	CTB1	CTB2	CTB3[1]	Full-Scale
Ca^{++}	1160	410	420	350
Na^{+}	480	1830	490	371
Mg^{++}	-	53	220	196
$SO_4^{=}$	1000	5080	2450	2014
Cl^{-}	2050	170	157	166
$CO_3^{=}$	-	-	95	-
Inhibitors	No	Yes	Yes	Yes
Gypsum Relative Saturation	0.75	0.90	0.80	0.65

[1] Simulates actual full-scale system

corrosion inhibitor used was not available at the time. A future test is planned to determine whether the corrosion inhibitor accounts for the discrepancies between the performances of the simulated and actual CTB.

ADDITIVES

The additive results reported show the effects of adding calcium chloride to the spray dryer feed. Concentrations up to 1 percent by weight (as chloride) in the fabric filter solids were tested. Testing was performed at pilot- and full-scale. Testing was also restricted to high sulfur operation since this was where reagent utilization improvement appears most desirable. Results relative to the fabric filter are presented in Figure 6. In the pilot-scale data, improved SO_2 removal results as the chloride level is increased. The full-scale results appear to show less improvement for the level of chloride addition; however, the full-scale results without chloride addition are also significantly lower than the pilot results. The difference in fabric filter cleaning cycle duration for the two systems (once per hour for the full-scale, once per 3 hours at pilot level) may account for much of the difference. This effect is further discussed below.

CLEANING CYCLES

SO_2 removal measurements across the single fabric filter compartment at the Arapahoe pilot unit indicate that the compartment cleaning frequency may impact the SO_2 removal across the fabric filter. Figure 7 is a plot of SO_2 removal versus time throughout a 3-hour cleaning cycle. SO_2 removal increases significantly during the first hour after cleaning, and less significantly during the second and third hours. Presumably, had the compartment been cleaned once per hour rather than once every 3 hours, a lower overall average SO_2 removal would have resulted. The average SO_2 removal across the compartment for the first hour of this cycle was 65 percent, while the average for the entire 3-hour cycle was increased to 76 percent. On the basis of fabric filter contribution to overall system SO_2 (as presented in Figures 3a, 3b, and 3c), the 1-hour average was 13 percent while the 3-hour

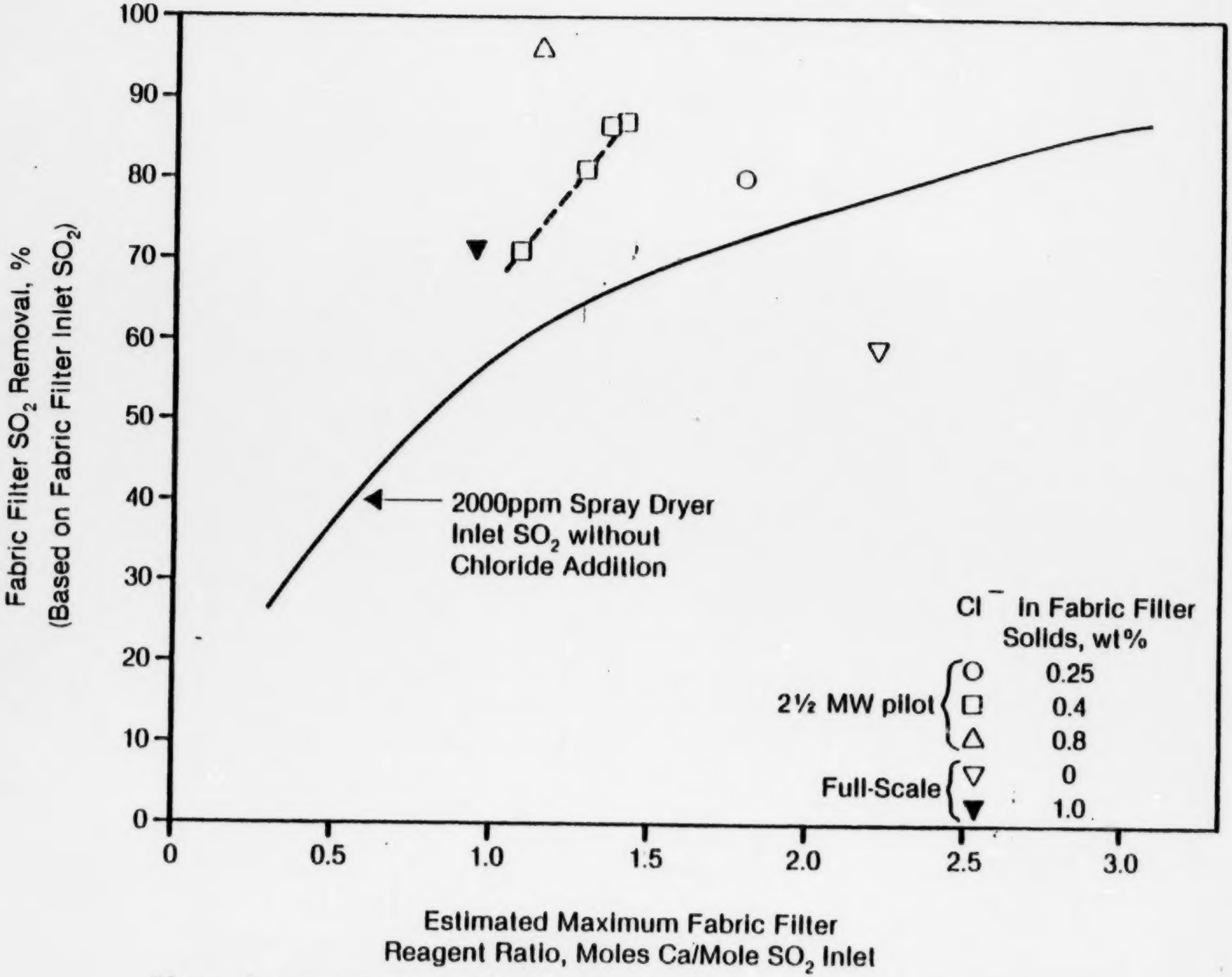

Figure 6. Fabric Filter SO_2 Removal Data From the Arapahoe Pilot-Scale System, Showing the Effects of $CaCl_2$ as a Performance Additive.

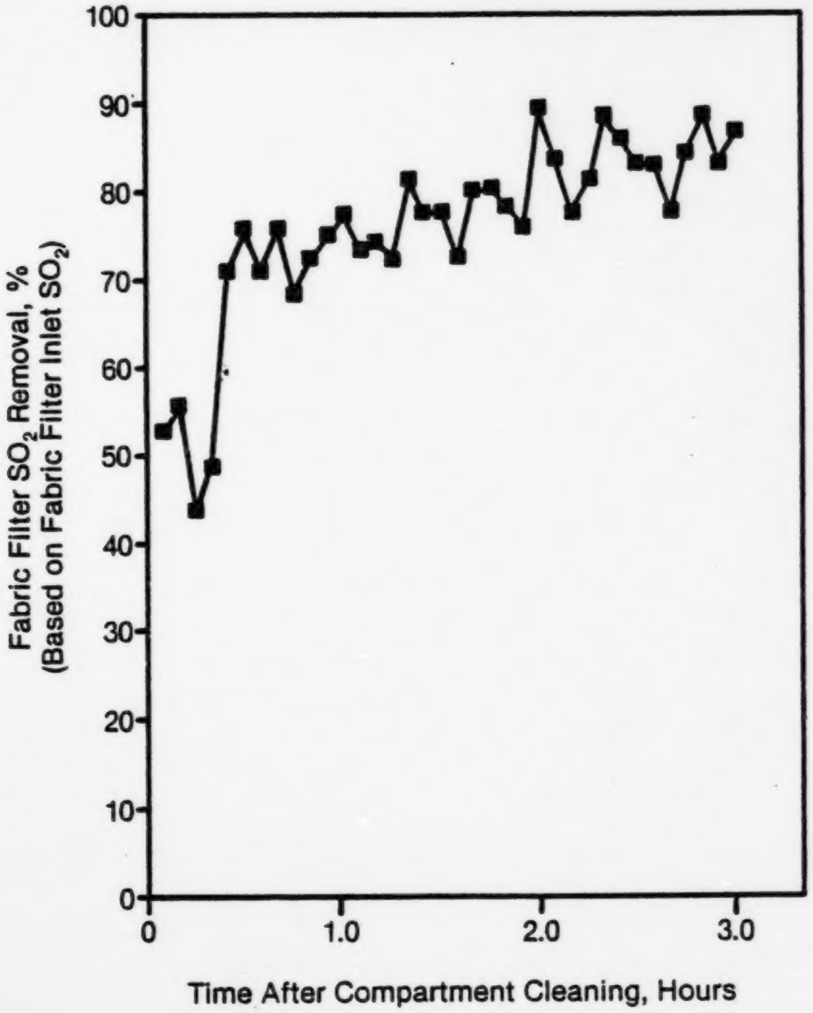

Figure 7. Fabric Filter SO_2 Removal Data From the Arapahoe Pilot-Scale System, Showing the Effects of Cleaning.

average was 16 percent. The tubesheet pressure drop (not shown) averaged 1.5 inches of H_2O for the first hour, and 2.2 inches for the entire 3-hour cycle.

Figure 7 is for a pilot unit test using CTB1 as makeup water for both dilu-tion and slaking and shows approximately an "average" effect of cleaning frequency. Some tests, particularly tests at high recycle ratios (9:1 to 12:1), show less of an effect of cleaning cycle duration on average fabric filter SO_2 removal. Others, particularly once-through tests, show a dramatic increase in SO_2 removal across the compartment during the first hour after a cleaning, and hence a greater effect of cleaning cycle duration on average SO_2 removal.

CONCLUSIONS

Fabric filters appear to be suitable for operation downstream of a spray dryer. Pressure drops appear lower than for fly ash only operation, even at much higher particulate loadings. The fabric filter can contribute significantly to overall system SO_2 removal. Fabric filter SO_2 removal appears to vary with operating variables in a manner similar to that across the spray dryer. Potential problems from the use of fabric filters downstream of spray dryers appear to be the possibility of corrosion on the clean side of the fabric filter compartments, and uncertainty about the ease of handling the relatively large quantities of solid waste product.

REFERENCES

1. Blythe, Gary M., et. al., "EPRI Spray Drying Pilot Plant Status and Results," presented at the joint EPA/EPRI Symposium on Flue Gas Desulfurization, Hollywood, Florida, May 17-20, 1982.

2. Rhudy, Richard G., and Gary M. Blythe, "EPRI Spray Dryer/Baghouse Pilot Plant Status and Results," presented at the Second Conference on Fabric Filter Technology for Coal-Fired Power Plants, Denver, Colorado, March 22-24, 1983.

3. Blythe, Gary M., and Richard G. Rhudy., "EPRI Spray Dryer/Baghouse Pilot Plant Status and Results," presented at the EPA/EPRI Symposium on Flue Gas Desulfurization, New Orleans, Louisiana, November 1-4, 1983.

4. Blythe, Gary M., and Richard G. Rhudy, "Field Evaluation of a Utility Dry FGD System," presented at the joint EPA/EPRI Symposium on Flue Gas Desulfurization, New Orleans, Louisiana, November 4, 1983.

5. Carr, Robert C., and Wallace B. Smith., "Fabric Filter Technology for Utility Coal-Fired Power Plants Part IV: Pilot-Scale and Laboratory Studies of Fabric Filter Technology for Utility Applications," JAPCA 34: 399 (1984).

6. Karlsson, Hans T., et. al., "Activated Wet-Dry Scrubbing of SO_2." Journal of the Air Pollution Control Association, Volume 33 No. 1, January 1983, pp 23-28.

NOVEL DESIGN CONCEPTS FOR AN 860 MW FABRIC FILTER USED WITH A DRY FLUE GAS DESULFURIZATION SYSTEM

by: Michael F. Skinner
Steven H. Wolf
Northern States Power Company
Minneapolis, Minnesota

John M. Gustke, P.E.
Donald O. Swenson, Ph.D.
Black & Veatch, Engineers-Architects
Kansas City, Missouri

ABSTRACT

Initial concerns with the application of fabric filters downstream of flue gas desulfurization systems using spray dryer absorbers centered on the potential "blinding" of the fabric filter bags by reaction of the moisture in the flue gas with the alkaline particulate on the bags. Three years of operation of the 100 MW spray dryer absorber and fabric filter installed at Northern States Power Company's Riverside Generating Station have demonstrated that bag blinding is not a significant problem.

However, corrosion of the fabric filter casing can be severe unless precautions are taken. This paper discusses novel corrosion protection design features for fabric filters located downstream of spray dryer absorbers. These design concepts were jointly developed by Northern States Power Company (NSP); Black & Veatch, Engineers-Architects (B&V); and Joy Manufacturing Company (Joy). The design concepts listed below are applied to the fabric filters that are being installed at NSP's 860 MW Sherburne County Generating Plant, Unit 3.

- Flue gas reheated between the spray absorbers and fabric filters.
- Fabric filter compartment wall temperature monitoring system installed.
- Fabric filter casing insulation thickness increased and insulation integrity improved.

- Air cavities eliminated by placing wall stiffeners inside casing and placing insulation against outside casing walls.
- Hopper crotch area insulation improved by insulating hopper support column.
- Thermal gaskets added on hopper discharge flanges.
- Insulation added between adjacent fabric filter compartments.
- Ambient air inleakage reduced by decreasing number of hinged access doors.
- Door seal materials selected using test results.
- Enclosures added around exterior compartment walkways.
- Individual casing isolated using guillotine dampers.
- After initial operation, spot coatings to be applied in problem areas to minimize internal casing wall corrosion.

These design concepts are not unique, but their combination to minimize casing corrosion is novel for spray dryer absorber applications.

INTRODUCTION

In November 1980, the 100 MW lime spray dryer absorber and fabric filter air quality control system[1] began operation at Northern States Power Company's (NSP) Riverside Generating Station. The Joy Manufacturing Company (Joy) fabric filter was installed downstream of the Niro spray dryer absorber to collect fly ash and flue gas desulfurization reaction products. Since the spray dryer absorber was installed as a test facility, the fabric filter is a "standard" utility reverse gas fabric filter with no special provisions for being downstream of the spray dryer absorber.

Prior to operation of the Riverside fabric filter, there was significant concern regarding the high potential for filter bag blinding in this application which is downstream of the spray dryer absorber. The high moisture content of the flue gas in conjunction with the alkaline material on the filter bags was believed to be conducive to the production of a cementacious cake on the filter bags. However, during three years of operation at Riverside, bag blinding has not been observed.[2-5] On the other hand, corrosion of the fabric filter has been significant in several locations and has necessitated repairs.[4,5] The amount of corrosion experienced in the Riverside fabric filter can be partially attributed to nontypical plant operating conditions (such as intermittent coal firing of the steam generator to maintain steam pressure) and to an extensive spray absorber test program.

After initial operation of the Riverside System, NSP, Joy, and B&V realized the need for special design features and operating procedures to minimize corrosion of fabric filters installed downstream of spray dryer absorbers. For NSP's 860 MW Sherburne Unit 3, which is under construction and will start up in 1987, the joint NSP, B&V, and Joy effort identified causes of corrosion in the Riverside fabric filter and developed cost-effective methods to minimize corrosion. The novel design concepts resulting from this joint effort are not unique. In fact, some of these features are installed in existing fabric filters in this type of application. However, the combination of all the corrosion protection features developed for the Sherburne Unit 3 fabric filter is new to the utility industry.

This paper identifies corrosion problems at Riverside and the design features which are incorporated into the Sherburne Unit 3 fabric filter to minimize corrosion. The Riverside and Sherburne Unit 3 fabric filter design parameters are listed in Table 1 for comparison. Corrosion problems at Riverside and design features incorporated into the Sherburne Unit 3 are addressed in the following categories.

(1) Flue Gas Temperature Control.
(2) Fabric Filter Insulation.
(3) Ambient Air Inleakage.
(4) Spot Coating Application.

TABLE 1. FABRIC FILTER DESIGN PARAMETERS

Parameter	Riverside 6, 7	Sherburne 3
Total Gas Flow, acfm (m^3/h)	420,000 (71,000)	3,450,000 (5,860,000)
Gas Temperature, F (C)	143 (62)	165 (74)
Approach Temperature, F (C)	18 (10)	40 (22)
Number of Filter Units	1	3
Compartments per Filter Unit	12	16
Bags per Compartment	250	384
Bag Diameter, Inches (m)	12 (0.3)	12 (0.3)
Bag Length, Feet (m)	35 (11)	33 (10)
Type of Bag	Woven Fiberglass*	Woven Fiberglass
Bag Cleaning Method	Reverse Gas	Reverse Gas
Gas-to-Cloth Ratio, acfm/ft^2 ($m^3/h.m^2$)**		
All compartments on line	1.3 (24)	1.9 (35)
One compartment cleaning per fabric filter	1.4 (26)	2.0 (37)
One compartment cleaning and one compartment out for maintenance	1.6 (29)	2.2 (40)

*Majority of the fabric filter compartments contain woven fiberglass bags.

**Fabric filter is sized to allow operation at 2.0 (37) gas-to-cloth ratio with the spray dryer absorber out-of-service. With the spray dryer absorber in-service, typically, two to four compartments are isolated to produce a 2.0 (37) gas-to-cloth ratio while the system is being tested. During normal operation, all compartments are in-service to avoid cold compartment walls.

FLUE GAS TEMPERATURE CONTROL

Fabric filters installed downstream of spray dryer absorbers operate in an environment with higher corrosion potential than that for conventional fabric filters.[6] A comparison of the fabric filter operating conditions developed for Sherburne Unit 3 and for conventional fabric filters is as follows.

	Spray Dryer Absorber Application	Conventional Application
Flue Gas Temperature in Fabric Filter, F (C)	140 to 180	250 to 350
Flue Gas Water Dew Point, F, (C)	125 (52)	108 (42)
Flue Gas Specific Humidity lb H_2O/lb flue gas (g H_2O/kg flue gas)	0.095 (95)	0.055 (55)

The combination of lower flue gas temperature, higher dew point temperature, and higher specific humidity increases the potential for condensation of moisture and sulfuric acid in the fabric filter.

At Riverside, in regions of low gas flow in the fabric filter compartments (near the tube sheet and in corners), the surface temperature of the casing wall can be 20 to 25 F (11 to 14 C) below the flue gas temperature. Thus, to minimize corrosion of the casing wall in these regions it is necessary to maintain the flue gas temperature at least 20 to 25 F (11 to 14 C) above the dew point (called 20 to 25 F approach temperature). To keep the compartment walls above the dew point, the flue gas entering the fabric filter at Sherburne Unit 3 will be maintained at a higher approach temperature of 40 F (22 C). Two methods were evaluated to produce this desired 40 F (22 C) approach temperature in the fabric filter: (1) maintain spray dryer absorbers outlet at 18 to 25 F (10 to 14 C) approach temperature, then reheat to 40 F (22 C) approach temperature prior to entering the fabric filters; and (2) maintain both the spray dryer absorbers outlet and fabric filters at 40 F (22 C) approach temperature. A comparison of the differential capital costs and present worth operating costs for these two methods is shown as follows.

	Differential Capital Costs $1,000	Differential Present Worth of Operating Costs for Thirty-five Years $1,000	Sum of Capital and Operating Costs $,1000
Maintain spray dryer absorber outlet at 18 to 25 F (10 to 14 C) approach temperature, then reheat flue gas to 40 F (22 C) approach temperature prior to entering fabric filter	285	Base	285
Maintain spray dryer absorber outlet and fabric filters at 40 F (22 C) approach temperature	Base	15,000	15,000

The difference in capital costs represents the additional costs of the bypass reheat ductwork and accessories. The difference in operating costs represents the increased lime consumption resulting from operating the spray dryer absorbers at a higher approach temperature compared to the operating costs due to decreased boiler efficiency resulting from extracting hot flue gas upstream of the air heater for reheat. As can be seen from this simplified analysis, the differential lime consumption cost is more than the cost of installing and operating the bypass reheat system.

The air quality control system arrangement and bypass reheat system for Sherburne Unit 3 is shown on Figure 1. Hot (700 F or 370 C) flue gas from the economizer outlet (above 3 percent of total gas flow to the fabric filter at design load) will be injected into the spray dryer absorber outlet ductwork. Using economizer outlet flue gas for reheat results in decreased boiler efficiency. Thus, it is desirable to minimize the use of economizer flue gas for reheat when load or ambient conditions permit. At Sherburne 3, a temperature monitoring system will be installed in each fabric filter compartment. Thermocouples will be installed in regions of low gas flows in each compartment to monitor the surface temperature of the wall. Based on the data provided by this temperature monitoring system, the amount of bypass reheat can be adjusted to maintain adequate wall temperatures and minimize corrosion in regions of low flow.

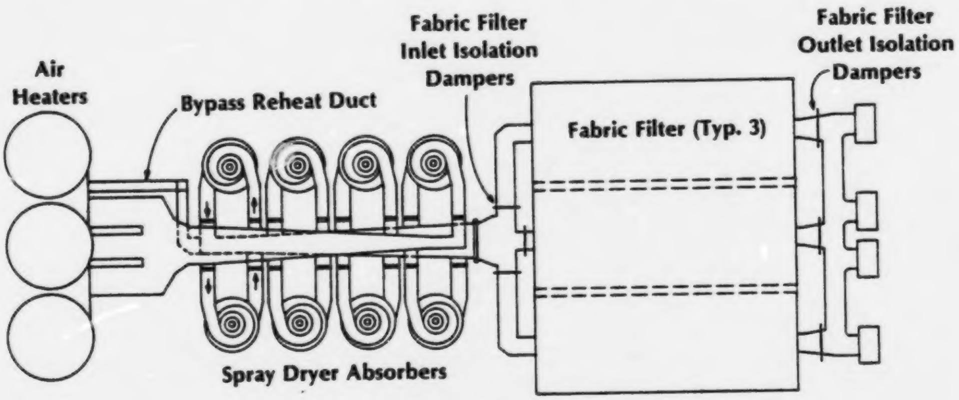
Air Heaters
Bypass Reheat Duct
Fabric Filter Inlet Isolation Dampers
Fabric Filter Outlet Isolation Dampers
Fabric Filter (Typ. 3)
Spray Dryer Absorbers

Plan View

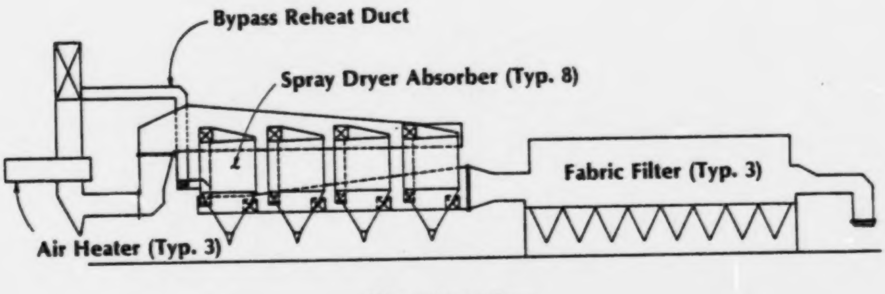
Bypass Reheat Duct
Spray Dryer Absorber (Typ. 8)
Fabric Filter (Typ. 3)
Air Heater (Typ. 3)

Elevation View

Figure 1. Sherburne Unit 3 Air Quality Control System

FABRIC FILTER INSULATION

Sufficient insulation is necessary to limit heat loss from air quality control equipment. The insulation thickness, however, does not significantly affect the bulk flue gas temperature downstream of spray dryer absorbers. In spray dryer absorber applications, the major effect of insulation thickness is on the fabric filter casing wall temperature. Figure 2 shows the calculated effect of insulation thickness on the bulk flue gas temperature and fabric filter casing inner wall temperature for Sherburne Unit 3. Even with no insulation on the fabric filter the bulk flue gas temperature does not decrease more than 10 F (6 C) when passing through the fabric filter. However, the casing wall temperatures are quite sensitive to the insulation thickness. Sufficient thickness is required to prevent extensive acid and water condensation on the interior walls. Two compartments on the Riverside fabric filter were reinsulated after two years of operation to determine if thicker insulation reduces wall corrosion. Increasing the insulation thickness from 4 to 5 inches did reduce compartment wall corrosion. Based on the Riverside results and the information presented in Figure 2, the fabric filter insulation for Sherburne Unit 3 will be five inches (13 cm) thick.

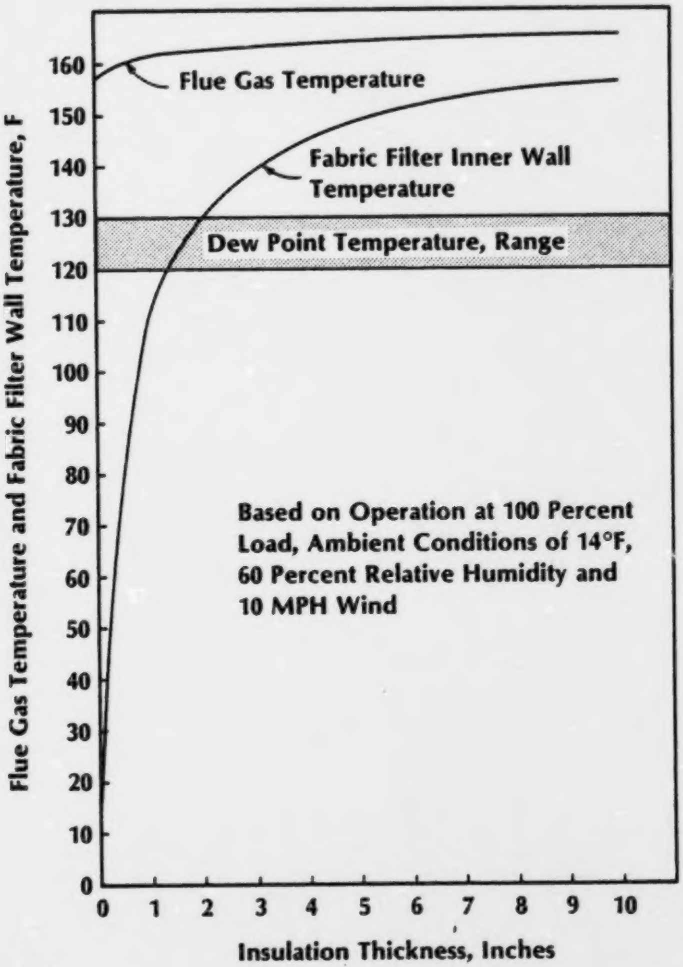

Figure 2. Effect of Insulation Thickness on Flue Gas Temperature and Wall Temperature

The quality of the insulation application is just as important as the thickness of the insulation. At Riverside an infrared thermal analysis after one year of operation revealed that significant heat leakage from the fabric filter was occurring at certain areas because of missing or damaged convection stops. Ambient air leakage into the cavity between the casing wall and insulation caused by improper convection stops defeats the protection provided by the insulation. All fabric filter compartment wall stiffeners for Sherburne Unit 3 are located inside the casing to eliminate air cavities between the casing wall and the insulation. The insulation, therefore, will be placed directly against the outside casing wall.

Another area in which significant heat loss occurs at Riverside is in the hopper crotch area along the outside walls. Figure 3 shows a detail of the typical insulation technique which is used at Riverside in the hopper crotch area. Also shown is the technique which will be used at Sherburne 3. The hopper support columns complicate the application of insulation in this area. Typically, insulation and lagging extend up to the middle of the hopper support columns. Movement of this support column damages the lagging and allows the insulation to bunch up. At Riverside, the insulation shifted in this area because of thermal cycling and opened up a path for heat loss. To minimize this problem at Sherburne 3, as shown on Figure 3, the insulation and lagging will entirely cover the support columns and tie into the top of the plate girders. Since the fabric filter will operate at relatively low temperatures (165 F or 74 C), this insulation will have little effect on the support column thermal deflection.

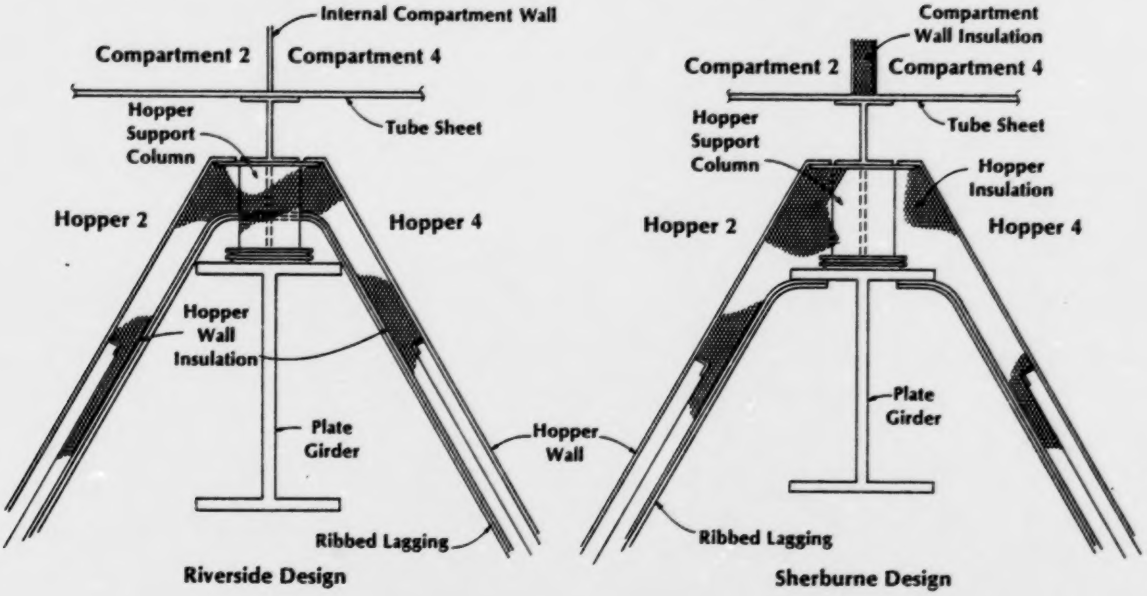
Internal Compartment Wall
Compartment 2
Compartment 4
Hopper Support Column
Tube Sheet
Hopper 2
Hopper 4
Hopper Wall Insulation
Plate Girder
Hopper Wall
Ribbed Lagging
Riverside Design
Compartment Wall Insulation
Compartment 2
Compartment 4
Hopper Support Column
Tube Sheet
Hopper Insulation
Hopper 2
Hopper 4
Plate Girder
Ribbed Lagging
Sherburne Design

Figure 3. Fabric Filter Crotch Area Insulation and Lagging Detail

An insulation detail which is being used at Sherburne 3 is a thermal gasket on each hopper discharge flange. The effectiveness of the hopper heaters is diminished if heat is conducted from the hopper walls to the ash handling equipment. Connecting bolts to the ash piping must still pass through this gasket (forming a heat conduction path); however, the heat transfer to the ash handling equipment is greatly diminished.

In addition to improved external insulation, Sherburne 3 will also have insulation between adjacent fabric filter compartments and between each compartment and the inlet and outlet gas plenums. At Riverside, acid and water condensation occurs on the walls of an on-line compartment when the adjacent compartment is out-of-service. As detailed on Figure 4, three inches (8 cm) of mineral wool insulation sandwiched between two 3/16-inch (5 mm) steel plates are between compartments and between each compartment and the gas plenums at Sherburne 3.

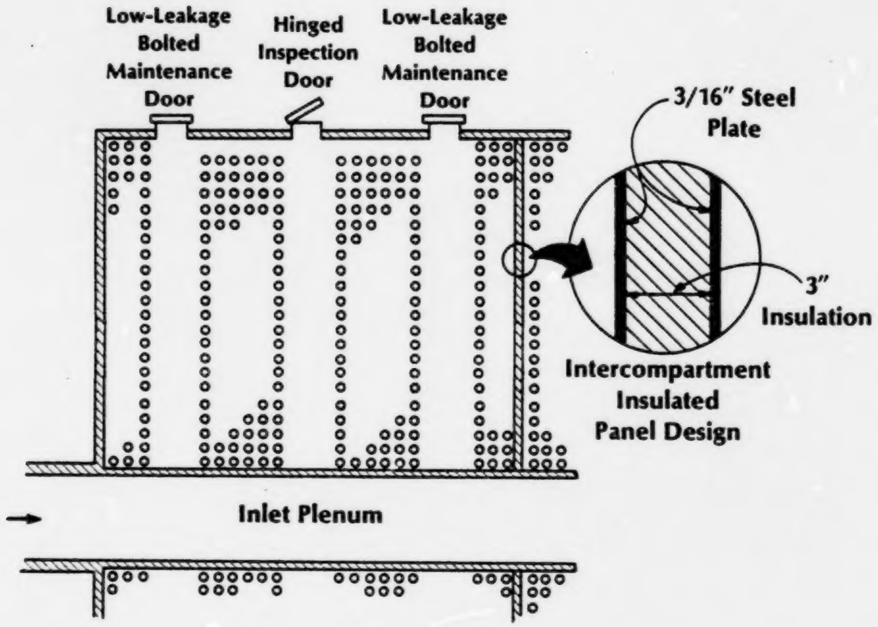
Low-Leakage Bolted Maintenance Door
Hinged Inspection Door
Low-Leakage Bolted Maintenance Door
3/16" Steel Plate
3" Insulation
Intercompartment Insulated Panel Design
Inlet Plenum

Figure 4. Fabric Filter Access and Insulation Details

AMBIENT AIR INLEAKAGE

Ambient air inleakage was identified as a cause of fabric filter corrosion around the doors at Riverside. Inleakage of ambient air causes cold spots on the casing walls, and if the inleakage rate is high enough, it can cause the bulk flue gas temperature to drop significantly. Figure 5 shows the effect of inleakage rates on the bulk flue gas temperature. An ambient air inleakage rate of less than two percent is expected for Sherburne 3. At this inleakage rate with the flue gas reheated to 40 F (22 C) above the dew point temperature, significant condensation is not expected even in the severest winter conditions. However, even this low level of inleakage can cause localized corrosion.

At Riverside, localized corrosion occurs around the access doors and compartment view ports on the access doors. Since view ports are a source of inleakage and are not used by maintenance personnel, they are not included in the Sherburne Unit 3 design. To further reduce inleakage, the compartment access doors for Sherburne 3 are separated into inspection doors and maintenance doors. As shown on Figure 4, the compartment interior walkways are arranged so that all of the walkways on a level can be reached by a single, quick-opening, hinged inspection door. During compartment maintenance activities when it is inconvenient to use only a single access door, one or more bolted maintenance doors in each compartment can be opened. These bolted maintenance doors are designed to have tighter seals than those on hinged inspection doors.

Due to the low flue gas temperatures, tight door seals are more critical on fabric filters downstream of spray dryer absorbers than on conventional higher temperature fabric filters. To determine the appropriate door seal material, various seals were tested by NSP at Riverside and by Joy in their laboratory. Unfortunately, the results do not agree with each other. In the laboratory, EPDM (ethylene-propylene-diene rubber) was the best door seal material. Low density fiberglass rope allowed inleakage twenty times greater than EPDM in the laboratory. However, at Riverside the low density fiberglass rope material remained soft and flexible and produced no visible signs of leakage, such as corrosion, on door frames. At Riverside, the EPDM material took on a set after only four months of operation. Visible signs of inleakage (corrosion) were apparent around the EPDM door seal. Additional door seal tests are being performed at Riverside to try to repeat these preliminary test results.

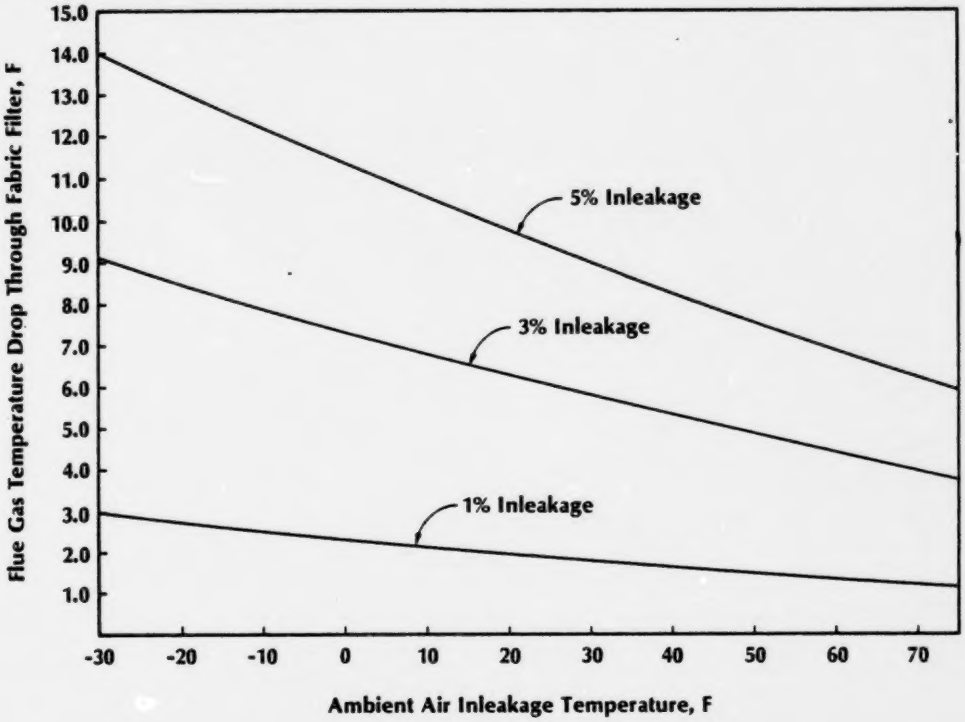

Figure 5. Flue Gas Temperature Drop Through Fabric Filter Versus Ambient Air Inleakage Temperature

As shown on Figure 6, the exterior compartment walkways around the fabric filters at Sherburne will be enclosed. The severe Minnesota winters prompted this design feature; however, the enclosure has secondary benefits in terms of limiting casing corrosion. The air space between the casing and enclosure helps insulate the fabric filter. Also the ambient air inleakage into the fabric filter will be preheated by the fabric filter heat loss into the enclosed area.

Another design feature of Sherburne 3 is that guillotine dampers will allow total casing isolation for each of the three fabric filter casings. Sherburne 3 is a cycling unit and is expected to operate for extended periods at reduced loads. Extended operating experience at Riverside with out-of-service compartments during reduced loads indicates that compartment poppet valves permit unacceptably high ambient air inleakage into isolated compartments. To reduce fabric filter heat loss and to allow extended on-line maintenance, NSP elected to install guillotine isolation dampers so that an entire fabric filter casing may be removed from service. The locations of the isolation dampers with repsect to the fabric filters are shown on Figure 1.

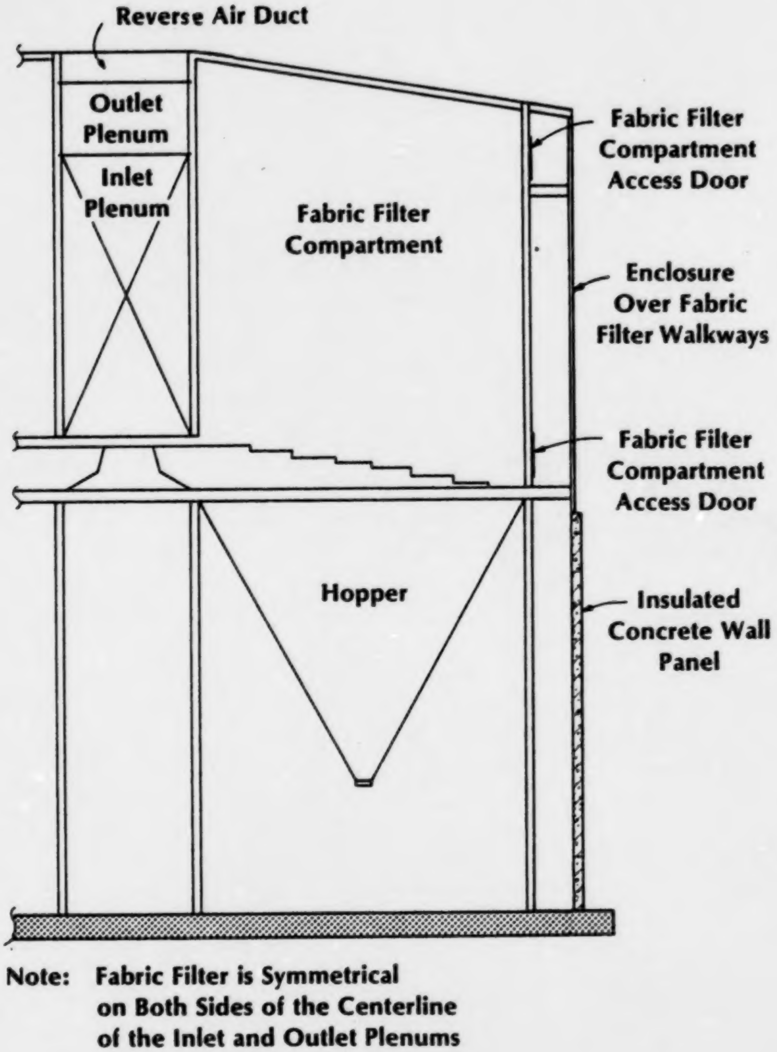
Reverse Air Duct
Outlet Plenum
Inlet Plenum
Fabric Filter Compartment
Fabric Filter Compartment Access Door
Enclosure Over Fabric Filter Walkways
Fabric Filter Compartment Access Door
Hopper
Insulated Concrete Wall Panel
Note: Fabric Filter is Symmetrical on Both Sides of the Centerline of the Inlet and Outlet Plenums

Figure 6. Fabric Filter Enclosure Profile

SPOT COATING APPLICATION

The corrosion protection design features which are being implemented at Sherburne 3 are expected to minimize corrosion; however, limited localized condensation may still occur. Metal support braces for insulation and support columns which penetrate the insulation and ambient air inleakage through door seals cannot be totally eliminated. To minimize the corrosion effects of condensation at Sherburne 3, the local areas where condensation occurs will be identified after start-up, sandblasted, and covered with a corrosion protection coating.

Spot coating of local areas experiencing corrosion has been successful at Riverside, where compartment access doors, door frames, and interior perimeters of doors have been cleaned and coated. Various corrosion protection coatings have been evaluated at Riverside. Based on six months of testing, a self-priming epoxy mastic is the most durable, cost-effective choice for this application. The corrosion which occurs in fabric filters does not appear to be as severe as that experienced in wet scrubbers. Thus, sophisticated coatings used in wet scrubbers are not currently needed for this application.

SUMMARY

The service environment inside fabric filters located downstream of spray dryer absorbers is considerably different from that inside conventional fabric filters. Based on observation from three years of operation at Riverside, corrosion in fabric filters downstream of spray dryer absorbers can be a major problem. To minimize fabric filter corrosion, Sherburne Unit 3 will have special design features which include bypass reheat for temperature control, improved insulation, reduced ambient air inleakage, and spot coatings.

Using these features will minimize the fabric filter casing corrosion. Subsequent operation of Sherburne Unit 3, Riverside, and other fabric filter installations downstream of spray dryer absorbers will provide additional information on effective corrosion prevention.

ACKNOWLEDGEMENTS

The authors wish to acknowledge those at Northern States Power Company, Black & Veatch, Engineers-Architects, and Joy Manufacturing Company who contributed the novel design concepts developed for Sherburne Unit 3.

REFERENCES

1. B. Brown et al., Performance Response of Dry SO_2 Removal System of Riverside Station, presented at the 43rd Annual American Power Conference, Chicago, Illinois, April 26-29, 1981.

2. J. M. Gustke, W. E. Morgan, and S. H. Wolf, Overview and Evaluation of Two Years of Operation and Testing of the Riverside Spray Dryer System, presented at the EPA/EPRI Eighth Symposium on Flue Gas Desulfurization, New Orleans, Louisiana, November 1-4, 1983.

3. G. M. Blythe et al., Field Evaluation of a Utility Dry Scrubbing System, presented at the EPA/EPRI Eighth Symposium on Flue Gas Desulfurization, New Orleans, Louisiana, November 1-4, 1983.

4. S. M. Kaplan et al., Dry Scrubbing at Northern States Power Company Riverside Generating Plant, presented at the EPA/EPRI Seventh Symposium on Flue Gas Desulfurization, Hollywood, Florida, May 17-20, 1982.

5. C. A. Sannes, Jr., M. F. Skinner, and S. H. Wolf, Riverside Spray Dryer and Baghouse Demonstration Program Test Results, presented at the 12th Biennial Lignite Symposium, Grand Forks, North Dakota, May 19, 1983.

6. M. L. Meadows, W. E. Morgan, and D. O. Swenson, Effects of Cycling Operation on Air Quality Control Equipment, presented at the EPRI Fossil Plant Cycling Workshop, Chicago, Illinois, November 2-4, 1983.

The work described in this paper was not funded by the U.S. Environmental Protection Agency and therefore the contents do not necessarily reflect the views of the Agency and no official endorsement should be inferred.

START-UP AND OPERATING EXPERIENCE WITH A REVERSE AIR FABRIC FILTER AS PART OF THE UNIVERSITY OF MINNESOTA DRY FGD SYSTEM

by: J.C. Buschmann, J. Mills
FLAKT, INCORPORATED
Environmental Systems Division
Knoxville, TN

W. Soderberg
University of Minnesota
Minneapolis, MN

ABSTRACT

A review of the start-up and operating experiences related to the Dry FGD System at the University of Minnesota is made with specific attention to the operation of the reverse air fabric filter. The system includes two separate gas trains, one connected to a stoker coal-fired boiler and the other to a pulverized coal-fired boiler, both using rotary atomization spray dryers operating with lime, once-through, for sulfur dioxide removal. Each system treats 120,000 ACFM flue gas. Operating parameters are reviewed and discussed with; 1) emphasis on the relative differences from conventional coal-fired operation, such as low temperature and pressure drop and ease of cleaning, and 2) enhancements derived from and contributing to the operation of the spray dryer, such as additional sulfur dioxide recovery.

SYSTEM DESIGN BASIS

The University of Minnesota Southeast Steam Plant is located downtown Minneapolis, on the banks of the Mississippi River. It consists of a Detroit stoker coal-fired boiler rated at 130,000 lb/hr of steam @ 450 psi and a Combustion Engineering pulverized fired boiler rated at 108,000 lb/hr of steam @ 450 psi. The two boilers drive a 12MW turbine and provide steam to the University. An analysis of the design coal is shown below. (Table 1)

TABLE 1. DESIGN COAL ANALYSIS - UNIVERSITY OF MINNESOTA

Proximate Analysis		
BTU	8700	8450
Total Moisture	24.55	25.11
Ash	8.85	9.09
Sulfur	0.71	0.73
Ultimate Analysis		
Carbon	49.40	50.18
Hydrogen	4.44	3.65
Sulfur	0.71	0.73
Oxygen	11.32	10.58
Nitrogen	0.73	0.66
Moisture	24.55	25.11
Ash	8.85	9.09
Ash Mineral Analysis		
Phosphorus Pentoxide	0.49	0.37
Silica	44.73	34.96
Ferric Oxide	4.08	8.30
Alumina	17.58	17.28
Titania	0.80	0.71
Lime	13.03	17.53
Magnesia	5.10	3.25
Sulfur Trioxide	12.23	14.75
Potassium Oxide	0.96	0.68
Sodium Oxide	0.44	1.87
Undetermined	0.66	0.30
Ash Fusion Temperatures		
Oxidizing		
Initial Deformation	2089	2130
Softening (H=W)	2203	2161
Softening (H-1/2W)	2234	2190
Fluid	2305	2264

The system design specification requires 70% removal of SO_2 and a maximum dust emission of .03 lb/mm BTU. Each boiler has its own dry scrubber and baghouse but share a common reagent preparation system. The design gas flow for each system is 120,000 ACFM at 375° F, (Figure 1).

Each FGD reactor is 24-1/2 feet in diameter, has a 22 foot cylindrical side wall, and a 60° cone bottom. The reactor has a roof gas disperser and side gas exhaust.

Each reactor has a single 150 Hp atomizer. The atomizer is driven by an Emerson frequency inverter drive through a 3600 rpm motor and a 4.4:1 speed increasing gear box manufactured by Sunstrand. The atomizer utilizes an abrasion resistant atomizer disk. The reactors, atomizer, and disk were supplied by Bowen Engineering, (Figure 2).

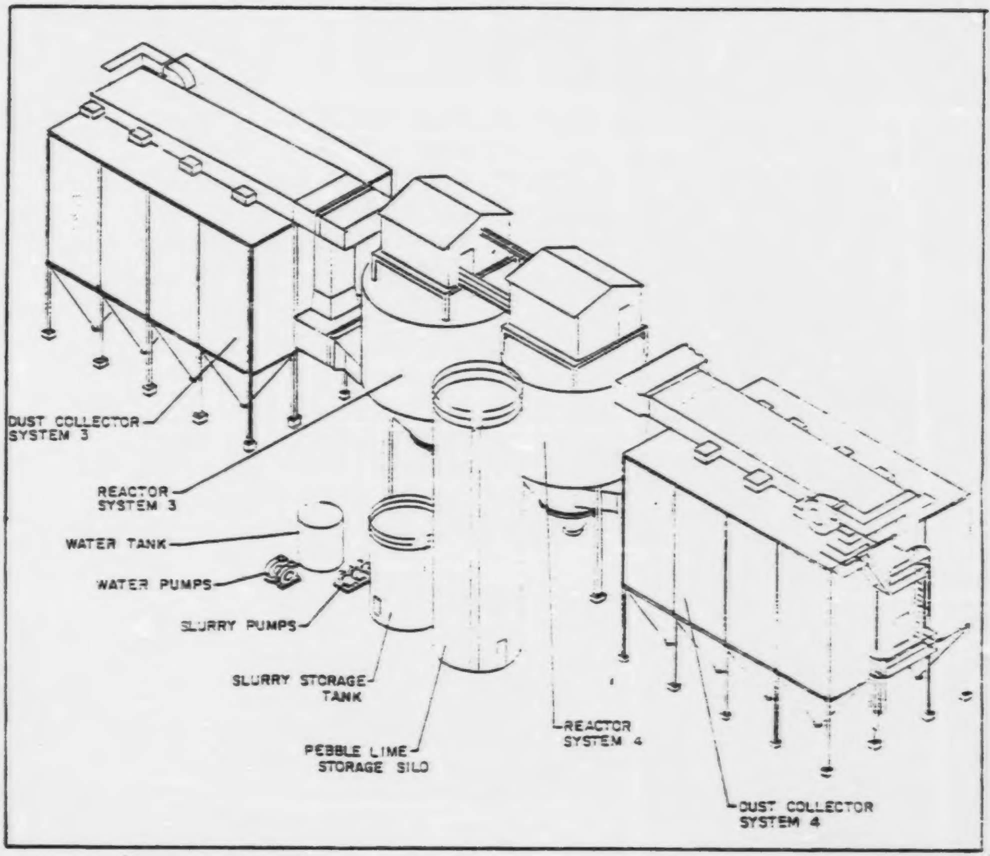
DUST COLLECTOR SYSTEM 3
REACTOR SYSTEM 3
WATER TANK
WATER PUMPS
SLURRY PUMPS
SLURRY STORAGE TANK
PEBBLE LIME STORAGE SILO
REACTOR SYSTEM 4
DUST COLLECTOR SYSTEM 4

Figure 1. University of Minnesota System General Arrangement

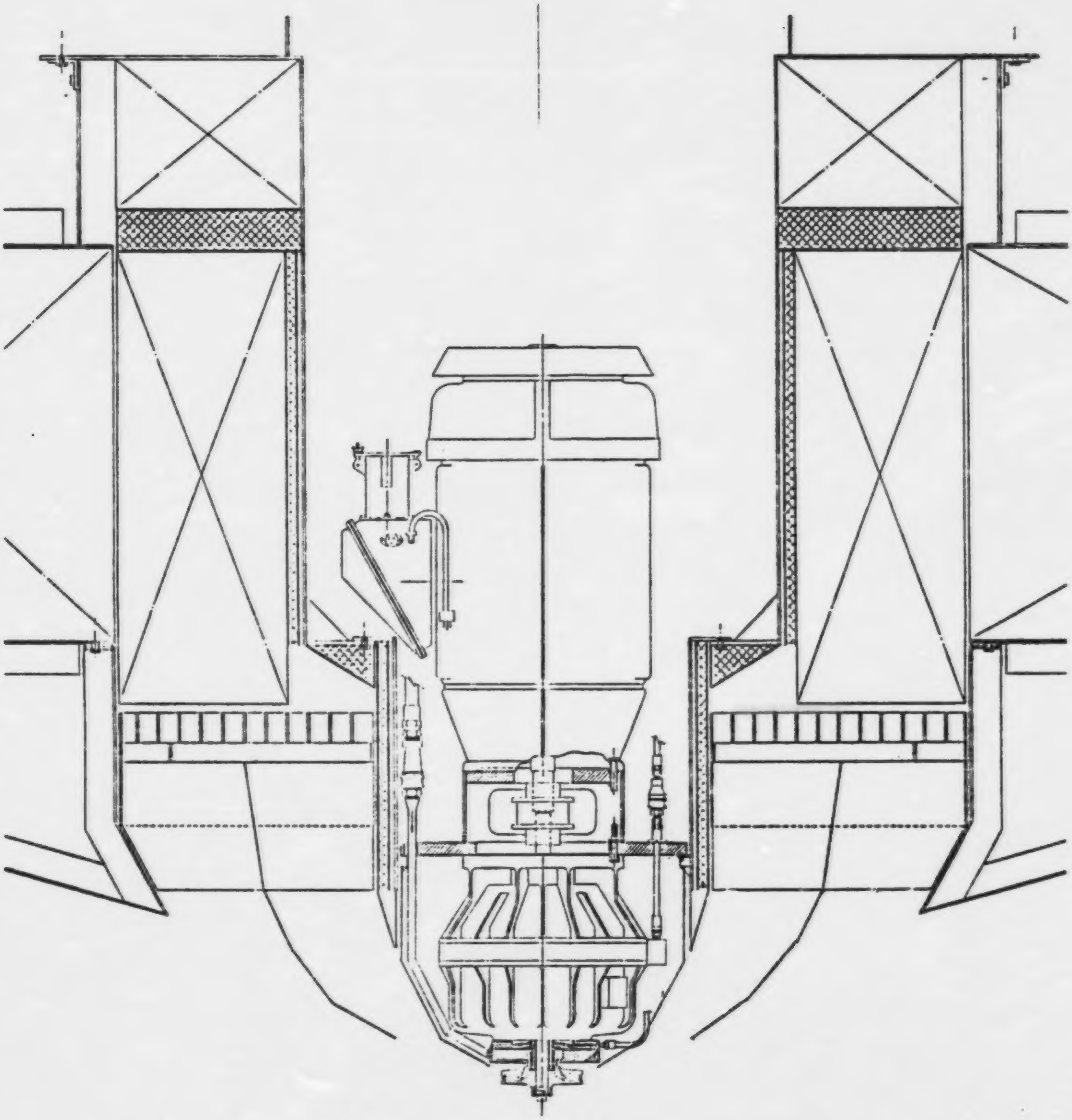

Figure 2. Cross Section of Atomizer and Gas Disperser

Each baghouse is a reverse air cleaned unit with 8 compartments, and a net net air-to-cloth ratio of 2.5:1 using fiberglass bags with a 10% teflon finish. There are 134 bags per compartment. Each bag is 8" diameter by 23'3" long. Bags are arranged in a 3-5-3 pattern in each compartment. Poppet type dampers are used for isolation and reverse gas cleaning. Reverse air-to-cloth ratio when cleaning is 1.5:1, (Figure 3).

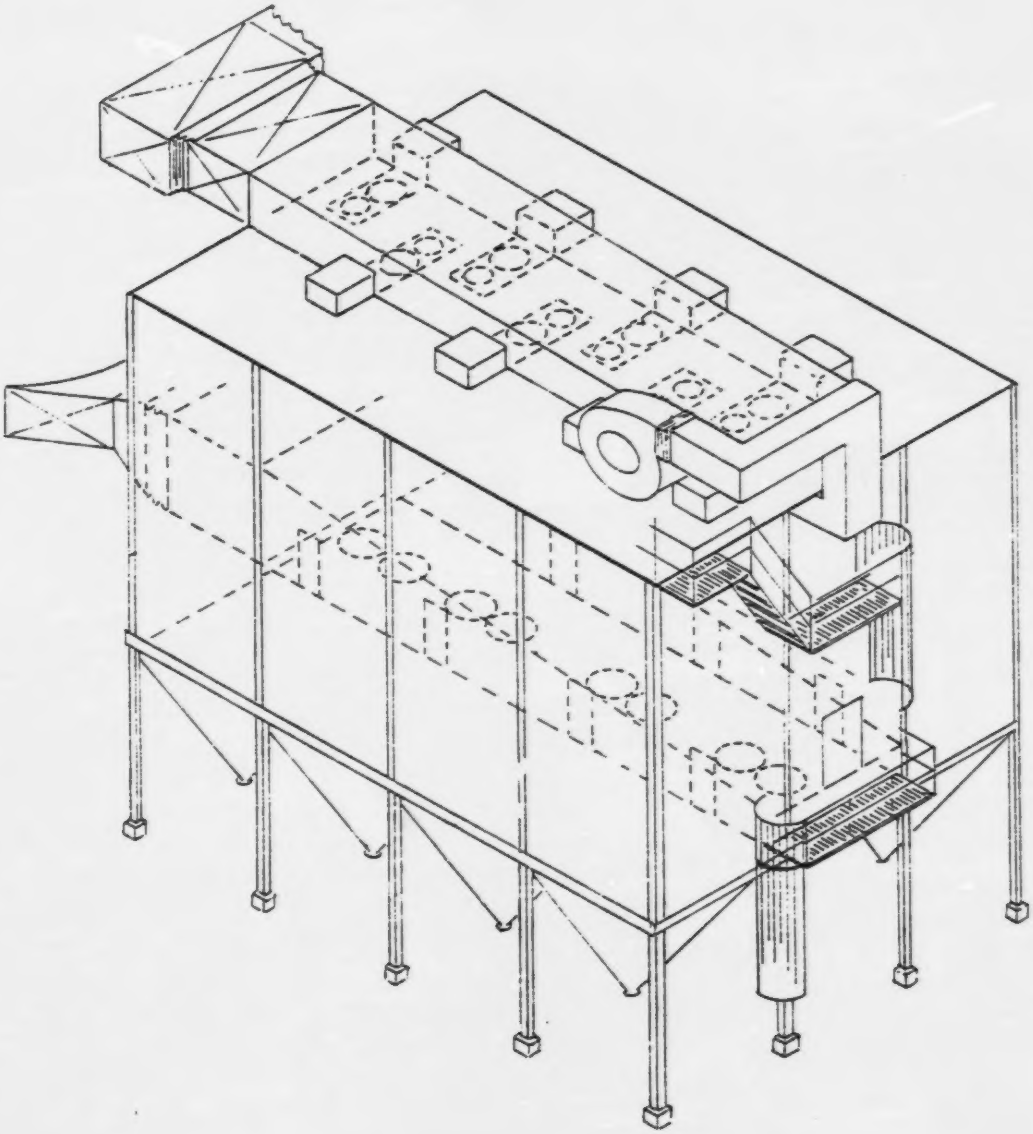

Figure 3. Baghouse Isometric View

The feed preparation system contains a 150 ton capacity lime silo, a 2 ton per hour Wallace & Tiernan lime slaker, a 4' diameter Sweco screen for grit separation and a 20,000 gallon lime slurry storage tank. A water supply tank and booster pumps are also included to provide regulated system water supply pressure. The feed preparation system is enclosed in a heated and ventilated building while the reactors and baghouses are installed outdoors. The lime slurry transfer pumps from slaker to storage tank are Warman centrifugal type, while the reactor feed pumps are Robbins & Meyers progressive cavity pumps.

The ash conveying system is a vacuum type pneumatic system provided by United Conveyor Corporation. It conveys from both baghouses and reactors to a common ash silo and truck unloading station. No recycle of ash or product is utilized in the FGD system.

OPERATING HISTORY

The stoker-fired boiler (Unit 4) first began operation in September of 1983. Start-up of the FGD system began in October and was mostly complete by January of 1984. Boiler operation has been varied with periods of low load, full load and shutdown intermixed throughout the period. Total running time has been approximately 6000 hours since start-up. The FGD system has been online and in compliance with emission requirements for 90% of this period. During periods of FGD unavailability, the boiler operation was unaffected and the baghouse continued to collect particulate. The problems causing system downtime have been corrected and we anticipate much better performance in the future. The pulverized coal-fired boiler (Unit 3) has had numerous problems with burner and windbox adjustments. These problems have delayed Unit 3 FGD system start-up until July of 1984. This start-up is still in progress.

START-UP PROBLEMS/SOLUTIONS

LIQUID DISTRIBUTOR

The Bowen/Sunstrand atomizer design utilizes a large (15") diameter feed distribution plate with two projecting feed pipes located immediately above the atomizer disk. (Figure 1.) The atomizer disk is much smaller (7-1/2") in diameter. A portion of the liquid spray coming from the disk contacted the upper side of the fixed feed plate and agglomerated into very large drops that could not be dried. This problem was solved by redesigning the feed plate to remove it from the spray zone around the disk. (Figure 4.)

ATOMIZER DISK

The Bowen supplied atomizer disk was 7-1/2" in diameter. When operated at its maximum speed of 16,000 rpm, the resulting tip speed was 530 FPS. The spray produced was not fine enough to produce dry product when the reactor outlet temperature was lowered below 170° F. The disk also had

ORIGINAL DESIGN

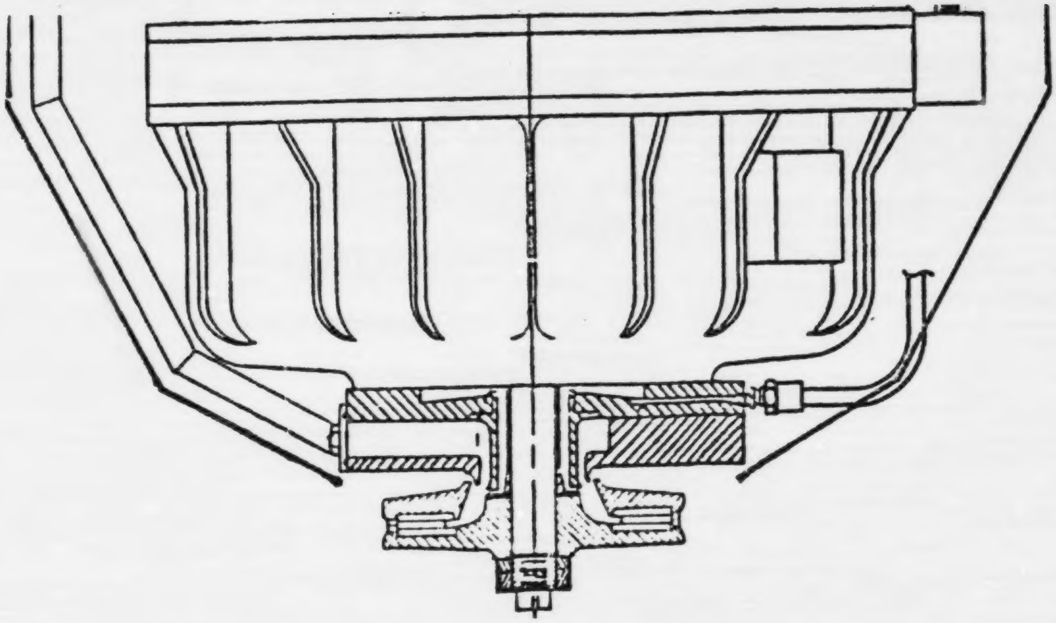

MODIFIED DESIGN

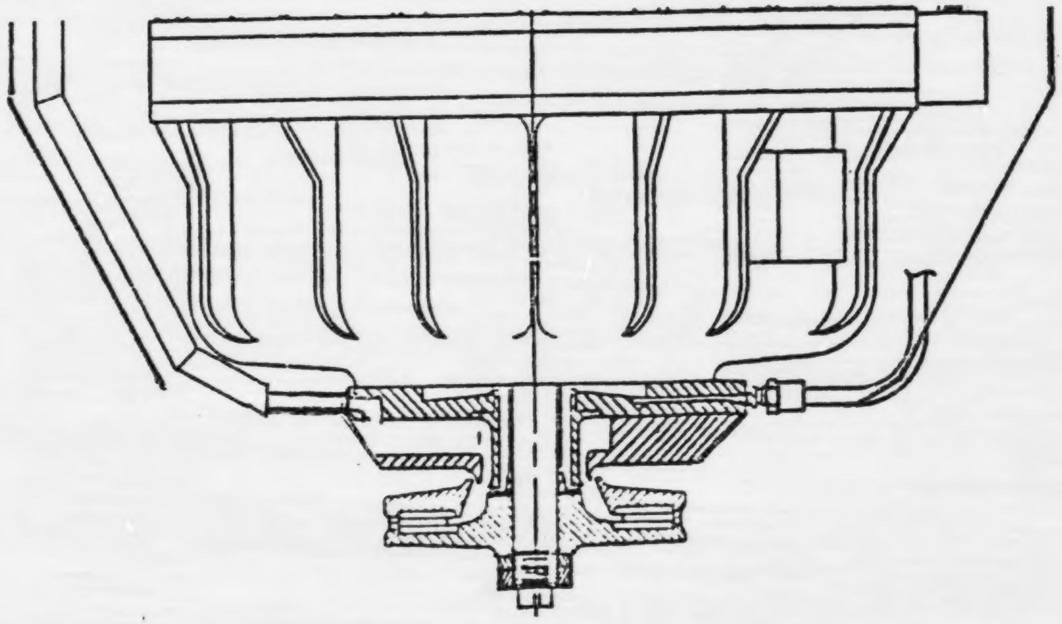

Figure 4. Liquid Distributer

a feed capacity much greater than required. The only partially filled disk suffered from predrying of the lime slurry inside the disk and ultimately plugged ports, and vibration problems. This same problem was reported by EPRI with the Bowen atomizer at the Arapahoe pilot plant.

We solved both of these problems by designing a new atomizer disk with a diameter of 9-5/8", giving a tip speed of 670 FPS. This disk was designed with only two slurry outlets, each 8mm in diameter. The original disk had 12 ports, each 6mm X 10mm. The new FLAKT designed disk does not show any tendency to plug-up or become imbalanced. The better atomization from the new disk permits operation of the reactor at temperatures as low as 150° F, while still producing a dry product.

GAS DISPERSER

The Bowen gas disperser is a low pressure drop design that works well or near its design load. Unfortunately, it does not have a very wide turndown range. Below 65,000 ACFM the drying performance of the reactor deteriorates due to low velocities in the hot gas/spray mixing zone. This is not a problem on Unit 4 which runs at about 90,000 ACFM at full load and 60,000 ACFM at low load. However, the Unit 3 boiler only produces 65,000 ACFM at full load. We are modifying the Unit 3 gas disperser to give the correct design velocity at 65,000 ACFM. This will then allow a reasonable turndown range for this boiler as well. This is an example of the problems that overly conservative design specifications can cause. Owners and Architect engineers are urged to make realistic estimates of normal operating conditions so that vendors can properly size equipment. (Figure 5.)

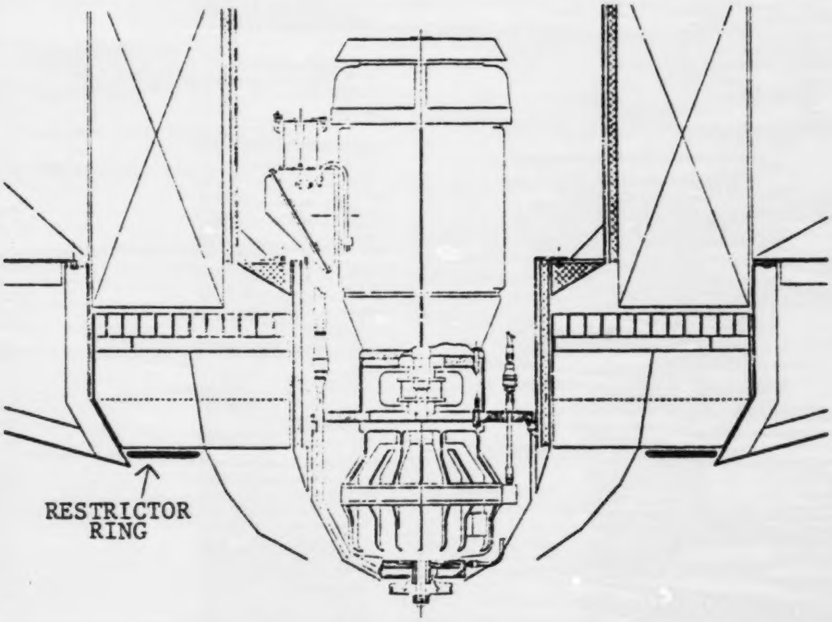

Figure 5. Cross Section of Gas Disperser with Restrictor Ring

BAGHOUSE

During a period of extremely cold weather (-35° F) the solenoid valves controlling the air cylinders operating the baghouse dampers froze up. This required manual damper actuation when cleaning was needed. The problem will be corrected by putting spot heaters on the solenoil valves.

More remarkable were the problems we did not have. Even though the outside temperature was often below zero and occasionally -35° F, there were no problems with condensation or corrosion in the casing, doors, or tube-sheet. There were also no problems with discharge of dust from the hoppers.

ASH CONVEYING

The reactor ash conveying system is a vacuum pneumatic system using ambient air. During periods of sub-zero weather, the cold conveying air and exposed outdoor conveying pipeline would cause the residual moisture in the FGD dust to freeze. This plugged the pipe fairly quickly. The solution to the problem was insulating the pipeline and pulling the conveying air from inside the boiler building where it was reasonably warm.

During the early phases of start-up, we had occasional problems with large (3" diameter) chunks of solid material plugging the conveying line. Now that the spray dryer is running smoothly, we no longer form these large pieces and have no conveying problems.

FEED PREPARATION SYSTEM

We have had a few problems associated with cold weather and freeze protection. These were solved by relocating lines and adding heat tracing. From a process and mechanical standpoint, the equipment has been remarkably trouble free.

CURRENT SYSTEM PERFORMANCE

The Unit 4 FGD system runs whenever the boiler runs, and follows load as required by the University. The lime slaking system is run batchwise. The reactor consumes the 20,000 gallons of lime slurry stored in about two days. The slaker is then run for about 8 hours to refill the tank. Lime slurry is stored at 20% solids and then is diluted to 10% solids before being atomized into the reactor. The reactor operates at temperatures as low as 150° F while producing a dry dust. Based on spot checks and calculations, SO_2 removal is normally 90% or higher. Continuous SO_2 monitors supplied by the University are not yet in service, so we have to keep the system operation safely below the required SO_2 emission level. When these monitors are in service, the control system will be set to minimize lime consumption while just meeting SO_2 emission requirements.

Baghouse inlet grain loading is about 4 grains per actual cubic foot. Gas temperature is typically 160° F. Pressure drop is typically 2" of wg just after cleaning. The pressure drop will rise slowly until 5" wg is reached. The cleaning cycle is then automatically restarted. The typical interval between cleaning cycles is 12 to 24 hours. Outlet opacity is less than 5%. This excellent performance appears to be the result of the porosity and good cake release of lime dust when mixed with fly ash. We have seen reasonably good cleaning if the compartment is isolated and no reverse air is applied. No bag failures have been reported to date. Low temperature operation after the FGD system does not appear to have any negative effect on baghouse operation. Corrosion and hopper discharge problems have been non-existant. We attribute this success to good door seals, all compartments on line most of the time, and sufficient hopper heating.

SUMMARY

We view dry FGD as a superior alternative to wet FGD for SO_2 removal. It can also result in unusually good fabric filter operation in properly designed systems.

SPRAY DRYER/BAGHOUSE EXPERIENCES ON A 1000 ACFM PILOT PLANT

by

Wayne T. Davis
Gregory D. Reed

Civil Engineering Department
The University of Tennessee
Knoxville, TN 37996

and

Tom Lillestolen
Flakt, Inc.
Knoxville, TN 37923

ABSTRACT

This paper summarizes the results of a research effort conducted during 1982-1984 in which a 1000 ACFM spray dryer/fabric filter pilot plant was utilized to obtain performance data on SO_2 removal using a $Ca(OH)_2$ slurry. Data are included on the performance of the spray dryer and the spray dryer/baghouse as a combined system which clearly shows the benefits of the baghouse as a means of enhancing the overall removal. Physical/Chemical analyses of the products are also included. A discussion is also included of the operational problems encountered during the testing program.

The performance data shows that the spray dryer/baghouse can be operated with efficiencies in excess of 90% under specified operating conditions.

SPRAY DRYER/BAGHOUSE EXPERIENCES ON A 1000 ACFM PILOT PLANT

OVERVIEW

This report summarizes results of a pilot test program conducted during 1982-1984 in which research was conducted on a 1000 ACFM spray dryer/fabric filter sulfur dioxide removal system located on a slipstream of the flue gas at the University of Tennessee steam plant. The primary objective of this study was to develop stoichiometric ratio data using a $Ca(OH)_2$ slurry. Secondary objectives were to 1) identify the effects of recycle of the spray dried product and 2) identify the nature of the reacted compounds.

Operating conditions for the tests reported herein were maintained at constant conditions throughout the test program at the following values (except where otherwise noted):

ACFM: 1050 ± 25 ACFM
SO_2 concentration: 1100 (wet basis) ± 100 ppm
Approach to wet bulb temperature: 16 - 20° F
Inlet temperature: 300° F ± 10° F
Slurry conditions: lime slurry
lime slurry + continuous recycle
lime slurry + continuous recycle + flyash

The test program consisted of 1) conducting performance tests on the spray dryer and/or the spray dryer/fabric filter system in which the SO_2 removal efficiency was determined as a function of stoichiometric ratio, and 2) collection and analysis of the slurries, and spray dryer and bag house products. These latter analyses included measurements of slurry viscosity, and analyses of the products including total sulfur, specific surface area, moisture content, and carbonate (CO_3) content. A description of the experimental system and test procedures is included in the following section, followed by the results.

TEST PROGRAM

EXPERIMENTAL DESCRIPTION

Figure 1 is a schematic diagram of the pilot test facility which was constructed in 1980 on a slipstream of the University of Tennessee Riley stoker fired boilers. The original system consisted of a slaking system control room, a seven foot diameter spray drying chamber with a variable speed Stork-Bowen AA-6 Spray Machine (5000-21000 rpm) and 6" diameter centrifugal atomizer

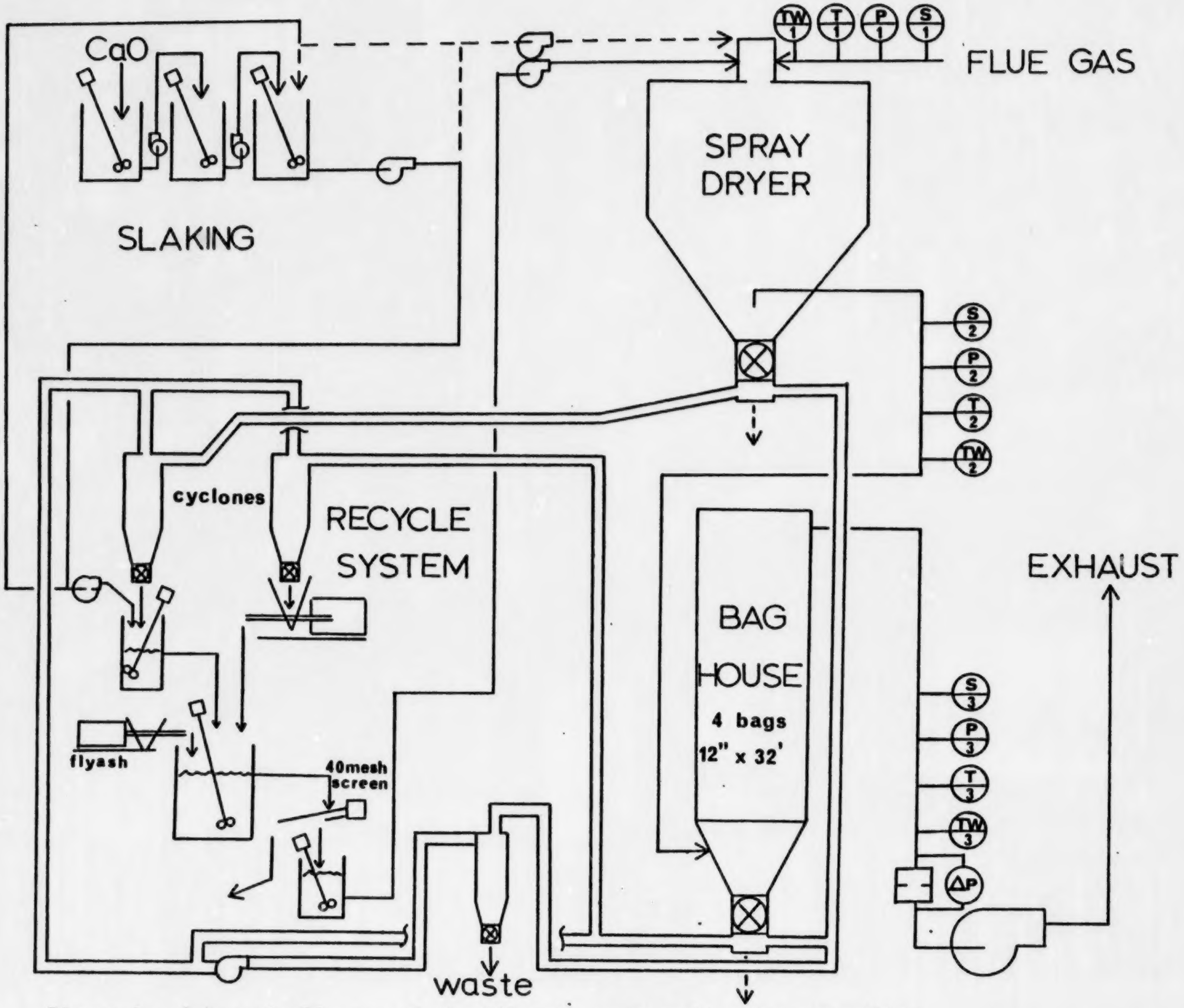
CaO
SLAKING
FLUE GAS
TW 1
T 1
P 1
S 1
SPRAY DRYER
S 2
P 2
T 2
TW 2
cyclones
RECYCLE SYSTEM
BAG HOUSE
4 bags
12" x 32'
EXHAUST
S 3
P 3
T 3
TW 3
ΔP
flyash
40mesh screen
waste

Figure 1: Schematic Diagram of the Pilot Spray Dryer/Bag House Facility.

with 6 nozzle inserts, and a low energy shaker baghouse with four 12" x 32' fiberglass filter bags (bottom entry).

A continuous pneumatic recycle system was installed in 1983. This system provided a continuous partial recycle of the dried product collected in the spray dryer. Since the baghouse was periodically cleaned (rather than continuously cleaned), the baghouse product was pneumatically conveyed to a cyclone separator, collected in a screw feeder, and partially recycled back into the slurry feed as needed. The lime feed, spray dryer recycle, and baghouse recycle were mixed in an intermediate mixing tank, and screened through a 40 mesh vibrating screen prior to delivery to the atomizer. This technique was found to be a necessity for successful operation at solids concentrations in the 15-35% solids ranges to prevent clogging of the slurry lines and atomizer nozzles due to the small volumetric flow rate of the delivery system (less than 0.30 GPM with 1/4" ID lines). Further it was found that it was necessary to continuously recycle the lime slurry between the final slaking room mixing tank and the recycle tanks located at the spray dryer in order to prevent plugging in the transport lines when the atomizer feed rate was terminated.

The system provided for continuous monitoring of the static pressure, temperature, and SO_2 concentrations at the inlet and outlet of the spray dryer and the baghouse. (Ports 1, 2, and 3, respectively). The sampling locations for these are indicated in Figure 1 by the symbols P, T, and S, respectively. Continuously extracted samples of flue-gas were transported through heat traced lines to one of three analyzers: two Lear Siegler SM810 analyzers and a TECO Model 800/Model 40 analyzer. Dependent on the availability of analyzers data were acquired simultaneously at multiple ports or sequentially. Wet bulb temperatures were measured at all three ports by a hand-held wetted wick thermometer and/or thermocouple (symbol TW in Figure 1).

Temperature control was accomplished by a dilution air damper located upstream of the inlet sampling ports of the spray dryer. The concentration of SO_2 (1100 ppm) was maintained by controlled supplemental injection of SO_2 vapor obtained from tanks of liquid SO_2.

TEST PROCEDURES

All data reported herein represent individual tests of 45 minutes to 1 hour duration. A single one hour evaluation consisted of monitoring 21 different parameters including disk speed, SO_2 concentrations at Ports 1-3, temperature at Ports 1-3, available CaO (by HCl titration), orifice pressure drop (flow rate), static pressures at Ports 1-3, lime slurry flow rate, barometric pressure, wet bulb temperatures at Ports 1-3, ambient temperature, air in-leakage rate, recycle ratio of product to lime, and recycle ratio of fly ash to lime.

SUMMARY OF RESULTS

$Ca(OH)_2$ SLURRY (NO RECYCLE)

The results of a series of tests in which $Ca(OH)_2$ slurry was injected and atomized into the spray dryer are shown in Figure 2 which shows the overall relationship between SO_2 removal efficiency and stoichiometric ratio (SR) for

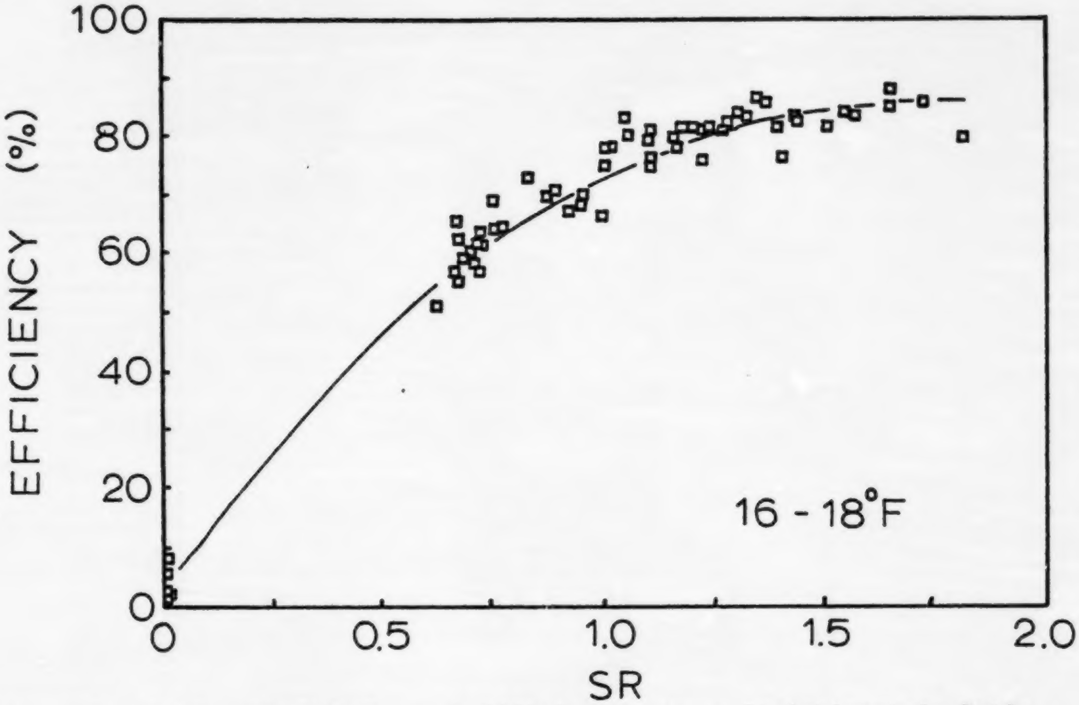

Figure 2: Sulfur Dioxide Removal Efficiency versus Stoichiometric Ratio at an Approach of 16 - 18 °F.

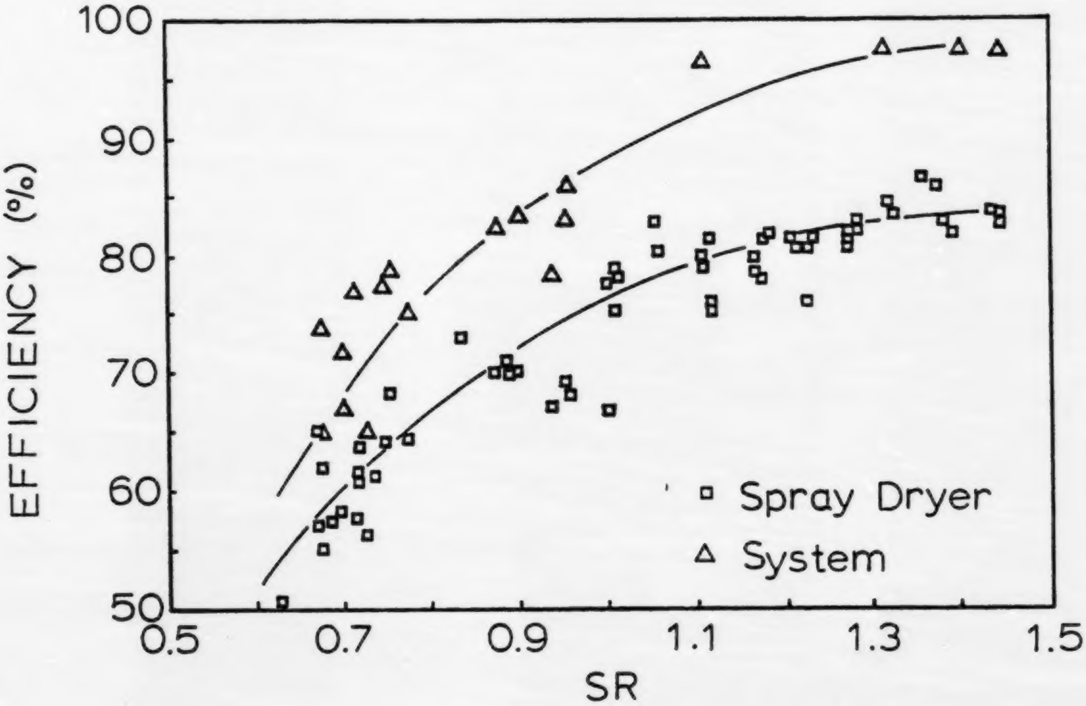

Figure 3: Comparison of Spray Dryer and Overall Removal Efficiencies.

the range of 0-1.8 SR for the spray dryer only. These data were collected at an approach to saturation of 16-18°F. In this report the stoichiometric ratio refers to the ratio of the number of moles of $Ca(OH)_2$ injected to the moles of SO_2 entering the system. On this basis the theoretical ratio is 1.0 for a perfect reaction. In general the data indicate that "near-stoichiometric" conditions can be achieved up to 60% efficiency. At 60% efficiency, SR = 0.7 and the utilization of $Ca(OH)_2$ was approximately 85%. The SO_2 removal efficiency at SR = 0 (water injection with no lime) ranged from 0-10% suggesting a minimum effect of the UT boiler fly ash on removal.

Further, the data exhibited a significant decrease in utilization as stoichiometric ratio was increased. At a SR = 1.0, the efficiency was approximately 75% (utilization = 75%), and at a SR = 1.2, the efficiency was 80% (a utilization of only 67%). It is also evident that the individual data points fluctuated about the mean value. For example at a SR = 1.2 the efficiency values actually varied from 74% up to 84%.

Figure 3 was restricted to efficiencies of 50-100% and an SR of 0.5-1.5 to provide more detail. Also shown in Figure 2 is a superposition of the data for overall SO_2 removal across the spray dryer/fabric filter system for comparison to the "spray dryer" data. For the overall system, near stoichiometric ratios were achieved up to SR = .8. For the data collected at SR > 1.1, the SO_2 removal efficiency was greater than 95%. Values above 97% were within the error of measurement of the SO_2 analyzers and could not be determined accurately. The importance of the fabric filter as a reactor/contactor for enhanced SO_2 removal is obvious from these data.

It should be noted that the above results are for a specific set of operating conditions. Extrapolation of the data to other operating conditions (temperature, SO_2 concentration, approach to saturation, or fly ash loadings/chemical composition) may not be possible. This can be illustrated by a comparison of the above data to a similar set of data in which the only significant operating parameter changed was the approach to saturation. Figure 4 shows a comparison of data collected at an approach to the wet bulb temperature of 16-18° F to that collected at an 18-20° F approach. This two degree shift in the approach to saturation resulted in an observable shift in the efficiency at a given stoichiometric ratio.

EFFECT OF RECYCLE

In the more recent test programs (1983-1984) more emphasis has been placed on the effect of recycling a portion of the waste product from the spray dryer and/or baghouse in an effort to improve on the utilization of CaO at the higher stoichiometric ratios. Tests were conducted at both of the operating conditions previously described (16-18°F and 18-20°F approaches to saturation) in an effort to quantify the potential benefits of recycle. The recycled materials consisted of various amounts of spray dried products and fly ash being added to the $Ca(OH)_2$ slurry fed to the spray dryer. Fly ash was injected by a screw feeder into the mixed slurry at a rate corresponding to approximately 3 grains mixed/ACFM (equivalent to a typical flue gas emission rate) since the loading contributed by the UT boilers was generally less than 0.3 grains/CF. The fly ash was obtained from TVA's Kingston steamplant (low alkalinity ash) and had a mass mean diameter of 7.8 μm and a geometric standard deviation of 1.7-1.9.

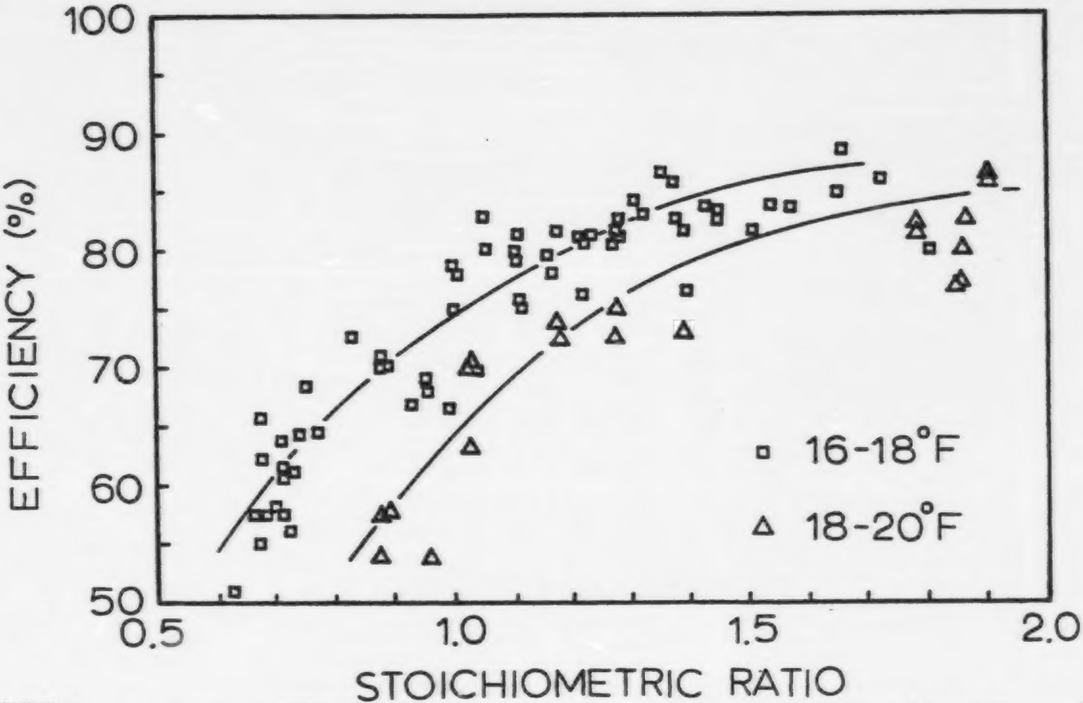

Figure 4: Comparison of Performance for Two Different Approaches to Saturation.

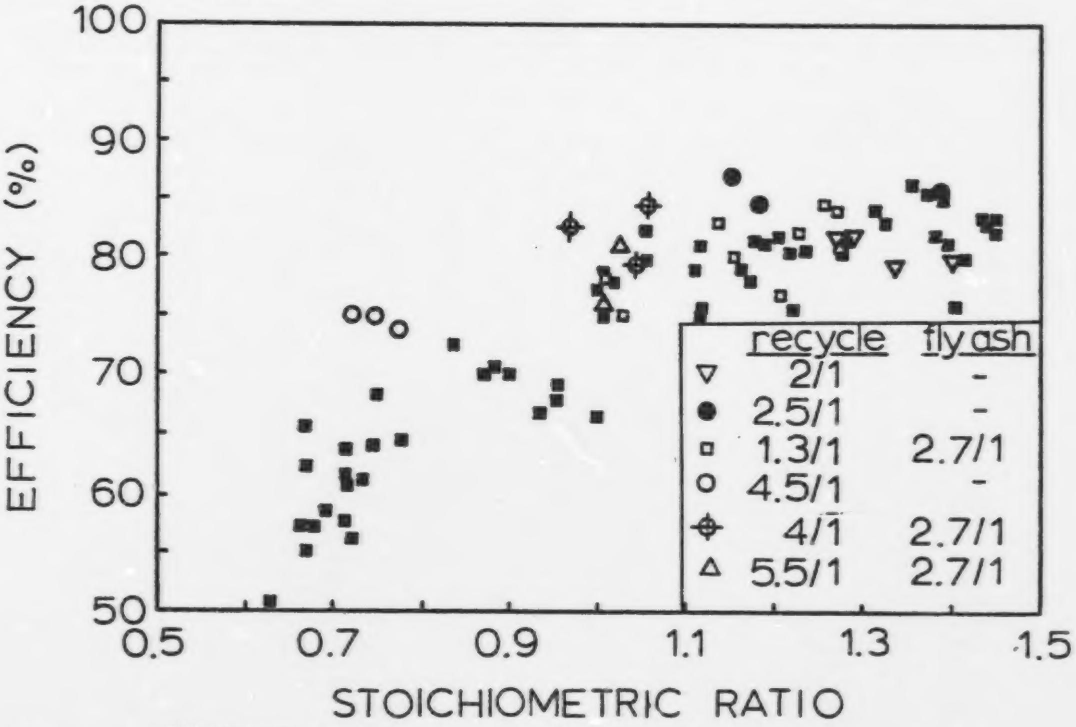

Figure 5: Comparison of Recycle Data to Baseline Data (■) for the Spray Dryer.

Figure 5 is a summary of the continuous recycle test data which were obtained at various concentrations of recycle product and fly ash at 16-18° F across the spray dryer. For these data, the quantity of recycle product is reported as the mass ratio of product to new $Ca(OH)_2$ as CaO (lb/lb). A 4/1 ratio of product to lime corresponded to approximately 33% solids at a stoichiometric ratio of 1.2. No effect was observed for tests in which only fly ash was recycled or tests in which the product recycle ratio was less than 2/1. However a positive enhancement was generally obtained when the ratio of product/lime exceeded 2/1.

A similar series of tests have been conducted at the 19-20°F approach to saturation in which the slurry concentration was maintained at 35% solids. The results of these tests are shown in Figure 6. These recycle tests consisted of "spray dryer product", "baghouse product", and "recycle product plus fly ash". No significant difference was observed between the different types of recycle. In general, the recycled product improved the utilization. One of the data sets was collected on the same day, all conditions remaining constant except for the recycle product addition. The efficiency was enhanced from 82 up to 86% with a simultaneous decrease in stoichiometric ratio from 1.38 down to 1.19. While the above data tend to show some improvement in utilization with the use of recycle, further testing is being conducted to more clearly understand the mechanisms involved and the interaction between the recycled product, fly ash and the new $Ca(OH)_2$ slurry. One additional benefit of recycle is that the moisture content of the products collected in the recycle mode have been observed to be typically in the 2-5% range, whereas the mositure content of the product without recycle ranged from 2-20% with a typical values of 10%. This may result in a product which is easier to handle, particularly in those systems where the outlet temperature is near the saturation point.

ANALYSIS OF PRODUCTS

Detailed chemical analyses were conducted on the products collected from the tests shown in Figure 2. Analyses included the measurement of the specific surface area, sulfur content, moisture content and the carbonate content utilizing the techniques or instruments shown below:

Product Analyses

Measurement	Instrument or technique
Surface area (m^2/g)	Micromeritics Model 2200 (modified BET Technique)
Sulfur content (%S)	Fisher Model 470
Mositure content (% H_2O)	Weight loss at 105° C
Carbonate content (% CO_3)	Acidification/Capture of CO_2 gas

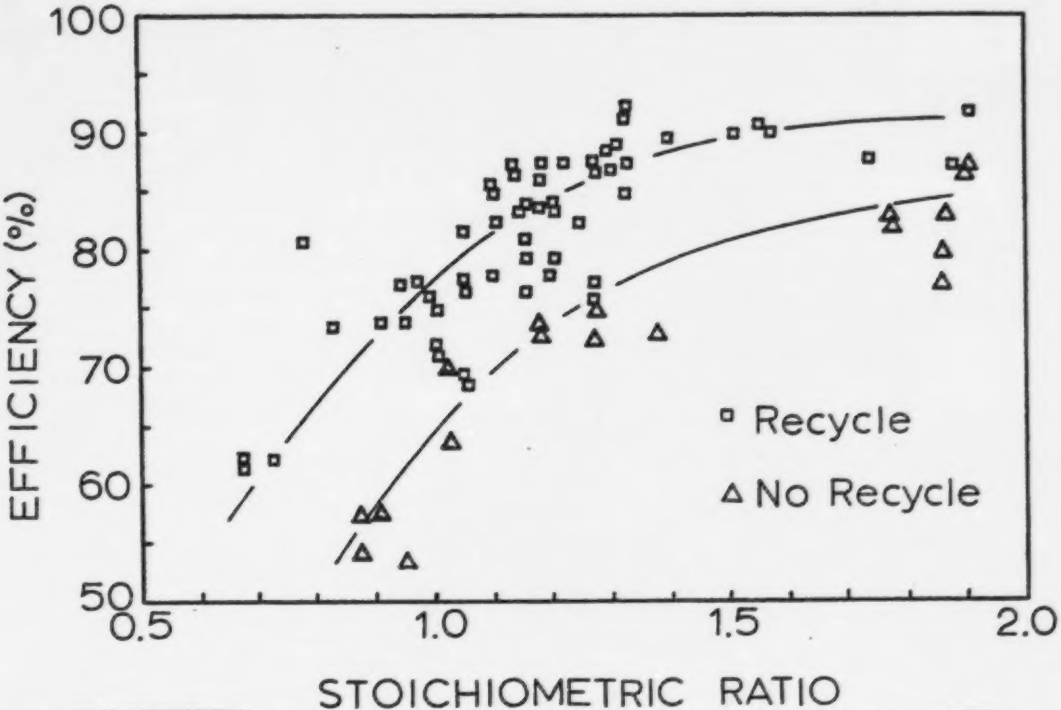

Figure 6: Comparison of Recycle Data (35% solids) to Baseline Data for the Spray Dryer.

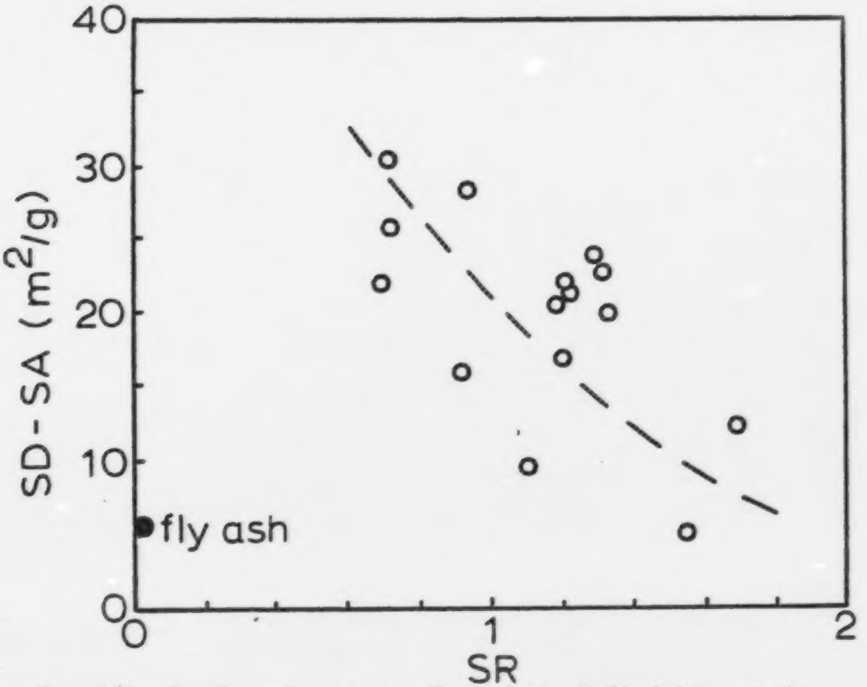

Figure 7: Specific Surface Area as a Function of Stoichiometric Ratio.

The surface area of the products ranged from 30 down to 5 m^2/g with a tendency toward decreasing surface area as the stoichiometric ratio of the lime was increased. (See Figure 7). The UT fly ash collected during the tests with no lime slurry had approximately 5 m^2/g of surface area. Previous tests on 23 different fly ashes have revealed a range of 0.21-12.52 with an average of 1.59, indicating that the spray dried products have significantly greater surface area than fly ash (1).

The moisture content as stated earlier, ranged from 2-20% with a typical value of 10%; however no dependency on stoichiometric ratio was observed.

The product sulfur content is shown in Figure 8 as a function of stoichiometric ratio. Based on a 1 to 1 molar ratio between calcium and sulfur the theoretical percent sulfur values are given as follows assuming specific end products:

Compound	% Sulfur
$CaSO_3 \cdot 1/2\ H_2O$	24.8%
$CaSO_4$	23.5%

The data presented in Figure 8 appear to approach these values at stoichiometric ratios of less than 0.8 where the reaction is nearly stoichiometric. The combination of decreased utilization and the greater than theoretical quantities of $Ca(OH)_2$ injection accounts for the decreased sulfur content at higher stoichiometric ratios.

The carbonate analysis data are shown in Figure 9. The solid line in the figure represents the calculated carbonate content that would be expected if all of the $Ca(OH)_2$ which did not react with sulfur dioxide in the spray dryer had reacted with CO_2 to form $CaCO_3$. These data indicate that very little carbonate is formed at the lower stoichiometric ratios due to the efficient utilization of the Ca/Sulfur reaction. However, at higher stoichiometric ratios it is evident, under the conditions of these tests, that almost all of the $Ca(OH)_2$ that didn't react with the SO_2 did react to form the carbonate end product. Based on the reactivity of $Ca(OH)_2$ and $CaCO_3$ it can be hypothesized that the conversion of the hydroxide to the carbonate may decrease the potential reactivity of the product in the limited reaction time of the spray dryer chamber.

CONCLUSIONS

This study has shown that the performance of a $Ca(OH)_2$-based spray dryer can be improved significantly by utilizing a baghouse as the final collector, and by partial recycling of the reacted products. Recycle ratios of greater than 2/1 were found to increase the efficiency at a constant stoichiometric ratio. Analyses of the collected products showed that the $Ca(OH)_2$, which did not react to form a sulfite/sulfate end product, reacted with CO_2 to form a carbonate end product.

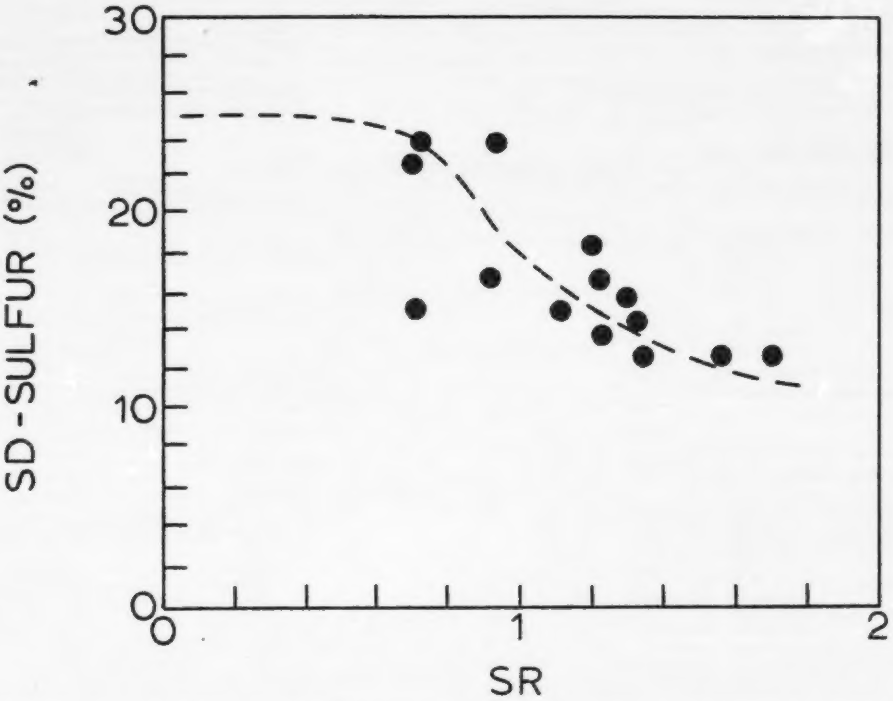

Figure 8. Sulfur Content as a Function of Stoichiometric Ratio

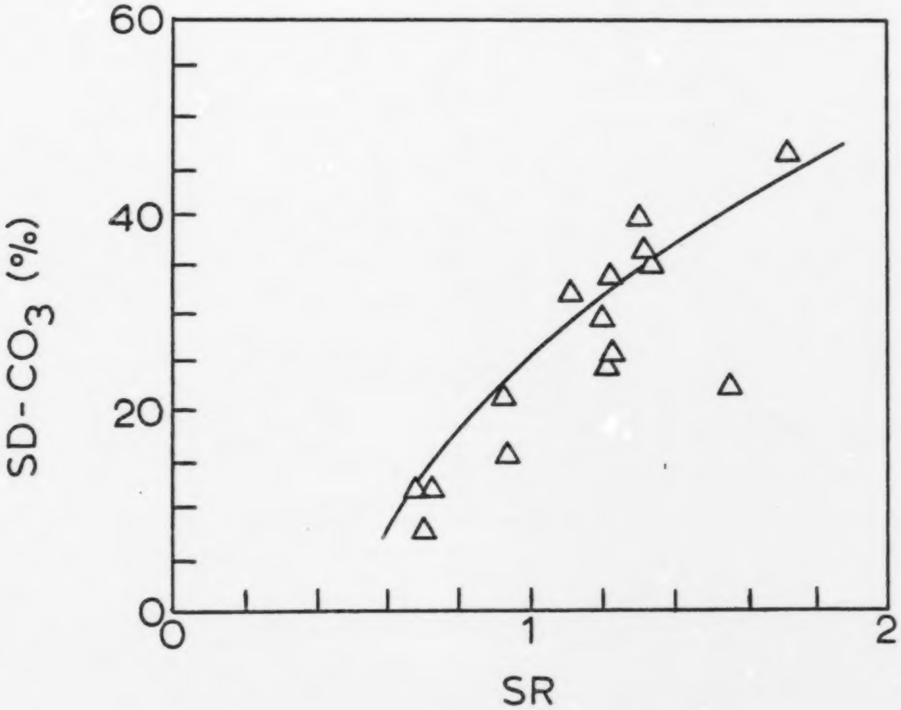

Figure 9. Carbonate Content as a Function of Stoichiometric Ratio

Further research is needed to identify the specific reactions and mechanisms involved in the improvements associated with recycle of the reacted products.

REFERENCES

1. Davis W.T., and G.D. Reed, "Reactivity of Fly Ashes in a Spray Dryer FGD Process," DOE/FC/20492-TI, available through NTIS, May, 1983.

DISCLAIMER

The work described in this paper was not funded by the U.S. Environmental Protection Agency and therefore the contents do not necessarily reflect the views of the Agency and no official endorsement should be inferred.

Session 21: DRY SO_2 REMOVAL II

Theodore G. Brna, Chairman
U.S. Environmental Protection Agency
Air and Energy Engineering Research Laboratory
Research Triangle Park, NC

DESIGN AND OPERATION OF THE BAGHOUSE AT HOLCOMB STATION, UNIT NO. 1

By: B. R. McLaughlin - United Engineers & Constructors Inc.
Englewood, Colorado 80112

R. D. Emerson - Sunflower Electric Cooperative, Inc.
Garden City, Kansas 67846

ABSTRACT

Sunflower Electric's Unit No. 1 at Holcomb Station is rated at 280 MW (net) and burns low sulfur sub-bituminous coal from Powder River Basin of Wyoming. Flue gas desulfurization and particulate removal is accomplished by a "dry" lime scrubber followed by a baghouse.

Because of this location, operation of the baghouse must be coordinated with operation of the steam generator and the dry scrubber. Compared to boiler operation only, flue gas conditions leaving the dry scrubber are characterized by high dust loading and low temperatures. Particulates entering the baghouse are a combination of boiler fly ash and products of desulfurization and the relatively low temperatures are due to lime based reagent slurry injected into the scrubber modules.

In addition to presenting design criteria for the baghouse, details of the hopper ash collecting and transfer system are included. Ash conveying is by mechanical drag link conveyors.

Operation of the unit on coal began in early June of 1983. In addition to summarizing some problems and successes of operation for almost a year, results of initial baghouse start-up as well as operation during the tune-up period of the scrubber will be presented.

PLANT DESCRIPTION

The plant site is located in western Kansas in the town of Holcomb near the Arkansas River. Coal is supplied from the Rojo Caballos mine in the Powder River Basin of Wyoming by rail. The coal is classified as a low sulfur, sub-bituminous coal with a typical sulfur content less than 0.5% and a HHV of 8300 BTU/lb.

The power block consists of a GE turbine rated at 319 MW and a B&W steam generator with a continuous rating of 2,500,000 lbs/hr. Steam conditions are 2400 psig, 1000F/1000F at the turbine throttle. Maximum expected gross output from the unit is 348 MW when operating with the turbine inlet valves wide open, 5% over pressure and a 2½ in H_gA condenser back pressure.

First coal was on June 3, 1983. During the first year of operation load demands have been variable causing the unit to operate anywhere from full load to 25% of maximum continuous rating (MCR). As is typical during the first year of operation, the unit has also been through a number of cold starts.

Emissions control is by a 'dry' scrubber/baghouse combination which accomplishes both sulfur dioxide and fly ash particulate removal in one system. It is supplied by Joy Manufacturing Co. and Niro Atomizer Inc. The 'dry' scrubber, baghouse and all associated support systems such as the reagent (lime based) preparation and feed system is referred to as the flue gas cleaning system.

LICENSING CONSIDERATIONS

This flue gas cleaning system enabled Holcomb Station to demonstrate that the Best Available Control Technology (BACT) is used to meet the emissions limitations required by the New Source Performance Standards (NSPS) and as stipulated in its Prevention of Significant Deterioration Permit (PSD). Emissions limitations for particulates are 0.03 lbs/MBTU and the maximum sulfur dioxide level is 0.48 lbs/MBTU. Regardless of the sulfur dioxide emissions the unit must always remove at least 70% of the boiler flue gas sulfur dioxide levels. The NSPS requires that the system be operated at, or above, the specified minimum removal efficiencies on a continuous basis.

As part of the demonstration a detailed evaluation between a baghouse and an electrostatic precipitator was performed. The baghouse was evaluated as the preferred choice because of the following reasons:

- It represented the most economical choice to meet the stringent emissions limitations
- Ability to produce a constant emissions level over a wide range of inlet conditions that may vary due to changing coals or operation of the dry scrubber

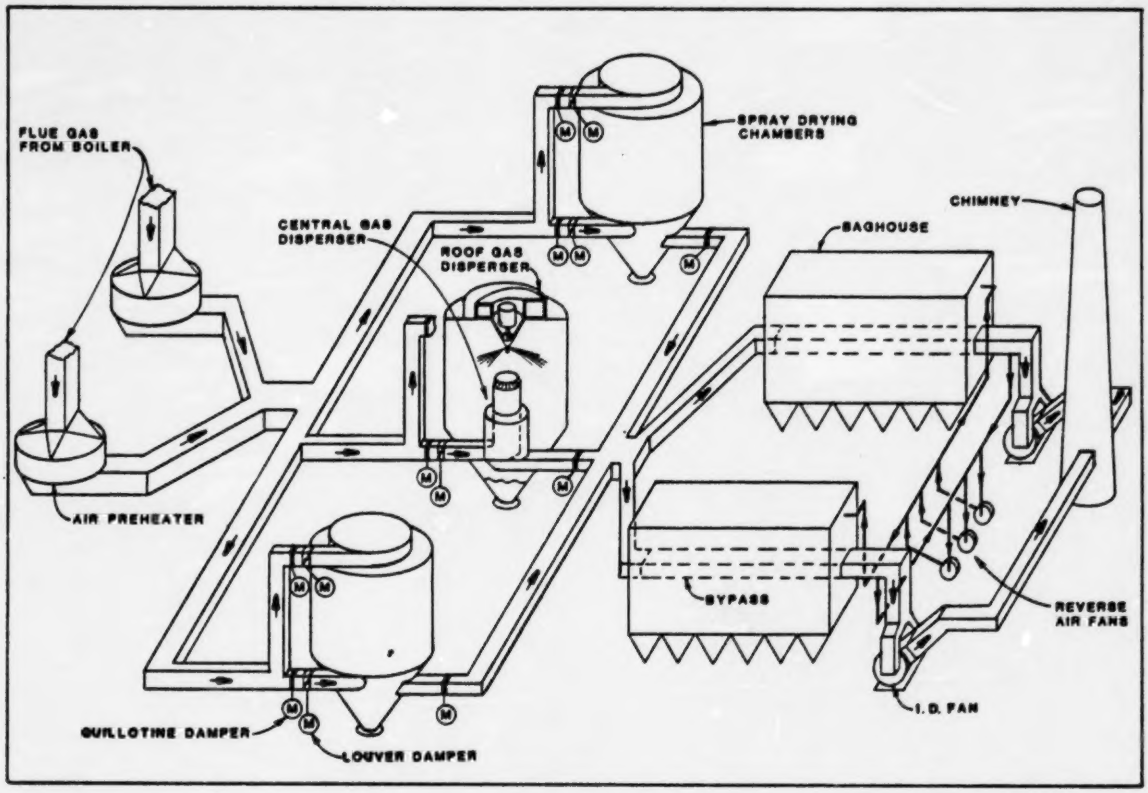
FLUE GAS FROM BOILER
SPRAY DRYING CHAMBERS
CHIMNEY
CENTRAL GAS DISPERSER
ROOF GAS DISPERSER
BAGHOUSE
AIR PREHEATER
BYPASS
REVERSE AIR FANS
I. D. FAN
GUILLOTINE DAMPER
LOUVER DAMPER
M

Figure 1 : Flue Gas Handling

- Ability to isolate individual compartments for maintenance without shutdown of the baghouse
- In general, it seemed the better system to place behind a dry scrubber whose full scale utility experience at that time was lacking

GENERAL DESCRIPTION OF FLUE GAS CLEANING SYSTEM

As shown on Figure 1 flue gas from the boiler airpreheaters enters the spray drying chambers through an internal central gas disperser and a roof gas disperser. In the chambers the flue gas comes into contact with a spray of prepared slurry composed of lime and recycled waste powder which has been removed from the spray dryers and baghouse. The lime chemically reacts with the SO_2 in the flue gas transforming the gaseous SO_2 into dry reaction products, consisting primarily of calcium sulfite and calcium sulfate. Design of the spray dryers is to promote proper gas distribution thereby ensuring the particles are dry before reaching the walls of the spray dryer and the baghouse.

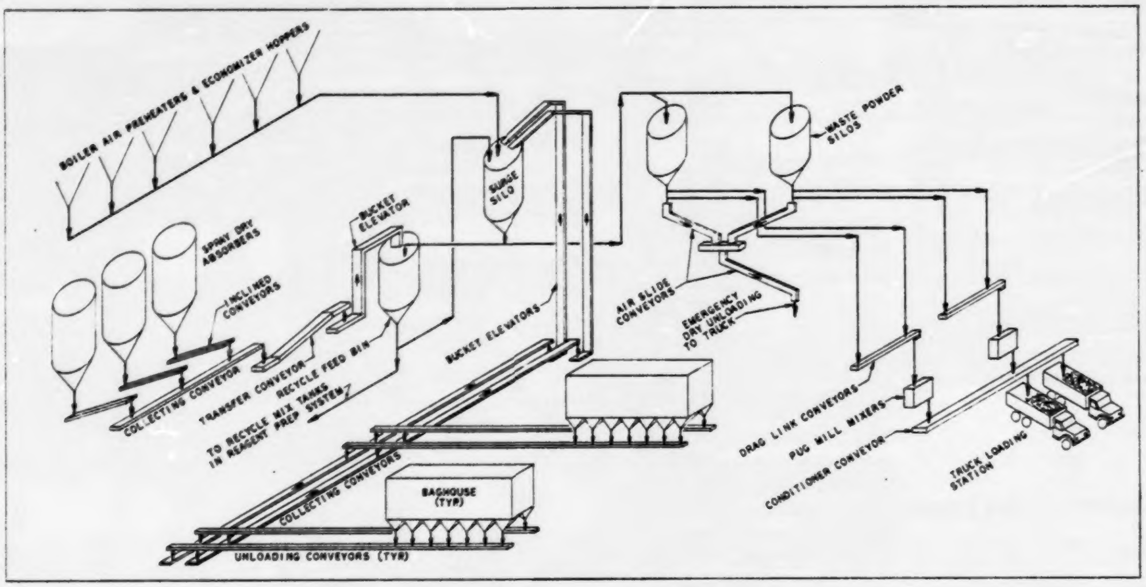
BOILER AIR PREHEATERS & ECONOMIZER HOPPERS
SPRAY DRY ABSORBERS
INCLINED CONVEYORS
COLLECTING CONVEYOR
TRANSFER CONVEYOR
BUCKET ELEVATOR
RECYCLE FEED BIN
TO RECYCLE MIX TANKS IN REAGENT PREP SYSTEM
SURGE SILO
BUCKET ELEVATORS
COLLECTING CONVEYORS
BAGHOUSE (TYP)
UNLOADING CONVEYORS (TYP)
WASTE POWDER SILOS
AIR SLIDE CONVEYORS
EMERGENCY DRY UNLOADING TO TRUCK
DRAG LINK CONVEYORS
PUG MILL MIXERS
CONDITIONER CONVEYOR
TRUCK LOADING STATION

Figure 2 : Fly Ash / Waste Powder Handling System

A portion of the dry material falls to the bottom of the spray dryer and is removed. As shown in Figure 2, the removed material is recycled back to the reagent preparation and feed system. Waste powder is recycled to make use of the unreacted lime and the available fly ash alkalinity. It also provides a substrate to promote SO_2 removal, increases particle size growth and improves slurry drying in the chamber. By increasing the percent solids in the feed better drying of the products should result. A basic premise in spray drying is that a thicker slurry will dry better. Although it had been expected that sufficient material would fall from the spray dryers, provisions were incorporated to transfer waste powder from the baghouse to the reagent preparation system.

The flue gas leaving the spray dryers containing fly ash and reaction products next enters the baghouse for removal. In addition to removing particulates the baghouse also removes sulfur dioxide. This is due to the sulfur dioxide reacting with the residual lime content in the layer of dust which accumulates on the bag surface area.

The cleaned gas exits the baghouse through the Induced Draft (ID) Fans and is routed to the stack and the atmosphere. The Continuous Emissions Monitoring (CEM) system is located in the stack and measures opacity, SO_2 NO_x, CO and O_2 continuously. The CEM system is an extractive type system except for the in-line opacity monitors.

BAGHOUSE DESIGN

Inlet flue gas design conditions for the baghouse with and without operation of the spray dryers are as shown in Table 1. These are calculated values based on the unit at MCR burning a coal with a 1% S and 12% ash content; 80% removal of SO_2; and a 50F approach temperature to adiabatic saturation (ADSAT) entering the baghouse. Although more SO_2 removal would occur in the spray dryers at a lower approach temperature and with less lime consumption it was felt that a hotter temperature would ensure safer operation for the bags, the baghouse structure, ID Fans and chimney - especially during any upset conditions in the spray dryers. The predicted reagent stoichiometry at these conditions based on lb-moles of lime consumed to lb-moles of SO_2 removed was 1.38.

Table 1: Baghouse Inlet Design Conditions

Item	Without Scrubbing	With Scrubbing
Flue Gas flow, lbs/hr	3,900,000	4,038,234
Flue Gas flow, acfm	1,339,823	1,274,186
Temperature, (F)	253	179
SO_2 concentration, lbs/hr	8,696	2,083
Dust loading, lbs/hr	41,741	66,587
Dust loading, gr/acf	5	7
H_2O in flue gas, % weight	8.2	15.3
Pressure, inches WG	+30,-35	+30,-35

Other process characteristics assumed were 30% drop-out of particulates in the spray dryer modules; minimal SO_2 removal in the baghouse; a 40-45% slurry, by weight of solids, being sprayed into the atomizers; and a minimum contribution of the alkalinity in the recycled ash to the available lime in the slurry. As shown in Table 2 a high percentage of the ash is calcium oxide. During the early stages of design it was unknown how much of this calcium oxide would be converted to calcium hydroxide and actually be available for sulfur dioxide removal. A small percentage of SO_2 removal across the baghouse was assumed because of the relatively high approach to ADSAT.

Table 2: Design Ash Analysis

Item	Average	Range
Silica, SiO_2	31.12	18.48 - 43.76
Ferric Oxide, Fe_2O_3	5.22	3.58 - 6.86
Alumina, Al_2O_3	16.67	11.39 - 21.95
Titania, TiO_2	1.44	1.00 - 1.88
Lime, CaO	24.32	16.48 - 32.16
Magnesia, MgO	4.44	1.86 - 7.02
Sulfur Trioxide, SO_3	13.33	5.77 - 20.89
Phosphate Pentoxide, P_2O_5	0.89	0.19 - 1.59
Potassium Oxide, K_2O	0.41	0.05 - 0.77
Sodium Oxide, Na_2O	1.29	0.31 - 2.27

These conditions were also developed for a number of cases at lower loads, and lower SO_2 and ash coal analyses. One characteristic worth noting is the change in the ratio of recycled product to raw lime added as the % inlet SO_2 and ash concentrations are reduced. For example, at the design condition of 1% sulfur and 12% ash the predicted ratio of recycle to raw lime was about 4 to 1. With a 0.33% sulfur and 9% ash the ratio was approximately 18 to 1. More recycle proportionately is needed to compensate for the more dilute solution being sprayed into the chambers at the lower sulfur dioxide concentration.

BAGHOUSE OPERATION

Each of the two (2) fabric filter units treat 50% of the flue gas and consists of a number of compartments arranged in two (2) parallel rows with a common inlet, outlet and reverse air manifolds running between the rows. Filter bags are suspended within each compartment.

In general the main process steps associated with operation of the baghouse are filtering; first dust settling; bag collapse by reverse air pressurization; second dust settling; bag reinflation; and then back to full flow filtering.

As shown in Figure 3 flue gas from the spray drying chambers enters the inlet manifolds and into the hoppers and upwards into the inside of the bags where the dust particulates are trapped. The filtered gas passes through the bags into the compartment and then through the outlet valves into the outlet manifold. The ID Fans draw the flue gas through the entire system and the baghouse is under a negative pressure i.e., air leakage is into the baghouse.

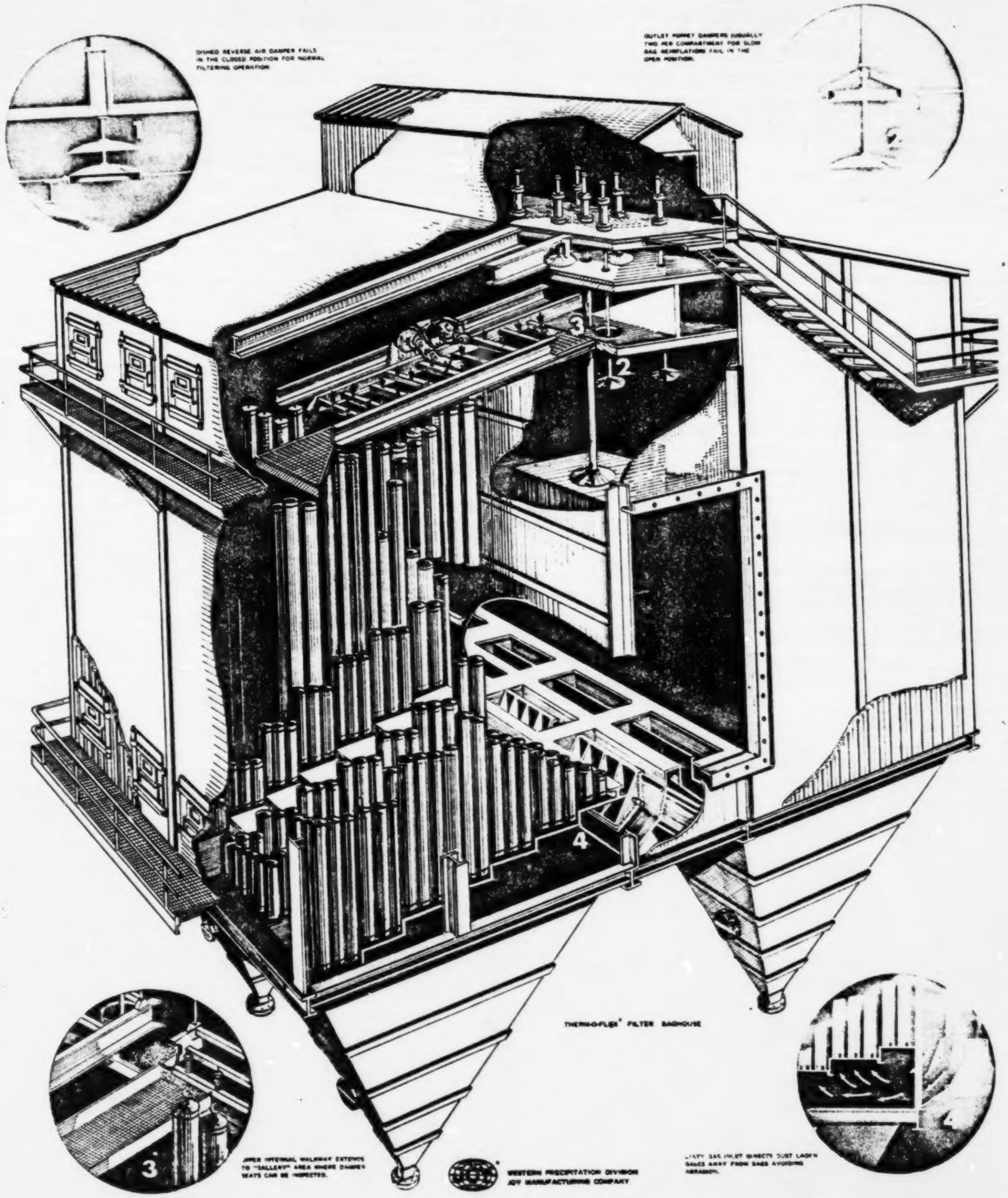
DISHED REVERSE AIR DAMPER FAILS IN THE CLOSED POSITION FOR NORMAL FILTERING OPERATION
OUTLET POPPET DAMPERS USUALLY TWO PER COMPARTMENT FOR SLOW GAS REINFLATIONS FAIL IN THE OPEN POSITION.
2
3
2
4
THERM-O-FLEX® FILTER BAGHOUSE
3
UPPER INTERNAL WALKWAY EXTENDS TO "GALLERY" AREA WHERE DAMPER SEATS CAN BE INSPECTED.
WESTERN PRECIPITATION DIVISION
JOY MANUFACTURING COMPANY
4
DIRTY GAS INLET DIRECTS DUST LADEN GASES AWAY FROM BAGS AVOIDING ABRASION.

Figure 3: Cross Sectional View of Baghouse

Ash build-up on the inside of the bags periodically requires cleaning. Reverse air fans take filtered gas from the outlet manifold and pressurize the compartments in sequence causing the bags to collapse and release the accumulated ash into the hoppers. The reverse air fans which run continuously also provide sealing of the bypass poppet valves. Ash removal from the hoppers is by a mechanical drag-link conveying system to disposal or recycle to the scrubber reagent preparation system. Selection of a mechanical conveying system was due to the unique flue gas characteristics caused by the dry scrubber/baghouse combination.

EQUIPMENT SUMMARY

The baghouse is supplied by the Western Precipitation Division of Joy Industrial Equipment Company. Details of the baghouse and the ash conveying system are as shown below and are followed by the rationale for the selected fabric filter, the mechanical ash conveying system and a discussion on the model study:

Dimensions - Each baghouse has a length of 126 ft, width of 73 ft and a height of 94 ft. There are 14 compartments per baghouse for a total of 28.

Fabric filters - Each compartment has 286 bags per compartment for a total of 8008 bags for both baghouses. Gross filter area is 820,019 ft^2 and the net filter area with two (2) compartments out for cleaning and two (2) out for maintenance is 702,873 ft^2. The gross air-to-cloth ratio without scrubbing is 1.63 and 1.55 with scrubbing. The net air-to-cloth ratio, which also includes gas volumes from the reverse air fans, is 2.03 without scrubbing and 1.93 with scrubbing. Details of the bags and fabric are as shown in Table 3.

Method of Cleaning - Reverse air. Three reverse air fans (2 operating and one on standby) supply warm clean air from the outlet duct to reverse air plenums. Each of the fans supply approximately 43,000 acfm at normal operating pressure conditions.

Hoppers - Pyramid type each with a capacity of 4485 ft^3. Each hopper is equipped with a 10kw heater, nuclear type level indicating system, electric vibrator, aeration pads supplied with heated air, capped pokeholes and a bottom slide gate for isolation.

Dampers - Each compartment has one (1) butterfly inlet damper; two (2) poppet type outlet valves and two (2) poppet reverse air valves. Each outlet and reverse air poppet valve is on the same shaft. Internal bypass is accomplished by five (5) 6 ft diameter double (coaxial) poppet valves which allows gas to bypass filters directly to stack. Bypass is actuated when inlet gas temperature exceeds 450 F, drops below 150 F or if the baghouse pressure drop exceeds 10 in. WG. Compressed air consumption for damper actuation and other controls is estimated at approximately 100 scfm. Compressed air is supplied from the main plant compressors and is dried to -40F.

Hopper ash removal system - Each hopper has a 10 in mechanical dual tipping valve with a rated capacity of 117 cfh of ash. The dual valves are operated in sequence to provide an air seal to prevent ambient air from entering the hoppers and are provided with an override counterweight gravity mechanism. Mechanical drag link conveyors are located under hoppers and have a capacity of 36 tons/hour.

Controls - The main control panel is equipped with redundant programmable logic controllers (PLC). Remote panels serve as interface panels which house the remote I/Os for the multiplexing system, hopper heater controls and damper controls. SO_2 analyzers and the ADSAT meters (wet wick type) are located in the outlet duct of each baghouse. Pressure drop is measured across the entire baghouse system as well as individual compartments.

Insulation - Outside surfaces including hoppers have 4" insulation and cladding. Internal partitions between compartments have a nominal 3 inches of insulations to help reduce the temperature of an isolated compartment.

Compartment Venting - Each compartment has four access doors (2 at the top and 2 near the base) which provide ventilation by natural circulation. A keyed safety interlock system for the access doors is provided.

Fabric Filter Selection

Filter material selection was based on testing and investigation made at the Joy/Niro demonstration facility at Northern States Power's Riverside Station in Minneapolis, Minnesota. The characteristics of the fabric chosen are as shown in Table 3. The bag chosen in general can be classified as a fully plied, texturized, fiberglass bag with a teflon coating. The selected bag exhibited the best dust collection efficiency, lowest pressure drop and longest bag life. These characteristics can be attributable to the relatively high yarn count, texturizing of the fabric and the teflon coating.

The high yarn count allows more surface area for the dust to collect to and more passages for the gas to pass through thereby reducing pressure drop. Texturizing aids in collecting the dust and release of the dust during bag collapse. The teflon coating has shown to penetrate deep into the thinner yarn thus creating a form of lubrication between the yarns.

This lubrication combined with the thinner yarn results in a fabric that is flexible and collapses easier, thereby reducing stress during repeated bag collapses and reinflation. As stress is reduced a longer bag life can be expected.

The selection of this particular bag enabled Joy to respond to a 3-year bag guarantee and meet the required pressure drop limitations. Bag life is an important consideration because of the expense involved with replacement. It is estimated that a 7-man crew can replace all 28 compartments, that is, 8008 bags in about 5 months.

Table 3: Fabric Filter Specification

Manufacturer	Menardi Southern
Style	601 T
Fiber content	DE Glass
Weight after finish, oz/yd	9.5
Thread count per inch (warp x fill)	54 x 30
Weave	3 x 1 Twill
Warp yarn	150 1/2
Fill yarn (texturized)	150 1/4
Permeability, (cfm/ft^2 at 0.5 in WG)	45-75
Mullen Burst	350 min.
Type of finish	Teflon B
Weight of finish (% of fabric weight)	10% min.
Bag Diameter	12 inches
Bag length	32.6 ft
Rings per bag	7
Ring finish	Mild Steel with epoxy coating
Bag tensioning	Compression spring with steel rod
Maximum Inlet Temperature	500F

Mechanical Conveying System

The more popular choice for ash collection from a baghouse directly treating boiler flue gas is a pneumatic system. However, the selection of the mechanical conveyor is based on the flue gas characteristic leaving the spray dryer modules. That is, the flue gas has more moisture at a lower temperature; the ash is not completely dry and contains the products of desulfurization, namely calcium sulfate and calcium sulfite. It was estimated initially that the ash could contain up to 1-2% moisture by weight.

Therefore, it was decided that to reduce the possibility of crusting of the top layer of ash in a hopper the material should always be moving downward in the hopper. In essence during normal operation the hoppers were to be treated as 'chutes' and not for storage.

Both the pneumatic and mechanical conveying were, however, evaluated as workable systems but the mechanical system exhibited the following advantages and was selected:

- Continuous removal (or as much as possible) of the ash would eliminate or substantially reduce the possibility of caking
- Reduce the amount of false air introduced into the hoppers via the air pads for ash fluidization
- Claimed easier maintenance
- Lower installed cost

As mentioned earlier the tipping valves are provided with an override counterweight gravity mechanism. This causes the valves to fail open when a significant amount of ash accumulates in the hoppers. Therefore, the removal capacity of an open valve is only dependent on the maximum removal capacity of the underneath conveyor.

Model Study

A model study was performed to determine the flue configuration needed to provide an acceptable flue gas and particulate distribution. A 1/16 scale model was constructed of clear plexiglass and flow tests were performed by running ambient air through the model.

Testing was performed on the model as originally constructed and was modified mainly by adding turning vanes until the objective of the tests were reached. That is, a flue arrangement which ensured proper velocity profile control; uniform dust distribution to the baghouse compartments; minimize dust deposition in flue gas passage items; and verify that the system flue gas pressure drop under full scale operating conditions would be within design.

Boiler flue gas conditions similated were 40, 60, 80 and 100% of MCR.

OPERATION

This section will cover start-up, early operation and problems encountered concentrating on how operation of the boiler and spray dryers affects the baghouse. The results of EPA compliance testing and contract performance tests are also included as well as a discussion of bag replacement rate to date.

Start-up and Early Operation

After a 12-month construction schedule the baghouse was ready to support the early boiler start-up activities such as boilout, steam blows and first steam to turbine. Figures 4 and 5 show the baghouse during construction. Early boiler operations were performed with the ignition fuel, i.e., natural gas, which also provides low-load stabilization with coal firing. During early operation with gas and coal the internal bypass of the baghouse was used. It was thought that the high moisture content in the natural gas at the low flue gas temperatures leaving the airpreheaters would be harmful to the bags.

The first filtering sequence is critical to subsequent operation of the baghouse. High moisture content in the flue gas can cause the bags to be 'blinded' leading to very high pressure drops, manual cleaning of bags or even bag replacement. Therefore, flue gas was not allowed to enter the fabric filters until a stable combustion process had been reached. Stable was defined as combustion entirely on coal, flue gas temperatures well above the acid dew point (250F was selected) and a constant boiler load. These conditions were reached about 2 weeks after first coal because of the start-up sequence of the five coal pulverizers. Once a few cleaning cycles of the bags had been completed the bags were deemed sufficiently conditioned to accept the products of desulfurization and related lower flue gas temperatures. After this, start-up of the spray dryer system had to be carefully controlled as not to adversely affect the baghouse. The amount of moisture being introduced into the flue gas must be carefully controlled such that the temperatures are continually maintained above the acid and water dewpoint.

This was accomplished by spraying with only water first then a dilute lime slurry such that the temperature of the flue gas entering the baghouse was maintained at 200F (approximately 70F above ADSAT). Once this mode was well established recycle material was added to increase the solids content of the reagent feed to approximately 30-35% and spraying down to 180 F. As the process developed the amount of recycled material was increased to a 45-55% solids content.

During this time the stringent restart and shutdown procedures for the baghouse such as a hot air purge at shutdown, were followed. It is imperative these be performed religiously for successful operation.

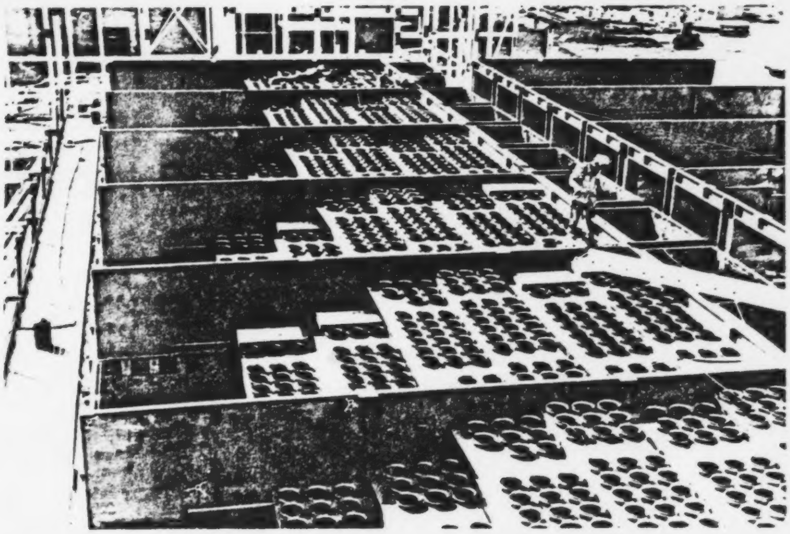

Figure 4: Baghouse Thimble Floor

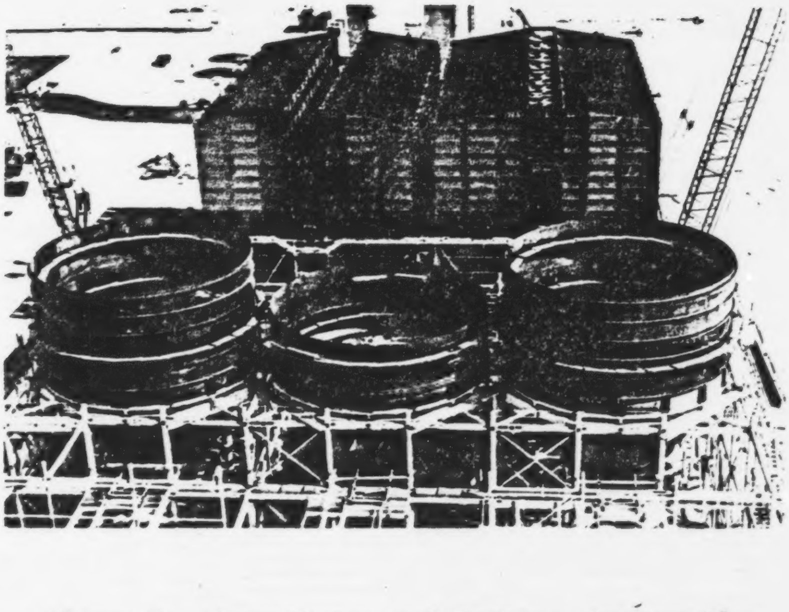

Figure 5: Spray Dryers and Baghouse Construction

Early Problems

During start-up and early operation the 'usual' controls and equipment problems were encountered and these were quickly remedied. However, certain process related problems developed which required more effort to resolve.

One such problem, which was rather interesting, showed how operation of the baghouse affects the ash removal system and the SO_2 removal and control system.

Originally, the compartment cleaning cycle was set on the 'delta pressure' initiated mode. With low boiler loads coupled with the light ash loading the cleaning cycle would be started once every 10-12 hours. Once started it would take approximately one hour to clean all 14 compartments. The set point for initiating the cleaning cycle at these loads was approximately 4 in. WG.

As the baghouse would remove SO_2 after a uniform layer of dust had built up on the bags, the sudden release of the dust during cleaning resulted in essentially no removal across the baghouse until the dust layer could be re-established. During this time the SO_2 analyzer downstream of the baghouse would then send a signal to the scrubber to increase the percent removal of SO_2 by adding more lime to the reagent feed. This resulted in more lime being added than was necessary.

With the huge amount of ash falling into the hoppers the mechanical conveyors at times had problems keeping up with the ash loading. Specifically, the bucket elevator conveyor could not keep up with the collecting conveyor. This would cause ash in the collecting conveyor to back up and be carried back by the top flights. This conveyor would then be compacted with ash and trip due to overload. This would in turn stop all the unloading conveyors. The condition was made worse when both baghouses cleaned at the same time.

The solution at least conceptually was to optimize dust cake build-up on the bags such that a more continuous SO_2 signal would be provided when cleanings were factored in; provide a more uniform ash loading to the conveying system; and ensure that the maximum pressure drop is not exceeded or is set within a certain range to accommodate these conditions.

The actual fix was to operate the baghouse cleaning cycle on a combination 'continuous' and 'delta pressure' initiated mode. It is now set such that when the overall pressure drop is less than a predetermined set point (which is adjustable) one compartment is cleaned every 50 minutes on a continuous basis. If the pressure drop increases to the set point due to higher flue gas flow rates due to higher loads, for example, the 'delta pressure' mode will take over and as many compartments will be cleaned until the pressure drop for the entire baghouse drops below the set point. After this the cleaning cycle reverts back to the continuous cycle. To augment this controls change, the speed of the unloading conveyor has been reduced from 30 fpm to 20 fpm by a sprocket change thereby making the unloading conveyor speed more compatible with the collecting conveyor and bucket elevator. Adjusting the cleaning cycle and reducing the conveyor speed has accomplished the desired objectives.

A similar problem with overloading of the conveyors was caused during a sudden loss of flue gas flow due to an ID Fan or boiler trip. This caused the bags to collapse and release all the dust into the hoppers. Again the conveyors couldn't keep up with the ash loading. The solution was that upon sensing a pressure drop of 'zero' the unloading conveyors are tripped. The operator would then start the unloading conveyors one-at-a-time until the collecting conveyors can keep up with the ash. This problem however has been reduced by the aforementioned fix.

The mechanical conveyors had exhibited mechanical problems early in operation mostly due to construction and fabrication problems. However, these have been resolved and the conveyors as well as the mechanical 'tipping' valves have been operating satisfactorily and appear to be low maintenance items.

As mentioned earlier the baghouse not only has to be coordinated with operation of the boiler but the spray dryer systems as well. This also includes upset conditions. Moisture excursions have occurred in the spray dryers which resulted in solids forming on the chamber walls and cone section. However, the spray dryers have shown to be an effective remover of wet particles preventing them from reaching the baghouse. During normal operation the ash in the spray dryer hoppers and baghouse hoppers has been dry and has not adhered to the hopper walls. The ash in the spray dryers is usually less than 2% water by weight while the baghouse ash is less than 0.5%.

This material cannot be allowed to get wet at any place in the process. Because of the cementitious nature of this material it sets-up very quickly. The unconfined compressive strength of the material leaving the pugmill mixer, where approximately 30% by weight water is added, is about 350 psi. Testing under controlled conditions has produced much higher compressive strengths.

Compliance Testing

EPA compliance testing was performed on February 1, 1984. The unit was operated at 330 MW and measurements were taken at the test ports in the chimney fiberglass flue.

The three particulate runs yielded an average particulate emissions level of 0.0345 lbs/MBTU. Rounding off the average to the 0.03 limit was not acceptable so the unit was deemed to be non-compliant. During the test the opacity was measured at 14%

The problem was quickly diagnosed as broken bags in two(2) compartments and a plugged purge seal air line. The purge line forms a gas tight seal on the bypass valves to prevent uncleaned flue gas from migrating directly to the outlet duct. The required fix of replacing the broken bags and removing the solidified fly ash from the purge seal air line was made immediately and compliance testing was rescheduled for March 7.

During this test measurements yielded an average of 0.0188 lbs/MBTU, thereby meeting the standard and the emissions criteria.

Performance Tests

On April 11 tests were performed to measure the performance of the flue gas cleaning system. Items measured were reagent stoichiomietry, system pressure drop, stack particulates and baghouse air in-leakage.

Before testing began the system was determined to be in a steady state condition. This was accomplished by measuring the available calcium hydroxide of the powder at various points in the process. The analysis yielded values in the range of 4-6% and was indication the system was at steady state.

During the day of the test the unit was operated at loads from 323 MW to 333 MW. The composition of the coal actually burned during the test is as shown in Table 4.

Table 4: Proximate Coal Analysis

Item	Percent
Moisture	30.08
Ash	6.29
Volatile Matter	30.12
Sulfur	0.38
Fixed Carbon	33.13
HHV of 8236 BTU/lb	

The results of the data measured are as shown in Table 5. Measurements were only taken on the spray dryer inlet ports and the stack monitoring ports.

Table 5: Performance Test Results

Item	Spray Dryer Inlet	Stack Outlet
Gas Volume, acfm	1,498,333	1,268,000
Gas Flow, lbs/hr	3,983,433	3,741,400
Gas Temperature, ^{o}F	260	184
Particulate loading		
a) gr/acfw	1.3	0.0032
b) lbs/hr	16,693	34.6
c) lb/MBTU	4.56	0.0107
SO_2 loading		
a) ppm, wet	320	55
b) lbs/hr	3006	502
c) lbs/MBTU	0.82	0.1559
O_2, % weight(wet)	6.0	6.7
Gas Moisture, % weight	6.7	8.7

The results by the following categories are as follows:

SO_2 Removal - The SO_2 removed across the entire system was maintained at 81%. Based on instrumentation the percent removal of SO_2 across the baghouse based on that leaving the boiler was 20-25%.

Reagent Consumption - The average measured stoichiometry was 1.10 with a lime consumption rate of 2550 lbs/hr. Approach to ADSAT was maintained at 50F during the test with an average temperature of 177F entering the baghouse. The temperature of 184F in the stack is due to the heat of compression of the ID Fans.

The percent slurry feed was maintained at 50-55% solids. It was estimated that the ratio of recycle solids to raw lime added was roughly 20 to 1. Most of the recycle material was taken from the baghouse as an estimated 5-10% drop out of ash was experienced in the spray drying chambers.

Particulate Removal - As shown in the table the particulate emissions was much less than the emissions standard. Based on lbs/MBTU the particulate removal efficiency was 99.76%. During the test period the opacity ranged from 1.0 to 2.5%.

Pressure Drop - A water filled manometer was used to measure the pressure drop across the system, i.e. from the air preheater discharge to the ID Fans and from the fans to the chimney. This was deemed more reliable than static measurements because it would dampen the variations in the system due to reverse air cleanings, dampers closing, etc. However, it was checked against static head measurements.

The pressure drop with 3 spray dryers was 10.7 in. WG and with 2 spray dryers was 14.3 in. WG. During the tests the baghouse was placed in the 'delta pressure' initiated cleaning mode with a set point of 4.8 in WG. Baghouse A required on the average approximately 3 cleanings per hour and Baghouse B about 4 cleanings per hour. The difference in cleanings was due to ID Fan B being slightly biased over ID Fan A. Because of the savings in pressure drop it is intended to run 3 modules continuously if slurry velocities can be maintained at levels where plugging will not occur.

Air Inleakage - Based on O_2 values taken from Orsat analyses air inleakage across the Baghouse B was determined to be 1.4% and essentially 0 across Baghouse B, each well below the 2% air inleakage guarantee.

Bag Replacement

During the first year of operation a total of 40 bags out of the 8008 installed have had to be replaced. Not all of the bags replaced were the result of bag failure. Some were replaced because of improper installation, manufacturer defects and installed bags destroyed by the failure of an adjacent bag. Sometimes a bag which has failed can whip around and destroy adjacent bags. Of the 40 bags replaced 10 have been diagnosed as having 'failed'.

Therefore, the first year replacement rate is 0.5% with a failure rate of less than 0.2%. The predicted failure rate was 1% for the first year of operation.

To provide an early indication of a compartment with a broken bag the stack opacity is recorded on the baghouse panel to compare it with the bag cleaning sequence. In effect when the stack opacity decreases upon isolation of a compartment for cleaning it is usually indication that the compartment has a broken bag or an accumulation of ash in the bag thimble floor.

SUMMARY

The baghouse has been operating satisfactorily characterized by pressure drops within design, low air inleakage rates, low bag replacement rate, and more importantly yielding emission rates lower than the standards. It essentially has had an availability of 100% and has not limited the output of the unit.

In tracing the steps from design, start up and operation of the baghouse the reasons for the success of the installation seem to be as follows:

- Incorporate flexibility in design to accommodate variable flue gas and particulate loading conditions.
- Pay attention to details of design and construction.
- Verify design of flue gas passage items with model testing.
- Select fabric filter and bag design to suit actual operating conditions.
- Carefully coordinate initial start-up of boiler and spray dryer with the baghouse to ensure flue gas conditions are suitable for the fabric filter.
- Attention to restart and shutdown procedures.
- Select an ash conveying system consistent with the application.

The work described in this paper was not funded by the U.S. Environmental Protection Agency and therefore the contents do not necessarily reflect the views of the Agency and no official endorsement should be inferred.

AN UPDATE OF DRY-SODIUM INJECTION IN FABRIC FILTERS

by:

R. Hooper and R.C. Carr
Electric Power Research Institute
3412 Hillview Avenue
Palo Alto, California 94304

G.P. Green
Public Service Co. of Colorado
550 Fifteenth Street
Denver, Colorado 80202

V. Bland and L.J. Muzio
KVB, Inc.
18006 Skypark Blvd.
Irvine, California 92714

R. Keeth
Stearns-Catalytic
925 S. Niagara Street
Denver, Colorado 80219

ABSTRACT

Injection of dry-sodium powders into the inlet plenum of fabric filters (baghouses) has been demonstrated to be an effective flue gas desulfurization (FGD) technique. On a full-scale utility boiler, injected sodium products have been shown to meet New Source Performance Standards (NSPS) of 70% removal for low-sulfur coal applications. Higher levels of SO_2 removal have also been demonstrated with the injection of greater quantities of sodium reagent. The low capital cost and simplicity of the dry-injection process make it particularly applicable in retrofit applications. Supply of sodium reagents is becoming increasingly more abundant as several chemical commodity suppliers expend both research and venture capital dollars to enter the potential utility market. To date, sodium bicarbonate reagents have been shown to provide better sodium utilization than sodium sesquicarbonate reagents. Recent economic estimates confirm a much lower capital cost required for the dry-injection technology when compared to lime spray drying. The levelized cost of dry-injection is sensitive to reagent cost and utilization. Tests are proceeding at the Electric Power Research Institute's Arapahoe Test Facility to evaluate injection procedures and several upgraded reagents.

The work described in this paper was not funded by the U.S. Environmental Protection Agency and therefore the contents do not necessarily reflect the views of the Agency and no official endorsement should be inferred.

INTRODUCTION

The process of combining SO_2 and particulate control using dry-sodium reagents is gaining increased utility interest. This paper reviews and updates events relevant to the use of dry-sodium-based injection technology within the industry with emphasis on system simplicity, reagent availability, technology viability, and system economics.

The Electric Power Research Institute (EPRI) is interested in evaluating the advantages and disadvantages of dry-sodium injection because the technology has the potential to greatly simplify hardware requirements, and to significantly reduce the capital requirements for both new and retrofit SO_2 control applications. Evaluating the importance of simplicity is qualitative, but may be weighted heavily by utility concern about operation and maintenance of emission control equipment.

EPRI began studying dry-sodium injection in 1977. To date, it has published feasibility study results(1), bench-scale investigation results(2), and full-scale demonstration results obtained in testing at the 22 MW Cameo station of the Public Service Co. of Colorado(3). An economic evaluation of dry-sodium injection is scheduled to be published soon. Work is now being conducted at EPRI's Arapahoe Test Facility in Denver to characterize and assess potential new dry-injection reagents for utility applications.

SIMPLICITY

Figure 1 is a simplified flow schematic of a coal-fired power plant with dry-sodium injection for SO_2 control. Unit processes are much the same as those required for coal handling: transportation, storage, pulverization, and injection.

With dry-sodium injection, the sodium reagent is fed into the hot flue gas stream (nominally at a temperature of 300°F) ahead of a baghouse and downstream of the air heater. In the ductwork, the sodium bicarbonate in the reagent particles decomposes to sodium carbonate (Na_2CO_3) in a "popcorn" fashion, forming an open, porous microstructure and exposing more particle surface area. The reagent reacts with the SO_2 in the flue gas and subsequently collects along with fly ash on the bags in the baghouse as part of the dustcake, further removing SO_2. Both the spent reagent and the filtered fly ash on the bags are then removed in the normal course of bag cleaning and collected for disposal. Typically, 70-80% of total SO_2 collection occurs in the baghouse, and the remaining 20-30% in the ductwork.

Dry-sodium injection offers a number of advantages over alternate SO_2 collection options. These include:

- Capital costs are significantly lower because of the comparative simplicity of the process.

- Only equipment already in common use at coal-fired power plants is required.
- No wet slurry or sludge is required.
- The systems are easily retrofitted to boilers equipped with baghouses.
- Power costs are low.
- Scaling and corrosion are minimal.
- Flue gas reheating is not necessary.

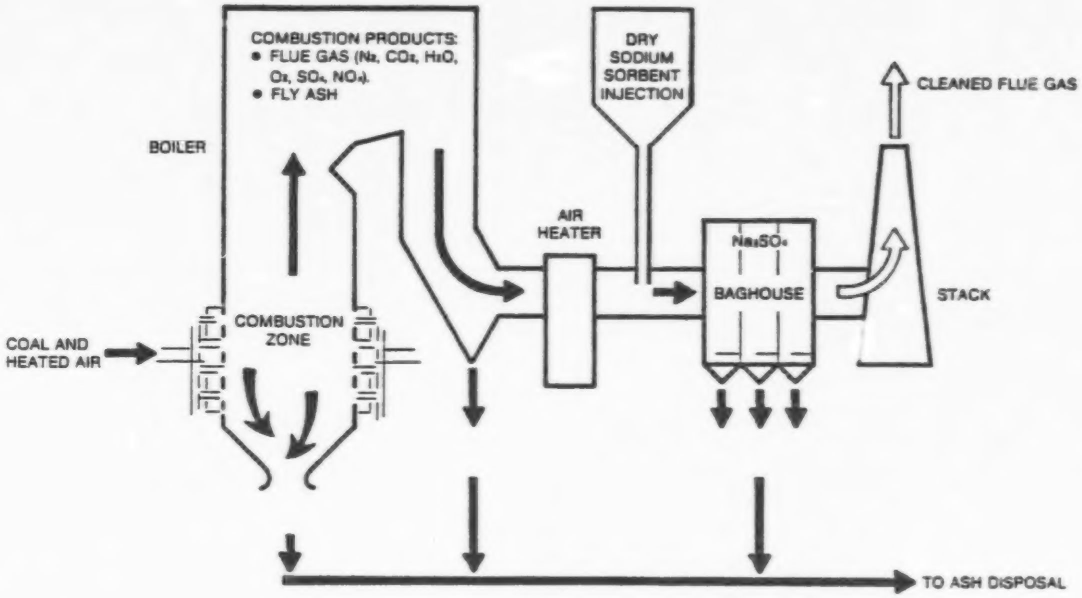
COMBUSTION PRODUCTS:
• FLUE GAS (N_2, CO_2, H_2O, O_2, SO_x, NO_x).
• FLY ASH
BOILER
DRY SODIUM SORBENT INJECTION
CLEANED FLUE GAS
AIR HEATER
Na_2SO_4
BAGHOUSE
STACK
COMBUSTION ZONE
COAL AND HEATED AIR
TO ASH DISPOSAL

Figure 1. Schematic of a coal-fired power plant with dry-sodium injection for SO_2 control.

REAGENT AVAILABILITY

Sodium reagents which have received most utility and supplier attention include nahcolite (naturally occurring sodium bicarbonate, $NaHCO_3O$), trona (naturally occurring $NaHCO_3 \cdot Na_2CO_3 \cdot 2H_2O$), and sodium sesquicarbonate (a trona analogue, $NaHCO_3 \cdot Na_2CO_3 \cdot 2H_2O$). Huge supplies of both nahcolite and trona are estimated to exist in the United States: over 30 billion tons of nahcolite, and in excess of 85 billion tons of trona.

Nahcolite is the preferred reagent because of its high bicarbonate content and, in tests conducted to date, its high sodium utilization. While it is not presently mined as raw ore in the United States, efforts are underway to obtain and process it through solution mining. In contrast, trona is commercially available in large quantities. Both have been shown to easily achieve 70%-plus SO_2 removals.

Given the promise of dry-sodium injection for SO_2 control, several companies have recently expressed interest and/or begun offering processed reagents for use by utilities. A list of these companies is given below in Table 1. This list demonstrates the dramatic turnaround in available suppliers of reagent. Only a few years ago, no firm suppliers could be identified.

TABLE 1
SUPPLIERS OF SODIUM-BASED REAGENTS - 1984

Allied Chemical Corporation
Cominco American
Church & Dwight Company, Inc.
Industrial Resources, Inc.
FMC Corporation
Kerr-McGee Chemical Corporation
Stauffer Chemical Company
Texas Gulf Chemicals Company

This potential for improved product availability has increased the level of utility interest in a more detailed analysis of dry-injection. Also, and significantly, these suppliers are developing improved processed reagents which have substantially lower fractions of inert material. This means less inert material to be transported and stored by the utility, thereby lowering overall reagent costs.

A VIABLE TECHNOLOGY

The technical aspects of dry-sodium injection have been studied by several researchers over the past few years. The most important aspect is the utilization of sodium in the reagent. Figure 2 illustrates SO_2 removal versus NSR (normalized stoichiometric ratio) for low-sulfur (0.5%), western coal obtained with nahcolite, at the bench-scale, and at Cameo. Sodium utilization (calculated as SO_2 removal divided by NSR) is shown to improve substantially from the bench-scale to the full-scale. A major reason for this improved utilization is now believed to be associated with reagent particle size distribution. The reagent at Cameo was pulverized much finer than those for the bench-scale research. Results published by other researchers are similar to those reported on the bench-scale; the results from the Cameo demonstration reported the highest sodium utilization of any previous work.

SO_2 removal versus NSR at Cameo is shown in Figure 3 using trona, nahcolite, and soda ash. The data in this figure support the view that SO_2 removal is viable for low-sulfur (0.5%), western coal for both trona and nahcolite. However, this data (as those of previous investigators) also demonstrates the diminishing relationship of sodium utilization with increasing NSR values above 0.7. Until recently, no mechanism has been suggested that explains this phenomenon.

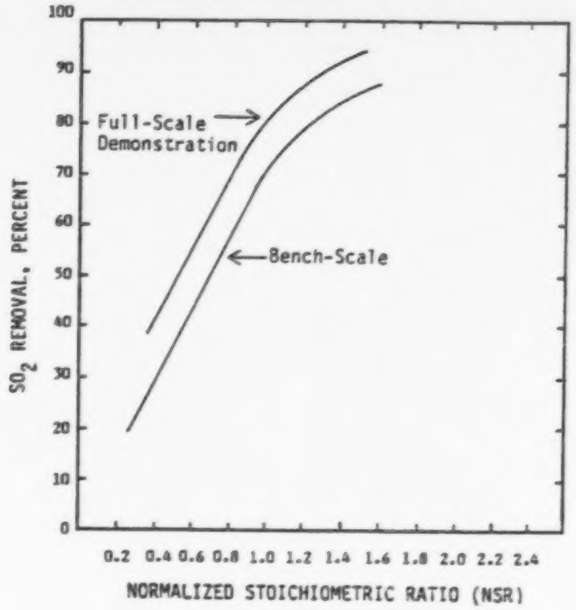

Figure 2. SO_2 removal vs. NSR for nahcolite illustrating improvement in results reported from the bench-scale to the full-scale. Tests conducted with low-sulfur (0.5%), western coal.

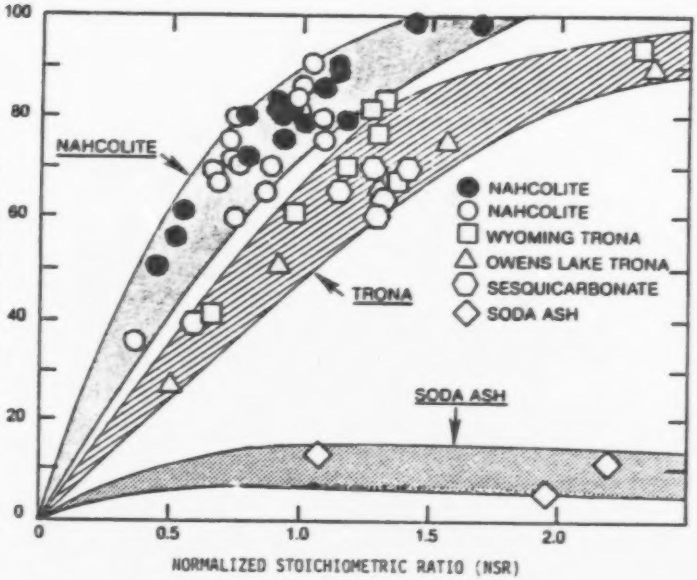

Figure 3. SO_2 removal vs. NSR from full-scale demonstration at Public Service Co. of Colorado's Cameo station. Tests conducted with low-sulfur (0.5%), western coal.

EPRI is currently conducting pilot-scale research to evaluate sodium utilization of the numerous new reagents now being offered. This work is being conducted by KVB, Inc. at Arapahoe. Although results are preliminary, they do indicate that particles must be small enough to follow the gas stream and to distribute uniformly among the bags. For example, if one region of the bag is getting more than an average share of reagent, this means another region is being starved of reagent. Accordingly, overall reagent utilization drops.

Figure 4 shows a family of curves relating SO_2 removal to NSR using sodium bicarbonate reagent. Each curve relates to material of different average particle diameter. For the lowest curve, average reagent particle diameter is approximately 100μm; for the middle curve, average diameter is approximately 60μm; for the upper curve, the average diameter is approximately 20μm. BET surface area was between 0.1 to 0.2 m^2/gm for the three materials prior to injection, and increased five to 10 times upon decomposition from bicarbonate to carbonate. Therefore, each of these materials is relatively close in surface area during the reaction of carbonate with sulfur This data is believed to substantiate the postulate that, with reagents of comparable surface area, the controlling factor in achieving high sodium utilization is particle size. The key, then, is to have a reagent particle size sufficiently small (less than 20μm) to ensure that the reagent will remain in and follow the gas stream as it enters the hopper region and distributes uniformly among the bags. Fortunately, sodium reagents are easily pulverized to small particle sizes with conventional equipment.

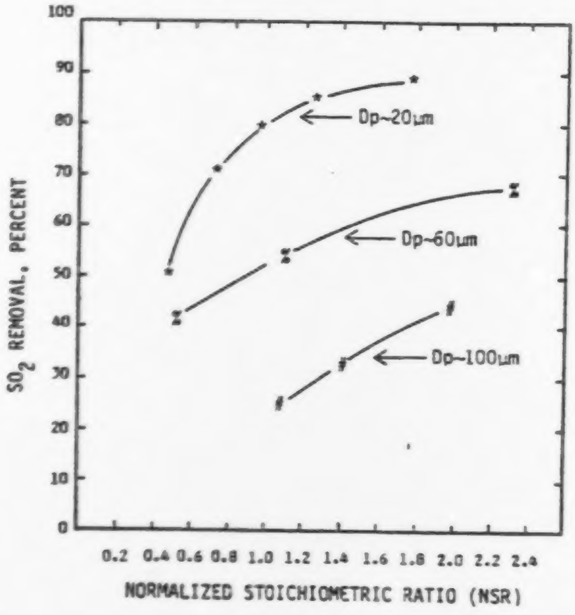

Figure 4. SO_2 removal vs. NSR for sodium bicarbonate illustrating the dependence of SO_2 removal to the average particle diameter injected into the flue gas duct.

These findings are important when considering injection design criteria, reagent pulverization requirements and techniques, and possibly baghouse inlet transition and hopper designs. For example, the requirements on a pulverizer for dry-injection might be slightly more demanding (i.e., finer particle required) when the boiler load is reduced and the gas flows are lessened. The carrying velocity into a baghouse compartment hopper needs to be sufficient to keep a reagent particle from falling out; and the reagent distribution needs to remain somewhat uniform across the tubesheet. This underlines the importance of a good aerodynamic modeling effort relating to the injection system and baghouse designs.

These results were obtained using sodium bicarbonate provided by several different suppliers. Sodium sesquicarbonate and light soda ash will also be tested at Arapahoe this year. The effect of reagent particle size on SO_2 collection and reagent utilization will continue to be documented as will the effect of baghouse temperature on the utilization of sodium. Two further and important issues will be reported at the conclusion of the current work. They are: the effect of the injection of dry reagents on baghouse pressure drop, and the effect of inlet SO_2 concentration on sodium utilization.

SYSTEM ECONOMICS

In retrofit applications, dry-sorbent injection would clearly be an attractive choice because of its simplicity, low capital cost, and minimal land and power requirement.

To assess the economics of dry-sorbent injection on new plants, EPRI recently sponsored a study conducted by Stearns-Catalytic(4). This work compared the costs of commercially available spray dryer systems with commercially sized nahcolite and trona all-dry injection systems physically and chemically similar to those reported at Cameo. The analysis was performed using EPRI economic premises for a new, hypothetical power plant located in Kenosha, Wisconsin, consisting of two 500 MW units burning 0.5% low-sulfur, western coal, and with an assumed 30-year plant life.

Results showed the capital costs of trona and nahcolite dry-injection systems at about \$25/kW, compared to approximately \$115/kW for spray drying (Figure 5). On a levelized cost basis, trona injection was least expensive, followed by nahcolite injection and spray drying (Figure 6). These results were found to be highly sensitive to the delivered price of the sorbent, sulfur content of the coal, and SO_2 removal requirement. Cost for waste disposal and the size of the generating plant were found to be important, but less significant. Since this economic analysis was for a hypothetical power plant site, it does not take into account site-specific considerations. Consequently, any electric utility considering the technology is encouraged to conduct an analysis of its own for each plant site.

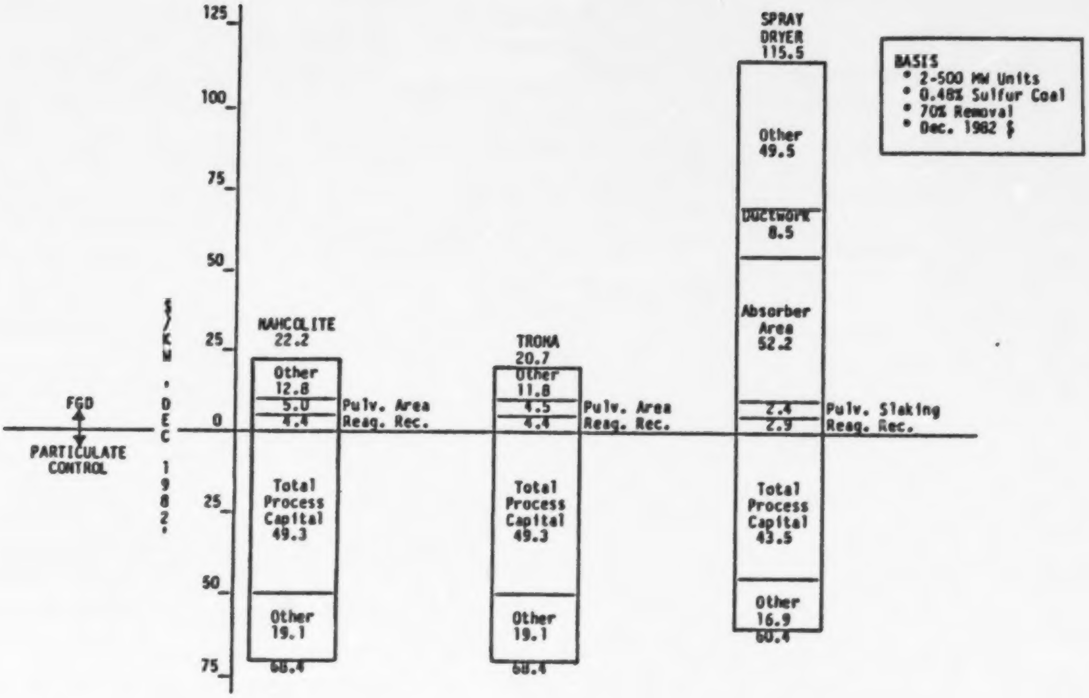

Figure 5. Capital costs (December 1982) for nahcolite injection, trona injection, and spray dryer systems at a hypothetical power plant in Kenosha, Wisconsin.

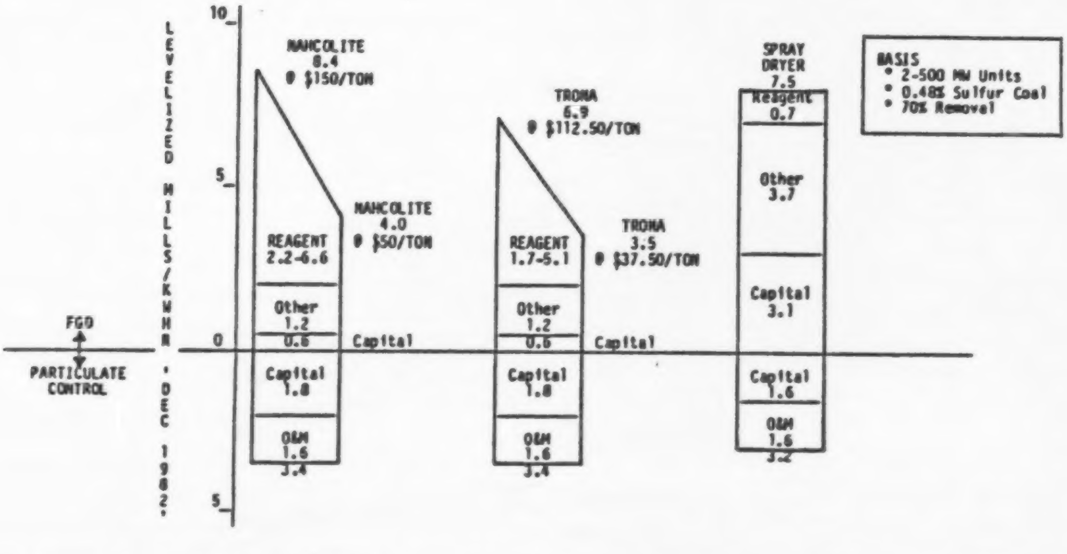

Figure 6. Distribution of levelized costs (December 1982) for nahcolite injection, trona injection, and spray dryer systems at a hypothetical power plant in Kenosha, Wisconsin.

SUMMARY

The few and simple unit processes required to successfully operate a dry-injection system make the technology an attractive, economic alternate for SO_2 control on coal-fired power plants. The interest of several large, potential suppliers in entering the market is especially promising in terms of making available better performing and lower cost reagents. Dry-sodium injection systems designed to optimize reagent utilization will provide benefits in all areas of the technology, minimizing reagent and solids handling requirements, hopefully lowering levelized costs, and reducing the sodium levels in the fly ash waste product.

REFERENCES

1. Bechtel Corporation, "Evaluation of Dry Alkalis for Removing Sulfur Dioxide from Boiler Flue Gases," FP207, October, 1976, Electric Power Research Institute, Palo Alto, CA.

2. L.J. Muzio, J.K. Arand, "Bench-Scale Study of the Dry Removal of SO_2 with Nahcolite and Trona," CS-1744, March, 1984, Electric Power Research Institute, Palo Alto, CA.

3. L.J. Muzio, T.W. Sonnichsen, "Demonstration of SO_2 Removal on a 22 MW Coal-Fired Utility Boiler by Dry Injection of Nahcolite," CS-2894, Vol. 1, March, 1983; Vol. 2, June, 1984, Electric Power Research Institute, Palo Alto, CA.

4. R.W. Scheck, D.J. Naulty, A.E.E. Gallagher, R.P. Grimm, D.A. McDowell, R.J. Keeth, J.E. Miranda, "Economic Evaluation of Dry Injection FGD Technology," RP-1682-1, Electric Power Research Institute, Palo Alto, CA, 1984.

REMOVAL OF SULFUR DIOXIDE AND PARTICULATE USING E-SOX

by: Leslie E. Sparks, Geddes H. Ramsey,
Richard E. Valentine and Cynthia Bullock
Particulate Technology Branch
Industrial Environmental Research Laboratory
Environmental Protection Agency
Research Triangle Park, N. C. 27711

ABSTRACT

Research aimed at developing a low cost retrofit system, called E-SOX, for combined particulate and SO_2 removal is described. The E-SOX concept centers on recent advances in ESP technology that makes it possible to reduce the size of ESP required for particulate control. Results of mathematical modeling and limited pilot scale experiments on the feasibility of collecting SO_2 in the freed space are discussed. The results show that the concept is technically feasbile. Modest (40-65%) levels of SO_2 removal are possible with lime as the reagent. High (over 90%) levels of SO_2 removal are possible with sodium carbonate as the reagent. Order of magnitude economic analysis shows that the process is economically feasible. Plans for additional experimental and theoretical work are presented.

REMOVAL OF SULFUR DIOXIDE AND PARTICULATE USING E-SOX

INTRODUCTION

Because of the concern over acid rain and the resulting interest in low cost methods for reducing sulfur dioxide (SO_2) emissions from existing plants, the Particulate Technology Branch has begun theoretical and experimental work to combine advanced ESP and SO_2 removal technologies in an existing ESP. This process, called E-SOX, combines advanced ESP technology and spray dryer technology to remove particulate and SO_2 in the same physical equipment.

Advanced ESP technology provides the means for collecting particles with high efficiency in relatively small ESPs. The technology can be used to reduce the required size of new ESPs or to free space in an existing ESP that can be used to collect SO_2.

This paper describes experiments and modeling which demonstrate the technical feasibility of E-SOX in retrofit situations.

CONCEPTUAL DESIGN

The basic idea of E-SOX is to turn the existing ESP into a combination spray dryer and advanced ESP. The conceptual design can best be understood by considering a hypothetical ESP used to control particulate emissions from a boiler firing high sulfur coal. Such an ESP would have a specific collector area (SCA) of 41.3 sec/m based on actual gas flow conditions with three 3 m long electrical sections in series. This size ESP is adequate to meet a particulate emission standard of 43 ng/J when collecting fly ash from a high sulfur coal.

The following modifications would convert the ESP to E-SOX:

1. Remove the wires and plates in electrical section 1.
2. Install a bank of spray nozzles at the inlet of electrical section 1. These nozzles should produce fine drops with diameters between 15 and 30 μm.
3. Install prechargers (either cooled pipe or other design) at the inlet of sections 2 and 3.
4. Replace the normal discharge electrodes in sections 2 and 3 with large diameter wires.

The removal of wires and plates in section 1 provides a space for SO_2 removal. At typical gas velocities in an ESP (1 to 2 m/sec), section 1 would provide about 1.5 to 3.0 sec residence time for SO_2 removal and drop evaporation.

The precharger and large diameter wires added to sections 2 and 3 convert the remainder of the ESP from single-to multi-stage. This conversion will compensate for the reduction in SCA from 41.3 to 27.5 sec/m. As is discussed later, this multi-stage ESP configuration makes it possible to meet the 43 ng/J particulate emission standard assumed for the plant.

The design goal for the E-SOX system is continued compliance with the particulate emission limits of 43 ng/J for the plant and 50 to 60% SO_2 removal. A particulate emission standard of 43 ng/J is typical of the particulate emission standards required of most existing power plants.

MODELING

E-SOX is designed to use part of the existing ESP as the reaction chamber for SO_2 removal. This means that all SO_2 removal and drying must occur in 1 to 2 sec residence time. If drying is not complete by this time, severe operating problems are likely in the active ESP sections following the reaction zones.

The spray dryer model developed by Damle (1) was used to determine the feasibility of collecting SO_2 in the 1 to 2 sec residence time available in the inlet section of an ESP. An example of the model projections is shown in Figure 1. The model predictions show that, if the droplet diameter is less than 30 μm, the solids entering the ESP should be dry and significant SO_2 removal is possible.

The modeling was favorable enough to warrant a limited experimental study aimed at verifying the model projections.

EXPERIMENTAL

The experiments were conducted in the IERL-RTP in-house ESP pilot plant. The pilot ESP is a four-section single-lane pilot plant capable of operating from ambient to 350°C. Sampling ports are located at the ESP inlet, the ESP outlet, and between each pair of electrical sections of the ESP.

The configuration for these experiments is shown in Figure 2. Sections 1 and 2 were converted to SO_2 reaction chambers by removing the wires. The SO_2 was injected at point A located before the gas distribution plate. Scrubbing liquid was injected at point B using two sonic spray nozzles. These nozzles are two fluid nozzles and produce drops of 5 to 10 μm in diameter. SO_2 was measured at four locations (C, D, E, and F). Location C provided about 0.5 sec of residence time; location D, 1.3 sec; location E, 2.1 sec; and location F, 3.7 sec.

For the E-SOX tests the pilot plant was operated with a gas inlet temperature of 150°C and a gas flow rate of about 0.487 am^3/sec at 150°C. The ESP was operated under about 5 cm H_2O negative pressure to ensure that no SO_2 was released into the room. SO_2 and air flow rate were measured to determine the air leakage into the ESP. These measurements showed about

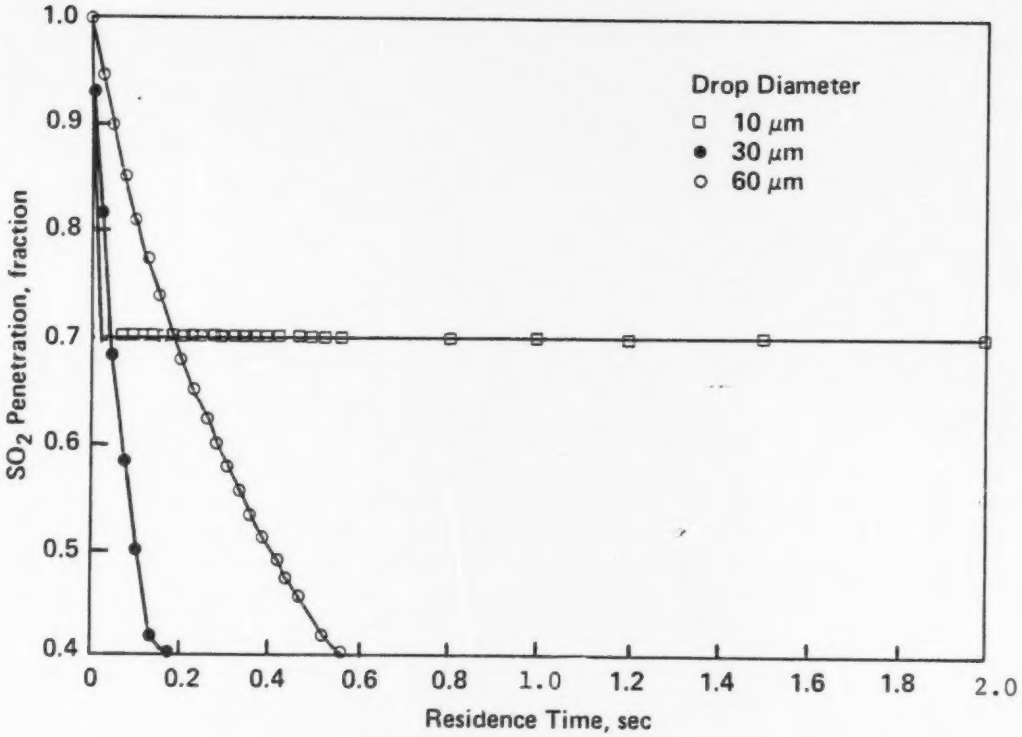

Figure 1. Predicted SO_2 removal for E-SOX.

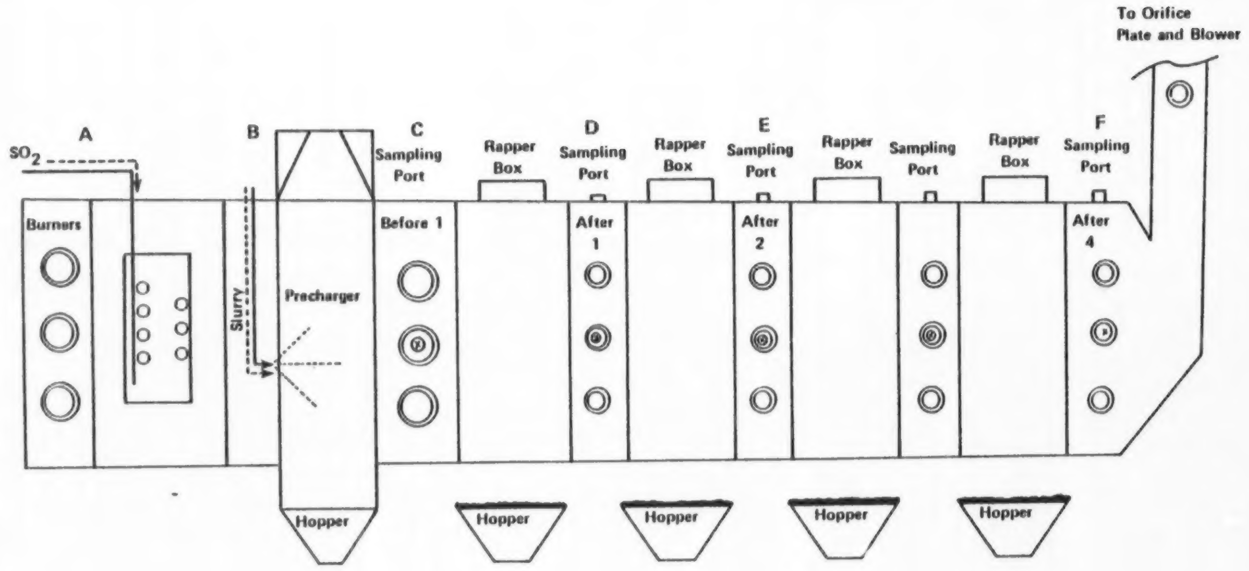
To Orifice Plate and Blower
A
SO_2
B
C
Sampling Port
Rapper Box
D
Sampling Port
Rapper Box
E
Sampling Port
Rapper Box
Sampling Port
Rapper Box
F
Sampling Port
Burners
Slurry
Precharger
Before 1
After 1
After 2
After 4
Hopper
Hopper
Hopper
Hopper
Hopper

Figure 2. Sketch of pilot plant modified for E-SOX.

5% inleakage between the inlet and the sampling ports at the end of section 2. There was 20% inleakage between the ESP inlet and the ESP outlet. The E-SOX performance data were corrected for this inleakage.

SO_2 was measured with a TECO analyzer that was zeroed and spanned periodically. The SO_2 injection rate was between 1100 and 1500 ppm.

Preliminary measurements were made to determine the uniformity of the SO_2 concentration in the ESP. Horizontal traverses were made at three vertical locations at each sampling location. These measurements showed no vertical stratification of the SO_2, but a slight horizontal stratification. Because there was no vertical stratification, all experimental measurements were made using the center port at each sampling location. A multipoint horizontal traverse was made to account for the small amount of horizontal stratification.

Two sets of experiments were conducted: sodium carbonate was used as the scrubbing reagent for the first set; and lime was used for the second. The experimental procedure was the same for both sets of experiments SO_2 readings were made at all sampling locations with the scrubbing liquid off. The scrubbing liquid was turned on and the system allowed to come to steady state. Then SO_2 measurements were made and the scrubbing liquid was turned off. The SO_2 measurements were then repeated. For a typical run the maximum difference between the two scrubbing-liquid-off measurements was less than 20 ppm; i.e., the inlet SO_2 concentration varied by less than 20 ppm.

RESULTS

Sodium Carbonate

Initial experiments were conducted using sodium carbonate solution as the scrubbing liquid. The results of these measurements are summarized in Figures 3 and 4.

The SO_2 concentration dropped rapidly during the initial 0.5 sec. The SO_2 concentration then dropped nearly linearly for the remainder of the time in the ESP. The initial rapid decrease in SO_2 is due to the reaction of SO_2 with the evaporating drops. During this phase the mass transfer of SO_2 to the drops is rapid, as is the reaction with the dissolved SO_2 and the sodium carbonate.

The linear phase is due to the reaction of the SO_2 with dry sodium carbonate particles. The gas-solid mass transfer is much less efficient than the gas-liquid mass transfer. However, the reactivity of sodium carbonate is high enough to ensure that considerable SO_2 is removed after the drops have evaporated.

The data in Figure 3 indicate that significant SO_2 removal is possible with E-SOX at reasonable stoichiometry. At high stoichiometry, over 90% removal can be realized.

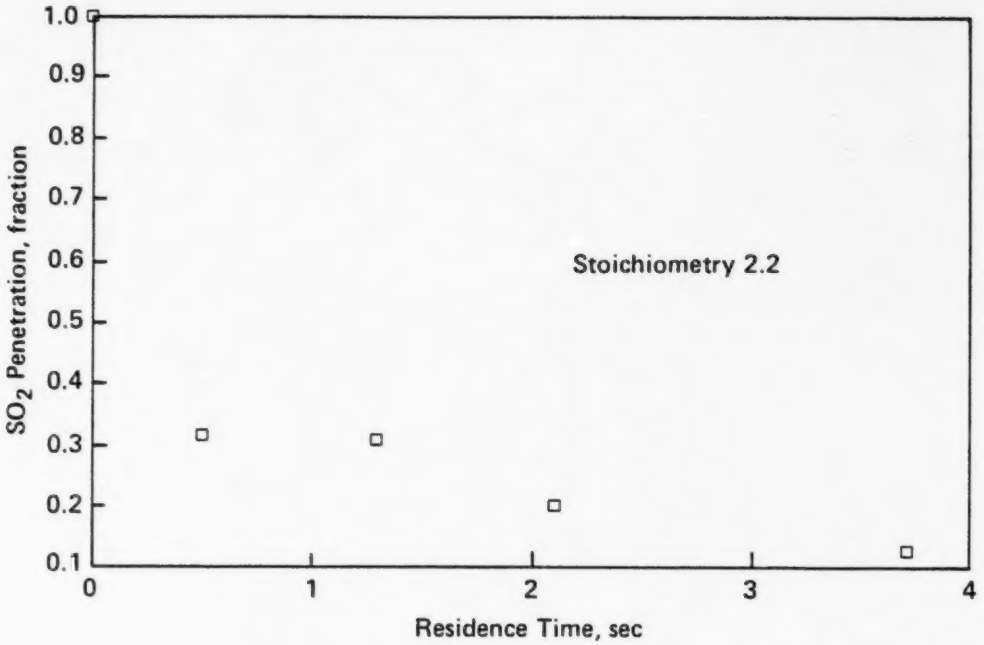

Figure 3. E-SOX SO_2 penetration vs. time.

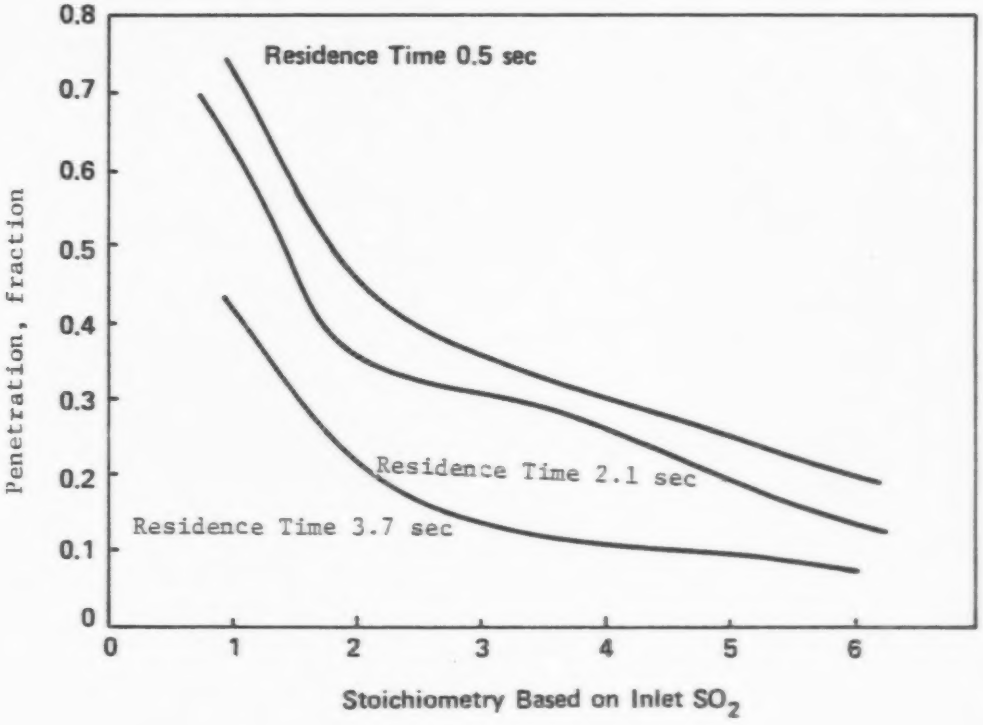

Figure 4. E-SOX experimental data for sodium carbonate

Lime

Because the results with sodium carbonate were encouraging, experiments were conducted using hydrated lime as the alkaline material. A slurry of lime and water was injected through the same nozzles used during the sodium carbonate experiments. The results of the lime experiments are shown in Figures 5 and 6.

The results in Figures 5 and 6 demonstrate that with lime all the SO_2 removal is obtained during the initial phase when SO_2 is collected by the evaporating drops. The dry lime used in these particles was not reactive enough to allow measurable SO_2 removal due to the dry lime particles. This indicates that the major advantage of sodium carbonate as compared to lime is the high reactivity of the dry sodium carbonate particles. Some of the highly reactive limes, being studied in conjunction with other retrofit SO_2 removal systems, may increase the SO_2 capture efficiency of E-SOX with lime to near the levels obtained with sodium carbonate.

The experimental data for both lime and sodium carbonate show that the design goals of the E-SOX system can be achieved with either reagent. A residence time of 1 sec is sufficient for 60% SO_2 removal with E-SOX and lime.

PARTICULATE COLLECTION EXPERIMENTS

E-SOX's success depends on its ability both to provide 50-60% SO_2 removal and to meet particulate emission limitations. Therefore, experiments were conducted to simulate the particulate collection of an E-SOX ESP. In these experiments lime slurry was injected through the spray nozzles. Fly ash was injected through sand blast guns, as is normal for the operation of the pilot plant for fly ash experiments. The ESP was converted to multi-stage configuration with cold-pipe prechargers installed in sections 1 and 3 and large wires installed in sections 2 and 4. The SCA of the ESP for these tests was about 11 sec/m.

Calibrated cascade impactors were used to determine the particle size distribution entering and leaving the multi-stage ESP. The impactor data were used to calculate the penetration as a function of particle diameter for the multi-stage ESP.

The results of the experiments are shown in Figure 7. The data in Figure 7 were used to estimate the performance of an ESP that was converted to E-SOX. The calculations were performed by converting the penetration as a function of particle diameter data in Figure 7 to migration velocity as a function of particle diameter, see Figure 8. These data were then used to calculate the performance of an E-SOX ESP collecting fly ash with a typical size distribution (mass mean diameter 15 μm, geometric standard deviation 3.5) and E-SOX solids with a size distribution typical of those generated in our experiments (mass mean diameter 3 μm, and geometric standard deviation 3.5). The overall mass penetration of the ESP was

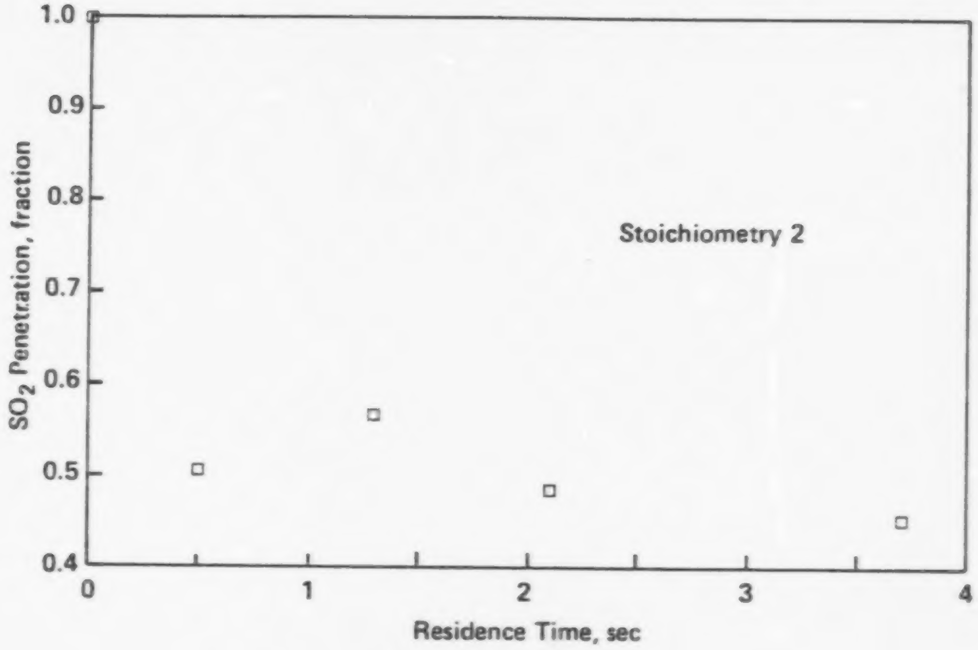

Figure 5. Penetration vs. time for lime.

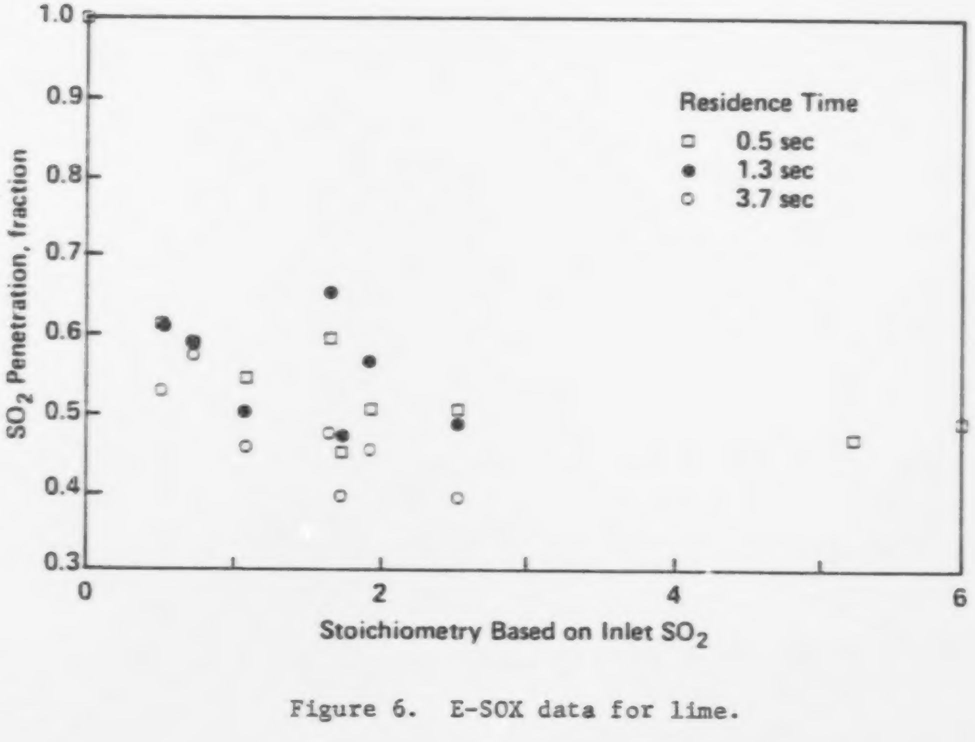

Figure 6. E-SOX data for lime.

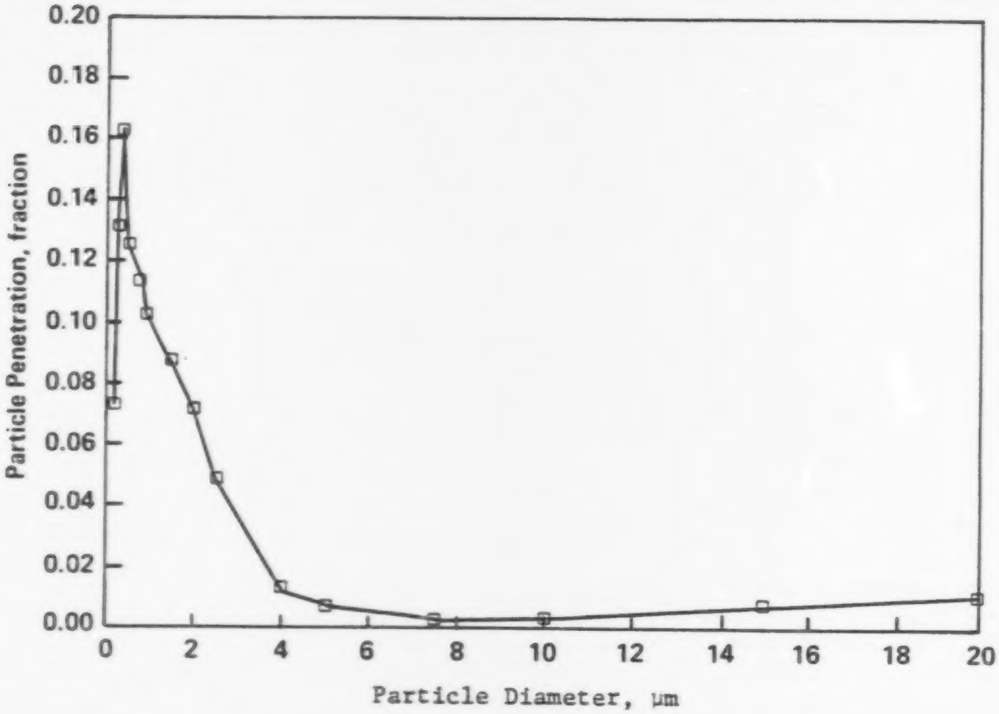

Figure 7. Results of E-SOX ESP experiments

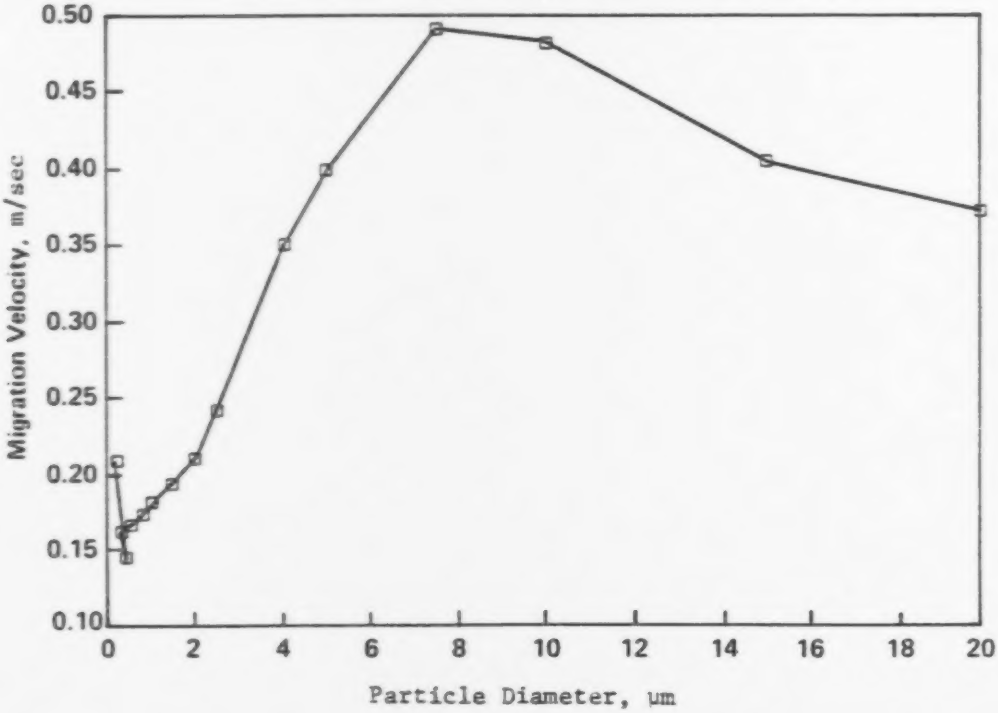

Figure 8. Migration velocity vs. particle diameter.

determined by integrating over the two size distributions. The results were corrected for sneakage and reentrainment using procedures similar to those used in the EPA/SoRI ESP model. (2)

The results of the particle collection calculations are shown in Figure 9. Note that the mechanical conditions of the ESP, as characterized by the uniformity of the gas flow distribution and the gas sneakage, are important factors. The mechanical conditions must be representative of current good practice if the particulate emission limitations are to be met.

ECONOMICS

A study estimate of the economics of E-SOX was conducted to determine the economic feasibility of the system. The capital costs of E-SOX were estimated by first analyzing the process diagram for the E-SOX system, Figure 10, to identify equipment that was required by other SO_x removal processes. This analysis showed that the lime handling system and the reacted lime waste disposal systems were common to most FGD processes. Because these two items, the lime handling system and the extra waste disposal system, are common to E-SOX and spray drying, the portion of the E-SOX capital cost due to these items was based on costs of the same two items for spray drying.

The capital costs of the cold-pipe precharger were based on experience gained from fabrication of a 5 MW pilot plant. The costs of the large diameter wire retrofit were based on discussions with nozzle vendors.

The cost analysis showed that the major costs were associated with the lime handling system followed by the costs of waste disposal--the two components with the firmest costs. The costs of the cold-pipe precharger, large diameter wires, and spray system were a small part of the total costs. Thus, even a factor of two error in estimating these costs would have little impact on the total economics of E-SOX.

The results of the capital cost study are shown in Figure 11. Also shown in Figure 11 are the costs of wet limestone FGD removal processes. Note that E-SOX is at least competitive with current technology and appears to offer significant cost advantages.

CONCLUSION

The experimental data and the modeling based on that data show that E-SOX is capable of providing 50-60% SO_2 removal in an existing ESP while meeting a particulate emission standard of 43 ng/J. The economic analysis shows that E-SOX has cost advantages when compared with other methods of SO_2 control.

Research is continuing to improve and verify the SO_2 and particulate removal models for E-SOX. Also a series of in-house experiments with the entire system of SO_2 removal and multi-stage ESP is planned for early 1985. A large pilot scale evaluation of E-SOX may take place in 1986.

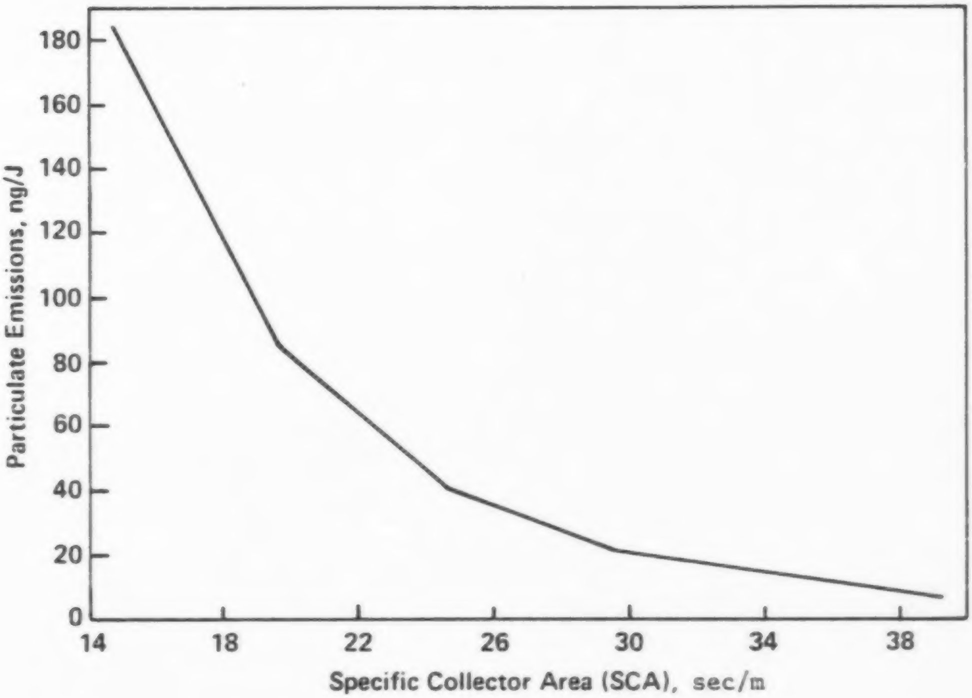

Figure 9. E-SOX predicted particulate emissions.

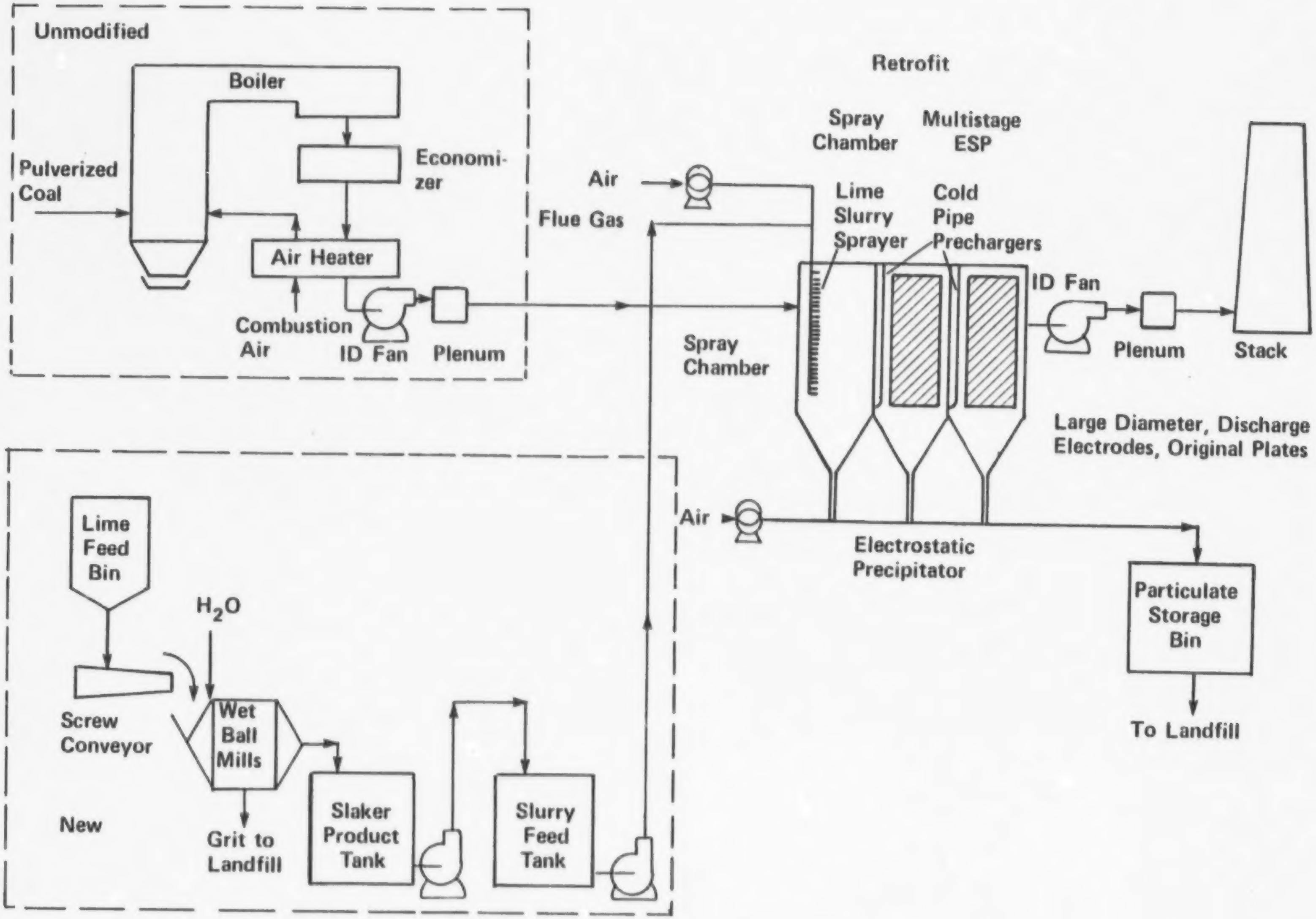
Unmodified
Boiler
Pulverized Coal
Economizer
Air Heater
Combustion Air
ID Fan
Plenum
Retrofit
Air
Flue Gas
Spray Chamber
Multistage ESP
Lime Slurry Sprayer
Cold Pipe Prechargers
ID Fan
Plenum
Stack
Spray Chamber
Large Diameter, Discharge Electrodes, Original Plates
Air
Electrostatic Precipitator
Particulate Storage Bin
To Landfill
Lime Feed Bin
H_2O
Screw Conveyor
Wet Ball Mills
Grit to Landfill
Slaker Product Tank
Slurry Feed Tank
New

Figure 10. Process flow diagram for E-SOX.

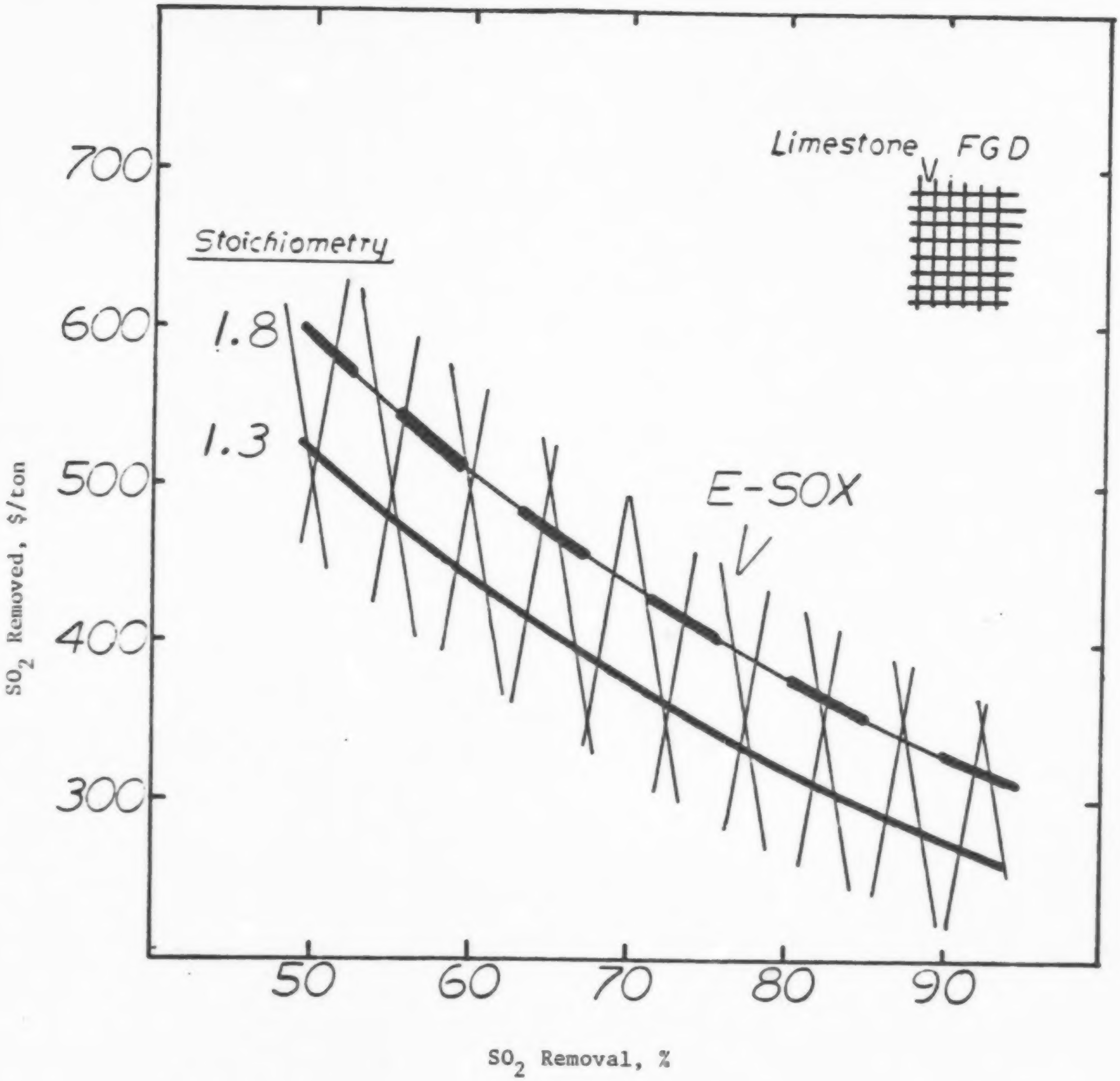

Figure 11. Cost effectiveness of E-SOX process.

Research is also planned to reduce the amount of lime required for a given level of SO_2 removal. Reducing the amount of lime reduces the particulate burden on the multi-stage ESP and can significantly reduce the capital and operating costs of the system.

ACKNOWLEDGEMENTS

The economic analysis for E-SOX was conducted by John Milliken of IERL-RTP.

REFERENCES

1. Damle, A.S. and L. E. Sparks, "Modeling of SO_2 Removal in Spray-Dryer Flue-Gas Desulfurization System." Paper presented at the Fifth Symposium on the Transfer and Utilization of Particulate Control Technology. U. S. EPA and EPRI, Kansas City, MO, August 27-30, 1984.

2. Faulkner, M. G. and J. L. DuBard, "A Mathematical Model of Electrostatic Precipitation (Revision 3)," Volumes I and II, and source code tape EPA-600/7-84-069a,b,c (NTIS PB84-212-679, PB84-212-687, PB84-232-990), U. S. EPA, IERL-RTP, N.C. 1984.

COMPARISON OF DRY INJECTION SYSTEMS AT NORMAL AND HIGH FLUE GAS TEMPERATURES

by: Robert M. Jensen, William Dunlop,
George C. Y. Lee and Duane Folz

ABSTRACT

At normal flue gas temperatures, the sulfur dioxide removal capability of a dry injection system using nahcolite as the reagent is limited to approximately 70%. The stoichiometry and capability of nahcolite to remove sulfur dioxide improve with increasing flue gas temperature.

This paper compares technical, operating and economic considerations for dry injection with baghouse systems operating at normal (270°F) and high (550°F) flue gas temperatures. The high temperature system has regenerative air preheaters ahead of and after the baghouse. The hot system eliminates coldend problems for the regenerative air preheaters and provides greater heat recovery from the flue gas. High sulfur eastern and low sulfur western coals are burned in two 500-MW pulverized coal-fired power plants at Kenosha, Wisconsin. The study shows that the hot system is marginally competitive with the normal temperature dry injection system and with the spray dryer/baghouse system for low sulfur coal. For high sulfur coal, the hot system is competitive with the normal temperature dry injection system.

INTRODUCTION

Injection of dry powdered nahcolite into a gas stream before it enters a baghouse removes sulfur dioxide from the gaseous products resulting from the combustion of fossil fuel. Some removal of the SO_2 takes place in the gas stream, and most of the removal takes place in the filter cake on the bags in the baghouse.

Dry FGD systems include the spray dryer/baghouse system in which the spray dryer removes most of the SO_2 and some additional SO_2, and practically all of the particulates are removed as the gas passes through the filter cake of dry alkaline material from the spray dryer. This paper is concerned only with the dry injection system that uses nahcolite and a baghouse to remove both SO_2 and particulates. Its purpose is to compare capital, operating and electricity costs as well as advantages and disadvantages of normal (270°F) and high (550°F) temperature dry injection systems. It also examines whether there is any cost advantage related to coal sulfur content.

EARLY HISTORY OF THE DRY INJECTION BAGHOUSE SYSTEM

Pioneering efforts to remove a gaseous pollutant from fossil fuel flue gas by dry injection ahead of a baghouse began in the early 1960s when Bechtel conducted a small pilot baghouse test program for Southern California Edison Co. (SCE). That program, using limestone injection, removed sulfur trioxide from oil-fired flue gas. Its success led to the construction of the baghouse on the 320-MW oil-fired Unit 3 of SCE's Alamitos Station in Long Beach, California. This was the first utility baghouse.

The first use of nahcolite to remove SO_2 from flue gas was a bench-scale test program by T.A. Kittleman and R. Borgwardt of the National Center For Air Pollution Control of the Department of Health, Education and Welfare (HEW) in Cincinnati, Ohio during 1968. Using a synthetic flue gas, this program demonstrated that nahcolite would remove SO_2 from flue gas and that it is as reactive as commercial sodium bicarbonate for this application.

In February 1969, SCE experimented with a pilot baghouse at Alamitos and confirmed that nahcolite would remove SO_2 from oil-fired flue gas. When it became necessary in 1970 for SCE to reduce SO_2 emissions, nahcolite was not available, and pure sodium bicarbonate was not a practical alternative. SCE then switched to a low sulfur fuel oil and gas, and the baghouse was mothballed. During 1973-1974 SCE anticipated they might have to burn high sulfur residual oil and overhauled the baghouse. The overhaul included installation of a new suit of bags.

Also during 1969, another program, funded by HEW to test dry injection, was conducted at Public Service Electric & Gas Co.'s coal-fired Mercer Generating Station near Trenton, N.J. That test program[1] confirmed that nahcolite will remove SO_2 from coal-fired flue gas, and it demonstrated that percentage removal and stoichiometry both improve with increasing gas temperature.

PREVIOUS COST ESTIMATES

Other investigators[2,3,4] have compared costs for dry injection for coal-fired flue gas with wet FGD systems and with the spray/dryer baghouse system. These cost comparisons, as well as the cost comparisons in this paper, are for two standard EPRI 500-MW units located in Kenosha, Wisconsin. EPRI estimating procedures and economic factors are as given in the EPRI Technical Assessment Guide, TAG, (P2410-SR).

SCOPE

Cost estimates in this paper begin at the economizer gas outlet and end at the inlet to the chimney. Previous cost estimates have begun at the airheater gas outlet. This difference in scope derives from two objectives: first, the hot system avoids or minimizes some of the shortcomings of regenerative airheaters; and second, it takes advantage of the fact that nahcolite utilization is better at higher flue gas temperatures. In order to compare these estimates with previous estimates we have added airheater costs to the previous estimates.

Reference here to a conventional dry injection system is for one that starts at the airheater gas outlet where the temperature of the gas leaving the airheater is some margin above the acid dew point. Figures 1 and 3 show conventional dry injection systems with 270°F gas temperature leaving the regenerative airheaters. These are compared with a proposed arrangement, Figures 2 and 4, which, for convenience, can be called the "hot baghouse system." Here the flue gas temperature leaving the first stage regenerative airheaters and entering the baghouse is 550°F. The gas leaving the baghouse then enters another stage of air heating using either regenerative or recuperative airheaters. Flue gas passes in series through the first stage airheaters, the baghouse, and then the second stage airheaters. Primary air and secondary air pass in series through the second stage airheaters, the first stage airheaters, and then to the furnace wind box and the pulverizers.

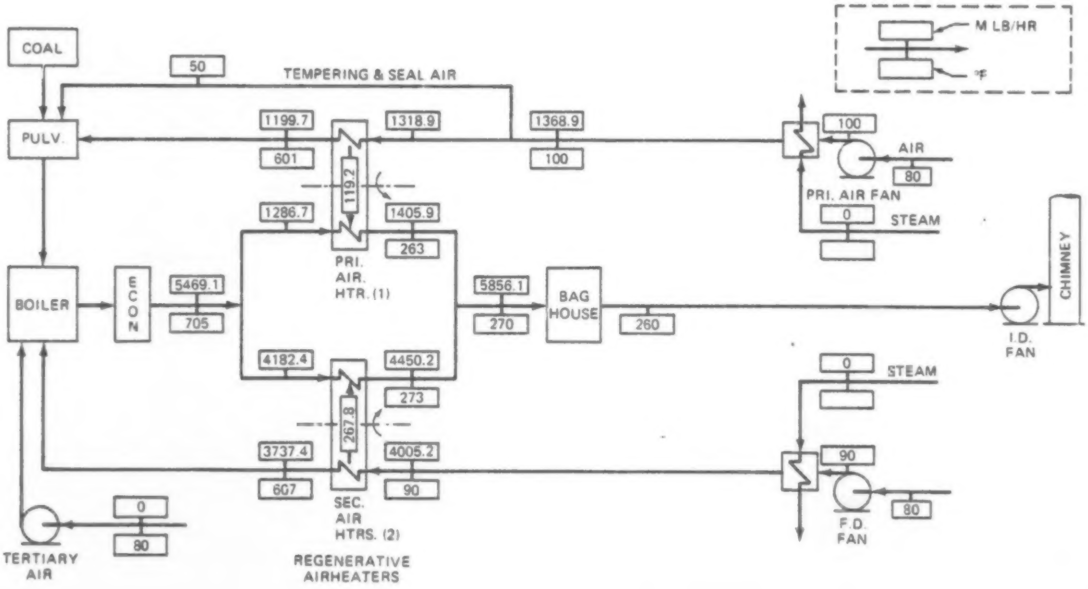
M LB/HR
°F
COAL
50
TEMPERING & SEAL AIR
PULV.
1199.7
601
1318.9
119.2
1368.9
100
100
AIR
80
PRI. AIR FAN
0
STEAM
1286.7
1405.9
263
PRI. AIR. HTR. (1)
BOILER
ECON
5469.1
705
5856.1
270
BAG HOUSE
260
CHIMNEY
I.D. FAN
4182.4
4450.2
273
267.8
0
STEAM
3737.4
607
4005.2
90
90
F.D. FAN
80
0
80
TERTIARY AIR
SEC. AIR HTRS. (2)
REGENERATIVE AIRHEATERS

Figure 1. Standard baghouse low sulfur coal (Case 1A).

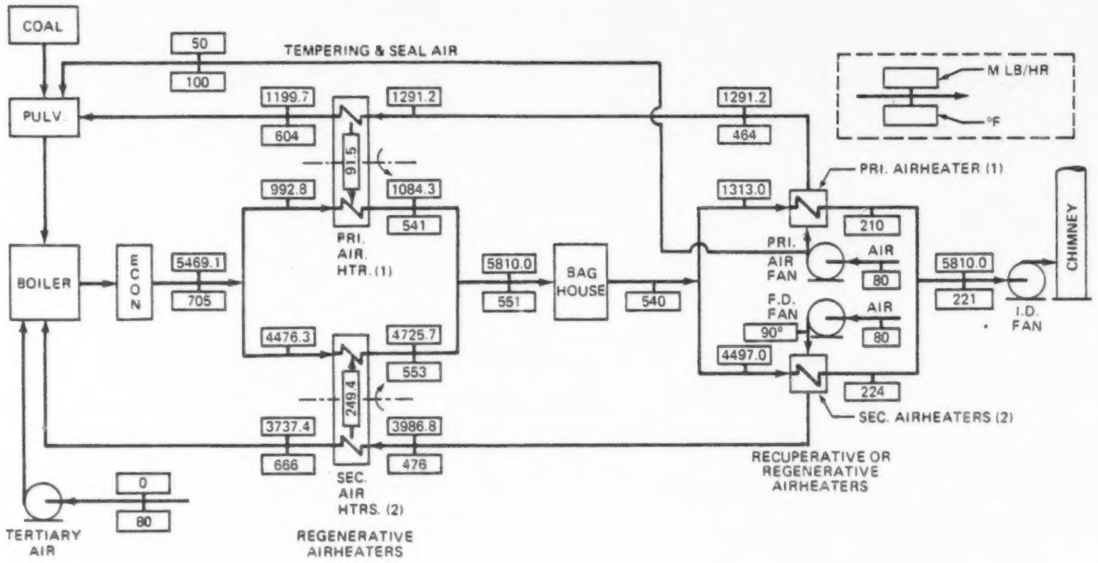
COAL
PULV.
BOILER
ECON
50
100
TEMPERING & SEAL AIR
1199.7
604
1291.2
91.5
992.8
1084.3
541
PRI. AIR. HTR. (1)
5469.1
705
5810.0
551
BAG HOUSE
540
4476.3
4725.7
553
249.4
3737.4
666
3986.8
476
SEC. AIR HTRS. (2)
REGENERATIVE AIRHEATERS
0
80
TERTIARY AIR
1291.2
464
1313.0
PRI. AIRHEATER (1)
210
PRI. AIR FAN
AIR
80
F.D. FAN
90°
AIR
80
4497.0
224
SEC. AIRHEATERS (2)
RECUPERATIVE OR REGENERATIVE AIRHEATERS
5810.0
221
I.D. FAN
CHIMNEY
M LB/HR
°F

Figure 2. Hot baghouse low sulfur coal (Case 1B).

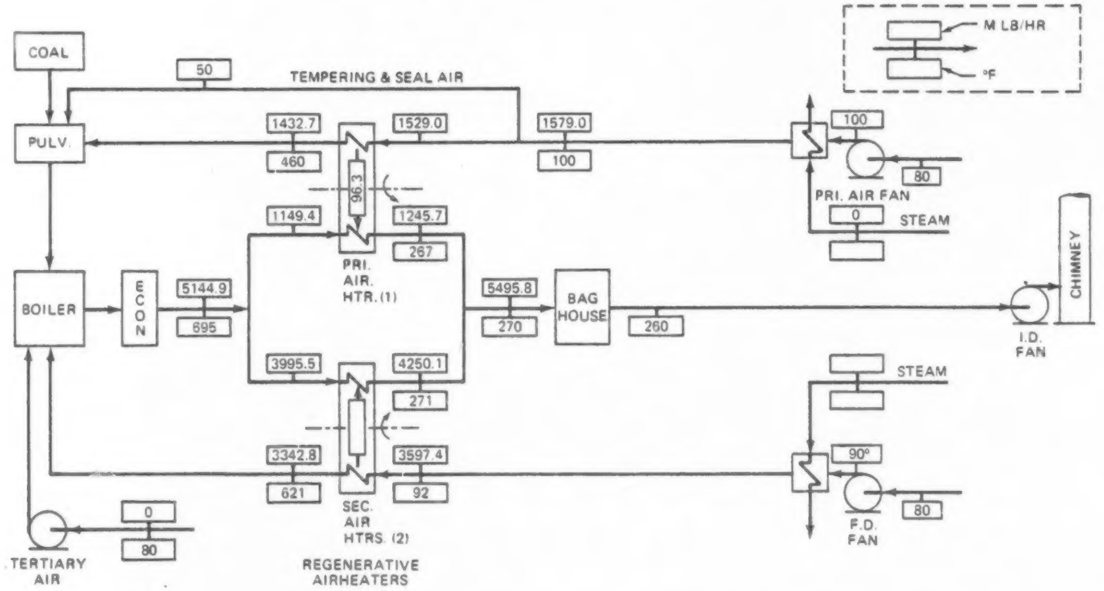
COAL
PULV.
BOILER
ECON
50
TEMPERING & SEAL AIR
1432.7
460
1529.0
96.3
1579.0
100
1149.4
1245.7
267
PRI. AIR. HTR. (1)
5144.9
695
5495.8
270
BAG HOUSE
260
3995.5
4250.1
271
3342.8
621
3597.4
92
SEC. AIR HTRS. (2)
REGENERATIVE AIRHEATERS
0
80
TERTIARY AIR
100
80
PRI. AIR FAN
0
STEAM
STEAM
90°
80
F.D. FAN
I.D. FAN
CHIMNEY
M LB/HR
°F

Figure 3. Standard baghouse high sulfur coal (Case 2A).

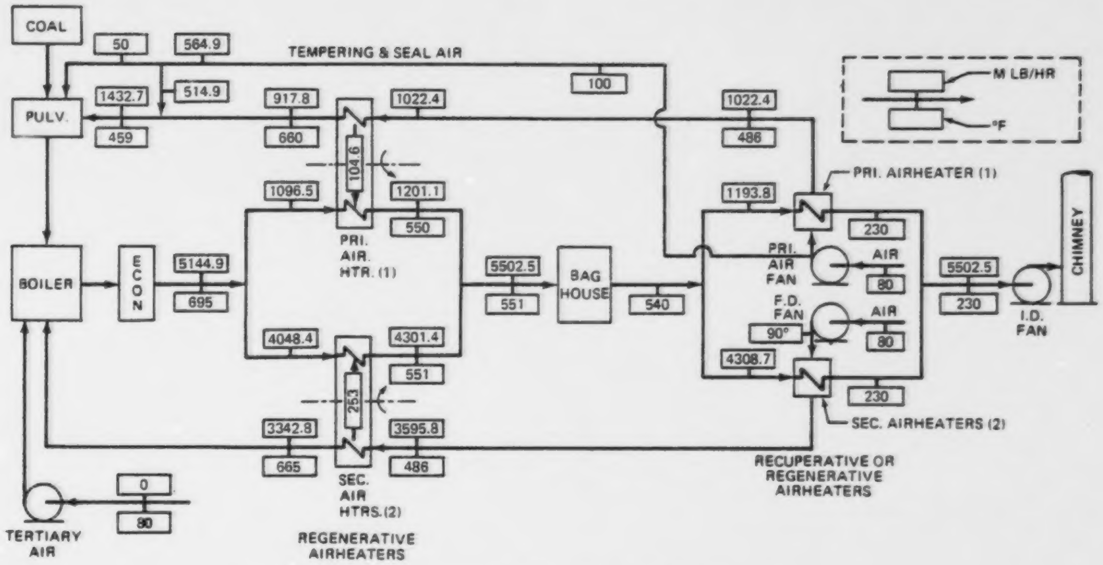
COAL
50
564.9
TEMPERING & SEAL AIR
100
1432.7
514.9
PULV.
459
917.8
660
1022.4
104.6
1022.4
486
M LB/HR
°F
1096.5
1201.1
550
PRI.
AIR.
HTR. (1)
1193.8
PRI. AIRHEATER (1)
230
CHIMNEY
BOILER
E
C
O
N
5144.9
695
5502.5
551
BAG
HOUSE
540
PRI.
AIR
FAN
AIR
80
5502.5
230
I.D.
FAN
F.D.
FAN
90°
AIR
80
4048.4
4301.4
551
4308.7
230
253
SEC. AIRHEATERS (2)
3342.8
665
3595.8
486
RECUPERATIVE OR
REGENERATIVE
AIRHEATERS
0
80
TERTIARY
AIR
SEC.
AIR
HTRS.(2)
REGENERATIVE
AIRHEATERS

Figure 4. Hot baghouse high sulfur coal (Case 2B).

ADVANTAGES AND DISADVANTAGES OF CONVENTIONAL DRY INJECTION SYSTEMS

ADVANTAGES

Compared with all other FGD systems and with a hot baghouse system, the conventional dry injection system has the lowest capital cost, the fewest components, the smallest space requirement, and the lowest pressure loss. The system is simple, flexible and tolerant of a wide range of coals and operating conditions.

DISADVANTAGES

The conventional dry injection system limits heat recovery from the flue gas. This in turn limits reduction in fuel cost. This system also limits SO_2 removal by nahcolite to about 70%. Air leakage from the high temperature airheaters increases the size of the backend system and the gas volume to be handled by the I.D. fans. Regenerative airheaters cause some recirculation of fly ash from the gas side to the air side. For a 500-MW coal-fired unit this may be on the order of 3 to 5 tons per hour of fly ash in the air going to the furnace wind boxes. Regenerative airheaters are designed and the materials of construction are selected to minimize coldend corrosion. Variations in gas temperature across the airheater gas outlet and in coal and operating conditions usually cause coldend corrosion in spite of design margins and other safeguards. Disadvantages of the conventional dry injection system include the limitations and shortcomings of conventional regenerative airheaters and the limitation on percentage of SO_2 removal.

ADVANTAGES AND DISADVANTAGES OF THE HOT BAGHOUSE SYSTEM

ADVANTAGES

Increasing the gas temperature leaving the first stage airheaters from a typical 270°F to 550°F reduces the size and cost of the airheaters. Air leakage is reduced which in turn reduces the gas flow and size of the rest of the system. Fly ash recirculation is lessened and coldend corrosion is eliminated. Increasing gas temperature reduces the amount of nahcolite needed to remove the required amount of sulfur dioxide and it also enables this system to achieve higher (greater than 70%) percentages of SO_2 removal.

The treated gas leaving the baghouse and entering the second stage airheaters will have practically no fly ash, very little SO_2 and practically no SO_3. These heaters can therefore be made of lower cost materials because the corrosive and abrasive constituents have been removed. More importantly, because of the removal of the SO_3, the acid dew point is lowered significantly and thus permits greater heat recovery with less risk of corrosion. Greater heat recovery reduces fuel cost. Reducing the amount of injected nahcolite reduces reagent cost, the waste produced, and the cost of waste disposal.

The hot baghouse system can be used for retrofit applications by removing baskets from existing regenerative airheaters.

Bags made of woven fiberglass with silicone/graphite finish are selected for the hot baghouse because they have been used for many years in applications with normal temperatures of 550°F and swings to 600°F.

DISADVANTAGES

The reduction in cost of the first stage airheaters does not compensate for the additional cost of the second stage airheaters. Increasing the gas temperature increases the gas flow volume and therefore the size of the baghouse. Increasing the gas temperature increases gas viscosity and therefore the pressure loss across the baghouse. The hot baghouse system entails more air ducts as compared with the conventional dry injection system.

BASES FOR COMPARATIVE ESTIMATES

EMISSIONS

Particulate emissions are less than 0.03 lb/10^6 Btu heat input. SO_2 removal is 70% for the low sulfur coal and 90% for the high sulfur coal.

COALS

Coal and ash properties are the same as published in EPRI CS-1428.

GAS QUANTITIES

Gas quantities and temperatures are as shown in Figures 1, 2, 3, and 4.

REAGENT

The reagent is 97% refined nahcolite. The price, ready for injection, is $160 per ton shipped by rail from northwestern Colorado and delivered to the plant in Kenosha, Wisconsin.

STOICHIOMETRY[1,4,5,6]

Reagent stoichiometry and utilization are as follows:

Case	1A Std.BH Low S	1B Hot BH Low S	2A Std.BH High S	2B Hot BH High S
Stoichiometry	0.75	0.71	1.25	1.0
Utilization	93.3	98.6	72.0	90.0

AIRHEATERS

Airheaters are vertical shaft regenerative heaters. The estimates are based on regenerative heaters for both airheaters stages; however, air and gas flows shown on Figures 2 and 4 are for recuperative second stage heaters.

MATERIAL HANDLING

The material handling system for the reagent includes unloading from railcars, 25-day onsite storage in concrete silos, a day bin for each boiler and pneumatic transport systems for transfer and injection complete with blowers, controls, and metering devices. Injection is into the gas inlet duct of each baghouse compartment. The ash handling systems are conventional pneumatic systems arranged for discharge to trucks for transport to the waste disposal area.

WASTE DISPOSAL

All costs for waste disposal are included in the operating costs for waste disposal. This is a cut-and-fill type of disposal in which a cut is made for some amount of waste which is then covered by material from the next cut. This pay-as-you-go arrangement conserves capital cost. The facility includes the necessary impermeable lining with the leakage detector monitors, topsoil cover and planting.

COMPARATIVE ESTIMATES

The estimate summaries are shown graphically in Figures 5, 6, and 7. The conventional dry injection system is compared with the hot baghouse system and with a spray dryer/baghouse system. Comparisons of these systems are made for low sulfur and high sulfur coal. The estimates are for capital costs, operating and maintenance costs, and 30-year levelized busbar cost.

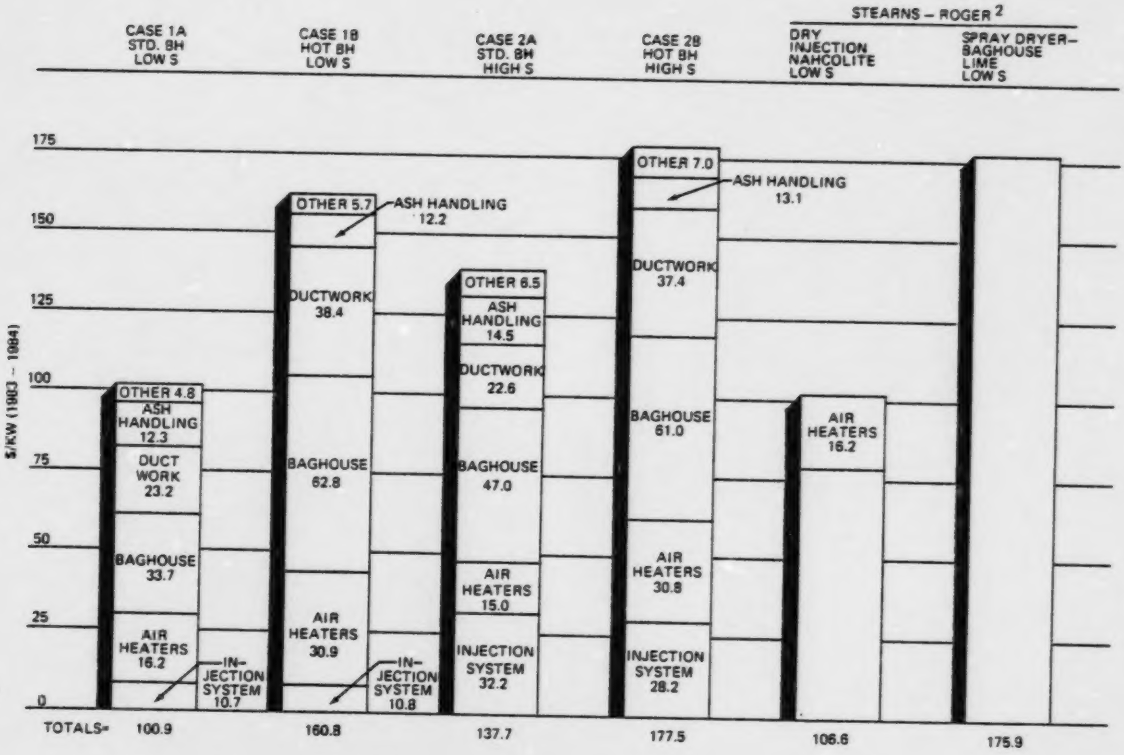

Figure 5. Capital cost.

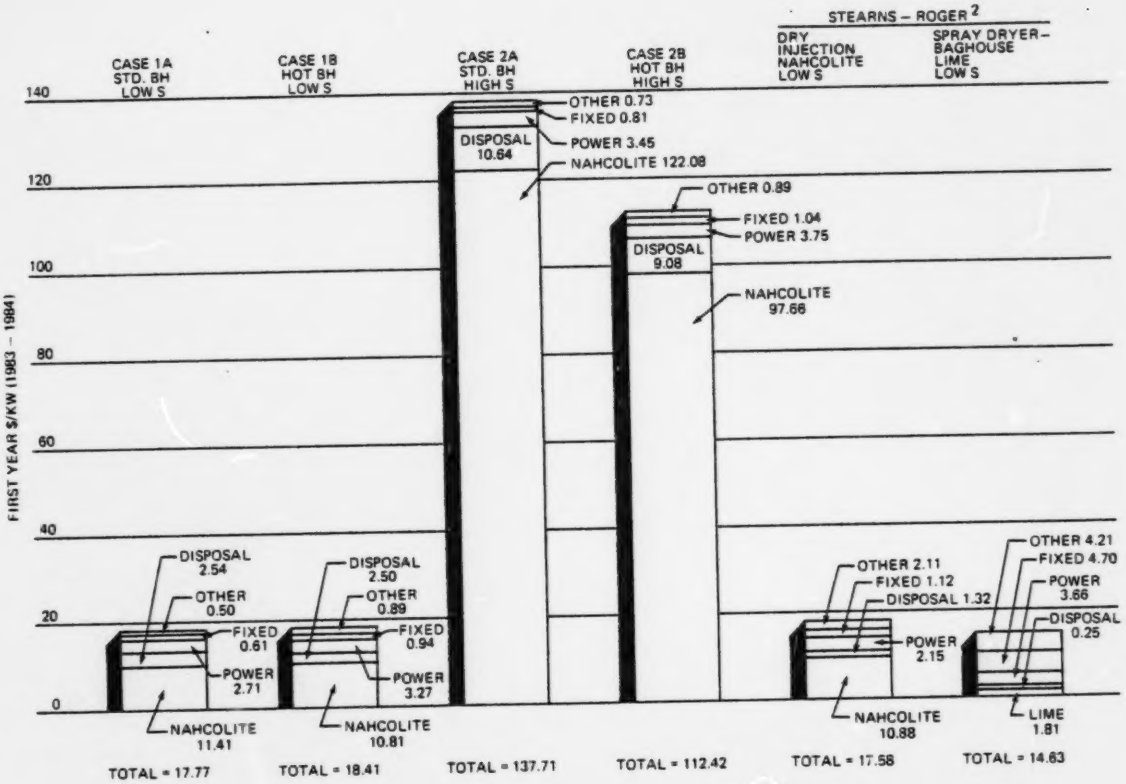

Figure 6. First year operating cost.

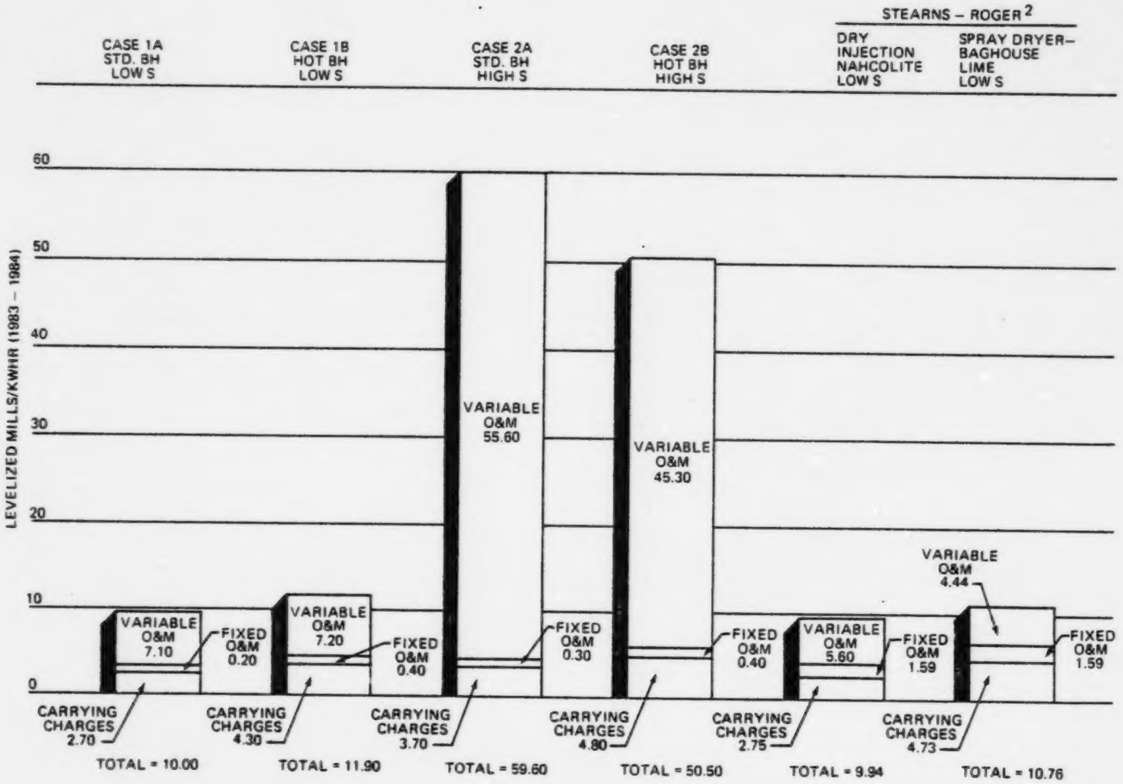

Figure 7. Levelized busbar cost.

CONCLUSIONS

For low sulfur coal on the basis of 30-year levelized busbar cost there is a significant advantage in favor of the conventional dry injection system: 10.0 mills/kWhr versus 11.9 mills/kWhr. However, this system is not suitable for applications that have to remove more than approximately 75% of the SO_2.

For high sulfur coal the hot baghouse system is competitive in capital cost with the spray dryer/baghouse system, but it is not competitive on first year operating cost and levelized busbar cost.

For high sulfur coal the hot baghouse system is competitive with normal temperature dry nahcolite injection in first year operating cost and levelized busbar cost but not in capital cost. The advantage in first year operating cost and levelized busbar cost is primarily due to the significantly lower reagent cost for the hot baghouse system. This advantage is very slight for low sulfur coal.

The costs included in this study do not include the value of the elimination of airheater coldend corrosion, the value of the reduction in the amount of fly ash recirculation, nor the value of the fuel cost reduction for the hot baghouse scheme.

The fuel cost reduction for Case 1B compared with Case 1A, assuming fuel cost at $2.00 per million Btu and a capacity factor of 65%, is $410.000 per year per unit. Additional fuel cost saving can be made by eliminating the requirement to heat the air leakage in the second stage regenerative airheaters. This can be accomplished by using recuperative airheaters or possibly liquid couples for heat recovery after the baghouse.

The potential benefits of the hot baghouse scheme warrant further investigation. Low temperature heat exchangers such as recuperative heaters and liquid couples may improve the economics for the hot baghouse scheme by eliminating the heat loss in the air leakage of regenerative heaters and by heat transfer by pipe instead of ducts. The economics may also be improved by determination of the cost savings for eliminating coldend corrosion and fly ash recirculation in the high temperature regenerative airheaters. The major benefit that can be derived from the hot baghouse system is the extension of nahcolite dry injection to higher levels of SO_2 removal.

ACKNOWLEDGMENTS

The authors are grateful to the following companies that provided prices, technical information, and other assistance in the preparation of these estimates:

Babcock & Wilcox
Combustion Engineering, Inc.
North Atlantic Technologies, Inc.
Research-Cottrell
Wheelabrator-Frye, Inc.
Fuller Co.
Church & Dwight Co., Inc.
Lake Minerals Corp.

Their assistance does not imply that they agree or disagree with this paper.

The work described here was not funded by the U.S. Environmental Protection Agency and therefore the contents do not necessarily reflect the views of the Agency and no official endorsement should be inferred.

REFERENCES

1. Chaffee, R. and Liu, H. Final report on evaluation of fabric filter as chemical contactor for control of sulfur dioxide from flue gas. Public Health Service of Department of Health, Education and Welfare, National Air Pollution Control Administration, Contract No. PH22-68-51 (1969).

2. Naulty, D.J., Scheck, R.W., McDowell, D.A., and Hooper, R. Economics of dry FGD by sorbent injection. EPRI Second Conference on Fabric Filter Technology for Coal-Fired Power Plants, 1983.

3. Green, G.P., Carr, R.C., and Hooper, R.G. Technical and economic evaluation of dry sorbent injection for SO_2 control using sodium compounds. Paper 84-43.1 Presented at A.P.C.A. Annual Meeting, (1984).

4. Lutz, S.J., Christman, R.C., McCoy, B.C., Mulligan, S.W., and Slimak, K.M. Evaluation of dry sorbents and fabric filtration for FGD. EPA-600/7-79-005 (1979).

5. Shah, N.D., Teixeira, D.P., and Muzio, L.J. Bench-scale evaluation of dry alkalis for removing SO_2 from boiler flue gases. In: Proceedings of the First Symposium on the Transfer and Utilization of Particulate Control Technology (1978).

6. Muzio, L.J., Sonnichsen, T.W., Green, G.P., Brines, H.G., and Hooper, R.G. 22-MW coal-fired demonstration of dry SO_2 scrubbing with sodium sorbent compounds. In: Proceedings of the Second EPRI Conference on Fabric Filter Technology for Coal-Fired Power Plants, 1983.

ACID RAIN CONTROL OPTIONS - IMPACT ON PRECIPITATOR PERFORMANCE

by: Victor H. Belba, Fay A. Horney, and Donald M. Shattuck
Stearns Catalytic Corporation
P.O. Box 5888
Denver, Colorado 80217

ABSTRACT

There are numerous proposals before Congress for reducing the acid rain problem. The many technologies mentioned in the proposed legislation include coal switching, coal washing, coal blending, fluid bed combustion, limestone injection multistage burner (LIMB), flue gas desulfurization (FGD), least emission dispatch, unit retirement or doing nothing. Some of these, such as coal switching, coal blending, coal washing and LIMB can have an adverse effect on the performance of an existing electrostatic precipitator (ESP). Such performance reductions can result in load limitations and/or the need for retrofitting flue gas conditioning or replacing the particulate control systems. This paper discusses the various sulfur dioxide reduction options and their effects on an ESP. The effects of ash from Powder River Basin, Montana, Illinois, and Appalachian high and low sulfur coals are compared to demonstrate the impact of coal switching on ESP performance.

INTRODUCTION

Over the past several years, over 24 bills have been proposed in the Senate and House with respect to acid rain. Fourteen of these bills require sulfur dioxide (SO_2) and nitrogen oxide (NO_x) emission reductions and are directed primarily at the electric utility industry.

In general, the bills are directed at the Acid Deposition Impact Region (ADIR) which comprises the 31 states which border on and are east of the Mississippi River and the District of Columbia. The total SO_2 emission reduction called for by the proposed legislation ranges from 8 to 12 million tons per year in the ADIR. In general, each state within the ADIR will be required to reduce its annual SO_2 emissions by the ratio of all the actual 1980 utility emissions in the state in excess of 1.2 lbs/MMBtu to the total utility emissions in all the ADIR states in excess of 1.2 lbs/MMBtu.

The overall compliance period stated in many of the bills is typically ten years. This includes a two-year period for each state or utility to establish a compliance plan; a six-year period to effect fuel switching; six years to establish contracts for the installation of SO_2 control systems; and by the tenth year, full compliance must be in effect.

To date, none of the Federal bills have passed; however, several states have bills pending in their legislatures. New York has passed legislation requiring a two-step approach (1). The first phase of New York's bill requires an SO_2 reduction by utilities and major industries totaling 100,000 tons (12 percent of state emissions) by 1988 (1). The second phase requires the establishment of an administrative mechanism to facilitate achievement of a 30 percent reduction by the early 1990's. The 30 percent goal is about equivalent to an emission rate of 1.0 lb/MMBtu for New York utilities.

Of the many technologies for SO_2 reduction suggested by the proposed Federal legislation, coal switching, coal blending, coal washing, and LIMB appear to be some of the more economical and technically feasible approaches. However, changes to the ash and flue gas properties by changing the coal or by injecting additives to the boiler can adversely impact the performance of an existing ESP as well as the boiler and other equipment. Such performance reductions can result in load limitations and/or the need for retrofitting flue gas conditioning or replacing the particulate control system.

PREMISES

To demonstrate the impact that such SO_2 control strategies can have, we imagined a typical 225 MW, pulverized coal-fired unit located in the Eastern United States. We assumed the unit has a cold-side ESP, albeit a small one by today's standards, with a specific collection area (SCA) of 165 sq. ft/1000 ACFM for the high sulfur Appalachian coal currently being fired in the unit. We also assumed a typical furnace and boiler design to provide some idea as to what impact such coal changes might have in these areas.

We selected seven U.S. coals to study the impact of coal changes on SO_2 reduction and on ESP and unit performance. A high sulfur Appalachian coal was assumed to be the coal which is currently being fired. This coal is called the base coal and most comparisons are made relative to it. An Illinois coal was selected as another likely high sulfur eastern coal. The other five coals were selected as candidates for coal switching and blending to reduce SO_2 emissions. The specific coal analyses that were selected as being representative of these coal fields are presented in Table I.

Each of the seven coal analyses considered is not meant to represent the entire range of constituents possible for each coal field. There are coals available in each of the seven classifications that would provide completely different results from those presented here.

TABLE 1. COAL AND ASH ANALYSES ALTERNATE COALS

	BASE COAL Appalachian High Sulfur	Illinois	Appalachian Medium Sulfur	Appalachian Low Sulfur	Utah	Montana Powder River Basin	Wyoming Powder River Basin
ULTIMATE ANALYSIS (As Received)							
Moisture (%)	2.9	11.2	5.92	6.3	5.2	17.6	23.9
Carbon (%)	73.6	64.1	70.9	71.42	68.2	57.1	50.2
Hydrogen (%)	5.05	4.65	4.63	4.52	5.22	4.02	3.52
Nitrogen (%)	1.5	1.2	1.33	1.0	1.3	1.0	0.7
Chlorine (%)	0.1	0.05	0.08	0.02	0.01	0.02	0.01
Sulfur (%)	3.3	3.1	2.03	0.3	0.7	0.4	0.5
Ash (%)	8.5	8.3	9.98	8.68	8.0	6.5	7.6
Oxygen (%)	5.05	7.4	5.13	7.26	11.37	13.36	13.57
BTU PER POUND	13580	11760	12870	12660	12305	9780	8450
ASH ANALYSIS							
SiO_2 (%)	38.62	50.47	45.77	53.24	65.3	35.03	27.86
Al_2O_3 (%)	23.97	16.82	28.41	32.37	16.3	14.69	16.96
Fe_2O_3 (%)	25.87	19.98	19.33	4.5	4.35	7.68	4.97
CaO (%)	2.8	3.68	1.68	0.5	4.46	20.34	35.12
MgO (%)	0.76	0.84	0.81	0.65	1.95	4.63	5.64
Na_2O (%)	0.96	0.67	0.51	0.42	1.97	7.08	0.66
K_2O (%)	1.84	2.72	1.6	3.95	1.63	0.93	0.95
TiO_2 (%)	1.07	0.95	1.03	1.3	0.89	1.0	1.33
P_2O_5 (%)	1.05	0.08	0.4	0.1	0.22	1.13	1.66
SO_3 (%)	2.6	2.6	0.46	1.4	2.51	6.4	3.0
Other (%)	0.46	1.19	0	1.57	0.42	1.09	1.85
HARDGROVE GRINDABILITY	65	50	75	80	50	48	44

The three western coals were selected based on potential SO_2 reductions and the feasibility, either demonstrated or potential, of shipment to the east. We did not consider the capacity of the mines to meet the potential reduction requirements nor the ability of the existing transportation systems to meet the demand.

COAL CHANGES

Switching to a different coal with a lower sulfur content, blending coals with lower sulfur contents, and washing coals to remove pyritic sulfur seem to be technically simple and economical solutions to reducing SO_2 emissions. However, changing the coal and ash analyses of the coals fired in the boiler will result in changes in the particulate and flue gas properties which can reduce the performance of the existing ESP. Should the new coal result in a higher quantity of ash carrying over from the boiler, the ESP will be called upon to perform more efficiently to achieve a certain outlet emission limitation. Also, changes in the chemical composition of the flue gas and ash can result in boiler deratings due to such factors as slagging and fouling of furnace and convection pass surfaces, erosion of boiler tubes and a reduction in pulverizer capacity.

Impacts of such coal changes on ESP performance were evaluated by using a precipitator performance model developed by Stearns Catalytic (2). The ESP specific collection area (SCA) required to meet the particulate emission standard of 0.1 lbs/MMBtu was determined for each coal by using the performance model. Knowing the flue gas volume generated for each coal, as determined by stoichiometric calculations and assuming total air of 139 percent, we then determined the minimum square footage of collecting area required to meet the emission standard.

The impact of each coal change was then expressed by a ratio of the square footage of the existing ESP to that required for the new coal or blend. Such a ratio is a good approximation of the unit derating that would be required to provide a sufficient gas flow volume reduction in combination with the existing collection area to provide a large enough SCA for compliance with the emission limitation.

A ratio that equals 1.0 suggests that the existing ESP has sufficient collection area with the unit at full load to meet the standard. For example; if the ratio is 0.5, the existing collection area is one-half of what is required; or, the unit will have to operate at 50% of full load or less to comply with the 0.10 lb/MMBTU emission standard. For ratios greater than 1.0, the existing ESP is sufficiently large with some contingency.

The possible impact of coal changes on boiler performance was evaluated by assuming a typical boiler design. The important parameters are:

- Flue gas design and/or operating temperatures and velocities in the furnace and at the inlet and outlet of the convection passes
- Pulverizer capacity and number
- Furnace plan and surface area

Such information can be used to determine the impact of slagging in the furnace and fouling and erosion of the convection passes of the boiler for each coal considered. For example, a particular ash may be more abrasive than the ash for which the convection pass velocities were originally designed. To avoid excessive erosion of the tubes, the gas velocity through the convection passes can be reduced by limiting the load at which the unit operates. The ratio of the design velocity to the maximum velocity desirable for ash from the coal under consideration is a good approximation of the maximum load the unit can maintain without subjecting the tubes to excessive erosion. As in the case of the ESP, a ratio of 1.0 or greater indicates that convection pass tube erosion is not a concern with the coal under consideration, and a load limitation need not be imposed. A ratio of, for example 0.60, indicates that a load limitation of 40% must be imposed; that is, the unit should not be operated above 60% so that erosion is prevented.

Similarly, ratios for slagging and fouling indicate load limitations that would be necessary to prevent problems due to such phenomena. The pulverizer ratio indicates whether or not a load limitation will result due to a reduction in pulverizer capacity because of coals that are less amenable to grinding.

The philosophy and procedures used in performing such an analysis of boiler impacts are outlined in Reference 3. These techniques are, in general, similar to conventional boiler design analyses. Stearns Catalytic has computerized such techniques to allow these analyses to be performed quickly for a variety of coals.

COAL SWITCHING

The possible SO_2 reductions achievable and the accompanying impact on ESP performance by switching to the various coals are summarized in Table 2.

TABLE 2. COAL SWITCHING - ESP IMPACT

Coal	Percent Sulfur	Lb SO_2/ MMBTU	Percent SO_2* Reduction	ESP**
BASE Appl. Hi. S	3.3	4.86	0	1.19
Illinois	3.1	5.28	+8.5	1.01
Appl. Med. S.	2.03	3.16	-35	0.88
Appl. Lo. S.	0.8	1.26	-74	0.62
Utah	0.7	1.14	-77	0.79
Montana PRB	0.4	0.82	-83	0.74
WYO. PRB	0.5	1.18	-76	0.44

* Percent reduction relative to Base Coal - Appalachian high Sulfur

** Unit derating (fraction of full load) due to alternate coal's impact on ESP performance at 0.1 #/MMBtu.

Note that by switching to either the Appalachian low sulfur coal or the three Western coals, substantial SO_2 reductions of 74 percent or more can be achieved. The greatest reduction, 83 percent, is reached by switching to the Montana coal. This is close to the 84 percent SO_2 reduction required by the current New Source Performance Standard (NSPS) for SO_2 emissions. Note that these SO_2 emission reductions are relative to the Appalachian high sulfur coal (base coal).

A 76 percent SO_2 reduction is required to meet the 1.2 lb/MMBtu SO_2 limitation mentioned in most of the Federal legislation. The three western coals meet that criteria with the Appalachian low sulfur coal coming close. The only coal emitting less than the 1 0 lb/MMBtu emission rate which may be required by the New York legislation is the Montana coal. The SO_2 emission rates used here are based on the assumption that 100 percent of the sulfur contained in the coal is converted to SO_2, and 100 percent of the heat input is from the new coal.

The impact on the ESP of switching to these coals is demonstrated in the last column of Table 2. The ratio of 1.19 for the Appalachian high sulfur coal indicates that we are fortunate at this generating station. The small ESP that was installed on this unit years ago is more than adequate to collect the ash from this one, specific, high sulfur coal. In fact, we have a contingency of 19 percent additional collection area at full load.

Remember that the analysis presented here is based on only one coal analysis for each of the seven coal fields represented. In reality, the analyses from any field can vary considerably, and it's possible that the ESP ratio for any of the seven coals could vary by as much as plus or minus 20 percent. Also, there is a certain amount of inaccuracy inherent in any model. We estimate that the possible error in the ratio is plus or minus five percent.

Despite the high sulfur content of the Illinois coal, its ESP ratio indicates that the ESP is just large enough to meet the 0.1 lb/MMBtu particulate emission limitation. This is due in part to the high ash content of the Illinois coal. Also, the Illinois coal contains slightly less sodium which promotes ash precipitability, and slightly higher contents of calcium, magnesium and potassium which detract from an ash's precipitability.

Switching to the other coals results in SO_2 reductions; however, ESP performance reductions come along with the bargain. Despite the very low sulfur content of the Montana coal, the load limitation at 74 percent of rated load due to impacts on the ESP performance is not as great as for other coals. In fact, switching to the low sulfur Appalachian coal, with a sulfur content on a lb/MMBtu basis of over one-and-a-half times that of the Montana coal, requires a load limitation at 62 percent of rated capacity. The superior performance of ash from the Montana coal in the ESP is due primarily to the ash's high sodium content.

The worst ash with respect to ESP performance is from the Wyoming Powder River Basin coal. This is due to the relative lack of any constituents, such as sodium or sulfur that aid ESP performance. A load limitation to 44 percent of full load would result by switching to this particular coal.

Other factors must be considered if a major load limitation is imposed to allow a coal switch. The gas velocities through the ductwork may be so reduced that ash dropout may be a problem for both structural considerations and as a possible source of ash reentrainment and increased dust loading during unit load changes. Also, the velocity may decrease so much through the ESP that its performance will actually degrade. However, the velocities are so high through many ESPs of the vintage with which we are concerned that considerable load reduction could be tolerated without adversely affecting ESP performance.

The ESP ratios presented in Table 2 were based upon meeting a particulate emission limitation of 0.1 lb/MMBtu. Many state particulate emission limitations for existing sources are as high as 0.25 lb/MMBtu or even greater. Therefore, Figure 1 has been included to demonstrate the impact on required ESP size of emission limitations which are higher or lower than 0.1 lb/MMBtu.

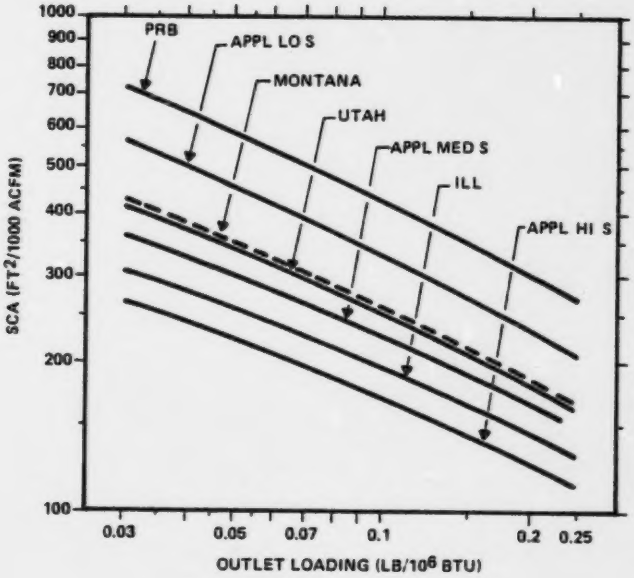

FIGURE 1. SPECIFIC COLLECTION AREA VERSUS OUTLET LOADING

In some cases the opacity standard will prevail over the mass emission standard. Twenty percent opacity roughly works out to 0.1 lb/MMBtu for many Eastern coals. However, ash from many Powder River Basin coals is notorious for having extremely fine particle size. Often an ESP will be sized to achieve 0.03 lb/MMBtu, even if the mass emission standard is only 0.1 lb/MMBtu, just to ensure compliance with an opacity standard of 20 percent.

"What's Good For The ESP is Bad For The Boiler, and Vice Versa". This rule of thumb is particularly true with respect to slagging and fouling. One may be able to locate a coal that is a good candidate for switching due to its SO_2 reduction potential and good performance of the ESP. However the ash properties that enhance ESP performance can require a load limitation due to fouling and slagging. Impacts on the boiler and other equipment also must be evaluated. Table 3 demonstrates these impacts from the seven coals considered in this paper.

TABLE 3. COAL SWITCHING - BOILER IMPACTS

Coal	Slagging	Fouling	Erosion	Pulverizer	Coal Rate
BASE Appl. Hi. S	0.98	0.85	0.99	1.00	1.00
Illinois	0.91	1.00	0.94	0.72	1.17
Appl. Med. S.	1.04	1.10	0.95	1.02	1.06
Appl. Lo. S.	1.04	1.16	0.91	1.02	1.08
Utah	1.04	0.95	0.91	0.76	1.11
Montana PRB	0.80	0.54	0.92	0.57	1.43
Wyo. PRB	0.71	1.16	0.89	0.46	1.68

The values in Table 3 represent load limitations required to accommodate a change to the specific coal due to slagging and fouling, erosion and reductions in pulverizer capacity. Also included is the ratio of the coal firing rate (in tons/hr) for the candidate coal to the base coal.

The base coal which is currently being firing in this fictitious unit turns out to be an adequate coal, within the realm of accuracy, in terms of furnace slagging and erosion of convection passes. The slagging and erosion ratios of 0.98 and 0.99 are accurate to within plus or minus 3 percent and 5 percent respectively. This high sulfur Appalachian coal may require a load reduction to 85 percent of full load if fouling cannot be controlled by more frequent soot blowing of the convection passes.

The worst coal with respect to slagging and fouling is the Montana Powder River Basin coal. These coals are famous for good ESP performance despite their low sulfur contents. The good ESP performance is due to high ash sodium content which unfortunately, also causes slagging and fouling. Also, firing the Montana coal results in a load limitation to 57 percent of full load due to pulverizer capacity. This is due to the lower grindability of this coal, and the necessity to fire it at high rates because of its relatively low heating value.

The Wyoming Powder River Basin coal also requires substantial reductions in load due to boiler problems. The largest of its limitations is a load reduction to 46 percent of capacity due to impacts on the pulverizer.

Except for the Montana coal, the greatest load restrictions for the four low sulfur coals are due to the ESP. Fouling and pulverizer limitations are the limiting factor for the Montana coal at ratios of 0.54 and 0.57 respectively.

COAL BLENDING

Coal Blending is a way to achieve modest reductions in SO_2 while, hopefully minimizing negative impacts on the ESP and boiler. For this analysis we considered blends of the Appalachian Low Sulfur and the Utah coal with the base coal in proportions such that a 30 percent reduction in SO_2 is achieved. The ratios for both the ESP and the boiler impacts are determined in the same manner as for coal switching. The impacts of these blends and the base coal on ESP performance are compared in Table 4.

TABLE 4. COAL BLENDING - ESP IMPACT

Blend	Percent Sulfur	Lb SO_2/ MMBtu	Percent SO_2* Reduction	ESP**
BASE ***	3.3	4.86	0	1.19
Appl. Lo. S. + BASE	2.21	3.31	-30	0.98
Utah + BASE	2.19	3.29	-30	1.06

* Percent reduction relative to base coal

** Unit derating (fraction of full load) due to blend's impact on ESP Performance at 0.1 lb/MMBTU.

*** BASE COAL - Appalachian High Sulfur

Within the range of accuracy, this analysis indicates that the existing ESP will be adequate for these blends. However, for these blends there is no size contingency for degradation of ESP Performance between maintenance outages due to grounded discharge electrodes or other problems.

Table 5 compares the impacts of the blends and the base coal on boiler performance. No serious boiler deratings are indicated for the blends with the exception of a potential fouling problem for the base coal and the Utah blend. Depending upon the amount of overdesign in the soot blowing system, it may be possible to cope with the potential fouling problem by an increased soot blowing schedule.

TABLE 5. COAL BLENDING - BOILER IMPACTS

Blend	Slagging	Fouling	Erosion	Pulverizer	Coal Rate
BASE *	0.98	0.85	0.99	1.00	1.00
APPL. LO. S. + BASE	1.04	1.00	0.97	1.01	1.02
UTAH + BASE	1.04	0.83	0.97	0.95	1.02

* Base Coal - Appalachian High Sulfur

By trial-and-error analysis, these and other blends could be optimized to maximize SO_2 reduction while minimizing boiler and ESP impacts.

COAL WASHING

Much of the Appalachian coal used in the Eastern U.S. today is being washed. Coal washing is an effective way to clean pyritic sulfur from coal through mechanical, float and sink processes. An effective chemical process to remove organic sulfur from coal has not yet been developed. In fact, the effectiveness of mechanical methods are dependent upon how finely divided the pyrites are. Larger chunks of pyrites are more easily removed.

Currently there are no reliable methods to predict washed coal analyses from raw coal analyses. Therefore, a derating analysis as done above for the raw coals and blends was not performed. We can only offer some generalities.

We do know that in general, the quantity of ash will be reduced by coal washing, and in general, the analyses of the coal fired will be more consistent. The reduction of the amount of ash which must be collected by the ESP will reduce the required collection efficiency. However, in general, the reduction in sulfur will reduce the performance of the ESP. It is possible that other ESP performance enhancers such as sodium can be removed from the coal, especially if in soluble forms.

Washing may not be an overall effective strategy at removing large quantities of SO_2 emissions from power plant stacks. Due to the finely divided nature of the pyrites found in most western coals, in general, only a 10 percent sulfur reduction can be expected. To achieve a 30 percent or greater reduction of sulfur for most eastern coals, deep washing may be required.

Deep washing has been observed to result in major unit deratings and other problems. The product that results from deep washing is, in general of fine particle size. Such fine coal if it is not creating dusting problems when it is being handled can adsorb large quantities of moisture from rain or snow. The adsorbed moisture makes the coal difficult to handle in conventional coal handling equipment. Such coal is very prone to severe freezing in winter. Wet coal tends to reduce pulverizer capacity and hang up in coal feeders. Such hang-ups can totally shut a unit down with flame-outs; a dangerous situation due to the explosion and fire potential in the furnace and flue gas train.

It has been observed that most of the moisture adsorption occurs while the coal is stored on its pile. One method to reduce adsorption on a deep washed product is to provide a covered coal storage area.

GAS CONDITIONING

Gas conditioning is a potential means of improving ESP performance and can perhaps allow the switch to a coal or blend of coals with less than ideal properties. Sulfur trioxide (SO_3) injection ahead of the ESP and the addition of sodium, in the form of sodium sulfate or carbonate, to the coal are two promising methods of ash conditioning.

Sulfur trioxide conditioning is done primarily to reduce ash surface resistivity and has been used successfully on Eastern and Western coals. Recent successful experience with SO_3 gas conditioning of a Wyoming Powder River Basin coal suggests that over a 30 percent reduction in required SCA can be realized (4). A greater improvement in ESP performance would be required for the specific Wyoming Powder River Basin coal selected for study in this paper (See table 2). Even if adequate ESP performance were achieved by gas conditioning the ash from the Wyoming coal, the impacts of this coal on the existing pulverizers and furnace slagging would become the limiting factors in switching to this coal (See table 3).

Of the low sulfur coals considered in this paper, the Appalachian low sulfur coal holds the greatest promise of being fired with minimal boiler impacts. The amenability of this coal's ash, as well as any ash, to SO_3 gas conditioning can only be determined by test burns of the candidate coal while testing the impact of ash conditioning.

Sodium addition to the coal can reduce the intrinsic resistivity of the ash. It is also believed that sodium can contribute to the ash's tendency to agglomerate, and thus effectively increase the particle size. The low sodium, low sulfur coals are potential candidates for this type of conditioning provided the boiler is not already experiencing slagging and fouling problems. The candidate coal analyses can be adjusted to account for the addition of sodium and then analyzed for ESP and boiler impacts. As in the case of any type of conditioning final selection of sodium conditioning would be dependent upon the results of test burning of the candidate coal(s) while conditioning.

LIMB

Recently, Limestone Injection with Multistage Burners (LIMB) has been touted as an effective way to reduce SO_2 emissions. To estimate the impact of LIMB on ESP performance, we assumed that a 30 percent reduction of SO_2 is possible. We assumed that the injection rate must be 2 moles of limestone per mole of SO_2 in the boiler to achieve the 30 percent reduction. This expected SO_2 removal rate and stoichiometric ratio are based on past experience with limestone injection.

The coal and ash mineral analyses for each of the seven coals were adjusted to account for the limestone injected. A striking observation is that for the higher sulfur coals, the ash content on a lb/MMBtu basis almost doubles due to the limestone injection. The lower limestone injection rates have less of an impact on the ash content of the low sulfur coals.

Intuitively, we feel that LIMB will have a devastating impact on ESP performance due to the injection of large quantities of limestone, which is typically considered to have a low precipitability. Our curiosity overcame our caution, and we decided to try the coal and ash analyses adjusted for limestone injection in our ESP performance model. Currently there is no data to calibrate the model for limestone injection, although theoretically the increased quantities of CaO in the ash will be accounted for by the empirical model. The results of this analysis are presented in Table 6.

TABLE 6. LIMB - ESP IMPACT

Coal	Percent Sulfur	ESP**	ESP***
BASE			
Appl. Hi. S	3.3	1.19	0.52
Illinois	3.1	1.01	0.50
Appl. Med. S.	2.03	0.88	0.48
Appl. Lo. S.	0.8	0.62	0.44
Utah	0.7	0.79	0.50
Montana PRB	0.4	0.74	0.58
Wyoming PRB	0.5	0.44	0.39

* LIMB - Limestone injection multistage burner - Limestone injected to effect 30 percent SO_2 reduction relative to coal without LIMB combustion.

** Unit derating for coal without limestone injection per Table 2.

*** Unit derating (fraction of full load) due to impact of coal and ash properties and LIMB on ESP.

The model suggests that the large quantities of limestone make the ash about equally difficult to collect for most coals. The effect on ESP performance wasn't as devastating as we might have guessed. LIMB combustion for most of the coals would require load limitations to around 50 percent of capacity to maintain compliance with the 0.1 lb/MMBtu particulate emission standard. The model suggests that the high sodium of the Montana coal boosts the performance of its ash slightly above that of the other coals. The Wyoming Powder River Basin ash is still the worst performer. The ESP suffered a reduction in performance for all coals relative to the data presented in Table 2 which involves no limestone injection.

Due to the lack of data available, we are not prepared to make definitive predictions of boiler deratings required to facilitate LIMB combustion.

ECONOMIC IMPLICATIONS

A complete economic analysis of such SO_2 reduction options is beyond the scope of this paper. However, once the various options have been screened to select the most technically appropriate options for each unit in a utility's generating system, a complete economic analysis of the options on a system-wide basis must be performed so as to minimize the economic impact to the utility. Site-and system-specific factors must be considered, such as:

- Remaining life of each unit
- Delivered costs of each coal alternate and blend
- Rate assumed for coal cost escalation
- Delivered cost of reagents
- Costs of unit deratings
- Each unit's capacity factor
- Applicability of the bubble concept for system-wide compliance
- Required overall percentage of SO_2 reduction
- Applicable economic factors

Stearns Catalytic recently assisted a mid-western utility in selecting and costing potential acid rain control strategies (5). It was estimated that a 67.5 percent SO_2 reduction would be required for this utility.

Various SO_2 control options, including coal charges and LIMB, were reviewed for each unit in the utility's system. The costs were identified for the viable technologies for the 12 coal-fired units on this system. It was found that coal switching could be a very attractive means to control SO_2 emissions on many of the units. However, a market analysis of current coal prices and escalation rates for candidate deep mined Western coals indicated that high fuel costs may possibly rule out coal switching.

It was found that least cost compliance for the utility dictated SO_2 scrubbers (90 percent efficiency) on four units, atmospheric fluidized beds (80 percent SO_2 removal) on two other units, and no change on the remaining six units.

A computer program was essential for the completion of this study and also allowed alternates and costs to be optimized for SO_2 reductions greater than and less than the 67.5 percent level. The analysis indicated that there was a point of rapidly diminishing cost effectiveness for system-wide SO_2 reductions above 61 percent on the system.

CONCLUSIONS

Potentially significant SO_2 reductions can be achieved by switching to coals of lower sulfur content. However, in general, some unit derating may be required for the existing ESP to provide compliance for the lower sulfur coals. Also, unit derating may be required due to inpacts of the coal on the furnace, boiler and pulverizers.

Modest SO_2 reductions are feasible by blending coals. Blends can be optimized so that minimal, if any, impact on ESP performance results.

It is doubtful that the deep coal washing required to provide even modest SO_2 reductions from high sulfur eastern coals will provide more benefit than problems. Deep coal washing provides a product that is not amenable to present day coal handing equipment and pulverizers.

Gas conditioning may be an option to mitigate the negative impacts of these ashes on ESP performance. A test burn of the alternate or blended coal candidates would be required to verify their impacts on boiler performance and the amenability of the ash to gas conditioning.

LIMB combustion perhaps will not be an attractive option in many cases due to the large quantities (Stoichiometric ratio of 2) of limestone that must be injected and to the 50 percent load reductions thought to be necessary for the ESP to cope with performance reductions.

In any event, final selection of the optimum SO_2 reduction option can only be made on a unit-by-unit basis after considering a complete economic analysis of the utility's entire system.

NOTICE

The work described in this paper was not funded by the U.S. Environmental Protection Agency and therefore the contents do not necessarily reflect the views of the Agency and no official endorsement should be inferred.

REFERENCES

1. "States Passing Acid Rain Legislation", FGD/FGC NEWSLETTER, The McIlvane Company, No. 75, July 30, 1984.

2. F. A. Horney and V. H. Belba, "An Impirical Model of Cold-Side Precipitator Performance Based upon Coal and Ash Chemistry", IEEE Transactions on Industry Applications, October 1982.

3. F. S. Nolte and F. A. Horney, "Boiler Derating for Coal-Water Mixtures" Coal Technology '83, Volume 4 (Proceedings of the 6th International Coal and Lignite Utilization Exhibition and Conference; Houston, Texas; November 1983).

4. B. J. Eskra and B. G. McKinney, One years Operating Experience with SO_3 Conditioning on a large Coal-Fired Unit's Electrostatic Precipitator. 75th Annual Meeting of the Air Pollution Control Association, New Orleans, LA; June 1982.

5. J. E. Damon, et. al, An Approach for Selecting Cost Effective Acid Rain Control Technologies, Paper No. 84-43.8, Presented to the 77th Annual Meeting of the Air Pollution Control Association; San Francisco, California; June 1984.

Session 22: OPERATIONS AND MAINTENANCE I

Richard E. McRanie, Chairman
Southern Services Inc.
Birmingham, AL

COMPARISON OF U.S. AND JAPANESE PRACTICES IN THE SPECIFICATION AND OPERATION AND MAINTENANCE OF ELECTROSTATIC PRECIPITATORS

by: Michael F. Szabo
PEI Associates, Inc.
11499 Chester Road
Cincinnati, Ohio 45246

Charles A. Altin
Ebasco Services, Inc.
145 Technology Park
Norcross, Georgia 30092

William B. Kuykendal
Industrial Environmental Research Laboratory
U.S. Environmental Protection Agency
Research Triangle Park, North Carolina 27711

ABSTRACT

This paper compares the practices of major Japanese and U.S. companies in the utility and steel industries with regard to their procedures for specifying, operating, and maintaining electrostatic precipitators. It also provides information on the predominant designs used in each country and the frequency of various operating problems. Different approaches to solving typical operating problems are discussed. The descriptions of Japanese practices are based on interviews conducted during the authors' recent visit to Japan.

Some ESP operation and maintenance problems are common to Japan and the U.S., including wire breakage, reentrainment, hopper pluggage, and discharge system problems. The lack of back-corona problems reported in Japan could have been masked by the additional particulate collection that occurs in the flue gas desulfurization (FGD) system. Backup FGD particulate collection is designed into all utility plants in Japan.

This paper has been reviewed in accordance with the U.S. Environmental Protection Agency's peer and administrative review policies and approved for presentation and publication.

INTRODUCTION

The purpose of this paper is to compare the specification and operation and maintenance (O&M) practices of Japanese companies with regard to electrostatic precipitators (ESP's) against those used in the United States. The basis for these comparisons are 1) the authors' 1983 trip to Japan to visit a number of major sources using ESP's for the purpose of discussing O&M practices, and 2) available knowledge of U.S. practices. The goal is to highlight any practices that appear to improve long-term reliable operation of ESP's.

Because the utility and steel industries were the major types of Japanese sources visited (see Table 1), they are the focus of the comparison.

BACKGROUND

One of the main purposes of the 3-week trip to Japan in July and August 1983 was to meet with the Institute of Electrostatics' Committee on Operation and Maintenance 1) to discuss the O&M manuals for ESP's and fabric filters that PEDCo Environmental is preparing for EPA/IERL-RTP and the set of three manuals covering specifications, operations and maintenance, and upgrading of ESP's on utility boilers that Ebasco is preparing for the Electric Power Research Institute; and 2) to discuss the O&M manuals that the Institute of Electrostatics is preparing based on a systematic survey of ESP operating problems. The latter include recommendations for proper O&M procedures which, after a review period, probably will become incorporated into the Japanese Industrial Standards.

The authors also visited the Japanese Environmental Protection Agency and the Ministry of International Trade and Industry (MITI), which regulates industry in Japan. It was interesting to learn that both agencies believed that large industrial users already have adequate O&M practices and that O&M manuals are therefore not needed. They did admit, however, that smaller sources may not be as well controlled because they do not have as many certified air pollution control engineers.

Several other large sources that were visited during the trip are summarized in Table 1. Two of the major ESP manufacturers in Japan (Sumitomo and Mitsubishi) were also visited to solicit their ideas on proper O&M.

One interesting observation made during the trip was the way the geography of Japan influences the approach to pollution control from large emitting sources. Japan is a relatively small country, and all of the plants that we visited are located near residential areas. These plants had pollution control agreements with the local prefecture, and many performed continuous monitoring of SO_x, NO_x, and particulate, the results of which were telemetered to an office in the local prefecture. In contrast, many of the large powerplants in the United States are located in areas remote from residential areas, where the local impact for emissions is not as severe as in Japan. Emission data for sources that are located closer to populated areas, however, are not telemetered to the local pollution control agency.

TABLE 1. COMPANIES VISITED DURING 1983 TRIP TO JAPAN

Company	Plant name	Source type
Electric Power Development Company	Isogo Power Station	Utility
Kawasaki Steel	Chiba Works	Integrated Iron and Steel
Tokyo Electric Power Company	Nakosa Power Station	Utility
Chubu Electric Power Company	Chita Power Station	Utility
Nippon Steel Company	Oita Works	Integrated Iron and Steel

Set pollution standards at major Japanese emitting sources can only be exceeded for short periods of time (a matter of minutes) before the plant is required to switch to a lower-sulfur fuel or shut down. Reportedly, stipulated emission regulations are rarely exceeded. In the United States, malfunctions at major emitting facilities resulting in excess emissions may be allowed to continue (depending upon the location) for hours or days before the plant is required to reduce the load or shut down for repair. Much greater pressure is exercised in Japan for control of emissions because of the proximity of major emitting sources to residential areas.

OPERATING PROBLEMS

O&M PROBLEMS AND APPROACH TO O&M IN THE UNITED STATES

Several surveys have been conducted in the United States to determine O&M problems associated with ESP's. The most common operating problems (listed in approximate order of importance) have been 1) the discharge electrode, 2) dust removal systems, 3) collecting plates, 4) rappers/vibrators, and 5) insulators. With the decline in the use of weighted-wire ESP's, the discharge electrode failure problem has been reduced, but dust removal problems remain high on the list of reported problems.

PEI has also summarized data from inspections conducted on 75 ESP installations controlling a total of 42×10^6 acfm. Table 2 summarizes the results of this survey, which covered ESP's in the utility industry (22), pulpmill recovery boilers (27), cement kilns (17), and miscellaneous industries (9). In contrast to the problems listed above, the most common operational problems found were power input and dust reentrainment. Problems with gas throughput, dust removal, and rapper timing all ranked about equally, but

TABLE 2. RANKING OF MOST COMMON PROBLEMS IN 75 ESP'S INSPECTED[a]

Design	Number of problems	Maintenance	Number of problems	Operation	Number of problems
1. Instrumentation	15	Rapper system	23	Power input	19
2. Corona power input	12	Air inleakage	13	Reentrainment	16
3. Sectionalization	9	Alignment	11	Gas throughput	5
4. Gas velocity	5	H.V. insulator	9	Solids removal system	4
5. Accessibility	5	Ash conveyor	5	Rapping timing	3

[a] From PEI Associates in-house data.

well below the former two problems. Maintenance problems center around the rapping system, air inleakage, alignment, and high-voltage insulator failures; dust removal ranks as the least common maintenance problem.

Large U.S. users' approach to O&M is generally to use plant personnel to perform maintenance activities and to call in the manufacturers as needed to provide advice and spare parts. Major rebuilds, however, are normally performed by the manufacturer. The dedication to providing an adequate O&M program varies greatly and depends on the company. In general, the best O&M programs are found among the larger users because more capital is allocated for this purpose. Just as important as capital, however, is the need for management support of O&M activities and a means of effective communication among operators, maintenance personnel, and a coordinator of O&M activities.

O&M PROBLEMS AND APPROACH TO O&M IN JAPAN

No surveys of O&M problems in Japan were available for comparison with the U.S. experience. As mentioned previously, the Institute of Electrostatics is now conducting the first systematic survey on O&M. Upon its completion, the results regarding ESP operating problems will be summarized.

Table 3 presents a summary of the results of our interviews with various Japanese vendors and users to estimate which O&M problems appear to be the most common. In general, the O&M problems experienced by these vendors and users are not substantially different from those experienced in the United States. One major difference, however, is that ESP's applied to utility coal-fired plants in Japan do not have the hopper pluggage problem that plagues U.S. installations. The apparent reason is that Japanese plants keep their hoppers as close to the gas temperature as possible, which minimizes agglomeration of the ash and subsequent pluggage problems.

TABLE 3. SUMMARY OF ESP O&M PROBLEMS REPORTED BY JAPANESE PLANTS

Company	Reported O&M problems
EPDC - Isogo	Wire breakage, rapper problems
TEPCO - Nakosa	No data - new units
oil-fired units	Rapping, opacity
Chubu Electric - Chita	Discharge system erosion/corrosion, wire breakage
Kyushu Electric - oil-fired units	Rapping problems, wire breakage
Kawasaki Steel - Chiba	Corrosion - ESP shell Conveyors - chain breaks - shearpin breaks Hopper pluggage - foreign objects
Nippon Steel - Oita	External corrosion

All of the manufacturers that we visited are now using rigid-frame ESP's, which has resulted in a substantial decrease in wire breakage problems. The rigid-frame design also allows manufacturers to use higher plate heights (up to 52-ft plates are now in service), which help conserve precious space at the plant.

Corrosion was the major problem reported at the Japanese steel plants that we visited, which is consistent with the experience of the U.S. steel companies.

Upsets are relatively rare at major source emitters because the plants cannot violate emission regulations for more than a few minutes without having to shut down. Some utility coal-fired plants have ESP's with efficiencies in the range of 98 to 99 percent and utilize the chloride stripper section of the FGD system as a particulate polisher. There are no bypass systems such as those found in the United States.

Opacity Problems During Rapping

Another operating problem that occurs frequently on the ESP's installed on oil-fired boilers is increased opacity during rapping. Two of the utilities we visited are using the following procedures to solve this problem:

1. Discharge electrodes are rapped continuously.
2. Collection electrodes are rapped infrequently (every 6 hours at one plant and every 20 hours at another) for 15 to 30 minutes per chamber with the power off and the inlet and dampers closed to prevent reentrainment.

At one plant this procedure must be done at night, as the plant must reduce boiler load to close off an individual ESP chamber. At the other plant, the procedure was designed into the operation of the plant so that two chambers out of eight can be isolated without reducing load or violating emission regulations. This company is planning to adopt this procedure for their coal-fired units as well.

Control Circuits for Control of Back Corona

Both of the manufacturers we visited are working on intermittent energization systems to help prevent back corona and to effect savings in operating costs. Also under development is a troubleshooting circuit for ESP's, which would be used in conjunction with the automatic control circuit and would provide problem diagnosis capability for the operator in the main control room. Both of these systems may find their way to the Japanese market in the near future.

General Approach to O&M

The Japanese companies' approach to O&M was very interesting and different from U.S. practices. An outside company, usually a subsidiary of the parent company, is responsible for performing the maintenance functions at the plant. The vendors are often invited to participate in annual inspections or are called to help troubleshoot specific problems if central engineering cannot determine the cause of a problem or if a review of the records indicates that a problem is developing. The companies we visited indicated that they follow the manufacturer's recommended O&M procedures and generally do not develop site-specific O&M manuals.

Although the subsidiary company that performs the maintenance is really just an extension of the parent company, this more formal arrangement (as opposed to having people at the plant do the maintenance work) contributes to a reduction of O&M problems through regular preventive maintenance.

Air Pollution Control Engineers' Examination

Another practice that was developed a number of years ago in Japan and has continued is that of requiring Air Pollution Control Engineers to take certification examinations. All plants must have certified Pollution Control Engineers. The level of expertise required is tied to the size of the plant. The Fugitive Dust Emission Control Engineer takes a simpler examination. Another classification is a Pollution Control Manager, whose certification test has more emphasis on the regulations and less on technical aspects. The category requirements for the engineers' tests are indicated by Roman numerals in the following listing:

	Type of pollutant	
Plant size	Hazardous	Nonhazardous
Large >40,000 Nm^3/h	I	III
Small <40,000 Nm^3/h	II	IV

Classification category I denotes the highest technical level of expertise. Personnel at a large plant must become certified in Areas I and III, whereas those in a small plant must qualify in categories II and IV. The Pollution Control Manager must also be certified in Categories II and IV. Applicants must correctly complete 60 percent of all the problems and 40 percent of those in each area of the test.

The committee for this exam, which is run by MITI, has 12 members for each pollution control area (air, water/solid waste, and noise/vibration). To date, 360,000 people have passed the exam in all pollution control areas. The overall passing rate is slightly less than 30 percent (40% - air, 40% - water/solid waste, 20% - noise/vibration). About 125,000 people took the initial exam 12 years ago; the average is now 25,000/year. MITI has prepared a textbook that engineers must study before taking the exam. The Table of Contents of this book is summarized in Table 4. This text is updated every 4 years.

TABLE 4. CONTENTS OF HANDBOOK FOR AIR POLLUTION CONTROL ENGINEERS IN JAPAN

I. INTRODUCTION

1) Status of Air Pollution in Japan
2) Mechanism of Pollutant Generation
3) Effects of Air Pollution
4) Government Responsibility in Controlling Pollution

II. COMBUSTION AND SOOT CONTROL TECHNOLOGY

1) Fuel Types
2) Combustion Calculation
3) Methods of Decreasing Soot Generation
4) De-SO_x Technology
5) De-NO_x Technology

III. DIFFUSION OF PARTICULATE EMISSION IN AIR

1) Evaluation of Particulate Soot Generation Diffusion
2) General Description of Diffusion Technology
3) Basics of Diffusion
4) Temperature Gradient, Meteorological Conditions, Ocean Effects, City Heat
5) Diffusion Calculations
6) Diffusion Models

IV. POISONOUS/HAZARDOUS AIR POLLUTION CONTROL

1) Generation Methods
2) Control Measurement
3) Emergency Countermeasures (when hazardous materials are discharged)

V. DUST CONTROL TECHNOLOGY (PARTICULATES)

1) Definition of Particle Size Distribution
2) Principle and Operation of Particulate Control Devices
3) Properties of Gases and Dusts Specific to Different Industries
4) Maintenance and Operation of Control Devices
5) Canopy Hoods, Ducting, and Fans

VI. MEASUREMENT TECHNOLOGY

1) Methods for Testing Solid, Liquid, and Gaseous Fuel
2) Measuring Instruments for Combustion Control, Flow Meters and Combustion Monitors
3) Analytical Methods - SO_2 in Combustion Gas
4) Analytical Methods - NO_x in Combustion Gas
5) Measurement of Particulate (Japan Industry Standard)

APPENDIX

- Dust Measurements: 1) Fugitive
  2) Practical Measurements - SO_2
  3) NO_2, CO, Oxidants, HC
- Regulations: 1) Related to Air Pollution

A bypass program is also available through which qualification as an Air Pollution Control Engineer can be attained. This involves a 3-6 day course and a simpler examination. This is done to ensure that enough people get qualified throughout Japan. About 30 percent of the presently qualified people did so through the bypass program. This percentage is higher in the smaller air pollution source companies. Overall, the qualification program is believed to have improved the O&M expertise of plant personnel.

SPECIFICATION PROCEDURES

JAPANESE SPECIFICATION PROCEDURES

Japanese companies generally utilize in-house expertise (they do not use architectural-engineering--A/E--firms) when preparing bid specifications, and manufacturers must respect the experience and requests of the user when responding to an RFP. Although price is usually the deciding factor in choosing a vendor, large users need reliable equipment and are willing to pay additional money to get it. Plants usually have a manufacturer of choice, although some of the plants we visited were operating different brands of ESP's. The manufacturers have a set of guidelines that determine the minimum level of design; i.e., an ethical guideline that must be agreed to before membership in the association of manufacturers is granted.

The time period for developing a specification and choosing a manufacturer for a large ESP user typically takes from 1½ to 2 years. This procedure was described as follows:

1. The company undertakes an initial investigation and then develops preliminary specifications.
2. The company holds discussions with several manufacturers, and pilot tests are conducted at this time.
3. The company receives preliminary proposals from manufacturers.
4. The company rejects all unqualified manufacturers after pre-bid meeting.
5. The company prepares specifications for qualified vendors, indicates the budget limits, and establishes minimum detailed design parameters.
6. After explaining contract conditions, the company receives bids from manufacturers, and the costs are put in a safety deposit box.
7. The proposals are reviewed technically by the company; if anything is unsatisfactory, the manufacturers are asked to reconsider (and requote the price if necessary) so that all bids are on the same technical level.

8. Results are sent to procurement, and the lowest price wins. (Ductwork and ash handling are not included with these bids.)

During construction, the user may visit factories to inspect electrical equipment electrodes and rapping machine motors to check structural steel for defects, in addition to checking each stage for the ESP erection process, and checking electrical performance during the trial operation stage.

No payment is made to the ESP manufacturer until after the initial performance guarantee is met. In the United States, 5 or 10 percent of the cost is usually withheld until the performance guarantee is met. After the initial trial, the company checks the internals of the equipment. The final stage of the trial involves an inspection by MITI, which follows the final performance inspection by the company. After 3 months of operation, a final acceptance test is conducted with the design fuel listed in the specification, and the title for the ESP is transferred from the manufacturer to the purchaser.

An inspection is made 1 year from the start of operation. All parts inside and out are checked and repaired if necessary, and a report is prepared. Each ESP is backed by a 2-year performance and materials guarantee (except for damage caused by the user).

For new plants, the Japanese EPA requires a survey of the environment 1 year in advance of the start of construction. Local area residents also can comment on the report that MITI submits to EPA.

An air pollution agreement between the new plant and the local government is completed, and construction begins. MITI conducts an annual inspection during construction of the plant, and local people can also participate in these inspections.

After the plant is in operation, the Japanese EPA can change regulations for that area if monitoring by local government shows an increase in ambient pollution. Data on NO_x and SO_x are telemetered to the local government on a continuous basis.

Use of Combustors

Two of the major ESP manufacturers in Japan (Mitsubishi and Sumitomo) have built special test furnaces that are equipped with a pilot scale ESP for testing the fly ash characteristics of various coals that an ESP-equipped power station is considering for use. These furnaces burn coal at rates of 30 and 50 kg/h, and both have plate-type ESP's for collection of fly ash. Low-sulfur imported coals are the ones most frequently tested. Bulk resistivity is measured in a laboratory adjacent to the test furnace. The coals are then ranked in various levels, based on the precipitability of the fly ash as measured by the resistivity test. Different coals can be blended and the effect on resistivity measured, which can help to reduce resistivity and improve performance.

For an average test, the test furnaces generally operate 2 to 3 weeks at a time and use 5 to 7 tons of coal. Current density and gas temperature can be modified, conditioning agents can be added if desired, and the ESP's are equipped with a separate section for testing new electrodes or a charging system. Opacity is also monitored. The pulverizers for the coal can be set to match the grind that would typically be found at a coal-fired power station.

The sizing of ESP's is based on the results of these test furnace burns in conjunction with the chemical composition of the ash and a computer program that utilizes a variation of the Matts-Öhnfeldt equation. These test furnaces appear to help considerably in reducing uncertainty with respect to sizing new ESP's.

U.S. SPECIFICATION PROCEDURES

In contrast to Japan, most large users of ESP's in the United States utilize architectural-engineering (A/E) firms to serve as an intermediary between the purchaser and the equipment supplier. The A/E firm is essentially responsible for the design of the ESP, and the trend in the past few years has been for the A/E firm to specify a minimum specific collection area (SCA) that the manufacturer must meet, as well as the other items, such as aspect ratio, electrical sectionalization, and transformer-rectifier (T-R) set ratings. This trend has been the result of past problems of unrealistic design parameters resulting in low collection efficiencies.

With this approach, all manufacturers bid on the same size ESP, assuming that they all agree that the prescribed size is large enough to provide an adequate safety margin. If there is a possibility that the SCA might change (as a result of additional testing or investigation of sizing variables), the purchaser will request costs for a range of sizes or the cost for a single size with correction factors to increase or decrease the cost based on the final size that is agreed upon.

Some large companies use their own in-house staff to prepare specifications and deal directly with the manufacturers in selecting an ESP. In effect, the manufacturer becomes the A/E firm.

Although U.S. manufacturers use procedures and equations similar to those used in Japan to size ESP's, the U.S. manufacturers do not have the benefit of the test furnaces currently in use in Japan. Pilot testing is the usual alternative in cases where little or no data are available on the fuel to be used.

Another interesting comparison concerns the application of ESP's at coal-fired utilities. In Japan, the ESP efficiency is relatively low at 98 to 99 percent, and additional particulate collection is provided in the chloride stripper section of the FGD system. The SCA of these ESP's is in the 300 to 400 range. In the United States, new coal-fired utility ESP's are designed for efficiencies in excess of 99.5 percent because the ESP must account for essentially all of the particulate removal. The FGD system is not depended upon for additional backup particulate control.

SUMMARY/CONCLUSIONS

GENERAL COMMENTS

Overall, we believe the trip yielded considerable perspective on the Japanese approach to the specification and O&M of electrostatic precipitators. We were impressed by the cleanliness and attention to proper maintenance at the plants we visited. In most cases, plant stacks showed no visible emissions. Instrumentation was excellent and was generally located in the main control room for easy reference by operators. Most of the information provided by the Institute of Electrostatics' O&M Committee regarding O&M practices, bid specification procedures, and design practices was substantiated during the course of our visits to plants and manufacturers. Particularly interesting is the conservativeness of Japanese industry in the type of particulate control devices used; e.g., fabric filters are not utilized on either coal-fired utility boilers or dry-process cement plants, whereas they receive considerable use in these areas in the United States. Apparently both the Japanese companies who use ESP's and vendors believe that the ESP performs adequately, and they favor the ESP because it is the more energy-efficient of the two devices.

O&M PRACTICES

Based on our conversation with manufacturers and on the plant visits, we concluded that there is a deep commitment among major sources to keeping their pollution control equipment operating at its design efficiency and that the control equipment is treated as if it were a part of the plant process. Whether this same attitude prevails at smaller sources is not known.

The reason for the dedication to proper O&M is obvious: if the control equipment fails to operate properly, the plant must shut down. This is part of the agreement between the plant and the local prefecture. Not letting the plant produce excessive emissions then becomes a matter of pride. The need for stringent measures is apparent after visiting these plants. They are so close to the residential areas that excessive emissions have a definite local impact. To the extent that emissions from smaller industries also pose a nuisance to the local populace, they likely are under a similar amount of pressure to limit emissions.

Some specific ESP O&M problems are similar to those found in the United States: wire breakage, rapping-related reentrainment, hopper pluggage, or discharge system problems. All manufacturers are now utilizing rigid-frame designs, so wire breakage problems should diminish in the future. Hopper problems in utility ESP's do not seem to be a problem in Japan because the temperature in the hoppers is relatively high (110°-130°C). Although Japanese plant personnel did not indicate sodium depletion and back-corona to be a problem for hot-side ESP's, the effects of these problems could be masked by the additional particulate collection that occurs in the FGD system. The reduced importance of the ESP because of the backup FGD particulate collection that is designed into all of the utility plants is a major difference in design practices between Japanese and U.S. utilities.

As mentioned earlier, the maintenance of control equipment at the companies visited is generally performed by a subsidiary company. Even though the people performing the maintenance are employees of the parent company, this more formal arrangement (rather than having people at the plant do the work) may contribute to better job performance. Most U.S. companies use plant personnel for routine maintenance and call upon the manufacturer or other outside help for major repairs or additions. Commitment to proper O&M varies in the United States and depends greatly on the attitude of the management at a particular company.

BID SPECIFICATIONS

The typical bid specification procedure used by large sources in Japan takes about 2 years for a typical ESP, and considerable time is spent in upfront study before the official specification is issued. Japanese companies do not use A/E firms as many U.S. companies do. Extensive checks are made by the company during construction and start-up. This type of cooperation (plus the fact that the major industries will generally spend enough money to get good reliability) helps reduce the number of problems connected with installation and start-up.

In Japan, the use of pilot-scale test furnaces to evaluate the collectability of various coals is a valuable tool for more accurate specification of the size of new ESP's. This type of facility does not exist in the United States at this time.

CONCLUDING COMMENTS

One final observation concerns the relationship between government and industry in Japan. The cooperation between the two parties with regard to pollution control is much greater than in the United States. Regulations are based on a consensus between the government and industry so that industry accepts the regulations and proceeds to abide by them. The Japanese practices reported in this paper in regard to bid specifications and O&M practices appear to work well and enhance the long-term high performance of ESP's installed on major polluting sources.

Differences in the political structure, culture, geography, and population density of Japan and the United States influence the development, implementation, and enforcement of air pollution regulations. Thus, it is difficult to say with confidence that what is beneficial in one country will also be beneficial in the other country.

We hope, however, that the preceding discussion has provided the reader with some insight into pollution control practices in Japan, and how they compare with those in the United States.

ACKNOWLEDGMENT

The authors wish to thank Dr. Senichi Masuda, University of Tokyo, who set up the agenda for this trip to Japan, and all of the companies and university people who allowed us to visit their plants and laboratories. Their gracious hospitality resulted in a trip that was well planned and coordinated as well as providing us with a perspective on the geography, culture, and politics in Japan that affect their approach to pollution control.

OPERATION AND MAINTENANCE MANUALS FOR ELECTROSTATIC PRECIPITATORS AND FABRIC FILTERS

by: Michael F. Szabo
Ronald D. Hawks
Fred D. Hall
Gary L. Saunders

PEDCo Environmental, Inc.
11499 Chester Road
Cincinnati, Ohio 45246

ABSTRACT

This paper describes the purpose, audience, and content of operation and maintenance (O&M) guideline manuals for electrostatic precipitators and fabric filters that are presently being prepared for EPA. The audiences being targeted are plant engineers, O&M personnel, and state and local enforcement officials. The choice of these audiences and the topics being covered in the manuals were reviewed by a panel of more than 30 government and industry representatives involved in some phase of control device O&M. After describing how these manuals will be used, the paper focuses on the O&M problems associated with: 1) use of fabric filters on coal-fired utility boilers, and 2) use of electrostatic precipitators on kraft pulp mill recovery boilers. Both of these applications will be included in the manuals as appendices.

This paper has been reviewed in accordance with the U.S. Environmental Protection Agency's peer and administrative review policies and approved for presentation and publication.

BACKGROUND

In recent years, both government and industry have shown increasing interest in the proper operation and maintenance (O&M) of electrostatic precipitators (ESP's) and other kinds of pollution control equipment. This interest stems from the knowledge that O&M practices have a definite impact on the ability of a control device to operate at or near design efficiency over a longer period of time. Once the source has attained initial compliance, a combination of indifference, restricted funding, lack of knowledge, or limited personnel historically has tended to result in inadequate maintenance programs. Under pressure of federal and state control agencies to maintain compliance with regulations, industries have improved their O&M practices and, in many cases, have found that proper O&M is very cost-effective.

This increasing interest in promoting proper O&M has created a need for informative O&M manuals to assist both source personnel and agency inspectors. In December 1982, EPA contracted with PEDCo Environmental to prepare these manuals. The main goal of each of these manuals is to bring together in a single document the information that has been developed through EPA and other organizations and the O&M practices and procedures that have been developed and proven by users. The manuals were to be identical in concept, differing only in the subject area covered. They were to be written as an educational document, not as an enforcement tool.

The remainder of this paper describes the procedure used to determine the audience, scope, and content of the ESP and fabric filter O&M manuals, followed by examples of the information contained in the manuals in the form of the characterization of O&M problems related to the use of ESP's on recovery boilers in kraft pulp mills, and to the use of fabric filters on coal-fired utility boilers. Details on both of these applications are included in the manuals as appendices.

USE OF AN ADVISORY PANEL

One of the first tasks of the project was to establish an advisory panel to assist the EPA project officer in establishing specific user needs and in reviewing program plans for the technical manuals. It was also believed that such a panel would be helpful in identifying sources of information for inclusion in the technical manuals. The selected 33 members of the advisory panel included 17 with government-oriented interests and 16 with industry-oriented interests. They were chosen from EPA Headquarters and regional office personnel, state and local control agency personnel, trade association personnel, industry users, and control device manufacturers.

ESTABLISHING USER NEEDS, MANUAL SCOPE, AND CONTENT

A questionnaire was sent to each of the 33 panel members asking for input regarding the following:

1) Which group(s) would be potential users of the manuals and would most benefit from a manual focusing on their needs.

2) Specific needs of likely users.

3) The content and scope of topics and level of detail necessary to meet these needs.

4) The availability of O&M-related data suitable for inclusion in the manual or use in its preparation.

Discussion of Questionnaire Results

The results of the 24 responses to the questionnaire are discussed in the following paragraphs.

Question 1 requested panel members to give opinions regarding which groups the O&M manuals should focus on and to assign a relative priority for each group. The questionnaire listed three government-related job categories (state or local inspector, state or local permit writer, and EPA regional office - SIP review), three industry-related job categories (plant operators, plant maintenance personnel, and plant environmental engineer), and "consulting engineering firm" and "other (specify)" categories. Responses from persons in government-related jobs gave nearly equal priority to government- and industry-oriented jobs--with a slight emphasis toward industry. Industry responses placed almost total high-priority emphasis on industry-related jobs and secondary emphasis on government classifications. Overall, the high-priority emphasis was on industry use, and the distribution among industry classifications was nearly equal. The bulk of high-priority emphasis in governmental jobs was on the inspector classification.

The clear preference was for an O&M manual directed to industry employees representing all three job types. Secondary preference (with high-priority emphasis) was for the state/local inspector category. Providing O&M manuals for the use of consulting firms was not regarded as a priority item.

Question 2's purpose was to define the needs of the listed user groups by suggesting for review the possible needs for each user group (see Table 1, Section A). Both government- and industry-oriented respondents indicated that the user needs provided as examples were representative of actual user needs as they perceived them and that the brief one-line "guideline" statements (examples) were acceptable as a general statement of these needs.

TABLE 1. SUMMARY OF USER NEED AND MANUAL TOPICS PRESENTED TO THE ADVISORY PANEL FOR CONSIDERATION

A. User needs	B. Suggested manual topics
State or Local Inspector--Guideline documents on setup and implementation of inspection procedures for evaluating source O&M.	Operational Theory--Design and performance equations, reentrainment effects, charging and collection mechanisms, resistivity effects, conditioning, pressure drop, cleaning mechanisms, fabric types.
State or Local Permit Writer--Guidelines for writing O&M procedures for permits or determining whether O&M procedures submitted by a source are adequate; information on design aspects would also be required.	O&M-Related Design Considerations--Instrumentation, access, safety, materials of construction, quality control.
EPA Regional Office - SIP Review--General manual on the state-of-the-art in design and O&M.	Proper Operating Practices--Start-up/shutdown, normal operation, preventive maintenance.
Plant Control Equipment Operators--Guidelines for proper operation during all phases of operation as well as for evaluating equipment performance on a daily basis; i.e., trends analysis.	Malfunctions--Information related to common causes of equipment malfunctions or poor performance, and corrective measures once performance has deteriorated.
Plant Maintenance Personnel--Guidelines on inspections, preventive and corrective maintenance, and troubleshooting.	Troubleshooting--Techniques and procedures for detection of deteriorating performance and components.
Plant Environmental Engineer--Guidelines on bid specifications and a wide range of trends analysis related to performance of specific components and control devices as a whole.	Inspection Procedures--Procedures to follow for evaluating the performance of control devices.
Consulting Engineering Firm--Guidelines on troubleshooting and methods for improving performance.	Recordkeeping--Covering both performance trends analysis and troubleshooting.
	Case Histories--Good and bad examples of control device O&M.

Question 3 attempted to explore two issues--first, the primary audience (or user) groups for the manuals, and second, the subject content of a manual to meet the needs of the user group selected (see Table 1, Section B).

With respect to selection of user groups, both industry and government respondents favored plant personnel as the target users. Government respondents indicated that the preferred "users" within the government and industry classifications were state/local inspectors and plant environmental engineers. Industry respondents suggested plant environmental engineers and control equipment operators among the industrial job classifications and state/local inspectors among the governmental classifications. The combined responses from government and industry representatives (without respect to "level of detail") yielded the following priority listing of user groups:

Plant environmental engineer	(134)
Plant equipment operators	(111)
Plant maintenance	(97)
State/local inspectors	(95)
State/local permit writers	(45)
Consulting firms	(38)
EPA Regional offices	(22)
Other	(10)

With respect to manual topics and level of detail, the patterns of response from government and industrial panel members were similar. For example, both suggested a high level of detail on inspection procedures and a low level for operational theory in a manual for state/local inspectors. Similarly, both groups suggested a high level of detail for operating practice and a low level of theory for an audience of plant equipment operators.

Question 4 concerned O&M data about which the panel members might be knowledgeable (or to which they might have access) and would be useful in manual preparation. It also inquired about the availability of such data. A number of respondents indicated that they could provide useful data.

A nonstructured response was received from several panel members as a result of the invitation in the cover letter and questionnaire for candid comments and input on any relevant matters associated with O&M manual content, user audience, or user needs. A digest of these additional comments from the respondents was provided to the EPA project officer for review.

DEVELOPMENT OF DETAILED OUTLINES

The next step was the preparation of a detailed program plan for the O&M manuals. Based on the responses of the advisory panel members, annotated outlines were prepared for both the ESP and fabric filter manuals. The audiences addressed were those given the highest priority in the advisory panel responses; i.e., plant environmental engineers, plant operation and maintenance personnel, and state/local inspectors. The technical level of the material was aimed at a college-educated/degreed individual, and the targeted degree of detail was to provide enough information on the covered topics to allow the plant to prepare its own site-specific O&M manual.

Each manual contains the following basic sections plus basic matter and appendices:

1. Introduction
2. Overviews of Theory, Design, and O&M Considerations
3. Performance Monitoring
4. Performance Evaluation, Problem Diagnosis, and Correction
5. Operation and Maintenance Practices
6. Inspection Methods and Procedures
7. Safety
8. Model O&M Plan

Index
Glossary
Appendices (sections on specific problems, example checklists, and recordkeeping forms)

The presentation of information is structured somewhat differently in each manual. The text of the ESP manual presents general, across-the-board procedures that are applicable to ESP's in a number of industries and then focuses on O&M procedures and problems for specific industries in separate appendices (kraft pulp mill recovery boilers, cement, iron and steel, and municipal incineration). Use of ESP's on utility coal-fired boilers is not given major emphasis; thus, overlap with the current EPRI-sponsored manuals on ESP bid specifications and O&M is minimized. The fabric filter manual text, in contrast, uses the major gas stream characteristics (temperature, pressure drop, gas volume, chemical composition) for analysis of fabric filter O&M across several different industries. This manual also gives more attention to relative O&M needs for small versus large installations. Use of fabric filters in the utility industry is covered in an appendix.

Annotated outlines were sent to the advisory panel for review, and the response to the content of the outlines was generally favorable. All of the responses that were obtained were sorted according to outline section and were used as memory joggers of advisory panel comments during the preparation of the manuals.

EXAMPLES OF INDUSTRY-SPECIFIC O&M PROCEDURES AND PROBLEMS COVERED IN THE MANUALS

Two examples of special appendices presented in each of the O&M manuals are briefly summarized in the following sections. One example covers the use of ESP's on recovery boilers in kraft pulp mills, and the other covers the use of fabric filters on utility boilers.

KRAFT PULP MILL RECOVERY BOILERS AND THE USE OF ESP's

This appendix is one of four industry appendices contained in the ESP O&M manual, and was chosen because it represents a major industrial market for ESP's. The other three industry appendices contained in the ESP manual are cement, iron and steel, and municipal incineration. Each of the appendices characterizes its respective process, discusses the impact of the process characteristics on ESP design parameters, and summarizes the major O&M problems and means to minimize these problems.

Kraft Recovery Boiler Operation

The kraft recovery boiler or furnace is an indirect water-walled steam generator used to produce steam and recover inorganic chemicals from spent cooking liquors. The fuel used in the boiler is spent concentrated cooking liquor (black liquor). The black liquor is sprayed into the furnace at an elevated level in the combustion chamber and is burned as it falls through the combustion zone. Combustion gases produced by the burning of the liquor are passed through the heat exchanger section of the boiler before being exhausted to a particulate control device. The gases are cooled to about 800°F* in the boiler tube bank before passing into the economizer. Temperature of the gas leaving the economizer is about 750°F, and is reduced in either indirect- or direct-contact evaporators.

The three types of direct-contact evaporators used in the industry are the cyclone, venturi, and cascade. All result in substantial removal of particulate emissions (50 to 85 percent).

The indirect-contact evaporators use a noncontact tube-and-shell design to evaporate the black liquor. The fume exiting the furnace is condensed to a fine particulate consisting of sodium sulfate (Na_2SO_4) and sodium carbonate (Na_2CO_3), collectively known as salt cake.

Boiler and O&M Practices that Affect Uncontrolled Particulate Emissions

The rate of uncontrolled particulate matter from a recovery boiler and the resulting loading to an ESP depends on a number of interrelated boiler operating variables. The effects of a number of these boiler parameters on particulate emission rates and suggested O&M practices to minimize particulate loadings are shown in Table 2.

Recovery Boiler ESP's

Both the weighted-wire rigid-frame and rigid-discharge electrode-type ESP's are utilized on kraft recovery boilers. Two methods of salt cake removal are utilized. In one method, the salt cake is allowed to fall into an agitated pool of black liquor in the bottom of the ESP. In the second method, the salt cake falls onto a flat bottom of the ESP shell, where a drag chain physically moves the material to a discharge screw. Pyramid-type hoppers with rotary air locks and slide-gate discharges are not often used for kraft recovery boiler ESP's because of hopper pluggage problems.

The ESP's utilized on the newer indirect-contact-type boilers are sized larger than ESP's for the direct-contact process because of higher particulate loadings.

---

* To convert to metric equivalent, please use the conversion factor listed at the end of this paper.

TABLE 2. SUMMARY OF THE EFFECTS OF RECOVERY BOILER PARAMETERS ON PARTICULATE EMISSION RATES AND SUGGESTED O&M PRACTICES TO MINIMIZE PARTICULATE LOADINGS

Parameter	Change	Effective particulate emission rate	Effective O&M practices
Firing rate, lb of BLS/h*	Increase	Increase	Establish baseline conditions for inlet and outlet grain loading, air volume, and temperature to the ESP as a function of firing rate; compare monitored data against these baselines. Be aware of the acceptable range for firing rate and reevaluate periodically; keep appropriate personnel aware of changes in boiler operation that affect firing rate, and when parameters are outside of acceptable ranges.
Black liquor heating value, Btu/lb BLS, and solids content, %	Increase	Increase	These values are dependent on several process variables in the pulping process (digesters, evaporators, wood species, and harvest conditions), and can vary significantly. This variability makes these parameters difficult to control; the environmental engineer must know how much variation in the inlet grain loading the ESP is designed to handle.
Primary air, % of total air	Increase	Increase	Keep primary air to no greater than 45 percent of total air volume to minimize particulate and sulfur emissions.
Secondary air, % of total air	Increase	Increase	Keep secondary air in the range of 40 to 65 percent of total theoretical air.
Total combustion air (excess air)	Increase	Increase	Keep excess air between 110 and 125 percent of theoretical air; <110 percent causes incomplete combustion, and >125 percent causes an increase in SO_3, which is absorbed in the particulate and makes it sticky; this causes fouling of heat exchanger surfaces and problems in removal from ESP plates and wires. Develop empirical relationships between excess air and primary air.
Char bed temperature, °F	Increase	Increase	Directly affected by firing rate and amount of combustion air, and thus subject to the same O&M practices.

* Black liquor solids.

Proper O&M Practices In Specific Problem Areas

The four major problem areas for recovery boiler ESP's are flue gas volume, gas distribution and sneakage, salt cake removal, and corrosion. Adequate corona power must also be maintained for optimum collection efficiency.

Flue Gas Volume--

Because ESP performance is affected by total gas volume, a good operating practice is for the operator or environmental engineer to estimate the volume based on the black liquor firing rate, flue gas oxygen, and temperature. Most plants monitor flue gas oxygen at the economizer outlet rather than at the ESP outlet. An estimate of the flue gas volume must be based on ESP outlet conditions, and the inspector should be equipped with portable temperature measurement equipment (i.e., thermometer or thermocouple) and portable oxygen measurement equipment (e.g., a Fyrite oxygen analyzer). The flue gas volume may be calculated from a plant-specific F-factor (dry standard cubic feet/pound BLS)* corrected for flue gas oxygen, moisture, and temperature. (The F-factor for a typical black liquor is approximately 51 dscf/lb BLS.) Temperature and oxygen measurements should be made at the outlet of each chamber where possible (accessible).

The following method is used to calculate the flue gas volume at the ESP inlet or outlet. Corrections made for the flue gas oxygen are for dry standard gas volume, not wet gas volume.

$$Q = \left[\frac{BLS}{min} \left\{ \left(F_{dry} \; \frac{20.9}{20.9 - \%O_2} \right) + F_z \right\} + F_s + F_E \right] \left(\frac{T_s + 460 \; ^{\circ}R}{528^{\circ}R} \right)$$

where Q = flue gas volume, acfm.
BLS = black liquor solids firing rate to the boiler.
F_{dry} = F-factor for black liquor solids in dscf/lb BLS.
$\%O_2$ = oxygen content of flue gas at ESP inlet in percent.
F_z = standard cubic feet of water vapor generated from combustion of hydrogen per pound of black liquor solids.
F_s = standard cubic feet of water vapor added to flue gas stream as a result of soot blowing.
F_E = standard cubic feet of water vapor evaporated in direct-contact evaporator.
T_s = temperature of the flue gas at the ESP inlet in °F.

When flue gas oxygen increases above normal ranges, the source of inleakage should be identified immediately and appropriate repairs made to reduce the inleakage. Failure to reduce the inleakage will not only cause excess emissions, but the cooling effect of the ambient air may also cause low-power input, excess sparking, and corrosion.

---

* Black liquor solids

Calculated values for superficial velocity through the ESP should be in the range of 2.5 to 4.0 ft/s, and the lower values generally are recommended. Obviously, as the superficial velocity in an ESP decreases, treatment time will increase. Also, if the superficial velocity exceeds 8 ft/s, not only will the treatment time drop, but reentrainment of captured particulate may occur as a result of the high velocity stripping material off the ESP plate. Thus, it is important to consider the gas volume through the ESP. Gas volume is especially critical if there is a possibility of high excess air levels resulting from air inleakage or improper boiler operation, or if high gas volumes could occur from overfiring the recovery boiler.

Another value that should be checked as an operating practice is the actual SCA. This value relates the total available plate area to the gas volume (ft^2/1000 acfm) and, when compared with design or baseline values, indicates ESP performance capabilities. Generally, an increase in the SCA (actual) means improved performance, but actual SCA can be compared with design or baseline values only if other parameters have not changed.

Gas Distribution and Sneakage--

Proper gas distribution into the ESP is very important to allow the salt cake particles to have adequate residence time in the ESP. A well-designed distribution system is necessary for good ESP operation. An effective operating practice is to keep the distribution system clean. This is accomplished by rappers and periodic inspection.

A series of baffles perpendicular to the gas path are used above and below the plates to keep the flue gas in the electrostatic treatment zone, and prevent gas sneakage. Gas sneakage allows a portion of the particulate-laden flue gas to bypass the electrically charged area. As a result, collection efficiency is reduced.

In otherwise well-designed and well-operated ESP's, gas sneakage and gas distribution problems may account for more than 50 percent of the total particulate emissions. An increase in ESP input power cannot result in the capture of particulate matter in a gas stream that bypasses the treatment zone.

The baffle plates must be designed so that they do not interfere with the normal dust removal system. They must not extend too far below the treatment zone, but they must be low enough to present sufficient resistance to minimize gas sneakage. In wet-bottom ESP's, the proximity of these baffle plates to the black liquor pool may cause them to be subject to increased possibilities of acid dew point corrosion. The placement and integrity of these baffles should be checked during each internal inspection.

Salt Cake Removal--

The collected dust removed from the collecting surfaces must be disposed of properly. In the kraft recovery process, the collected salt cake is recycled to the recovery boiler by combining it with the black liquor. This recycling of the salt cake is usually accomplished in the bottom of the ESP.

Relatively few recovery boiler ESP's have hoppers. These ESP's are typically flat-bottomed with a ribbon-mixer, paddle-mixer, or drag-chain conveyor to move the salt cake to a pool, trough, or tank of either black liquor or water for recycling to the recovery boiler. Chain breaks, misalignment of the drags, sprocket failures, and motor failures are typical malfunctions. Areas near these liquid recycle points and baffles between fields and the shell walls may be prone to corrosion due to heat loss and the raising of the acid dew point temperature. Emphasis should be placed on detecting these problems, thus minimizing excess emissions.

The conveying system or mixing system must be sized properly to remove the quantity of dust recovered under normal maximum operating conditions. Undersized equipment may allow buildups that can seriously affect long-term ESP performance. In addition, the dust conveyor system must adequately cover the ESP bottom and minimize the area that is "out of reach" of the conveyor system.

The buildup of these deposits or the failing of the conveyor system can have long-term effects on ESP performance. If a buildup were to reach the treatment zone, permanent damage to the ESP components might result; e.g., warpage of the plates or rigid discharge frames and misalignment of wire-weight guide frames. In addition, temporary misalignment of wires or plates may result from the pressure of moving plates and wires, T-R's may be tripped out because of wire plate contact, and resuspension of the dust may occur because of the dust piling up in the treatment zone. The most serious problem, however, is the distortion of the ESP internal components. This distortion will reduce the ESP performance capabilities. The usual indication of a material buildup is the tripping of a T-R set (although there are many other causes for this) along with apparent discharge problems. Records should indicate the time and location of the occurrence, the corrective actions taken, and when normal operations were restored. A gas-load test will provide preliminary indications of permanent damage, and an air-load test should be performed at the next outage to determine if significant damage and deterioration occurred. An internal inspection of the ESP should reveal the nature and extent of any damage incurred. In any event, continuous liquor level monitoring is required.

Corrosion--

Corrosion appears to be the most serious maintenance problem in long-term operation of recovery boiler ESP's. Corrosion attacks the ESP shell and internal components. Advanced corrosion is accelerated by air inleakage through corroding areas in the ductwork, around access doors, or in areas near the liquor/flue-gas interface in wet bottom units. The rate of corrosion is increased in the colder areas of the ESP. Localized cooling occurs when heat loss through the shell is highest; i.e., where outside stiffeners or structural columns are attached to the shell. Corrosion in internal areas reduces rapper effectiveness so that dust cannot be effectively removed from ESP collection surfaces. In addition, structural members can be weakened or destroyed.

A survey by the Technical Association of the Pulp and Paper Industry (TAPPI) of 19 noncontact recovery boilers installed between 1974 and 1979 indicated that 63 percent had some corrosion problems and 26 percent had severe corrosion problems.[1] Based on the operating conditions of the 19 boilers, the average temperature of those with serious corrosion problems was 361°F. The average temperature of those reporting no corrosion problems was 384°F.

The primary corrosive agent in kraft recovery boiler ESP's is sulfuric acid. Flue gases from the boiler contain H_2O vapor with a high concentration of SO_3. The SO_3 vapor combines with the water present to form sulfuric acid vapor (H_2SO_4). As the temperature of the gas stream is reduced, the H_2SO_4 vapor becomes saturated and forms an acid mist.

The most severe area of corrosion in wet bottom ESP's is in the area above the liquid level and below the treatment zone. This area is baffled and is not a part of the main gas volume passing through the ESP. Vapors from the black liquor in the bottom are extremely corrosive. The activity of the vapors increases with high oxygen and sodium sulfide concentrations.[2] Also water vapor raises the local dew point temperature. The temperature of the black liquor is normally below 180°F and results in a cool shell temperature surrounding the liquor. This cool shell temperature results in a gradual decrease in shell temperature between the treatment zone and liquor level. The lower wall temperature is usually below the acid dew point and near the moisture dew point (which is typically around 165°F). The temperature within the ESP is not uniform, and the temperature of the shell varies due to contact with structural members, degree of insulation, exposure, and orientation. Areas of low gas circulation in the ESP typically have the lowest temperature and highest rate of corrosion.

The maintenance of a uniformly high temperature in the ESP is important in reducing the rate of corrosion. The temperature may be increased by:

1. Reducing air inleakage.
2. Insulating the shell.
3. Heating the shell.

Maintaining Adequate Corona Power--

A key indicator of ESP performance is the corona power, which is a useful value for determining whether ESP performance has changed significantly. In general, the corona power in a recovery boiler ESP increases from inlet to outlet, as dust is precipitated out of the gas stream. Secondary current values are generally about 0.02 to 0.03 mA/ft^2 in the inlet field and increase to 0.08 to 0.09 mA/ft^2 in the outlet field.

Specific corona power, which may also be calculated for the entire ESP or for individual chambers, is calculated by the following equation:

$$\text{Specific corona power} = \frac{\text{total corona power (W)}}{\text{total gas volume (1000 acfm)}}$$

The volume obtained by the modified F-factor (divided by 1000) is substituted into this equation. In general, the higher the value of the specific corona power is, the higher the ESP removal efficiency will be. Thus, one may determine whether ESP performance would be expected to increase or decrease by evaluating the specific corona power.

Typically, the specific corona power needed to meet NSPS for kraft recovery boilers is usually above 400 W per 1000 acfm. Acceptable performance may be obtained with lower specific corona power values, however, if there are no major problems with power distribution, inleakage, or rapper operation. Although the specific corona power may be indicative of ESP performance, it should not be used as a sole indicator. The inspector must rely on his/her experience and general knowledge of the ESP applied to the recovery boiler in question to draw any final conclusions regarding overall ESP performance.

To detect and help prevent decreases in corona power caused by misalignment, dust cake buildup, insulator failure, etc., the boiler operator should record T-R meter readings at least twice per shift. The operator also should plot ESP power levels by field (inlet to outlet) for each chamber. Deviations from optimum values (determined from baseline or normal values) should be used to evaluate internal ESP conditions and to analyze potential emission levels. If recent V-I curves are not available, the operator should request the plant environmental engineer or electrician to produce a V-I curve for each field. Data from the V-I curves should be used to target the inspection of the rappers, the gas distribution system, and local cooling, and to check for inleakage. Serious deviations from normal values should be evaluated with respect to their impact on potential emission levels.

OPERATION AND MAINTENANCE OF UTILITY FABRIC FILTER INSTALLATIONS

A discussion of operation and maintenance of fabric filters in the electric utility industry is included as an appendix in the fabric filter O&M manual. This was done because of the importance of the utility industry as a major source category, the relative newness of the fabric filter as a control device in the utility industry, and the realization that fabric filters will probably see increasing use in the future.

Since 1973, rapid growth has occurred in utility commitment to fabric filter technology. By the first quarter of 1984 more than 110 fabric filters were either in operation or under design or construction, with an associated generating capacity of more than 20,000 MW.[3] This is illustrated in Figure 1.

Although the data base on O&M problems is not large in comparison to ESP's on utility boilers, it was felt that a summary of existing O&M data would be useful to the user of the manual. The appendix covers types of fabric filters in use, monitoring and maintenance problems, and case history summaries for a number of installations.

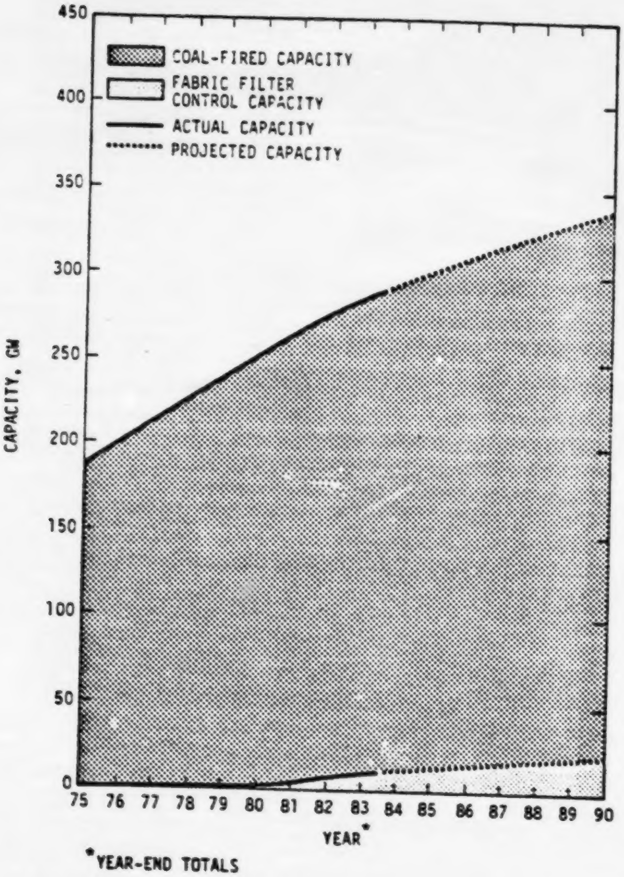

Figure 1. Actual and projected coal-fired generating capacity and effective fabric filter capacity, 1984.[3-9]

Types of Fabric Filters in Use

Fabric filters are normally classified by fabric cleaning method. The three primary cleaning methods are shake-deflate, reverse-air, and pulse-jet. Only the first two are widely used in utility applications, and the reverse-air method is by far the most prevalent. Of the 72 utility boilers equipped with fabric filters as of June 1981, 9 were of the shake-deflate design, 2 were of the pulse-jet design, and all the rest were of the reverse-air design.

Pulse-jet fabric filters work well for the shorter, small-diameter bags found on smaller-scale industrial applications. Because utility systems require much larger units in terms of bag dimensions and other design aspects, the pulse-jet systems are less effective. Also, coated fiberglass bags are generally used for utility applications because of their durability in high-temperature, potentially acid environments. Since the more-brittle fiberglass material tends to wear out rapidly when flexed, it is not suitable for pulse-jet units.

Fabric filters used in utility applications, although similar in basic design, differ significantly from those used in typical industrial applications. Utility fabric filters may be 10 to 100 or more times larger than industrial fabric filters. Because of their larger size and the stricter emission guidelines imposed upon these boilers (even at start-up and shutdown), fabric filters become critical to the operation of the powerplant. Therefore, more attention is directed toward such factors as operation and maintenance, energy efficiency, bag life, and preventive maintenance strategies. Other constraints also affect the design and operation of fabric filters for utility applications. For example, the temperature of flue gas from utility boilers is significantly higher than that encountered in many industrial applications, and the abrasive qualities of the ash also must be considered. The flue gas also contains significant moisture and acid constituents that require high temperatures (above 250°F) to be maintained to preclude acid dewpoint problems and moisture condensation on the bags. If the high temperatures are not maintained, corrosion, bag fabric decay, and bag blinding can result.

In an effort to maintain the temperature of the flue gas to the fabric filters, utilities have installed flange-to-flange insulation. Even with this insulation, localized corrosion may occur at any heat sinks where supports and ground-mounted structural beams are welded to the fabric filter framework. Precautions also must be taken in the downcomer sections or hoppers of the fabric filters. Corrosion may occur on the walls, and the ash may agglomerate in the hoppers when lower surface temperatures cause condensation. Some low-sulfur Western coals yield alkaline ashes that tend to "set up" when wetted, which further complicates the problem of ash removal. Care also must be taken to prevent inleakage of ambient air in the ash removal system, as this too reduces the flue gas temperature.

Because fly ash is abrasive, some design feature must be implemented, particularly at the gas inlet, to minimize the initial impact of the inlet gas stream on the bag fabric. No standard design is available that ensures adequate flow distribution of the flue gas (and therefore, fly ash) through the fabric filter. Some installations have no means of distribution other than the wedge-shaped inlet manifold; others have baffles, turning vanes, or combinations of the two.

In some instances, louvred dampers or butterfly valves are used, but poppet valves at the inlet and outlet of the compartments are most commonly used for flow control. On reverse-gas cleaning applications, both economics and a desire to achieve a "gentle" reinflation dictate the number and size of poppet valves at the outlet.

Except at the sites of the two pulse-jet installations, woven fiberglass is the bag material most often used. The coatings vary, but most are Teflon (10 percent by weight). A survey taken in 1981[9] indicated that those plants not using Teflon (roughly 13 percent) were using a silicon-graphite coating or one of the recently introduced acid-resistant finishes. The woven bags are typically attached to the tube sheet by means of thimbles 8 to 12 in. in height. Tube-sheet thimbles are used to prevent erosion of the bag material due to fly ash particles entering the bags from the hopper.

As mentioned earlier, utility and industrial fabric filters differ in several ways. For example, gas velocity in electric utility systems may be as high as 4 million acfm as opposed to 100,000 acfm in typical industrial applications. Energy costs resulting from ductwork and dust cake resistance pressure drop are generally much greater for utilities. In addition, utilities do not benefit from a product recovery credit of the collected material as many industries do. High flue gas temperatures in utility applications limit the choices of bag fabrics. The volume, flow, temperature, composition, and particulate concentration of the flue gas entering the fabric filters in utility applications vary greatly with the boiler load, and the fly ash represents a wide and often unpredictable range of coal properties.

Monitoring

Utility applications typically incorporate more monitoring devices than industrial fabric filter systems do to track the operation of the system and its related equipment. Monitoring and alarm devices display and/or record the gas flows and pressure losses within the system, compartmented isolation events, inlet and outlet temperatures, operation and sequencing of the cleaning apparatus, particulate emissions exiting the stack, and bag failures (i.e., severe plugging or rupture). Outlet opacity monitors are typically installed to satisfy environmental regulations, but they are also useful in detecting problems before they become serious. For example, when bag rupture problems were encountered at the Harrington Station of Southwestern Public Service Co., workers were able to pinpoint failures in the specific compartment through the use of opacity meters.

The outlet opacity monitor should be observed during normal filtering operation and during compartment cleaning. A gradual increase in opacity during filtering indicates a worsening bag or compartment leak (assuming the monitor itself is performing properly). During cleaning, a very clean filter will show almost no change in opacity as compartments are removed, cleaned, and put back into service. A drop in opacity when a compartment is removed from service indicates that the compartment has a leak. The opacity will also normally increase immediately when that particular compartment is put back in service.

The opacity may also increase momentarily when a given compartment is removed, because of the disturbance of an accumulation of ash in the other compartments resulting from the sudden increase in gas flow in these compartments due to the removal of a compartment.

Pressure gauges, level indicators, and gas flow and temperature monitors also provide data for early detection of problems. Thus, it is apparent that good monitoring systems, dedicated maintenance, and quality control in the fabrication and installation of bags lead to greatly improved service and substantial savings in labor and repair costs.

Operation and Maintenance Problems and Precautions

Fabric filters have performed well on utility boilers. Design removal efficiencies for all fabric filters range from 99.4 to 99.9 percent, and in many cases, actual efficiencies have exceeded the design efficiencies. Opacities are typically below 5 percent. Pressure drops range between 3 and 12 in., with newer installations showing values at the lower end of the range.[3]

Assuming proper fabric filter design and proper bag installation, the most critical concern is start-up and shutdown. Several typical maintenance problems and precautions are introduced briefly here and are summarized for a number of specific installations.

Operating Factors--

Operating factors of concern on fabric filter systems include the cleaning system, the bags themselves, the ash-removal system, and overall system integrity.

Operators must be careful not to clean the bags too frequently. When bags are cleaned too frequently, the overall average pressure drop is higher because the dust cake is not as heavy and is harder to remove. Also, frequent cleaning weakens the material and shortens bag life.

Operators must minimize the potential for problems associated with start-up and shutdown. If at all possible, the fabric filter system should be heated thoroughly (e.g., by gas firing the boiler or by some other means) before the sulfur-laden gas from coal firing is allowed to enter the collector. If the fabric filter applied to a coal-fired unit is cold at start-up, moisture from the flue gas will condense on the bags and walls, and the SO_3 in the gas will combine with the moisture to form sulfuric acid, which may result in corrosion and fabric decay. Also, moisture may cause blinding of the fabric when residual fly ash and water seal the air passages in the fiber weave. During shutdowns and forced outages, fabric filters should be purged as thoroughly as possible to remove moisture and sulfur-laden gases as the collector cools.

Operators should observe the performance of the reverse-air valve and compressor system to ensure adequate bag cleaning during the cleaning cycle. Operators also must carefully observe the fabric filter monitoring equipment to detect bag failures as early as possible. A serious bag failure can cause damage to surrounding bags.

Maintenance Factors--

During bag replacement, care must be taken to minimize the risk of damage to other bags as a result of snags and punctures with tools and equipment. As the utility industry has become more familiar with fabric filter technology, problems relating to improper maintenance procedures have diminished in number.

Maintenance personnel must be certain that bag tensioning devices are properly adjusted and in good condition. One of the primary causes of bag failure can be traced to improper bag tensioning. The bags also must be properly installed. Improper installation may cause the bag to rupture and/or become dislodged. When this occurs, other bags can also be damaged.

Fabric filters are well maintained at most utility applications. The changeout time for 12-in.-diameter, 36-ft-long fiberglass bags is 15 to 20 minutes (two men). In most fabric filters, insulation is placed between compartments. Some also have ventilation systems to cool the compartments quickly, which permits personnel to work comfortably and safely while replacing bags while the rest of the baghouse is still in service.[3]

SUMMARY OF OPERATING PROBLEMS AT SELECTED PLANTS[10-13]

The O&M histories of 10 plants were evaluated. These plants were chosen based on the availability of O&M data. Little data were available for larger installations (500 MW and greater) because the applications at these facilities are so recent. The results of this analysis are summarized in Table 3.

COMPLETION OF MANUALS

Both the ESP and fabric filter O&M manuals will be completed by the end of September 1984. These drafts will be circulated to the Advisory Panel for review. Final reports are scheduled for the end of November 1984.

CONVERSION FACTORS

To convert British units, used in this paper, to metric equivalents, please use the following:

British	Times	Yields Metric
°F	5/9(°F-32)	°C
ft	30.48	cm
ft^2	0.093	m^2
ft^3	28.32	liters
in.	2.54	cm
lb	0.454	kg

TABLE 3. SUMMARY OF OPERATION AND MAINTENANCE PROBLEMS AT 10 UTILITY PLANTS UTILIZING FABRIC FILTERS[10-13]

Plant	Size, MW	Start-up date	Major O&M problems	Comments
Martin Drake No. 6	8[illegible]	1978	Erratic temperature instrument readings	Minimized thermocouple junctions and extended wiring to thermocouple sensor; overall operation reported to be very satisfactory.
			General bag cleaning problems accompanied by increased ΔP, tensioning mechanism problems, and loss of poppet valve operation due to cold weather freeze-up of control air lines	
Kaw No. 1 No. 2 No. 3	44 44 68	1979 1979 1980	High ΔP due to boiler operations; i.e., gas temperature falls below dewpoint	Cyclic operation of the boilers on high-sulfur coal with frequent excursions below dewpoint is thought to be a major influence on operating problems.
			Reverse-air fan and fan motor bearing failure on Units 1 and 2	
			Inability of Units 1 and 2 to reach design efficiency	
Clay Boswell No. 1 No. 2	69 69	1979 1979	Poor tensioning resulted in replacement of several hundred bags	Problems not considered critical, and improved operation has been noted since start-up.
			Flue gas temperatures below dewpoint cause poor cleaning effectiveness and high ΔP	
			Initially could not reach design efficiency	
			Reverse-air fan and fan motor bearing failure	
			Ash-handling system--vacuum blowers experienced erosion and pluggage from ash carryover in the transport air	
Kramer No. 1 No. 2 No. 3 No. 4	23 23 23 36	1977 1977 1977 1977	Experiments with dolomitic lime as precoat resulted in bag blinding	Discontinued lime precoat--used flyash coating
			Reverse air fan bearing failure and bent shafts	
Coyote No. 1	410	1981	Higher-than-normal flue gas temperature caused high failure rate of polyester fabrics	Replaced polyester with acrylic material
Brunner Island No. 1	350	1980	High bag failure rate from improper tensioning (1981 - 209; 1982 - 877), which also resulted in high ΔP because of frequent shutdown for maintenance	Sonic horns have reduced ΔP significantly

TABLE 3 (continued)

Plant	Size, MW	Start-up date	Major O&M problems	Comments
			Valve operators, control system, and tensioning mechanism	
Sunbury No. 1 No. 2	175	1973	No major O&M problems reported. ΔP has risen to 6 in. in recent past from previous level of 3 in.	Two fabric filters control eight boilers. Mechanical collectors precede fabric filters
North Valmy No. 1	250	1981	Valve problems during cold weather	Utility is generally satisfied with the operation of the fabric filter; high overall efficiency has been maintained, except during bag failures. Changes in bag type, increased frequency of bag shaking, and redesign of shaker support mechanism have improved performance; utility generally satisfied with operation of fabric filters.
			Ductwork corrosion and expansion joint failures	
			Casing and door seal leaks have caused some corrosion	
Harrington No. 2 No. 3	350 350	1978 1980	High ΔP on occasion	
Monticello No. 1 No. 2	575 575	1978 1979	High ΔP	Tensioning problems with bags were resolved, which improved bag life.
			Short bag life	
			Casing and door seal leaks resulting in corrosion and flue gas distribution problems	
			Reverse-air fan and fan motor failures	
			Ash system pressure blower erosion	

REFERENCES

1. Henderson, J. S. Final Results for Noncontact Recovery Boiler Electrostatic Precipitators. TAPPI, 63(12), December 1980.

2. Stockman, L., and A. Tansen. Gvensk Papersteiden. 62, 907 to 914(1959). Abstr. Bull. Inn. Paper Chem. 30, 1164 to 1165 (1960). The Paper Industry, June 1960. p. 215.

3. Carr, R. C., and W. B. Smith. Fabric Filter Technology for Utility Coal-Fired Power Plants: Journal of the Air Pollution Control Association, 31(2): 178-181, 1984.

4. U.S. Department of Energy. Inventory of Power Plants in the United States. Office of Utility Project Operations. DOE/RA-0001, December 1977.

5. U.S. Department of Energy. Inventory of Power Plants in the United States - December 1979. Energy Information Administration. DOE/EIA-0095(79), June 1980.

6. U.S. Department of Energy. Inventory of Power Plants in the United States - 1980 Annual. Energy Information Administration. DOE/EIA-0095 (80), June 1981.

7. U.S. Department of Energy. Inventory of Power Plants in the United States - 1981 Annual. Energy Information Administration Office of Coal, Nuclear, Electric, and Alternate Fuels. DOE/EIA-0095(81), September 1982.

8. Personal communication from Mr. Skeer, Office of Policy Planning and Analysis, U.S. Department of Energy, August 1983.

9. Piulle, W., and R. Carr. Operating History and Current Status of Fabric Filters in the Utility Industry. Proceedings: First Conference on Fabric Filter Technology for Coal-Fired Power Plants, Denver, Colorado, July 15-17, 1981. CS-2238. p. 1-5.

10. Piulle, W., and R. Carr. 1983 Update, Operating History and Current Status of Fabric Filters in the Utility Industry. In: Proceedings of Second Conference on Fabric Filter Technology for Coal-Fired Power Plants, Denver, Colorado, March 22-24, 1983. EPRI CS-3257. p. 1-5.

11. Carr, R. C., and W. B. Smith. Fabric Filter Technology for Utility Coal-Fired Power Plants; Journal of the Air Pollution Control Association, 31(2), March 1984.

12. Electrical Power Research Institute (EPRI). Proceedings of First Conference on Fabric Filter Technology for Coal-Fired Power Plants. EPRI CS-2238, February 1982.

13. EPRI. Proceedings of Second Conference on Fabric Filter Technology for Coal-Fired Power Plants. EPRI CS-3257, November 1983.

AN UPDATE OF THE PERFORMANCE OF THE CROMBY STATION FABRIC FILTER

by: M. Gervasi
Philadelphia Electric Company
Phoenixville, PA 19460

J. R. Darrow and J. E. Manogue
W. L. Gore & Associates, Inc.
Elkton, MD 21921

ABSTRACT

In late 1980, the Philadelphia Electric Company installed a fabric filter at Cromby Station - Unit 1, located in Phoenixville, PA. The fabric filter (a sidestream unit), in conjunction with the refurbished mechanical separators and electrostatic precipitator, brought the unit into compliance with the 1979 consent decree particulate emission rate of 0.65 pounds per 10^6 Btu heat input.

From the initial start-up, the baghouse did not perform as expected. The pressure drop has been higher than design and the bag life has been shorter than anticipated. This paper describes the modifications to the collector and compares the performance of standard woven fiberglass versus PTFE membrane/woven fiberglass.

INTRODUCTION

Cromby - Unit 1 is a 160 megawatt (Mw) Babcock and Wilcox radiant, drum type boiler, designed to burn pulverized eastern coal at a rate of 60 tons per hour. The original air pollution control system consisted of a mechanical collector and an electrostatic precipitator. In 1980, a side-stream fabric filter was installed. The baghouse receives ash transport gas from the mechanical collector through a series of cyclones. In addition, it takes the conveying air from the precipitator ash transport system after a second set of cyclones (Figure 1).(1)

In late 1982, a particulate scrubber and MgO flue gas desulfurization (FGD) system were added. The FGD system was designed to utilize the gas from the baghouse for reheat. The gas from the baghouse can also enter upstream of the FGD system in the event of an opacity problem. This is undesirable since it increases reagent consumption and reheat costs by approximately $49,000 per month and can exceed scrubber design flow rate.

The fabric filter, manufactured by Enviro-Systems and Research, Inc., was designed for the following specifications:

Gas Flow:	45,000 acfm (max.)
Gas Temperature:	400°F (max.)
Inlet Grain Loading:	3.0 grains/actual cubic foot (acf)
Outlet Grain Loading:	0.03 grains/acf
Coal:	Western Pennsylvania and West Virginia
Configuration:	4 modules, 224 bags each
Gas to Cloth Ratio:	3.84:1 (gross) 5.12:1 (net)
Bag Size/Construction:	5" ϕ x 10' long grooved snap top reinforced cuff bottom
Bag Material:	Woven fiberglass with acid resistant finish, 16.9 oz/yd^2, double beam, 2/2 broken twill, thread count 48 x 28 (W x F), air permeability 30-55
Cleaning Method:	Pulse jet, on-line or off-line cleaning (with venturies)

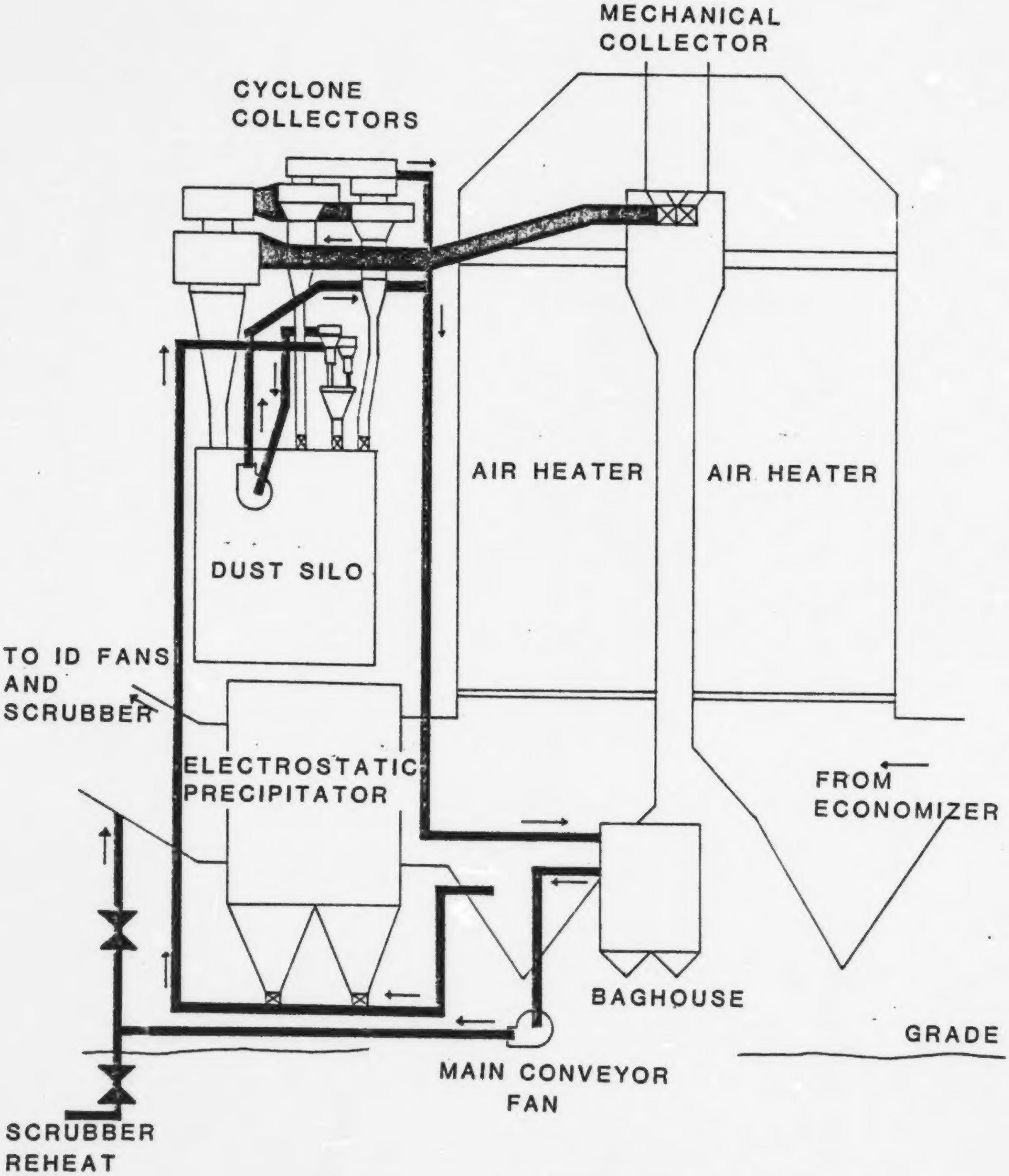
MECHANICAL COLLECTOR
CYCLONE COLLECTORS
AIR HEATER
AIR HEATER
DUST SILO
TO ID FANS AND SCRUBBER
ELECTROSTATIC PRECIPITATOR
FROM ECONOMIZER
BAGHOUSE
GRADE
MAIN CONVEYOR FAN
SCRUBBER REHEAT

Figure 1. Fly ash collection system.

FIRST YEAR OF OPERATION

December 29, 1980, the baghouse was placed in service. The cleaning mode was on-line. During the first week of operation, the flange-to-flange pressure drop approached 10 inches of water. The manufacturer advised that a pressure drop of greater than 10 inches may adversely affect the integrity of the bags. It was decided to reduce the airflow through the baghouse to maintain this pressure drop limit. This was achieved by throttling the main conveyor fan inlet damper.

On February 28, 1981, three bags were removed for analysis to determine if the high pressure drop was due to bag blinding. The examination of the bags revealed that the permeability as-received was less than 0.7 cubic feet per minute/square foot of cloth area at 0.5 inches of water differential pressure. The explanation of the low permeability was that a sufficient amount of fine particulate in the dust was present to plug the fabric. It appeared that the bag blinding caused the high pressure drop.

In March, the unit was tested for compliance. During the test, the flow had to be limited to 75% of design to maintain the 10 inches of water pressure drop limit. The test results showed that although the inlet grain loading was twice the design value, the emission rate met the required standards.

In April, to reduce bag wear, the pulse air pressure was decreased from 90-100 psig to 65-80 psig. This had no effect on the baghouse pressure drop.

At the end of May, one compartment of bags was air lanced from the backside. This reduced the pressure drop temporarily. However, within one week the pressure drop became excessive again. In late June, all modules were air lanced and precoated. Again, this helped, but only for a few days. It was decided to investigate alternative bag materials.

A bag test program started in August. Two Teflon® felt, two fiberglass felt, and two woven fiberglass (original bag material) bags were installed. One of each was precoated with limestone. After one month, all the bags were removed and sent to a laboratory for analysis. All the bags were found to be blinded. It was believed the fineness of the dust was responsible for bag blinding. The mass median diameter of the dust found on the bag was 3.95 microns. As a result of the bag analysis, it appeared that woven glass was the best media of the three for this application.(2)

Because bag analyses indicated the blinding was caused by small particulate, it was decided to install a cyclone bypass to increase the median particle size entering the baghouse. The bypass connected the mechanical collector ash transport duct to the cyclone outlet duct. It was believed that the coarse particles would form a cake and help prevent fines from plugging the fabric. During the annual outage, November and December 1981, the partial cyclone bypass was installed. At the same time, new woven fiberglass bags and cages were installed and the secondary cyclones were replaced.

With these modifications completed, various baghouse control and cleaning system problems corrected, and more operating experience, it was believed the pressure drop problem would be solved.

SECOND YEAR OF OPERATION

Late January 1982, the baghouse was precoated with limestone (0.1 lb/sq ft of cloth) and placed into service. Within six weeks, the pressure drop climbed to 10 inches. During this period, the pulse pressure was increased from 62 psig to about 80 psig in an effort to contain the pressure drop.

Mid-February 1982, unit compliance and baghouse performance were tested. The emission rates were 0.348 lb/10^6 Btu for the unit and 0.012 grains/acf for the baghouse. The baghouse inlet grain loading was 3.97 gr/acf (average) with the partial cyclone bypass operating.(3) It is interesting to note the grain loading was lower than during the first compliance test because the precipitator ash transport cyclones had been replaced, which increased their efficiency.

Over the next few months, the pressure drop continued to climb. During this time, the pulse cleaning interval was reduced from 7 seconds to 1 second; the pulse pressure was increased to 90 psig and off-line cleaning was instituted in an effort to stop the ΔP increase. Finally, the gas flow was reduced to keep the ΔP less than the 13.5 inch alarm set point.

In June there was an economizer tube leak. The baghouse was inspected and no evidence of a moist cake was found. About ten days after the unit came back on-line, the baghouse flow was reduced again to keep the pressure drop down. At the end of June, it was decided to return to on-line cleaning. It was also decided to adjust the flow to maintain a 10 inch maximum pressure drop across the tube sheet.

In July, a bag was removed for analysis. It was found to be blinded, with an as-received permeability of 0.7.(4)

The effect of the cyclone bypass was tested in August. The results were as follows:

	Bypass Closed	Bypass Open
Airflow	42,000	41,000
Grain Loading	1.6 grains/acf	3.4 gr/acf
Median Particle Size	4.3 μm	18 μm

Although the bypass did increase the mean particle size, as it was designed to do, it did not solve the pressure drop problem, as hoped. It appeared that the bags were blinding due to the fineness of the ash and the cyclone bypass did not reduce the quantity of fines. It was decided to close the cyclone bypass to reduce the grain loading to the baghouse.

At this same time, an ash analysis was performed. It showed that $CaSO_4$, about 1%, and carbon were present.(5) Since these agents can act as binders, it was decided that the dust cake formation should be closely studied with the next set of bags.

The unit came down in September for the scrubber tie-in. At this time, the following baghouse system modifications were made:

- Rebagged using same woven fiberglass material
- Installed Staclean™ diffusers in place of the venturies
- Installed seats on inlet and outlet dampers
- Modified pulse sequence to random
- Changed photohelic setting to initiate cleaning at 3 inch ΔP
- Converted back to off-line cleaning
- Pulse air pressure increased to 110 psig

September 19, a fly ash precoat was applied to the bags and the baghouse was put into service. The initial pressure drop was about 4.5 inches, but climbed to 9 inches over the next three months. During this period, a bag analysis (microscopic examination) program was conducted.(5) A new bag, a precoated bag, a six-hour bag, a one-week bag, and a forty-day bag were analyzed.

The new bag was examined and found to be of high quality in workmanship. It was found that the coating (acid resistant finish) did not contribute to the adhesion of the fly ash to the glass.(5)

Examination of the precoated bag showed that fly ash was not well bound to the fiberglass. In addition to the light coating of fly ash on the upstream side, approximately 1% of the ash penetrated to the backside. The fly ash appeared to be an excellent precoat because it formed a porous cake and had no binding agents present.(5)

The bag from start-up (six hours of service) had 30-40% by weight of soot, from oil firing, in the dust cake on upstream side. A trace of oil was also detected. The oil could act as a glue causing future problems with cake release.(5)

The best evidence of this blinding mechanism was found on the one-week sample bag. Both sides showed a well bound cake of fly ash spheres and carbon flakes (up to 400 microns thick on the upstream and 250 microns on the downstream side). The presence of the downstream cake could inhibit cleaning action and accelerate blinding. An analysis of the binder showed 20-30% $CaSO_4$ and 60-90% of an unidentified organic.(5)

The 40-day bag showed the following:

1. Increase of dust cake thickness on both sides of bag

2. Three mechanisms causing agglomeration and adhesion
    a. Organic glue
    b. Calcium and magnesium sulfate
    c. Carbon flake

Based on this bag/dust analysis program, it appeared that bleed-through and agglomeration were causing the bag blinding.

After 58 days of operation, another bag was removed for testing. The permeability, as received was 0.7; visual inspection showed no visible fabric on the inside or out; after cleaning, it was noted that the textured surface of the bag was on the inside.(4)

Because standard fiberglass bags were repeatedly tried and subsequently blinded, Cromby Station management decided to rebag with GORE-TEX® membrane filter bags. These bags had a microporous membrane of expanded polytetrafluoroethylene laminated to the surface of 16.8 oz./sq. yd. of Teflon® B coated fiberglass.

The high cost of these bags was offset by a performance guarantee of 12 months' life and 8 inches (maximum) flange-to-flange pressure drop. The guarantee required:

1. Maximum of 70 psig pulse pressure

2. Remove Staclean diffusers/install venturies (cut off at throat)

3. Inlet baffle modification

to provide a more gentle cleaning action and minimize direct impingement of fly ash on the bags.

The station installed new igniters to reduce soot and oil carryover at start-up. This was done because the bag/dust analysis program indicated soot/oil act as bonding agents, causing fly ash to adhere to the bags. Larger blowpipes were also installed. (Note: W. L. Gore & Associates, Inc. did not feel this was necessary because efforts were made to reduce cleaning energy/bag wear for longer bag life.)

THIRD YEAR OF OPERATION

Early March 1983, the bags were precoated with fly ash and the baghouse was put in service. Within one week, the pressure drop stabilized at 4.0-4.5 inches w.g. (flange-to-flange) with the cleaning cycle being initiated at a $\Delta P = 6.5$ inches w.g.

Because of previous bag problems, a detailed bag analysis program was initiated. This included permeability testing, strength testing (tensile, MIT flex, mullen burst) and visual inspection. The bags were removed after precoating, ten hours, one week, three weeks, one month, three months, nine months, and one year of operation. These results are summarized in figures 2 through 7.

Figure 2 shows the as-received permeabilities decreased from 9 to about 1.5 after one year of operation. The permeability after cleaning (vacuuming front side at 15 inches w.g.) dropped from 6.3 for the one-month bag to 1.8 for the one-year bag.(4) The difference between the as-received and after-cleaning permeabilities indicates a reduction in cleanability. The field data for the baghouse showed a residual (after cleaning) pressure drop of 4.5-5.0 inches flange-to-flange when cleaning every 15 to 30 minutes in July 1983; by July 1984, the residual pressure drop increased to 6-7.5 inches across the system with an interval between cleaning cycles of 0-10 minutes. The slow deterioration of the permeabiities agrees with the increased pressure drop and cleaning frequency.

The permeability profiles, figures 3 and 4, show that the nine-month and twelve-month bags are blinded (permeability ≤ 1.0) at the top. This concurs with the visual reports of dust impregnated into the inside, top two feet of the bag.(4) It appears that dust from the clean air plenum is being pulsed back into the bag.

The strength of the bags have decreased slightly during the twelve months of service. Values at this time are not indicative of any degradation problems. (See figures 5, 6, and 7.)(4)

In addition to the above testing, microscopic examination of the dust/bag surface was conducted on a new bag, a bag with ten hours of service, and a bag with one week of service. The new bag showed the presence of a barrier layer (GORE-TEX membrane) firmly bonded to a woven fiberglass fabric with an anti-abrasion coating (Teflon B). Both the ten-hour and the one-week bags showed no penetration of particles through this barrier layer.(5)

The one-week bag had a significant decrease in the amount of carbon particles from oil combustion, and their nature was more representative of carbon from coal firing. This lack of oil soot indicated effective cleaning and good release, which precluded long residence times. The shorter residence time of dust on the membrane, as compared to that of the woven fiberglass, limited the agglomeration mechanisms described previously.(5)

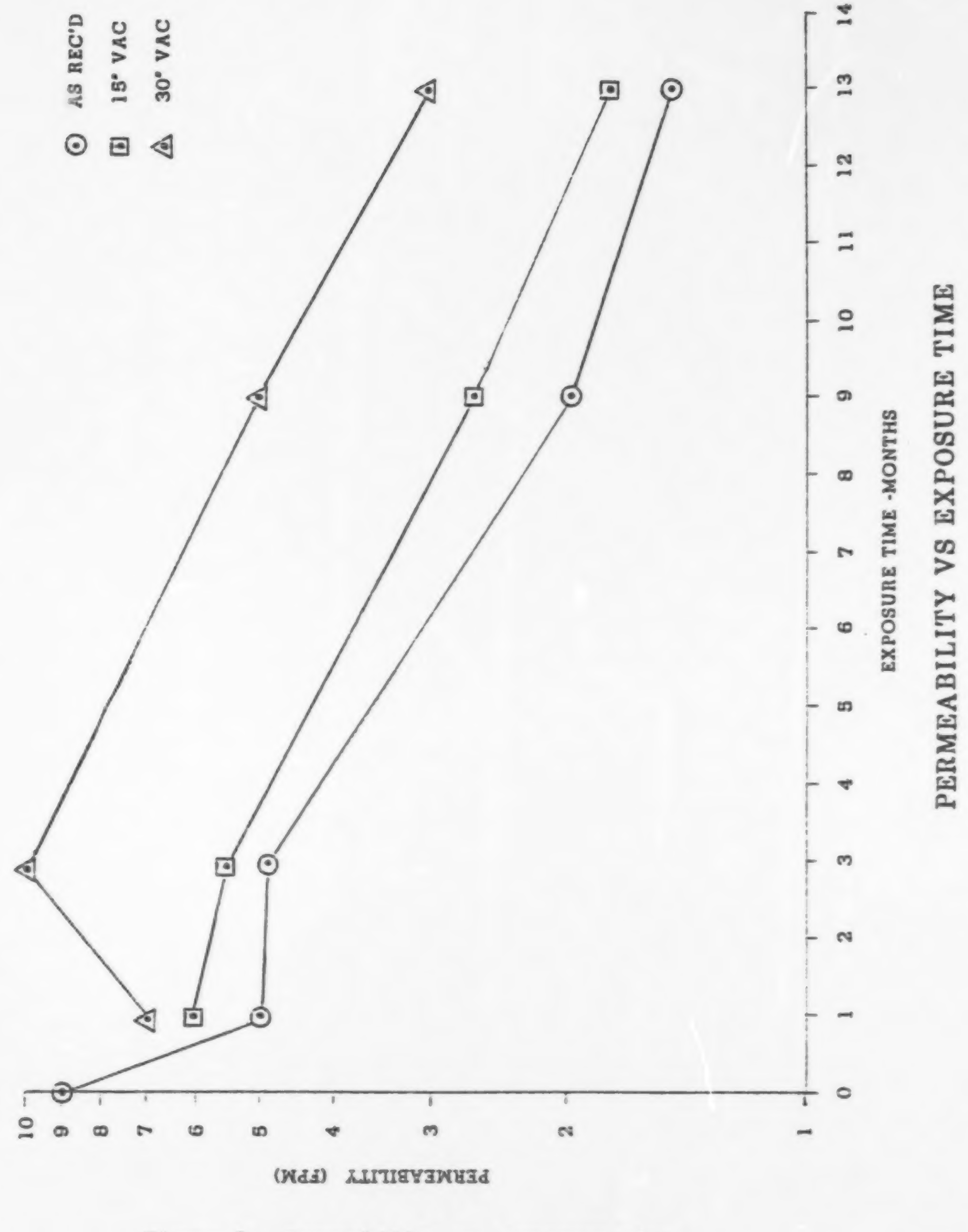

Figure 2. Permeability vs. exposure time.

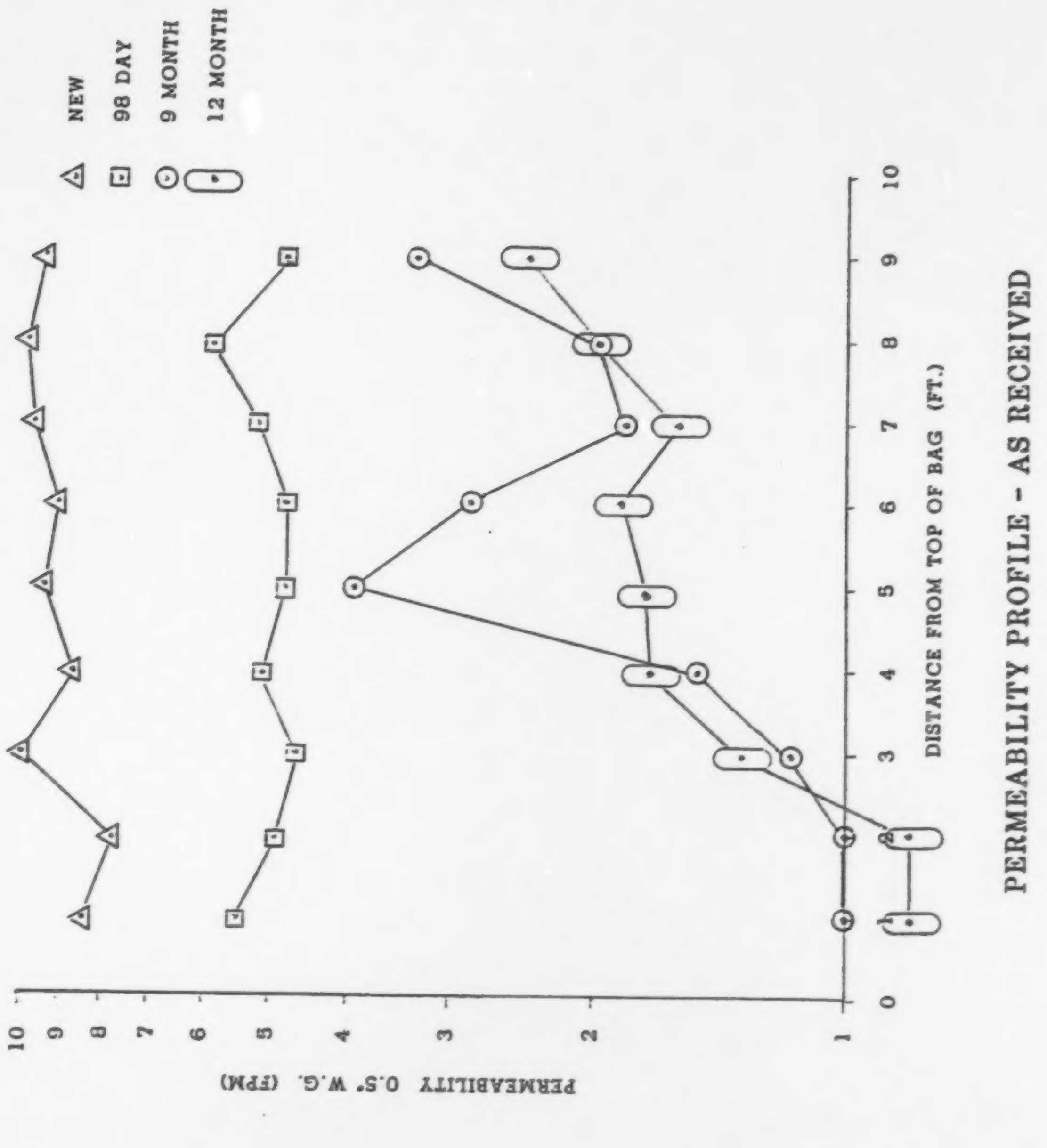

Figure 3. Permeability profile - as received.

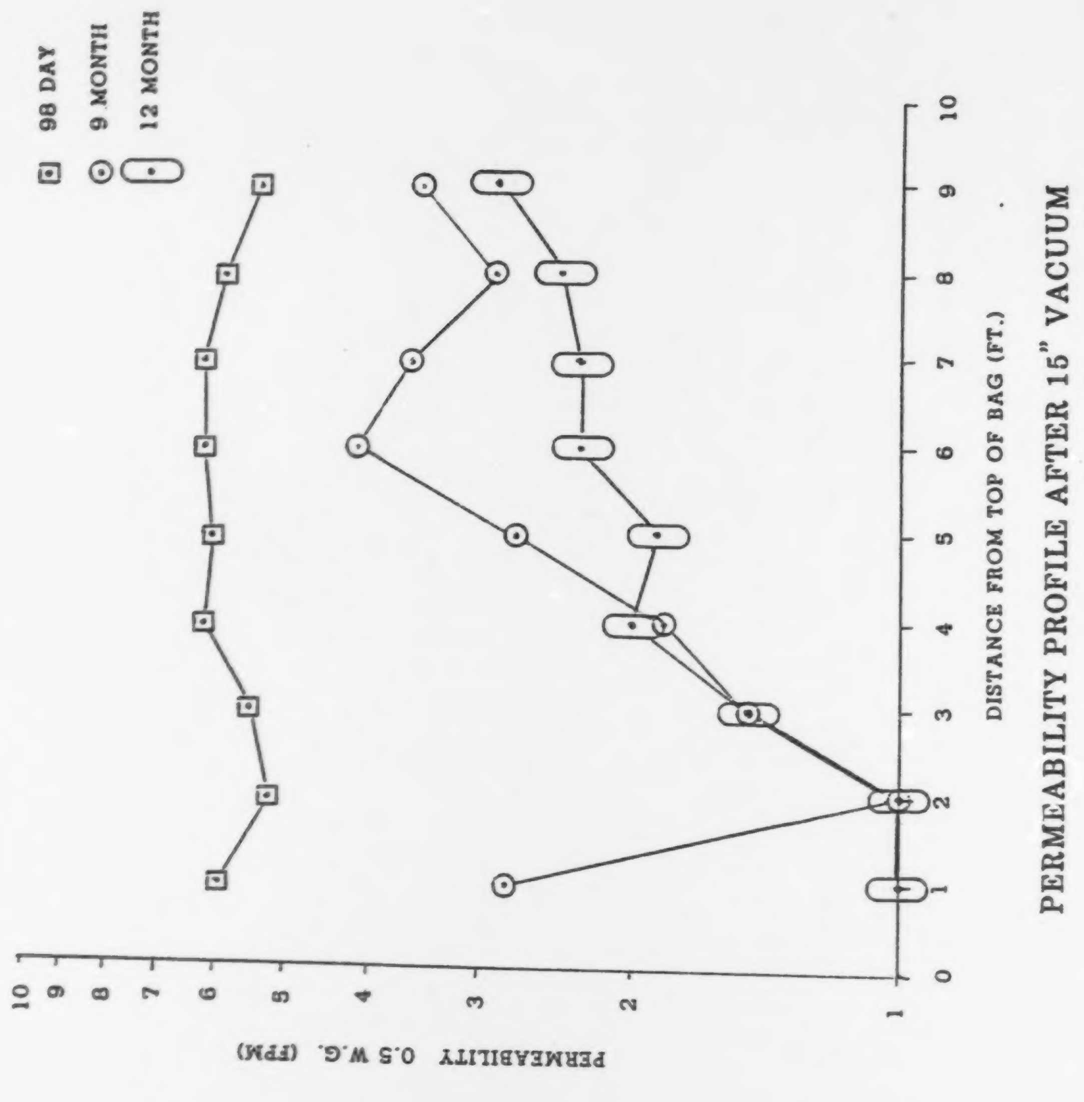

Figure 4. Permeability profile after 15" vacuum.

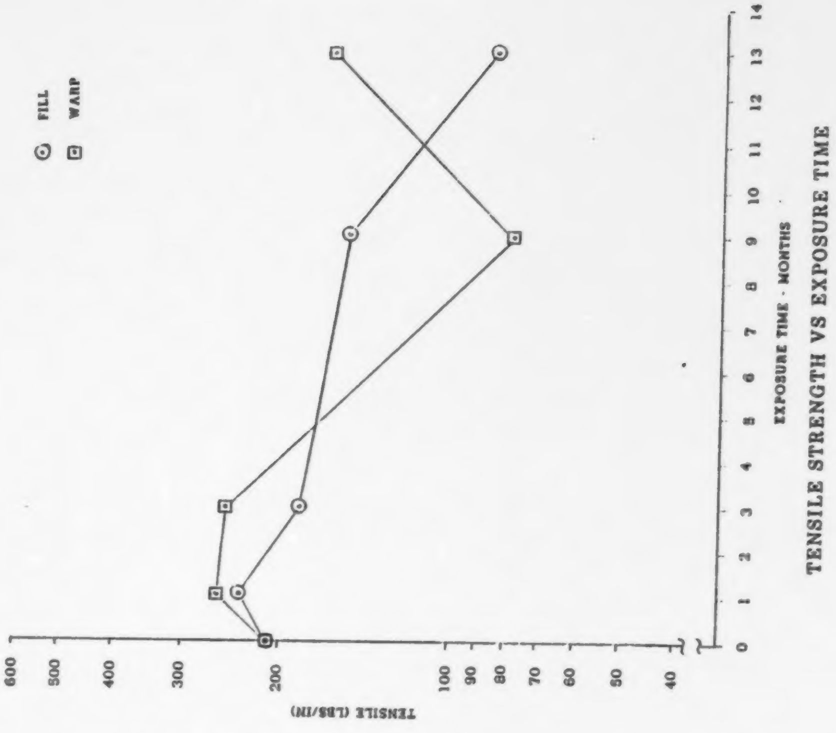

Figure 5. Tensile strength vs. exposure time.

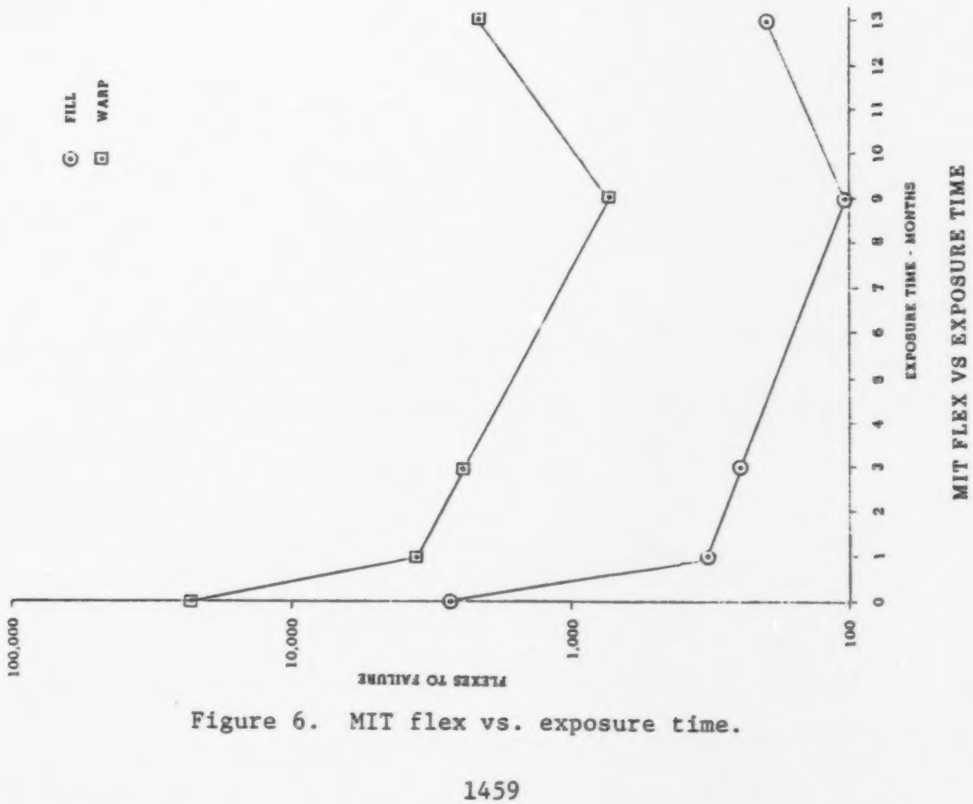

Figure 6. MIT flex vs. exposure time.

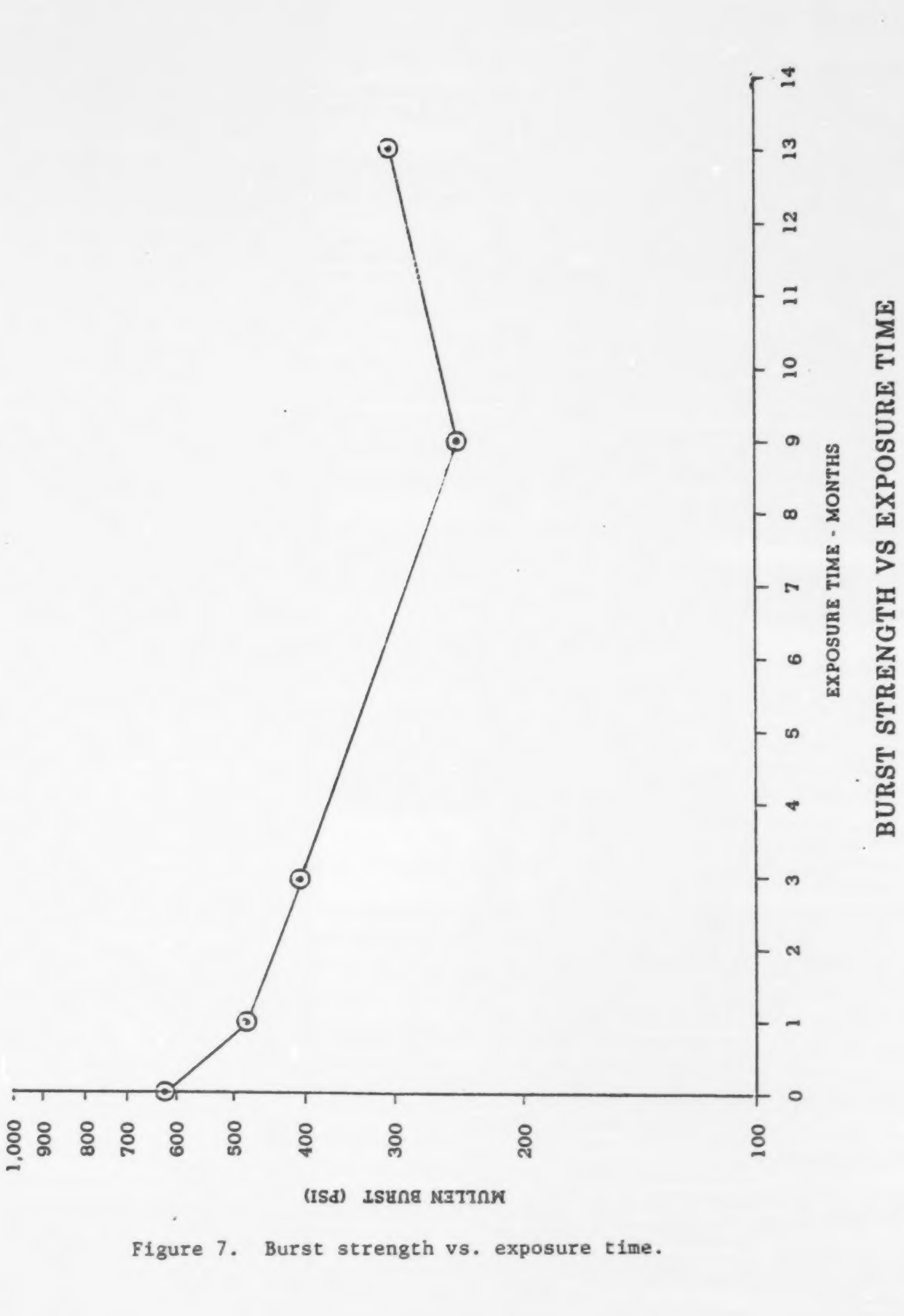

Figure 7. Burst strength vs. exposure time.

The high efficiency and excellent release properties of the membrane prevented particle penetration and lessened agglomeration, which in turn stopped the blinding process.

CONCLUSION

Using standard woven glass bags, the pressure drop across the baghouse system would increase to over 10 inches w.g. within a short perid of time. In spite of multiple modifications to the baghouse, the increasing pressure drop would cause the gas flow to the baghouse to be throttled back. The reason for this high ΔP was bag blinding (initially thought to be due to fine particulate, now appeared to be a combination of fines plus binding agents).

With the GORE-TEX membrane filter bags, this pressure drop has not reached 10 inches and no airflow reductions have been necessary. The effect of the reduced baghouse flow is increased gas flow to the scrubber.

Based on 1983 FGD system operations, increased reagent and reheat costs amount to approximately $1.09 per month for each acfm that goes to the scrubber instead of the baghouse. For instance, a 25% flow reduction to the baghouse would increase the scrubber operating costs by $12,262 per month (0.25 x 45,000 x $1.09 = $12,262). This reduction could cause the scrubber flow rate to exceed design levels. In addition, the reduced baghouse flow decreases the efficiency of the mechanical collectors and increase the particulate loading the precipitator and scrubber.

Although the membrane filter bags were initially more expensive ($70,000 installed) than the woven fiberglass ($35,000 installed), the savings in operating and maintenance costs of the baghouse and scrubber more than offset this premium.

Based on previous experience, Cromby Station will rebag using GORE-TEX membrane filter bags during the outage scheduled for mid-October 1984.

The work described in this paper was not funded by the U.S. Environmental Protection Agency and therefore the contents do not necessarily reflect the views of the Agency, and no official endorsement should be inferred.

®Teflon is a registered trademark of E. I. du Pont de Nemours & Co., Inc.

™Staclean is a trademark of Staclean Diffuser Company.

®GORE-TEX is a registered trademark of W. L. Gore & Associates, Inc.

REFERENCES

1. Ingram, T. J., Biese, R. J. and Jacob, R. O. Upgrade of Fly Ash Collection Capability at the Cromby Station. In: Fourth Symposium on the Transfer and Utilization of Particulate Control Technology.

2. Lamport, S. Tex Lab, Inc. Report 4279, Aug. 1981.

3. Gilbert/Commonwealth, Inc. Report 10-0353-000-1.

4. Greiner, G. et al. ETS, Inc. Report 82-243-L and 83-294-L.

5. Bayard, M. Particle Data Lab. Project I-6949, I-7055, I-7159, and I-7245.

CRITICAL ELECTROSTATIC PRECIPITATOR PURCHASING CONCEPTS

By: Charles A. Altin
Ebasco Services Incorporated
Norcross, Georgia 30092

Dr. Ralph F. Altman
Electric Power Research Institute
Chattanooga, Tennessee 37411

ABSTRACT

Over the last two decades, the electric utility industry has been faced with ever more stringent environmental regulations. This regulatory pressure coupled with political and public awareness, has resulted in utilities having to substantially, and in some cases, dramatically increase capital expenditures for the control of air pollution. When considering these expenditures and the impact of noncompliance with emission regulations on plant operations, it is mandatory that the utility purchase electrostatic precipitators which can produce consistently high-performance levels while maintaining extremely high availability levels.

This paper discusses those critical purchasing concepts which affect the ultimate quality and performance levels of precipitators. Specific issues are performance-oriented versus design specifications; material only versus deliver and erect contracts; performance versus wide-range fuels; precipitator size selection; bidder qualification; and performance guarantees.

CRITICAL ELECTROSTATIC PRECIPITATOR PURCHASING CONCEPTS

Electric utilities have been purchasing electrostatic precipitators for more than 60 years. Over these years, our understanding of the electrostatic precipitation process has improved while allowable emission limits for coal-fired electric generating stations have decreased.

Traditionally, the electrostatic precipitation process has dealt with those physio-chemical-electrical relationships between the equipment and the nature of the particles to be collected. However, in this paper, we wish to include the method by which one actually purchases a precipitator under the definition of "electrostatic precipitation process." The purchasing process has often been overlooked because precipitators have been considered as just another piece of equipment and have not been given the same priority or significance as the steam generator or turbine generator. However, in today's regulatory environment, this approach can result in marginal or noncompliant operation. This situation can lead to fines, load limitations, and/or plant shut downs. The legal emission standards placed upon utilities require that extreme care and sound judgement be utilized in the purchasing process to obtain desired performance levels.

If the history of a marginally or poorly performing unit is reviewed, special attention should be focused on those decisions which lead to the selection of the precipitator. Invariably, the analyses will reveal that "compromises" were made in the hope of obtaining a more "cost-effective" design. Sometimes the changes are made principally or even solely in an effort to make the offer more competitive. Pressures of this kind sometimes overshadow engineering judgements and engender significant risk. The consequences of these risks have come to be understood only after the unit has gone into operation. In light of this past experience, it is clear that the purchasing process can be the single most important activity the utility can engage in to produce a precipitator which consistently achieves compliance with emission regulations.

PROCUREMENT CYCLE

The purchasing process can be viewed from the sequencing of the following events:

- Alternative equipment study (hot vs. cold side precipitators vs. fabric filters vs. wet scrubbers)
- Preparation of draft technical specifications and drawings
- Preparation of commercial terms and conditions
- Qualification of potential precipitator suppliers
- Review by qualified supplier of draft specifications, terms and conditions
- Preparation of final "Request for Proposal" (RFP) package
- Supplier proposal preparation
- Proposal evaluation
- Contract award
- Contract administration

SEQUENCING OF ACTIVITIES

Once a decision is made as to the specific level of particulate matter emission control required for a plant or project, then overall schedules and cost estimates must be developed. In terms of the foregoing event sequence, the following generic schedule requirements are suggested:

- Alternate equipment study - three (3) to six (6) months depending upon the extensiveness of the study.
- Draft technical specification preparation - up to three (3) months.
- Draft commercial terms and conditions - up to two (2) months - concurrent with specification preparation.
- Qualification of potential suppliers - up to two (2) months - must either be performed prior to or concurrent with specification preparation.
- Qualified supplier review of draft specifications - four (4) to six (6) weeks.
- Preparation and issuance of RFP - one (1) to four (4) weeks depending upon the nature of qualified supplier comments.
- Proposal preparation - two (2) to three (3) months depending upon scope of supply and proposal activity level of the qualified suppliers.
- Proposal evaluation - Two (2) to six (6) months depending upon the number of proposals and the quantity of technical and commercial exceptions.
- Contract award including evaluation review - one (1) to two (2) months.
- Contract administration through initial performance testing - twenty (20) to forty (40) months depending upon scope of supply, magnitude of the work and project schedule requirements.

PERFORMANCE ORIENTED VERSUS DESIGN SPECIFICATIONS

Over the years, two distinct approaches with respect to precipitator specification philosophy have been utilized. The first approach, commonly referred to as a "performance" specification, sets forth only a desired performance result and scope of supply. The precipitator supplier is then charged with the responsibility to use its own standards, procedures, and judgements in the design of the precipitator. Under this concept, the utility would accept essentially whatever design features and margins the supplier deems necessary. By and large, the supplier would select sub-suppliers without providing the utility with a review or approval function.

Generally, a true performance specification would consist of the following:

- Inlet design conditions
- Design collection efficiency
- Fuel characteristics

- Performance warranty statement (efficiency, electric power consumption and flue gas pressure drop)
- Scope of supply
- Standard commercial terms and conditions

The supplier would then include in its proposal a basic, although limited, description of the equipment to be provided. Major portions of the proposal are usually incorporated into the purchase order in order to provide some description of the equipment to be furnished.

The other approach to specification philosophy is termed "design" or "detail" specifications. This approach requires the utility to develop a specification which not only incorporates the elements of the performance specification, but also sets forth design standards in greater or lesser detail. These detail design standards can include such features as the minimum number of transformer-rectifier sets, hoppers, rappers, and most importantly, specific collecting areas. This assures that all proposals would be similar in terms of essential equipment characteristics and meet minimum design criteria. Proposal evaluation should be simpler and quicker, and there is greater assurance that the equipment will meet the performance warranty. Further, utility preferences for sub-suppliers would be addressed in the design specifications. Moreover, the supplier's proposal would not be incorporated into a purchase order due to the nature of the design specification, thus avoiding or minimizing any misunderstandings relating as to what is to be furnished by the supplier.

In comparing performance oriented and design specifications, the design specification offers the utility the greater degree of latitude in factoring into the precipitator design its own experience and those of others. Further, design specifications provide both the utility and supplier with a clearer understanding of the responsibilities and duties of each party in order to comply with the provisions of the Contract. This will lead to fewer misunderstandings and conflicts during the execution of the Contract.

MATERIAL ONLY VERSUS DELIVER AND ERECT CONTRACTS

The utility has a choice as to whether it wishes the precipitator supplier to furnish only the material or to provide both the material and the erection thereof. For the "material only" contract, the supplier's material warranty will be limited to only providing for the repair or replacement of a defective part or system. As a result, the utility would be responsible for the removal and reinstallation of such affected equipment. Based on years of experience, the cost of removal and reinstallation may be anywhere from one (1) to ten (10) times the cost of the defective material. Therefore, significant and unanticipated costs can be incurred by the utility for "warranty repair or replacement" work.

"Material only" contracts must contain the requirement for a representative of the supplier to be on-site during all construction activities associated with the precipitator. This representative is commonly referred to as an "erection consultant or advisor." It must be noted that this erection consultant has no on-site erection supervisory responsibility and can only advise the utility's erection contractor. The erection consultant's primary function, as a practical matter, is to protect the interests of the supplier from the standpoint of recording any deviations from the supplier's erection instructions and tolerances.

Therefore, the utility must exercise extreme care and diligence in assuring that the erection consultant is experienced with the supplier's equipment since there seems to be a great deal of personnel mobility within this area of endeavor. Further, the consultant must exercise prudent judgement in applying erection tolerances in such a manner as to realistically reflect construction realities. Further, it is most important that the erection consultant work the same hours as the construction crew, even if it means overtime and/or having two (2) erection consultants, one for each shift, if the work is to be performed on a double shift basis. Moreover, the erection consultant must be given every opportunity to alert the utility to any potential deficiencies in erection. This function should be offered through regular meetings with the constructor's supervisory personnel and the utility on-site representatives. In addition, the erection consultant should provide a weekly report to the utility and precipitator constructor. Further, the supplier should provide with its proposal a "critical item sign-off" sheet which would be used in the field. The erection consultant must sign-off and accept each and every critical item or notify the utility's management of nonacceptance conditions so that corrective action can be taken. This point cannot be overemphasized since it can be to the supplier's advantage to claim that any failure to attain performance and/or fulfill material warranties is due solely or principally to construction deficiencies over which the supplier had no control.

On the other hand, contracts which require the precipitator supplier to erect the material it furnishes, commonly referred to as "deliver and erect" contracts, provide for unified responsibility. This unified responsibility prevents potential claims that the utility did not properly erect the equipment should there be a warranty problem. Further, in terms of the material warranty, it would be on a furnish and install basis, sometimes referred to as an "in-place" warranty under the concept of "warranty in kind." This "in-place" warranty offers potential financial benefits to the utility by avoiding the expenditure of non-appropriated or maintenance funds during the warranty period, which can be functionally as long as three (3) years after unit trial operation. It must be noted that the supplier will mark up the cost of the erection service some relatively small percentage to account for overhead, profit and warranty reserve. It is clear that "deliver and erect" contracts offering unified responsibility are preferable in terms of limiting the utility's risk, although there is an additional cost, usually a small percentage, associated with this approach.

PERFORMANCE FUEL VERSUS WIDE RANGE

When establishing a fuel specification for the design and purchase of electrostatic precipitators, the utility is faced with planning for an uncertain future. This future from a precipitator standpoint, revolves about environmental regulations, variability in fuel properties, domestic economic conditions, and the impact of worldwide political unrest on foreign energy sources with the cascading effects on the domestic energy market. Therefore, when planning new generating capacity or performance upgrading of existing facilities, the interactive relationship between fuel quality and electrostatic precipitator performance must be examined.

Utilities have traditionally utilized three approaches to developing fuel characteristics for precipitator specifications. These approaches are (1) performance fuel, (2) narrow range, and (3) wide range of characteristics. The "performance fuel" concept is similar to that employed in steam generator specifications. In essence, a specific fuel is identified and the performance warranty is dependent upon this one fuel. This concept requires that the utility be absolutely certain that this specific fuel is not only available during the performance tests, but that this fuel or a sufficiently similar fuel is available over the life of the unit. From a precipitator standpoint, this concept is really only applicable for mine-mouth or captive mining operations with extensive analyses of known reserves . The second concept, narrow range of characteristics, involves identifying a specific geographic region of the country or coal formation from which the utility wishes to purchase fuel. A range of fuel characteristics, would then be developed which would be based upon a relatively large number of mines. The third concept, wide range of characteristics, involves selecting such a broad range of characteristics as to functionally include all coals within a very large geographic area. An example of this concept would be "to be able to fire any coal east of the Mississippi River."

In terms of current fuel market conditions and based upon past experience, the performance fuel concept approach is generally not applicable because of the potential unavailability of that specific fuel some three to four years after the purchase of the precipitator. Compounding this problem is the approach which might be taken by the utility's fuel purchasing group which may be more interested in obtaining the lowest fuel cost regardless of the impact on precipitator performance. This situation is mitigated by a close and ongoing working relationship between the utility's engineering and fuel purchasing groups.

When considering the benefits and disadvantages of designing precipitators for either a narrow or wide range of fuel characteristics, the overall economic impact on the plant must be evaluated. This evaluation would include the impacts on the steam generator, coal and ash handling systems, precipitator and flue gas desulfurization system. Capital expenditures along with operating costs would have to be included in the evaluation. Such a study was presented at the Conference on Electrostatic Precipitator Technology for Coal-Fired Power Plants in 1982 by C. A. Altin in his paper entitled, "Electrostatic Precipitator Sizing Impact on Coal Purchasing Practices."

In the final analysis, the utility should so select and establish the range in fuel characteristics for precipitators in such a manner as to provide the utility with the greatest cost-effective latitude in responding to a changing fuel market. In essence, a "best balance" approach should be pursued between investment costs and long term operating costs.

PRECIPITATOR SIZE SELECTION

There is one critical aspect of precipitator design which has created and will continue to create the greatest opportunity for differences of opinion among precipitator experts. That question is how to select the appropriate precipitator sizing factor. The question has been asked for over 50 years, and will probably be asked for some time to come.

Pioneering work in the field of electrostatic precipitation was conducted by Dr. Fredrick Cottrell in the United States and Sir Oliver Lodge in England during the late 1800's and early 1900's. Initial application of precipitators were in the industrial sector of our economy during the first quarter of the 20th century. The first full-size utility application of a precipitator to a pulverized coal-fired steam generator occurred in 1923 at a unit of the Detroit Edison Company.

Between that first utility installation and the precipitators installed today, significant strides have been made in hardware design along with an understanding of the fundamental processes involved. These equipment improvements have been fostered by the differing perspectives developed by numerous suppliers. This tended to produce different insights into the precipitation process and hence sizing practices.

Since the suppliers basically sponsored their own research work, the work was and still is considered proprietary and therefore not publicly available. This discrete, non-publicized work resulted in unique data bases for each supplier. Even today, with all of the governmental and private institutionally funded research projects, the suppliers' data bases still provide the basis upon which suppliers base their guarantees. This situation makes it very difficult for the utility to independently establish precise precipitator sizing.

Recognizing the limited precipitator sizing resources available to the utility, a practical approach must be taken in order to develop a minimum precipitator size with which the utility will be confident. It has often been said that sizing should be left to the suppliers because they are the ones who are taking the commercial risks. But in fact the utility is assuming considerable risk. Consider that the current federal air pollution regulations permit fines of up to $25,000 or even $50,000 a day for each knowing violation. In addition, federal laws even provide for the issuance of orders for power plants to be shut down until the problems are corrected. Shutdowns of large units may result in costs between $500,000 to $1,000,000 a day to the utility in terms of lost generation, replacement power and interest on the investment. These liabilities stem from the fact that the utility has the sole and nontransferable legal responsibility to make the precipitator comply with the applicable emission standards. These are real commercial risks to the utility, and they overshadow those of the supplier by up to one order of magnitude.

Considering the risks to the utility, it is absolutely essential that the utility be confident of the precipitator size. This confidence can be generated by development of the utility's own sizing procedures, selecting only qualified suppliers to bid on the project, extended performance warranties, or increased levels of financial liability on the part of the supplier. Over the years, these techniques have been employed either singly or in combinations. The utility should consider utilizing all of these techniques to increase the probability of successful precipitator operation. The prudent sizing procedure would be to employ all of the following techniques to develop a "consensus" size:

- Empirical models based on units firing the same or similar coal
- Mathematical simulation models
- Test burns in full or pilot size units
- Size selections developed by qualified manufacturers.

These techniques will result in distinct size requirements for each case studied. It still becomes the responsibility of the utility to identify exactly what performance level is required for each particular coal and ultimately select the size which is believed to attain the objective. This approach suggests a "consensus" size with a guiding rule that the minimum size should not be less than the largest size submitted by the qualified supplier. However, the largest size, if significantly different than those of other suppliers, must be thoroughly examined by the utility to assure of its applicability to the project. This size selection process occurs prior to the "request for proposals." Once the utility establishes a minimum precipitator size and then applies design margins, the minimum design size is then established. This minimum design size is then set forth in the specifications, and the bidders may be instructed that any offering which does not exactly conform to this minimum may be considered "nonresponsive." Coping with the nonresponsive proposal situation presents the utility with options ranging from permitting the bidder to revise its proposal to rejection of the proposal. Whatever action is taken by the utility, the issue of fairness to an individual bidder versus all bidders must be addressed while adhering to the utility's purchasing policy and guidelines.

Further, it should be kept in mind that, should a supplier believe that the minimum size is too large, then the supplier's risk can only be reduced by supplying a larger precipitator. This reduced perceived risk could be reflected either in lower levels of warranty reserve requirements, thus reducing the price, or improved performance warranty levels, which could be to the supplier's benefit in terms of proposal evaluation. Hence, the continued use of minimum precipitator sizes is prudent from the standpoint of reducing the utility's ultimate financial risk.

SUPPLIER QUALIFICATION

One of the most critical aspects in purchasing an electrostatic precipitator is to select the suppliers who will offer proposals from which the utility must choose. Although the supplier selection process is often seen as merely nothing more than gathering the names of all the companies engaged in manufacturing precipitators, the selection process has far reaching implications as to whether performance warranties will be achieved on a continuous basis. Some view the process as a way to ensure competitive pricing. The questions which must be asked are, "How many suppliers are needed to assure competitive prices?"; and "Which suppliers have demonstrated a clear cut track record of having reliable equipment, prudent sizing criteria, commercial commitment to resolving problem jobs, and a continuing effort in developing precipitator technology?" The following discussion presents concepts which should be at least considered when selecting qualified precipitator suppliers for a particular project.

ASSEMBLY OF SUPPLIER EXPERIENCE

In order to obtain the information necessary for the implementation of a rational qualification procedure, a meeting should be held with each of the prospective bidders. These meetings serve the purpose of exchanging information relative to the project. Usually, utility personnel from both the engineering and purchasing staffs will describe the project in terms of technical requirements such as fuels, removal efficiency and scope of supply, and commercial requirements such as limitations on escalation or lump sum fixed pricing, extended material and performance warranties, liquidated damages, and schedule. The supplier would usually be requested to provide the following information:

- Review of equipment design features
- Discussion of sizing philosophy and history
- Presentation of current research and development projects
- Installation list
- Performance test reports on similar projects
- Discussion of problem jobs
- Quality assurance program
- Staff qualifications
- Schedule adherence analyses of previous projects
- Identification of manufacturing facilities
- Financial value of recent contracts
- Annual financial report
- Bank references
- Utility references
- Listing of any pending litigation

This information will serve as the basis for the evaluation conducted by a team of utility personnel. This team normally consists of personnel from the utility's engineering, purchasing, legal, construction, and quality assurance departments. The team approach is suggested in order to bring specialized talents and perspectives to bear and to limit the overall time spent in the selection process. The advantage of these efforts will become evident when evaluating the proposals.

COMMERCIAL EVALUATION

Each utility normally has its own commercial criteria for determining qualification for a bidders list. Considering the cost and regulatory significance of the precipitator, it is prudent to employ specific screening procedures. These procedures tend to center about the suppliers' ability to assume a new liability and how it has discharged its responsibilities on previous contracts.

A Dun and Bradstreet rating of the supplier is often the beginning of the evaluation. Depending upon the utility's corporate policies and the potential value of the project, some minimum rating may be required as a first screening level. This type of screening is based on a "go/no go" concept. The second level of screening would be an analysis of past annual reports, bank references, and possibly a current financial statement. Again, this analysis would establish a "go/no go" level which the supplier must pass in order to be considered further. The third screening level would be whether the supplier has recently completed a contract with a value similar to that of the proposed precipitator project. The fourth level of screening involves an assessment of the liability to the supplier of any outstanding litigation in which the supplier is involved. The utility's legal staff would normally be in contact with the supplier's counsel to determine the exact nature and status of the litigation. In essence, the determination would have to be made under the premise that should the supplier lose all or a major portion of the litigation, could the supplier be significantly impaired in fulfilling future contracts. The final screening level, and possibly one of the more influential, is the utility's past history with a particular supplier in terms of meeting schedule requirements, treatment of material and performance warranties, contract extras, and the resolution of problem jobs.

Supplementing the foregoing screening levels, the utility may wish to investigate the supplier's manufacturing facilities, subcontractor facilities, quality assurance programs, discussions with other utility users of the supplier's equipment, and possible plant site visits.

It must be recognized that the commercial evaluation factors must be judged with regard to the economic conditions existing at a specific point in time and in all probability are substantially subjective in nature. However, it is more appropriate to use subjective screening procedures in the bidder qualification phase rather than in the proposal evaluation stage since the expense of preparing a proposal is substantial. Therefore, it is suggested that this procedure be used to assure that the bidders list only contains those suppliers from whom the utility would be happy to purchase equipment.

CRITERIA FOR SELECTION INCLUDING RELATIONSHIP TO SPECIFICATION

Once the commercial evaluation has been completed and a tentative bidders' list has been established, an experience and a technical evaluation would then be performed. This evaluation concerns itself with the technical features of the precipitators, sizing track records, number of units in service and/or under contract, operational flexibility, and reliability. In essence, each of the tentative bidders is evaluated in terms of overall precipitator experience and technical merit of specific design features.

The supplier's total experience should be evaluated in terms of a summation of the megawatt ratings of all cold-side precipitators on domestic coal-fired plants in operation since 1970 and/or currently on order. This time frame represents the relevant experience in terms of recent emission requirements, sizing philosophy, and fuel characteristics. Each supplier's installation list would then be credited in terms of megawatts in the experience evaluation process.

This evaluation should attempt to put the supplier's experience into the proper perspective relative to the total range of activities from the engineering phase through operation. Consequently, the amount of credit accorded may be categorized into (1) those units which have passed guaranteed performance levels; (2) units which are operating but have not been tested to date; (3) units which are operating but have failed to pass performance guarantees; (4) units under construction; and (5) units which are in the engineering phase. Each phase of the work demonstrates a certain capability. In any evaluation of experience, the major portion of the credit should be given to those units which have passed performance guarantees.

These criteria for crediting megawatts can be modified to reflect a utility's concern or special requirements. Typical modifying factors are:

- Consider only those precipitators operating on a particular type of fuel.
- Consider only those precipitators with a certain minimum collection efficiency.
- Consider those precipitators with tested outlet emissions of a certain level or less.
- Consider those precipitators which have failed their performance guarantees only if they represent a small percentage of those precipitators which have passed their performance guarantees.
- Consider only those precipitators applied to a certain megawatt size or larger.
- Apply a multiplying factor to those precipitators where the supplier had responsibility for both material and erection as opposed to material only contracts.

This experience screening level will result in establishing a "credited megawatt" rating for each supplier. The ratings level can range from a very small number to approximately 10,000 credited megawatts. The utility will have to decide what specific level of experience is appropriate to the proposed project. Only those potential suppliers who meet an experience level acceptable to the utility, would then be considered for further evaluation.

The final screening level involves evaluating the remaining potential suppliers from the aspect of the technical merit of their respective designs in relationship to project requirements. A typical technical merit evaluation can consider the following design aspects:

Discharge Electrodes

- Electrode configuration
- Type of electrode mounting
- Type of electrode support
- Potential for electrode and support expansion or distortion
- Internal electrode assembly bracing
- Type of rapping system
- Rapper location (in or out of gas stream)
- Rapper maintenance features
- Rapper segregation and energization
- Type of automatic voltage controller

Collecting Electrodes

- Plate thickness (18 or 16 gauge)
- Upper plate support
- Bottom plate spacers and bracing
- Plate spacing experience (9,10, or 12 inch)
- Type of rapping system
- Rapper location (in or out of gas stream)
- Rapper maintenance features
- Number of plates rapped by any one rapper (one, two, three, or four)
- Rapper segregation and energization

Size Selection

- Data base
- Methodology
- Specialized fuels

Of course, this list of design aspects should be modified to suit the utility's specific needs. However, the design aspects should reflect realistic concerns and the relative importance of individual parameters in terms of enhanced precipitator performance. Typically, the maximum ratings are converted to a numerical system for ease in establishing an overall rating.

The application of both the commercial and technical evaluation criteria will probably result in a bidders list containing a manageable number of suppliers. The number of suppliers must be large enough to assure competitive pricing while recognizing that the period of time permitted for evaluation is usually limited, regardless of the number of bidders. Hence, when considering that there is a certain minimum period of time and effort associated with reviewing and properly evaluating each proposal, the need for a limited number of bidders is clear. Further, courtesy bids do not serve the interests of the utility or supplier since those bids consume the time and resources of both parties.

QUALIFIED SUPPLIERS' REVIEW AND COMMENT OF DRAFT SPECIFICATIONS

The development of a precipitator specification is a significant undertaking. Moreover, proposal preparation may require a supplier to expend upwards of $250,000 for a major project. Therefore, it behooves both the utility and supplier to assure that the specification accurately reflects the utility's needs, desires, and requirements. This will reduce the incidence of alternate equipment quotations or even re-bidding with the preparation of entirely new proposals.

In order that the specifications reflect the utility's requirements, it is suggested that the qualified precipitator suppliers be given the opportunity to review the specifications prior to their release in a request for proposal. This review on the part of the qualified supplier should address the following as a minimum:

- Minimum specific collecting area (SCA)
- Maximum collecting electrode height
- Maximum gas velocity through the precipitator
- Minimum aspect ratio
- Minimum treatment time
- Minimum number of mechanical fields
- Minimum number of electrical fields and bus sections
- Number of precipitators and chambers
- Precipitator arrangement
- Precipitator control system

Ideally, the qualified supplier would review all of the specifications, not just the precipitator, but also the attachment specifications. However, time constraints usually limit the level of review to only the precipitator specification. The supplier can use two techniques for reviewing the specification. The first technique involves an in-depth analysis based upon cost-effective benefit considerations of each of the significant design requirements. This technique requires a significant effort on the part of the supplier. The second technique involves reviewing the specification from the standpoint of identifying those requirements which would make the supplier's proposal "non-competitive" in terms of its standard or normal design practices or scope of supply. These "non-competitive" requirements would have to be individually studied and evaluated in terms of whether (1) the requirement is a physical impossibility, (2) the requirement is not part of the supplier's original equipment design concept, or (3) the requirement has proved to be ineffectual on previous designs. These "non-competitive" aspects of the specifications should be carefully reconsidered by the utility.

The utility must realize that the suppliers' comments may be quite valuable, however they must be examined very carefully to prevent the intent of the original specification from being changed. Also, the utility may be subjected to comments from some suppliers, implying that the utility should not be concerned about detailed specifications or that specific features are not necessary. These comments must be viewed from the standpoint that competitive pressures may be the motivating factor.

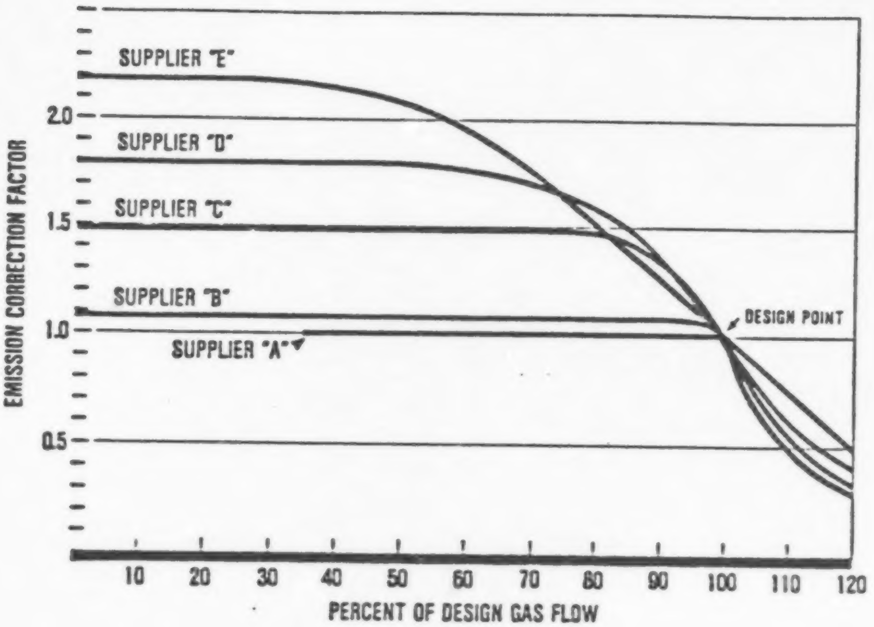

Figure 1. Guarantee performance curve gas flow vs. emission correction factor

If these curves in Figure 1 represented the purely technical relationship between gas flow and performance, all curves would coincide. However, this is not the case. It is apparent that Supplier 'A' is engendering the least risk while Supplier 'E' is assuming the most risk. From the utility's standpoint, Supplier 'E' is offering the most attractive performance curve because it states that at lower gas flows, there is considerable margin in the design. This added design margin reduces the utility's risk in meeting design emission levels and/or its ability to achieve acceptable emission levels under adverse operating conditions.

Utilities should also be aware of the effect of an outlet stopper and how it relates to the performance warranty curves. In essence, an outlet stopper states that whenever a certain emission level is achieved, the warranty is then deemed to have been satisfied in full, even though the precipitator is not producing the collection efficiency stated in the contract or as adjusted by the correction curves. The original reason given for the outlet stopper concept was that one could not reliably measure emissions less than 0.1 pounds/million BTU. In actuality, many precipitators in the 1960 to early 1970 era, passed performance tests by meeting the outlet stopper. The problem with an outlet stopper becomes apparent when performance curves are considered in connection with this limit. The curves may indicate a collection efficiency of 99.8 percent or higher at nondesign point conditions, while the outlet stopper could be satisfied by efficiencies in the low 99 percent range. It is therefore

In the final analyses, qualified suppliers' review of the specification can be beneficial by identifying potential problems and resolving them prior to the issuance of a request for proposal. This will benefit the supplier by having to prepare only one proposal while making the utility's evaluation less complicated. This will permit the utility to concentrate its efforts on the evaluation of the real issues.

PERFORMANCE WARRANTIES

If all precipitators met their design emission levels, there would be no need for the supplier to offer performance assurances, and utilities would have absolute confidence in meeting emission standards. However, when facing the realities of the electrostatic precipitation process, it is apparent and necessary that the supplier make specific assertions as to the performance of its equipment. This assertion is commonly referred to as a "performance warranty". The performance warranty reflects the degree of confidence a supplier has in its technology and a level of commercial risk it is willing to accept "to get the order".

Generally, the performance warranty will cover parameters such as collection efficiency, outlet emission, opacity, flue gas pressure drop, power consumption, and unit availability. The key to a performance warranty is that it must be clearly stated, and there must be a straightforward and reasonable mechanism for the administration of the warranty.

Precipitators are designed to achieve a specific collection efficiency at a particular set of process conditions, sometimes referred to as a design point. This design point usually represents the "worst case" combination of parameters. These worst case parameters would be maximum flue gas flow, maximum flue gas temperature, maximum fuel ash content, minimum fuel sulfur content, and minimum fuel heating value. This worst-case design point is frequently a fabricated condition which, in all probability, may never be attained. Further, it would be almost impossible to produce this worst-case design point during the performance tests. Hence, suppliers are requested to provide a projection of precipitator performance for a range of conditions. These projections are usually presented in graphic form and referred to as guaranteed performance correction curves. These curves are supposed to inspire confidence in the equipment by predicting improved performance levels for non-design point conditions. For example, if the emission level at 80 percent of design flow coincides with the value read from the appropriate correction curve, then it would be presumed that should the maximum gas flow be encountered, the design emission level would be met. The basic problem with these performance curves is that although they may be based on technical principles, the curves are really commercial curves and must be treated as such. Again, these curves represent a certain perceived risk level the supplier is willing to accept for a particular project. The perceived risks can vary dramatically with each supplier. This variation in perceived risk is illustrated in Figure 1 which relates an emission correction factor to gas flow.

suggested that if an outlet stopper is to be accepted, it should be set low enough to inspire confidence that the unit could meet performance requirements at the design point. As an alternative, the outlet stopper could be replaced by adjustments in the performance curves. This idea may have been the reason Supplier "A" chose the straight line curve in Figure 1. It can not be overemphasized that the utility must be careful in determining the exact nature of the performance warranty offered by each supplier.

The consideration and evaluation of power consumption warranties requires the utilities to exercise the utmost care. This care is required because, to date, there is yet to be developed a reliable, publically available method for correlating power consumption with fuel properties, collection efficiency, and precipitator internal configuration. For the most part, the data developed by each supplier tends to be unique and limited in its scope and applicability. Predicting power consumption becomes even more difficult when dealing with specific fuels for which the supplier has no data. Therefore, the utility must investigate the basis and reasonableness of supplier claims and warranties.

Power consumption warranties have been a major evaluation factor and have actually determined which supplier receives the award. Each supplier calculated its power consumption in a particular manner with certain assumptions. The methodology and assumptions can create situations where power consumption levels vary by a factor of five (5). It is unlikely that such great differences will exist in reality. Therefore, extensive discussions with each supplier must be undertaken to determine the bases of the consumption levels. In essence, when modern specifications establish minimum precipitator sizing and other feature-related criteria, the bids will be extremely close in physical configuration. Thus, power consumption levels should not dramatically vary.

Precipitator electrical loads can be broken down into those associated with (1) transformer-rectifier sets, (2) hopper heating, (3) insulator purge and heating, (4) control room heating and air conditioning, and (5) lighting. The principal loads are associated with the transformer-rectifier sets and hopper heating. When the specification establishes the minimum number of hoppers and their capacity, essentially all bids would consume the same level of power. Therefore, the only remaining variable load is that of the transformer-rectifier sets. Considering that the power consumption will be a function of discharge electrode geometry, gas and particle electrical properties, automatic voltage controllers, and electrode cleanliness, attention must be directed to potential differences in equipment to substantiate power consumption levels.

If one were to consider various bids and presume, due to advances in equipment design, that discharge electrode configuration will be the predominant factor in power consumption, then transformer-rectifier set power consumption levels should not vary by more than 25 percent for the same conditions. Of course, all of the foregoing would not support variations in power consumption of up to 500 percent. Therefore, the utility can take one of the following approaches: (1) ignore power consumption warranties, (2) establish a minimum consumption level under which the bidder would receive no credit, or (3) prorate consumption levels of all bidders so that the difference between high and low is on the order of 25 to 50 percent. In the final analysis, the utility must exercise prudent judgement in evaluating power consumption warranties in light of the lack of a cohesive and reliable data base. Further, the utility must take care as to not place suppliers in the position where misrepresentation or unwarranted risk is encouraged.

PERFORMANCE TESTS

Currently a "two test" concept is utilized to determine if the precipitator can fulfill the performance warranty. Generally, the first test 'A', is conducted within three (3) months of the unit's commercial operation date. At this time, tests are performed to determine compliance with contract collection efficiency, outlet emission, opacity, power consumption, and flue gas pressure drop warranties. This test more or less characterizes precipitator performance in an as "new" condition. The second test, 'B', usually is conducted twelve (12) to twenty four (24) months after having passed test 'A'. Test 'B' only addresses collection efficiency, outlet emission and opacity. In order for test 'B' to be enforceable in terms of the performance warranty, it is imperative that the material warranty extend through test 'B' to avoid the supplier from claiming "the reason that the equipment failed was due to subcomponents which were inoperable due to material failure and/or poor maintenance practices.

Another aspect of the performance warranty is the requirement that the supplier promptly and diligently pursue those corrective actions required under the material and performance warranties. The concept requires that a cumulative period of time, ie 550 elapsed calendar days, be established in which the supplier can complete any and all warranty repairs. Of course, the elapsed time for each event would be computed from the time the supplier is notified in writing that a condition exists which requires corrective action, and until that time when the corrections are effected and completed and the utility so notified in writing. Delays in making the equipment available to the supplier would be excluded from the time accounting. Should the supplier fail to complete the corrections in the time allotted, then the supplier would forfeit a sum of money. The forfeiture of money would not relieve the supplier from its responsibilities under the contract, but merely acts as a way to prompt responsive action on the part of the supplier.

CONCLUSION

Utilities should approach the electrostatic precipitator procurement process as the single most important and active step it can take to assure that desired performance levels will be met. The utility must decide on a specification approach (performance, design or a blend), scope of supply (material or deliver and erect), and fuel selection (performance, narrow or wide range) which best meets its specific project requirements. Further, the utility must be assured that the precipitator supplier is qualified to perform the work and will meet its contractual obligations. When all of these activities are carefully and diligently pursued during the procurement process, a precipitator capable of providing many years of satisfactory performance should result.

The work described in this paper was not funded by the U.S. Environmental Protection Agency and therefore the contents do not necessarily reflect the views of the Agency and no official endorsement should be inferred.

REDUCING ELECTROSTATIC PRECIPITATOR POWER CONSUMPTION

By

Joseph P. Landwehr, P.E.
Air Quality Design Section Chief

and

George Burnett, P.E.
Air Quality Control Senior Engineer

Burns & McDonnell Engineering Company

ABSTRACT

The current trends for minimizing the operating cost of electrostatic precipitators (ESPs) include methods for reducing electrical power consumption. One method applies to new ESP designs and includes specifying a guaranteed power consumption which requires design optimization by the ESP manufacturer. A second method consists of using a centralized control system to regulate normal operating power of all transformer-rectifier (T/R) sets.

This paper presents available techniques for determining the potential for power savings in ESP design and operation. Theoretical and practical considerations for reducing T/R power with the least sacrifice of collection efficiency area examined. Both classical methods and sophisticated computer models for predicting ESP performance as a function of power input are used to evaluate the effect of reducing power input. Actual results of power reduction testing for a high-efficiency ESP on a coal-fired utility boiler are presented. Procedures for power consumption testing to satisfy guarantees and bonus/penalty clauses are also presented.

INTRODUCTION

THE LATE 1970s

To help control life cycle costs of high-efficiency electrostatic precipitators (ESPs) power plant owners and architect-engineers began to require power consumption guarantees. ESPs, designed to meet new source performance standards, consumed up to 1 percent of the gross generating capacity. Power consumption guarantees, however, caused ESP manufacturers to optimize their designs to meet guaranteed collection efficiency at reduced power input to the high-voltage supplies.

To verify the guarantees power consumption measurements were taken during precipitator performance tests. Automatic voltage controls were adjusted manually to reduce power input while still meeting guaranteed collection efficiencies. Afterwards, voltage controls were returned to automatic because of the impractical and unsafe nature of continuous manual operation. The power input increased to normal operating values. With automatic power reduction controls not yet generally available, plant owners could not easily take advantage of the potential for power savings.

TODAY

The application of microprocessors for practically every type of plant control has become widespread. The application of microprocessor controls for ESPs has led to the development of centralized control systems that regulate normal operating power consumption of each high-voltage power supply. These centralized control systems can be applied to either analog- or digital-type automatic voltage control systems and represent a major step in reducing precipitator power consumption.

This paper presents available techniques for determining the potential for power savings in ESP design and operation. Theoretical and practical considerations for reducing T/R power with the least sacrifice of collection efficiency are examined. The results of both classical methods and sophisticated computer models are presented for predicting ESP performance and are used to evaluate the effect of reducing power input. The results of field tests to reduce power on a high-efficiency ESP on a coal-fired utility boiler are presented. Considerations for power consumption testing and for designing are also presented.

DESIGN CONSIDERATIONS

There are three primary areas of power input required by a dry-type ESP for industrial processes:

1. Fan horsepower required to overcome the gas flow resistance to flow.
2. Power required by low-voltage auxiliary equipment.
3. Power required by high-voltage power supplies normally called transformer-rectifier (T/R) sets which produce the dc corona power used for particle charging.

Before examining ways to reduce power consumption, it must be assumed that the objective of reducing power consumption is to reduce operating costs without decreasing particulate removal and without increasing maintenance costs caused by equipment deterioration.

FAN HORSEPOWER

Probably the most difficult place to reduce power consumption in a cost-effective way is the fan horsepower area. The total pressure differential across a high-efficiency ESP is almost negligible due to the low gas velocities (250-300 fpm) even at maximum flow. Most of the pressure loss in a large ESP is due to losses in ductwork and across flow distribution devices.

Small units have simple inlet and outlet ductwork arrangements and, therefore have smaller pressure differentials. ESPs on units 200 MW (800,000 acfm) and larger usually require complex ducting to minimize the plant area (and cost) required. Turning vanes are often used to obtain uniform flow of gas and dust throughout the ductwork system resulting in a reduction in pressure drop as a desirable side effect.

Pressure loss caused by friction in ducts depends on the particular ductwork arrangement, but losses are mainly due to: (1) straight runs of duct, (2) elbows, (3) inlet and outlet transitions, and (4) gas flow distribution devices. The most obvious way to reduce pressure loss through straight runs, elbows, or otherwise is to lower the gas velocity by increasing the duct size. Ductwork cross-sectional area is generally limited by the minimum gas velocity required at low loads to prevent dust fallout in horizontal runs. However, ductwork arrangements without horizontal runs and incorporating ash handling equipment at the bottom of vertical runs, although expensive, should not be overlooked. The potential for dust fallout at low loads should be carefully evaluated because the buildup of hard deposits could be detrimental to proper flow distribution and significantly increase pressure loss at full-load operation.

The use of turning vanes in elbows is a cost-effective way to reduce pressure loss. The use of additional vaning beyond what is usually required for uniform gas flow, however, is generally not cost-effective. Normally, rectangular ducts with miter elbows are used. The use of three or four small arcs or angular turning vanes achieves about 90 percent of the possible reduction in pressure loss. Larger vanes which subtend the full (90-degree) turn, or even airfoil vanes, may further reduce pressure loss, but are generally not considered cost-effective. The use of radius elbows with large arc vanes, which in theory results in the lowest pressure loss, should be evaluated where power costs and/or duct velocities are exceptionally high.

Gradual inlet and outlet transitions can be effective in reducing pressure drop. Transitions from low velocities to high velocities, such as ESP outlet nozzles, should be designed for static pressure regain while inlet nozzles are primarily designed to provide a uniform gas distribution to facilitate particle collection within the precipitator. An ideal configuration may not be possible because of space limitations and dust fallout considerations. Futhermore, although low velocity may result in dust fallout, minor dust accumulation may be acceptable in these transition areas and therefore allow a more cost-effective design.

A gas flow model study can provide data necessary to estimate the effectiveness of various gas flow control devices including internal turning vanes. However, model studies are usually performed for only one ductwork arrangement. Model studies typically recommend turning vanes to maintain uniform flow and other alternatives for reducing pressure drops are not evaluated. On larger units, particularly where the costs of station services are relatively high, the ductwork sizing and arrangement should be evaluated and selected based on life-cycle cost. This evaluation should include the cost of fan horsepower.

AUXILIARY EQUIPMENT

Most of the auxiliary equipment for an ESP requires relatively low power. Insulator heaters, insulator purge air heaters and blowers, and hopper heaters, however, can be major users of electrical power. If designed without regard to power conservation, heaters can use as much power as the transformer-rectifier sets themselves.

The operation of auxiliary equipment generally has no effect on ESP performance. However, misdirected attempts to reduce power consumption can be detrimental. For example, if the flow or temperature of heated purge air to high-voltage insulators is reduced, performance may be reduced immediately as a result of arcing at minimum clearance areas. Insufficient temperature can result in condensation of moisture and dust buildup on insulators, also causing arcing and/or cracking of insulators. Reduction of hopper heater power in combination with cold ambient temperatures and hygroscopic ash, can lead to hopper pluggage and ultimately to grounding of the associated high-voltage electrical sections.

CORONA POWER

The greatest potential for power reduction in ESPs lies in the area of corona power. ESP theory thus far has not been able to adequately quantify the effects of such phenomena as sparking, reentrainment, and back corona especially in the high-efficiency range where a large percentage of the particles collected are submicron-sized. Actual tests, however, have shown that at certain operating conditions it is possible to achieve higher collection efficiency at lower power input.

MINIMIZING POWER CONSUMPTION ON EXISTING PRECIPITATORS

A typical high-efficiency precipitator design has a capacity for approximately 1,400 watts of corona power per 1,000 acfm (Figure 1). Once this "typically designed" capacity has been installed and tuned, assuming the application is correct, the operating corona power level falls in at approximately 1,100 watts. Due to the location of this power level on this operating curve, it can be seen that a significant power savings is possible with only minor changes in removal efficiency. When corrections for excessive rapping reentrainment, back corona, or sparking problems take place simultaneously with the power reduction, the removal efficiency may actually be increased while corona power is reduced.

Gas volume is inversely proportional to removal efficiency. Reducing the gas volume may be achieved by monitoring CO, O_2 or CO_2 levels and thereby trimming excess air to the boiler. Control of excess air levels can allow reduced corona power without decreasing removal efficiency and permit even further power savings in fan horsepower.

CLASSICAL PRECIPITATOR MODELS

A problem to be overcome when studying the power requirements of an existing precipitator is accurately predicting the effect of a particular change on the precipitator's performance. Various procedures attempt to describe the three fundamental phases of the precipitator process:

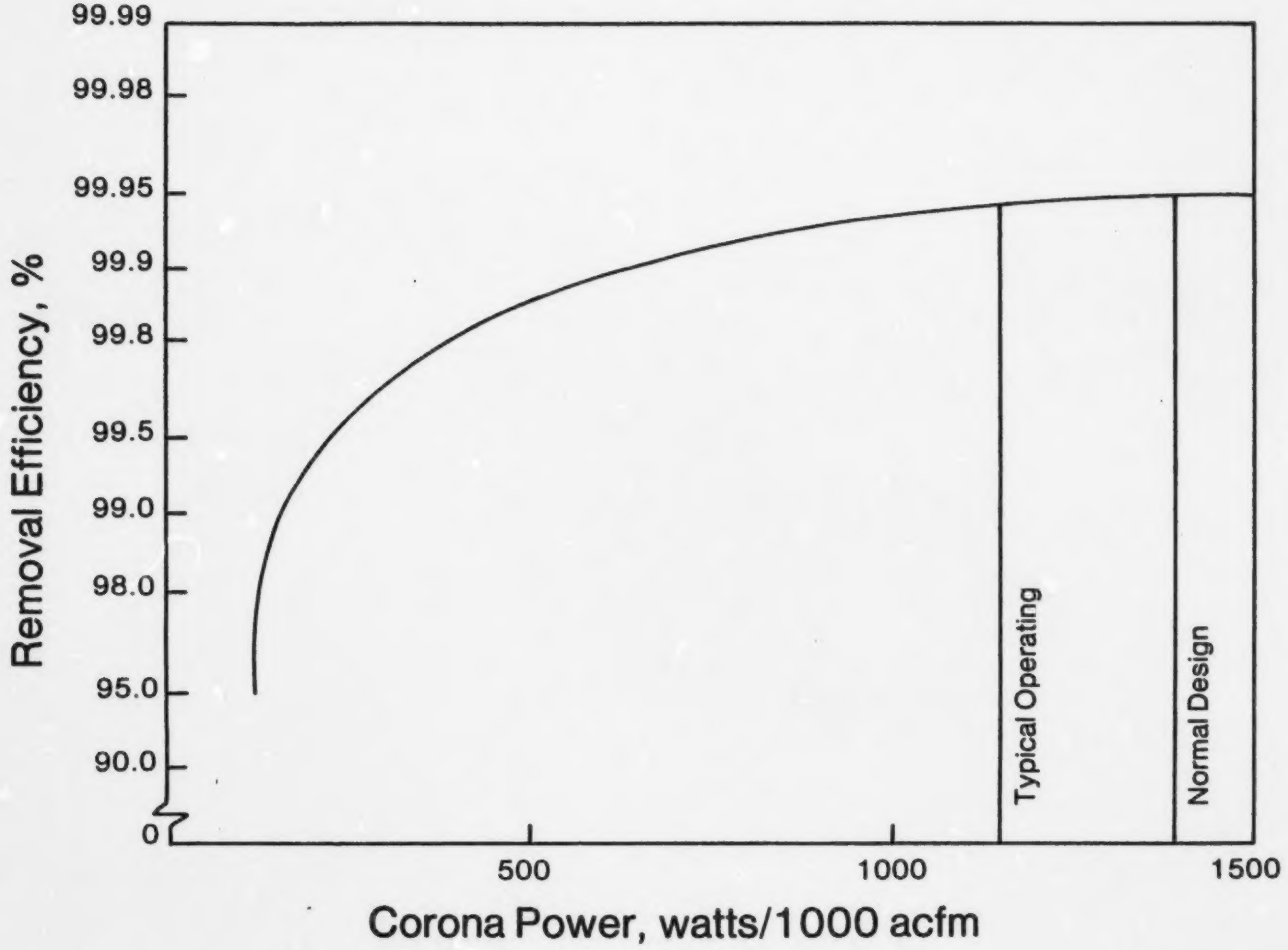

Figure 1. Removal Efficiency versus Corona Power

1. Particle charging.

2. Particle collection.

3. Removal of the collected particles from the system.

The Deutsch-Anderson equation and the Matts-Ohnfeldt modifications (Figure 2) are popular methods used to design and evaluate precipitators; but both have several limitations. They are empirical equations and do not account for all the factors which affect the ESP process. For example, they assume a uniform particle concentration at any cross section within the precipitator. They assume a constant migration velocity for all particles regardless of size or shape. They assume a perfectly uniform gas flow distribution. They do not acknowledge the existence of back corona, sparking effects or rapping reentrainment. They do not provide information concerning performance changes caused by the more subtle design modifications, such as discharge electrode spacing or changes in the number of fields within the same size precipitator casing and they ignore the effect of operating the equipment designed to remove the collected dust particles from the hoppers.

The Matts-Ohnfeldt modification does provide a mechanism for correcting the various shortcomings by incorporating a "catch-all" correction factor to force the equation results to agree with reality. The selection of this correction factor, however, requires a large base of past performance results. Since a large base of experience is needed to determine appropriate values for the migration velocity and constants involved, most organizations are unable to use these procedures to evaluate a precipitator in detail.

COMPUTERIZED PRECIPITATOR MODEL

The Southern Research Institute has developed a program for the EPA which can provide insight into the effect of various design and operating parameter changes. This program gives an organization without a large base of performance results the ability to predict the effects of various energy-saving schemes on precipitator performance. The program is based the exponential form of the Deutsch-Anderson equation. Some of the problems created by the various assumptions made are dealt with by taking advantage of the computer's ability to perform redundant operations with high speed. Essentially, the program breaks the actual precipitator into many smaller precipitators to minimize the effect of such assumptions as uniform particle size and constant electrical conditions. By this procedure, the need for empirical correction of the predicted result is reduced. However, empirical corrections are still made to adjust the results for some as-yet unmodeled effects such as rapping reentrainment, gas bypassage of electrical regions, nonuniform gas velocity distributions, particle concentration gradients and corona wind. Further modeling improvements should continue to reduce the number of empirical corrections required.

Although access to a large base of performance results is not needed, the model is not simple to use. Considerable time and effort must be invested in learning how to properly apply the program if it is to be used with success. Also, the program currently requires the use of a mainframe computer. Effort is underway to make the program available for public use on microcomputers,

Deutsch - Anderson Equation:

$$\text{Removal Efficiency} = 1 - e^{\left[\frac{-wA}{V}\right]}$$

Matts-Ohnfeldt Modification:

$$\text{Removal Efficiency} = 1 - e^{\left[\frac{-w_aA}{V}\right]^k}$$

Where:

w = migration (drift) velocity (an empirical constant)

w_a = average migration velocity (an empirical constant)

A = nominal collection plate area

$= 2(n-1) \times H \times (L_1 + L_2 + L_3, \text{etc.})$

where: n = number of collection plates per field

H = height of collection plates

L_1 = length of collection plates in 1st field

L_2 = length of collection plates in 2nd field

L_3 = etc.

V = volumetric gas flow rate

k = correcting factor (and empirical constant)

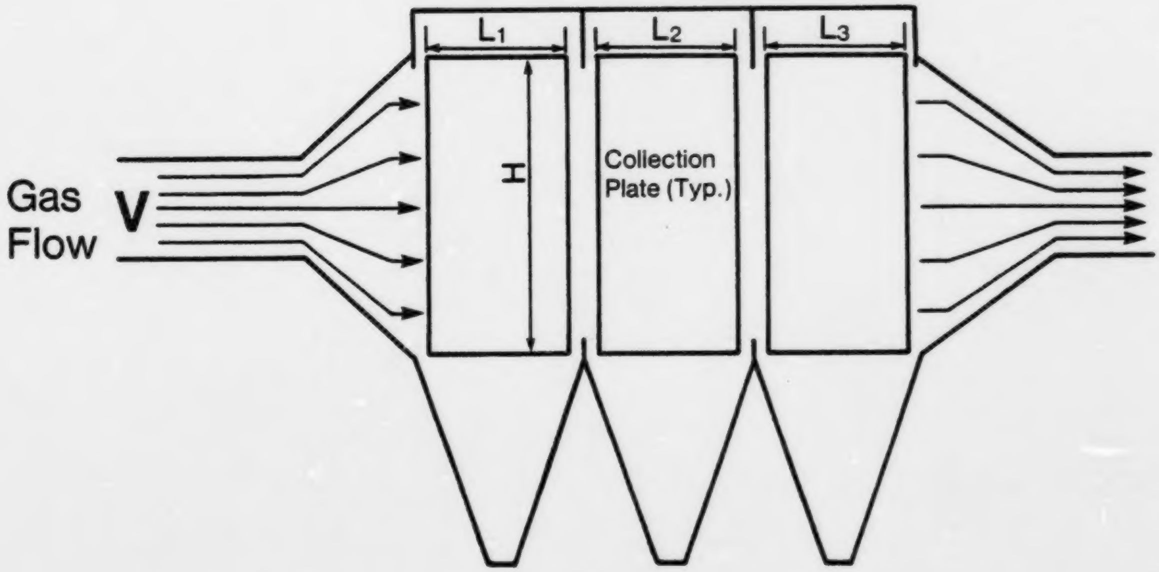

Figure 2. Empirical equations for electrostatic precipitator removal efficiency.

but as of this writing it has not been completed. This will eventually prove beneficial since it will make the program accessible to a wider range of users.

During the process of converting the program for use on microcomputers, the selection of a number of the less significant variables is being simplified or eliminated. Currently there are over 50 variables involved, some of which may not be needed and some of which may have little or no effect on the results, depending on how the program is applied. For example, an inexperienced user might make adjustments to the corona wire radius expecting to analyze a proposed discharge electrode design change. Depending the value of certain other variables, however, changing the corona wire radius will cause no change in the predicted result. Or, the resistivity value may be altered in an attempt to evaluate the possibility of changing the coal supply. The model does not have a procedure to specifically alert the user to a possible resistivity problem; therefore, the results may be impractical for use with that particular precipitator. The user may not realize this until it is too late to avoid a costly change in plans. However, if certain values in the program output are examined, there are ways to determine if the resistivity used may cause a problem and therefore affect the reliability of the final removal efficiency predicted.

Interpretation of the results must be performed carefully to avoid incorrect conclusions. The user must know how to analyze and interpret the results to ensure proper actions. However, once experience has been gained with the model and the model user understands its limitations as well as the internal procedures used in the program, evaluation of various energy-saving plans can become routine.

EVALUATION OF THE AVAILABLE POWER REDUCTION

Several things should be accomplished when evaluating a proposed microprocessor control system. The following can serve as a guide in this evaluation:

1. Conduct field testing and inspections (internal when possible) to determine the actual effect of the various power reduction schemes.

2. Through use of the previously discussed computer program, model the precipitator that is to receive the control system so that the reduction procedures can be optimized and the greatest possible savings gained.

3. Evaluate the economic feasibility of the proposed control system.

Field testing and computer modeling should go hand in hand. Field testing provides specific input needed to place a dollar value on the possible savings. It also verifies the ability to perform the projected power reduction without exceeding the emission and opacity requirements and helps verify the predictions of the computer model. The computer model, on the other hand, provides valuable insight to the most advantageous method for applying the proposed power reduction in the field. It also allows theoretical determination of the available cost savings, and helps determine the effect of changes in operating conditions which would otherwise be difficult or expensive to verify through actual field testing.

The field testing must be thorough enough to provide all the necessary information and should be designed to address any specific concerns of the prospective user of the control system to give them the confidence to use the system to the full extent of its capabilities. Depending on the decision-making criteria to be used, the test may include EPA Reference Method testing or simply take advantage of the opacity monitoring equipment already installed.

To illustrate the evaluation process, we recount the procedures and results of an evaluation performed for a utility located in the western United States. The objectives of the evaluation were as follows:

1. Determine how much the overall power consumption could be reduced without significant degradation of the removal efficiency, using the opacity monitor readings as the indicating parameter.

2. Determine the practicality of load-indexed power reduction as a normal mode of operation.

3. Address the utility maintenance staff's concern over transformer-rectifier (T/R) controller instability after extended periods of low-power and no-power operation.

4. Address the utility operation staff's concern over exceeding the design dust loading to the downstream wet scrubber caused by the possible inability of a centralized ESP control system to react to rapid changes in resulting in periods of increased dust load to the precipitator (increasing unit load, for example) operation of the generating unit. load, for example).

5. Evaluate the economic feasibility of a proposed microprocessor-based precipitator supervisory control system.

Field testing was performed and operating data was collected to achieve each of the above objectives. To determine the overall power reduction available without degradation of removal efficiency, the values of ESP and related operating parameters were obtained from the unit's computerized data logging system on a 1-minute interval, while 5 percent step reductions were manually applied to the dc voltages indicated on the individual T/R controllers. Power consumption data were recorded from the load centers supplying power to the precipitator and from the T/R controllers during these step-wise reductions.

To determine the practicality of using load-indexed power reductions, the testing described above was performed while the power station was operating at a high load (97 percent of the maximum continuous rating (MCR) of the unit) and at a low load (65 percent MCR). This resulted in information to develop the relationship between unit generating load and a start point for power reduction by the proposed supervisory control system.

To address the utility's concern over T/R controller instability after extended periods of low-power or no-power, the normal operating condition of a fourth-field T/R controller was recorded. The upstream T/R controllers were then reduced in power and the fourth-field T/R controller was deenergizedwhile the upstream T/R controllers remained at reduced power. The fourth-field controller's response was monitored when it was later reenergized. This provided data for evaluating the controller's instability after no-power operation.

The normal operating condition of another fourth-field T/R controller while the upstream T/R controllers were reduced in power. This fourth-field T/R controller was then reduced in power as well. Afterwards, all T/R controllers were returned to full-power operation. This provided data for evaluating the controller's instability after low-power operation.

To address the utility's concern over exceeding the inlet dust loading capacity of their wet scrubber, the computer model was used to simulate a 200 percent dust-load increase at the inlet to the precipitator with the ESP at reduced power. The model was used due to the difficulty and expense of artificially increasing the dust load by a controlled amount. The program variables were selected and the model was validated by comparing the model results with the results of EPA Method 5 testing. Then the program was rerun with a 200 percent dust load increase to determine the dust loading at the precipitator outlet and, consequently, at the wet scrubber inlet.

To evaluate the economic feasibility of the proposed supervisory control system, the power savings determined during the previously described field testing was adjusted for generating unit availability and efficiency, fuel analysis, and fuel cost data to provide a value for the power savings in dollars per year.

The results obtained for each objective were as follows:

1. At 97 percent of unit MCR, a power savings of at least 1.1 megawatts (MW) for the 575-MW unit was available. At 65 percent of unit MCR, a power savings of at least 1.3 MW was available. For test purposes the power reductions had been scheduled to continue until a significant deterioration in opacity occurred. However, reductions were stopped when various T/R controllers began to trip on undervoltage. The tripping was caused by reaching the preset voltage limits within the controller circuitry. Further power reductions could have been made by circumventing the low-voltage limits, taking care not to allow voltage to drop below the ionization voltage, however, these adjustments were not attempted. At the point where T/R tripping began, the opacity had increased less than 1 percent.

2. Through use of the computer program and the precipitator operating parameters measured during the field testing load-indexed power reduction was shown to be a viable procedure and can be applied to improve on the operating characteristics of some currently available supervisory control systems.

3. T/R controllers quickly (within a matter of seconds) return to stable, full-power automatic voltage control after extended periods of low-power and no-power operation.

4. A 200 percent increase in precipitator inlet dust loading did not exceed the designed dust load capacity of the downstream wet scrubber even under reduced power operation. Note that because of the design of the supervisory control system being evaluated, the precipitator power is increased during periods of such increased demand on the system.

5. The cost of the supervisory control system could be recovered within 2 years. This payback was considered very good, especially since the fuel costs were low ($0.99 per million Btu delivered).

TESTING FOR GUARANTEED POWER CONSUMPTION ON NEW UNITS

Field testing (as described above) is obviously not possible for new ESPs in the design or construction stage. Performance and power consumption data may be obtained from similar installations or from ESP pilot plants. Depending on the amount of similarity or the sophistication of the pilot plant, however, such data may not accurately represent the new ESP. Computer models can be used to predict potential power savings; however, a guaranteed power consumption value by the ESP manufacturer is probably the best estimate of actual operating power required to meet the specified particulate removal efficiency.

When power consumption guarantees are specified, test procedures for determination of penalty or bonus values should be established prior to the bidding. Testing specifications which clearly define the scope of the test and detailed procedures will prevent unnecessary arguments in the contract closeout stage in case the tested power consumption and/or performance does not coincide with the guarantee. The power consumption testing procedures must include:

1. Who is to be financially responsible for conducting the test and who is to be responsible for evaluation of the penalty/bonus value?

2. What components are to be included in the testing? That is, which components? For example, hopper heaters, seal air blowers, rappers, T/Rs, etc.?

3. When is the testing to be accomplished? For example, will it be conducted when the unit is first considered in commercial operation, within 1 year of that time, or at the time the contractor turns the equipment over to the owner? Will the power consumption test be accomplished in conjunction with the performance test?

4. How will the testing be conducted? That is, what measurements will be made and where? How long will the measurement be made? Will they be averaged over some time period? What criteria are to be established for operation of the unit? How will the data be

manipulated to determine the penalty/bonus value? What value will be assigned for a unit of power above or below the established design amount?

MICROPROCESSOR CONTROL SYSTEM FEATURES

When the potential power savings from operating an ESP at reduced corona power is sufficient to justify the initial cost, a supervisory mircoprocessor control system should be considered for both new and existing ESPs. Such a control system should have the capability for maximizing the power savings and should be designed for the owner's needs. The following list contains only some of the features that should be considered when evaluating a supervisory control system for use in reducing corona power:

1. Power Balancing Capabilities: Does the system actually balance the power input of the various controllers on a field-by-field and row-by-row basis or does it simply back power down on all controllers until opacity is increased to some level? A balancing capability can provide optimum power reduction without deteriorating the outlet emissions, and allow compensation for any T/R set which may be out of service.

2. Back Corona Analysis/Compensation: Does the system analyze and evaluate the existence of back corona and make appropriate adjustments to reduce its effect?

3. Single-Component Dependency: Does the system depend heavily on the performance of one piece of equipment such as the opacity monitor, which may prove to be a maintenance headache?

4. Rapper Supervision: Does the system analyze the optimum rapping sequences and initiate rapping when needed or just provide an adjustable timer to slow it down and speed it up?

5. Self-Diagnostics: Does the system have self-diagnostic routines to check itself and advise the user of potential trouble?

6. Expandable: Can the system be expanded later as additional uses become apparent?

7. Operator Adjustments: Does the system allow operator adjustment of variables such as setback, quench time, current and voltage limits, rate of rise, etc.?

8. Software Algorithms Availability: Is the software available to the user or is that considered proprietary by the supplier?

9. Power Consumption Data: Does the system provide information concerning power consumption for all T/R sets? What additional data logging capabilities are available?

10. Feed-Forward Capabilities: Does the system have a feed-forward capability or does it just increase power input after some preset emission limit is reached?

11. Failsafe Procedures: Does the system failsafe to the original automatic voltage control?

These and other features should be evaluated to determine which control system provides the greatest power reduction capability.

SUMMARY

Efforts to reduce power consumption by electrostatic precipitators should begin early during the design phase of the new plant. Ductwork arrangements and precipitator designs, auxiliary equipment and high voltage power supplies should be evaluated to determine cost-effective ways to reduce average operating power usage. Fan horsepower required to overcome ductwork losses should be considered during initial ductwork layouts and prior to selecting the design gas velocities. The design requirements and actual need for each type of auxiliary equipment should be determined on a case-by-case basis. To optimize the detailed design by the ESP manufacturer, a power consumption guarantee which coincides with the guaranteed removal efficiency should be specified. When the combination of power cost, plant operation and precipitator size is evaluated, a supervisory control system to meet the particular needs of the plant operator should also be considered.

Power reduction strategies for existing precipitators are similar to those for new designs. Simply reducing power consumption is not generally cost-effective. Installing additional equipment, such as turning vanes to reduce pressure drop or supervisory control systems for high voltage power supplies, is more likely to be economically attractive. The evaluation of such additional equipment for existing plants has a distinct advantage in that actual tests can be conducted to determine the economic benefit prior to actual installation.

The work described in this paper was not funded by the U.S. Environmental Protection Agency and therefore the contents do not necessarily reflect the views of the Agency and no official endorsement should be inferred.

* * * * *

Session 23: OPERATIONS AND MAINTENANCE II

Peter R. Goldbrunner, Chairman
Burns & Roe
Oradell, NJ

DESIGN CONSIDERATIONS TO AVOID COMMON FLY ASH CONVEYING PROBLEMS

by: Gus Monahu PE
Ash Systems Engineering, Inc
Elk Grove, IL 60007

Walter Piulle
Electric Power Research Institute
Palo Alto, CA 94303

ABSTRACT

Almost all fossil fueled steam generators have some sort of ash handling equipment and very few of these systems are considered to be totally satisfactory.

One of the main reasons for this, is the lack of an independent data base by which designers and users can assure themselves in advance that a system under consideration will do the job. The equipment vendors have regarded the underlying engineering to be proprietary and have guarded it relentlessly.

This paper presents five areas of consideration (and the methodology) which do not require proprietary knowledge to apply, and which should assist in specifying, designing and maintaining pipe line ash conveyors.

The paper addresses

- system capacity
- conveying velocity
- solids/air ratio
- conveyor layout
- pipe line conveyor construction

as they apply to dilute phase vacuum conveyors, which are by far the most prevalent in the United States, but the principles discussed offer insight to all types of pneumatic fly ash conveyors.

DESIGN CONSIDERATIONS TO AVOID COMMON FLY ASH CONVEYING PROBLEMS

BACKGROUND AND SCOPE

The suppliers of ash handling equipment have long considered the engineering underlying their systems to be proprietary and have guarded it zealously. As a result there is very little specific information available by which those interested in designing, specifying or maintaining ash handling systems can do so independently, with any degree of confidence.

Because of this lack of a data base and the often conflicting claims of the vendors of ash handling equipment, offerings are usually not examined and verified to the extent that other power house auxiliaries are.

The predominant work horse type particulate (fly ash) handling system in the U.S. is the vacuum pneumatic dilute phase pipe line conveyor, Figure 1. It is this type of system that this paper addresses. We will suggest some parameters and a methodology which an owner or engineer can use to help assure that a satisfactory system is being procurred, or alternately to suggest areas for improving existing, unsatisfactory systems.

The scope of this paper is limited to design considerations, not hardware. We will speak of hardware in generic or general terms, but do not make or imply comparisons between different types of equipment from different vendors.

There are numerous, subtle, ash handling system problems that go beyond the scope of a paper such as this. There are also a number of faults, including line plugging, excess line leakage, pipe failure and excessive abrasive wear that can be alleviated by attention to the parameters suggested here.

The topics discussed are

- system capacity
- conveying velocity
- solids/air loading
- conveyor layout
- pipeline conveyor construction

These five items, when not adequately addressed, account for a significant number of the problems in vacuum pneumatic ash (particulate) handling systems.

To examine each of these parameters we should define or discuss some of the applicable terms.

A glossary of these terms follows:

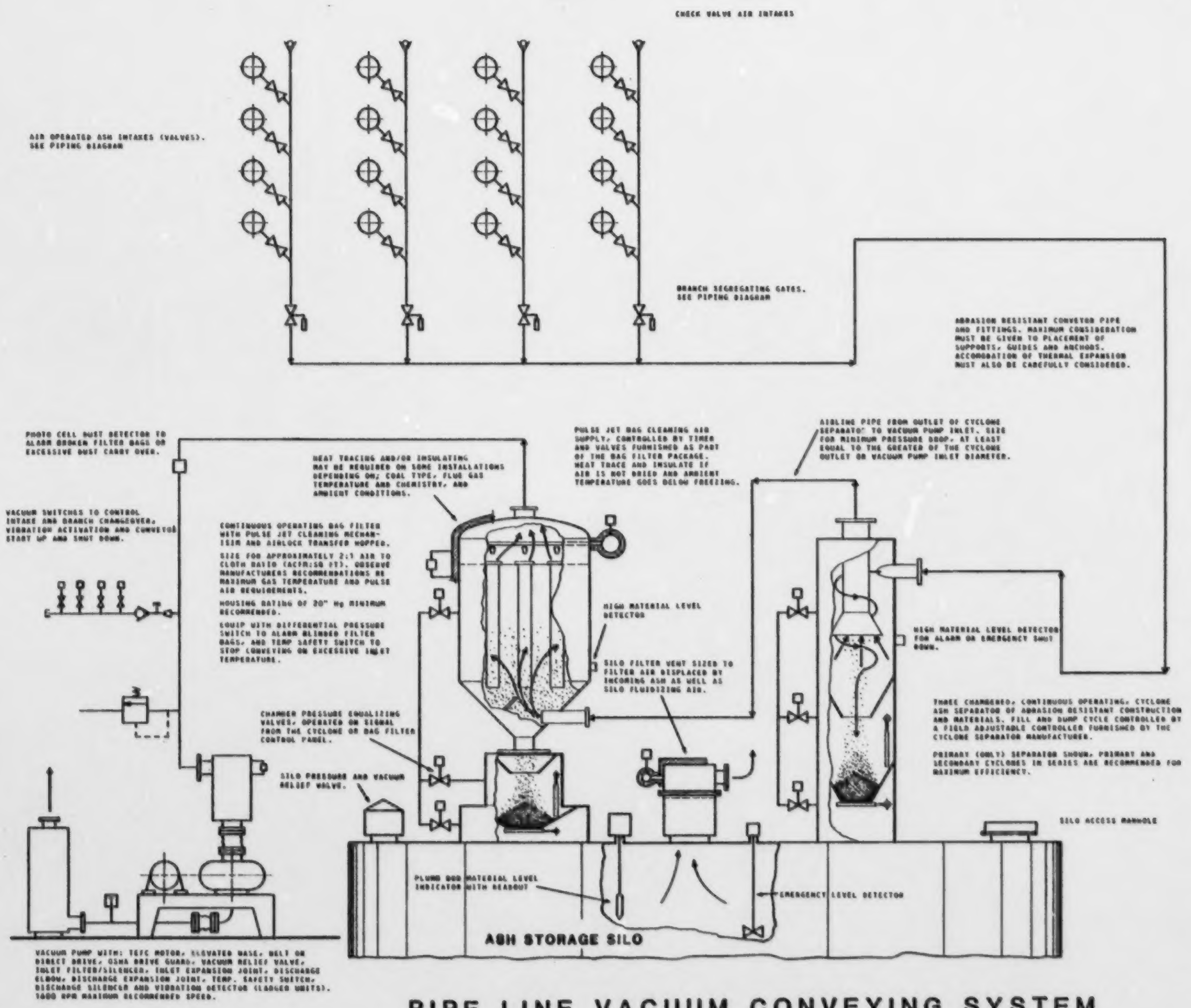
CHECK VALVE AIR INTAKES
AIR OPERATED ASH INTAKES (VALVES). SEE PIPING DIAGRAM
BRANCH SEGREGATING GATES. SEE PIPING DIAGRAM
ABRASION RESISTANT CONVEYOR PIPE AND FITTINGS. MAXIMUM CONSIDERATION MUST BE GIVEN TO PLACEMENT OF SUPPORTS, GUIDES AND ANCHORS. ACCOMODATION OF THERMAL EXPANSION MUST ALSO BE CAREFULLY CONSIDERED.
PHOTO CELL DUST DETECTOR TO ALARM BROKEN FILTER BAGS OR EXCESSIVE DUST CARRY OVER.
HEAT TRACING AND/OR INSULATING MAY BE REQUIRED ON SOME INSTALLATIONS DEPENDING ON; COAL TYPE, FLUE GAS TEMPERATURE AND CHEMISTRY, AND AMBIENT CONDITIONS.
PULSE JET BAG CLEANING AIR SUPPLY, CONTROLLED BY TIMER AND VALVES FURNISHED AS PART OF THE BAG FILTER PACKAGE. HEAT TRACE AND INSULATE IF AIR IS NOT DRIED AND AMBIENT TEMPERATURE GOES BELOW FREEZING.
AIRLINE PIPE FROM OUTLET OF CYCLONE SEPARATO" TO VACUUM PUMP INLET. SIZE FOR MINIMUM PRESSURE DROP. AT LEAST EQUAL TO THE GREATER OF THE CYCLONE OUTLET OR VACUUM PUMP INLET DIAMETER.
VACUUM SWITCHES TO CONTROL INTAKE AND BRANCH CHANGEOVER, VIBRATION ACTIVATION AND CONVEYOR START UP AND SHUT DOWN.
CONTINUOUS OPERATING BAG FILTER WITH PULSE JET CLEANING MECHANISIM AND AIRLOCK TRANSFER HOPPER.
SIZE FOR APPROXIMATELY 2:1 AIR TO CLOTH RATIO (ACFM:SQ FT). OBSERVE MANUFACTURERS RECOMMENDATIONS RE MAXIMUM GAS TEMPERATURE AND PULSE AIR REQUIREMENTS.
HOUSING RATING OF 20" Hg MINIMUM RECOMMENDED.
EQUIP WITH DIFFERENTIAL PRESSURE SWITCH TO ALARM BLINDED FILTER BAGS, AND TEMP SAFETY SWITCH TO STOP CONVEYING ON EXCESSIVE INLET TEMPERATURE.
HIGH MATERIAL LEVEL DETECTOR
SILO FILTER VENT SIZED TO FILTER AIR DISPLACED BY INCOMING ASH AS WELL AS SILO FLUIDIZING AIR.
HIGH MATERIAL LEVEL DETECTOR FOR ALARM OR EMERGENCY SHUT DOWN.
THREE CHAMBERED, CONTINUOUS OPERATING, CYCLONE ASH SEPARATOR OF ABRASION RESISTANT CONSTRUCTION AND MATERIALS. FILL AND DUMP CYCLE CONTROLLED BY A FIELD ADJUSTABLE CONTROLLER FURNISHED BY THE CYCLONE SEPARATOR MANUFACTURER.
PRIMARY (ONLY) SEPARATOR SHOWN. PRIMARY AND SECONDARY CYCLONES IN SERIES ARE RECOMMENDED FOR MAXIMUM EFFICIENCY.
CHAMBER PRESSURE EQUALIZING VALVES, OPERATED ON SIGNAL FROM THE CYCLONE OR BAG FILTER CONTROL PANEL.
SILO PRESSURE AND VACUUM RELIEF VALVE.
SILO ACCESS MANHOLE
PLUMB BOB MATERIAL LEVEL INDICATOR WITH READOUT
EMERGENCY LEVEL DETECTOR
ASH STORAGE SILO
VACUUM PUMP WITH: TEFC MOTOR, ELEVATED BASE, BELT OR DIRECT DRIVE, OSHA DRIVE GUARD, VACUUM RELIEF VALVE, INLET FILTER/SILENCER, INLET EXPANSION JOINT, DISCHARGE ELBOW, DISCHARGE EXPANSION JOINT, TEMP. SAFETY SWITCH, DISCHARGE SILENCER AND VIBRATION DETECTOR (LARGER UNITS). 1800 RPM MAXIMUM RECOMMENDED SPEED.

PIPE LINE VACUUM CONVEYING SYSTEM figure 1

SOURCE: ELECTRIC POWER RESEARCH INSTITUTE (1)

Guide - a restraint on a pipe line conveyor which restricts lateral movements, but allows axial movement.

Hanger - a support on a pipe line conveyor suspended from above which allows some random movement. In the case of a spring hanger, at a controlled rate.

Dilute Phase - Generally taken to be two phase conveying where the solids to fluid loading is in the range of 25 -30 lbs. per lb., or less.

Loading - the ratio by weight, of solids to fluid in two phase pipe line flow. Usually expressed in lbs/lb. Loading is sometime expressed in lbs. of solid per cf of fluid but this is less common.

Capacity, Net - the specified capacity of the ash handling system over a sustained period of time, this should include allowances for; sequencing, irregularities of feed, instrumentation lag and component response, and be based on an average conveying distance from an "average intake".

Velocity, or conveying velocity, if not further defined is usually taken to be the superficial velocity or the calculated velocity of a volume of fluid thru a pipe of given cross section. This takes the familiar form:

$$V = Q/A \quad \text{eg} \quad V = \frac{\frac{80\ \text{lb}}{\text{min}} \times \frac{\text{ft}^3}{.075\ \text{lb}}}{.0352\ \text{ft}^2} = 3030 \text{ ft per min.}$$

The velocity so defined is usually used in two phase pipe-line conveyor specifications and literature. In truth it is neither the actual velocity of the fluid or the solid but for the sake of convention we will continue to use it in this context.

Velocity, Starting - the fluid velocity thru a pipe line required to entrain a given sample of particulate into the fluid stream starting from rest at the bottom of the pipe. Starting velocity is determined empirically.

Velocity, Saltation - the particle velocity in two phase flow at which the particles pass back and forth between entrained flow and sliding flow. During saltation solids are concentrated in the bottom part of the pipe. At less than the saltation velocity the particles will settle out of the fluid stream.

Collection Points - although a typical ash handling system serves mill reject and bottom ash collection devices, our paper concerns itself only with particulate collection points, i.e the precipitator or fabric filter, the air heater hoppers and to a lesser extent the economizer hoppers, figure 2.

General characteristics of the particulate at each of these collection points are:

Precipitator or bag house particulate as "seen" by the conveying system can be generalized as 50 to 400 microns @ 275°F to 350°F in cold side precipitators and in the range of 50 to 150 microns at 400° to 800°F in hot side precips. The particulate is size classified by the electrostatic precipitator with the

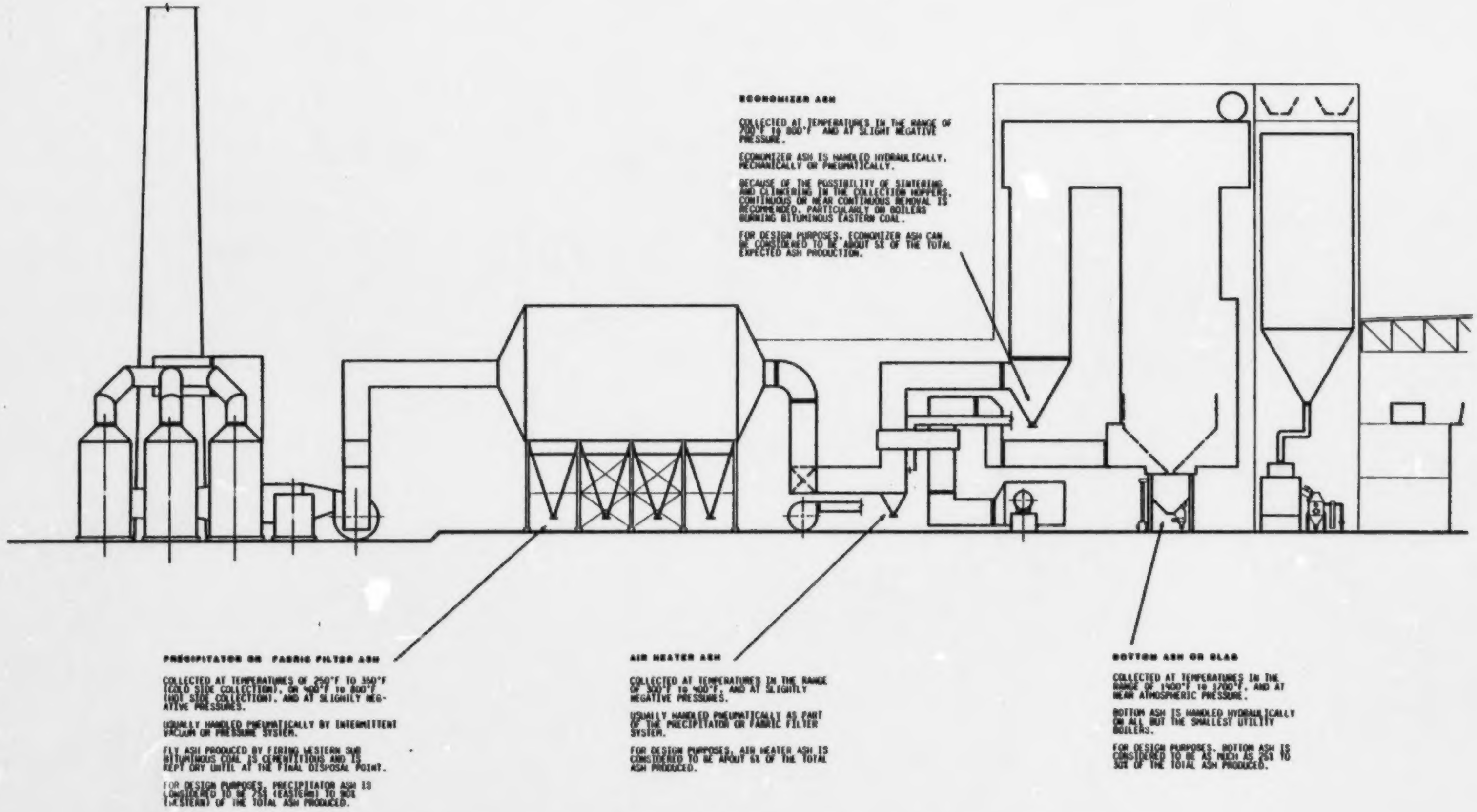

ECONOMIZER ASH

COLLECTED AT TEMPERATURES IN THE RANGE OF 700°F TO 800°F AND AT SLIGHT NEGATIVE PRESSURE.

ECONOMIZER ASH IS HANDLED HYDRAULICALLY, MECHANICALLY OR PNEUMATICALLY.

BECAUSE OF THE POSSIBILITY OF SINTERING AND CLINKERING IN THE COLLECTION HOPPERS, CONTINUOUS OR NEAR CONTINUOUS REMOVAL IS RECOMMENDED, PARTICULARLY ON BOILERS BURNING BITUMINOUS EASTERN COAL.

FOR DESIGN PURPOSES, ECONOMIZER ASH CAN BE CONSIDERED TO BE ABOUT 5% OF THE TOTAL EXPECTED ASH PRODUCTION.

PRECIPITATOR OR FABRIC FILTER ASH

COLLECTED AT TEMPERATURES OF 250°F TO 350°F (COLD SIDE COLLECTION), OR 400°F TO 800°F (HOT SIDE COLLECTION), AND AT SLIGHTLY NEGATIVE PRESSURES.

USUALLY HANDLED PNEUMATICALLY BY INTERMITTENT VACUUM OR PRESSURE SYSTEM.

FLY ASH PRODUCED BY FIRING WESTERN SUB BITUMINOUS COAL IS CEMENTITIOUS AND IS KEPT DRY UNTIL AT THE FINAL DISPOSAL POINT.

FOR DESIGN PURPOSES, PRECIPITATOR ASH IS CONSIDERED TO BE 75% (EASTERN) TO 90% (WESTERN) OF THE TOTAL ASH PRODUCED.

AIR HEATER ASH

COLLECTED AT TEMPERATURES IN THE RANGE OF 300°F TO 400°F, AND AT SLIGHTLY NEGATIVE PRESSURES.

USUALLY HANDLED PNEUMATICALLY AS PART OF THE PRECIPITATOR OR FABRIC FILTER SYSTEM.

FOR DESIGN PURPOSES, AIR HEATER ASH IS CONSIDERED TO BE ABOUT 6% OF THE TOTAL ASH PRODUCED.

BOTTOM ASH OR SLAG

COLLECTED AT TEMPERATURES IN THE RANGE OF 1400°F TO 1700°F, AND AT NEAR ATMOSPHERIC PRESSURE.

BOTTOM ASH IS HANDLED HYDRAULICALLY ON ALL BUT THE SMALLEST UTILITY BOILERS.

FOR DESIGN PURPOSES, BOTTOM ASH IS CONSIDERED TO BE AS MUCH AS 25% TO 30% OF THE TOTAL ASH PRODUCED.

PULVERIZED COAL FIRED BOILER - ASH COLLECTION POINTS

PARTICULATE COLLECTION POINTS　　figure 2

SOURCE: ELECTRIC POWER RESEARCH INSTITUTE (1) coarsest ash collected in the front hopper and the finest at the rear.

Bag house or fabric filter catch is uniform thru the collector hoppers and usually in the range of 100 microns at 250°F to 350°F.

Air heater particulate - usually slightly coarser than precipitator ash and fairly uniform in size. Air heater ash ranges in size from 100 to 800 microns and are collected at temperatures in the range of 250°F to 400°F.

Economizer particulate - while classified as particulate, contains pebble and stone like particles between 1/4" and 2" in size, frequently with a high combustible content. The normal temperature range varies between 600°F and 900°F.

It should be pointed out that because of the temperatures, size distribution and combustible content, intermittent pipe line conveyors are not the best way to transport economizer ash, but this is still the most common method.

REQUIRED CAPACITY

A frequent complaint in pipe line ash handling systems is that of inadequate system capacity which results in excessively long operating cycles, which do not allow adequate time for maintenance and may not even keep up with the collection of ash. It is possible that the inadequate capacity is a result of system deterioration or changed operating conditions, (eg, burning coal with a higher than design ash content). While some of these conditions can be dealt with, basic system inadequacy cannot be overcome. This raises the question, what should the specified capacity be?

The traditional, industry rule of thumb is to specify a handling capacity of two times the particulate collection rate. This is intended to provide time for maintenance and repairs between conveying cycles.

This rule of thumb can certainly be varied depending on site specific circumstances. If redundant key equipment is installed capacity can be less. If, on the other hand multiple conveying systems share a single component, capacity should be greater. The required conveying capacity is also influenced by the amount of ash storage available in the collection hoppers, and the willingness to utilize that storage.

The expected collection rate on which capacity is to be based is somewhat arbitraily established. The boiler and collection equipment manufacturers should be consulted for guidance.

We can generalize the following quantities for design:

Pulverized coal boilers:

- Precipitators or bag houses 75% to 90% of total ash

- Air heaters 5% of total ash
- Economizers 5% of total ash

Stoker fired boilers:

- Bottom ash (handled pneumatically) 60% of total ash
- Siftings hoppers 5% of tota ash
- Rear pass hoppers 7% of total ash
- Economizer (if used) 5% of total ash
- Air Heater (if used) 5% of total ash
- Precipitator or baghouse 20-30% of total ash

Example:

A pulverized coal boiler fires 63 tph coal having a design ash content of 10.35 %. The expected collection of particulate is

Precipitator 63 tph x .1035(%) x .80(%) = 5.22 tph
Air heater " " x .05(%) = 0.33 "
Economizer " " x .05(%) = 0.33 tph

total particulate collected = 5.88 tph

With a total calculated particulate collection rate of approximately 5.9 tph, a removal and handling systems of approximately 12 tph net capacity would be appropriate. The gross capacity of the system should be 10 to 20% greater to allow for start-up, sequencing, erratic material feed and shut down.

Having decided on a system capacity (in tph) we can now turn our attention to conveyor size and conveying velocity.

Velocity is the major item of disagreement among equipment vendors. Those advocating a low velocity cite reduced wear and power requirements as justification. The proponents of conveying at higher velocity point to reduced tendency to plug the pipeline and increased allowances for system deterioration

Both are correct as far as they go, unfortunately the user doesn't feel very confident about making a decision either way.

We are all agreed that the optimum velocity is the minimum one that will reliably and consistantly do the job. The disagreement is on what that velocity is. Fortunately there is a parameter which can be used to more objectively specify conveying velocity. This is Owens' Criteria (2) which we will examine after we decide on the conveyor size.

CONVEYOR SIZE

Having determined the required system capacity we can now make a reasonable estimate of the required pipe size.

With an assumed maximum loading of 25 lbs. ash/lb. air, and an assumed initial conveying velocity of 3500 fpm, the following table relates the maximum theoretical gross capacity in tph to pipe diameter.

Table 1. Maximum Capacity vs. Pipe Diameter

pipe dia. inches	pipe area sq. ft.	air flow lbs/min	solids loading lbs/min	max capacity tph
4	0.088	23.1	557	16.7
6	0.198	51.9	1297	38.9
7	0.270	70.6	1765	52.9
8	0.352	92.4	2310	69.3
9	0.446	116.9	2922	89.7
10	0.550	144	3600	108
12	0.790	207	5175	155

Again this a maximum capacity for a given pipe size based on the loading and velocity limits we have set. The actual capacity will probably be lower due to a number of factors, including:

- feed rate out of collection hopper
- feed rate into the conveyor intake
- cycle efficiency of the system
- length and routing of pipe line conveyor
- temperature and/or altitude
- possible lower velocity
- possible lower loading ratio

In our example we require a net conveying capacity of 12 tph. A gross capacity 10 to 20% greater would be used to design the system. We therefore need a system capacity in the range of 13.2 tph to 14.4 tph. For purposes of further illustration we will speak of a 15 tph system.

It is reasonable and conservative to use one pipe size larger than indicated as an allowance against any of the listed conditions. In our example a 15 tph capacity system is required. This would indicate (according to table 1) a 4" system. It would be more practical to increase one size and examine a 6" diameter pipe line conveyor.

OWENS' CRITERIA (2)

As mentioned earlier the trade offs of reducing or increasing velocity are excessive wear or increased tendency to plug. The optimum velocity is the minimum that gives assurance against plugging. Owens' criteria which predicts the velocity at which saltation occurs is a very useful tool in determining the required minimum velocity. The authors, based on a proprietary study (3), recommend that Owens' criteria for the dilute phase pneumatic transport of ash be equal to at least 0.2.

This recommends Owens Criteria

$$0.134 \frac{m^2 T \ f_f}{d^4 \ P \ \rho_p \quad D_p} = 0.2$$

where m = air flow- lbs/min.
d = inside diameter of pipe - inches
T = flue gas temperature - °R
f_f = Darcy friction factor
D_p = particle diameter - feet [1]
ρ_p = particle density - lbs/ft^3
P = starting conveyor pressure - lbs/in absolute
use 14.7 for vacuum conveying systems

The friction factor f_f can be determined using principles of fluid mechanics and the Moody diagram. For flow thru commercial steel or cast pipe and with the temperatures and fluid viscosity encountered in ash handling, A friction factor in the range of 0.018 to 0.024 is appropriate.

since $m = V \times A \times \rho_f$

where V = velocity in fpm
A = area of pipe i.d. in ft^2
ρ_f= density of fluid (flue gas) in lbs/ft^3

We can solve directly for V, the required conveying velocity.

$$V = \left(\frac{.2 \times d^4 P \times f_f \times D_p}{.0134 \times T \times f_f} \right)^{\frac{1}{2}} \cdot \frac{1}{A \ \rho_f}$$

To continue our example, input data is

d = 6"
T = 300 °F = 760 °R
f_f = 0.02

---

(1) particle size is taken from the sieve which passes 60% of the sample

D_p = 150μ = 4.9×10^{-4}ft
ρ_p = 126 lb per ft^3 (sp gr = 2.0)
P = 14.7 psia
ρ_f = 0.052 lbs/ft^3 (density of air at 300° F

The density of air (flue gas) at any given temperature can be readily calculated using the Gas Laws, but Table 2 following, gives a ready reference.

Table 2. Air Density at Other Than Standard Temperature

T°F	T°R	Air Density lbs/cu ft
70	530	0.075 lbs/ft
250	710	0.056
300	760	0.052
400	860	0.046
500	960	0.041
600	1060	0.037
700	1160	0.034

Solving our equation yields:

$$V = \left(\frac{.2 \times 6^2 \times 14.7 \times 4.9 \times 10^{-4}}{.0134 \times 760 \times 0.02} \right)^{.5} \times \frac{4 \times 144}{\pi \times 6^2 \times .052} = 3326 \text{ fpm}$$

and $m = V \times A \rho_f$

$= 3326 \times .196 \times .052 = 33.9$ lbs per min air

$$\text{ash} = \frac{15t}{hr} \times \frac{2000 \text{ lb}}{ton} \times \frac{hr}{60 \text{ min}} = 500 \text{ lbs per min.}$$

LOADING

Loading has already been defined as the weight ratio of solids to fluid (air, flue gas etc). It is a measure of conveyor efficiency. Obviously if we are transporting 20 lbs of ash with each lb of air our operation is more efficient than if we are transporting only 5 lbs per lb.

While we want optimum loading, it is not always within our control to obtain it. Loading is a function of design capacity and also of conveyor length and configuration. Pipe sizes are available in finite steps. A six inch conveyor could be used for both a 15 tph system or a 25 tph system. At the same velocity the latter system would of course have the higher concentration of ash, i.e. a higher loading.

If a pipe line conveyor is operating at a lower loading than designed for, wear is accelerated. This reduced loading can be due to; air leakage into the conveyor, slow feed out of the collection hopper or obstruction in the line. When loading is reduced the vacuum producer can pull more air (this is analagous to a water pump operating "down the curve"). The greater air flow means greater velocity and hence increased wear. It should be kept in mind that conveyor line wear increases exponentially with velocity.

Because some owners wish to keep the collection hoppers empty (probably to alleviate other problems), they operate their pipe line conveyors continuously. The hoppers are always nearly empty, the feed of ash into the conveyor is light and the loading is low. The results are high velocity and wear.

As we can now appreciate, loading is an important parameter that does not always get the attention or thought that it merits. The writers recommend loading limits of 5 lbs per lb to 25 lbs per lb and a target range of 15 lbs per lb to 22 lbs per lb.

Using our 15 tph example again (from the previous page):

the solids rate = 500 lbs/min
the air rate = 33.90 lbs/min

Therefore the loading is:

500/33.90 = 14.75 lbs per lb

This is acceptable although at the low end of our 15 to 22 lb per lb target range. In actual practice it would be worthwhile to recheck; Owens Criteria, velocity and loading for a 4" conveyor. The final decision would be based on considerations such as power requirement, motor size, vacuum pump size etc.

At this point we have decided on reasonable conveying capacity and conveying velocity and have a realistic idea of required pipe size and the loading.

This should be included in the specifications issued to vendors who should be asked to support non-compliance, with calculations.

CONVEYOR DETAILS

Next to be considered is layout. All pipeline conveyors will have changes of direction so elbows or tees of different configurations are used.

Conveyor Configuration

At every change of direction in the pneumatic pipe line conveyor, the particle velocity is reduced. This decrease in particle velocity occurs because the particles scrape around the outside of the bend where they have been thrust by momentum and centrifugal force, thus slowing down.

If this reduction in velocity is great enough, the partical velocity may go below the velocity of saltation and material will settle out in the pipe. If enough material settles out, pipe plugging is likely. After coming out of the change of direction, the particles will normally accelerate again.

The greatest danger (from a plugging standpoint) occurs when there are two or more changes of direction close together in the pipe line. If a second change of direction occurs before the ash has accelerated and is at a lower than design velocity, the further slowing at the second bend can lead to slugging and plugging. Because of the physics involved, which are beyond the scope of this paper, sucessive turns in the same direction are more detrimental than alternating turns.

As a rule of thumb, changes in direction should be at least ten pipe diameters apart. For example, in an 8" pipe line conveyor there should be straight section of pipe at least 80" long between successive changes of direction.

Inclines

All but the shortest inclines should be avoided. In horizontal runs particles drop down to the surface of the pipe and then are re-entrained into the flow. On inclined surfaces the contact on the bottom of the pipe is for a longer period of time resulting in increased power requirements and increased pipe wear.

Parenthetically, on vertical runs there is minimal particle impact on the pipe wall. This results in low pipe wear which is fortunate since vertical pipe runs are usually the least accessible for maintenance.

Transitions (Increasing Pipe Size)

Head Loss, or the power required to transport the particulate in a pipe line is geometrically proportional to velocity. The velocity increases (as the conveying fluid expands) from intake to the end of conveyor where the pressure is lowest). If we minimize velocity we can minimize head loss, and hence the power required, however, we do not want the initial velocity to be less than that indicated by Owens' criteria.

One way to minimize velocity for a given mass flow is to increase the pipe size (area). However, we need a minimum initial velocity as discussed earlier. This can be done by expanding the conveyor to a larger pipe size at a point where the solids velocity has accelerated so that the resulting decrease in velocity (at the increase in pipe area) still does not allow salation to occur. It is not necessary to maintain the originally determined conveying velocity since the ash is already in motion rather than being slowly introduced into the conveyor as at a feeder or intake.

The allowable percentage reduction in velocity is a subject of some debate, with velocities in the range of 60% to 85% of original being advocated. The authors recommend the velocity at the transition (to larger pipe) be not less than 75% of the calculated design velocity determined by Owens' Criteria.

PIPE LINE MATERIALS

Because fly ash is a hard, abrasive material, and abrasive wear of system components is common place, there has been a trend to harder and more brittle alloy pipe. This is not always beneficial.

High hardness alloy pipe should be avoided on systems handling high temperature ash and should be carefully re-considered on positive pressure systems.

Although the conveyed ash is usually in suspension in the moving air stream, there are times when the ash particles drop to and rub along the bottom of the pipe. This has two effects; wear is greatest at the bottom of the pipe and temperature rise is greatest there.

In a system serving a hot side precipitator, or in the branch serving the economizer hoppers, there can be a very significant difference in temperature between the top of the pipe and the bottom. This temperature difference means the bottom of the pipe wants to expand linearly to a greater extent than the top of the pipe. Normally the pipe would bow because of this differential expansion. Since high hardness alloy pipe is brittle, it does not bow but could break instead if the ΔT, and stresses become great enough.

Broken pipe is the utlimate conveyor line failure, and is not offset by abrasion resistance. On those systems with ash temperatures in excess of 500°F, the use of welded steel pipe is recommended. When this is done, it is important that the I.D. of the pipe match the I.D. of the cast fittings to minimize turbulence and aggravated wear.

The use of welded steel pipe or tube will provide a tight, flexible conveyor where the advantages outweigh the loss of abrasion resistance.

Pipe Couplings, Anchors and Expansion Joints

A surprising number of complaints regarding pipeline conveyors, stem from inadequate or incorrect pipe coupling and anchoring systems. The resulting problems are more pronounced on high temperature systems, but the potential for problems exists on all pipe line conveyors.

When a conveying system is in operation it is subjected to both static and dynamic forces and both internally and externally imposed movement. All collection hoppers served by pipeline conveyors undergo some movement in heating up from the cold, or off line temperature, to the maximum operating temperature. The movements that concern us are those of the interface to the ash handling system, i.e. the hopper outlets.

As shown in figure 3 these thermal growth movements occur in all three planes of orientation.

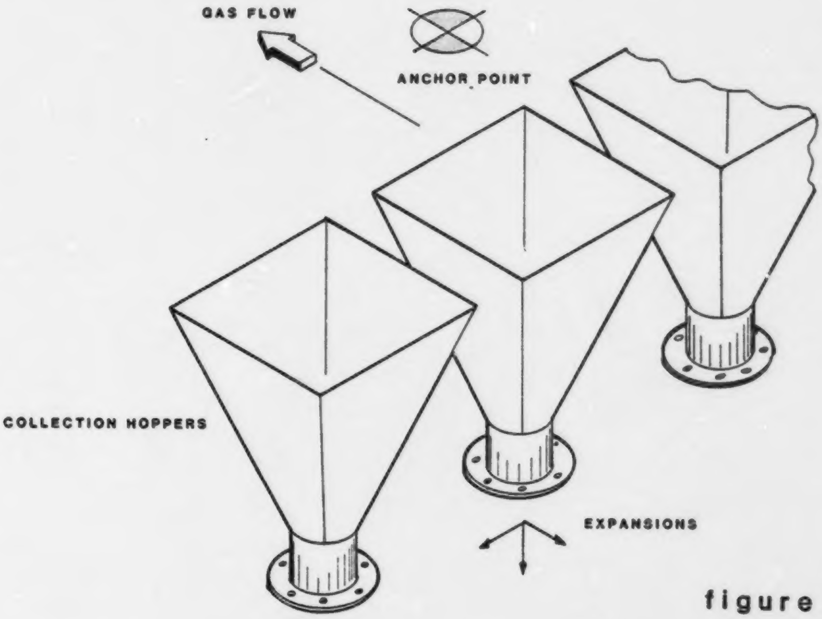

figure 3

THERMAL MOVEMENTS of COLLECTION HOPPERS

Since the ash handling equipment is rigidly connected to these outlets, the movements must be accomodated by the ash conveyor while the leak free integrity of the conveyor is maintained. If small, the movements can be accomodated in the couplings connecting the conveyor components together. If of a larger magnitude, expansion joints should be employed.

Where provision for expansion is inadequate, the pipeline can pull apart or break and the forces due to expansion can bind gates preventing them from opening or closing completely.

By way of example, if an 18 ft. length of 8" cast alloy pipe were completely constrained while heated from 70°F to 250°F, the axial force developed by the pipe would be in excess of 500,000 pounds. The developed forces are certainly sufficient to break the pipe, pull apart connections and bind line gates and valves. All of these lead to greatly reduced system capacity or even total system failure.

To avoid these problems and assure that the expansion joints will perform as intended, a carefully engineered system of pipe supports, guides and anchors should be provided.

Generally anchors are required at each change of direction of the pipeline conveyor, at the outlet of most expansion joints and near the inlet of most line gates. By "anchors" we mean the restriction of all movement in any direction, with respect to the "earth", or plant structure. On those systems using plain end, rather than beveled or flanged end pipe and fittings, the anchors at each change of direction are especially important.

While some portions of the pipe line conveyor must be anchored, there are other parts that should be free to move axially, laterally or in combination. This is accomplished (respectivelly) by the use of pipe guides which allow axial movement only, and spring hangers which allow lateral movement at a controlled rate.

Spring hangers would be used to support the conveyor in proximity to the collection hoppers which move. The spring hangers would allow the pipe to move with the hoppers to which it is attached while providing support of the pipe and connections.

Guides would be used on long runs of pipe to allow thermal growth into the expansion joint(s) provided to accomodate it.

CONCLUSION

If the user will consider and apply the parameters presented here; capacity, velocity, loading, layout and pipe line details, more satisfactory conveyors will result. In fact, if the user examines each in the detail suggested, he will be capable of reviewing vendor designs and recommendations from an informed perspective.

The work described in this paper was not funded by the U.S. Environmental Protection Agency and therefore the contents do not necessarily reflect the views of the Agency and no official endorsement should be inferred.

REFERENCES

1. Ash Handling Reference Manual . Palo Alto, CA: Electric Power Research Institute, 1984 . RP-1835-4

2. Owens, J., In: Fluid Mech 20 (1964), p. 225

3. Brown, M.W., Monahu, G.T., unpublished study of fly ash conveyor failures.

FEASIBILITY OF USING PARAMETER MONITORING AS AN AID IN DETERMINING CONTINUING COMPLIANCE OF PARTICULATE CONTROL DEVICES

by: Joseph Carvitti, Michael F. Szabo, and William Kemner
PEDCo Environmental, Inc.
Cincinnati, Ohio 45246

ABSTRACT

This paper on the feasibility of parameter monitoring as a continuing compliance tool includes a discussion of the relationships between parameters and emissions or performance, and the accuracy, reliability, and cost of parameter monitoring compared with other methods of measuring emissions. Also included is a discussion of the appropriate uses of parameter monitoring, the current availability of documented data, data needs for future implementation of parameter monitoring, and the interaction required between the source and the control agency to assure cooperation in the implementation of the concept. The paper presents the results of a preliminary assessment to 1) ascertain the feasibility of using parameter monitoring to measure continuing compliance of stationary sources, 2) identify examples of its current application, and 3) identify issues that would need to be addressed in widespread use of parameter monitoring.

The following potential advantages make parameter monitoring appear to be an attractive tool for ascertaining continuing compliance:

- Provides an inexpensive check on proper operation and maintenance.
- Provides diagnostic assistance during malfunctions.
- Permits the efficient use of control agency personnel.
- Establishes a strong basis for compliance determination.
- Allows the source to initiate corrective action without control agency involvement.

A major hindrance to widespread application of parameter monitoring appears to be the lack of a large body of data documenting the use and importance of parameter monitoring in the day-to-day operation of stationary sources.

The work described in this paper was funded by the U.S. Environmental Protection Agency and has been reviewed in accordance with the U.S. Environmental Protection Agency's peer and administrative review policies and approved for presentation and publication.

INTRODUCTION

The concept of parameter monitoring is not new. Various sources have used this approach for many years as a process control for product quality and quantity. Also, control equipment operators have used it in the operation and maintenance of their equipment and as a relatively unsophisticated indicator of equipment performance. Some of the parameters commonly monitored in the pollution control field include pressure drop in scrubbers and fabric filters, and voltage and current levels in electrostatic precipitators. These parameters have been used as a qualitative measurement of the performance levels or capabilities of this equipment.

The following potential advantages make parameter monitoring appear to be an attractive tool for ascertaining continuing compliance:

- Provides an inexpensive check on proper operation and maintenance.
- Provides diagnostic assistance during malfunctions.
- Permits the efficient use of control agency personnel.
- Establishes a strong basis for compliance determination.
- Allows the source to initiate corrective action without control agency involvement.

A major hindrance to widespread application of parameter monitoring appears to be the lack of a large body of data documenting the use and importance of parameter monitoring in the day-to-day operation of stationary sources.

While the air pollution control regulations of several states specifically include parameter monitoring for stationary sources, most include only general provisions regarding good engineering practice in the operation and maintenance (O&M) of emission control equipment. Still other state regulations merely allude to parameter monitoring through process monitoring requirements, process or control equipment operating conditions, or operating permit requirements.

This evaluation of the feasibility of parameter monitoring as a continuing compliance tool includes not only the relationships between parameters and emissions or performance, but also the accuracy, reliability, and cost of parameter monitoring compared with other methods of measuring emissions (i.e., continuous emission monitors (CEM's) and stack tests). Also included is a discussion of the appropriate uses of parameter monitoring, the current availability of documented data, data needs for future implementation of parameter monitoring, and the interaction required between the source and the control agency to assure cooperation in the implementation of the concept.

PEDCo utilized a number of its own previous O&M studies, process and pollution control literature, and contacts with trade associations and state control agencies to perform this feasibility analysis. These sources provided several good examples of existing parameter monitoring programs for particulate and other gaseous (SO_2, hydrocarbon) sources in several states, some initiated by the source using the approach and some by the control agency responsible for stationary source activities. Based on this information, three use categories were determined to be the most feasible for parameter monitoring: 1) as an indicator of proper O&M, 2) as an indicator of probable compliance, and 3) as a basis for compliance determination. The rationale for each use is explained.

APPLICATION OF PARAMETER MONITORING IN A CONTINUOUS COMPLIANCE CONTEXT

For many years industry has monitored various process parameters to improve quality control, improve safety in the workplace, improve product yield, and provide a means of accounting for raw materials and product use, to name a few. In the environmental control field, certain control device parameters have always been measured, and these parameters have been used with varying levels of sophistication to provide an indication of how well the device is performing. Figure 1 illustrates the relationship of various activities common to the concept of parameter monitoring. These early data sources and the theory of control devices suggest that a parameter monitoring approach for estimating stationary source performance is technically feasible. Unfortunately, because this method of estimating performance is relatively new and adequate background data are scarce, parameter monitoring has not been widely adopted.

The goal of parameter monitoring is to provide a useful tool to operators and control agency personnel in the following ways:

- As a guide to arriving at an optimum maintenance schedule
- As a diagnostic tool capable of detecting/preventing malfunctions
- As a performance guideline
- As a process optimization guide
- To assure that appropriate corrective action has been taken in the case of malfunctions
- To assure considerations in future designs
- To assess compliance on a continuing basis

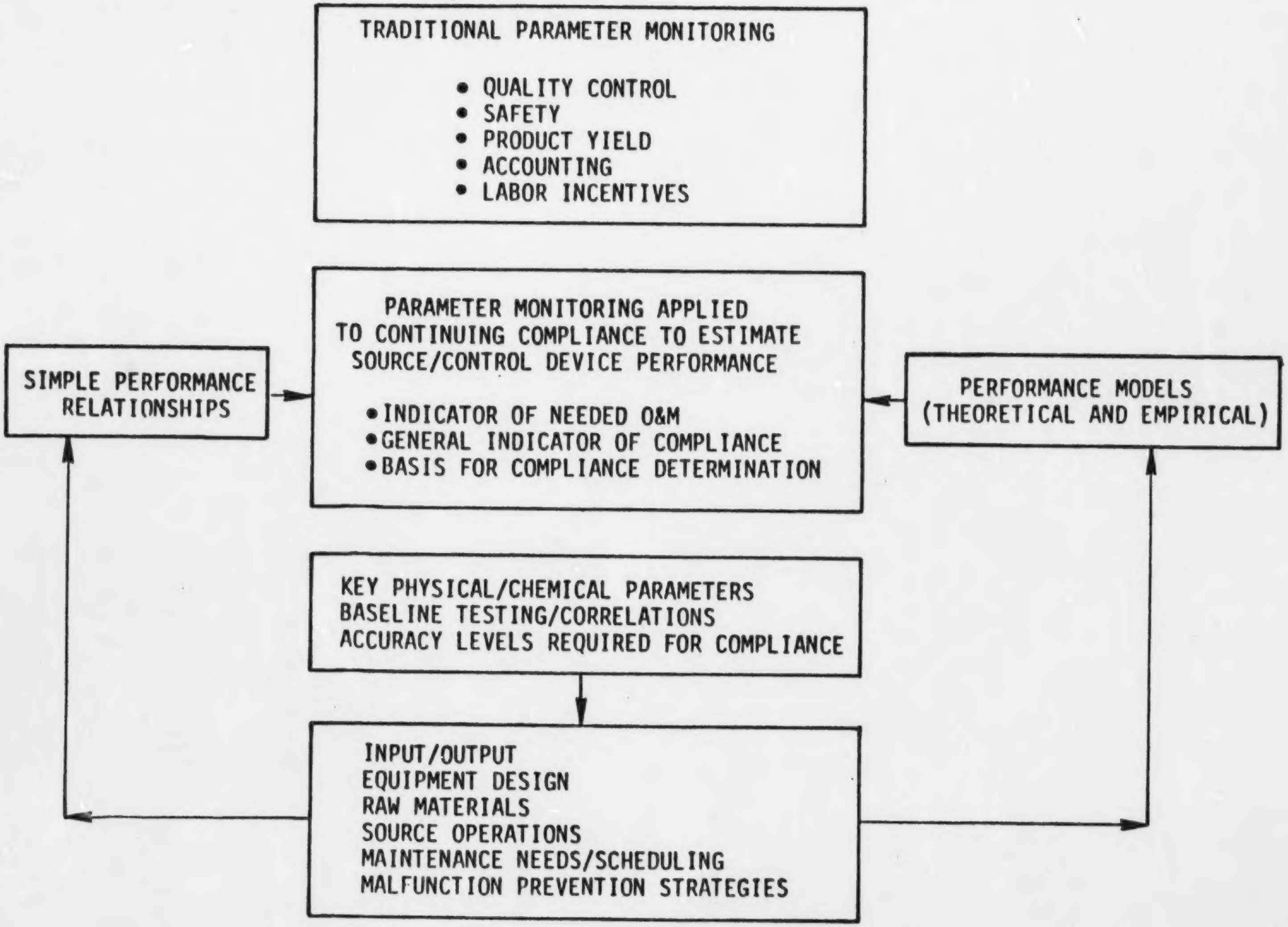
TRADITIONAL PARAMETER MONITORING
• QUALITY CONTROL
• SAFETY
• PRODUCT YIELD
• ACCOUNTING
• LABOR INCENTIVES
SIMPLE PERFORMANCE RELATIONSHIPS
PARAMETER MONITORING APPLIED TO CONTINUING COMPLIANCE TO ESTIMATE SOURCE/CONTROL DEVICE PERFORMANCE
•INDICATOR OF NEEDED O&M
•GENERAL INDICATOR OF COMPLIANCE
•BASIS FOR COMPLIANCE DETERMINATION
PERFORMANCE MODELS (THEORETICAL AND EMPIRICAL)
KEY PHYSICAL/CHEMICAL PARAMETERS
BASELINE TESTING/CORRELATIONS
ACCURACY LEVELS REQUIRED FOR COMPLIANCE
INPUT/OUTPUT
EQUIPMENT DESIGN
RAW MATERIALS
SOURCE OPERATIONS
MAINTENANCE NEEDS/SCHEDULING
MALFUNCTION PREVENTION STRATEGIES

Figure 1. Scope and uses of parameter monitoring.

The use of parameter monitoring for these purposes will require clearly defined goals that will be beneficial to all participants, i.e., both the source and the control agency.

DATA ELEMENTS NECESSARY FOR DEVELOPING PARAMETER MONITORING

The first step required in the development of parameter monitoring for a particular source/control device application is to gather the major data elements. This entails the following:

1) Identification of important source or control device parameters
2) Generation of baseline parameter/emission data
3) Determination of desired/acceptable parameter ranges
4) Monitoring of specified parameters for maintenance within the required range

Not all of these elements would be necessary in every case of parameter monitoring.

Required Data Element 1: Identification of Important Parameters

Identification of important parameters to be considered for monitoring requires investigation of the design, operation, and physical/chemical variables of a system. A parameter is an independent variable that affects the functional capabilities of a system and, ultimately, the performance of a control device in reducing air pollutant emissions. For the source operator, the ideal parameters will represent a controllable process or control device variable such as temperature, pH, power input, pressure drop, etc. so that required conditions can be achieved and maintained. In the case of the control agency officer, parameters such as opacity or particle size distribution can be used as indicators of expected performance and to develop parameter/ emission relationships even though the operator cannot necessarily control the levels of these parameters.

Considerable work has already been done on identification of parameters that can be used as performance indicators. Two general approaches are followed: 1) identification of control device parameters across all source categories and 2) if necessary, identification of system/device parameters for a specific source category type. Examples of the first type of identification are given in Table 1. Identifying parameters requires an understanding of the relationships between process operations, the physical and chemical properties of the emission, and the principles of controlling the emission. This basic identification step involves a literature search for data, discussions with vendors, and a review of operating data available from actual source operations. The first two sources (vendors and literature search) usually provide immediate assistance in identifying control device parameters. The use of source-specific data, however, requires study of the process and control configuration. Information sources such as background documents for NSPS and AP-42 emission factors also can be useful in the preliminary identification effort. In many cases, only the relationship

TABLE 1. MONITORING PARAMETERS THAT INDICATE PERFORMANCE OF PARTICULATE CONTROL DEVICES

Equipment type	Parameter	Indication
A. Particulate control devices		
Fabric filters	Hopper level/dust removal system	If hopper fills, dust can be reentrained.
	Pressure drop	If too low, indication of ruptured or leaking bag.
Mechanical collectors/cyclones	Pressure drop	High pressure drop across collector may indicate poor inlet conditions or plugging, both of which reduce efficiency. Low pressure drop could be caused by erosion; this also can result in low efficiency.
	Hopper level/dust removal system	Incomplete removal will result in reentrainment.
Wet scrubbers (particulate)[a]	Flow monitors	Liquid: Feed rate determines quantity of liquid available for formation of particle-collecting droplets.
		Pressure at which liquid is introduced governs size (surface area) of droplets; higher pressures produce smaller (greater surface area) droplets for better collection.
		Gas: Insufficient gas flow reduces inertial effects of particles and decreases collection.
	Pressure drop	Across a venturi, sufficient pressure drop/kinetic energy of gas is necessary to fragment the scrubbing liquid to form particle-collecting droplets. High gas velocity also promotes particle inertial collection.

[a] The above applies basically to high-energy or spray-type scrubbers. In other packed-type scrubbers, measurement of the feed rate of scrubbing liquid can ensure sufficient liquid for absorption.

(continued)

TABLE 1 (continued)

Equipment type	Parameter	Indication
Electrostatic precipitators	Secondary voltage (v)/current (I) meters - VI curves	Direct measure of power input to ESP; can be correlated directly with emission levels.
	Flue gas temperature	Deviation from design can either increase or decrease resistivity and degrade or improve collection efficiency, respectively.
	Moisture	Moisture content of ESP inlet gas can lower resistivity, thus enabling collection of high resistance particles, or it can cause corrosion if combined with low temperatures.
	Fuel sulfur content	Inversely proportional to resistivity, low-sulfur fuel can degrade performance if ESP is not designed for it.
	Rapping rate	If improperly set, could result in reentrainment or, if insufficient, particles can build up and insulate collection plates, thus decreasing efficiency.
	Rapping intensity	If too high, particle reentrainment, fatigue, or failure of discharge electrode may occur. If too low, collection becomes less efficient as particles build up and insulate plates.
	Hopper level indicators	Full hopper can lead to reentrainment or short and burn out discharge electrodes.
	Flow rate	If too high, reentrainment occurs and efficiency decreases. If too low, poor gas distribution and reduced efficiency may result.

development is required because of the amount of work already performed on identification of important parameters.

Required Data Element 2: Generation of Baseline Parameter/Emission Data

Baseline testing can consist of any number of tests, depending on predictive capabilities of the data desired. Baseline testing is similar to ordinary source compliance testing (stack testing) except for one major difference--the parameter levels are recorded for those parameters identified in Data Element 1 while the stack test is being conducted. The extent of baseline testing determines the ultimate usefulness of the data. If, for example, testing is done under only one set of conditions, a later set of observed conditions can only be used for the qualitative prediction of expected changes in emissions over a small range of conditions similar to the baseline conditions. Quantitative predictions require the use of multiple baseline tests, the ultimate accuracy being proportional to the number of tests performed.

Since baseline testing is costly (minimum of $6000 for two data points), it is wise to rely on the theory of the process mechanics or control device operation to select only those conditions that represent reasonable operations preferably in a compliance mode. The baseline study thus verifies the existence of the theoretical relationships that were established for use in the design of a system. Baseline data also can be used to develop performance curves by providing the site-specific values that provide an empirical modifier to increase the accuracy of the performance curve.

Required Data Element 3: Determination of Acceptable Parameter Levels

Determining acceptable parameter levels for source operation entails engineering and statistical evaluation of the baseline data. The engineering evaluation of an operation is often conducted prior to baseline testing, and thus the statistical evaluation of baseline data is used to establish a site-specific relationship and the ranges of parameter levels. This evaluation can consist of full baseline testing followed by rigorous statistical analysis and determination of parameter ranges, or merely of extended observation of normal parameter levels followed by a specification of acceptable levels within ± x of the norm. Both methods have been used.

An important aspect of the feasibility of parameter monitoring is that the established relationships and parameter levels must be indicative of source operations. Also, several items must be addressed when specifying parameters: the methods used to monitor parameters; the levels that indicate noncompliance or the need for maintenance or operational adjustments; recordkeeping and reporting procedures; and the methods used to determine compliance. Specifications of unreasonable levels of any parameter will seriously affect the success of the use of parameter monitoring.

Required Data Element 4: Monitoring of Specific Parameters

Ideally, the parameters to be monitored will be those for which monitoring instrumentation is currently in place or easily available. The main idea is to provide economical and reliable substitutes for periodic stack testing or continuous emission monitoring by incorporating continuous parameter monitoring.

The source and control agency must mutually decide whether a possible decrease in accuracy in return for a more continuous indication of compliance is acceptable. They must also agree on the level of sophistication required. For example, a simple manometer across the throat of a scrubber is an accurate and reliable means of monitoring pressure drop. To provide a continuous recorder for pressure drop will require a much more expensive instrument. In practice, the maintenance burden of the recorder may discourage the plant, and if so, the instrument will fall into disrepair. In such an instance, the simple manometer may well be the best practical approach for both parties. In other situations, actual compliance status may be difficult to determine. It is possible in these cases, however, at least to observe degradation of control equipment performance and to ascertain the probable corrective action that is necessary.

USES OF PARAMETER MONITORING INFORMATION

The existing or potential parameter monitoring uses that have been identified as being applicable for sources and/or control agencies are as follows:

- As an indicator of proper operation and maintenance - Simple physical or chemical indicators can be used to qualitatively evaluate the performance of a control device and point up the need for maintenance. These simple parameters form the basis for control equipment design. For example, vendors often specify power input, pressure drop, or temperature in their operating manuals. Simple monitoring of such parameters reveals how well a control device is functioning. This approach can be used at virtually any source.

- As an indicator of probable source performance - Data generated by a large number of sources during relatively unsophisticated baseline studies have been used to develop a list of various functions that define the effects of monitored parameters on control device performance. These simple functions are sometimes used to make cursory assessments of compliance. By comparing the performance functions applicable to a specific source with general industrywide relationships, one can sometimes ascertain whether the equipment is operating in a compliance mode. This approach can be used easily at sources incorporating devices that are highly dependent on parameter levels for proper operation.

- As a basis for compliance determinations - Detailed correlations can be established between certain parameters and emissions to permit accurate estimation of source emissions and determination of compliance status. This level of parameter monitoring is most often practiced by industrial sources requiring control of a process, rather than control of emissions. Constant monitoring of process parameters has led many manufacturing firms to establish optimum levels of the parameters shown to have the greatest impact on product quality, quantity, and appearance.

Many sources have used parameter monitoring in the past to help operate and maintain their process and control equipment. These past applications, however, have mostly been rudimentary and unsophisticated. The use of monitoring process and equipment parameters to judge the operation of pollution control equipment has been limited. Most efforts have been expended by sources wishing to perform troubleshooting or by control agencies suspecting noncompliance problems. Incorporation of parameter monitoring activities, however, need not be delayed until a source experiences upset or compliance problems. More sources and agencies are begining to realize this fact, as witnessed by the number and variety of parameter monitoring activities which have recently been implemented.

Indicator of Proper O&M

This approach can be integrated into the source's preventive maintenance schedule. A source that observes the levels of various parameters on a regularly scheduled basis (daily or other) will eventually be able to determine the range in which those parameters fall during both normal and abnormal operating conditions. A benefit to the source of such an approach is that the control agency will most likely have more confidence in the compliance status of a source that uses parameter monitoring to analyze both process and control equipment O&M and malfunctions. Thus, the use of parameter monitoring as an indicator of proper O&M also becomes an indirect indicator of compliance. An alternative approach is to monitor only those parameters that do not require the purchase of additional equipment. These data, collected in a parameter monitoring scheme, will eventually indicate if enough data are being collected or if additional parameters must be monitored to detect malfunctions and ensure proper O&M.

Applicable Situations--

Virtually every source operator relies at least partially on instrumentation and on indicators of equipment malfunction; e.g., an oil leak as an indication of a worn-out seal, excessive noise or vibration as an indication of worn bearings, or reduced flow or pressure as an indication of an upstream blockage or fluid leak. These situations alert the operator to perform required maintenance before the problem gets worse. Similarly, virtually any source can perform some type of parameter monitoring to aid in detecting equipment malfunctions or diagnosing probable control equipment upsets. The intent is to bring about more planned, cost-effective, and improved O&M, and to promote a more thorough understanding of potential problem conditions on the part of the source.

Some states include provisions for parameter monitoring in the pollution control regulations, either as monitoring requirements or operating conditions. The State of Iowa, for example, specifies that a maintenance plan and a parameter monitoring program are required at sources experiencing numerous malfunctions. If malfunctions persist after adoption of the monitoring program, the control agency can compare the parameter levels prior to the malfunction with those during normal conditions to determine if maintenance was performed and the malfunction was indeed unforeseen or unavoidable. The agency can then grant or deny an exemption based on this determination.

Iowa regulations also contain general provisions pertaining to compliance testing. Control officers in the State request that certain key parameters be monitored by the source during its initial compliance test. The control officers then review the levels of these parameters during inspection. If operation falls within the ranges of the conditions defined by the compliance test, performance is believed to be similar to that when the source was tested. If operation falls outside this range, the State either requests the necessary maintenance be performed to put operations back in range, or initiates a compliance test. This approach is feasible because the inspectors are familiar with the sources. Some stationary sources have operated for years with only an initial compliance test; all subsequent maintenance requirements and compliance determinations have been based on the parameter levels observed during this test.

Whether used by a source to schedule maintenance or by a control agency to determine the avoidability of a malfunction, similar approaches can be implemented quickly and inexpensively. Such approaches add little financial burden. A source operator can show a good faith effort by using parameter changes to assist in the proper operation and maintainance of process and control equipment and to serve as a malfunction warning system.

Indicator of Probable Source Performance

Certain operating parameters of control devices are known to provide some indication of control device performance. Similarly, some variables in source operations (e.g., changes in raw materials) are known to affect the level of emissions from that source. Relationships between these variables and emission levels can be used to estimate the performance of a source with respect to compliance with emission limits. The approach is analogous to establishing conditions of an operating permit. Although actual emissions are unknown, compliance with the operating permit is proven by maintaining the conditions it has set forth. The accuracy of emission estimates is likely to vary widely; however, the estimates are judged to be accurate enough to indicate probable compliance.

Applicable Situations--

This approach has two benefits. First, it provides the control agency with a basis for determining compliance that is probably more accurate and well formed than the basis used for typical SIP inspection compliance determinations. Second, it helps in the response to a citizen's complaint against a source. An inspector can request the records for the period in question to determine if parameter levels were in acceptable ranges at the time of the complaint. This reduces the necessity for personal observation on the part of the inspector. It can also supply the source with the necessary data to defend its operations against unsubstantiated reports of pollutant releases.

The performance of most control devices can be defined by the parameter levels observed during operation versus those for which the system was designed. Table 1 lists many of the known relationships between operating parameters and particulate control device performance that can be used to form the foundation of this level of parameter monitoring, in which the estimated performance of a control device is based on the observed parameter range during operation.

As an example, a new ESP has recently been installed to upgrade control capabilities. At current operating levels the ESP is overdesigned, and emission rates of less than 0.02 $lb/10^6$ Btu have been observed. The extent of overdesign, however, has caused problems with the ash removal system operation. It was discovered that too much of the particulate was being captured in the inlet fields. By utilizing the ESP power meters and reducing ESP power, the plant was able to spread collection out in the ESP thus reducing emissions by eliminating hopper overload. These ESP power levels, which are recorded every shift, are being used to optimize ESP performance. This not only provides an indicator of compliance, but also of proper operation and required maintenance.

Another example is found at a 180-tons/h batch asphalt concrete plant which monitors pressure drop across a scrubber and adjusts this value according to the mix type. Base mixes require an 18-in. pressure drop for compliance, whereas surface mixes require a 26-in. pressure drop. Water flow rate is not varied to achieve the required pressure drops; instead, the throat size is varied. In this way, the plant is able to meet the 0.3 gr/scf and 0 percent opacity standard for all products.

A final example is a power plant. Most utility boilers are well instrumented. The example plant burns low-sulfur coal (0.5 to 0.8 percent sulfur). Large ESP's with 48 transformer-rectifiers (T/R's) and an SCA of >750 ft^2/1000 acfm are used to control particulate emissions. Because of the high-resistivity ash produced by the low-sulfur coal, back corona can be a problem. Plant personnel daily establish maximum ESP performance by performing gas load tests (generating a V-I curve) and determining the point of back-corona onset. The T/R controls are set to operate below this back-corona onset, and ESP performance is thus optimized. Opacity levels between 6 and 15 percent are usually maintained by this method, and compliance problems normally associated with high resistivity and back-corona are avoided.

In summary, all of the applications presented have assisted either the operators or control agency personnel in ascertaining the operability of a system and the probable compliance status of that system. Although in none of these cases is it possible for the control agency to state that a source is emitting at a rate of x lb/h, it can state that, based on the parameter levels observed, a source is likely to be in or out of compliance. [This is the usual objective in State Implementation Plan (SIP) compliance inspections.] If parameter levels are outside acceptable ranges, a full compliance test can be justified.

Models for Linking Parameter Monitoring to Performance

All the preceding examples rely on "empirical" relationships, either qualitative or quantitative, between performance and indicator parameters.

Another alternative is the use of models that predict performance on the basis of the fundamental theory of the operation of the control device. Various parameters are used as input to these models, which can be used to predict future performance of a control device (i.e., permit review), or estimate performance at any given point in time. Such models are validated by generating baseline data, either at a specific site or for a group of similar sources, depending on the accuracy required.

No detailed discussion of these models will be presented, but some of the more common ones include the Contact Power Theory model, the ESP power equation, the EPA/Southern Research Institute ESP model, and the fabric filter model (1,2,3).

Basis for Compliance Determinations

Many of those involved in the design and analysis of control devices believe it is possible to make accurate and quantitative predictions regarding the performance of control devices by using various parameters. The idea is to build on the basic physical or chemical properties of a process or control unit and specifically define the relationships that are present. To obtain the most representative results and to suppress site differences, this is done on a case-by-case basis. Once a reasonable relationship is ascertained, the emissions can be predicted for various operating levels. Regardless of the product being manufactured (steel, ink, cloth, glass, etc.), certain process parameters, such as scrap content, reaction temperature, drying temperature, or cool down rate, must be monitored and controlled to generate the desired quality results in the end product. Because there is less profitability in controlling process emissions, there is less impetus to apply similar quality control procedures to pollution control devices. Public awareness, fines for noncompliance, and costs incurred in demonstrating compliance have slowly begun to make it desirable to develop such procedures for pollution control. This approach, the most sophisticated use of parameter monitoring, is discussed here.

Applicable Situations--

The situations to which this approach is applicable are not as easily defined as those for the two earlier approaches. It is clear, however, that control device models can be refined to accommodate site-specific emission predictions. The most complex situation requires monitoring of both process and control device parameters. Some cases (presented later) have been discovered in which control device parameters are sufficient in themselves to predict emissions; in these cases the assumptions required pertain to the stability of the pollutant levels in the uncontrolled emission. It is definitely easier to use the approach when the source has a constant emission rate. The goal is to arrive at a relatively simple procedure by which to account for the influencing variables.

Required Elements--

The success of this approach to parameter monitoring is contingent upon an accurate definition of the effect of operating variables on emissions.

Therefore, all four data elements of parameter monitoring must be incorporated, and particular attention must be given to identification of parameters and baseline studies.

Because the baseline testing required for this approach can become extensive, only those parameters known to affect emission rates should be monitored. The baselining can be conducted on a case-by-case basis and the actual testing can be designed to include either the full operating range of the plant or control device or only the operating range that will achieve compliance. Obviously, the second test design is more economical. In both cases some pretest definition of the conditions during the test must be established. Information from vendors can assist in defining reasonable operating ranges.

The accuracy of this approach depends on the amount and quality of the baseline data, including the response of emissions on changes in parameter levels, and the variability of the pollutant concentrations. A process in which emissions can vary greatly, such as in the steel industry, will require more baseline tests than one in which emission characteristics are fairly constant. Similarly, a process having little variation in pollutant loading will produce better results because fewer variations will have to be explained.

A parameter monitoring approach using nomographs to ease calculations has reportedly been used by a major utility to ensure compliance in the event of failure of a section of an ESP. An ESP is kept in compliance with particulate emission regulations by reducing boiler load.

Figure 2 presents a typical nomograph. The top graph illustrates collection efficiency of a four-field ESP with 24 bus sections as a function of the gross boiler load, depending on the number of bus sections out and whether they are in series or parallel. The bottom graph shows the required ESP efficiency needed to meet a state regulation of 0.38 $lb/10^6$ Btu as a function of the ash content of coal (assuming 11,000 Btu/lb coal).

Knowing the ash content of the coal being fired and knowing which bus sections of the ESP are inoperative, an operator can tell from the top graph how much the boiler load must be reduced to keep emissions in compliance with regulations. Charts of this type must be developed for each boiler-ESP combination.

Comparison of Parameter Monitoring With Other Monitoring Methods

The purpose of this discussion is to briefly compare the use, feasibility, status, accuracy, reliability, and cost of parameter monitoring to the two other available monitoring approaches: CEM's and stack tests.

General Description of the Three Major Monitoring Approaches--

The following three approaches are currently available for determining probable source performance or actual compliance status: 1) stack testing (the reference method for emission rates), 2) continuous emission monitoring,

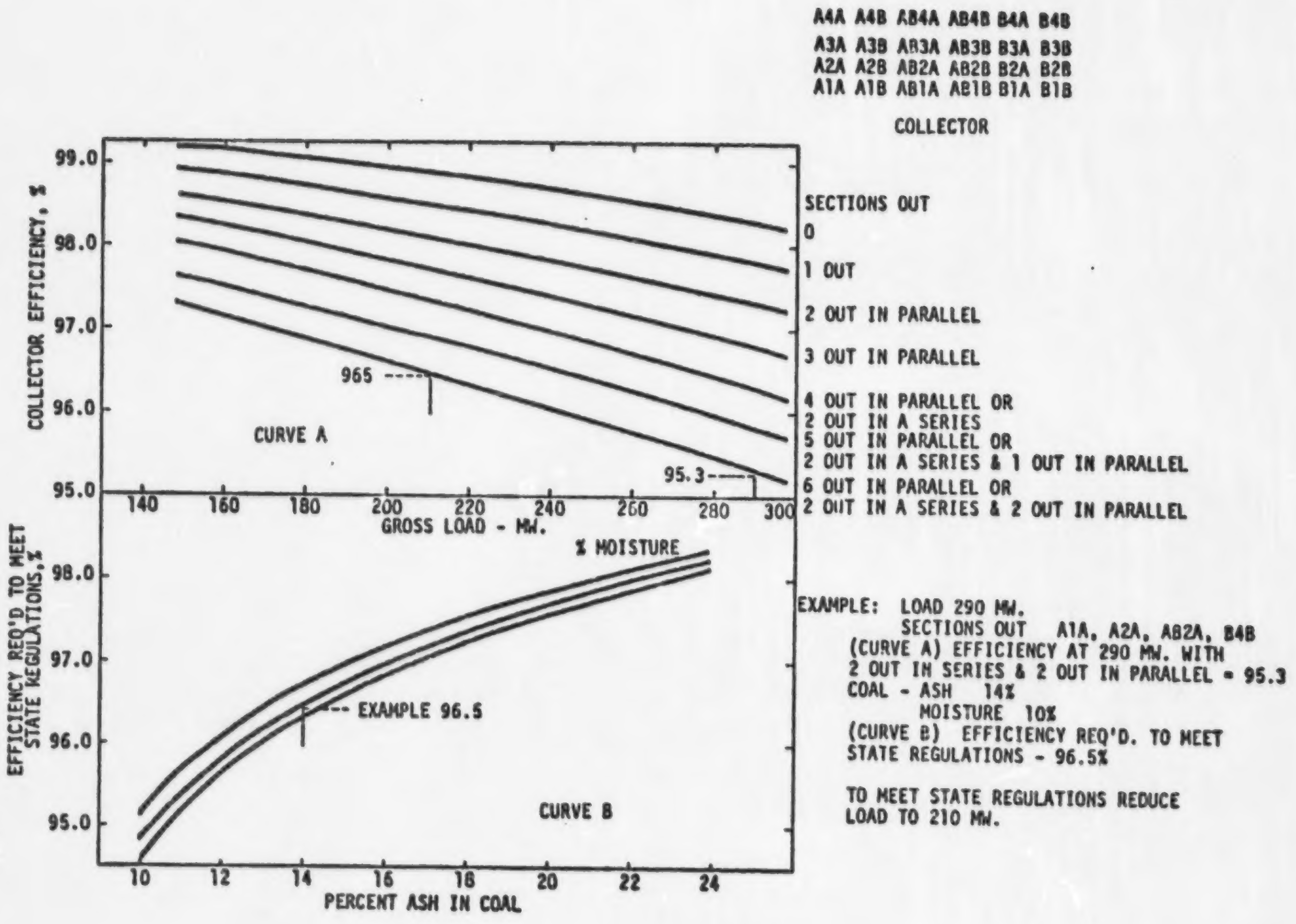

EXAMPLE: LOAD 290 MW.
SECTIONS OUT A1A, A2A, AB2A, B4B
(CURVE A) EFFICIENCY AT 290 MW. WITH
2 OUT IN SERIES & 2 OUT IN PARALLEL = 95.3
COAL - ASH 14%
MOISTURE 10%
(CURVE B) EFFICIENCY REQ'D. TO MEET
STATE REGULATIONS - 96.5%

TO MEET STATE REGULATIONS REDUCE
LOAD TO 210 MW.

Figure 2. Operating curve to meet emission regulations with partial malfunctions of ESP.

and 3) monitoring of parameters for subsequent comparison with compliance conditions. Although all three approaches have been used in industry, the use of CEM's and parameter monitoring has been somewhat limited. Stack testing, the most widely used approach, has been conducted on virtually every kind of source type and for all kinds of pollutants.

The parameters discussed in this report that have used monitoring as a performance indicator include current/voltage (power input), pressure drop, liquid/gas, gas/air flow rate, and residence time. Although not absolutely necessary, recording devices provide a permanent record of the measured values. Although these parameters may often be successful as indicators of proper O&M, their use to estimate emissions is a function of (1) the accuracy of the actual monitoring device, and (2) the accuracy of the correlation models or equations which utilize monitored parameter levels and emissions. Monitoring devices are available that can accurately measure the parameter in question. In only a few cases, however, has the accuracy of a correlation between parameter levels and emissions actually been established.

Comparison of Uses--

A qualitative comparison of the use, feasibility, status, accuracy, reliability, and cost of these three approaches is presented in Table 2. To the extent possible, quantitative estimates have been made for various uses.

Comparison of Feasibility Status--

All of the monitoring approaches discussed in this report have been demonstrated to some extent. Obviously CEM and stack testing are the most publicized, and both are clearly feasible. The status of the various parameter monitoring uses vary. The simpler, more accepted uses (i.e., as indicators of proper O&M or probable source compliance) have been proven feasible in several situations. The more advanced the approach, the fewer the applications found. Almost every parameter identified has been used for screening purposes, and represents necessary required design information.

Comparison of Accuracy--

As stated previously, the accuracy of a parameter monitoring approach to estimating emissions depends on the following: 1) ability of the parameter or performance equation to reflect changes in control device performance, and 2) accuracy of the monitoring device. The monitoring devices are seldom the limiting factor in arriving at an accurate relationship. More often, the pollutant stream being treated displays nonuniform characteristics that may contribute to subtle changes in the behavior of monitored parameters. For instance, the resistivity of a coal ash may change substantially between coal supplies, and thus change the power distribution within an ESP. If resistivity is not a monitored parameter, the accuracy of the parameter monitoring results will be less than optimum. Parameter monitoring is thus believed to be most accurate when 1) the performance of a control device or process is highly dependent on the parameter, and 2) the pollutant concentrations within the gas stream do not vary much. The comparison in Table 2 reflects this in the rankings. The accuracy of parameters in the ±10, 20, 30, or 40 percent

TABLE 2. COMPARISON OF APPROACHES FOR ESTIMATING PARTICULATE EMISSIONS

Monitoring approach	Applicable process/ device	Use code[a]	Status code[b]	Accuracy code[c]	Reliability code[d]	Cost		
						Equipment[e], $	Maintenance	Testing[f]
1) Parameter monitoring								
Current/voltage (power)	ESP	1	5	5(a)	5	<1,000	1 h/week	0
		2	4,3	3	5			2-6
		3	1	4	4			9-20
ΔP (power)	Scrubbers	1	5	5(a)	5	<1,000	1 h/day	0
		2	4,3	3	5			2-6
		3	2	3	4			9-15
	Mechanical collectors	1	5	5(a)	5			0
		2	4,3	3	5			2-6
		3	1	2	3(a)			9-15
	Fabric filters	1	5	5(a)	3(a)			0
		2	2	1	3(a)			2-10
		3	Not determined					NA
L/G	Scrubbers	1	5	5(a)	5	<2,000	1 h/day	0
		2	4,3	5(a)	5			2-6
		3	1	2	3(b)			9-20
Aspiration rate/delivery pressure	Coking	3	2	5(b)	5	<1,000	1 h/day	9-15
2) Continuous monitoring of opacity	Any	3	5	4	2	15,000	1 h/shift	$7,000
3) Stack testing	Any	3	5	3	1	NA	NA	$3,000

[a] Use Codes

1 - Indicator of proper O&M
2 - Indicator of compliance
3 - Compliance determination

[b] Status Codes

5 - Feasibility demonstrated at several sources
4 - Feasibility demonstrated for screening purposes
3 - Design basis
2 - Limited use demonstrated
1 - Theoretical

[c] Accuracy Codes

5 - 100% qualitative confidence in indicating
  a) Malfunction or maintenance needs
  b) Compliance
4 - ±10% possible
3 - ±20% possible
2 - ±30% possible
1 - ±40% possible

[d] Reliability Codes

5 - Results highly reproducible with little uncertainty
4 - High reliability with some uncertainty
3 - a) Uncertain
  b) Other parameters also required
2 - Reliability depends on O&M of monitoring equipment
1 - Not reliable or only periodic readings

[e] Recording device can increase equipment costs by $1,500 - $10,000.

[f] For the parameter monitoring approach, only the number of baseline tests required is presented.

NA = not applicable.

range is based either on observed accuracies of earlier studies, or qualitatively on the dependence of performance on parameter levels. In the case of continuous emission monitors, the accuracy is given as that required in the Federal performance standards. For stack testing (the reference method), accuracies of ±10 percent relate more to precision than to accuracy.

Comparison of Reliability--

Within the context of the comparison in Table 2, the notion of reliability encompasses two basic ideas: 1) whether the parameter being monitored is capable of tracking the performance of a control device so as to allow its use in a parameter monitoring application, and 2) whether the instrument chosen to monitor the parameter is capable of measuring and displaying the parameter levels confidently. In addressing the first point, most of the parameters identified in this report can be used individually to track performance and hence indicate a malfunction or to define a maintenance need. As the intended use of an approach becomes more quantitative in nature, however, it becomes more difficult to reliably establish the true performance of a control device. Thus, parameter levels can be used reliably to identify fluctuations in performance. Less confidence can be placed on the results of parameter fluctuations, however, when making a determination of the compliance status of a particular source. In the latter case, conclusions are less reliable. It should be noted, however, that different reliability levels are acceptable for compliance determinations if the relationship and results satisfy the requirements of the control agency.

In regard to the second point, most parameter monitoring equipment is relatively simple and parameter levels can be monitored almost continuously with only minor maintenance required to preserve the integrity of the readings. Conversely, a CEM requires a substantial amount of attention to provide reliable results. If properly maintained, a CEM will provide a reliable indication of compliance; however, such maintenance efforts will range from 3 to 8 hours per day for calibration and repair. Without this information, the integrity of the reading is severely sacrificed. Thus, the high on-line availability of most parameter monitoring instrumentation gives better reliability at lower cost than CEM's.

Stack testing, in comparison, provides accurate results and reliable compliance information, but only for one point in time. If baseline data are taken at the time of the test, however, and used with suitable parameter monitoring during periods between stack tests, a reliable indication of continuing compliance can then be developed.

Comparison of Costs--

The ranges of equipment costs given for parameter monitoring devices in Table 2 are very general and merely reflect the relatively low cost of such equipment. These costs assume only minor installation costs and manual recording of data. The costs for applications that require special care in installation, automatic recording or control devices, or multiple units must be adjusted accordingly. The costs for CEM equipment include installation. Equipment costs for stack testing are factored into the total testing costs.

Maintenance costs are given in terms of hours per shift, day, or week and represent likely averages. Equipment with a few moving parts or simple electronic equipment will require minor attention. The maintenance time presented for these devices represents replacement time throughout the year and periodic cleaning and equipment checks. Devices needing more attention (for minor calibration, leak checks, or line cleaning) will require an additional hour per day. Analyzers for CEM's or other parameters that make use of reagents or more sophisticated techniques will require an additional hour per shift for calibration, cleaning, and repairs. Some analyzers actually require a dedicated maintenance person. Once again, maintenance costs are factored into the stack testing costs.

Testing, the final cost factor, represents the number of baseline tests required to develop a parameter monitoring approach, the certification cost for a CEM, or the actual costs of conducting a stack test. The number of baseline tests required is based on the simplicity of the parameter/emission relationship and the number of other variables affecting the relationship. In all cases it is assumed that an indication of proper O&M can be obtained without baseline testing. For an indication of compliance, baseline testing is always required except in a few well-defined situations. Other than in these few situations, a minimum of two good baseline tests is required. To be representative of a good test, the results of the testing should fall within the values on the performance curve of a well-known relationship. The need for baseline testing beyond this minimum number can then be ascertained by observing the deviation of the baseline results from these known relationships. For compliance determination at a complex facility, a minimum of nine baseline tests allows a source to generate data at a variety of parameter conditions. The correlation between the parameter condition and emissions will then indicate whether adequate baseline testing has been performed. Sources that show wide variations in pollutant concentrations will require more baseline tests than sources that show relatively stable emission so as to provide a better definition of the confidence range.

CONCLUSIONS

The three approaches to using parameter monitoring in continuing compliance are 1) as an indicator of proper O&M, 2) as an indicator of compliance, and 3) for determining compliance status. Establishment of a parameter monitoring approach requires identification of important parameters, generation of baseline data, determination of acceptable parameter levels, and monitoring parameters to ensure that levels are maintained within specified ranges.

Parameter monitoring has been used in the past and is beginning to be incorporated into the formal regulatory framework. Its ultimate success is contingent upon arriving at a valid relationship between parameter levels and emissions. Parameter behavior is also identified as an important consideration in the design of pollution control devices and in the operation of many manufacturing facilities. The following observations were made in regard to the various methods available for determining the continuing compliance status of a source:

- Although stack testing is accurate and relatively inexpensive, it only provides evidence of compliance at the time of the test. Because these tests are performed periodically (anywhere from once every year to every five years), it cannot provide assurance of continued compliance.
- While CEM's are effective, they are also costly, both from the standpoint of initial cost and maintenance.
- Parameter monitoring offers an indication of continued compliance and is considerably less expensive (from the standpoint of both initial cash outlay and maintenance) than the CEM. Also, in some cases it is just as accurate.

REFERENCES

1. Semrau, C. T. Correlation of Dust Scrubber Efficiency. JAPCA Vol. 10, No. 3, June 1960.
2. Mosley, R. B., Anderson, M. H., and J. R. McDonald. A Mathematical Model of Electrostatic Precipitation (Revision 2). EPA-600/7-80-034. February 1980.
3. Dennis, R., and Klemm, H. A. A Working Model for Coal Fly Ash Filtration. In: Second Symposium on the Transfer and Utilization of Particulate Control Technology. Volume I, Control of Emissions From Coal-Fired Boilers. EPA-600/9-80-039c. September 1980.

AIR POLLUTION CONTROL:
MAINTENANCE COST SAVINGS FROM THE WASHING, PATCHING AND REUSE OF BAGS USED IN FABRIC FILTERS

by: Frank L. Cross, Jr., P. E., President
Cross/Tessitore & Associates, P. A.
Orlando, Florida 32812

ABSTRACT

One of the highest costs in operating a fabric filter is bag replacement. Reduced bag life is the result of poor design, improper bag selection and poor operation and maintenance.

This paper discusses how the replacement costs of bags can be reduced by the use of a field-operated spindle-type washing device. Techniques are described for washing and patching bags, the cost and type of equipment used in the maintenance program, the labor involved, and the cost savings and improved performance that can be obtained.

These details are based upon a phosphate rock bulk-handling facility located at Tampa, Florida, with over ten baghouses ranging from 10,000 to 70,000 cubic feet per minute in capacity.

INTRODUCTION

Industrial facilities that have particulate problems generally use baghouses as a part of their emission control scheme. Two of the highest costs in the operation and maintenance program for baghouses are the replacement of bags and the energy requirements to overcome the pressure drop through the system. Techniques that increase bag life and reduce energy consumption will save money for the facility.

FACILITY DESCRIPTION

The facility that has been chosen for review currently operates a bag washing and patching operation as a part of its baghouse maintenance activities. This phosphate-ore bulk-handling facility has a through-put of approximately six million tons per year, utilizing 14 baghouses ranging in size from 5,000 to 120,000 actual cubic feet per minute (ACFM). (See Table 1).

TABLE 1. TYPES OF BAGHOUSES*

Source	Baghouse Type	Gas Flow (ACFM)	No. Bags	Bag Diam. (inches)	Bag Length (feet)	No. Units
Rail car dumper	Micro-pulsaire	120,000	1152	4	8	1
Storage dumper	Am. Air Filter	79,000	312	6½	14	4
Ship loader	Standard Havens	52,000	420	6½	9	1
Other "A"	Micro-pulsaire	4,500	64	4	8	5
Other "B"	†Micro-pulsaire	11,000	144	4	8	1
Other "C"	Micro-pulsaire	8,000	100	4	8	2

*All baghouses are of the pulsejet type, using 16 oz. polyester bags with cages.

†Tunnel belt baghouse.

BAG CLEANING AND PATCHING OPERATION

The facility has found that it is advantageous to clean and repair the bags on a regular schedule rather than a) replace torn bags when visible emissions violations occur, or b) replace all bags when the pressure drop becomes excessive.

This bag maintenance procedure is performed twice per year for all bags, except for those in the tunnel belt baghouse, which are washed three to four times per year.

The bags from an entire baghouse (for smaller units) or a section of the baghouse (for larger units) are removed, washed, dried, patched, and stored for replacement (Figure 1). This means that two sets of bags are generally in use -- those in the baghouse and those being cleaned and patched.

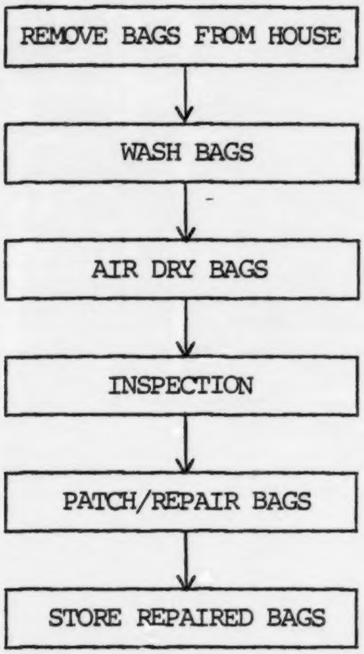

Figure 1. Flow diagram of bag maintenance procedure.

BAG WASHING AND PATCHING EQUIPMENT

The maintenance foreman has developed a rather unique washing device (Figure 2). The bags, with cages in them, are washed under pressure by pulling them slowly past a rotating water spray. If the bag is badly coated on the outside, it is first washed with a wand from the outside and then internally with the bag washing machine[1] (Figure 3).

---

[1] The key to the washing device is the rotating union at the end of the machine. (Dueblin Co., 1919 Stanley St., Northbrood, IL 60062).

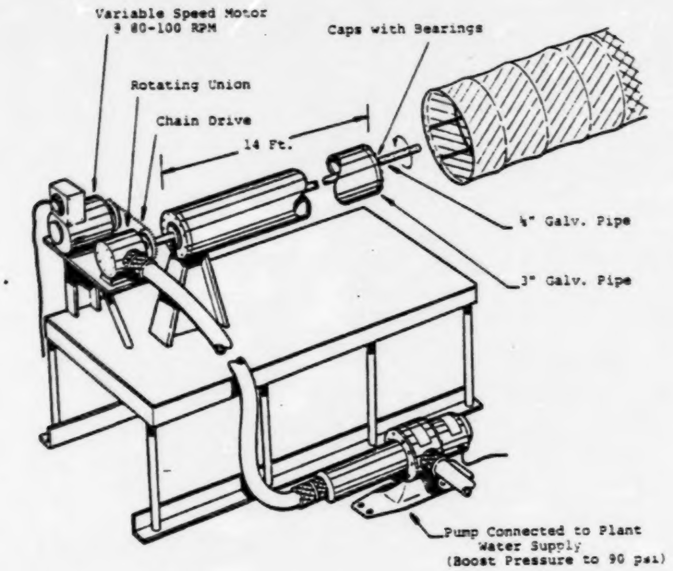
Variable Speed Motor
@ 80-100 RPM
Caps with Bearings
Rotating Union
Chain Drive
14 Ft.
½" Galv. Pipe
3" Galv. Pipe
Pump Connected to Plant
Water Supply
(Boost Pressure to 90 psi)

Figure 2. Diagram of bag washing machine.

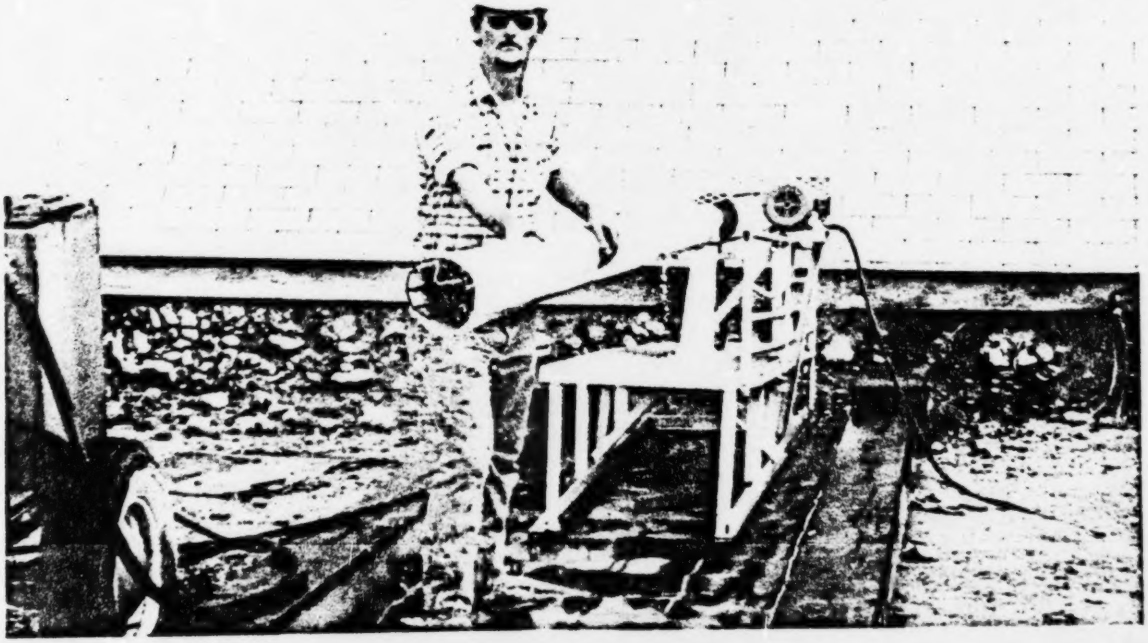

Figure 3. Photograph of bag washing machine in operation.

The cleaned and dried bags are then inspected for pinholes, which are for the most part due to rusty cages. The majority of these holes occur ar the cage rib joints. Coating the metal cages with plastic is not a sufficient solution to this problem. Patching of these holes is done with a hot melt adhesive gun.[1] Figure 4 shows the method of storage for the bags.

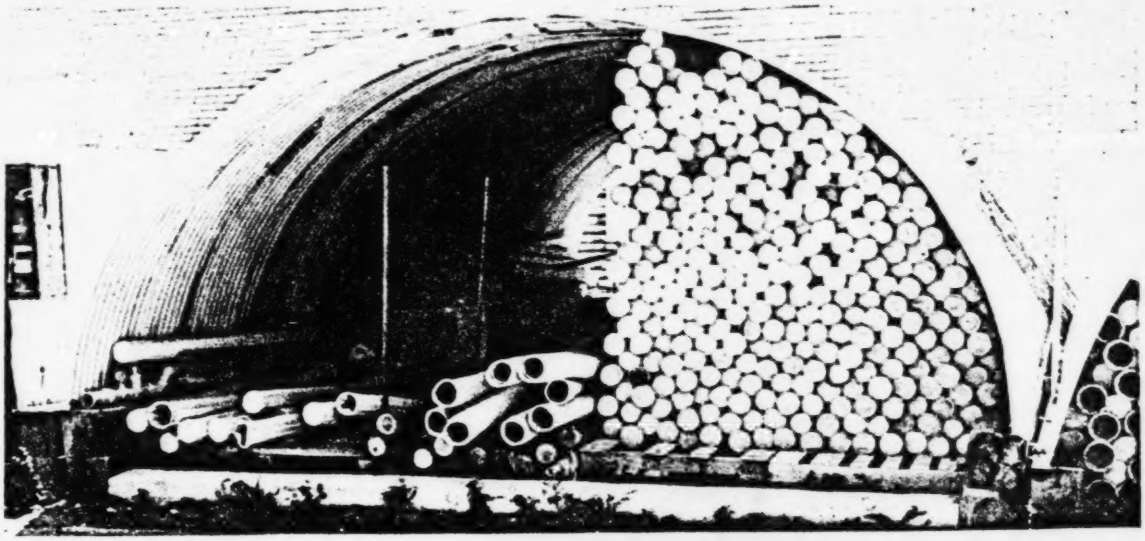

Figure 4. Storage of bags -- dirty, drying, and clean.

Bags are now replaced only when they:

a) are too thin for further use;

b) have been patched excessively (usually eight patches is limit used.

The advantages of this system are:

a) increased bag life from 1½ to 2 times normal life (i.e. a two-year-life bag can be used for three to four years);

b) reduced pressure drop after washing by 1 to 1½ inches H_2O.

---

[1] Polyester patches are cut from other bags with a C. S. Osborne 1½" diameter Arch Punch. The electric hot melt gun used is the Hipermatic TE. The adhesive used is Dexter Hysol Hot Melt.

FINANCIAL BENEFITS OF BAG MAINTENANCE

The cost to build and install a washing machine is minimal and can be done with spare scrap metal. The critical item is the $75 rotating union. At the installation discussed, a $1200 pressure-washing unit was used to boost the nozzle pressure to 900 psi. The washing unit at this facility was also used for other purposes, and a booster pump connected to the plant water supply would normally be ample to operate the wand and washing machine.

The increased pressure drop in the polyester bags between washings is between 1 and 1½ inches H_2O. If the bags were replaced rather than washed, the pressure drop would be approximately the same. Although this is not correct and there would be some pressure drop reductions, this has been left out of the cost analysis.

The net savings in washing and patching bags rather than replacing them would approach $12,000 for a bulk-loading facility of this type and size (Table 2).

The work described in this paper was not funded by the U. S. Environmental Protection Agency and therefore the contents do not necessarily reflect the views of the Agency and no official endorsement should be inferred.

The work described in this paper was not funded by the U.S. Environmental Protection Agency and therefore the contents do not necessarily reflect the views of the Agency and no official endorsement should be inferred.

TABLE 2. ECONOMICS OF BAG MAINTENANCE PROGRAM

Source	Cost per Bag (in $)	No. Bags Repaired Annually	[*]Bag Cost Savings/ Yr (in $)	[†]Labor to Clean (in days)	[‡]Labor to Patch (in days)	[§]Labor Cost/Yr (in $)	[#]Labor Savings/Yr (in $)
Rail car dumper	3.69	500 units/ yr (1152 total)	2908	12	7½	441	2467
Storage bldg (4)	8.54	75 (312)	7789	12	4½	399	7390
Ship loader	6.00	100 (420)	1230	4	1½	133	1097
Other "A" (5)	3.69	20 (64)	368	3	1½	105	264
Other "B" (1)	3.69	30 (144)	244	1	½	49	195
Other "C" (2)	4.40	25 (100)	330	2	3	67	263

[*] Based on (bag cost x number of bags) ÷ 4 years (assuming 2-year bag life, extended to 4 years). Includes cost of bag replacements if bags were not repaired.

[†] Washing takes approximately one day (8 hours) to wash 100 bags.

[‡] Patching/inspection takes approximately 1½ days to patch 100 bags. Bags are washed and patched two times per year.

[§] Labor rate at $14 per hour (salary and overhead).

OPTIMIZING THE PERFORMANCE OF A MODERN ELECTROSTATIC PRECIPITATOR BY DESIGN REFINEMENTS

by: Donald H. Rullman, Vice President
Lurgi Corporation
River Edge, New Jersey 07661

Franz Neulinger, Manager
Lurgi GmbH
Frankfurt, West Germany

ABSTRACT

The continued development of optimal internal components, electrical control systems, and gas flow testing technologies is essential to the fullest functional performance of the modern electrostatic precipitator for economic application toward potentially tightening process particulate emission standards. This paper addresses the design logic, development, and full scale application of increasing gas passage width from the common 200 mm to 300 mm (8 inch to 12 inch) widths to a 400 mm (or 16 inch) width. Results of the consequently needed adaptation of electrode geometry, especially for the inhibition of back ionization, will be discussed in this context. The type of gas flow-technological tests which must be performed in order to ascertain optimal precipitator configuration for best possible flow, will also be described.

Further, the advantaged use of microcomputers versus analog type controls for high voltage control, is presented. A superordinated, central process computer assumes the functions of control, supervision, and optimization of an inplace precipitator, thereby minimizing clean gas dust content and overall electrical energy consumption.

WIDE PASSAGE SPACING

According to conventional sizing criteria (typically the Deutsch formula), the effective surface area of collection electrodes built into an electrostatic precipitator is a measure of the maximum possible collection efficiency. In the past, this view resulted in relatively small passage widths of between 8 inches (200 mm) and 12 inches (300 mm) in precipitators, which made it possible, with reasonable standards of erection alignment accuracy, to accommodate the largest possible collection areas in casings of specified dimensions.

However, tests in pilot and large-scale plants have shown that it is possible to increase passage width above the aforementioned values and thereby to decrease the collection area accordingly, without affecting the efficiency of the electrostatic precipitator.

After carrying out extensive tests both in the laboratory and in large-scale plants, in recent years Lurgi has been installing more and more electrostatic precipitators with passage widths of 16 inches (400 mm). Measurements show that the collection efficiency and the clean gas dust content of these precipitators compares favorably with those of precipitators with the same size casing having conventional passage widths and thus a correspondingly larger collection area.

Introduction of larger passage widths thus offers an interesting opportunity to reduce investment costs, while the energy consumption remains more or less unchanged. The Deutsch formula is the traditional basis of the process design of electrostatic precipitators:

$$\eta_{total} = \frac{C_{inlet} - C_{clean}}{C_{inlet}} = 1 - e^{-w \cdot A_n/\dot{V}} \qquad (1)$$

in which

η_{tot} = total collection efficiency
C_{inlet} = raw gas dust content
C_{clean} = clean gas dust content
w = effective migration velocity
A_n = collection area
$\dot{V}$ = main volume flow

This formula is based on a simple model concept and is occasionally given in modified form.

Effective migration velocity (w-value), which is a measure of the velocity component of the particles to be separated perpendicular to the gas flow, is of utmost importance. This velocity may be viewed as the integral average value of many variables. These include, for example, particle-size distribution and properties of the particles to be separated, temperature, pressure and composition of the gas, attainable field strength, discharge current density and distribution, distribution of gas to the individual passages, etc. Also included are gas flow parameters (within the precipitator) which are influenced by gas velocity, passage width, field height and field length. Effective migration velocity is therefore a complex variable dependent upon many factors. It may be viewed as a process characteristic, similar to a heat transfer coefficient in the design of heat exchangers or to a rate of reaction constant in the design of chemical reactors.

In addition to viewing the w-value as a process variable containing all the parameters not taken into account by the basic Deutsch formula, classical theory makes it possible to calculate the movement of an individual particle (w_{th}) when under the influence of voltage and gas flow in the vicinity of collection electrodes.

A mathematical relationship for particles $> 1\ \mu m$ can be derived from the equilibrium of forces of Coulomb-force and Stokes's law of resistance.

$$w_{th} \sim \frac{E^2 \cdot d}{\eta} \qquad (2)$$

w_{th} = theoretical migration velocity

E = electrical field intensity in the vicinity of the collection plates

d = particle diameter

η = dynamic viscosity of the gas

From such equation it can be deduced that migration velocity is a function of the square of the field intensity and thus of the voltage applied.

Higher gas viscosity values, normally associated with high temperatures, reduce migration velocity. Migration velocity is also reduced as particle-size becomes smaller; but, in the case of particles with diameters of below 0.2 - 0.5 μm, migration velocity rises once again due to diffusion which then comes into effect and becomes an overriding factor.

Certain technical publications, in recent years, have dealt with factors influencing effective migration velocity (1 - 4). The relationships between gas velocity, precipitator length, passage width and w-value are demonstrated particularly clearly by Güpner's investigations. (3)

The dependence of effective migration velocity on passage width is particularly interesting:

If, for example, one were to remove every second collection electrode and the associated discharge electrodes from an electrostatic precipitator without changing the casing dimensions, thus doubling passage width, then according to the Deutsch equation, collection efficiency should be reduced since collection plate area is halved.

However, this phenomenon has not been observed. The reason for this can be demonstrated by measurements taken in a pilot plant. A test precipitator was operated in a slip stream off a large scale plant and the passage width was increased from 250 to 375 mm.

Figure 1 (top) shows the w-value calculated on the basis of the measurements taken along the length of the precipitator. It can also be seen that the w-value, with a passage width of 375 mm, is consistently higher than it is with a passage width of 250 mm. As shown in Figure 1 (top), the curves are essentially parallel.

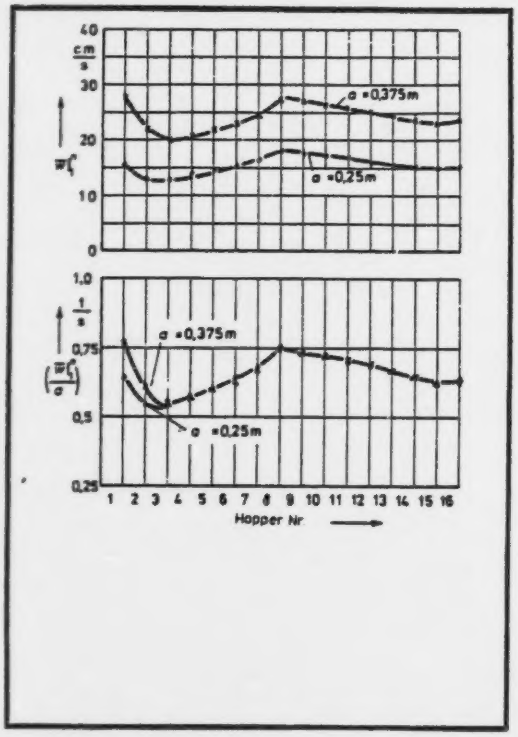

Figure 1. Comparison of w-Values at 250 and 375 mm Passage Spacing.

The plotting of the relationship w/a as a function of precipitator length produces practically identical curves, i.e. the same collection efficiency values exist at every part of the precipitator. The total collection efficiency value of wide passage spacing is just as high as that of the precipitator with a narrow passage spacing (Figure 1 - bottom) and the w-value has increased proportionately to passage width. One thus obtains the same clean gas dust content values.

Tests carried out on pilot precipitators can reproduce the qualitative character of the mechanisms of separation process, but experience demonstrates that the applicability of these test results to industrial plants is limited.

In recent years, Lurgi has been providing more and more precipitators, downstream of industrial plants, with passage widths increased to 16 inches (400 mm). It has been observed that, even in large-scale plants, effective migration velocity increases proportionately to passage width, but only on the condition that the same specific discharge current is reached when the maximum applicable voltage - or sparkover voltage - is applied. Since the discharge current density depends on the ratio of discharge electrode clearance to passage width, the discharge electrode spacing was also enlarged.

Extensive comparative data testing was conducted in two industrial plants, one a cement plant, and the other an electrical power plant. In both cases, the electrostatic fields were provided with rows of plates with different clearances (thus enabling a direct comparison between collection efficiencies). Test results of both plate arrangements will be examined in the following.

CEMENT PLANT PROCESS TESTS

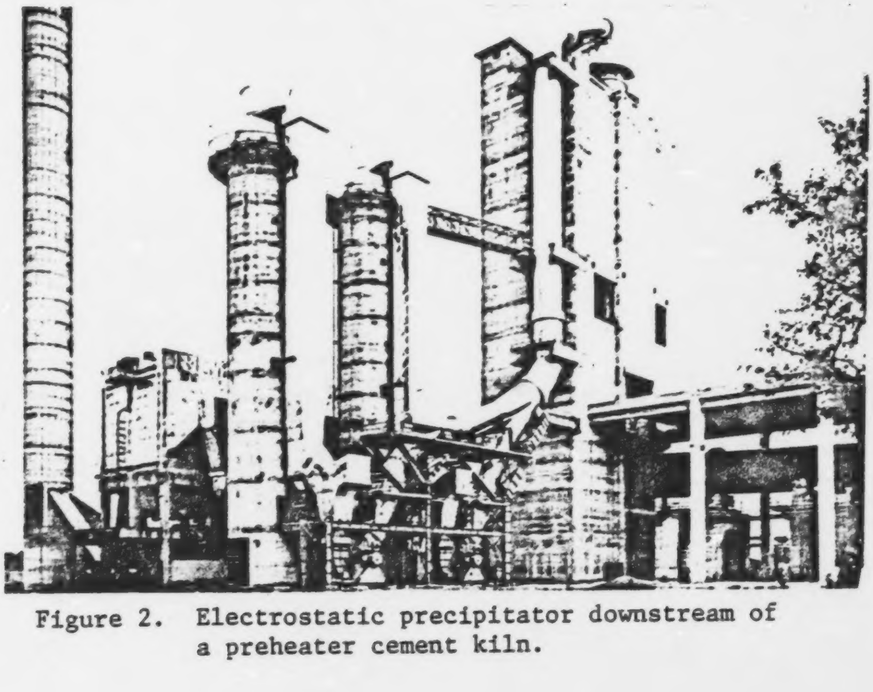

Figure 2. Electrostatic precipitator downstream of a preheater cement kiln.

A large-scale pilot plant (see Figure 2) was installed in a cement plant in order to clean waste gases from a pre-heater.

As shown in the plant flow diagram (Figure 3), waste gases from the kiln were conveyed via 3 two-chamber, two-field precipitators.

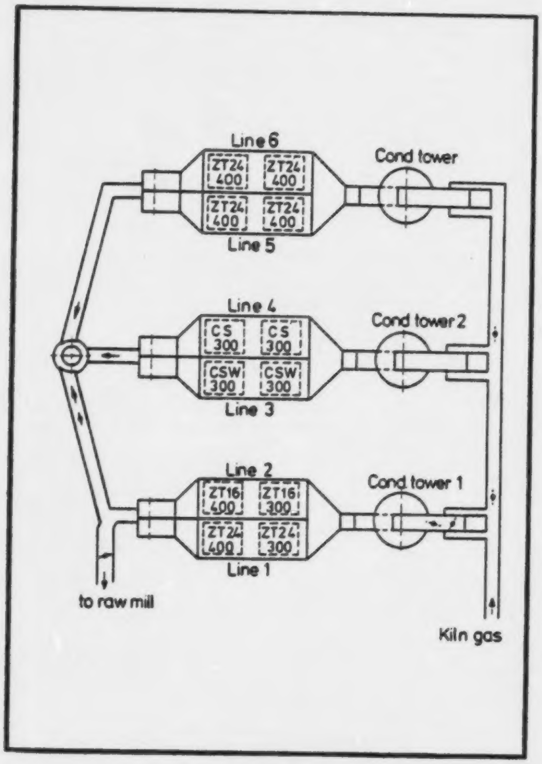
Line 6
ZT24 400
ZT24 400
ZT24 400
ZT24 400
Line 5
Cond tower
Line 4
CS 300
CS 300
CSW 300
CSW 300
Line 3
Cond tower 2
Line 2
ZT16 400
ZT16 300
ZT24 400
ZT24 300
Line 1
Cond tower 1
to raw mill
Kiln gas

Figure 3. Schematic view of the dust collection system.

Whereas tests in lines 3 and 4 were carried out entirely with collection and discharge electrode combinations having a passage width of 300 mm, precipitator lines 1 and 2 allowed a direct comparison to be made between the different configurations, since the large passage width was used here for secondary cleaning.

Evaporative coolers located upstream of the precipitators also made it possible to vary the gas temperature and water dew point and thus to influence dust resistivity.

Table 1 shows the values of some important operating and measured data for two temperature ranges (gas temperatures 340°C/155°C).

TABLE 1. COMPARISON OF TEST RESULTS (PW 300 vs. 400 mm)

gas temperature	[°C]	340		155	
gas passage width	[mm]	300	400	300	400
ratio of GPW	$\frac{400}{300}$	1,33			
voltage U	[kV]	29,6	52	44,4	65
ratio of voltage	$\frac{U_{400}}{U_{300}}$	1,75		1,46	
collection efficiency	[%]	97,3	98,2	97,3	98,1
ratio of w-value	$\frac{w_{400}}{w_{300}}$	1,46		1,45	

As may be deduced from Table 1, with wide passage spacing it was possible to achieve an out of proportion increase in the maximum applicable voltage in the above-mentioned temperature ranges, or an increase in field strength. The specific discharge current remained at the same high level in every case. Hence, the total discharge current decreases proportionately to the clearance ratio in fields with wide passage spacing.

As far as dust separation is concerned, greater efficiency and thus lower stack emission levels can be achieved with a passage width of 400 mm. The ratio of the w-values (factor 1.45) produces an improvement which is out of proportion to the passage widths (factor 1.33).

Similar testing of a precipitator applied on a coal fired utility boiler, which was originally provided with two collection fields, produced similar examples of the efficiency of a precipitator with wide passage spacing. Stricter clean air standards made it necessary to install two extra fields, in which a passage width of 400 mm was provided, compared to the original equipment passage width of 265 mm in the original (first) two fields.

The collection effect of the individual sections could be measured by first connecting the fields to and then disconnecting them from the system and by precisely monitoring the individual incoming and outgoing gas streams.

Test results were similar to results of the cement kiln precipitator. Although the passage width ration (400 mm/265 mm) was only 1.51, the maximum high-voltage values and thus the w-value ratio were increased above this factor. In this case, the 400 mm passage width lead to a disproportionate improvement in collection efficiency in the precipitator, thus achieving a lower clean gas dust content and an increase in precipitator collection efficiency.

Although a good deal of work by worthy institutions and companies has been conducted to attempt to explain the phenomenon of the w-value increase in units with wide passage spacing, there are still gaps in theory. Nevertheless, there are several logical considerations which may be used to explain the phenomenon.

For example, it can be proven by calculation and measurement that an increase in field intensity in the vicinity of the collection electrodes goes hand in hand with the increased passage width, and consequently, that the w-value, according to equation 2, is influenced by the square of field intensity. Moreover, assuming the same close erection tolerance of the plates, minor inaccuracies in the spacing of the plates are of less importance, with the beneficial result that the applicable voltage and hence the average field intensity can be increased.

Another theory is that an increase in plate spacing and the corresponding reduction of collection areas, decreases those effects which have a negative bearing on collection in the boundary layer area of the plates. Such effects are: reverse ionization, re-diffusion of particles which have not been separated and the raising of dust by ionic wind.

Economically, the use of wider passage spacing designs make it possible to reduce the plant costs due to reduced material, production and erection costs. An area of resulting cost increase involves the transformer-rectifier sets, which must be designed to produce higher d.c. voltages. However, net investment costs are still reduced, especially for larger precipitator plants.

ELECTRODE DESIGN

In general, an optimum increase in migration velocity by means of a wide passage spacing may be achieved provided the design configuration of the discharge and collection electrodes is optimized. Homogeneity of the electrical field has a decisive effect on the level of voltage which may be attained. In this respect, a tubular precipitator is ideal, since the lines of force radiate outwards from the emitter in a completely symmetrical pattern ensuring a uniform current distribution.

In the case of parallel, passage-forming collecting plates, this situation is not so easy to bring about, as other criteria have also to be observed. For example: lateral rigidity, shape of the roll formed profile, stacking and erection simplicity, resistance to rapping stress, vibration properties and also dust retention ability and capacity to avoid dust reentrainment.

Figure 4 shows the distribution of current density for different types of collecting electrodes as measured in the laboratory. A flat plate is used as the control electrode.

The profiles indicate that current density distribution is very uneven in the case of the flat plate and also the flat plate with

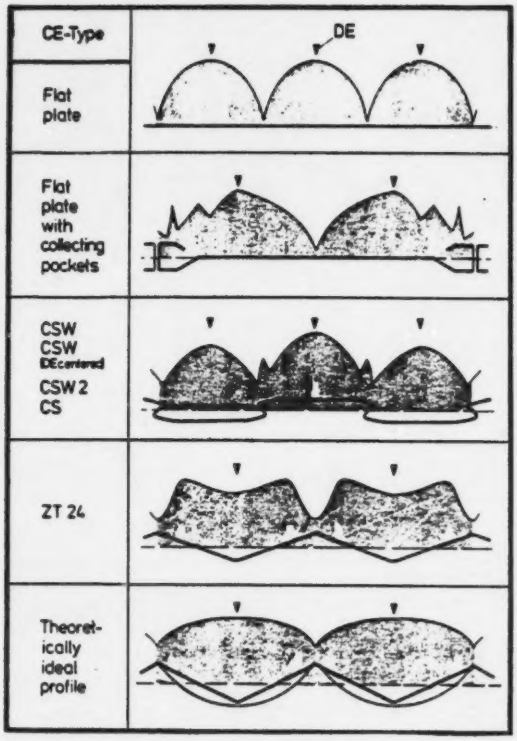
CE-Type
DE
Flat plate
Flat plate with collecting pockets
CSW
CSW DEcentered
CSW 2
CS
ZT 24
Theoretically ideal profile

Figure 4. Current density distribution.

collecting pockets, back ionization occurring at points with high specific flows. The aim of every collecting plate design should, therefore, be to produce as even a current distribution as possible, which leads at the same time to a maximum applicable voltage. The ideal shape would be a semicircular profile (bottom figure); this shape, however, would be extremely difficult to manufacture and lead to a substantial increase in material costs.

A successful compromise, in our opinion, is the so-called ZT electrode (wave-shaped). With its relatively even current density distribution, back ionization is markedly suppressed while the profile shape ensures a good dust-retaining capacity.

This ZT electrode arrangement specifically developed for broader passage widths is shown in Figure 5. With the discharge elements arranged in the middle, this electrode design comes close to providing the ideal conditions of a tube precipitator due to the approximately semi-cylindrical form of the plates.

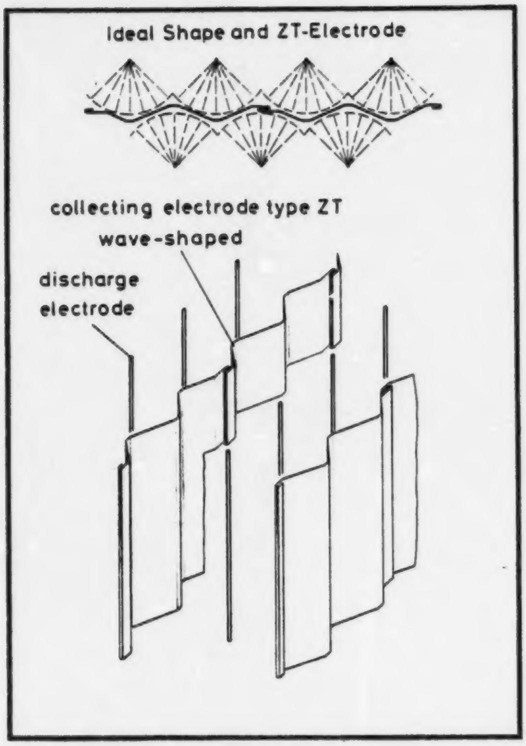
Ideal Shape and ZT-Electrode
collecting electrode type ZT
wave-shaped
discharge
electrode

Figure 5. Collecting Electrode Type ZT.

A further important factor to be taken into account in the design of collecting electrodes is the acceleration behavior. In our experience, at least 100 g should act on every part of the collecting electrode surface to guarantee efficient cleaning of the electrodes.

Figure 6 (comparison of acceleration values) compares the acceleration values of a shaped electrode and a flat plate (height 12 m/length 2.5 m). Both were rapped with a 5 kg hammer on the bottom supporting bar. As can be seen, the shaped electrode conducted the acceleration much better, with the result that 305 g was measured even at the point furthest from the point of impact of the hammer. With the flat plate, only 15% of this value was measured.

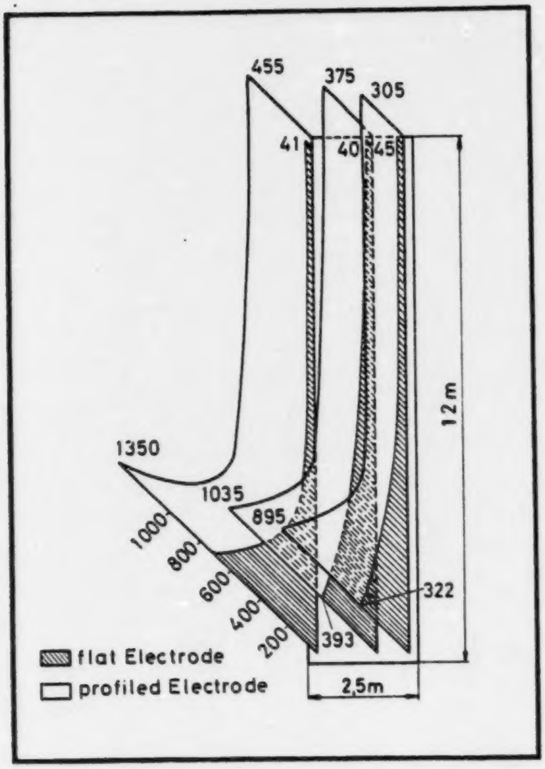

Figure 6. Collecting Electrodes Measurements of Acceleration.

A genuine comparison of different discharge and collecting electrodes is only possible if different variations are tested under the same gas and dust conditions. This means that parallel precipitators with different internals are installed downstream of the equipment to be dedusted (e.g. boiler, rotary kiln, fluidized bed kiln) and compared with regard to migration velocity.

Lurgi was able to perform such tests downstream of a preheater kiln in a cement works. In the first stage, different collecting electrodes were compared at different passage widths. The results with regard to the larger passage width were shown in Table I for different operating temperatures.

After proving the performance superiority of large passage widths, an enlargement of the kiln afforded the opportunity to install different design discharge electrodes in parallel units 5 and 6, each already modified with wide 400 mm passage width. Although it is not possible to discuss the results in detail here, it can be said that different discharge electrodes produce substantially different results under the same gas and dust conditions and that the electrodes have to be carefully matched to the shape of the collecting electrodes.

OPTIMIZATION OF ELECTROSTATIC PRECIPITATOR OPERATION BY THE USE OF MICROCOMPUTERS AND PROCESS COMPUTERS

INTRODUCTION

In recent years there has been increased interest and development work regarding the use of microcomputers and process computers for electrostatic precipitators. A principle reason for this is that, in recent years, emission standards for electrostatic precipitators have been progressively tightened. Particulate collection efficiencies of 99.98% and more are not unusual nowadays and this high performance level inevitably results in the construction of larger electro-precipitators. In the cement industry, for example, electrostatic precipitators with collector plate areas of 10,000 m^2 (108,000 ft^2) are normal. In the utility industry, areas of more than 100,000 m^2 (1,080,000 ft^2) are frequently encountered.

Larger precipitator sizes result, of course, in increased power consumption, with specific power input normally rising more steeply as particulate content decreases. For instance, an electrostatic precipitator applied on a cement kiln rated at 4.500 tpd and with an average mill capacity of about 400 tph has a connected power of approximately 2 MW. For a 1,300 MW electrical power plant, connected power of the precipitators may be as high as 20 MW or more. These are electrical power consumption levels which command conservation measure attention.

STATE OF THE ART

The principle of electrostatic precipitation is well known and well proven. A high voltage transformer rectifier set produces a negative voltage which is then applied to the discharge electrodes of the electrostatic precipitator.

Gas molecules in the particulate laden gas stream flowing by the discharge electrode receive a negative charge from the electrode emitted corona. These negatively charged gas molecules in turn impart a charge to dust particles in the gas stream which migrate under the influence of the electric field to the collecting electrodes where they are deposited.

The high voltage transformer rectifier set requires a control system, and in recent years these have been analog control systems.

The principle of the analog control system is seen in Figure 7. The high voltage in the electrostatic precipitator is increased to the flashover limit. Upon flashover, the voltage drops to zero and the thyristors are blocked during a so-called deionization period which enables restabilization of the ionized gas passage; this normally lasts for 20 milliseconds.

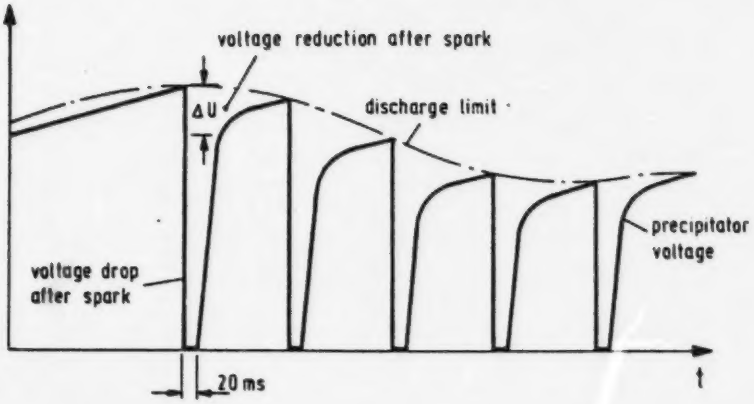

Figure 7. Principle of an Analog Control System.

Afterwards, the voltage is rapidly increased according to a defined curve up to a specific level, from where it is once again slowly raised to the flashover limit, the voltage rise also proceeding according to a defined curve. In such control systems these three (3) parameters - voltage reduction, deionization time and voltage increase - are adjustable but pre-fixed. Based upon empirical data, these operating parameters are generally adjusted to mean values. Accordingly, conventional analog control systems do not enable optimum adaptation to changing process conditions. Moreover, they provide no possibility for storing important, measured variables. To overcome these disadvantages of the conventional analog control system, attention has focused upon the unique capabilities of microcomputer systems.

SYSTEM COROMATIC, PRECICONTROL

Figure 8 gives a schematic of a two-stage system. The first stage - the so-called COROMATIC - comprises a microcomputer control system for each individual high-voltage unit. Moreover, there is a PLC for control and monitoring of all auxiliary drives of the electrostatic precipitator plant.

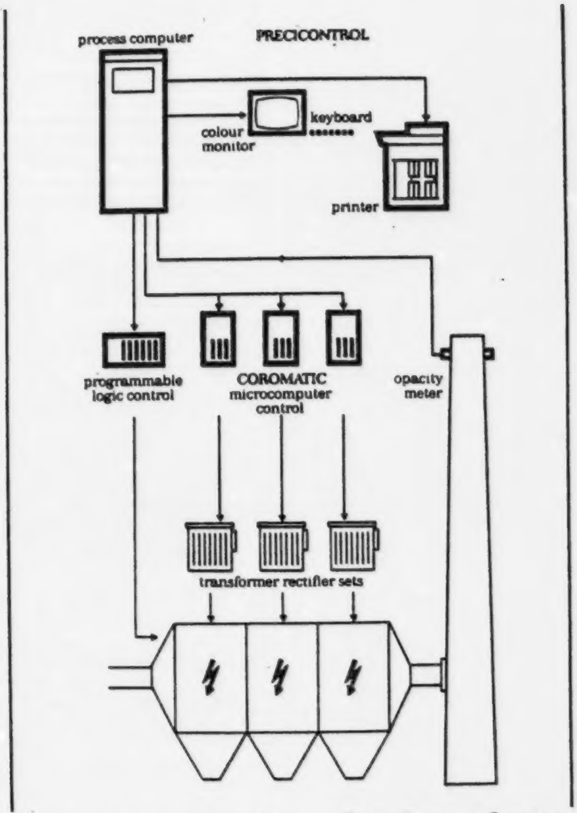
process computer
PRECICONTROL
colour monitor
keyboard
printer
programmable logic control
COROMATIC microcomputer control
opacity meter
transformer rectifier sets

Figure 8. Schematic - Two-Stage System.

The second stage - the so-called PRECICONTROL - consists of a process computer to monitor the overall precipitator plant, coordinate process control, optimize the dust collection efficiency and minimize operating costs.

Associated peripheral equipment includes a color monitor for parameter, process, and alarm displays, a process control terminal for operation of the plant, a printer for logging process and operating events, as well as data memory in the form of floppy disks for filing relevant process data.

COROMATIC

Concentrating upon the function of COROMATIC, the most important function of a transformer/rectifier set for electrostatic precipitators is to maintain the electrical field voltage at an optimum level under all operating conditions.

This voltage should be applied without interruption and, normally, at the highest values possible; that means, it should be controlled at a level immediately below the flashover limit. Continuous accurate detection of this process-dependent, constantly varying flashover limit is of paramount importance. To date, the only criterion available to determine this limit is the flashover itself. Accordingly, detection of flashover at all operating conditions is key for proper process control.

The top part of Figure 9 shows the curve of the high voltage in an electrostatic precipitator. The ripple content of the voltage is very high. In three cases, there are weak voltage drops, which indicate flashovers in the gas passage between the discharge and collecting electrodes. The bottom part of the figure shows the follow-up reference voltage. With a conventional analog control system, detection of a flashover was only possible if the high-voltage drop actually intersected the reference voltage. In this figure, this is not the case and, accordingly, the three flashovers which have occurred were not detected. This disadvantage can be overcome. COROMATIC digitalizes every half wave of high voltage into a series of measured values within a very narrow grid and stores these values in its memory. The succeeding half wave is equally digitalized and the values obtained are then compared with those of the preceding half wave. If the deviation of the compared values is inadmissibly high, a flashover is detected. A number of tests have shown that this type of flashover detection is far superior to that of the analog system. Thus, low intensity flashovers as represented in Figure 9 can be reliably detected.

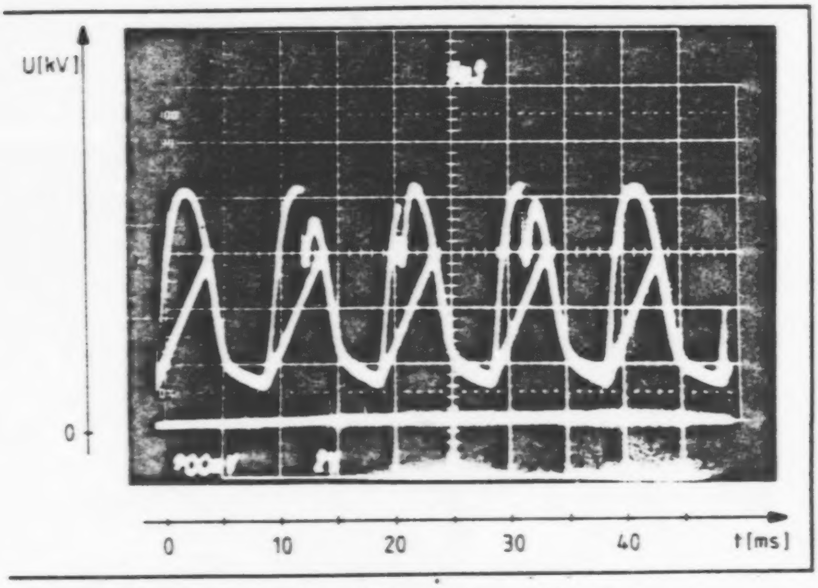

Figure 9. High Voltage Wave Shape.

Another important function of COROMATIC lies in the optimization of the voltage/time area and thus, the optimization of the dust collection efficiency. On one hand, the number of flashovers in a precipitator must be kept to a minimum to maintain electrode voltage as constant as possible and also to avoid damage to the electrodes. On the other hand, electrode voltage must be maintained at the highest possible level; which means that fluctuation of flashover limit in the precipitator must be constantly detected and controlled. An analog control system can only react with preset measures, set prior to start-up, to varying operating conditions.

COROMATIC, on the other hand, constantly adapts to varying operating conditions, since its memory permits the detection of rising, decreasing or constant flashover limits and hence rectification by applying variable scanning periods and steps. Thus, the scanning period is prolonged into the range of several minutes in the case of stable precipitator operation with constant flashover limit, while it is reduced into the range of seconds in the case of fluctuating operation.

The voltage/time area can be further optimized by optimum reaction to a flashover. This is achieved by adapting the voltage reduction to the curve of the precipitator characteristic, or to the current/voltage curve.

The current/voltage characteristics of an electrostatic precipitator may vary over a wide range from a very flat shape to an extremely steep one and also those representing a voltage maximum. Figure 10 shows three such typical characteristics. COROMATIC records the respective characteristics at defined intervals and stores them in its memory. If the

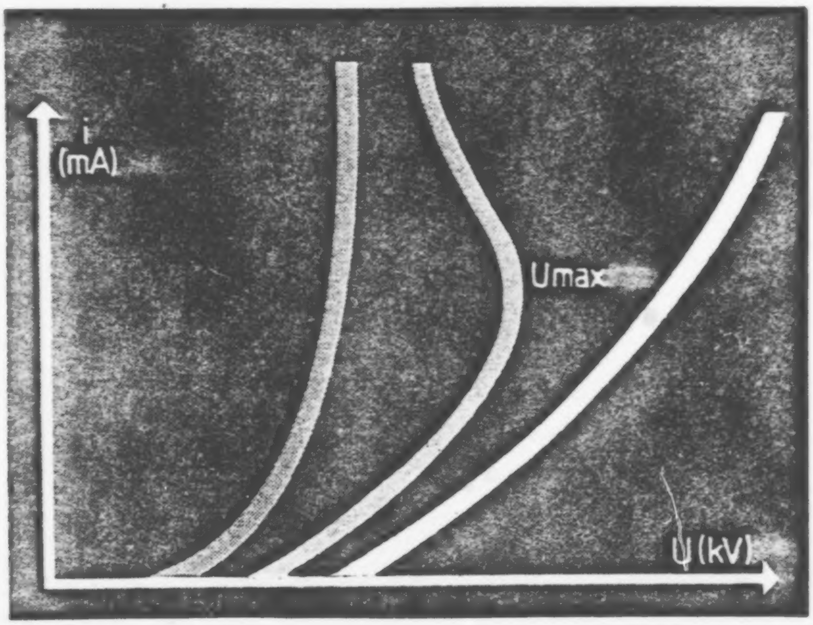

Figure 10. Typical Current-Voltage Curves.

characteristic is steep, a minor change in voltage causes a major change in current, the reverse effect taking place if the characteristic is flat.

To ensure that the transformer-rectifier set is optimally adapted to the operating conditions prevailing, COROMATIC calculates the steepness of the characteristic just recorded and decides on the basis of the result as to whether the adjustment of the voltage reduction after a flashover should be by current steps or by voltage steps, i.e. in the case of steep characteristics, control is by current steps, in the case of flat characteristics, by voltage steps. If the characteristic has a voltage maximum, COROMATIC adjusts to a value directly above the voltage maximum.

Moreover, the reaction to a flashover is optimized by adjusting the deionization time and the curve of voltage increase after a flashover via a programmed learning algorithm, the optimization criterion being the avoidance of sequence flashovers. Figure 11 shows some of the various reactions possible in the form of a graph. After the first flashover in the precipitator, COROMATIC reduces the voltage only slightly. If no further flashover occurs, the reaction on the next flashover will be the same. However, if there is a follow-up flashover after some time, the corresponding reaction is the next more severe level, namely voltage zero and rapid increase of the voltage to a defined level with a smooth slow increase to the flashover limit. If this measure is sufficient, i.e. if there is no further follow-up flashover, the reaction on the next flashver will be the same. Provided that this reaction produces desired results for the next five flashovers, a less severe level will be resorted to with the sixth flashover. Thus the reactions of COROMATIC are adapted

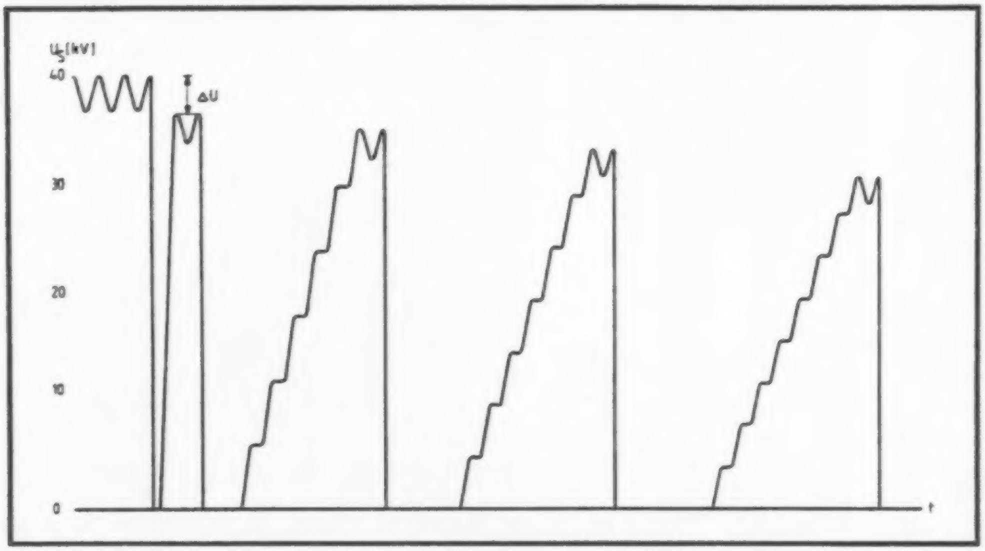

Figure 11. Reactions by COROMATIC to Sequence Flashovers.

to the different types of flashovers. In addition, the prevention of follow-up flashovers results in another increase in voltage/time area and thus in an improvement of the dust collection efficiency. A prolonged burning arc is detected when the voltage is below a specific value, the so-called under-voltage limit, and the current, at the same time, exceeds a specific value, e.g. 30% of the rated current. In such a case, operation will be stopped after a defined period of time.

All in all, a comparison of conventional analog control systems with COROMATIC shows clearly that optimum adaptation of flashover reaction to the varying process conditions enables an improvement in the voltage/time area and thus in the dust collection efficiency.

Figure 12 shows the reaction of an analog control system to a flashover with the associated high loss in voltage/time area. Figure 13 shows the reaction of COROMATIC to a flashover. The optimization of the voltage/time area is evident.

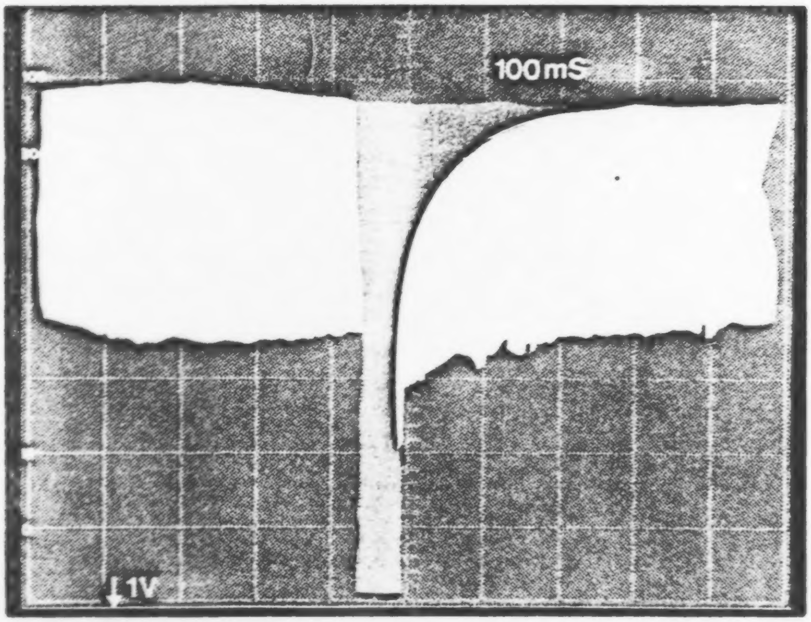

Figure 12. Flashover Reactor by Typical Analog Control.

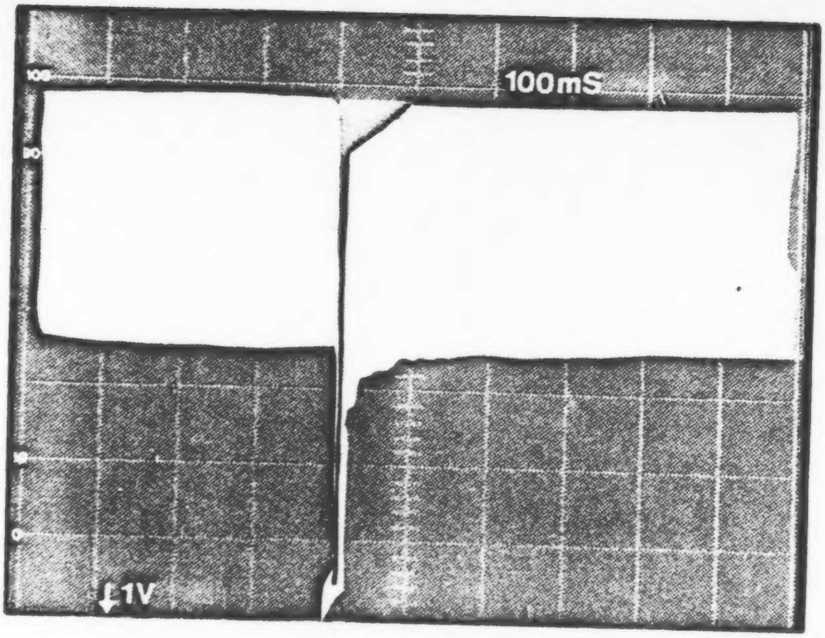

Figure 13. Flashover Reactor by COROMATIC.

In addition, COROMATIC is equipped with a special program to optimize the dust collection efficiency during rapping of the collecting electrode plates.

It is generally known that the electric forces of adhesion cause the dust to cling to the collecting electrodes. To reduce these forces of adhesion and to achieve optimum cleaning of the electrodes by rapping, COROMATIC reduces the voltage by a preset value during the rapping cycle and increases it again to the former level after completion of rapping. Figure 14 shows a large number of flashovers as they are caused by the churning up of the dust during rapping of the collecting electrodes. The sharp decrease of the high voltage due to the frequent flashovers is evident with the analog control system. Figure 15 enables a comparison with the high voltage behavior in COROMATIC-controlled plants. Here the voltage is slightly reduced at the beginning of the rapping cycle, any further voltage drop due to flashovers being prevented by means of a program. After completion of the rapping cycle, the high voltage is once again raised to its initial value.

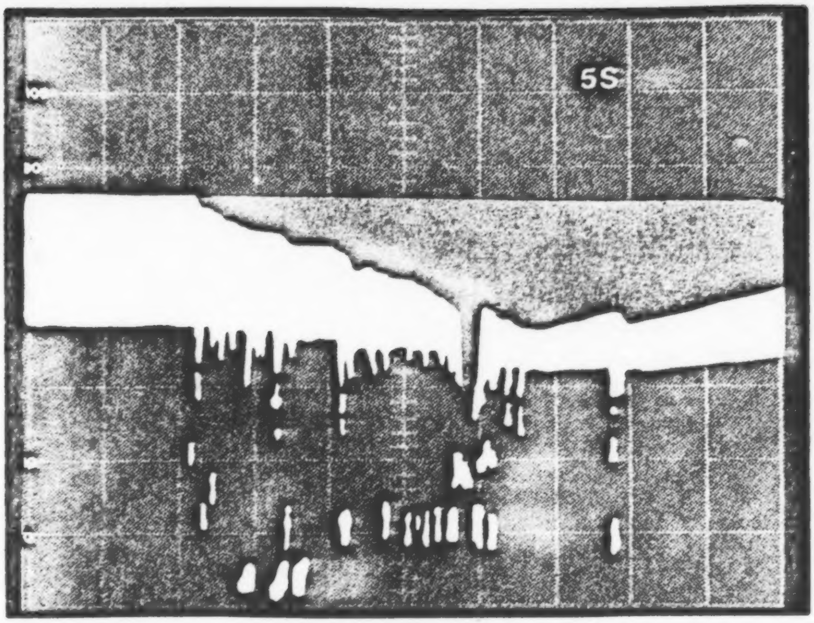

Figure 14. Flashover During Rapping - Typical Analog Control.

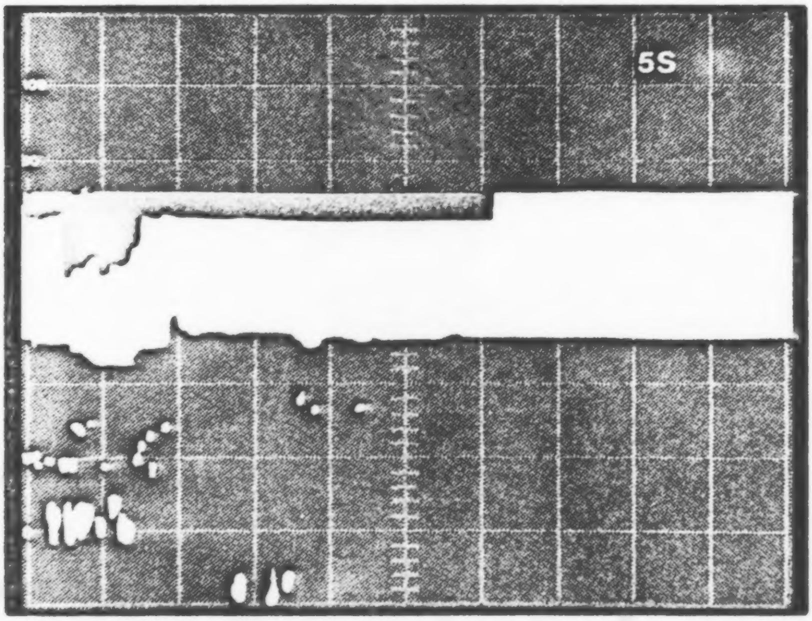

Figure 15. Flashover During Rapping - COROMATIC Control.

The improvement in the voltage/time area is considerable. Dust puffing at the stack is thus considerably reduced or even eliminated.

Comparative tests carried out with the conventional analog control system and COROMATIC have shown that at given operating conditions, considerably less dust is discharged to the environment with COROMATIC. Thus, COROMATIC enabled an improvement in the migration velocity by more than 8% depending upon the process. In other words, this means that up to 8% of the collecting electrode area can be dispensed with in COROMATIC-controlled plants, the special rapping program contributing a major share to this achievement.

Due to the evaluation of the precipitator characteristic, COROMATIC features yet another possibility for process-adapted operation. As has already been mentioned, COROMATIC adjusts to a value just below the voltage maximum in the event of a characteristic with voltage maximum. This is at the same time the point where optimum dust collection efficiency is achieved. In addition energy is saved by not applying the ineffective precipitator current. Compared with analog control systems, for instance, energy savings of more than 33% were reached in tests with a simultaneous improvement of the collection efficiency.

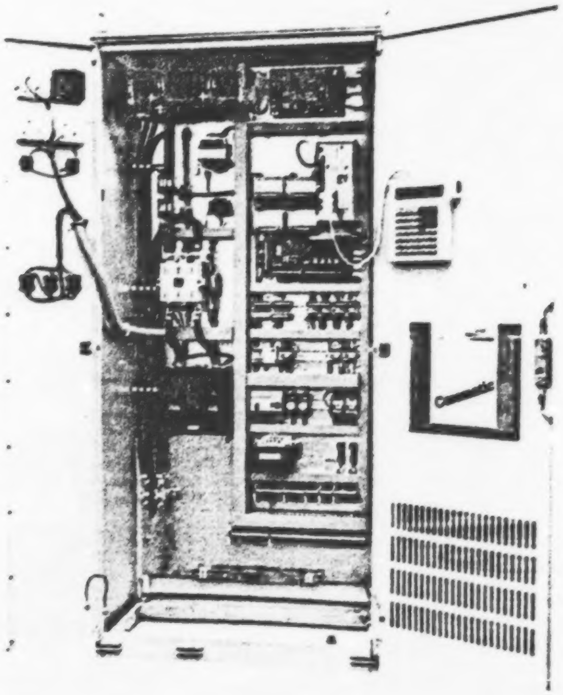

Figure 16. COROMATIC Control Cabinet.

Reproduced from best available copy.

All the functions mentioned so far are carried out by COROMATIC independently, so that even without the superordinated second stage, the use of this control system offers considerable advantages in electrostatic precipitator operation, as becomes apparent in the obvious improvement in the overall dust collection efficiencies. Figure 16 shows a control cabinet accommodating such a system and a portable keyboard.

It should be pointed out that COROMATIC is equipped with a data interface to transmit relevant factors to and receive commands from a superordinate process control system.

PRECICONTROL

Let us now have a closer look at the function of the process control system PRECICONTROL. The relevant input data required for PRECICONTROL from the preceding process are the inlet dust load, usually substituted by, for instance the fuel feed rate and/or mill output on the one hand, and the gas temperature, gas volume, the type of dust and the dust resistivity on the other hand. In addition, the relevant input data for the actual dust collection process are required, such as current and voltage of the individual precipitator zones, the precipitator characteristic, that means the profile of the current and voltage curve, the rapping signal, the electric power applied and, last but not least, the clean dust gas content.

The first important function of this system is the monitoring of the overall precipitator plant. This is realized by the indication and printing out of all error messages on the color monitor and the printer. Moreover, all switching operations carried out by the operator are recorded by means of the printer. The operating conditions of all units are signalled in the graphic display part of the color monitor. The filing of the operating data on a floppy disk enables the operator to trace back on previous operating events. Moreover, it would also be possible to coordinate maintenance via display.

Another important function of the PRECICONTROL system is process control. The process control terminal enables automatic start-up and shutdown of the overall electrostatic precipitator plant. In the event of several precipitators per boiler, it provides automatically for an even distribution of the gas stream over the individual precipitators. Moreover, the process control terminal permits remote control of the transformer rectifier sets and all auxiliary drives of the precipitator, such as, the rapping motors, insulator heating, etc.

By means of some pictures, it shall be shown how plant monitoring and process control are realized via a process control terminal and color monitor.

Figure 17 represents an overall display of the entire plant, showing the state of the individual drives and power consumers. Via the process control terminal, the overall plant can be started or shut down by pressing a key. The terminal also offers the possibility of selecting plant units down to the level of each individual drive for individual control. The principle underlying process operation and supervision is that of hierarchical organization.

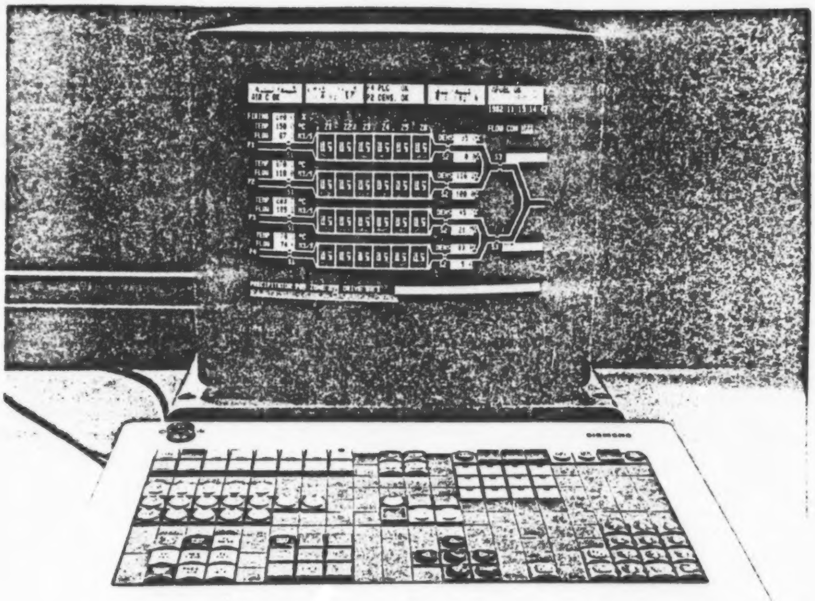

Figure 17. Process Control Terminal.

The operator can select different control levels starting with an overview of the overall plant as shown in Figure 18 down to an individual precipitator as can be seen from Figure 19.

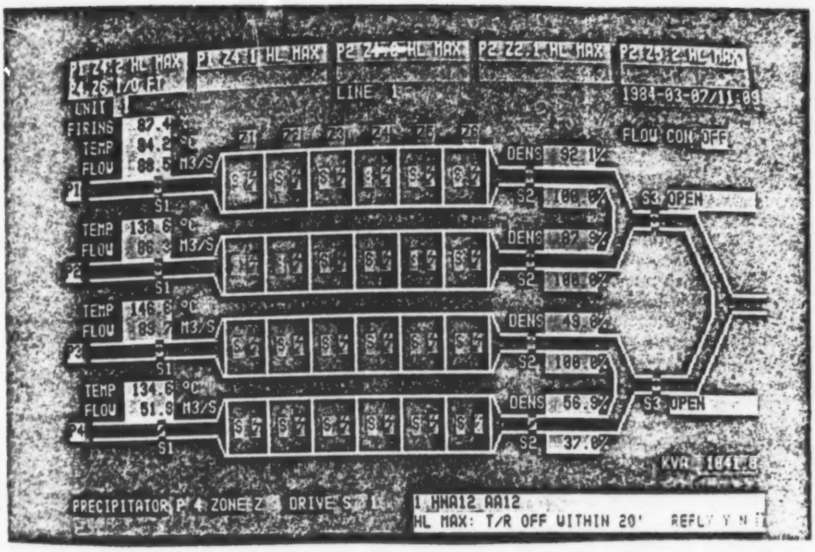

1984-03-07/11:09

PRECIPITATOR P 4 ZONE Z 3 DRIVE S 1

1 HMA12 AA12

HL MAX: T/R OFF WITHIN 20' REPLY Y N

P1 Z4.2 HL MAX
Z4 Z6 I/O F1
P1 Z4.1 HL MAX
P2 Z4.6 HL MAX
P2 Z2.1 HL MAX
P2 Z5.2 HL MAX
LINE 1
UNIT 1
FIRING 87.4
TEMP 94.2 °C
FLOW 88.5 M3/S
Z1
Z2
Z3
Z4
Z5
Z6
DENS 92.1%
FLOW CON OFF
P1
S1
S2 100.0%
S3 OPEN
TEMP 138.6 °C
FLOW 86.3 M3/S
DENS 87.9%
P2
S2 100.0%
TEMP 146.6 °C
FLOW 83.7 M3/S
DENS 49.8%
P3
S2 100.0%
TEMP 134.6 °C
FLOW 51.9 M3/S
DENS 56.9%
S3 OPEN
P4
S2 37.0%
KVA 1841.8

Figure 18. CRT Display of Entire System.

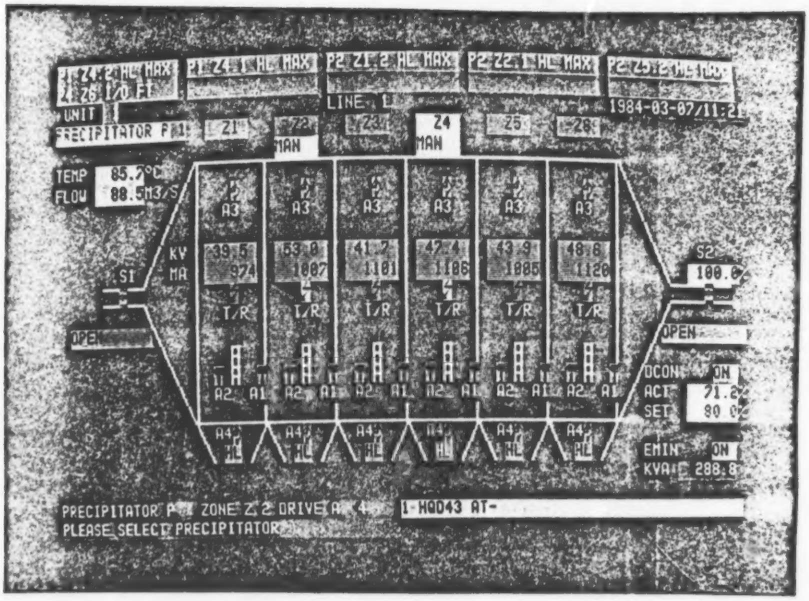

1984-03-07/11:2

PRECIPITATOR P 1 ZONE Z 2 DRIVE A 4

PLEASE SELECT PRECIPITATOR

1-HQD43 AT-

P1 Z4.2 HL MAX
Z4 Z6 I/O F1
P1 Z4.1 HL MAX
P2 Z1.2 HL MAX
P2 Z2.1 HL MAX
P2 Z5.2 HL MAX
LINE 1
UNIT
PRECIPITATOR P1
Z1
Z2
MAN
Z3
Z4
MAN
Z5
Z6
TEMP 85.7 °C
FLOW 88.5 M3/S
A3
KV
MA
39.5
974
53.0
1087
41.2
1101
47.4
1186
43.9
1085
48.6
1120
SI
T/R
S2
100.0
OPEN
OPEN
A2
A1
A4
HL
DCON ON
ACT 71.2
SET 80.0
EMIN ON
KVA 288.8

Figure 19. CRT Display of Individual Precipitator.

Figure 20 represents the display of an individual precipitator zone. The two uppermost lines of the display give information on the respective alarms existing in the overall plant. The graphic display part indicates the state of the individual drives (e.g. rapping motors) and other consumers (e.g. insulator heaters) by means of color signals and text. On the right in the display, the relevant actual data such as high-voltage value, current data and number of flashovers per minute are indicated.

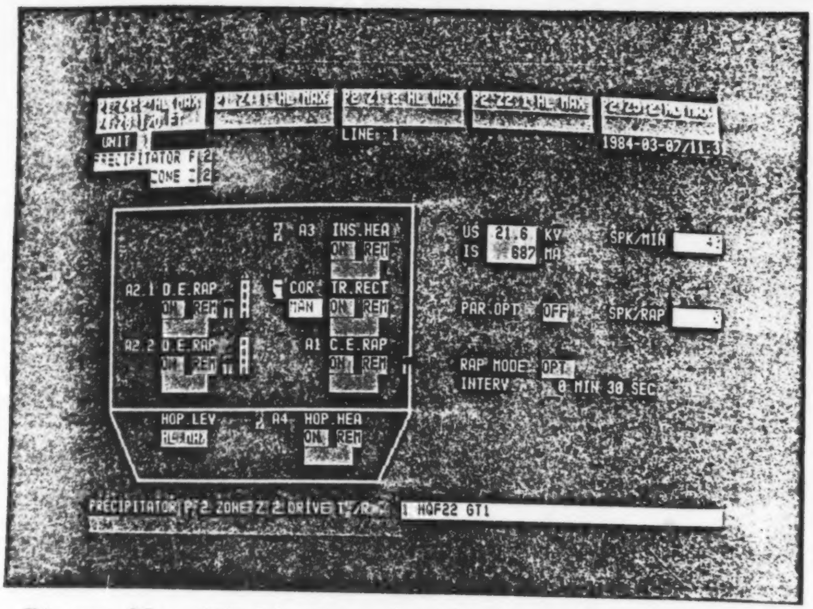
P2 Z1 2 HL MAX
P2 Z2 1 HL MAX
LINE: 1
1984-03-07/11:3
UNIT 1
PRECIPITATOR F 2
ZONE 2
A3
INS.HEA
ON REM
A2.1 D.E.RAP
ON REM
COR
MAN
TR.RECT
ON REM
A2.2 D.E.RAP
ON REM
A1 C.E.RAP
ON REM
HOP.LEV
HL MAX
A4
HOP.HEA
ON REM
US 21.6 KV
IS 687 MA
SPK/MIN
PAR.OPT OFF
SPK/RAP
RAP MODE OPT
INTERV 0 MIN 30 SEC
PRECIPITATOR PF2 ZONE Z 2 DRIVE T/R
1 HQF22 GT1

Figure 20. CRT Display of Individual Precipitator Zone.

Moreover, tables and curves of the measured variables can be displayed on the color monitor, for example the voltage and current levels in the various precipitator zones at defined times as shown in Figure 21. A special feature also enables "paging" through curves already filed.

The diversified possibilities of representing measured variables are supposed, on the one hand, to give the operator a rapid survey of the overall plant and on the other, to inform the plant engineer of the behavior of the electrostatic precipitator as a function of the different process parameters as well as to enable a quick and precise analysis of any failure occurring.

The printer furnishes operational records which serve for the chronological registration of process events such as switching messages, data inputs, error messages and so forth.

An external memory has been provided for the filing of data (e.g. current/voltage values for 24 hours, etc.). The wide range of possibilities leaves the individual user a free hand.

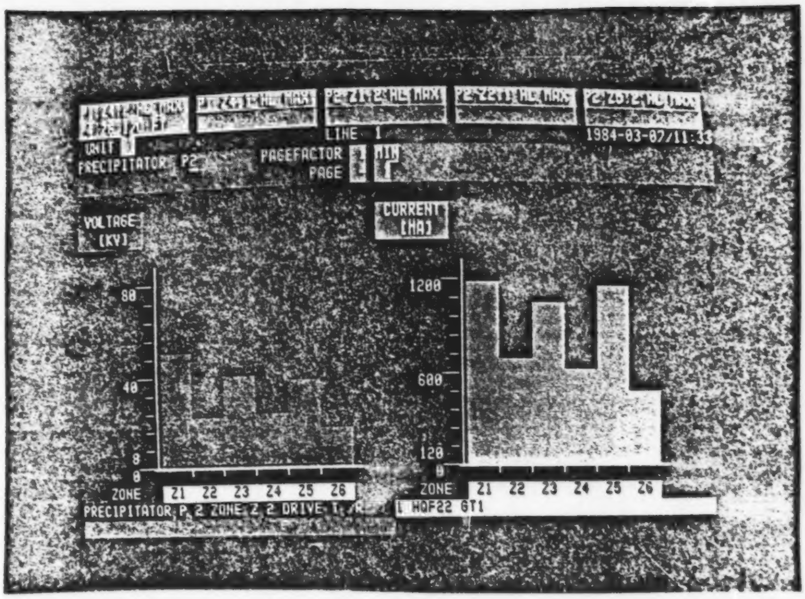

P2 Z1 2 AL MAX
P2 Z2 1 AL MAX
P2 Z6 2 AL MAX
LINE 1
1984-03-07/11:33
UNIT
PRECIPITATOR P2
PAGEFACTOR
PAGE
MIN
VOLTAGE [KV]
CURRENT [MA]
80
40
8
0
1200
600
120
0
ZONE 21 22 23 24 25 26
ZONE 21 22 23 24 25 26
PRECIPITATOR P 2 ZONE Z 2 DRIVE
HQF22 GT1

Figure 21. CRT Display of Voltage and Current in Individual Zone.

As already pointed out, PRECICONTROL has, however, to fulfill important tasks of process optimization apart from these functions of operational control. One of these further functions of the PRECICONTROL system is the optimization of the dust collection efficiency. This is achieved on the one hand, by minimizing the dust peak arising during plate rapping by changing the rate of voltage decrease during rapping. Also, the computer coordinates the collecting electrode rapping of all zones of a precipitator, that means only one precipitator zone is being rapped at a time, thus preventing increased dust emission due to accumulation.

Optimization of the rapping cycle - another function of PRECICONTROL - is to be understood as the constant adjustment of the rapping cycles which were set upon start-up to those that are responsive to varying operating parameters such as boiler or kiln load and/or dust resistivities. The term rapping cycle designates the time interval between two successive starts of the rapping drives. The top of Figure 22 shows the average dust emission as a function of the rapping cycle at 100% load. Minimum dust emission is attained at a defined rapping cycle which is known from empirical data. If the load changes to a value of, for example 50%, the raw gas dust content will be correspondingly lower and the rapping cycle optimum thus moved towards the right in accordance with the lower load. In the bottom part of Figure 22, you can see the average dust emission as a function of the rapping cycle at a defined dust resistivity. If the dust resistivity changes, this will inevitably disturb the electric conditions in the precipitator. With a low dust resistivity, for example, the dust can be allowed to build up more thickly on the collecting electrode plates

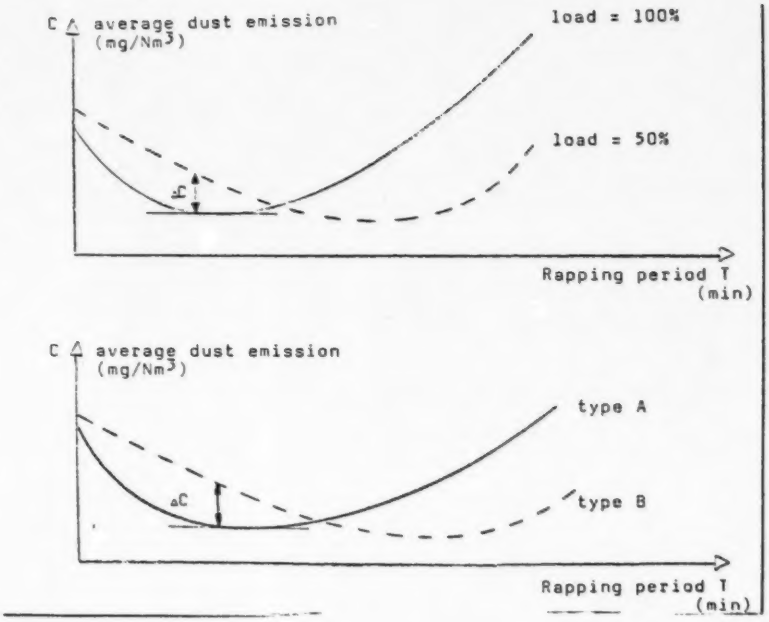

Figure 22. Dust Emission versus Rapping Cycle Period.

without the electric conditions being affected. As opposed to this, a high dust resistivity calls for a thinner dust layer on the collecting electrode plates, that means the rapping cycle has to be changed accordingly.

You might ask, how is the dust resistivity known? As already pointed out, the current/voltage curve of the electrostatic precipitator is stored in COROMATIC. By dividing the voltage by the current, a measure for the resistivity is obtained. This measure can be evaluated within the process computer by means of a special program. The rapping cycle is then optimized and adapted to the changed process conditions as a function of the result of this calculation.

Another important function of the PRECICONTROL system is the reduction of operating costs. This is achieved first by means of smoke density control which reduces the energy consumption of the electrostatic precipitator during partial load operation at a constant set point value. For this function, a relatively simple control circuit as shown in Figure 23 has been provided. Secondly, there is the energy minimizing program which goes some steps further. By continuously distributing the overall energy requirement to the precipitator zones operating at maximum efficiency, this

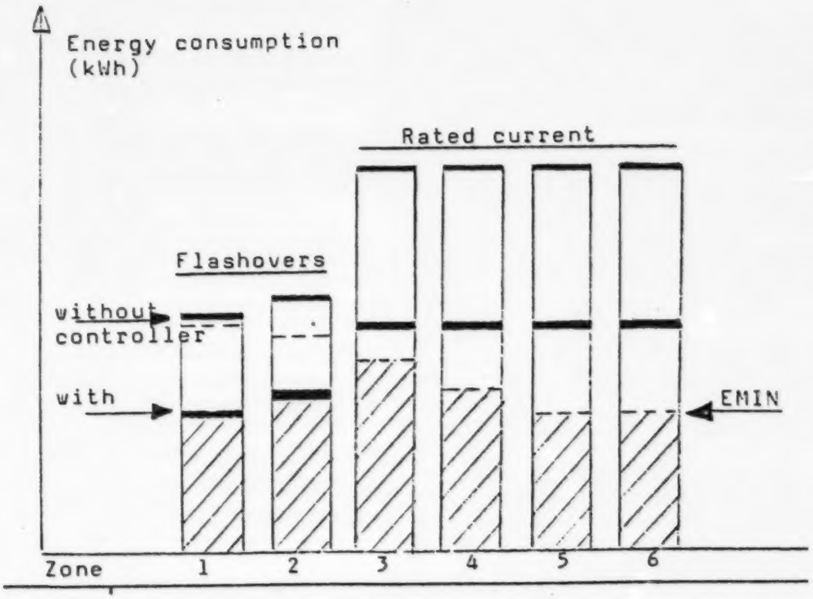

Figure 23. Energy Minimization with Precicontrol.

program enables energy savings without the dust collection efficiency being impaired. How is this possible?

All conventional control systems for transformer rectifier sets have been so designed that the maximum possible electric energy is supplied to the connected precipitator section. However, practice has shown that this is not always expedient since especially with steep current/voltage characteristics, an increase in current does not necessarily lead to an improved efficiency, that means there is a kind of saturation current which is ineffective. This phenomenon is frequently encountered with highly resistive dusts and it becomes particularly evident in characteristics with distinct voltage maxima. For these cases, a limitation to the voltage maximum has already been provided for in the program of COROMATIC.

The energy minimizing program in PRECICONTROL does, however, not stop at this point but attempts an elimination of this saturation current without any noticeable reduction in the collection efficiency of the electrostatic precipitator. For this purpose, it is essential to know the current voltage characteristics. As already mentioned, these are recorded by COROMATIC at regular intervals and transmitted to PRECICONTROL. Moreover, it is necessary to know the clean gas dust content, this value being available from opacity feedback to PRECICONTROL. In accordance with a programmed strategy, the power inputs of the transformer-rectifier sets are reduced as a function of the current-voltage characteristic and the location of the precipitator fields supplied, until a minor deterioration in the clean gas dust content is read. Any interferences, such as failure of a transformer rectifier set, load changes, etc. are, of course, taken into account.

The energy savings resulting from this strategy have been confirmed by several tests, one of them having been carried out in the Leimen Works of Heidelberger Zement AG. The measurements were carried out on an electrostatic precipitator with a collecting electrode area of 4,166 m^2 (45,000 ft^2). As can be seen from Figure 24, it was possible to achieve energy savings of 30.2 kW in the first field a similar savings of 20.4 kW was possible in the second field without affecting the collection efficiency. This results in total energy savings of approximately 70% as compared with conventional control systems. The same measurements were performed on electrostatic precipitators downstream of a 750 MW power station in Germany. In this plant, it was also possible to save 70% of the energy without impairing the collection efficiency of the precipitators. With a connected capacity of the precipitators of 1.6 MW, the savings come to a very large dollar amount.

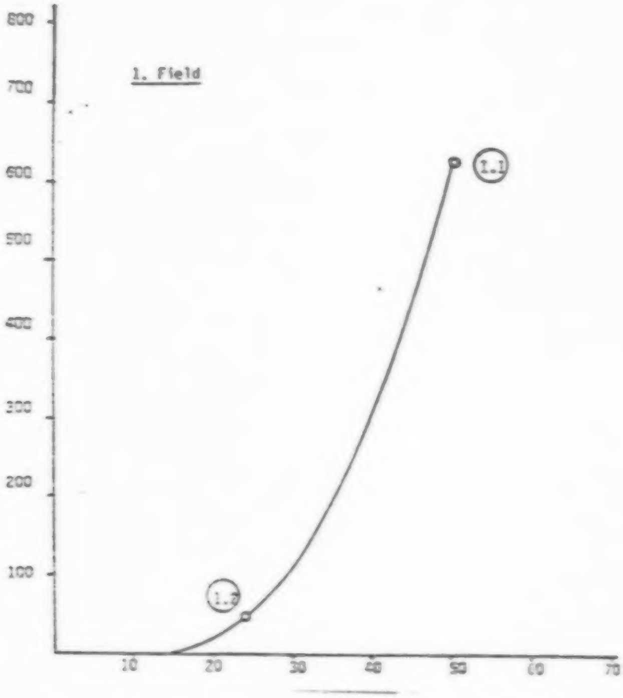

Figure 24. Energy Savings - Lieman Works - Field I

How about the availability of the overall PRECICONTROL system? In the event of a failure of one component, the startype layout will prevent a breakdown of the entire system. Each component, computer, PLC and COROMATIC system can continue operation independently. After a power failure, the components will automatically restart and continue operation once the voltage has returned.

What savings can be expected with the use of the PRECICONTROL system? Let us start with the installation costs which are much lower for PRECICONTROL than for conventional systems, since a large number of cables, switches, panel instruments, etc. can be dispensed with. PRECICONTROL requires only one data line each for communication between the individual components. As regards energy costs, savings up to 70% are possible. With frequent partial load operation, the 70% mark can no doubt even be exceeded. Moreover, the user friendly design reduces the number of shift personnel required and thus labor costs. As to reference plants, I would like to mention that about 400 high-voltage supply units are being equipped with COROMATIC or have already gone into operation all over the world. At present, six PRECICONTROL systems have been sold for large-size electrostatic precipitator plants. One PRECICONTROL system has been put into operation to date.

REFERENCES

1. Aureille, R. and Blanchot, P. Staub-Reinhalt, Luft 31, 1971. Number 9: 371, 375.

2. Masuda, S. Present Status of Wide-Spacing Type Precipitator in Japan. EPA Symposium, Denver, Colorado, July 1979.

3. Gūpner, O. Dissertation, University of Essen, 1976.

The work described in this paper was not funded by the U.S. Environmental Protection Agency and therefore the contents do not necessarily reflect the views of the Agency and no official endorsement should be inferred.

WEIGHTED DISCHARGE ELECTRODES - A SOLUTION TO MECHANICAL FATIGUE PROBLEMS

By
John A. Knapik
Neundorfer, Inc.
Willoughby, Ohio 44094

ABSTRACT

This paper discusses a specific aspect of discharge electrode failure, i.e. mechanical fatigue at the shroud-wire interface. This type of failure has been specifically addressed in a novel approach of changing the rigidity of the shroud in order to reduce the stress concentrations in the area of the interface.

It is demonstrated that using a close wound spring as the shroud material, as opposed to the solid shroud that is in common use, significantly reduces stress concentrations at the interface. This stress reduction would be expected to enhance fatigue life. Further, the design of the shroud provides for the electrode to be hot headed into the electrode end (button, hook, etc.), eliminating the need for crimping the shroud. This elimination of the crimp removes a source of sharp corners on the shroud, an area of high electrical stress.

INTRODUCTION

Weighted wire precipitator discharge electrodes have three primary modes of failure while in service:

1. failure from electrical arcing
2. failure from chemical attack
3. failure from mechanical fatigue

Solid metal shrouds on the ends of the discharge electrodes, having a diameter of from 2 to 4 times the diameter of the discharge electrode, were utilized to correct some of the causes of electrical arcing failures. This proved to be a good solution to the problem, but resulted in additional problems in some precipitator applications, specifically mechanical breakage of the discharge electrode at the wire/shroud interface. The resulting problem at times has been more frequent and annoying than the failures from electrical erosion.

This paper discusses testing that was conducted on a method to improve the shrouded end of a discharge electrode by continuing its ability to reduce electrical arcing related failures without the annoyance of mechanical fatigue induced breakage. This test quantifies and compares the strain response, hence stress response to rapping excitation, of two discharge electrodes, which were identical except for shroud design. Further, it discusses enhancements made on the upper and lower ends of the electrodes in order to minimize the possibility of an electrode failure.

DISCHARGE ELECTRODE FAILURES

ELECTRICAL EROSION

Electrical erosion failures in electrodes are caused by the dissipation of the sparking energy of an electrical section within the precipitator (a very high level of energy) into one small space on the discharge electrode over a very short period of time. This dissipation of current could be caused by a close clearance between the collecting and discharge electrode, an area of high electrical stress concentration (a cut in the wire, crimp in the shroud or sharp end on the attaching hardware), or an oscillating wire not properly tensioned.

The electrical erosion failure occurs after repeated spark strikes occur in the wire in the same area. This intense energy heats a small area of the wire to a molten state. After the energy is dissipated, the heat sink effect of the portion of the wire not disturbed by the spark cools the molten area very rapidly. This cooling can cause micro-cracks in the wire at the point of contact and/or embrittle the wire. Discontinuities in the strike area can lead to further strikes causing a reduction in wire material (cross sectional area) which succumbs to the tension imposed by the discharge electrode weight. (1)

CHEMICAL ATTACK

Discharge electrodes can be chemically attacked, resulting in a failure, if there is some chemical within the gas stream that will react with the material in the wire to corrode away sections of that wire. In the case of flue gas from an electric utility boiler the presence of SO_2 in the fuel leads to SO_3 in the flue gas. If the temperature of the gas is below its dew point, creation of H_2SO_4 can occur. This is one of the corrosive agents in flue gas. (2)

In the cement industry under certain conditions the alkali within the dust can be corrosive when present in a gas with a high concentration of moisture.

This is a very brief synopsis of two of the modes of failure of discharge electrodes with no attempt to identify corrective action needed to resolve these problems. These are presented solely for the purpose of making the reader aware of other types of failures before concentrating on one specific aspect of mechanical failures.

MECHANICAL FATIGUE

Mechanical fatigue occurs in discharge electrodes at points where the wire is at maximum stress. Points of maximum stress are at the wire/shroud interface or at any kink in the wire material.

The exact mechanism of the initiation of a fatigue failure is complex and is not completely understood. (3) The word fatigue is commonly used to describe repeated load phenomena. The word is a misnomer in the lay sense, in that the materials do not get "tired". Failure by fatigue is a progressive cracking and, unless detected the discharge electrode will rupture from this cracking.

If a repeated load (the load we are referring to is the load imparted to the electrode from rapping and the resultant vibration initiated) is large enough to cause a fatigue crack, the crack will start at a point of maximum stress. This maximum stress is usually due to a stress concentration. Stress concentrations can occur in the interior of the wire as the result of:

1. Inclusion of foreign matter
2. Voids in the material.

They can occur on the exterior surface of the electrode because of:

1. Scratches
2. Machining marks
3. Sharp corners
4. Abrupt geometry changes in the design (the wire/shroud interface).

If a stress concentration occurs in a region of high overall stress (in a discharge electrode this region would be the outer diameter of the wire) and if the effect of the stress concentration (the wire/shroud interface) is superimposed on this already high stress, then the chances of a fatigue crack developing under repeated loading are greatly increased.

After a fatigue crack is initiated at some point of stress concentration, the crack itself acts as an additional stress concentration. The crack grows with each repetition of the load until the effective cross sectional area of the wire is reduced to such an extent that the remaining portion will fail with the next application of the load (rappers). In a fatigue failure of an electrode there is no large amount of plastic deformation or "necking" down of the cross sectional area prior to failure. The fatigue failure appears somewhat as would the failure of a brittle material.

It may take thousands or millions of stress repetitions for a fatigue crack to grow to such an extent that it causes failure. The required number of repetitions depends on the magnitude of the stress, temperature and the chemical environment.

SOLUTION TO THE PROBLEM

The shroud is a very desirable feature on an electrode, however, the shroud/wire interface is an area of stress concentration and can lead to fatigue cracking from the stresses generated by rapping. A simplified solution is not to give a fatigue crack a place to start. This can be accomplished by a careful design of the shroud. This could be verified by measuring the strain at the outer diameter of the 12 ga. wire at the shroud/wire interface on a conventional wire vs. the resultant strain in the design solution. A close wound spring was chosen as the shroud for the design solution solely on the basis of a thought process that can best described in illustration (see Fig. 1).

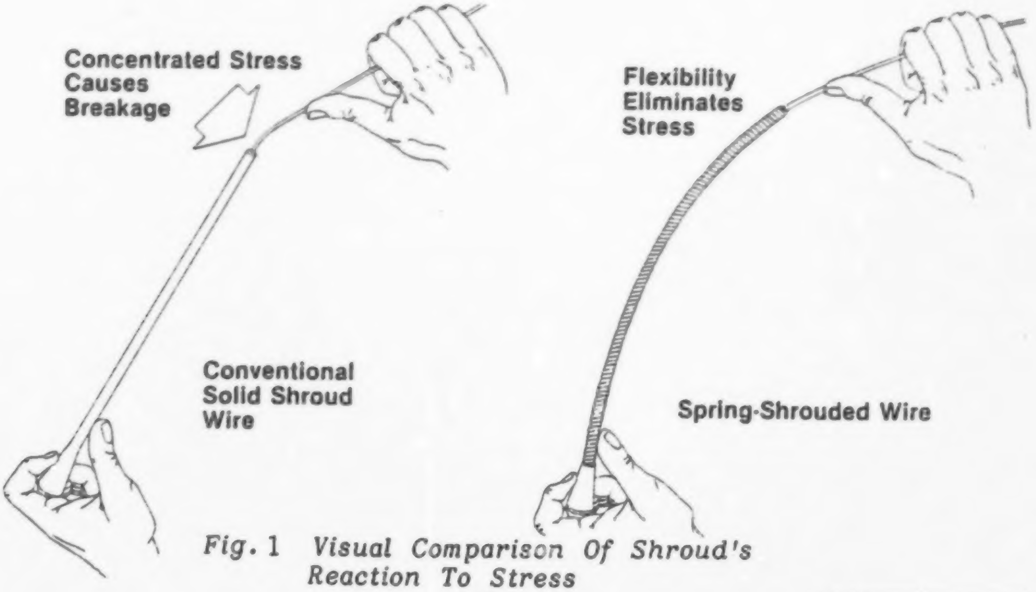
Concentrated Stress Causes Breakage
Flexibility Eliminates Stress
Conventional Solid Shroud Wire
Spring-Shrouded Wire

Fig. 1 Visual Comparison Of Shroud's Reaction To Stress

THE TEST TO MEASURE FLEXURAL STRAIN

Flexural strains were measured in two equal length electrostatic precipitator discharge electrodes subjected to the same vibratory excitation. The electrodes were under equal tension (25lbs.) and differed only in that one wire had a relatively stiff solid metal shroud while the other consisted of a relatively flexible close wound spring shroud. Flexural strain levels were measured for a range of excitation levels and frequencies. All tests were performed in the Structures Laboratory of the Department of Civil Engineering at Case Western Reserve University in Cleveland, Ohio. (See Fig.2 for Test set up)

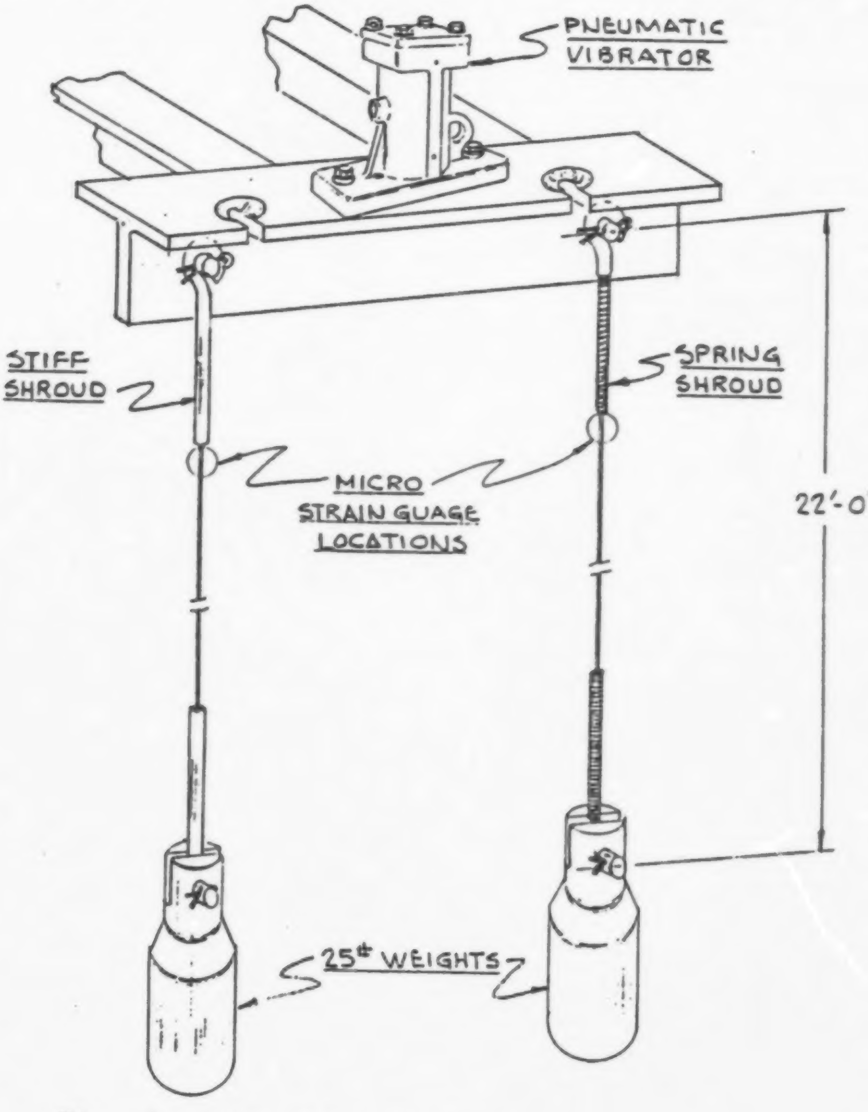
PNEUMATIC VIBRATOR
STIFF SHROUD
SPRING SHROUD
MICRO STRAIN GUAGE LOCATIONS
22'-0"
25# WEIGHTS

Fig. 2 Wire Test Fixture

Method of Measurement:

The strains were measured by means of electrical resistance strain gauges. The gauges employed were Micro-Measurement model EA06-050AH-120, configured as indicated on each electrode at the excited end. (See Fig. 3)

Half-Bridge Strain
Gage Configuration
For Flexural Strain
Measurement

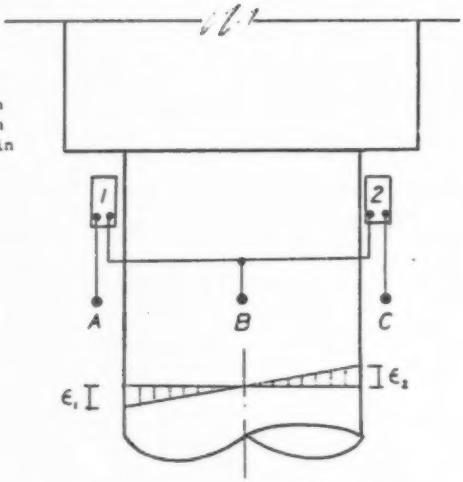

Fig. 3 Half-Bridge Strain Gage Configuration For Flexural Strain Measurement

These gauges have a gauge length of 50 mils and a grid width of 40 mils. The lot utilized had a gauge factor (g.f.) of 1.95. Since the gauges were placed in diametrically opposed positions on the electrodes and adjacent positions in the Wheatstone bridge circuit (See Fig. 4), the output signal was proportional to flexural strain and independent of axial strain. (If a situation of pure bending existed ($E_1 = E_2$), the actual flexural strains would be exactly half of the measured strain, as indicated in the formula.)

Wheatstone Bridge
Schematic

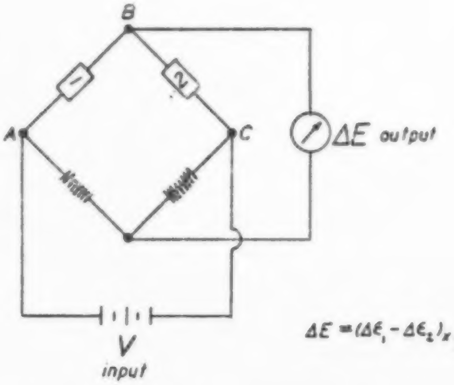

$$\Delta E = (\Delta\epsilon_1 - \Delta\epsilon_2) \times \frac{V}{4} \times g.f.$$

Fig. 4 Wheatstone Bridge Schematic

Data Recording:

The dynamic strain data was recorded from both electrodes simultaneously on a two channel Sanborn model 60-1300B strip chart recorder. Calibration of the recorder was accomplished by shunting a known resistance across one of the active arms of the Wheatstone bridge, thus producing a known resistance change. With knowledge of the gauge factor, this known resistance change could be converted to an equivalent strain, thus allowing calibration of the recorder. One millimeter on the strip chart was made equivalent to approximately 100 micro-strain (.0001). The calibration signals are included below. (See Figure 5)

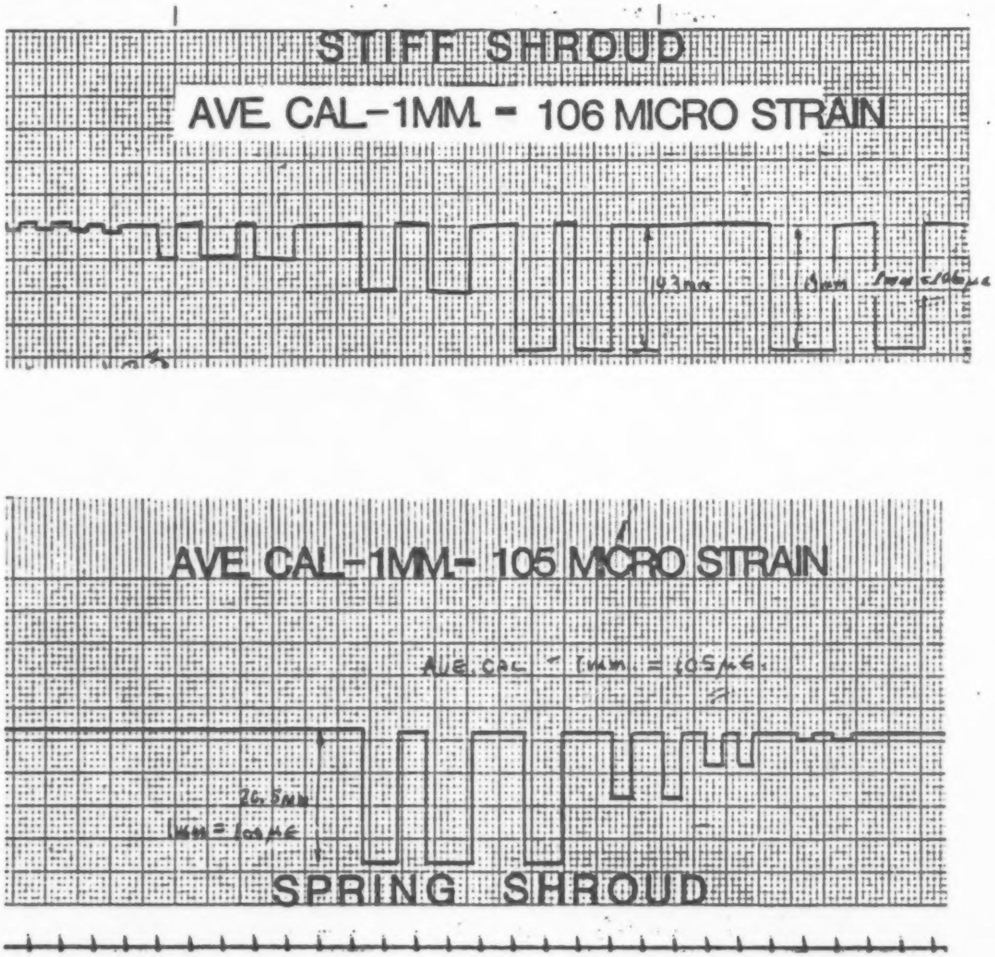

Fig. 5 Strip Chart Calibration

Test Specimens:

The specimens consisted of two electrostatic precipitator discharge electrodes, each approximately 22 feet in length. Each wire suspended a 25 lb weight. At the upper end the wires were attached to a steel frame simulating a wire frame in a precipitator. Each wire was terminated with identical hooks (similar to a Research Cottrell hook), one with a solid shroud and one with a spring shroud.

Also attached to the suspending frame was a pneumatic vibrator, capable of a range of excitation levels and frequencies. Air pressure ranging from 10 psi to 40 psi was supplied to the vibrator via a pressure regulator.

Test Results:

Figure 6 indicates the result of a sweep through the pressure input range to the pneumatic vibrator. As can be seen, the wires passed through critical frequencies, producing amplified responses at several pressure levels. Throughout the entire response range, however, the level of flexural strains for the spring shrouded wire were less than that for the solid shrouded wire. The difference in response is most extreme around the 20 psi input pressure level.

Figures 7, 8, 9, 10 and 11 indicate the results of "steady state" operation at input pressures of 20, 25, 30, 35, and 40 psi. Again the flexural strain levels were considerably lower for the spring shrouded wire, with the magnitude of the difference dependent upon the operating pressure (frequency).

The bottom recordings in figures 7, 8, 9, 10, and 11 represent the spring shrouded electrode and the top recordings represent the solid shrouded electrode.

CONCLUSIONS:

The introduction of a spring shroud considerably reduced flexural strains and hence flexural stresses for the precipitator discharge electrodes tested. The degree of reduction is a function of the vibration frequency and ranged from a slight reduction to more than a 90% reduction. The flexural strains remained small (approximately 150 to 200 microstrain or stresses of 4.5 to 6.0 ksi) for the spring shroud, while the flexural strains got quite large (approximately 675 to 700 microstrain or 20 to 21 ksi stress) for the solid shroud.

The most important parameter in determining fatigue life is the effective stress range to which a specimen is subjected. For the solid shrouded wire, with a total stress range(positive + negative) on the order of 40 ksi at the critical frequencies, a considerably reduced stress range exposure, would be expected to exhibit a similarly enhanced fatigue life.

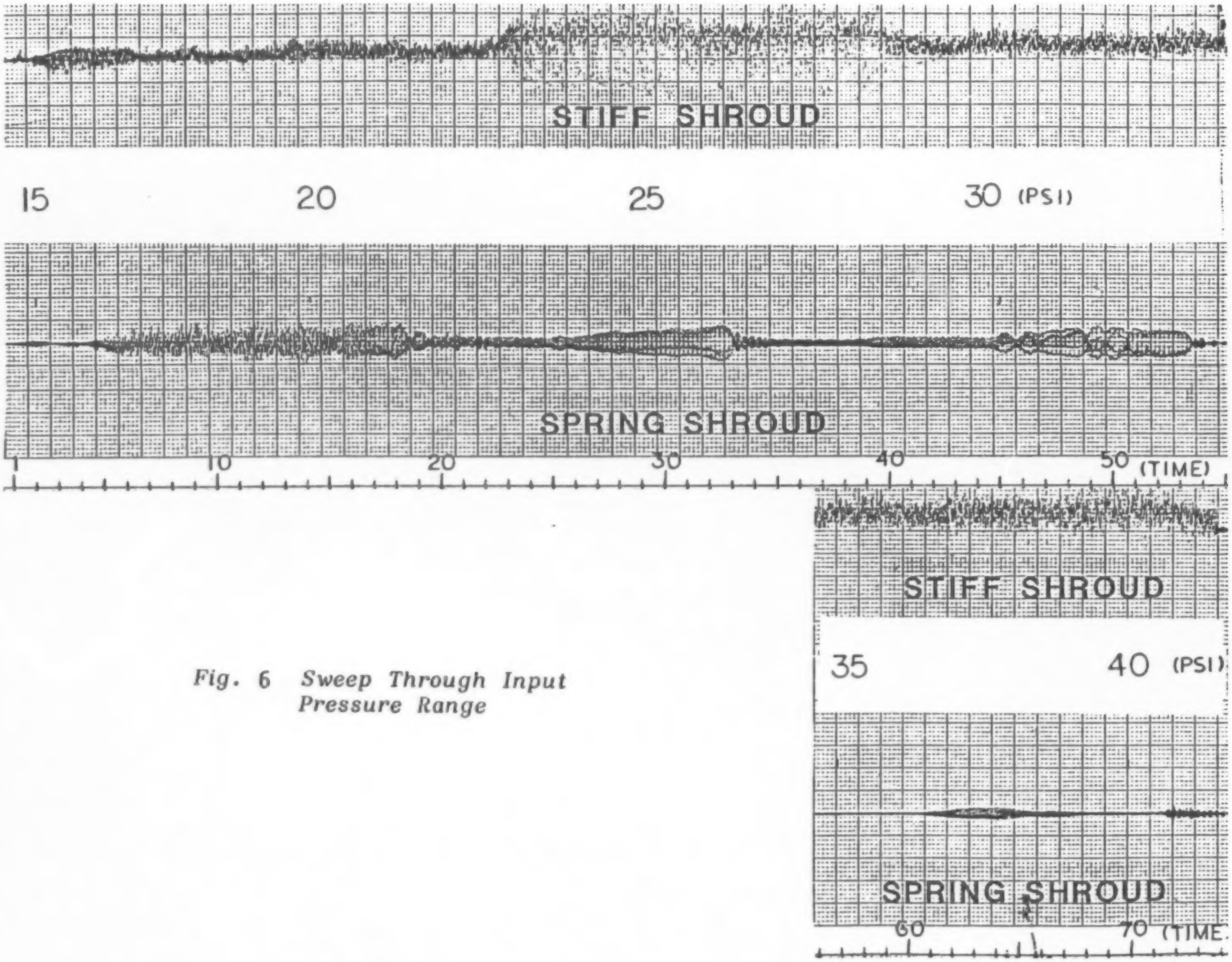

Fig. 6 Sweep Through Input Pressure Range

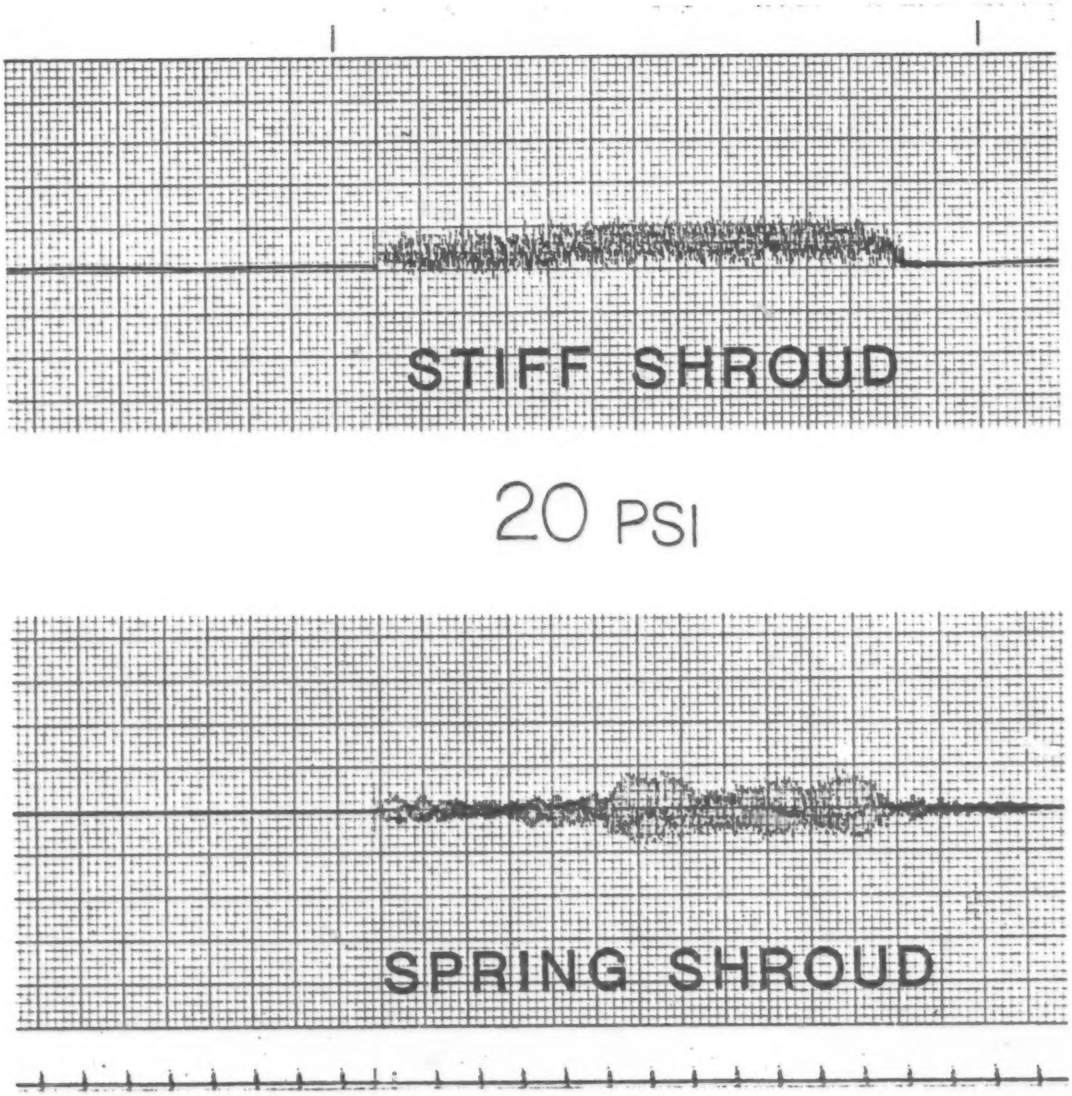

Fig. 7 Steady-State Operation @ 20 PSI

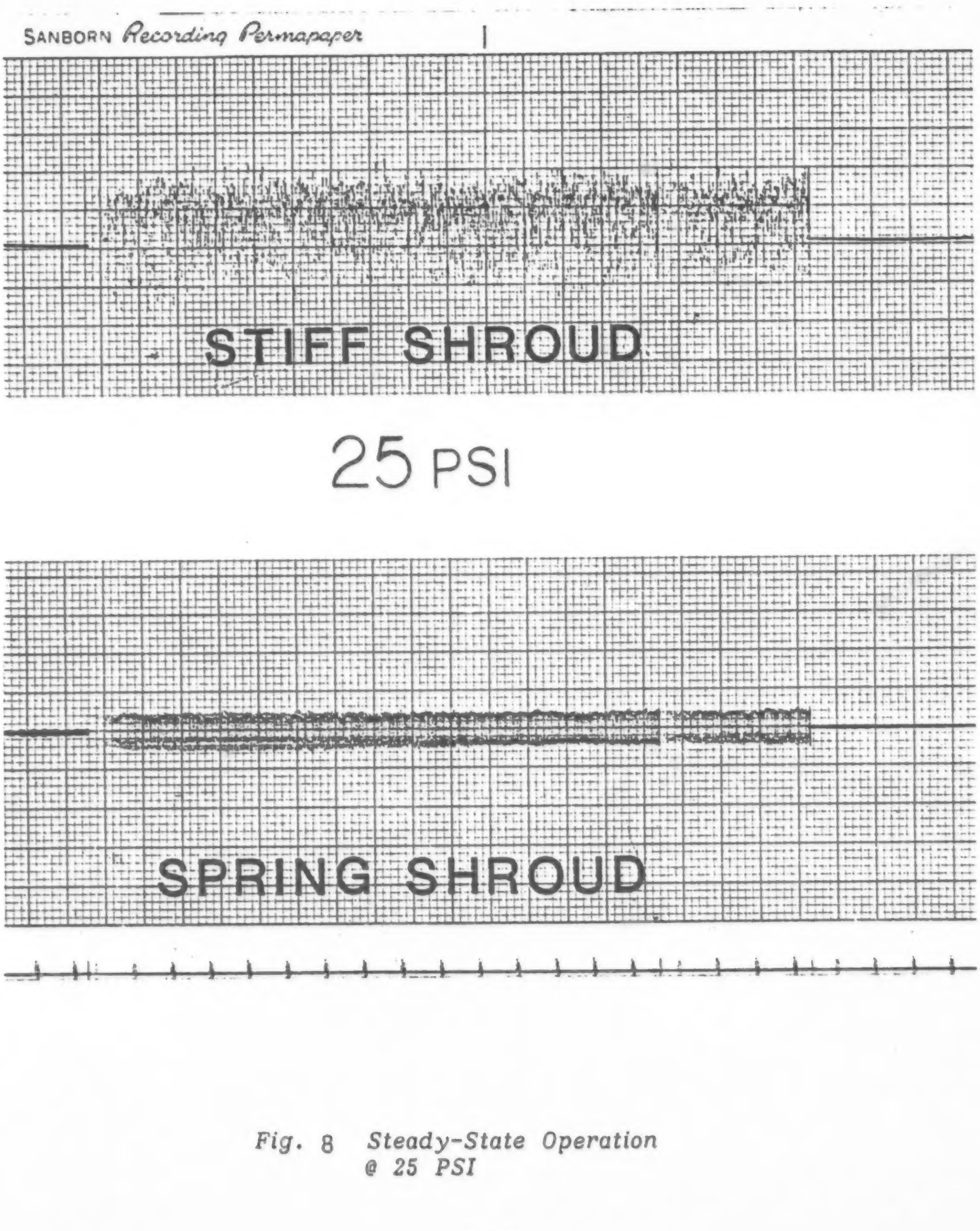

Fig. 8 Steady-State Operation
@ 25 PSI

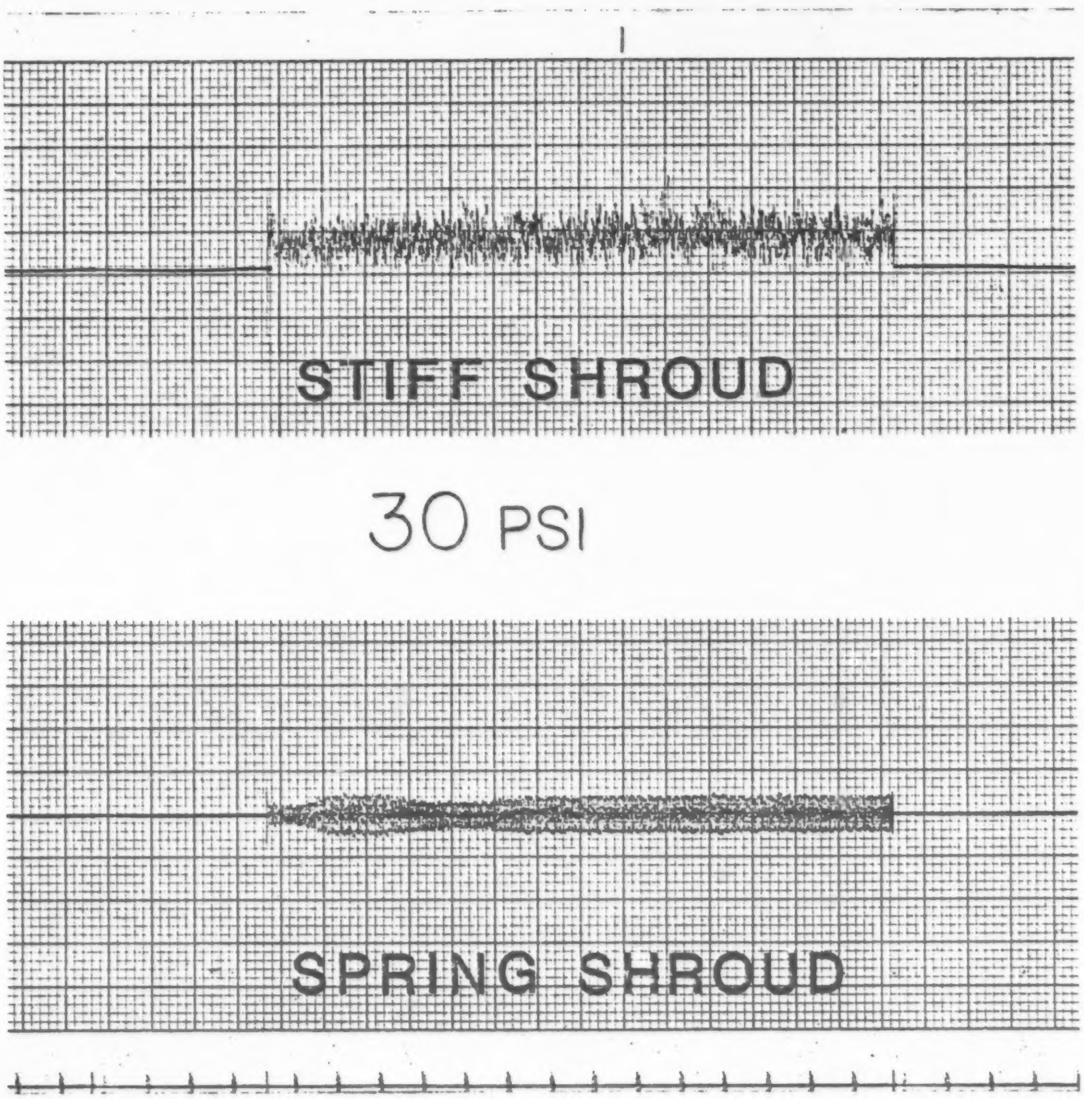

Fig. 9 Steady-State Operation @ 30 PSI

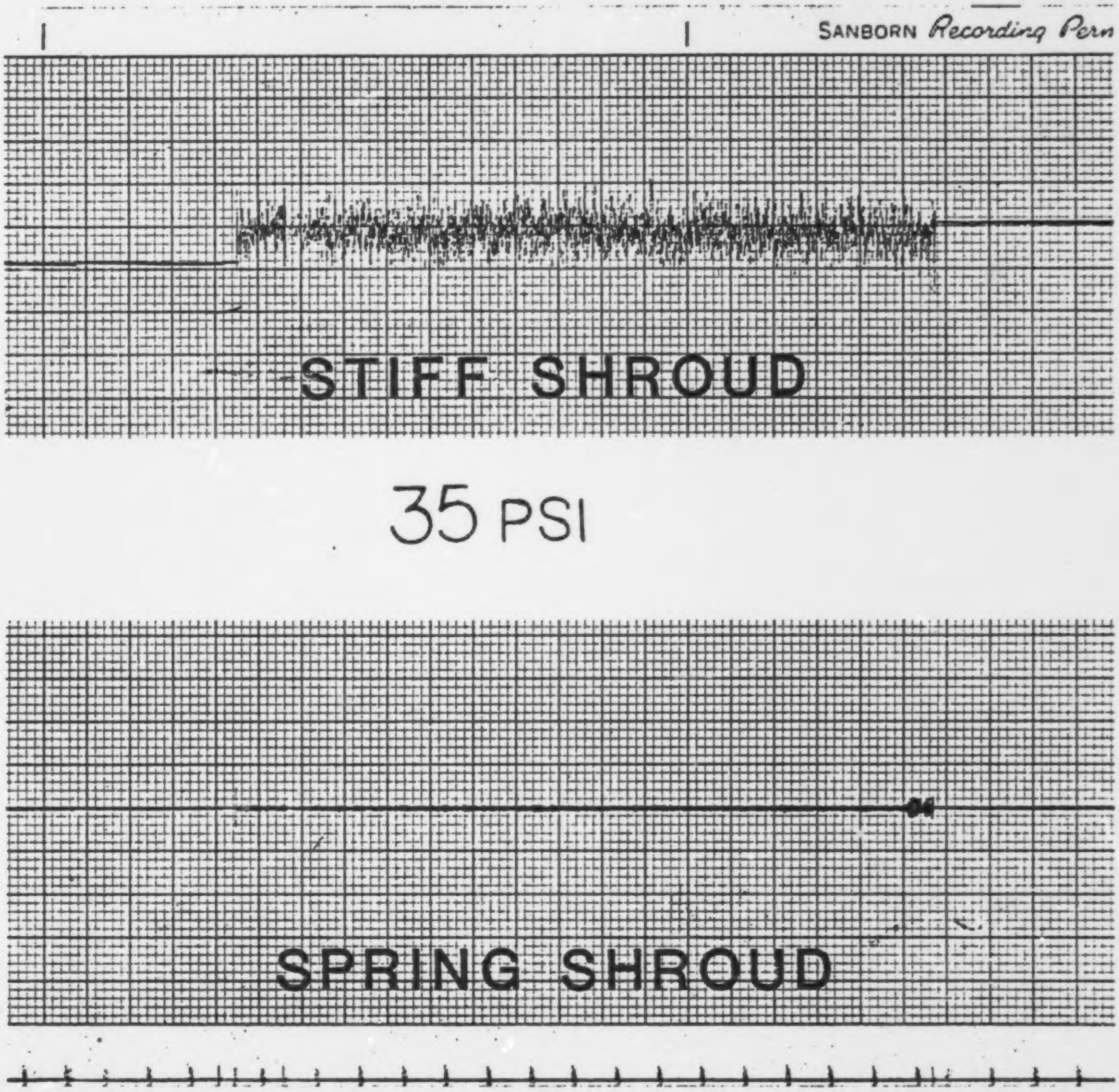

Fig. 10 Steady-State Operation @ 35 PSI

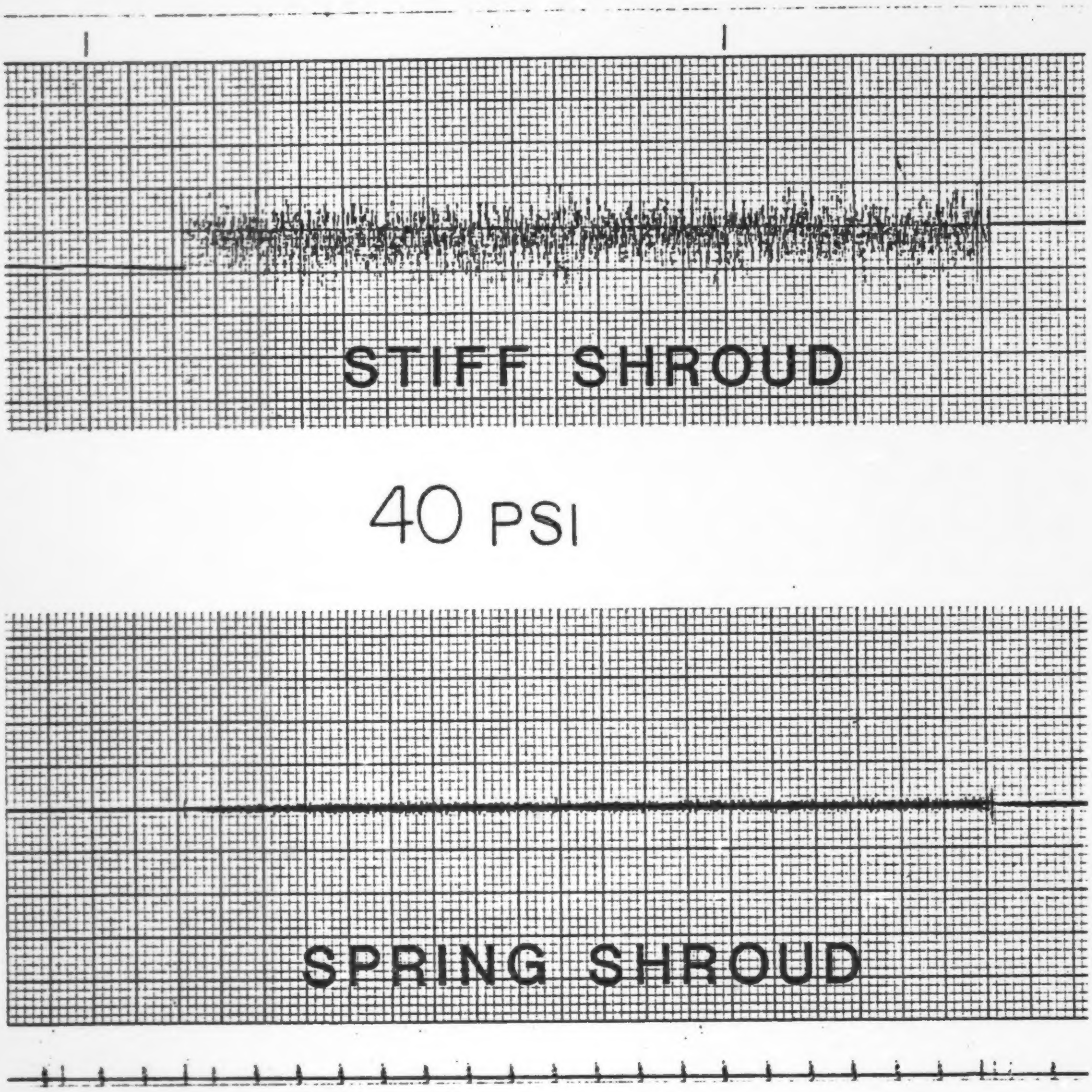

Fig. 11 *Steady-State Operation*
@ 40 PSI

There are additional benefits in the spring shroud design, in that the attachment of the wire is to the electrode end (button, hook, etc.) as opposed to being crimped in the shroud as is the practice of conventional wires. The advantage of this approach is the removing of the crimp which can be a source of high electrical stress concentration out of the proximity of the top of the collecting electrode, reducing the chance of sparkover. (See Fig. 12)

OPERATING RECORD

Thirty-two precipitators containing this new technology of shroud are in service as of this writing. It would be premature at this time to quantify an enhancement factor over the conventional shrouded wire for the spring shroud. Nevertheless, the test results demonstrate that the spring shroud reduces the stress concentration at the critical point in a discharge electrode (the shroud/wire interface).

ACKNOWLEDGEMENT

Our thanks to Professor Arthur A. Huckelbridge, Jr., D. Eng., P.E. of Case Western Reserve University for his assistance in conducting the strain measurements for testing.

DISCLAIMER

The work described in this paper was not funded by the U.S. Environmental Protection Agency and therefore the contents do not necessarily reflect the views of the Agency and no official endorsement should be inferred.

REFERENCES

1. Grady B. Nichols, Editor; "Electrostatic Precipitator Manual." Vol. 2, Chp. VII, Sec. 3.2 - 3.33 (March, 1976).

2. H. J. Hall and J. Katz, "Corrosion Problems and Solutions for Electrostatic Precipitators." Journal Air Pollution Control Assoc.: 26, pp. 312-317 (April 1976).

3. E. F. Byars and R.D. Snyder, "Engineering Mechanics of Deformable Bodies." International Textbook Company, Scranton, P.A. (1969)

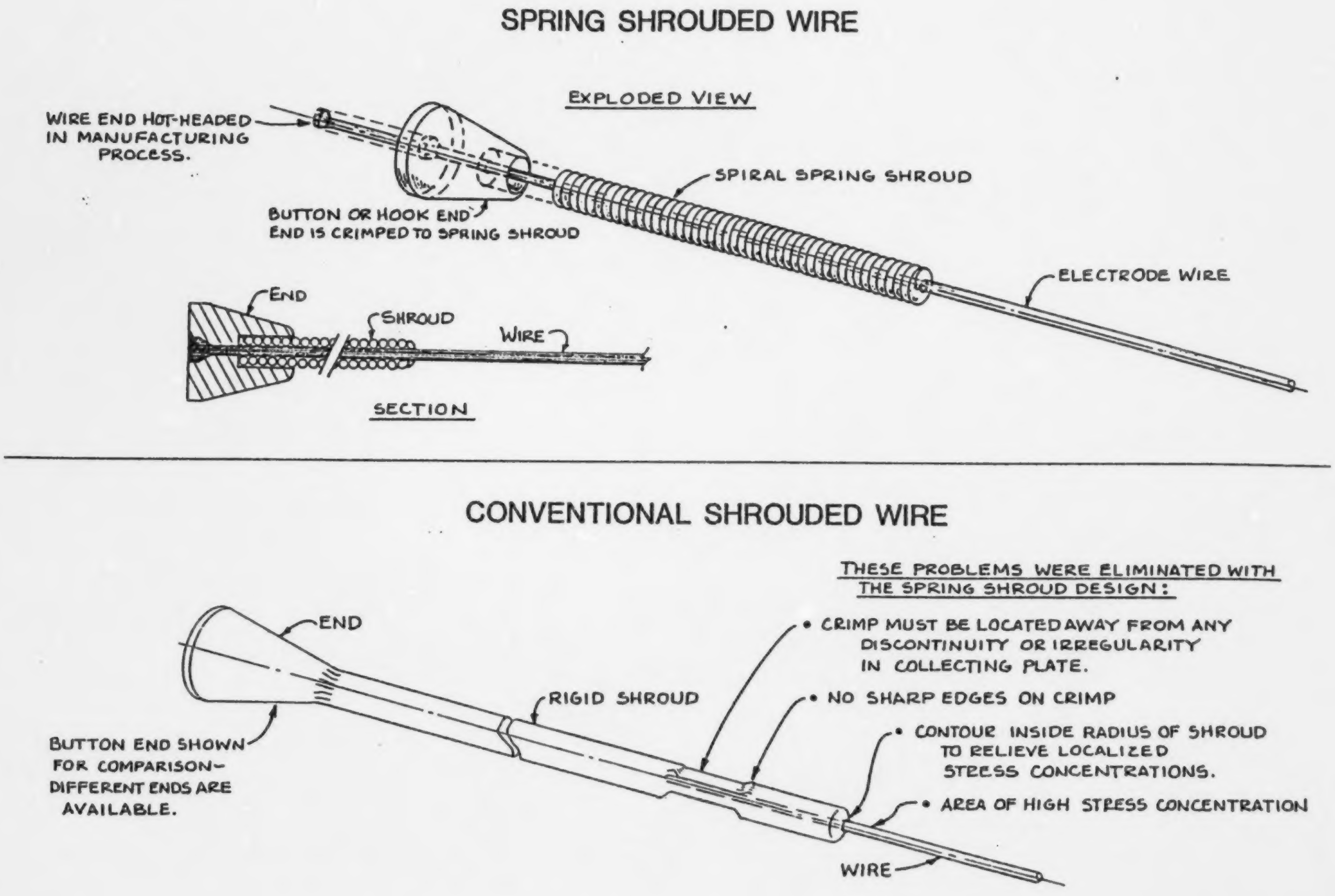

SPRING SHROUDED WIRE

CONVENTIONAL SHROUDED WIRE

EXPLODED VIEW
WIRE END HOT-HEADED IN MANUFACTURING PROCESS.
SPIRAL SPRING SHROUD
BUTTON OR HOOK END END IS CRIMPED TO SPRING SHROUD
ELECTRODE WIRE
END
SHROUD
WIRE
SECTION
THESE PROBLEMS WERE ELIMINATED WITH THE SPRING SHROUD DESIGN:
END
• CRIMP MUST BE LOCATED AWAY FROM ANY DISCONTINUITY OR IRREGULARITY IN COLLECTING PLATE.
RIGID SHROUD
• NO SHARP EDGES ON CRIMP
• CONTOUR INSIDE RADIUS OF SHROUD TO RELIEVE LOCALIZED STRESS CONCENTRATIONS.
BUTTON END SHOWN FOR COMPARISON– DIFFERENT ENDS ARE AVAILABLE.
• AREA OF HIGH STRESS CONCENTRATION
WIRE

Fig. 12 Comparison Of Spring Shroud V. Conventional Shroud

PAPER PRESENTED AT THE FOURTH SYMPOSIUM ON THE
TRANSFER AND UTILIZATION OF PARTICULATE CONTROL TECHNOLOGY
BUT NOT PUBLISHED IN PROCEEDINGS

MEASUREMENT OF THE ELECTROKINETIC TRANSPORT PROPERTIES OF PARTICLES IN AN ELECTROSTATIC PRECIPITATOR

by: Wallace T. Clark III, Robert L. Bond,
and Malay K. Mazumder
University of Arkansas
Graduate Institute of Technology
P. O. Box 3017
Little Rock, Arkansas 72203

ABSTRACT

A study of submicrometer particle behavior within a laboratory model, single stage, wire-and-plate type electrostatic precipitator (ESP) has been performed. A two-color, four-beam, two-dimensional laser Doppler velocimeter (LDV) was constructed to observe the two-dimensional kinetics of submicrometer diameter particles in the ESP. Particle migration velocity toward the collection wall was found to be dependent on particle position in relation to the wires and wall and on the voltage applied to the wires. This dependency indicates that particle electrokinetics is dependent upon the electric field magnitude. Values for migration velocity and downstream velocity were experimentally determined with the LDV system. These values were used to calculate the Deutsch-Anderson efficiencies which were in agreement with Climet particle analyzer efficiencies in the free stream of the ESP.

This paper has been reviewed in accordance with the U.S. Environmental Protection Agency's peer and administrative review policies and approved for presentation and publication.

INTRODUCTION

Electrostatic precipitators (ESPs) are widely used to control particulate emissions from certain large industrial processes. Although ESPs have been used since the beginning of the twentieth century, particle behavior within them is not well understood.

Although many investigators have spent much time and energy in precipitator studies, all such studies have been on particle collection efficiency for the entire unit. Until the work reported in this paper was begun no studies had been undertaken to determine particle migration velocities in ESPs.

Accurate particle velocity measurements are not possible with hot wire or hot film anemometers, pitot tubes, or any such device since they disturb the aerodynamic flow. On the other hand, a laser Doppler velocimeter (LDV) permits particle velocity measurement with no disturbance to either the flow or the particles. Since a single LDV system will measure particle velocities in only one dimension, a dual LDV system was necessary to measure particle velocities in both the downstream and cross-stream directions.

A laboratory model, single-stage, wire-and-plate type ESP was utilized in this work. The model was constructed of optically transparent materials so as to enable LDV observation of particles within the ESP. The roof, floor and outer walls of the laboratory ESP were constructed of Plexiglas. The inner walls (that is, the collection electrodes) were constructed of a metallic-oxide coated, electrically conducting (NESA) glass.

The laboratory model ESP is a positive discharge device. The discharge wires may be set to any potential from 0 through 50,000 volts D.C. The NESA glass collection electrodes were replaced with aluminum plates to check the conduction characteristics of the NESA glass. No significant difference was found between the voltage-current curves for the NESA glass and the aluminum plates.

The collection efficiency of commercial ESPs is at a minimum for aerosol particles between 0.1 and 1.0 micrometers in diameter. For this reason the aerosol particles introduced into the precipitator for experimental studies were 0.72 micrometer diameter 2-ethyl hexyl sebacate (BES), a nontoxic oil. The aerosol particle diameters were measured by a SPART analyzer (1) and a Climet particle analyzer. The bulk resistivity of the BES oil (2) used to manufacture the aerosol is 7.4 x 10^9 ohm centimeters. A Rapaport-Weinstock evaporator-condenser (3) was utilized to make the aerosol as monodisperse as possible. To remove any charge on the particles, they were fed through a neutralizer with a 10 mCi ^{85}Kr source.

EXPERIMENTAL RESULTS AND DISCUSSION

To realize the objective of characterizing the particle flow properties of the laboratory model ESP, aerosol was introduced into the flow at the upstream end of the ESP. The two-color, four-beam, two-dimensional LDV was focused onto several locations within a representative ESP section. Mean particle velocities and turbulence levels were ascertained for several discharge voltages.

The periodic and mirror symmetry of the laboratory model ESP permitted the majority of the data to be obtained from a single section within the unit. That is, particle and aerodynamic behavior from the corona wires to one wall (collection electrode) should be the same (mirror image) as the behavior from the wires to the opposite wall. Similarly, precipitation characteristics for the top half of the ESP should be mirror imaged in the bottom half. Finally, characteristics from one corona wire to the next should be repeated for any two other wires. This high degree of symmetry allows study of the ESP to be reduced to a single representative section, between the 10th and 11th wires; from those wires to one collection wall; and half-way between the ESP's ceiling and floor. Although only one such section has been strenuously studied, the properties described here have been observed in other sections.

Utilizing the LDV system, particle velocities were measured at 26 points within the ESP's area of investigation (Figure 1). Measurements were conducted with a gas flow rate of 2 meters per second at a temperature of 25^{o} centigrade. Aerosol was injected upstream of the settling chamber, at the inlet. The particle velocities were measured when discharge electrode voltages were sequentially set to 0, 35, 40, 45, and 50 kV. There was no significant increase in the current density at the collection walls between electrode voltages of 0 and 35 kV. Particle motion data were only acquired when a particle passed through both LDV sensing volumes simultaneously. The mean magnitude and direction for 250 such particles per observation point have been plotted on maps for each of the 26 observation points. These maps are a 1:1 representation of one section of the ESP; specifically, between discharge electrodes 10 and 11. (The interwire distance is 15.24 centimeters.) Particle motion is represented by vectors where magnitude is representative of the mean particle velocity (scale factor: 2.54 centimeters = 2 meters per second) and the angle is relative to the ESP axis and representative of the particles' mean flow direction.

With no voltage applied to the discharge electrodes, particle motion is fairly linear and the particles are moving downstream with the flow of the gas (Figure 2). It is noted that particle motion in row D, 1.27

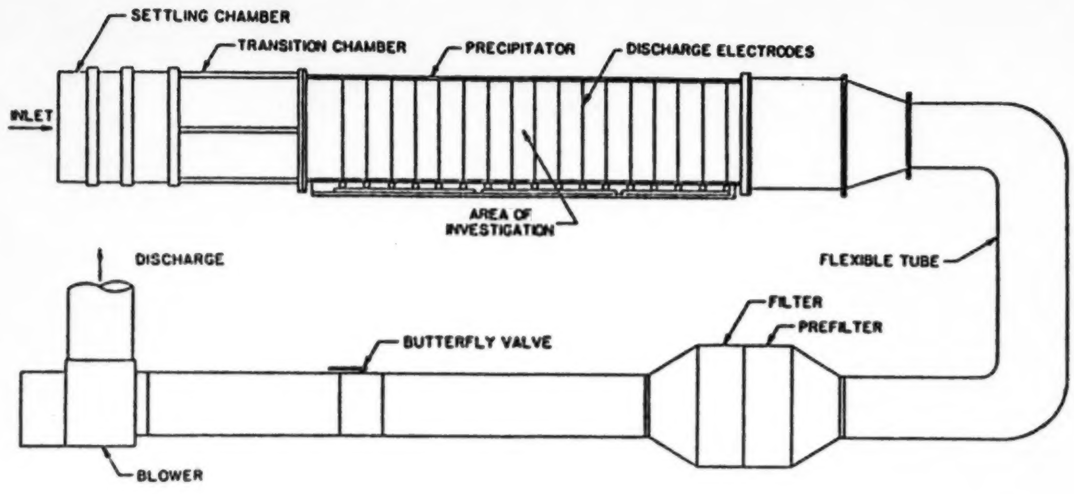
SETTLING CHAMBER
TRANSITION CHAMBER
PRECIPITATOR
DISCHARGE ELECTRODES
INLET
AREA OF INVESTIGATION
DISCHARGE
FLEXIBLE TUBE
FILTER
PREFILTER
BUTTERFLY VALVE
BLOWER

Figure 1. Diagram of the laboratory model electrostatic precipitator assembly.

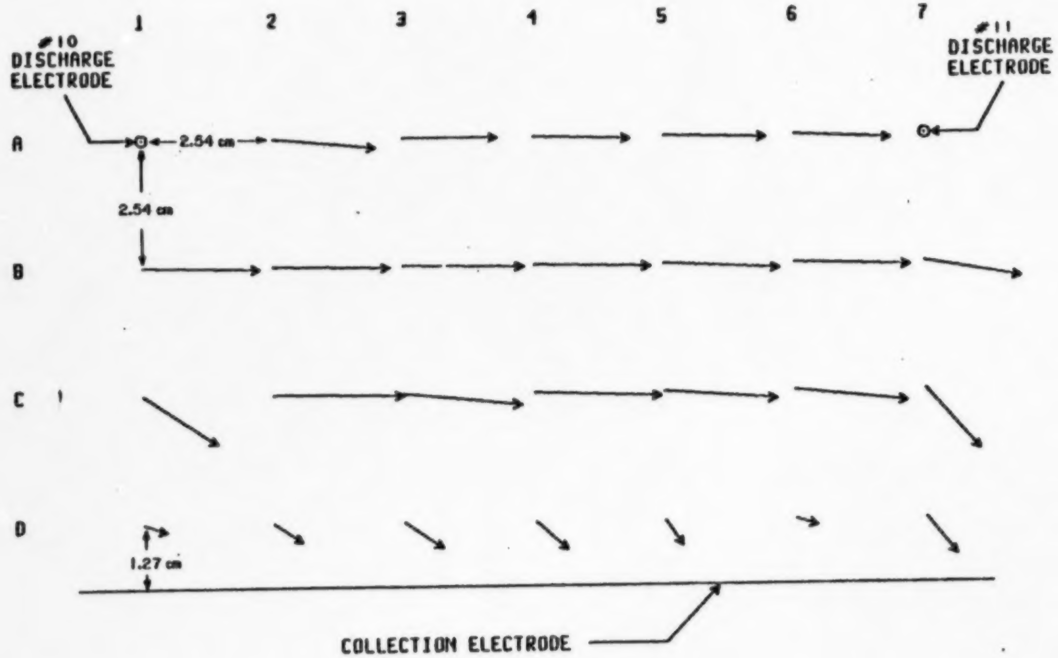
1
2
3
4
5
6
7
#10 DISCHARGE ELECTRODE
#11 DISCHARGE ELECTRODE
A
B
C
D
2.54 cm
2.54 cm
1.27 cm
COLLECTION ELECTRODE

Figure 2. Mean particle velocity map. $V_o = 0$.

Scale Factor: 2.54 cm = 2 meters/second.

Discharge to collection electrode distance = 8.89 cm.

Distance between discharge electrodes #10 and #11 = 15.24 cm.

centimeters from the collection electrode, tends to be toward the wall. This is indicative of shear stresses near the wall. With 35 kV on the discharge wires, particle motion is not as linear as in the previous case and the particles tend to move away from the discharge electrodes (Figure 3). Specifically, particle motion in columns 1, 2, and 3 is seen to be greatly altered by the high voltage at discharge electrode number 10 in position 1A.

With 40 kV applied it is observed that particle velocity toward the collection surface has increased throughout the section (Figure 4). Only in positions 3D and 4D has particle velocity toward the collection electrode been significantly reduced.

When 45 and 50 kV were applied, respectively, to the discharge electrodes (Figures 5 and 6) the downstream particle velocity decreased while the cross-stream or migration velocity increased. When 45 kV was applied (Figure 5), the downstream particle motion in positions 4B, 5B, 5C, and 5D seems to be nearly arrested. At 50 kV this arrested area moves upstream to positions 4C and 4D (Figure 6).

The particle collection efficiency of the ESP was calculated at three representative locations within the area of observation: 4A, 4C, and 4D. The efficiency was determined using the Deutsch-Anderson equation. Both the particle migration velocity and the volumetric flow rate were measured by the LDV system. With the voltage V_0 applied to the discharge wires set to 45 kV, efficiency at locations 4A and 4D was calculated to be 99.87 percent and 99.99+ percent, respectively. With V_0 adjusted to 50 kV, efficiency at location 4C was 99.99+ percent.

The efficiencies calculated using the LDV data compare favorably with the efficiencies calculated using the Climet particle analyzer data for locations 4A, the midstream, and 4C, the quarter stream. At location 4D, the boundary layer, there is a large discrepancy between the two calculated efficiencies. This discrepancy suggests that the Deutsch-Anderson equation adequately describes particle motion in the free stream of the ESP, but not near the boundary layer.

Velocity measurements acquired via the two-color, four-beam, two-dimensional laser Doppler velocimeter system indicate that the highest migration velocities for the given observation section occurred when the voltage applied to the discharge corona wires was 45 kV. These data are supported by concentration data taken with the Climet particle analyzer which indicates the highest efficiency is not necessarily at its greatest with maximum values of cross-stream (electrical migration) velocity. The Deutsch-Anderson calculated efficiency is in close agreement with the efficiency calculated using the Climet particle analyzer data in the free stream of the ESP. The Deutsch-Anderson equation is not an adequate predictor of particle migration velocity near or within the boundary layer of flow in the ESP; however, it is a good predictor of migration velocity in the free stream.

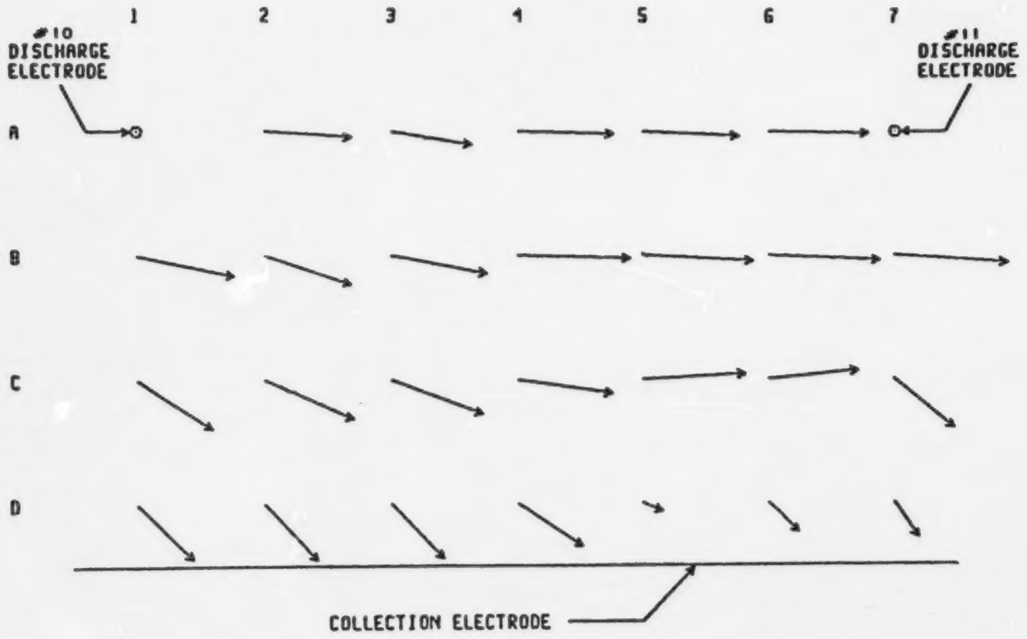
1
2
3
4
5
6
7
#10 DISCHARGE ELECTRODE
#11 DISCHARGE ELECTRODE
A
B
C
D
COLLECTION ELECTRODE

Figure 3. Mean particle velocity map. $V_o = 35$ kV.

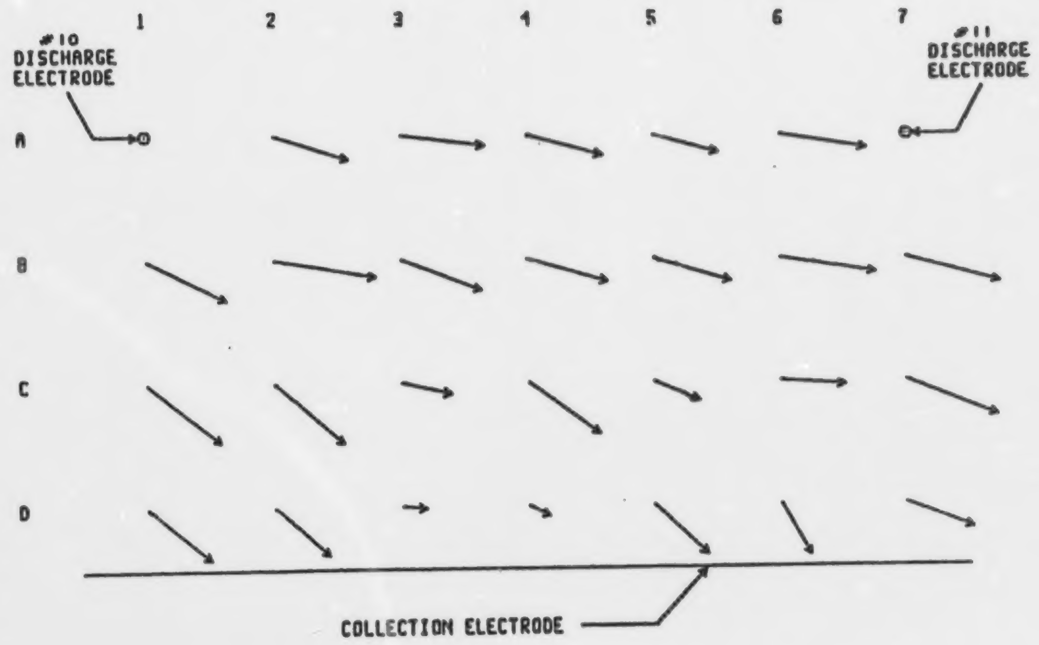

Figure 4. Mean particle velocity map. V_o = 40 kV.

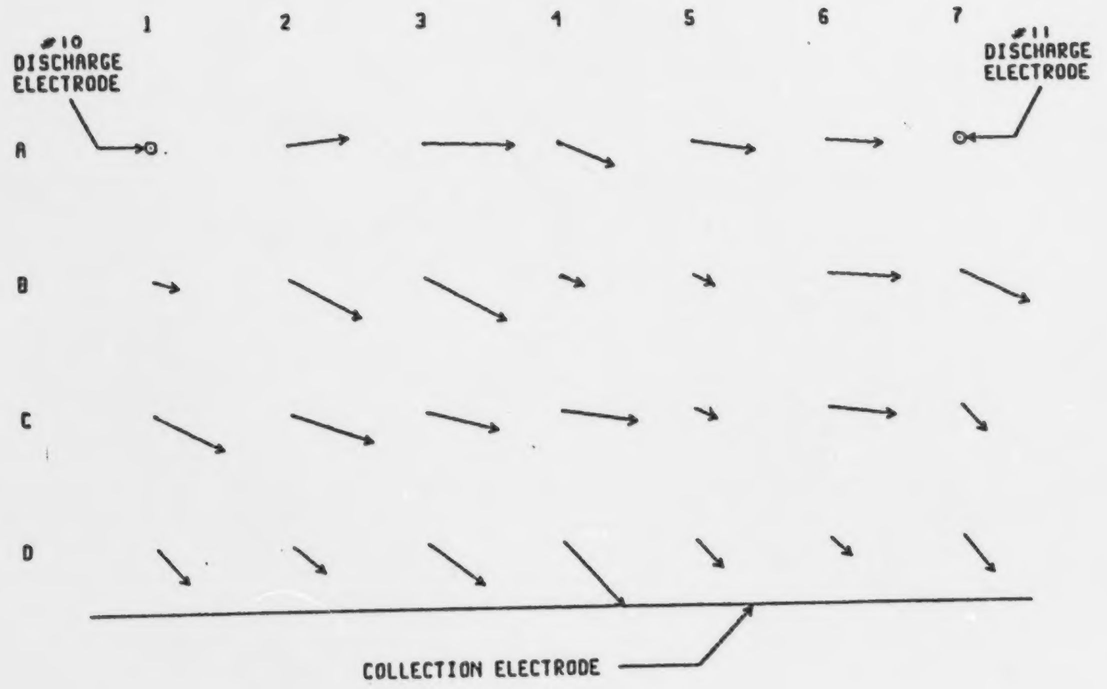

Figure 5. Mean particle velocity map. V_o = 45 kV.

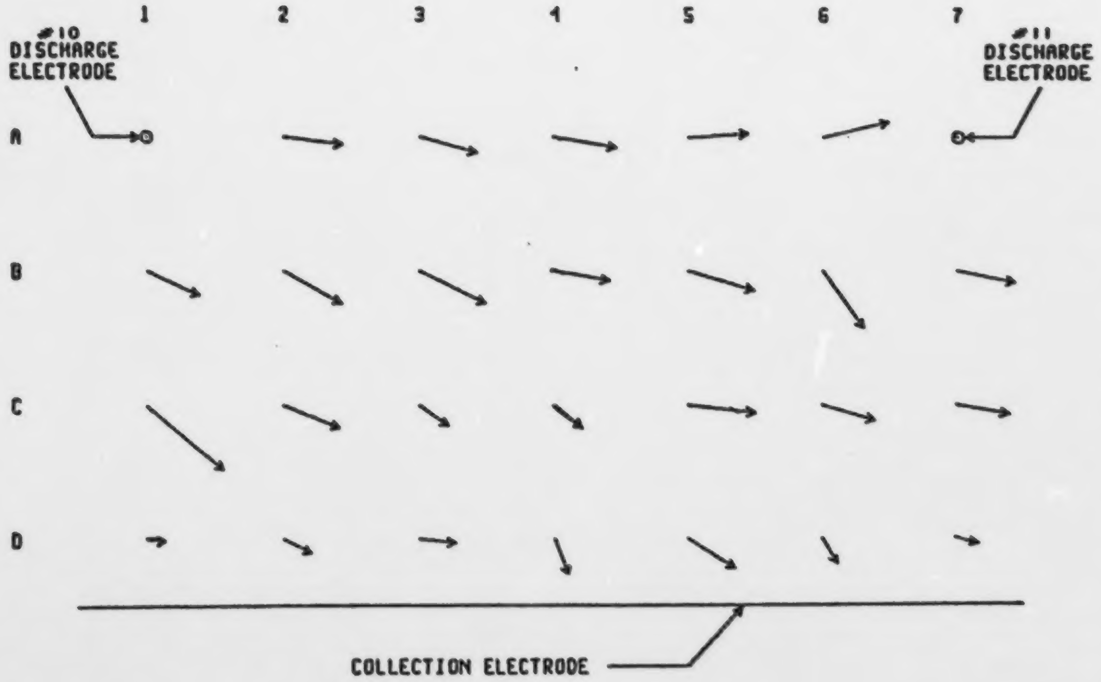

Figure 6. Mean particle velocity map. V_o = 50 kV.

REFERENCES

1. Mazumder, M. K., Clark III, W. T., Ware, R. E., McLeod, P. C., Hood, W. G., Straub, J. E., and Wanchoo, S. Application of Laser Doppler Instrumentation to Particle Transport Measurements in an Electrostatic Precipitator. In Third Symposium on the Transfer and Utilization of Particulate Control Technology, Vol. II, EPA-600/9-82-005b (NTIS No. PB 83-149591), July 1982, pp. 169-178.

2. Tang, Kunglin Hwang, "Measurement of High Resistance with an Electrooptic Crystal," M.S. Thesis, University of Arkansas, August 1983.

3. Davies, C. N. (ed.) Aerosol Science, Academic Press, Inc., New York, 1966, p. 11.

UNPRESENTED PAPER

ELECTROSTATIC PRECIPITATOR BUS SECTION FAILURE: OPERATION AND MAINTENANCE

by: Louis Theodore, Joseph Reynolds, Francis Taylor
Manhattan College
Riverdale, N.Y. 10471

Alan Filippi, Steve Errico
Consolidated Edison Company of New York
New York, N.Y. 10003

ABSTRACT

This work is an extension of a study recently reported in JAPCA (Dec., 1983): "ESP Bus Section Failures; Design Considerations", and addresses a common problem encountered with sectionalized electrostatic precipitators -- bus section failure. The first paper was directed mainly to those concerned with the design of ESPs and presented a method to calculate the probability of a unit being "out of compliance" (i.e., falling below a designated minimum overall collection efficiency) due to the occurrence of a given number of randomly located bus section failures.

This present paper extends the calculations to include the element of time and is intended to assist those involved with ESP operation and maintenance, particularly in scheduling outages and/or derating of units. The calculations are based on a statistical extrapolation from previous bus section failure rate data and provide an intelligent prediction as to when the unit can be expected to be out of compliance due to bus section failure. This calculational tool can be applied in one of two different modes depending on the type of prior information available. If an estimated number of bus section failures for the last several maintenance periods (i.e., periods between scheduled outages) is known, the first mode can be applied. If, however, the dates and locations of the bus section failures during the present period are available, the second mode should be used. Both modes provide the same type of information to the user: the probability that this unit will be out of compliance by the next scheduled outage (or, for that matter, by the end of any designated period of time). This information can be used to assist the user in determining the optimum time interval to employ in the scheduling of maintenance outages.

INTRODUCTION

This study is an extension of an earlier work, the results of which were recently published in a JAPCA paper entitled: "Electrostatic Precipitator Bus Section Failure: Design Considerations" (1). Both studies address a common problem encountered with sectionalized electrostatic precipitators -- bus section failure. While the first paper was directed mainly to those concerned with the design of ESPs, this work is primarily intended for those involved in ESP operation and maintenance. For more extensive details regarding either aspect of this project, the reader is referred to the final report prepared by the authors for Con Edison as part of Contract No. 4-20997.

The earlier study was presented in two parts: (a) a simplified procedure to estimate the effect of bus section failure on overall collection efficiency was developed, and (b) a technique to calculate whether or not a unit is "out of compliance" (i.e., operating below a designated minimum overall collection efficiency) due to the occurrence of a given number of bus section failures, was demonstrated. It was shown that the latter effect can only be expressed in terms of a probability, since the locations of the bus section failures have a profound effect on the amount by which the collection efficiency decreases. Most vendors ignore this fact when designing precipitators, either because it is too difficult to calculate or because they are not aware of the probability effect. A common practice is to "overdesign" the ESP without quantitative justification; e.g., an extra field is often provided to insure the unit's satisfactory performance if and when several bus sections fail.

Complete details of the calculational procedure used to determine the "out of compliance" probability were not provided in the previous paper and are discussed in the next section.

CALCULATION OF THE OUT-OF-COMPLIANCE PROBABILITY

The most important aspect of both the present and previous works is the calculation of the "out of compliance" probability. When several bus sections fail, the effect of these failures on the overall collection efficiency is a function of where the failures are located. Since it is usually impossible to predict which bus sections will fail, it is assumed that these failures occur randomly. (Note: This calculational procedure can easily be modified to handle cases where it cannot be assumed that the failure locations are random (1).) In order to determine, in rigorous fashion, the probability of whether or not the unit will be out of compliance after a given number of bus sections have failed, it is necessary to "test" all possible arrangements of the failure locations. The out-of-compliance probability is given by the percent of arrangements that result in overall efficiencies less than the minimum required to satisfy the legal standard. For large precipitators, however, the number of different arrangements of failure locations can be extremely large. For a unit of 64 bus sections with four bus section failures, for example, the number of arrangements can be shown to be

$$64!/(64-4)! = 15,249,024.$$

Since it is virtually impossible to test this number of failure location arrangements, a strictly rigorous approach is not practical. To generate the results presented in this paper, as well as those in the earlier work, a Monte Carlo technique (2,3,4) is employed. In this method, only a random sampling of the possible failure arrangements is tested. The arrangements to be tested are chosen by the use of random numbers, i.e., a set of random numbers are generated, equal in number to the number of bus section failures, and each of these random numbers is used to "choose" a particular bus section, which, during the calculation of the overall collection efficiency, is assumed to be out of commission. The accuracy of this approach depends on the number of arrangements used in the sampling. For all of the out-of-compliance probabilities listed in this paper, the number of failure location arrangements sampled was 5000, although reproducible results can be obtained with fewer runs, the number of runs depending on the accuracy required. The random numbers used were generated by the power residue method (5). These programs were written in FORTRAN and originally run on a VAX/780 (Digital Equipment Corporation) computer at Manhattan College; the programs were later modified to run on Con Edison's Hewlett-Packard system.

PRESENT STUDY

In the present study, the calculational procedure described above is extended to include the element of time. The calculations are based on a statistical extrapolation from previous bus section failure rate data and are intended to provide an intelligent prediction as to when the unit can be expected to be out of compliance due to bus section failure. The procedure can be applied in one of two different modes depending on the type of prior information available. The first mode applies to situations where the numbers of bus sections that have failed during the past several operating periods (i.e., intervals between scheduled outages) is known and can be used to estimate the number of failures expected during the next operating period. Usually this estimate is based on an extrapolation from the past numbers of failures. The second mode applies to situations where early failure rate data during the present operating period, such as the dates and locations of the failures up to the present time, are available. Both modes provide the same type of information to the user: the probability that this unit will be out of compliance by the next scheduled outage or by the end of any designated period of time.

THE FIRST MODE

To use the first mode, an estimate of the number of bus section failures expected by the end of the next operating period is required. This estimate should be based on the

number of failures that have occurred during each of the past several operating periods. The probability that any one bus section will fail during the next operating period is given by the ratio of the average number of bus section failures to the total number of bus sections in the unit. Assuming that the number of failures (hereafter also referred to as "failure number") in an operating period has a binomial distribution (6), a probability that a given number of failures will occur during the next operating period can be found. For example, if, during the current operating period, six bus section failures are expected in a precipitator containing 64 bus sections, the single bus section failure probability is 6/64. According to the binomial distribution, the probability of 6 failures occurring in this precipitator during the current period is 16.9%; of 7 failures occurring, 14.5%; etc. Several binomial probabilities for several failure numbers for this example are given below:

failure no.	1	4	5	6	7	10
probability	1.2%	13.4%	16.9%	16.9%	14.9%	3.9%

Using the binomial distribution in the manner described above, the probabilities associated with all possible numbers of failures (i.e., from zero to N, where N = the total number of bus sections in the unit) are determined. There are N+1 such numbers. These probabilities are used in conjunction with the Monte Carlo method to obtain the compliance probabilities, as described below.

A large number of "cases" or runs are next examined. In each case, two sets of random numbers are generated: the first set, a single random number, is used to assign a failure number for the next operating period; the second set, consisting of one random number for each of the failures (the number of these having been set by the first random number), is used to assign the "arrangement" (or locations) of the failures (as in the previous work). The assignment of the number of failures by the first random number must be compatible with the binomial distribution assumed earlier, i.e., those failure numbers with the higher probabilities of occurrence must have the higher chance (or frequency) of random number assignment. This is accomplished by dividing the random number range (0 to 1) into N+1 sub-ranges or "windows", one for each of the possible failure numbers. Since the size of each window is made proportional to the binomial probability calculated for that particular failure number, a very large number of runs will result in a set of binomially distributed failure numbers.

Once the failure number for a particular case has been determined, the locations of these failures are assigned by the second set of random numbers as previously described. The overall collection efficiency is then calculated and compared with the minimum efficiency required for compliance. When a large number of runs has been examined, the out-of-compliance probability is calculated from the number of arrangements or runs that resulted in efficiencies lower than this minimum.

ILLUSTRATIVE EXAMPLE 1

The Consolidated Edison Company of New York is considering plans to upgrade one of its electrostatic precipitators as part of the Ravenswood coal reconversion project. The existing unit was designed to operate at an efficiency of 99.00% and contains four separate high-voltage fields with eight parallel chambers for gas flow. The boiler is designed to utilize coal with a 8 lbs ash/million Btu content, but would burn coal with an ash content of 10 lbs/million Btu. To upgrade the unit, one high voltage field will be added and this is expected to raise the collection efficiency to 99.45%. In order to meet emission standards, the existing and upgraded units cannot operate below efficiencies of 98.55% and 98.82%, respectively.

From previous field data, the existing unit is expected to sustain five bus section failures during the next operating period. (a) Based on this estimate, what is the probability that the existing unit will be out of compliance by the next scheduled outage? (b) What is the out-of-compliance probability for the upgraded unit if 5 bus section failures are estimated for an operating period? ... if 7 bus section failures are estimated?

Solution: The calculated results for this problem are summarized in the Table 1. For the existing unit, it is found that, if 5 bus section failures are expected to occur before the next scheduled outage, the out-of-compliance probability is 70.0%. For the upgraded unit, this probability drops to 9.6% for 5 anticipated failures, and to 31.4% for seven.

This example clearly demonstrates the technical and economic merit of adding another high voltage field. The unit will not only operate more efficiently, but will also allow the boiler to fire a cheaper (higher ash content) coal.

TABLE 1. SUMMARY OF RESULTS FOR ILLUSTRATIVE EXAMPLE 1

	existing unit	upgraded unit	
no. of anticipated failures	5	5	7
probability for this number of failures	19.1%	18.7%	16.4%
out-of-compliance probability	70.0%	9.6%	31.4%

THE SECOND MODE

The second mode is employed to predict the out-of-compliance probability at the next scheduled outage when early bus section failure rate data for the present operating period are available. The method basically involves an extrapolation from these failure data and hence information from previous operating periods is not required.

By "early failure rate data" (hereafter also referred to as "time-to-failure" data) is meant the length of time, measured from the start of the present operating period, before each bus section failure occurred along with the location of that failure. In the calculations for this mode, the times of the failures are assumed to follow a Weibull distribution (7,8). This type of distribution has been found to be appropriate in describing failure patterns that are basically due to deterioration or wear.

Provided the start of the operating period is set at a time of zero, there are only two constants for the Weibull distribution equation that must be evaluated from the time-to-failure data. There are several methods by which this can be accomplished. It is the opinion of the authors that the method of "maximum likelihood estimations" (9) provides the best combination of convenience and accuracy for this particular application. Two types of data-censuring techniques are available with this method. Type I censuring is considered more appropriate because it takes into account not only the time to each failure that occurred, but also the time elapsed since the last failure.

Once the Weibull constants have been evaluated, the future time (usually the end of the current operating period) to which the data are to be extrapolated is chosen. Using the Weibull distribution, the probability of an individual bus section failing from the start of the operating period to that designated time can be calculated. The expected number of bus section failures (including the initial failures already observed) is then the product of this individual bus section probability and the total number of bus sections in the unit. As in the first mode, it is assumed that the number of future bus section failures is binomially distributed. The same technique as that used in the first mode to calculate the unit's out-of-compliance probability from the estimated number of bus section failures, or equivalently from the individual bus section failure probabilities, is then employed.

Although most of the calculations are the same for both modes, it should be pointed out that there are two advantages to using the second mode, if the necessary data are available. (a) During the course of the current operating period, the amount of time-to-failure data increases (whether more failures occur or not) and hence the out-of-compliance probability can be, and should be, continually updated. (b) Unlike the operating periods of fixed duration required in the first mode, the second mode provides the capability of altering the time to which the time-to-failure data are extrapolated. This aspect can be particularly useful if the next outage can be rescheduled. For example, suppose it is desirable that the unit not exceed a certain out-of-compliance probability, e.g., 20%. The time (measured from the present) corresponding to an out-of-compliance probability of 20% can be calculated and used to reschedule the next outage. This type of calculation is demonstrated in Example 2.

ILLUSTRATIVE EXAMPLE 2

For the upgraded unit at Con Ed's Ravenswood plant in Example 1, the following bus section failures have occurred since the last scheduled outage:

failure number	location (chamber,field)	time days
1	(4,2)	62
2	(7,4)	112
3	(8,1)	153
4	(1,3)	209

(a) Assuming that the last failure just occurred (i.e., that this analysis is being done on the 209th day), what is the probability that this unit will be out of compliance after 330 days, for which date a plant outage has been scheduled? It was recommended that the out-of-compliance probability not be allowed to exceed 10%. In keeping with this recommendation, will it be necessary to reschedule the outage, and if so, to what date? (b) Redo Part (a) assuming that three weeks have passed without the occurrence of another failure.

Solution: The results for this problem are summarized in Table 2. For each part, the data (including the 3-week time lapse without a failure in Part b) were used to determine the two Weibull distribution constants. The Weibull distribution was then applied to predict the number of bus section failures as well as the individual bus section failure probability (probability of failure for a given bus section that has not already failed). Using this individual probability in the binomial distribution, the probability for each failure number (i.e., the probability that a given number of failures would occur before the end of the operating period) was calculated; these were then used in the Monte Carlo technique to arrive at the out-of-compliance probabilities.

TABLE 2. SUMMARY OF RESULTS FOR ILLUSTRATIVE PROBLEM 2

Part (a):			
duration of operating period (days)	330	300	270
anticipated number of bus section failures	8.9	7.6	6.3
out-of-compliance probability (%)	50.4	27.1	9.5
Part (b):			
duration of operating period (days)	330	315	300
anticipated number of bus section failures	6.9	6.5	6.0
out-of-compliance probability (%)	18.1	11.6	6.6

For Part (a), the 50.4% out-of-compliance probability at the end of the 330-day operating period is unacceptable and the outage should be rescheduled (moved up). The results for a 300-day and a 270-day period indicate that the outage should be advanced by about two months if the recommended 10% maximum for the out-of-compliance probability is to be strictly adhered to. For Part (b), as expected, the addition of the 3-week time lapse without a failure decreased the out-of-compliance probability by a considerable margin. The probability for the 330-day period is still above the 10% limit, and indicates that the outage should be moved up by about three weeks.

This example demonstrates the advantage of using the out-of-compliance probability as a basis for the scheduling of maintenance outages. Without a method of quantifying this probability, this type of optimization is impossible.

SUMMARY

Calculational procedures aimed at helping those concerned with bus section failures in electrostatic precipitators have been presented in two phases. In the first phase, which was the topic of a previous paper and primarily intended for design purposes, a technique to enable alternate ESP designs to be quickly and conveniently compared and evaluated was developed. The second phase, which is the topic of this present paper and intended mainly for application in operation and maintenance, provides calculational procedures which should be useful in scheduling outages and/or derating units. These procedures are based on a statistical extrapolation from previous bus section failure data and provide an intelligent prediction as to when the unit can be expected to be out of compliance due to bus section failure. This model can be applied in one of two different modes depending on the type of prior information available. If the numbers of bus section failures for the last several operating periods are known, the first mode applies. If, however, the prior data extend from the beginning of the present maintenance period and the dates of the bus section failures during this period are available, the second mode would be used. Both modes provide the same type of information to the user: the probability that this unit will be out of compliance by the next scheduled outage. This information can be used to assist the user in determining the optimum time interval to employ in the scheduling of maintenance outages.

In conclusion, a calculational tool is now available that can provide quantitative ESP information on bus section failure for both design and operation/maintenance usage. The design aspect of the program can assist vendors, users, regulatory personnel, and consulting engineers in making rational decisions when evaluating alternate ESP designs. The operation/maintenance aspect can assist the user's field personnel in maintaining the unit in compliance and in scheduling outages.

FORTRAN programs to perform these calculations are operational on both main-frame and microcomputers at Manhattan College, and an extensive User's Guide for this program is available from Con Edison's Chemical Section.

ACKNOWLEDGEMENTS

Messrs. A. J. Buonicore, H. Engelbrecht, and M. Robinson served as consultants on this project. Thanks are also due to

Ann Kaptanis for typing the manuscript.

This study was supported by the Consolidated Edison Company of New York, Contract No. 4-20997, as part of that utility's Coal Conversion Project.

The work described in this paper was not funded by the U.S. Environmental Protection Agency and therefore the contents do not necessarily reflect the views of the Agency and no official endorsement should be inferred.

REFERENCES

1. L. Theodore, J. Reynolds, "ESP Bus Section Failures: Design Considerations", J. Air Poll. Control Assoc., 33: 1215-1218, 1983.

2. L. Theodore, A. Buonicore, Industrial Air Pollution Control Equipment for Particulates, CRC Press, 1976, P. 70.

3. A. Buonicore, L. Theodore, "Monte Carlo Simulation to Predict Collection Efficiencies of Centrifugal Separators", Paper No. 60d, 74th National A.I.Ch.E. Meeting, New Orleans, 1973.

4. J. Reynolds, L. Theodore, J. Marino, "Calculating Collection Efficiencies for Electrostatic Precipitators", J. Air Poll. Control Assoc. 25: 610-616, 1975.

5. B. J. Ley, Computer Aided Analysis and Design for Electrical Engineers, Holt, Rinehart and Winston, Inc., 1970, P. 534.

6. N. Mann, R. Schafer, N. Singpurwalla, Methods for Statistical Analysis of Reliability and Life Data, Wiley, 1974, P. 76.

7. E. Henly, H. Kumanato, Reliability Engineering and Risk Assessment, Prentice-Hall, Inc., 1981, P. 212.

8. Mann, Schafer, Singpurwalla, P. 127.

9. Mann, Schafer, Singpurwalla, P. 189.